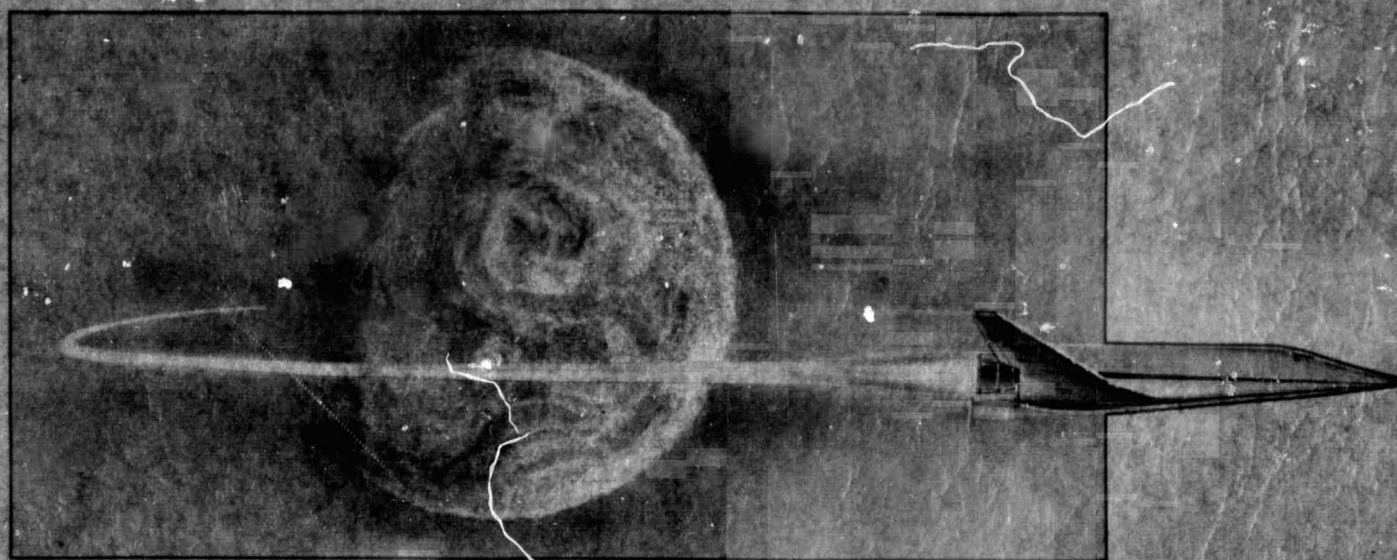


LMSC-A959837  
VOL I  
DECEMBER 22, 1969



**FINAL REPORT**  
**INTEGRAL LAUNCH AND REENTRY VEHICLE**  
**VOLUME I**  
**CONFIGURATION DEFINITION**  
**AND PLANNING**  
**PART A - SECTIONS 1 THROUGH 9**

3

5

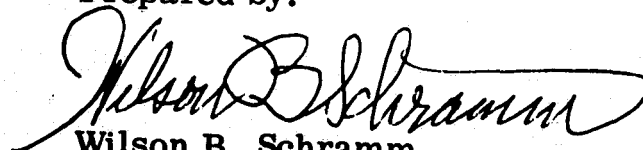
N70-31822

FACILITY FORM 602	_____	_____
	(ACCESSION NUMBER)	(THRU)
	526	1
_____	_____	
(PAGES)	(CODE)	
CR-102543	31	
(NASA CR OR TMX OR AD NUMBER)	(CATEGORY)	

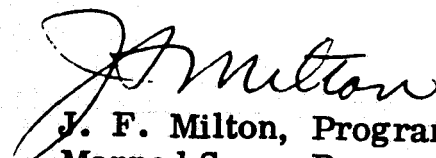
FINAL REPORT  
INTEGRAL LAUNCH AND  
REENTRY VEHICLE


Volume I  
Configuration Definition and Planning  
Part A - Sections 1 through 9

Prepared by:

  
Wilson B. Schramm  
ILRV Study Manager

Approved by:

  
J. F. Milton, Program Manager  
Manned Space Programs

  
F. C. E. Oder  
Vice President and Assistant General Manager  
Space Systems Division

## FOREWORD

This final report for the Integral Launch and Reentry Vehicle (ILRV) Study, conducted under Contract NAS9-9206 by Lockheed Missiles & Space Company under direction of the NASA Marshall Space Flight Center, is presented in three volumes. Volume I, Configuration Definition and Planning, contains results of the preliminary cost analyses, conceptual design, mission analyses, program planning, cost and schedule analyses, and sensitivity analyses, accomplished under Tasks 1 through 6. Volume II covers Task 7, Technology Identification; and Volume III contains results of the Special Studies conducted under Task 8.

Principal LMSC task leaders and contributors in performance of this study include:

Systems Integration	T. E. Wedge	Primary Engines	A. J. Hief
System Synthesis	J. E. Torrillo	Propulsion	L. L. Morgan
Mission Analysis	D. W. Fellenz	Integrated Avionics	J. J. Herman
Design	G. Havrisik	Safety	J. A. Donnelly
Cost	J. Dippel	Structures	P. P. Plank
Schedule	W. James	Thermodynamics	F. L. Guard
Test	R. W. Benninger	Aerodynamics	C. F. Ehrlich
Operations	K. Urbach	Weights	A. P. Tilley

The three volumes are organized as follows:

## Volume I - Configuration Definition and Planning

## Section

- 1 Introduction and Summary
- 2 System Requirements
- 3 Configuration Summary
- 4 Vehicle Design
- 5 Performance and Flight Mechanics
- 6 Aerodynamics
- 7 Aerothermodynamics
- 8 Structures and Materials
- 9 Propulsion

iii PRECEDING PAGE BLANK NOT FILMED.

Appendix A Drawings

Appendix B Supplemental Weight Statement

- 10 Avionics
- 11 Crew Systems
- 12 Environmental Control System
- 13 Reliability and Maintainability
- 14 System Safety
- 15 Operations
- 16 Test and Production
- 17 Cost and Schedules

Volume II - Technology Identification

Section

- 1 Introduction and Summary
- 2 Propulsion System Technology
- 3 Aerodynamics Technology
- 4 Aerothermodynamics Technology
- 5 Structures Technology
- 6 Avionics Technology
- 7 Bioastronautics Technology
- 8 Technology Development Program

Volume III - Special Studies

Section

- 1 Introduction
- 2 Propulsion System Studies
- 3 Reentry Heating and Thermal Protection
- Appendix A Rocket Engine Criteria for a Reusable Space Transport System
- 4 Integrated Electronics System
- 5 Special Subsonic Flight Operations
- Appendix B Summary of Electronics Component Technology (1972)
- Appendix C Requirements Definition Example (Propulsion)
- Appendix D Application of BITE to Onboard Checkout

CONTENTS

Section		Page
1	INTRODUCTION AND SUMMARY	1-1
2	SYSTEM REQUIREMENTS	2-1
	2.1 Mission Types	2-1
	2.2 Ascent Reference Orbit	2-1
	2.3 On-Orbit Delta Velocity	2-2
	2.4 Crew Size and Accommodations	2-3
	2.5 Mission Duration	2-3
	2.6 Payload Bay	2-3
	2.7 Return Cross Range	2-3
	2.8 Maximum Acceleration	2-4
	2.9 Design Contingency	2-4
	2.10 Docking Capability	2-4
	2.11 Guidance and Control	2-4
	2.12 Passenger/Cargo Accommodation	2-4
	2.13 Reliability and Safety	2-5
	2.14 Propulsion Requirements	2-6
3	CONFIGURATION SUMMARY	3-1
	3.1 Two-Stage Configuration Data	3-1
	3.2 Dissimilar Triamese Data	3-15
	3.3 Baseline Configuration Evaluation	3-26
	3.4 Alternate Configuration Approaches	3-37
4	VEHICLE DESIGN	4-1
	4.1 Two-Stage Vehicle-Design Description	4-2
	4.2 Triamese	4-14
	4.3 Pilot Vision Concept	4-18
	4.4 Personnel Escape Systems	4-19
	4.5 Launch Vehicle Attachment System	4-39
	4.6 Payload Bay Door Concept	4-42

Section		Page
	4.7 Orbiter Nose Cap Concept	4-44
	4.8 Orbiter Tank Support Concept	4-49
	4.9 Booster Thrust Structure Concept	4-50
	4.10 Booster Propulsion System Concept	4-52
5	PERFORMANCE AND FLIGHT MECHANICS	5-1
	5.1 System Sizing and Parametric Analysis	5-1
	5.2 Ascent Trajectory Analysis	5-18
	5.3 Reentry Maneuver Trajectory Analysis	5-21
	5.4 Jet Engine System Studies	5-45
6	AERODYNAMICS	6-1
	6.1 Orbiter Characteristics	6-8
	6.2 Return Booster Characteristics	6-11
	6.3 Composite Launch Vehicle Characteristics	6-15
7	AEROTHERMODYNAMICS	7-1
	7.1 Ascent Thermal Environment	7-1
	7.2 Reentry Heating and Thermal Protection	7-4
	7.3 Base Heating Environment and Candidate Material Systems	7-9
	7.4 Orbiter Plume Effects During Separation	7-15
8	STRUCTURES AND MATERIALS	8-1
	8.1 Design Criteria and Loading Requirements	8-1
	8.2 Materials	8-12
	8.3 Thermal Structural Concepts	8-16
	8.4 Vehicle Structural Arrangement	8-20
9	PROPULSION	9-1
	9.1 Primary Propulsion System	9-1
	9.2 Reaction Control System	9-18
	9.3 Subsonic Cruise Propulsion System	9-32
	9.4 Auxiliary Power/Hydraulic System	9-41

Section		Page
10	<b>AVIONICS</b>	10-1
	10.1 Electrical Power	10-1
	10.2 Guidance, Navigation, and Flight Control	10-11
	10.3 Communications	10-58
	10.4 Data Management	10-63
11	<b>CREW SYSTEMS</b>	11-1
	11.1 Crew Functions	11-1
	11.2 Crew Size and Composition	11-1
	11.3 Crew Compartment Configurations	11-2
	11.4 Crew Visibility Considerations	11-9
	11.5 Control and Display Concepts	11-13
	11.6 Habitability	11-17
	11.7 Crew Hazards Analysis	11-18
12	<b>ENVIRONMENTAL CONTROL AND LIFE SUPPORT</b>	12-1
	12.1 Atmospheric Supply and Control	12-1
	12.2 Thermal and Humidity Control	12-9
	12.3 Carbon Dioxide and Trace Contaminant Removal	12-10
	12.4 Food and Water	12-10
	12.5 Waste Management, Personal Hygiene, Medical Supplies	12-11
13	<b>RELIABILITY AND MAINTAINABILITY</b>	13-1
	13.1 Mission Success Design Criteria	13-1
	13.2 Reliability Models	13-2
	13.3 Maintainability Considerations	13-2
14	<b>SAFETY</b>	14-1
	14.1 Flight Safety	14-1
	14.2 Crew Safety	14-3
	14.3 Ascent Safety Propulsion Considerations	14-9
	14.4 Safety Tasks	14-12

Section		Page
15	<b>OPERATIONS</b>	15-1
	15.1 System Operations Profile	15-1
	15.2 Ground Operations	15-4
	15.3 Facilities and Operations	15-9
	15.4 Operations Management and Support	15-27
	15.5 Ground Support Equipment	15-30
	15.6 Logistic Mission Operations	15-35
	15.7 Docking Operations	15-37
	15.8 Logistics Cargo Transfer	15-46
16	<b>TEST AND PRODUCTION</b>	16-1
	16.1 Engineering Test Program	16-1
	16.2 Manufacturing	16-38
17	<b>COSTS AND SCHEDULES</b>	17-1
	17.1 Work Breakdown Structure	17-2
	17.2 Parametric Costing	17-2
	17.3 Bottom-Up Cost Estimate	17-20
	17.4 Schedules	17-38



Section 1  
INTRODUCTION AND SUMMARY

The Integral Launch and Reentry Vehicle Study was initiated by LMSC in March 1969, under direction of the Marshall Space Flight Center. The general objectives of the study were to assess technical feasibility, performance, and cost for development of reusable earth-orbital transportation systems that provide potential for an order of magnitude reduction in operating costs. A specific objective was to define baseline Space Shuttle configurations to perform the crew and passenger and logistics transport mission to support the large NASA Space Stations planned in the late 1970s and 1980s. The Space Shuttle, as presently conceived, is a versatile multimission vehicle system, based entirely on advanced liquid hydrogen and oxygen propulsion, with the capability of delivering 50,000 pounds to the nominal Space Station orbit at 270 nm and 55 degree inclination and returning to earth intact. The recommended vehicle design approach calls for a blend of advanced rocket and aircraft development techniques in a fully reusable Two-Stage configuration, consisting of an orbiter spacecraft and a flyback booster. Operations and facilities concepts provide for economical use at the high traffic rates forecast for routine common-carrier modes of space cargo and passenger flights in the decade of NASA and DOD space programs following IOC.

Significant aspects of the total system evaluation addressed in this final report include technical feasibility of the primary structural and propulsion concepts and technology requirements to achieve these developments; total payload performance for the nominal Space Station logistics mission; flexibility in performance and cross range to accommodate alternate missions; and the RDT&E and recurring operational costs.

Of the alternative approaches to design and development of a reusable Space Shuttle system investigated, several are not reflected in the baseline configurations. These alternatives and the rationale supporting various contractor and NASA decisions that

successively narrowed the range of alternatives are traced in Volume I, Section 3.4. Two prominent configurations investigated initially in the study are the Stage-and-One-Half/Star Clipper and the pure Triamese, each adhering to the preliminary study requirements for a 25,000-pound payload carried in a 3000-cubic foot cargo bay. Both concepts represent an orbiter development approach that could achieve the desired mission capability without relying on parallel development of a separate flyback booster, and both inherently require propellant crossfeed for full utility of all main propulsion engines at liftoff. The Stage-and-One-Half concept was conceived to achieve this objective through use of low-cost drop tanks and carrying all primary engines to orbit. The pure Triamese concept embodies a high degree of structural and propulsion commonality so that the orbiter and booster functions could be performed interchangeably by any element of the system. One concept is for a fully reusable vehicle; and the other, a partially reusable vehicle, with the principal cost elements concentrated in the orbiter.

Early in the study, new requirements forced system growth to a 50,000-pound payload, accommodated in 10,000-cubic foot bay. This typically increased the liftoff gross weight of candidate configurations by 70 percent. At this stage in development of these concepts, essentially no significant differences in total development and operational costs were identified; and another alternative, the Two-Stage fully reusable concept, with either parallel or tandem burning of the primary propulsion systems was introduced into the comparisons.

The remainder of the study revolved around resolution of key configuration sizing and evaluation discriminators as issues for evaluation and selection of the recommended baseline configurations. One such key issue was the drop tanks in the Stage-and-One-Half concept, eliminated by NASA to accommodate requirements for full reusability, omnidirectional launch capability and in consideration of the cost and inconvenience associated with drop-tank impact and disposal at the increased launch rates contemplated for joint NASA and DOD use of the shuttle. This step left only the pure Triamese concept dependent on propellant crossfeed for technical feasibility and achievement of its development objectives. One aspect of the pure Triamese concept is that the orbiter is required to carry variable-geometry wings in order to fulfill

the booster cruise-back function when it is used in booster application. The delta planform lifting body orbiter configuration applied in this study has inherently a sufficient subsonic L/D to accomplish approach and landing, and this proved to be a strong motivation in departing from the concept of rigorous commonality in the Triamese. Indications were apparent in LMSC trade studies that the doctrine of forced commonality between orbiter and booster elements could not be maintained and yet provide a competitive system gross weight. Vehicle sizing and optimization studies indicated cascading weight penalties for carrying elements for performing orbital and reentry functions in the booster and for carrying elements for performing cruise-back functions in the orbiter. Thus, the doctrine of forced commonality in structure and propulsion was abandoned and the need for crossfeed put in doubt. Only the dissimilar Triamese was carried forward into the final baseline configurations offered in this report. This configuration is essentially a Two-Stage fully reusable system, in which the booster is divided into two elements.

The remaining key question of parallel burn with or without crossfeed involved both configuration and operational implications. The weight savings provided by parallel burn with crossfeed over a pure tandem-burn condition is less than 2 percent in lift-off weight if the structural costs for crossfeed are not considered. The estimate of the structural weight for providing crossfeed is approximately 2500 pounds for a typical  $3.5 \times 10^6$  lb liftoff weight configuration. Hence, the advantage of a parallel burn plus crossfeed configuration over a pure tandem-burn configuration is about 1 percent, which is outweighed by the disadvantages in technical risk and complexity.

Burning the orbiter engines at 10 percent thrust during boost without crossfeed results in a 6 percent liftoff weight penalty, as compared to parallel burn with crossfeed. If the engines are initially burned at 100 percent thrust, the penalty is 10 percent. These penalties result from the necessity of providing the extra propellant storage in the weight-sensitive upper stage. These penalties are considered too high; therefore, operational Space Shuttle system should employ sequential burning of the stages. It is expected that there will be sufficient experience by the 1975 time period to warrant confidence in both on-orbit and during-boost starting of hydrogen/oxygen propulsion systems. During the development period, it may be feasible to

design the system initially for a parallel burn. If the system is initially sized for the sequential-burn condition, it can be flown at reduced payload in a parallel-burn condition during development and, after propulsion system experience and confidence are obtained, switched to the sequential burn mode with full payload capability. The recommended baseline configuration is a Two-Stage tandem-burn concept.

Alternative primary propulsion systems were carried throughout the study. These were the bell-nozzle and aerospike nozzle engine configurations at engine sea-level thrust values between 400,000 and 1,000,000 pounds. The shuttle concept that appeared to benefit most from the aerospike engine is the Stage-and-One-Half, in which all engines are burned from liftoff through orbit injection and the deep throttling capabilities and altitude compensation characteristics of the dual-throat aerospike are fully used. No clearly defined configuration installation and performance advantages could be determined for the aerospike engine in the Two-Stage, tandem-burn vehicle configurations.

Further discrimination among alternatives concerns cross-range potential. Cross range may not be a requirement for initial operational capability of the system, although in the interest of developing a highly versatile shuttle system, a capability for growth to at least a 1500-nm cross-range capability would be a highly desirable feature of any design. If the initial configuration of the orbiter is properly chosen, it can provide this capability by allowing for an increase in heat shield size and weight. The payload difference between a zero cross-range condition and 1500-nm cross-range condition is expected to be 10,000 pounds or less. The delta planform lifting body provides an additional attractive approach to the flight testing of the thermal protection system. Since the vehicle trims and is stable hypersonically through a wide range of angles of attack, the initial reentry tests may be performed at angles of attack for  $C_L$  max, where the peak temperature and the total heat are lowest. Then, as confidence in the thermal protection system is gained, the angle of attack can be reduced toward L/D max and gradually larger cross-range reentries performed.

The most significant issue in the final assessment of shuttle configurations is that of liftoff gross weight, which essentially is a measure of performance effectiveness, the

flight hardware inert weight, and the facilities and total program cost. Feasibility of the total system concept and the development planning, reflect significantly the impact of liftoff gross weight. The baseline Two-Stage configuration reported herein is sized to accommodate the nominal Space Station logistic mission with the full complement of reserves and contingencies embodied in the guidelines and with powered go-around for the orbiter landing mode. Analysis of inert weight growth sensitivity of the conceptual design based on historical trends in development of spacecraft from concept definition phase to operation indicates that the reserves and contingencies can accommodate mission requirements in an evolutionary development approach.

A significant contributor to launch system size and weight is the requirement that leads to selection of a jet engine system for powered go-around, since engines plus fuel must go to orbit and back. Development risk for the total program involves assessment of the dispersions anticipated due to weight growth in context with utilization of all contingencies and reserves, and with planned adjustments in requirements as the development program proceeds. This aspect is discussed definitively in Volume I, Section 3.3, which shows that a projected weight-growth penalty of 19,000 pounds in payload can be offset by eventual elimination of powered go-around in the operational phase or alternatively by reduction of flight performance reserves. With the recommended Two-Stage baseline configuration, a suggested concept is a planned minimum capability of 25,000 pounds at IOC for the nominal Space Station logistic mission, with identifiable growth potential to 50,000 pounds as performance reserves and contingencies are committed and as operational experience justifies elimination of some of the more costly options and requirements.

## Section 2 SYSTEM REQUIREMENTS

The requirements defined here form a basis for conceptual design of the ILRV baseline vehicles and support equipment. These requirements are consistent with desired characteristics defined by NASA in June 1969, and the conceptual design approaches presented in this report have been sized to meet all of these desired characteristics. The status of alternate requirements and design approaches is presented in Section 3.4, Alternate Configuration Approaches. Requirements for which future designs may deviate from the baselines are also identified parenthetically in this section.

### 2.1 MISSION TYPES

The vehicle is to be operationally flexible and capable of accepting a large variety of payloads, either cargo only or including passengers or mission-peculiar personnel, to accomplish the following mission types:

- Space Station/Base logistics
- Placement and retrieval of unmanned satellites
- Delivery of propulsion stages and payloads
- Delivery of propellants
- Experiment module/satellite service and maintenance
- Short-duration orbital mission

### 2.2 ASCENT REFERENCE ORBIT

Injection into the ascent reference orbit is not required, but performance beyond this orbit is definition of on-orbit delta velocity. Following are the particulars:

Perigee altitude: 45 nm  
Apogee altitude: 100 nm  
Inclination: 55 deg

Note: Ascent flight performance reserve of 3/4 of 1 percent of ascent ideal velocity.

### 2.3 ON-ORBIT DELTA VELOCITY

There will be an on-orbit delta velocity of 2000 ft/sec, including both main propulsion system and the translational capability of the H<sub>2</sub>/O<sub>2</sub> reaction control system (RCS). Propellants for on-orbit use will be stored partially in the main propulsion tanks and partially in extended-time storage tanks (up to 30 days), according to the following tabulation, which also shows a typical Space Station logistics mission  $\Delta V$  breakdown:

● With main tank propellants:	
Circularize at 100 nm	100 ft/sec
Transfer into 260-nm phasing orbit	558
Launch dispersion plane change	200
Total	858 ft/sec
● With extended-time stored propellants:	
Terminal rendezvous, docking, and undocking (RCS)	142 ft/sec
Deorbit	500
Contingencies	500
Total	1142 ft/sec
On-orbit total	2000 ft/sec

Note: For sizing purposes, it is to be assumed that only 142 ft/sec is to be used at the lower  $I_{sp}$  of the RCS.

## 2.4 CREW SIZE AND ACCOMMODATIONS

- Basic two-man crew with systems designed to be operable by one man in an emergency
- Crew cabin sized for an additional two men for mission-peculiar functions, with space for installation of mission-peculiar modular console (alternate approaches with two-man cabin to be studied further)
- ECS sized for four men total but expendables of baseline vehicles for the two-man crew only; additional expendables to be deducted from payload on missions with additional personnel (not applicable to two-man cabin alternatives)
- Landing visibility comparable to that of high-performance aircraft
- Shirtsleeve environment with 10 psi total pressure, 2.7 psia O<sub>2</sub> partial pressure, 7.3 psia N<sub>2</sub> partial pressure (These values are ILRV requirements; compatibility with Space Station/Base atmosphere is to be provided, but effects of possible increased pressure is not included in ILRV baseline sizing.)

## 2.5 MISSION DURATION

- Seven days self-sustaining an orbit
- Up to 30 days capability, with additional expendables provided from payload allocation

## 2.6 PAYLOAD BAY

- Bay sized to contain two alternate payload sizes:
  - 15-ft diameter, 60-ft long
  - 22-ft diameter, 30-ft long

## 2.7 RETURN CROSS RANGE

- Aerodynamic configuration adequate to meet DOD requirements
- Heat shield sizing to be based on 400-nm cross range
- Vehicle to be capable of reentry in high angle of attack, low L/D mode, with reduced cross range to provide more predictable (laminar) peak heating



## 2.8 MAXIMUM ACCELERATION

- Ascent: 3 g (eye balls in) with passengers, 4 g with crew only
- Reentry: 2 g (may be eyeballs down or out)\*

## 2.9 DESIGN CONTINGENCY

- Ten-percent of all dry weights design contingency allowed

## 2.10 DOCKING CAPABILITY

- Piloted hard docking to Space Station/Base
- Full automatic hard docking
- Undocked stationkeeping within 10 feet
- Shuttle-to-shuttle hard docking

## 2.11 GUIDANCE AND CONTROL

- Autonomous capability
- Restrictions to vehicle attitude of limited duration permissible for use of G&N sensors; otherwise no on-orbit attitude restriction
- One degree/sec<sup>2</sup> rotational acceleration, all axes
- One ft/sec<sup>2</sup> translational acceleration, all axes

## 2.12 PASSENGER/CARGO ACCOMMODATION

- Payload bay of basic vehicle to be designed to accommodate payload systems for either all-cargo or cargo-plus-passenger module for up to 50 people
- Design to allow for shirtsleeve transfer of crew and passengers to and from Space Station or Space Base
- Limited cargo transfer through personnel transfer hatches
- Large cargo transfer normally without EVA (Suited IVA in evacuated area is permissible in normal mode.)

\*Normal reentry will have peak of about 1.5 g, but some minimum range trajectories could exceed 2 g unless restricted. Penalty for restriction is small, and 2 g is reasonable maximum value for eyeballs down or eyeballs out.

## 2.13 RELIABILITY AND SAFETY

Adequate redundancy will be provided so that all subsystems fail operational with the failure of any critical component and fail safe with any second failure. Electronic systems should be designed for fail operational, with failure of two components providing any critical function and fail safe with a third failure. ("Fail operational" implies that mission capability remains after the failure; "fail safe" implies no effects of the failure lead to loss of life or equipment.)

Additional safety features include the following:

- Intact abort for operational vehicles
  - Primary abort mode through orbit
  - Return-to-base alternate mode for early portion of ascent
  - Multiple-engine design with zero deadband for single-engine-out condition (any engine)
  - Propellant expulsion to achieve landing weight by operation of remaining engines
- Highly reliable automatic landing system with zero-zero capability
- One time go-around capability for all landings for both booster and orbiter (alternates without go-around to be considered in future designs)
- Vehicle and launch site facilities for rapid, safe crew and passenger egress in case of prelaunch abort
- Basic vehicle to provide systems for crew egress after landing without ground system support and to accommodate payload system for safe passenger egress

## 2.14 PROPULSION REQUIREMENTS

- Bell-type, high  $P_c$ , hydrogen/oxygen primary engines with approximately 400,000 pounds of sea level thrust; minor resizing only to be needed if 400,000 pounds is chosen as engine specification level
- Three primary orbiter engines
- Sequential burn; orbiter engines started at staging
- Hydrogen/oxygen reaction control system
- Airbreathing engines fueled with JP-4 (alternate use of hydrogen-fueled airbreather to be further studied)

Section 3  
CONFIGURATION SUMMARY

Summarized in this section are baseline configuration data and evaluations and then alternate approaches.

3.1 TWO-STAGE CONFIGURATION DATA

Presented first are data on the 50,000-pound payload vehicle, then data on the 25,000-pound payload vehicle, in the following sequence:

- Design Summary and Geometry
- Propulsion/Performance Characteristics
- Vehicle Velocity Requirements
- Weight Summary
- Longitudinal Centroids (50 K case only)

DESIGN SUMMARY AND GEOMETRY (TWO-STAGE 50-K VEHICLE)

	<u>Booster</u>	<u>Orbiter</u>
Overall length (nose to fixed engine exit) (ft)	220	160
Overall length (nose to wing or fin tip)	237	179.5
Maximum span (ft)	200	101
Maximum body width (ft)	35	70
Maximum body height (ft)	38	27
Body volume - total (ft <sup>3</sup> )	140,000	
- propellant (ft <sup>3</sup> )	99,843	30,200
Body planform area (ft <sup>2</sup> )	14,740	5,720**
Body wetted area (ft <sup>2</sup> )	17,850*	15,000
Nose radius (ft)	3.0	3.0
Theo wing area (ft <sup>2</sup> )	12,000**	
Leading-edge sweep (deg)	51.5	78
Wing airfoil section	64-006	
Vertical tail area (two fins) (ft <sup>2</sup> )	3,100	1,540
Elevon area (ft <sup>2</sup> )	1,800	1,350
Tail rollout angle (deg)	35	30
Entry wing loading (psf)	34	46.4
Hypersonic L/D (trimmed)	0.57 at 60° $\alpha$	2 at 15° $\alpha$
Subsonic L/D <sub>max</sub> (trimmed)	7.5	4.66

\*Includes lower body surface blanketed by wing  
\*\*Aerodynamic reference areas

PROPULSION/PERFORMANCE CHARACTERISTICS (TWO-STAGE 50-K VEHICLE)

	<u>Stage 1</u>	<u>Stage 2</u>
Propellant/mixture ratio	7:1	7:1
Expansion ratio sea level vacuum	35:1 SL	35:1 SL and 150:1 vac
Specific impulse SL/vac (sec)	387.8 SL/428.5 vac	378.8 SL and 454.2 vac
Propellant fraction	0.850	0.763
Ideal $\Delta V$ (fps)	13,612	18,810
Mass ratio	2.69	3.64
Rocket engines	13 at 416K (SL)	3 at 487K (vac)
Thrust - sea level	5410K	
- vacuum	6000K	1460K
Flyback engine system		
Number/type	4 turbofan	4 turbofan
Maximum static SL thrust (lb)	135,000	87,000
SFC (1/hour)	0.43	0.50
Fuel (lb)	35,000	5600

VEHICLE VELOCITY REQUIREMENTS (TWO-STAGE 50-K VEHICLE)

*Ascent Ideal $\left(\frac{45}{100} \text{ nm}\right), 55^\circ$	Total (Subtotal)	Stage 1	Orbiter
	30,196	13,612	16,584
Inertial orbit velocity	25,882		
Losses			
Drag	-952	-931	-21
Gravity (including potential energy)	-3797	-3616	-181
Back pressure	-278	-252	-26
Thrust alignment } Maneuver }	-158	-9	-149
Earth rotation (gain) (Equiv initial vel)	+871	+871	-
Flight performance res ( $3/4\% \leq V$ )	226		226
Phasing Transfer 100 to 270 nm Circularize Rendezvous } 142 ft/sec Docking } at 1 ft/sec <sup>2</sup> } Orbit maneuvers Undocking Deorbit Orbit contingency	2,000		2,000
Total ideal velocity	32,422	13,612	18,810

\*Based on vacuum performance, this includes orbit velocity plus potential energy gained plus losses minus earth rotation velocity vector.

**WEIGHT SUMMARY (TWO-STAGE 50-K VEHICLE)**

Function or Condition	Booster	Orbiter	Stage
<b>Aerodynamic Surfaces</b>			
Wing	57,952	-	
Fin	-	4,601	
Elevon	-	9,000	
<b>Body Structure</b>			
Shell and frames	-	41,930	
Shell, frames, and tank domes	67,160	-	
Base shield	2,421	1,292	
Thrust structure	13,404	2,849	
Pressurized compartment	1,350	1,350	
<b>Induced Environment Protection</b>			
Body	18,741	30,618	
Wing	8,163	-	
Fin	-	4,656	
<b>Launch, Recovery, and Docking</b>			
Launch gear	15,000	5,000	
Landing gear	14,994	10,380	
Docking structure	-	500	
<b>Main Propulsion</b>			
Liquid rocket engine	58,720	12,493	
Airbreathing engine	32,341	20,806	
Rocket fuel container	-	13,392	
Rocket oxidizer container	-	10,647	
Rocket propellant systems	11,990	2,437	
Jet fuel container	2,653	421	
Jet propellant systems	455	433	

## WEIGHT SUMMARY (TWO-STAGE 50-K VEHICLE) (Continued)

Function or Condition	Booster	Orbiter	Stage
Orientation Controls, Separation and Ullage	4,387	2,059	
Prime Power Source	447	1,026	
Power Conversion and Distribution	8,563	4,082	
Guidance and Navigation	842	842	
Instrumentation	200	200	
Communication	141	141	
Environmental Control	1,181	1,231	
Personnel Provisions	636	636	
Crew Station Controls and Panels	612	612	
Range Safety and Abort	200	200	
Contingency	32,255	18,383	
Dry Weight	354,808	202,217	
Personnel	514	674	
Cargo	-	50,000	
Residual/reserve propellants and reactants	19,515	6,610	
ECS and prime power reactants	427	1,310	
Reaction control propellants	2,000	6,320	
Jet engine propellants	35,076	5,567	
Rocket engine propellants	2,344,297	705,571	
Launch Weight	2,756,637	978,269	3,734,906
Less main propulsion propellants	-2,344,297	-	-2,344,297
Stage Burnout Weight	-	-	1,390,609
Less main propulsion propellants	-	-669,507	



WEIGHT SUMMARY (TWO-STAGE 50-K VEHICLE) (Continued)

Function or Condition	Booster	Orbiter	Stage
Booster/Orbiter Burnout Weight	412,340	308,762	
Less ECS and prime power reactants,	-127	-485	
reaction control propellants, and	-2,000	-6,320	
orbit and retro propellants	-	-36,064	
Entry Weight	410,213	265,893	
Less prime power reactants and	-300	-825	
jet engine propellants	-35,076	-5,567	
Landing Weight	374,837	259,501	

LONGITUDINAL CENTROIDS (TWO-STAGE 50K VEHICLE)

All centroids are given in terms of feet and percentage of reference length. The reference length has its origin at the apex of the body sweep angle and ends at the base shield. The launch vehicle combined CG is given in the booster reference axis system.

	<u>Sta (ft)</u>	<u>% Ref L</u>
Launch Vehicle at Ignition	97	44.0
Launch Vehicle at Burnout	150	68.0
Booster at Entry (Ref L = 220 ft)	163	74.0
Booster at Landing	160	72.0
Orbiter at Ignition (Ref L = 164 ft)	115	70.2
Orbiter On-Orbit	120	73.0
Orbiter at Entry (50,000 lb payload)	121	73.5
Orbiter at Landing	121	73.5
Orbiter at Entry (no payload)	123	75.0

DESIGN SUMMARY AND GEOMETRY (TWO-STAGE 25-K VEHICLE)

	<u>Booster</u>	<u>Orbiter</u>
Overall length (nose to fixed engine exit) (ft)	211	154
Overall length (nose to wing of fin tip) (ft)	231	173
Maximum span (ft)		100
Maximum body width (ft)	35	60
Maximum body height (ft)	38	24
Body volume - total (ft <sup>3</sup> )		
- propellant (ft <sup>3</sup> )	81,000	22,800
Body planform area (ft <sup>2</sup> )		5,050*
Nose radius (ft)	3.0	3.0
Theo wing area (ft <sup>2</sup> )	10,914*	
Leading-edge sweep (deg)	51.5	78
Wing airfoil section	64-006	
Vertical tail area (two fins) (ft <sup>2</sup> )		1,370
Tail rollout angle (deg)	35	30
Entry wing loading (psf)		41.0
Hypersonic L/D (trimmed)	0.57 at 60° $\alpha$	2 at 15° $\alpha$
Subsonic L/D <sub>max</sub> (trimmed)	7.5	4.66

---

\*Aerodynamic reference areas

## PROPULSION/PERFORMANCE CHARACTERISTICS (TWO-STAGE 25-K VEHICLE)

	<u>Stage 1</u>	<u>Stage 2</u>
Propellant/mixture ratio	7:1	7:1
Expansion ratio sea level vacuum	35:1 SL	35:1 SL and 150:1 vac
Specific impulse SL/vac (sec)	387.8 SL/428.5 vac	378.4 SL and 454.2 vac
Propellant fraction	0.841	0.745
Ideal V (fps)	13,671	18,589
Mass ratio	2.70	3.58
Rocket engines	11 at 399K (SL)	3 at 467K (vac)
Thrust - sea level	4390K	
- vacuum	4860K	1400K
Flyback engine system		
Number/type	4 turbofan	4 turbofan
Maximum static SL thrust (lb)	118,000	68,000
SFC (1/hour)	0.43	0.50
Fuel (lb)	31,000	4400

VEHICLE VELOCITY REQUIREMENTS (TWO-STAGE 25-K VEHICLE)

	Total (Subtotal)	Stage 1	Orbiter
*Ascent Ideal $\left(\frac{45}{100} \text{ nm}\right), 55^\circ$	30,034	13,671	16,363
Inertial orbit velocity	25,882		
Losses			
Drag	-951	-931	-20
Gravity (including potential energy)	-3689	-3538	-121
Back pressure	-274	-250	-24
Thrust alignment } Maneuver }	-109	-9	-100
Earth rotation (gain) (Equiv initial vel)	+871	+871	-
Flight performance res (3/4% $\Delta V$ )	226		226
Phasing Transfer 100 to 270 nm Circularize Rendezvous } 142 ft/sec Docking } at $\leq 1 \text{ ft/sec}^2$ Orbit maneuvers Undocking Deorbit Orbit contingency	2,000		2,000
Total ideal velocity	32,260	13,671	18,589

\*Based on vacuum performance, this includes orbit velocity plus potential energy gained plus losses minus earth rotation velocity vector.

## WEIGHT SUMMARY (TWO-STAGE 25-K VEHICLE)

Function or Condition	Booster	Orbiter	Stage
<b>Aerodynamic Surfaces</b>			
Wing	54,244	-	
Fin	-	4,058	
Elevon	-	7,940	
<b>Body Structure</b>			
Shell and frames	-	36,776	
Shell, frames, and tank domes	57,760	-	
Base shield	2,121	1,142	
Thrust structure	10,876	2,906	
Pressurized compartment	1,350	1,350	
<b>Induced Environment Protection</b>			
Body	16,420	27,150	
Wing	7,640	-	
Fin		4,108	
<b>Launch, Recovery, and Docking</b>			
Launch gear	15,000	5,000	
Landing gear	13,127	8,295	
Docking structure	-	500	
<b>Main Propulsion</b>			
Liquid rocket engine	47,993	13,192	
Airbreathing engine	28,298	16,152	
Rocket fuel container	-	10,414	
Rocket oxidizer container	-	8,278	
Rocket propellant systems	9,568	2,547	
Jet fuel container	2,347	328	
Jet propellant systems	455	433	

WEIGHT SUMMARY (TWO-STAGE 25-K VEHICLE) (Continued)

Function or Condition	Booster	Orbiter	Stage
Orientation Controls, Separation and ullage	3,684	1,640	
Prime Power Source	447	1,026	
Power Conversion and Distribution	7,346	3,506	
Guidance and Navigation	842	842	
Instrumentation	200	200	
Communication	141	141	
Environmental Control	1,088	1,166	
Personnel Provisions	636	636	
Crew Station Controls and Panels	612	612	
Range Safety and Abort	200	200	
Contingency	28,240	16,054	
Dry Weight	310,635	176,592	
Personnel	514	576	
Cargo	-	25,000	
Residual/reserve propellants and reactants	16,975	5,264	
ECS and prime power reactants	427	1,304	
Reaction control propellants	2,000	5,205	
Jet engine propellants	31,039	4,341	
Rocket engine propellants	1,924,126	553,709	
Launch Weight	2,285,716	771,991	3,057,707
Less main propulsion propellants	-1,924,126	-	-1,924,126
Stage Burnout Weight	-	-	1,133,643
Less main propulsion propellants	-	-524,873	

WEIGHT SUMMARY (TWO-STAGE 25-K VEHICLE) (Continued)

Function or Condition	Booster	Orbiter	Stage
Booster/Orbiter Burnout Weight	361,652	247,118	
Less ECS and prime power reactants, reaction control propellants, and orbit and retro propellants	-127 -2,000 -	-479 -5,205 -28,836	
Entry Weight	359,525	212,598	
Less Prime power reactants and jet engine propellants	-300 -31,039	-825 -4,341	
Landing Weight	328,186	207,432	



3.2 DISSIMILAR TRIAMESE DATA

DESIGN SUMMARY AND GEOMETRY (TRIAMESE 50K VEHICLE)

	<u>Booster</u>	<u>Orbiter</u>
Overall length (nose to fixed engine exit) (ft)	182.5	160
Overall length (nose to fin or wing tip)	200	179.5
Maximum span (ft)	178	101
Maximum body width (ft)	29	70
Maximum body height (ft)	32	27
Body volume - total (ft <sup>3</sup> )	108,600	
- propellant (ft <sup>3</sup> )	59,000	30,200
Body planform area (ft <sup>2</sup> )	5,000	5,720**
Body wetted area (ft <sup>2</sup> )	14,200*	15,100
Nose radius (ft)	3.0	3.0
Theo wing area (ft <sup>2</sup> )	9,160**	
Leading edge sweep (deg)	51.5	78
Wing Airfoil section	64-006	
Vertical tail area (two fins) (ft <sup>2</sup> )	2,010	1,540
Tail rollout angle (deg)	35	30
Entry wing loading (psf)	32	46.4
Hypersonic L/D (trimmed)	0.5 at 60° $\alpha$	2 at 15° $\alpha$
Subsonic L/D <sub>max</sub> (trimmed)	7.5	4.66

\*Includes lower body surface blanketed by wing

\*\*Aerodynamic reference areas

PROPULSION/PERFORMANCE CHARACTERISTICS (TRIAMESE 50K VEHICLE)

	<u>Stage 1</u>	<u>Stage 2</u>
Propellant/mixture ratio	7:1	7:1
Expansion ratio SL/vac	35:1 SL	35:1 SL and 150:1 vac
Specific impulse SL/vac (sec)	387.8 SL and 428.5 vac	378.8 SL and 454.2 vac
Propellant fraction	0.826	0.763
Ideal $\Delta V$ (fps)	14,029	18,843
Mass ratio	2.77	3.64
Rocket engines	8 at 394 K (SL)	3 at 460 K (vac)
Thrust - sea level	3,480 K (ea module)	
- vacuum	3,480 K (ea module)	1,380 K
Flyback engine system		
Number/type	4 turbofan	4 turbofan
Maximum static SL thrust (lb)	96,000	87,000
SFC (1/hour)	0.43	0.50
Fuel (lb)	26,000 ea	5,600

VEHICLE VELOCITY REQUIREMENTS (TRIAMESE 50K VEHICLE)

*Ascent Ideal $\left(\frac{45}{100} \text{ nm}\right), 55^\circ$	Total (Subtotal)	Stage 1	Orbiter
	30,643	14,029	16,614
Inertial orbit velocity	25,882		
<b>Losses</b>			
Drag	-1238	-1230	-8
Gravity (including potential energy)	-4002	-3774	-228
Back pressure	-264	-264	-0
Thrust alignment } Maneuver }	-127	-3	-124
Earth rotation (gain) (Equiv initial velocity)	+871	+871	-
Flight performance (3/4% $\Delta V$ )	229		229
Phasing Transfer 100 to 270 nm Circularize Rendezvous } 142 ft/sec Docking } at $\leq 1 \text{ ft/sec}^2$ }	2,000		2,000
Orbit maneuvers Undocking Deorbit Orbit contingency			
<b>Total ideal velocity</b>	<b>32,872</b>	<b>14,029</b>	<b>18,843</b>

\*Based on vacuum performance, this includes orbit velocity plus potential energy gained plus losses minus earth rotation velocity vector.

**WEIGHT SUMMARY (TRIAMESE 50K VEHICLE)**

Function or Condition	Booster	Orbiter	Stage
<b>Aerodynamic Surfaces</b>			
Wing	45,568		
Fin	-	4,601	
Elevon	-	9,000	
<b>Body Structure</b>			
Shell and Frames		41,930	
Shell, Frames, and Tank Domes	53,502	-	
Base Shield	1,550	1,292	
Thrust Structure	7,789	2,862	
Pressure Compartment	1,350	1,350	
<b>Induced Environment Protection</b>			
Body	14,929	30,618	
Wing	6,418	-	
Fin	-	4,656	
<b>Launch, Recovery, and Docking</b>			
Launch Gear	9,000	4,741	
Landing Gear	10,603	10,380	
Docking Structure	-	500	
<b>Main Propulsion</b>			
Liquid Rocket Engine	34,045	12,544	
Air Breathing Engine	22,818	20,806	
Rocket Fuel Container	-	13,392	
Rocket Oxidizer Container	-	10,647	
Rocket Propellant Systems	6,705	2,448	
Jet Fuel Container	1,926	421	
Jet Propellant Systems	455	433	
<b>Orientation Controls, Separation and Ullage</b>	2,618	2,059	
<b>Prime Power Source</b>	447	1,026	

WEIGHT SUMMARY (TRIAMESE 50K VEHICLE) (Continued)

Function or Condition	Booster	Orbiter	Stage
Power Conversion and Distribution	5,743	4,082	
Guidance and Navigation	842	842	
Instrumentation	200	200	
Communication	141	141	
Environmental Control	962	1,231	
Personnel Provisions	636	636	
Crew Station Controls and Panels	612	612	
Range Safety and Abort	200	200	
Contingency	22,906	19,069	
Dry Weight	251,965	202,719	
Personnel	514	674	
Cargo	-	50,000	
Residual/Reserve Propulsion and Reactants	12,587	6,741	
ECS and Prime Power Reactants	432	1,310	
Reaction Control Propellants	1,500	6,337	
Jet Engine Propellants	25,476	5,580	
Rocket Engine Propellants	1,386,199	709,523	
Launch Weight	1,678,673	982,884	4,340,230
Less Main Propulsion Propellants	-1,386,199	-	-2,772,398
Stage Burnout Weight	-	-	1,567,832
Less Main Propulsion Propellants	-	-673,372	
Booster/Orbiter Burnout Weight	292,474	309,512	
Less ECS and Prime Power Reactants, Reaction Control Propellants, and Orbit and Retro Propellants	-132 -1,500 -	-485 -6,337 -36,151	
Entry Weight	290,842	266,539	
Less Prime Power Reactants and Jet Engine Propellants	-300 -25,476	-825 -5,580	
Landing Weight	265,066	260,134	

## LONGITUDINAL CENTROIDS (TRIAMESE 50K VEHICLE)

All centroids are given in terms of feet and percentage of reference length. The reference length has its origin at the apex of the body sweep angle, as seen in the plan view and ends at the base shield. The launch vehicle combined cg is given in the booster reference axis system.

	<u>Sta. (ft)</u>	<u>% Ref. L</u>
Launch Vehicle at Ignition	77	42.8
Launch Vehicle at Burnout	125	69.3
Booster at Entry (Ref L = 180')	129	71.8
Booster at Landing	127	70.5
Orbiter at Ignition (Ref L = 164')	115	70.2
Orbiter on Orbit	120	73.0
Orbiter at Entry (50-K Payload)	121	73.5
Orbiter at Landing	121	73.5
Orbiter at Entry (No Payload)	123	75.0

DESIGN SUMMARY AND GEOMETRY (TRIAMESE 25-K VEHICLE)

	<u>Booster</u>	<u>Orbiter</u>
Overall length (nose to fixed engine exit) (ft)	171	154
Overall length (nose to wing or fin tips) (ft)	191	173
Maximum span (ft)		100
Maximum body width (ft)	29	60
Maximum body height (ft)	32	24
Body volume - total (ft <sup>3</sup> )		
- propellant (ft <sup>3</sup> )	49,000	22,800
Body planform area (ft <sup>2</sup> )		5,050*
Nose radius (ft)	3.0	3.0
Theo wing area (ft <sup>2</sup> )	8,640*	
Leading edge sweep (deg)	51.5	78
Wing airfoil section	64-006	
Vertical tail area (two fins) (ft <sup>2</sup> )		1,370
Tail rollout angle (deg)	35	30
Entry wing loading (psf)	32	41.0
Hypersonic L/D (trimmed)	0.5 at 60° $\alpha$	2 at 15° $\alpha$
Subsonic L/D <sub>max</sub> (trimmed)		4.66

\*Aerodynamic reference areas

PROPULSION/PERFORMANCE CHARACTERISTICS (TRIAMESE 25-K VEHICLE)

	<u>Stage 1</u>	<u>Stage 2</u>
Propellant/mixture ratio	7:1	7:1
Expansion ratio SL/vac	35:1 SL	35:1 SL and 150:1 vac
Specific impulse SL/vac (sec)	378.8 SL and 428.5 vac	378.8 SL and 454.2 vac
Propellant fraction	0.814	0.745
Ideal ΔV (fps)	14,100	18,624
Mass ratio	2.78	3.58
Rocket engines	7 at 382 K (SL)	3 at 447 K (vac)
Thrust - sea level	2,670 K (ea module)	
- vacuum	2,870 K (ea module)	1,340 K
Flyback engine system		
Number/type	4 turbofan	4 turbofan
Maximum static SL thrust (lb)	86,000	68,000
SFC (1/hour)	0.43	0.50
Fuel (lb)	23,000 ea	4,400



VEHICLE VELOCITY REQUIREMENTS (TRIAMESE 25-K VEHICLE)

	Total (Subtotal)	Stage 1	Orbiter
*Ascent Ideal $\left(\frac{45}{100}\right)$ nm , $55^\circ$	30,498	14,100	16,395
Inertial orbit velocity	25,882		
<b>Losses</b>			
Drag	-1238	-1236	-2
Gravity (including potential energy)	-3887	-3733	-154
Back pressure	-263	-263	-0
Thrust alignment } Maneuver }	-99	-3	-96
Earth rotation (gain) (Equiv initial vel)	+871	+871	-
Flight performance res ( $3/4\%$ $\Delta V$ )	229		229
Phasing Transfer 100 to 270 nm Circularize Rendezvous } 142 ft/sec Docking } at $\leq 1$ ft/sec <sup>2</sup> } Orbit maneuvers Undocking Deorbit Orbit contingency	2,000		2,000
<b>Total ideal velocity</b>	<b>32,724</b>	<b>14,100</b>	<b>18,624</b>

\*Based on vacuum performance, this includes orbit velocity plus potential energy gained plus losses minus earth rotation velocity vector.

**WEIGHT SUMMARY (TRIAMESE 25-K VEHICLE)**

Function or Condition	Booster	Orbiter	Stage
<b>Aerodynamic Surfaces</b>			
Wing	42,920		
Fin	-	4,058	
Elevon	-	7,940	
<b>Body Structure</b>			
Shell and Frames		36,776	
Shell, Frames, and Tank Domes	47,109	-	
Base Shield	1,375	1,142	
Thrust Structure	6,425	2,930	
Pressurization Compartment	1,350	1,350	
<b>Induced Environment Protection</b>			
Body	13,425	27,150	
Wing	6,045	-	
Fin	-	4,108	
<b>Launch, Recovery, and Docking</b>			
Launch Gear	9,000	5,000	
Landing Gear	9,454	8,308	
Docking Structure	-	500	
<b>Main Propulsion</b>			
Liquid Rocket Engine	28,304	13,242	
Air Breathing Engine	20,460	16,182	
Rocket Fuel Container	-	10,452	
Rocket Oxidizer Container	-	8,309	
Rocket Propellant Systems	5,481	2,552	
Jet Fuel Container	1,611	328	
Jet Propellant Systems	455	433	
<b>Orientation Controls, Separation and Ullage</b>	2,265	1,640	
<b>Prime Power Source</b>	447	1,026	

WEIGHT SUMMARY (TRIAMESE 25-K VEHICLE) (Continued)

Function or Condition	Booster	Orbiter	Stage
Power Conversion and Distribution	5,044	3,506	
Guidance and Navigation	842	842	
Instrumentation	200	200	
Communication	141	141	
Environmental Control	904	1,166	
Personnel Provisions	636	636	
Crew Station Controls and Panels	612	612	
Range Safety and Abort	200	200	
Contingency	20,470	16,083	
Dry Weight	225,175	176,912	
Personnel	514	576	
Cargo		25,000	
Residual/Reserve Propulsion and Reactants	10,596	5,282	
ECS and Prime Power Reactants	432	1,303	
Reaction Control Propellants	1,500	5,214	
Jet Engine Propellants	23,021	4,348	
Rocket Engine Propellants	1,155,946	555,730	
Launch Weight	1,417,184	774,365	3,608,733
Less Main Propulsion Propellants	-1,155,946	-	-2,311,892
Stage Burnout Weight	-	-	1,296,965
Less Main Propulsion Propellants	-	526,860	
Booster/Orbiter Burnout Weight	261,300	247,505	
Less ECS and Prime Power Reactants, Reaction Control Propellants, and Orbit and Retro Propellants	-132 -1,500	-478 -5,214 -28,870	
Entry Weight	259,668	212,943	
Less Prime Power Reactants and Jet Engine Propellants	-300 -23,021	-825 -4,348	
Landing Weight	236,347	207,770	

### 3.3 BASELINE CONFIGURATION EVALUATION

The spectrum of concepts and design points carried into this final configuration evaluation includes both the fully reusable Two-Stage and the Triamese concepts at both 50,000-pound and 25,000-pound design payload. The comparative evaluation of the four baseline designs encompasses a basic technical and cost comparison and consideration of sensitivity and development risk. A plan is included in Section 3.3.3 for compensation of weight growth by management of operational requirements, reserves and contingencies. This evaluation demonstrates the superiority of the 50,000-pound payload Two-Stage approach over the other three baselines and verifies feasibility of this baseline design, even after consideration of projected weight growth.

#### 3.3.1 Basic Technical and Cost Comparisons

The Triamese system has only a small degree of commonality between the orbiter and the boosters. As discussed in Section 3.4.2, commonality in the structure subsystem was completely abandoned on the dissimilar Triamese in order to improve performance in a concept that promised smaller boosters than the optimized Two-Stage concept.

3.3.1.1 Reliability, Crew Safety and Mission Success. The existence of a pair of boosters on Triamese increases complexity and introduces failure modes not existing on Two-Stage. Furthermore, the additional booster crew increases communications problems. The triple separation maneuver is inherently less reliable, since a procedure with a given unreliability must be performed twice. In addition the probability of collision between the separated vehicles is increased.

Both Triamese boosters contain a large number of redundant subsystems to satisfy the triple redundant fail-safe reliability requirement.

Configuration synthesis is compromised by the need for simple load paths between the vehicles and the need for rapid removal of crews and passengers in the event of pad

abort. Also, sufficient clearance for crew ejection during R&D flights must be available. The triple-stacked system provides for minimum weight, but a triangular clustering could simplify the implementation of personnel safety requirements at the expense of structural efficiency.

3.3.1.2 Ground Handling. Triamese ground handling requires vertical assembly and probably vertical transportation on a crawler, whereas the Two-Stage system can be mated horizontally and towed to the launch site on the first stage landing gear.

3.3.1.3 Responsiveness to DOD Needs. Both Triamese and Two-Stage are capable of omniazimuth launch without hardware fallout. Since the staging velocity of the dissimilar Triamese is very nearly the same as that of the Two-Stage, there is essentially no difference in terms of accommodation of a large payload bay or regarding the impact of return payload on reentry wing loading and heat shield requirements.

3.3.1.4 Cost Comparison. The development costs and recurring costs per 1000 flights for Two-Stage and Triamese are tabulated below.

Payload	LB	2-Stage		Triamese	
		50-K	25-K	50-K	25-K
RDT&E	M \$	5512	5340	5525	5224
Recurring cost per 1000 Flights	M \$	1255	1145	1493	1356

As shown, the difference in development cost between the Two-Stage and the Triamese is within the noise level of the cost analysis. The primary advantage presumed for Triamese was to cut development cost by developing a small booster with extensive commonality with the orbiter. In dissimilar Triamese commonality in the structures was abandoned and only fractional commonality in other subsystems was retained. More Triamese vehicles have to be bought, and the flight test program would be more costly. In addition, it should be noted that the RDT&E term also pays for the initial operational capability.

A comparison of recurring costs and total program costs is given in Fig. 3-1 on the basis of a fixed cumulative payload of  $50 \times 10^6$  lb in 10 years. It is assumed that the learning experienced during the additional flights of the 25-K systems is compensated for by the additional vehicles that have to be purchased. On the basis of total transportation cost, the 50-K Two-Stage system is clearly superior.

### 3.3.2 Fixed Vehicle Sensitivities

Triamese has an inherently larger structural fraction in the boosters than does the Two-Stage. The move to a dissimilar Triamese has improved this situation slightly. The following table contains the fixed design point sensitivities of Two-Stage and dissimilar Triamese. It can be seen that the Triamese is always slightly more sensitive than the Two-Stage. The sensitivities of the 25-K payload vehicles are about of the same magnitude as those of the 50-K vehicle, which indicates that, on a relative basis, the smaller system is considerably more sensitive.

Payload	Stage	LB	Two-Stage		Dissimilar Triamese	
			50-K	25-K	50-K	25-K
$\partial \text{PLD}$	1	lb/sec	720	569	845	690
$\partial I_{sp}$	2	lb/sec	908	712	1065	870
$\partial \text{PLD}$	1	lb/lb	0.065	0.062	0.067	0.064
$\partial W_{\text{PROP}}$	2	lb/lb	0.176	0.183	0.170	0.177
$\partial \text{PLD}$	1	lb/lb	-0.151	-0.149	-0.153	-0.151
$\partial W_{\text{INERT}}$	2	lb/lb	-1.0	-1.0	-1.0	-0.1

### 3.3.3 Development Risk

An attempt was made to assess the dispersion of total program costs resulting from weight growth and consequent payload reduction of the Space Shuttle system. Subsequently, the use of weight contingencies and reduction of requirements is discussed to suggest how design performance can be regained by adjustment of requirements. This exercise was performed with Phase A weights used to simulate a Phase C situation.

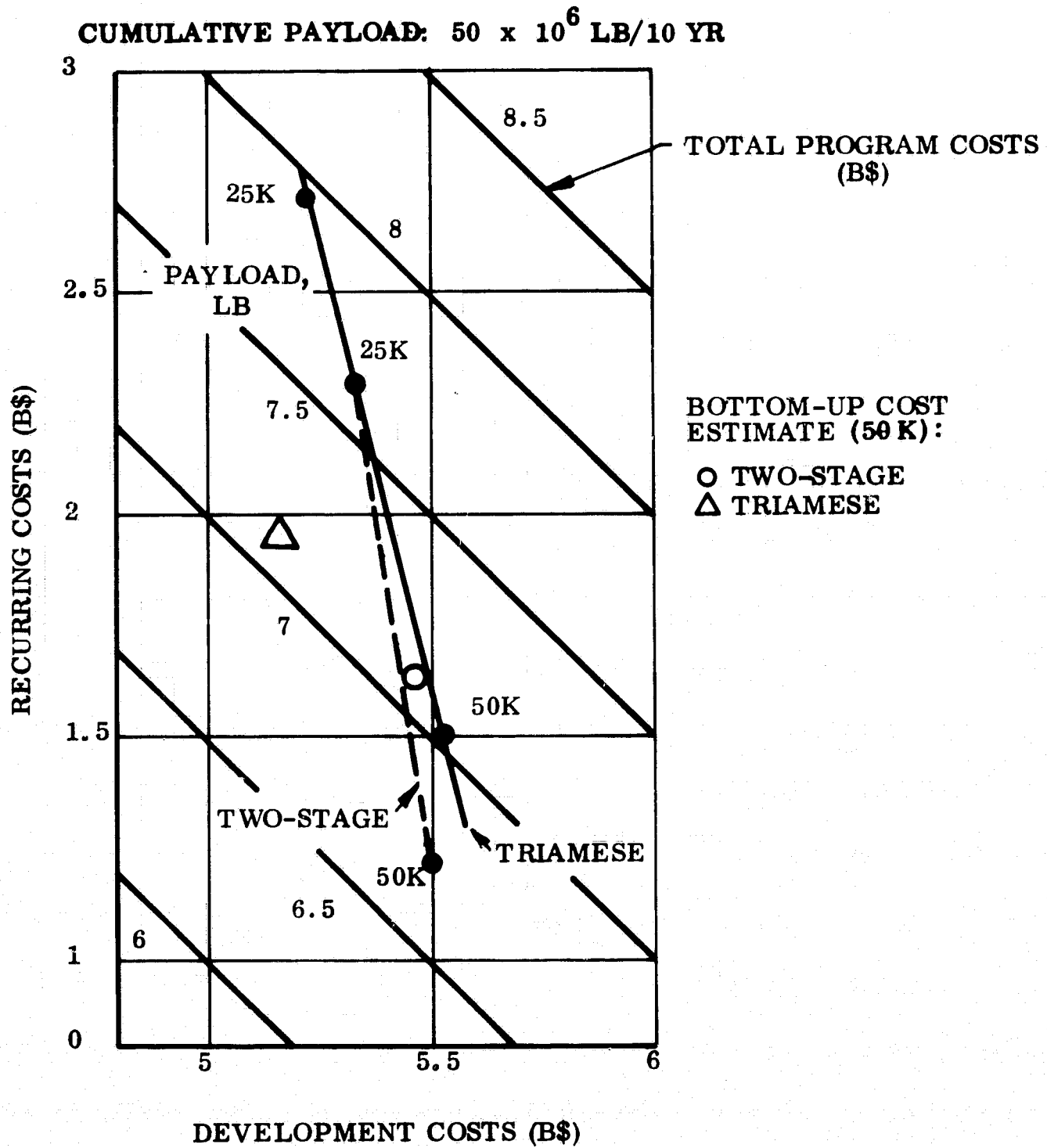


Fig. 3-1 Cost Comparison of Two-Stage and Dissimilar Triamese

3.3.3.1 Weight Growth. Weight growth historically occurs during all phases of vehicle design. The growth history is typically unpredictable until the acquisition phase is reached. During the conceptual and definition phases, the uncertainties regarding mission requirements and system definition provide an oscillating trend in predicted weight, which has been frequently biased by competitive posture. During acquisition, weight growth occurs more predictably as requirements are firmed up, and flight hardware is defined.

Statistically, weight growth seems to be related to complexity and design risk. Figure 3-2 is a graph showing weight growth due to all causes during acquisition of 19 space vehicles representing three levels of sophistication.\* Examples of typical candidates for each generation are first generation, Mercury or Apollo CM; second generation, Gemini; third generation, LMSC Agena D. The graph shows average weight growths of 35 percent, 15 percent, and 6 percent for first, second, and third generation designs.

Weight growth predictions are complicated by the fact that they do not fit neatly into any one generation. Although the Space Shuttle concept is clearly first generation, many elements of structure and equipment are based on mature concepts and designs. Thus, to make an assessment of total vehicle potential growth, it was assumed that the statistical growth percentages developed for vehicles could be applied with reasonable accuracy at the subsystem level.

An estimate of design maturity was made for each major system in the orbiter and booster, and growth factors from Fig. 3-2 were applied. Some systems might be split into two or more generations, thus some multiplying factors are weighted averages of the standard growth factors. The results, tabulated below, show an estimated growth of about 16 percent of the booster and 17 percent for the orbiter. Whether the technique described above or the magnitude of the growth values are rigorously accurate

---

\*Excerpted from a presentation by Charles Pullen of the Aerospace Corporation at the proceedings of the Government Industry Session on Weight Growth at the 1966 Annual Conference of the Society of Aeronautical Weight Engineers.



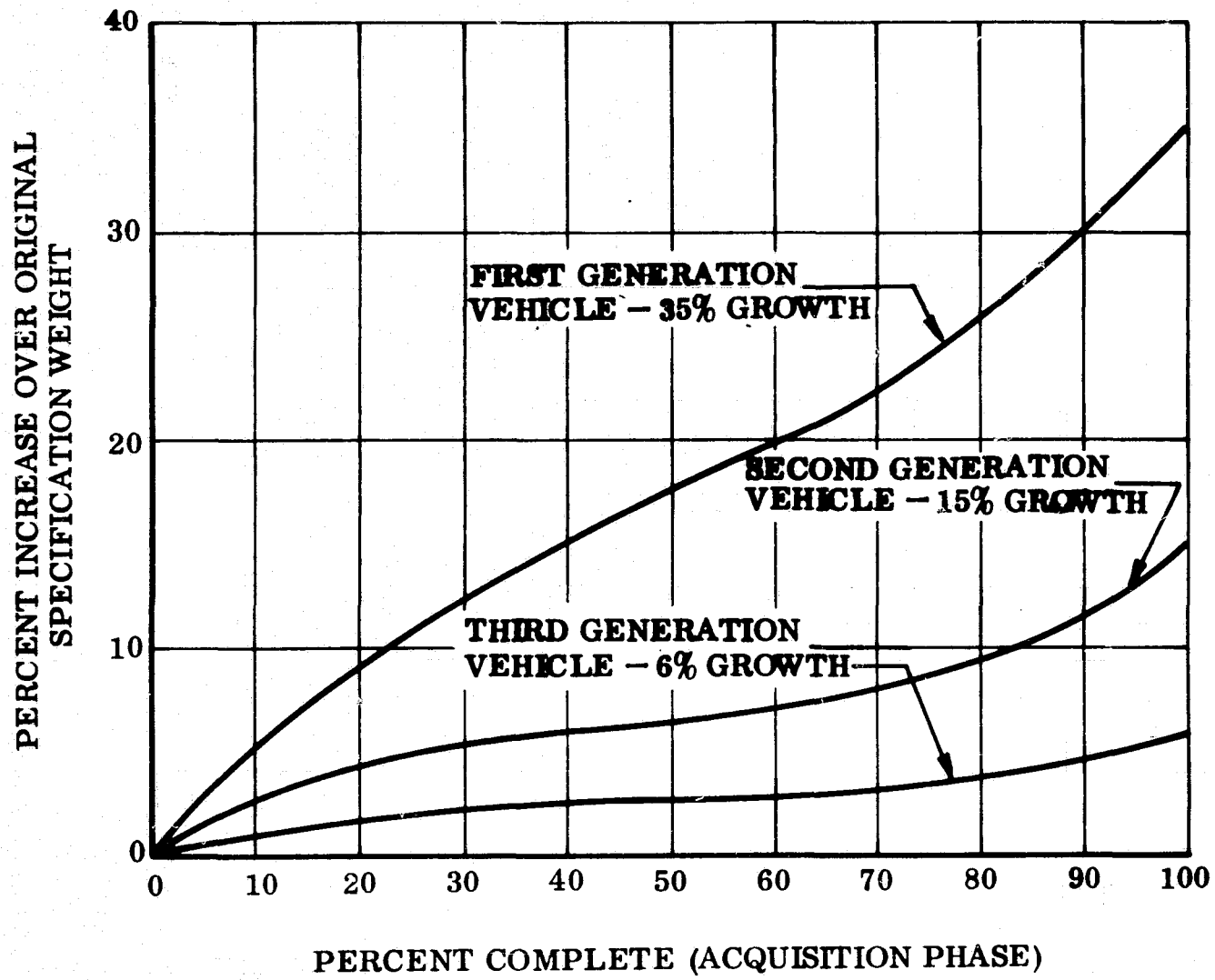


Fig. 3-2 Magnitude of Vehicle Weight Growth

is somewhat secondary in this analysis. The major point to be recognized is that weight growth is a historically substantiated condition with severity being dependent, in part, on complexity and technical risk. An assessment shows that most technologies to be applied are second generation at best; consequently, it is prudent to anticipate a weight growth in excess of that normally encountered in conventional aircraft design.

**ESTIMATED BOOSTER WEIGHT GROWTH**

<u>Item</u>	<u>Percentage of Dry Weight</u>	<u>Estimated Growth Factor</u>
Wing	18.0	1.15
Body Structure	26.1	1.20
Environmental Protection	8.3	1.35
Interstage Structure	4.7	1.15
Landing Gear	4.6	1.06
Rocket Engines	18.2	1.15
Jet Engines and Nacelle	10.0	1.06
Rocket Engine Systems	3.7	1.06
Jet Engine Systems	1.0	1.06
Orientation and Control	1.4	1.35
Electronic Systems	0.6	1.15
Environmental Control and Personnel Systems	0.6	1.06
Power Systems	2.8	1.06
Total Dry Weight	100.0	1.162

**ESTIMATED ORBITER WEIGHT GROWTH**

<u>Item</u>	<u>Percentage of Dry Weight</u>	<u>Estimated Growth Factor</u>
Aero Surfaces	7.4	1.15
Body Structure	25.8	1.20
Environmental Protection	19.2	1.35
Interstage Structure/Docking	3.0	1.15

ESTIMATED ORBITER WEIGHT GROWTH (Cont)

<u>Item</u>	<u>Percentage of Dry Weight</u>	<u>Estimated Growth Factor</u>
Landing Gear	5.6	1.06
Rocket Engines	6.8	1.15
Jet Engines and Nacelle	11.3	1.06
Rocket Engine Systems	14.4	1.10
Jet Engine Systems	0.5	1.06
Orientation and Control	1.1	1.35
Electronic Systems	1.1	1.15
Environmental Control and Personnel Systems	1.0	1.06
Power Systems	2.8	1.06
Total Dry Weight	100.0	1.777

3.3.3.2 Effect of Weight Growth on Program Cost. With a vehicle system presumed to be in the hardware stage, the effect of weight growth is payload reduction according to fixed design point sensitivities. The projected most likely weight growth based on historical trends is estimated at 17.7 percent for the orbiter and 16.2 percent for the booster(s) of both Two-Stage and Triamese. Out of these percentages, 10 percent are covered by the design margin. The effect on program cost of any parameter (p) variation that impacts payload (PLD) is described as:

$$\frac{\$ \text{ REC}}{\$ \text{ REC}}_{\text{NOM}} = \frac{1}{1 + \frac{1}{\text{PLD}_{\text{NOM}}} \sum \frac{\partial \text{PLD}}{\partial p} \Delta p} - 1$$

The parameter p may stand for weight growth as well as for other requirements.

Figure 3-3 shows the effects of the projected weight growth on recurring and total program costs associated with carrying  $50 \times 10^6$  lb of cumulative payload into orbit in 10 years. It can be seen that the costs of a 25-K vehicle are unproportionately more

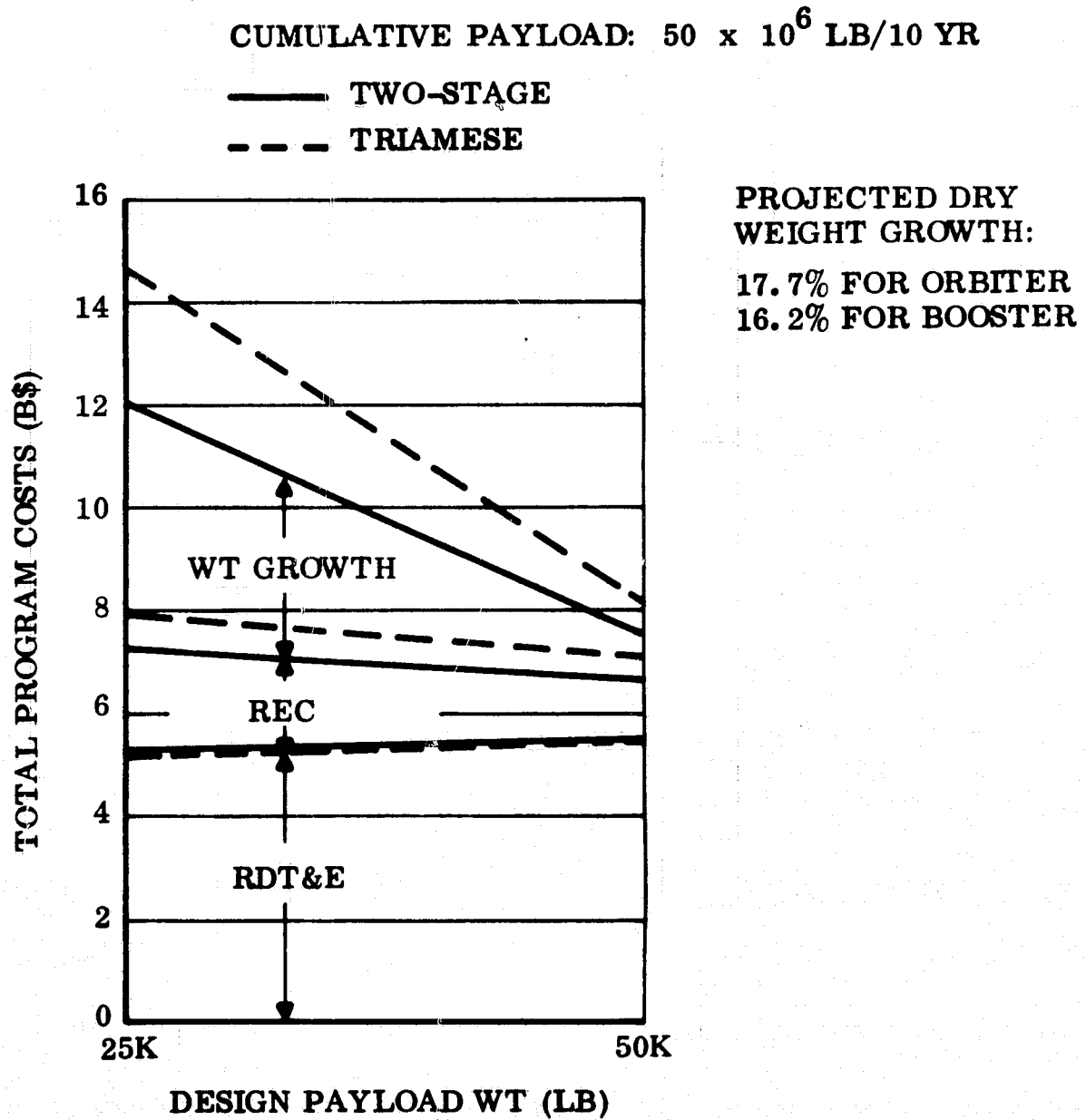


Fig. 3-3 Cost Effect of Weight Growth

affected than those of a 50-K vehicle for the same percentage weight growth. It can be argued that even this is an optimistic assumption for the smaller vehicle. The sensitivity of Triamese cost to weight growth is higher than for the Two-Stage. This effect is accentuated at the smaller vehicle size, at which program costs may almost be doubled as a result of weight growth.

**3.3.3.3 Requirements Reduction vs Weight Growth.** The prospect of weight growth poses the question for a performance recovery plan. The present systems are sized for full go-around capability on landing, and they provide for 2000 fps beyond injection. Both requirements can be reduced and result in considerable payload growth, as shown in Fig. 3-4 for the 50-K Two-Stage. Also entered is the latest set of requirements received from NASA. The reduction of turbofan size and fuel from the go-around condition to the 3-degree glide slope case increases payload by 19,000 pounds; a velocity reduction of 500 fps increases payload by 10,000 pounds; and additional payload growth may be obtained by an improvement in  $I_{sp}$ . The effect of a change in FPR on payload can also be seen.

A payload growth potential well in excess of 29,000 pounds is available to compensate for a projected weight-growth payload reduction of 19,000 pounds. This means that the considerable impact of weight growth on program costs can be avoided if requirements are adjusted accordingly.

It also means that the resulting 10,000 pound payload reserve can be converted into a 270,000 pound reduction of launch weight; i. e., it appears that a Two-Stage system meeting the reduced requirements with 50-K payload capability can be realized at  $3.5 \times 10^6$  lb launch weight including consideration of projected weight growth.

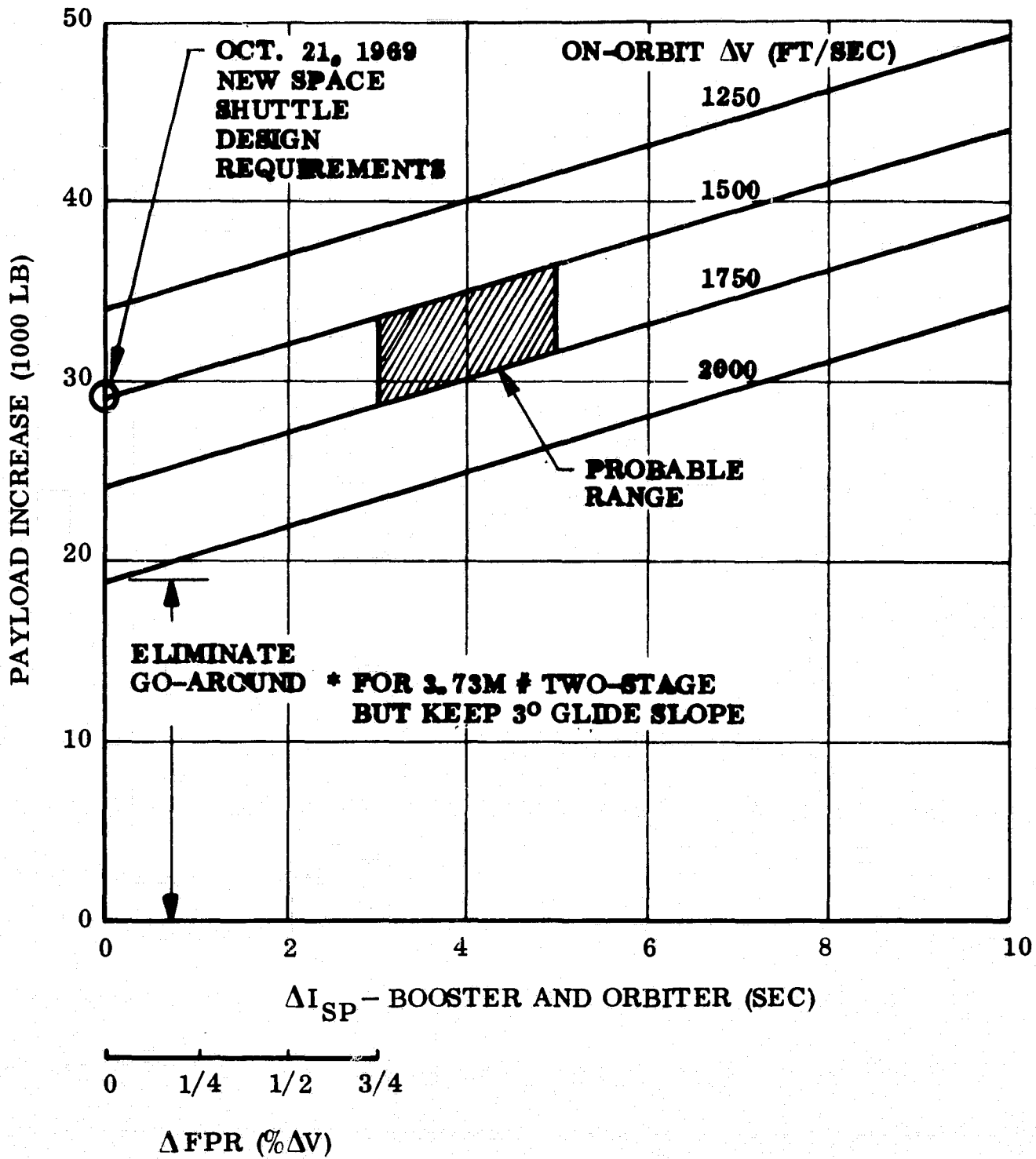


Fig. 3-4 Payload Growth Potential

### 3.4 ALTERNATE CONFIGURATION APPROACHES

#### 3.4.1 Introduction

During the course of the ILRV study, LMSC investigated a number of conceptual design alternatives in developing the baseline configurations described in this report. The status of several of the most important alternative approaches that are not characterized in the baseline designs is given in this section of the report.

There are, of course, design alternatives that were not studied because of the necessity to limit the scope of the ILRV study. Of particular significance is the possibility of alternate aerodynamic shapes. In the LMSC ILRV study, delta body orbiters, with and without variable-geometry wings, and booster configurations, with cylindrical bodies and fixed delta wings, were emphasized. While these approaches have superior characteristics for the Space Shuttle, other possibilities, which have not yet been studied in depth, may also offer promise. These include orbiters and boosters with cylindrical bodies and fixed or variable-geometry wings and blended wing-body orbiters

The design alternatives not used in the baseline systems that have been studied for ILRV fall into four categories:

- Those eliminated from further consideration during the study either by NASA direction or as a result of study evaluations (These cases are not discussed in detail in this report but reviewed briefly in Section 3.4.2 below. Reference is made to other appropriate documentation.)
- Those eliminated from further consideration by NASA decisions made after completion of the ILRV study technical effort (These cases are discussed in other sections of this report and are reviewed in Section 3.4.3 to clarify their status.)
- Those cases that represent NASA requirement changes after completion of ILRV technical effort (These two cases, elimination of operational go-around capability and reduction from 2000 ft/sec to 1500 ft/sec on-orbit delta velocity, are the only design requirements for which the ILRV baseline sizing deviates from current NASA requirements and desired characteristics. They are discussed in other appropriate sections of this report and are reviewed briefly in Section 3.4.4.)

- Those alternatives studied that remain valid alternatives to the baseline designs and for which further study is needed (These cases include thermal protection system design alternatives, structural material alternatives, integrated electronic system alternatives, crew cabin sized for basic two-man Space Shuttle crew only, pilot visibility system alternatives, and use of hydrogen fueled airbreathing engines. Each of these areas is discussed in appropriate sections of Volume I or Volume III of this report.)

### 3.4.2 Approaches Eliminated During Study

3.4.2.1 Two-and-One-Half Stage. For the first 3 months of the ILRV study (until NASA directed a discontinuance on June 10 1969), the Two-and-One-Half Stage concept was one of three being studied by LMSC; the other two were Stage-and-One-Half and Triamese. The Two-and-One-Half Stage concept was to reduce the propulsive requirements and vehicle size of the Stage-and-One-Half by reason of launching on an inexpensive solid or liquid first stage. At low traffic rates, this concept could be competitive; but when it became evident (by early June) that total NASA/DOD traffic for Space Shuttle is expected to exceed 100 flights per year, this concept was clearly noncompetitive.

The results of LMSC Two-and-One-Half Stage studies, summarized in LMSC-A951790, "Stage-and-One-Half with Solid Boost," dated July 11, 1969, show the ratio of Two-and-One-Half Stage recurring cost to that of Stage-and-One-Half to be 1.6 to 3.0, depending on staging velocity, at a launch rate as low as 20 flights per year. At 100 flights per year, the ratio is estimated to be in excess of 2.3 over the entire range of feasible staging velocities.

3.4.2.2 Stage-and-One-Half. Study of the Stage-and-One-Half concept was a major portion of the ILRV effort from its initiation on March 10, 1969, to August 8, 1969, when NASA directed that this effort be discontinued and the Two-Stage concept be substituted. While Stage-and-One-Half recurring costs would clearly be higher than those for Two-Stage, they were estimated to be equivalent to those for Triamese, which involves relatively high refurbishment costs (three vehicles for each flight). However, estimation of drop-tank production costs is subject to significant uncertainty, which could not be resolved by demonstration prior to the configuration selection date.



Also, the disposal of drop tanks on each flight would impose an operational inconvenience, which becomes increasingly significant at higher launch rates. NASA ILRV direction originally suggested a traffic of 4 to 12 flights per year; but, with the definition of six types of NASA missions in early June, coupled with DOD requirements, total traffic estimates have since increased to over 100 flights per year. While the drop-tank disposal problem could be solved even at these traffic rates by using techniques that include taking them to orbit on easterly launches and deorbiting them at convenient places on the first orbit, the growth of the system to other applications and still greater traffic would clearly be more inhibited with the Stage-and-One-Half than with a fully reusable approach.

Stage-and-One-Half data developed for the ILRV study are summarized in LMSC-A955317, "Space Shuttle Data," dated July 31, 1969.

3.4.2.3 Triamese With Structural Commonality. This basic Triamese concept, studied through early August, was an attempt to minimize development cost by using high commonality of structure in the orbiter and booster vehicles. The 50 K payload case, reported in LMSC-A955317, "Space Shuttle Data," dated July 31, 1969, had a launch weight of 5.9 million pounds. While this weight could be reduced with improved propellant packaging to about 5 million pounds, it could never become competitive in recurring cost to the 4.3-million pound dissimilar Triamese chosen as the baseline for the Triamese concept. Also, the orbiter dry weight for the basic Triamese would (even after size reduction) be about 40 percent greater than that for the dissimilar Triamese. The increased development cost for this heavier vehicle would offset the structural commonality savings in booster development to within about \$100 million. This is less than 2 percent of the total estimated development cost and well within the resolution of Phase A cost estimation.

In addition, the basic Triamese incorporates a significant technical disadvantage in requiring cross-feed from the booster to the orbiter engines during the boost phase; cross-feed can be eliminated in the dissimilar Triamese and Two-Stage cases. Cross-feed would not only impose an operational inconvenience but would also decrease system reliability; a significant effect would be an increase in the complexity of staging, which is one of the most critical events for the system.

The first configuration of dissimilar Triamese, reported in LMSC-A955317A, "Space Shuttle Data," dated September 12, 1969, included a retention of structural similarity at the forward portion of the booster. Cost estimates in that reference were based on an assumed 10 percent similarity, but further examination of the design indicates a value of not more than 5 percent. This advantage is more than offset in the baseline Triamese by improved propellant tanking efficiency and other cost and weight saving advantages, such as simpler provisions being required for pilot visibility in the booster.

Thus, the baseline Triamese booster structure optimized independently of the orbiter design and zero structural commonality is assumed for costing. Each Triamese booster is essentially a reduced-scale version of the booster for the Two-Stage configuration.

3.4.2.4 Cross-Feed During Boost. Cross-feed of propellants from the booster tanks to the orbiter engines, for either Two-Stage or dissimilar Triamese, could reduce the booster thrust requirement and decrease launch weight by 1 to 2 percent, by comparison to the baseline sequential burn approach. An additional advantage is that all engines would be started before liftoff.

Even though the booster dry weight would decrease with cross-feed, this reduction is largely due to a smaller number of engines, which would have little effect on development cost. Thus, total development cost would probably increase somewhat as a function of development of the valving and disconnect systems. Recurring costs for operation and maintenance of these systems could also override the savings of operating the slightly smaller system.

The valve and disconnect systems would have to be highly redundant and precise to minimize the effect on reliability. Even then, the effect on the probability of successful staging could not be disregarded, since failure to accomplish staging would be a catastrophic event. For the sequential burn system, failure to start all three orbiter engines is also catastrophic, but three-level redundancy is inherently provided and techniques for accomplishing reliable engine start have already been developed to a high level.

3.4.2.5 Parallel Burn with No Cross-Feed. Burning the orbiter engines at 10 percent flowrate during boost without cross-feed results in a 6 percent liftoff weight penalty, as compared to parallel burn with cross-feed. If the orbiter engines are initially burned at 100 percent thrust, the penalty is 10 percent. These penalties result from the necessity of providing the extra propellant storage in the weight-sensitive upper stage. These penalties are considered too high, so the operational Space Shuttle system should employ sequential burning of the stages. It is expected that there will be sufficient experience by the 1975 time period to warrant confidence in both on-orbit and during-boost starting of hydrogen/oxygen propulsion systems.

During the development period, it may be feasible to design the system initially for a parallel burn, as noted above. If the system is initially sized for the sequential-burn condition, it can be flown at reduced payload in a parallel-burn condition during development and, after propulsion system experience and confidence are obtained, switched to the sequential burn mode with full payload capability. The payload differential here is about 10,000 pounds for the Two-Stage vehicle with 50,000-pound payload capability.

3.4.2.6 Alternate Aerodynamic Shapes. While, as discussed in Section 3.4.1, not all the candidate aerodynamic shapes were investigated, certain significant conclusions were drawn for those investigated. Two important results are the following:

- o If the orbiter is a lifting body with a subsonic L/D of 4 or more, variable geometry wings should not be added.
- o Of several delta-shaped lifting body possibilities, the baseline orbiter based on the LMSC 8MX vehicle was chosen for its superior characteristics.

As presented in some detail in LMSC-A960088, "ILRV Interim Technical Review, Huntsville," August 21, 1969, and summarized in Volume III of this report, the use of variable-geometry wings added to the lifting body orbiter adds about 16 percent to the system launch weight, even after allowance for the additional propulsive requirements of the lifting body for go-around capability. The landing speed for the baseline vehicle is estimated to be 160 knots, and rollout distances are acceptable for 10,000-foot runways. Variable-geometry wings would reduce this speed by 10 to 15 knots, but would introduce an additional failure mode (failure to deploy); and they are not needed to meet the runway length requirements. Some penalty is taken in ferry range with the lower L/D of the

lifting body, but the cost effects of the resulting operational inconvenience are small as compared to the cost impacts of variable-geometry wing development and a 16 percent increase in launch weight. The ferry range could be extended with in-flight refueling.

Relative to delta body shapes, several cases were compared for their propellant volume efficiencies, which is a driving parameter for sizing both Two-Stage and Triamese orbiters. Competitors for the chosen baseline studied in some depth are the following:

- Case A - the proposed Triamese shape reported in LMSC-A955317, "Space Shuttle Data," dated July 31, 1969.
- Case B - a modified FDL-5B with side fins added to stabilize the vehicle with the more aft center-of-gravity for accommodation of Space Shuttle engines.

Surface-to-volume ratios for the chosen baseline were found to be about 30 percent lower than Case A and 20 percent lower than Case B. The Case B version includes an extended body surface, which tends to mediate the effect of the 20 percent penalty.

This version may warrant further investigation

3.4.2.7 Load-Carrying Tanks in Orbiter. In the studies on improving the volumetric efficiency of the orbiter, consideration was given to providing load-carrying propellant tanks, which nearly fill the available space within the vehicle. Designs of this type were reported in LMSC-A955317A, "Space Shuttle Data," dated September 12, 1969. Evaluation of this approach resulted in a return to the nonintegral tanks now represented in the baseline designs. The major difficulties with the load-carrying tanks are as follows:

- Complex load paths where the tanks are terminated to accommodate the payload cutout and landing gear cavities
- Thermal contraction of the tank around the payload bay during propellant loading
- The practical consideration of complex vehicle assembly and inspection

While these problems could be solved, the development time for this complex structure is not considered compatible with Space Shuttle requirements.

3.4.2.8 Space Shuttle Crew in Excess of Two Men. Initial investigations of the possibility of a flight engineer added to the crew were reported in LMSC-A955317A, "Space Shuttle Data," dated September 12, 1969. The baseline design approach, throughout the study and as used for the vehicle sizing of the baselines reported herein, is based on a two-man crew in a cabin sized for four men. The additional space is provided for mission-peculiar personnel. Alternate compartment layouts, sized for the two-man crew only, are discussed in Section 11. While the size of the basic crew compartment is subject to further study, further consideration of more than two men for the basic Space Shuttle crew was eliminated by NASA in October 1969. The issue now becomes the optimum design of the system so that two men can accomplish all Space Shuttle operational functions and one man can operate the system in an emergency. Mission-peculiar functions may still be assigned to additional personnel, who may be housed in the basic compartment, the payload bay, or in the airlock, which is also provided for EVA.

### 3.4.3 Approaches Recently Eliminated by NASA

3.4.3.1 Aerospike Engine. Throughout the ILRV study, the bell engine configuration has been the primary approach in defining the baseline primary propulsion system. Study of the alternate aerospike concept has been a major portion of the Special Study Task 8f, Propulsion System Parameters, which is reported in Volume III, Section 2.1, of this report. In October 1969, NASA decided to eliminate the aerospike from further consideration; however this type of engine should be reexamined for possible application in auxiliary propulsion systems.

3.4.3.2 Engine Thrust in Excess of 400,000 Pounds. During much of the ILRV study, Two-Stage and Triamese design concepts called for 500K to 700K engines with two engines on the orbiter and 10 or 11 booster engines for the 50K payload cases; as reported, for instance, in LMSC-A955317A, "Space Shuttle Data," dated September 12, 1969. In September, 400K engines were chosen for the baseline approach, as indicated in LMSC-A959125, "Space Shuttle Data, Two-Stage Summary," dated September 29, 1969.

Reasons for the selection of 400K include the following:

- It allows for the use of three orbiter engines, which meets the fail-operational requirement with single engine out.
- It reduces engine development cost by about \$140 million, as compared to that for a 600K engine, including the effect of less propellants required for test.
- The lesser estimated development time gives greater assurance of meeting the desired IOC date.

The primary effect of the large number of booster engines--13 on the baseline 50K Two-Stage vehicle--is to increase recurring costs somewhat. However, engine procurement and maintenance costs represent a fairly small fraction of total recurring costs; so the impact is not great.

NASA decided in October, to continue emphasis on the 400K case.

#### 3.4.4 Changed NASA Requirements

3.4.4.1 No Operational Go-Around Capability. The baseline concepts presented in this report include design for one-time go-around for a missed approach to landing to meet the desired characteristics established by NASA in June. Studies since that time have established that retaining this characteristic as an operational requirement imposes severe penalties on the system. The effect on launch weight for the 50K Two-Stage case is estimated to be from 14 percent to 20 percent, depending on the no go-around design chosen, i. e., whether engines for a 3 degree glide slope or the use of a dead-stick landing is considered.

NASA decided in October 1969, to eliminate go-around as an operational requirement, but to provide this capability during development. This approach allows for development and testing of the Space Shuttle automatic landing system to the level of confidence needed before the go-around capability is removed. The engine system used can also be employed to implement an engine kit for the self-ferry mode. The alternate landing system approaches are further discussed in Volume III, Section 5.2.10; and the effects on baseline vehicle sizing are covered in Section 3.3.3 of this volume.

**3.4.4.2 1500 Ft/Sec On-Orbit Delta Velocity.** The ILRV vehicle sizing has been based on 2000 ft/sec on-orbit delta velocity in response to NASA-desired characteristics established in June 1969. This included 500 ft/sec contingency in addition to conservative allowance to meet the requirements of the Space Station/Base logistics mission. NASA decided in October, to reduce the requirement to 1500ft/sec. The 500 ft/sec reduction is equivalent to about 8 percent reduction in launch weight for the 50K Two-Stage case. The effect on the baseline design is further discussed in this volume, Section 3.3.3.

Section 4  
VEHICLE DESIGN

This section covers the design of the Two-Stage and the Triamese reusable Space Shuttle vehicles.

For both, the orbiter is of the lifting body type with a delta plan form, whereas the boosters are of a wing-body arrangement, consisting of a delta wing and a cylindrical body.

The orbiter is similar in both systems; the difference is the additional support points required for the Triamese vehicle for attachment of the second booster. The payload bay on the orbiter is sized to carry the 50,000-pound payload and will accept the 22-foot diameter, 30-foot long payload; the 15-foot diameter, 60 foot long payload; or a combination of both.

The drawings describing the systems are contained in the appendix in the following order:

<u>Two-Stage System</u>	<u>Page</u>
Launch Vehicle General Arrangement (SKS 101069)	A-1
Booster General Arrangement (SKS 100969)	A-2
Booster Inboard Profile (SKS 101169)	A-3
Booster Structural Arrangement (SKX 100267)	A-4
Booster Main Propellant Lines (SKD 101569)	A-5
Orbiter General Arrangement (SKS 100769)	A-6
Orbiter Inboard Profile (SKS 100869)	A-7
Orbiter Structural Arrangement (SKW 101069)	A-8
Orbiter Main Propellant Lines (SKB 101569)	A-9
Launch Vehicle Two-Stage - 25 K Payload (SKJ 101669)	A-24



Triamese System

Page

Launch Vehicle General Arrangement (SKQ 100969)	A-10
Booster General Arrangement (SKG 100769)	A-11
Booster Inboard Profile (SKG 100369)	A-12
Orbiter General Arrangement (SKG 100969)	A-13
Orbiter Inboard Profile (SKG 100869)	A-14
Launch Vehicle - 25K Payload (SKJ 100769)	A-25

The following drawings show airframe system concepts that are generally applicable to both Two-Stage and Triamese systems:

Pilot Vision Study (Spacecraft) (SKE 100969)	A-15
Personnel Escape System Concept (SKJ 100169)	A-16
Personnel Escape System Concept (SKJ 100269)	A-17
Personnel Escape System Concept (SKJ 100369)	A-18
Launch Vehicle Attachment System (SKB 101069)	A-19
Payload Door Concept (SKM 10156)	A-20
Orbiter Nosecap Concept (SKR 060969)	A-21
Nosecap Concept (SKR 060669)	A-22
Orbiter Tank Support Concept (SKT 100969)	A-23
Booster Thrust Structure (SKQ 092969)	A-26
Booster Propulsion System (SKQ 101569)	A-27

**4.1 TWO-STAGE VEHICLE - DESIGN DESCRIPTION**

**4.1.1 Launch Vehicle (SKS 101069) (SKJ 101669)**

The position of the orbiter relative to the booster was influenced by the following requirements:

- Accessibility of the payload compartment in the orbiter
- Attachment points between orbiter and booster with minimum heat shield penetration
- CG travel during the ascent phase

The tip of the orbiter fin is at the booster base station. The geometric axes of the two stages are convergent toward the nose by 3 degrees.

The payload volume for the 25,000-pound payload launch vehicle (Dwg SKJ101669) (15 ft dia, 60 ft long; 22 ft dia, 30 ft long) is identical to that of the 50,000-pound payload vehicle. The orbiter contains 550,280 pounds of propellant. The  $\text{LH}_2$  is stored in one forward and two rear tanks, while the  $\text{LO}_2$  is carried in two amidships tanks. The maneuvering propellant is stored aft below the payload bay.

Propellant fill, drain, vent, and pressurization connections are all located in the base of both the orbiter and booster and hence provide for favorable ground servicing.

The mating and separation of the two vehicles entails a three-point attachment arrangement, with the two aft points as axial load carriers.

#### 4.1.2 Booster (SKS 100969 and SKS 101169)

The booster has an overall length from nose to wing tip of 237 feet and a maximum wing span of 200 feet. The maximum body height is 41 feet, while the vehicle height of body to wing tips is 47 feet and the taxi height is 59 feet.

The booster is a 51.5-degree sweep clipped aerowing vehicle, with 55-degree canted wing tips for directional stability. The wing has an area of approximately 12,000 square feet, with the lower surface canted up by 3 degrees. The forward cross-sections are basically flat bottom shaped and have a 5-degree inward sloped side to shadow behind the leading edge. The vehicle has a 3-foot radius spherical nose.

The lower part of the vehicle as seen from the side view is basically horizontal with just the nose section slightly cambered up. The wing is attached below the fuselage and permits expansion and contraction of the fuselage without constriction by the wing.

For the 25,000-pound payload vehicle the booster reference length (nose tip-to-base) is 210.1 feet. Eleven 400,000-pound thrust (sea level) bell-type rocket engines provide liftoff thrust. Propellant loading is 1,916,691 pounds, contained in two separate tanks. Four turbofan jet engines provide the necessary takeoff thrust of 148,500 pound. Overall dimensions are 230.8 feet long, 184.4 feet wide, and 89.5 feet high.

4.1.2.1 Structure (SKX 100269). The main fuselage, which is chiefly the cryogenic tankage, is constructed from aluminum planking, in which are incorporated integral T-section longerons. The structure is ring stiffened, again with a T-section, which is attached to integral risers, spaced to stress requirements between the longerons. The end bulkheads are gored sections, welded to a Y-ring, which also affords attachment points for the thrust structure, interstage section, and the cabin area.

The cabin is a pressurized area for pilot and crew with the same basic construction as the rest of the shell. The window section breaks away in the event of the necessity for crew ejection.

The wing is of a minimum-weight multibeam, multirib concept with corrugated heat shields on the top and bottom surfaces. The primary structures consist of tubular, circular-arc stiffened panels. The temperature on these surfaces is maintained at a low level by using insulation and corrugated heat shields. The latter are attached to the primary structure by flexible clips.

The major interfaces on the booster are for wing to fuselage and orbiter to booster.

Wing-to-fuselage connection is effected through a series of fixed and flexible joints. Approximately at the center of gravity of the LH<sub>2</sub> tank are mounted the drag-load attachment brackets, which constrain all movement between wing and fuselage, except that of contraction or expansion of its tank diameter. All other connections permit fore and aft temperature differential movement but no side shift.

All major loads resulting from the connection of the orbiter at the booster are routed through the thrust structure main beam system. Forward on the top surface between the two cryogenic tanks is a hard point, calculated to accept the orbiter nose tie-down loads necessary to stabilize the composite system. On the vehicle lower surface, aft

of the nose wheel housing, there is another hard point, designed to accept the thrust loads of the ground erection system.

The rocket engine thrust loads are routed from the engine gimbal point through a truss structure to a massive twin beam assembly. The beam assembly integrates with a conical longeron and ring stiffened interstage section, which spreads the loads evenly into the fuselage. The interstage is attached to the main fuselage by riveting to the tank Y-ring. In addition to the rocket loads, the thrust structure has also to transmit the cruise engine thrust and the reaction loads of the orbiter during boost and separation.

4.1.2.2 Subsystems. Provisions for most of the subsystem equipment is made at the forward nose section, behind the two-man crew compartment. The auxiliary power unit, however, is positioned, as in the orbiter, in the aft section of the booster to provide the auxiliary power for the actuation of the aerodynamic control surfaces.

4.1.2.3 Main Propulsion System. The booster has 13 high-performance rocket engines with fixed nozzles, using oxygen-hydrogen propellants at a mixture ratio of 7:1. The engines, installed at the aft skirt section, are arranged for a smallest base area with consideration for gimbal requirements during the ascent phase. The engine thrust structure is built up from a space frame concept. The engine nozzles are skirted by the body for protection during the return flight.

The oxidizer and fuel tanks are designed as the primary load-carrying structure. Their capacity is 2,051,260 pounds of  $LO_2$  and 293,037 pounds of  $LH_2$ , for a total impulse propellant of 2,344,297 pounds.

The  $LO_2$  flows from the forward tank via a single line to two manifolds just forward of the engines. The manifolds distribute the flow to seven and six engines, respectively. The  $LH_2$  is distributed directly from the tank to each engine via individual lines. (The booster main propellant lines are shown in SKD 101569.)

4.1.2.4 Subsonic Cruise Propulsion System. Four cruise-back fanjet engines, each rated at 38,600 pounds takeoff thrust, are mounted at the upper tail section by two primary supports with diagonal truss bracings.

The 35,000 pounds of jet fuel is shown stowed in the wing, but it may be located in the fuselage, if desired.

4.1.2.5 Main Propellant Lines (SKD 101569). Between the lower two engines, a panel mounted flush with the aft structure contains the inlets for fuel and oxidizer fill and replenish lines. The fuel vent outlet is also located on this panel.

The LH<sub>2</sub> tank is located just forward of the engines. A manifold located on the aft end of the fuel tank contains 13 outlets, one for each engine, and an outlet for the fuel fill line. Each of the engine feeder lines and fuel fill line is 8 inches in diameter. A 12-inch fuel vent line starting at the forward end of the fuel tank runs aft on the lower right-hand side to the inlet panel noted above. Three manifolded engines provide hydrogen gas pressurization for the fuel tank through a 6-inch line, which is tied into the fuel vent line. The 2-inch fuel replenish line is manifolded to each engine from which the fuel is circulated into the main fuel lines for cooling of the lines.

The LO<sub>2</sub> tank is located forward of the fuel tank. A 22-inch line, running aft on the lower left hand side, carries LO<sub>2</sub> to two manifolds, which distribute the oxidizer through 8-inch lines to each of the 13 engines. Venting of the oxidizer tank is by an 8-inch line at the forward end of the booster. A 6-inch oxygen pressurant line runs forward from the engine on the lower left-hand side of the booster to the forward end of the oxidizer tank. The three engines that provide pressurization for the fuel tank also provide oxygen pressurant for the oxidizer tank. A 2-inch manifolded replenish line provides LO<sub>2</sub> to each engine for effective feed line cooling.

Piping and tubing for the fuel and oxidizer lines are of stainless steel or other low expansion metal. Lines carrying fuel and oxidizer are insulated to the latest cryogenic practices. Bends are protected by gimbaled joints, and each tube contains one or more expansion or sliding joints.

4.1.2.6 Reaction Control System (RCS). The RCS propellants are stored in six hydrogen tanks and six oxygen tanks for a total usable propellants of 750 pounds. Two tanks each feed the forward thrusters, and the other tanks are located in the boattail to be used for the aft thrusters.

Fourteen RCS thrusters are located on the booster to perform pitch, yaw, and roll functions. Four of these thrusters, located in the nose section, provide a good moment arm for pitch and yaw corrections. Eight thrusters are placed in the wing for roll and pitch maneuvers, and two thrusters are mounted to the aft face for yaw functions.

4.1.2.7 Landing Gear. Based on a booster landing weight of 375,000 pounds, the tires selected are 56 x 16 type VII tires. The main landing gear has eight tires of 36-ply rating, while the nose landing gear has two tires of 32-ply rating. The arrangement of the gear is a tricycle type with a liquid-spring shock absorber system for the main gear.

#### 4.1.3 Orbiter (SKS 100769 and SKS 100869)

The overall length of the orbiter from nose to rudder is 179.5 feet, and a maximum width, as taken over the rudder tips, is 101 feet. The maximum height of the vehicle with wheels down is 55 feet.

The orbiter is a lifting-body shaped vehicle. The basic plan view is a delta, modified to produce an efficient distribution of volume. The sweep angle is 78 degrees, with a basic reference length of 164 feet, providing a plan view area of 5,717 square feet. The nose is ellipsoidal with a semimajor axis of 3 feet. The leading edge is a continuation of this 3-foot radius nose section with a slight increase toward the aft sections. The aft cross-sections are rolled out (+30 degrees from the vertical), adding benefit in pitch and yaw stability. The basic body has been cambered 6 degrees up on the nose ramp and 5.5 degrees on the boattail. The flap and elevon have been sized to approximately 23 percent of the 5,717 square foot plan view, or 1,300 square feet and have a maximum pitchup deflection of 30 degrees. The angular movement of 30 degrees can be achieved only when the two-position bell nozzle is in the retracted and pitchup position. The elevon portion of the flap is split to provide a left and right roll capability.

The fin, providing hypersonic directional and longitudinal stability, in addition to contributing to subsonic L/D maximum, has been sized to approximately 27 percent of the 5,717 square feet plan view, or 770 square feet, for each fin.

4.1.3.1 Structure (SKW 101069). The nose section is composed of the nose heat shield, outer shell, nose landing gear support structure, crew cabin structure, and outer heat shield.

The outer intermediate nose section shell has longitudinal joints, which permit removal of the main forward LH<sub>2</sub> tank from a completed vehicle. This panel arrangement reduces to a minimum the disruption of the other subsystems in the vehicle if a hydrogen tank must be replaced. Mounting points and load distribution longerons for support of the LH<sub>2</sub> tanks are provided in this intermediate nose section.

A portion of the payload bay is included in the center section. Here panels are also located for removal of the main LO<sub>2</sub> tank. The main landing gear bulkhead and the landing gear doors are included in this section. LO<sub>2</sub> tank attach points and load distribution longerons are also provided. The payload bay door is mission peculiar, so it is described separately.

The aft portion of the payload bay is included in the aft section. Support points and longerons for the main LO<sub>2</sub> and LH<sub>2</sub> tanks, as well as the orbit maneuver and de-orbit tanks, are provided. Rocket engine thrust structure attach points occur on the lower part of the aft payload bay, at the aft end continuation of the payload bay door jamb edge members, and at the upper longeron of the booster ascent thrust pad support structure.

A removable structural panel is provided for ease of fuel tank replacement.

The trim flap support bulkhead spans across the full width of the section and also serves as a carrythrough structure for the fin aft spar.

Both the left-hand and the right-hand fin and rudder assembly take the form of a typical two-spar fin, bolted to main frames and drag members on the aft section of the body. The rudder is also typical of aircraft design and construction. The reentry heat shield is attached to the outside surface of the basic structure.

The trim flap assembly consists of the forward panel, which is in one piece across the base of the vehicle, and two aft panels, which can be deflected differentially to provide roll control of the vehicle. These panels, of typical aircraft construction, are covered by a reentry heat shield. Several bearing concepts being evaluated include a flexural pivot, which has no sliding parts.

The structural system has a heat shield subassembly, consisting of a phenolic subpanel, to which is mounted the external metallic heat shield, the heat shield support clip, and microquartz and dynaflex insulation. The heat shield panel sizes are governed by the frame spacing, with the largest size being approximately 60 inches x 60 inches.

The cavity between the heat shield and the inner structural skin is used for circulating cooling air, which could be supplied by an external scoop during subsonic flight and by ground equipment after landing. This arrangement permits longitudinal members to be attached to the inside of the inner structural shell and not interfere with the passage of cooling air between the frames. In addition, the frame joints at the removable panels are accessible from the outside after a portion of the reentry heat shield is removed, thus making it easier to disconnect the frame joints in the removable panels.

In an alternate arrangement of the shell structure, the outer metallic heat shield is mounted directly to the corrugated skin panel, with the frames on the inside of the skin instead of outside. The cooling air is directed along the cavity of the corrugations. Disconnection of the frames for panel removal is achieved through access holes in the corrugated skin panel.

4.1.3.2 Subsystems. An auxiliary power system is provided to meet short-term peak demands not efficiently met by the electrical power system, principally the demand for hydraulic power to actuate aerodynamic control surfaces during reentry and landing, deployment of jet engines, and extension of landing gear. This system is a turbine-driven power unit, employing hydrogen and oxygen as reactants. Along with the



30 pounds  $\text{LH}_2$  and 30 pounds  $\text{LO}_2$  reactants, the system is located in the boattail near the principal power demand areas.

The fuel cells with 120 pounds of  $\text{LH}_2$  and 1000 pounds of  $\text{LO}_2$  reactants are positioned near the crew compartment.

Most of the components or equipment for the other subsystems (guidance, navigation, and flight control, data management, and communications) are located in the nose section near the crew compartment.

4.1.3.3 Main Propulsion System (SKT 100969 and SKB 101569). The orbiter has three high-performance rocket engines (with two-position nozzles), using oxygen-hydrogen propellants at a mixture ratio of 7:1. The three engines, installed in the tail section side by side, are separated for freedom to gimbal 8-degrees maximum with one engine out. The bell nozzles have been skirted by the upper surface of the body for maximum protection during reentry, creating an artificially lengthened vehicle over the basic 164-foot length. The engines are mounted on a welded tube space structure with joint fittings. The load paths are carried into built up beams, terminating near the aft bulkhead of the payload compartment.

The number of propellant storage tanks has been kept to a minimum, with one large nose tank holding 46,508 pounds impulse  $\text{LH}_2$ . Two slender side tanks straddle the payload compartment, each for a capacity of 290,808 pounds  $\text{LO}_2$ . Two more large tanks are located at the aft section, each providing 18,290 pounds of  $\text{LH}_2$ . These five tanks hold the total impulse propellant of 664,706 pounds to be used during the ascent phase. Two smaller tanks, located in the aft section under the payload compartment, are extended-time storage tanks. One holds 34,976 pounds of  $\text{LO}_2$ , and the other holds 5,358 pounds of  $\text{LH}_2$ . Of this propellant, 850 pounds  $\text{LH}_2$  and 3,420 pounds  $\text{LO}_2$  is scheduled for the reaction control system, with the remainder for on-orbit maneuver and retro usage. The propellant storage tanks are supported by a network of struts.

**4.1.3.4 Subsonic Propulsion System.** For landing go-around, a thrust of 74,219 pounds at 3000 feet is required. This is accomplished by four fanjet engines of approximately 25,000 pounds takeoff thrust each. The engines are normally stowed in the aft section and deployed individually as required. The location of the engines is favorable for the quality of ingested air, pressure recovery, distortion, and turbulence, as was determined on the wind tunnel model. Stored under the payload compartment is 6000 pounds of jet fuel.

**4.1.3.5 Main Propellant Lines (SKB 101559).** Liquid hydrogen is stored in three tanks. The largest of which is located in the forward portion of the vehicle. The other two tanks are mounted in the aft portion, just in front of the engines. Another LH<sub>2</sub> sump tank is located off center in between the two LH<sub>2</sub> tanks. Two 10-inch fuel lines connect each of the smaller LH<sub>2</sub> tanks with the large forward LH<sub>2</sub> tank. Another 10-inch line feeds fuel from the aft LH<sub>2</sub> tanks into the LH<sub>2</sub> sump tank. The exit of the LH<sub>2</sub> sump tank is provided with a short 11-inch trunk line, branching out into three separate 8-inch lines, which provide fuel to each of the three engines.

A 6-inch line, extending from the forward end of the large LH<sub>2</sub> tank to the rear of the vehicle, is for LH<sub>2</sub> venting. An LH<sub>2</sub> fill line, located at the rear, connects into one of the engine feed lines.

The two main LO<sub>2</sub> tanks, identical in size, are located immediately aft of the large LH<sub>2</sub> tank. They are interconnected at the exit with a 10-inch line and feed LO<sub>2</sub> to the sump tank through a 14-inch line. The LO<sub>2</sub> sump tank is located off center, next to the LH<sub>2</sub> sump tank. It is provided with a short 11-inch trunk line and, similarly to the LH<sub>2</sub> system, branches out into three 8-inch lines to feed LO<sub>2</sub> through the shortest route to each of the three engines. An LO<sub>2</sub> fill line, conveniently located at the rear, taps into one of the LO<sub>2</sub> engine feed lines.

**4.1.3.6 Reaction Control System (SKS 100869).** LH<sub>2</sub>/LO<sub>2</sub> propellants are used for the RCS, in which propellants are pumped from the low-pressure sump tanks (also called extended-time storage tanks) to the high-pressure gaseous O<sub>2</sub> and H<sub>2</sub> accumulator tanks. Four pairs of these accumulators are located near each thruster arrangement. The propellants are stored as liquid and supplied to the thrusters as a gas.

The 30 RCS thrusters, which perform attitude hold, attitude maneuver, and  $\Delta V$  translation, are arranged to provide three-axis functions such as slewing about any axis, attitude control, and translation along any axis.

The 30 thrusters are grouped into 12 small clusters (100 pounds) for limited cycling operations and 18 large clusters for attitude maneuvers and translation. The large thrusters are throttlable with a maximum thrust level of 3600 pounds. Four of the large thrusters are in the nose section. For the reentry phase the nose section is moved back to its flight configuration, covering the forward RCS thrusters. An alternative to be investigated is to penetrate the heat shield, allowing the forward thrusters to be used during the reentry operation.

At the aft section, six large and six small thrusters are clustered at each side. These clusters are deployable to satisfy operational phases. During launch, the clusters are stowed and insulated; in orbit they are fully deployed, allowing all the above mentioned functions. For reentry, the clusters are partially retracted, removed from the high-temperature areas but still permitting the necessary roll and yaw functions. This straight-line deployment eases nozzle alignment during all operational modes. Two more large thrusters are located at the upper aft center area, with one deployable and one fixed.

4.1.3.7 Landing Gear. Based on a landing weight of 260,000 pounds and a tricycle type landing gear arrangement, the tires have been sized. The main landing gear, consisting of two six-wheel walking beam clusters, have 34 x 11.0 - 28-ply tires, mounted on liquid-spring shock absorbers. The nose landing gear has two 32 x 11.50 - 15, 18-ply tires.

4.1.3.8 Payload Compartment. This compartment is configured in a cross fashion, providing space for either a 30 x 22 foot diameter payload, a 60 x 15 foot diameter payload, or a combination. A small cargo hatch is provided to the transfer station. The transfer station is connected by a passageway to the crew compartment.

4.1.3.9 Crew Compartment. The basic two-man crew compartment is capable of expanding to a four-man compartment. The compartment, designed for shirtsleeve operations, has three hatches - one for launch entry or emergency exit, one for access to the passageway, and the third for crew egress after landing. The environmental-control and life-support systems provide an  $N_2-O_2$  cabin atmosphere, with approximately 60 pounds of  $LO_2$  and  $LN_2$  stored outside the compartment. Inside the compartment is the equipment for atmosphere control, humidity control, carbon-dioxide removal, trace contaminant control, thermal control, food and water supply, and waste management.

## 4.2 TRIAMESE

### 4.2.1 Launch Vehicle (SKD 100969 and SKJ 101769)

In the process of selecting the arrangement of the Triamese launch vehicle, various possible combinations of orbiter and booster positions and orientations were considered. It was found that with the orbiter in an outside position the travel of the center-of-gravity of the launch vehicle during the boost phase of the ascent is prohibitively large. Hence, the orbiter must occupy the center position. Of the four arrangements possible with the orbiter in the center, the one selected affords symmetry and compactness, and with it the two boosters would have identical orbiter attachment structure.

For the 25,000-pound payload launch vehicle, the booster reference length (nose tip to base) is 169.2 feet. Seven 400,000-pound thrust (sea level) bell-type rocket engines per booster provide liftoff thrust. Propellant loading is 1,152,778 pounds, contained in two separate tanks. Four turbofan jet engines provide the necessary takeoff thrust of 107,300 pounds. All vehicles are in parallel alignment. Overall dimensions are 191 feet long, 178 feet wide, and 89.3 feet high.

The launch vehicle has the orbiter sandwiched between two booster stages, which are back to back.

The method of loading and unloading the Triamese launch vehicle causes some complications peculiar to this configuration. Since the payload compartment opens toward the top of the orbiter, it will be necessary to load large-sized payloads before erecting the booster on that side. To provide for boarding and disembarking passengers, there are passages from the payload compartment to doors on the sides of the orbiter. Emergency ejection of the crews, both booster and orbiter, in the conventional direction normal to the aircraft centerline is precluded in this configuration. A possible solution would require a programmed sequential ejection of the orbiter crew vertically upward, followed by ejection of the booster crews on trajectories approximately 45 degrees upward and clear of the opposite booster. In the case of the boosters, the same trajectory could be used for aircraft-type operations. The orbiter, however, would require other means for ejecting the crew in aircraft-type operations.

#### 4.2.2 Booster (SKG 100769 and SKG 100369)

The Triamese booster is derived from the same design concepts as the Two-Stage system booster. The structural arrangement is identical; and internal arrangement and design details are essentially identical to those of the Two-Stage booster, except for size, number of rocket engines, and minor differences.

4.2.2.1 Propulsion System. Locations and construction of the load-bearing main propellant tanks are similar to those of the Two-Stage system. Volume of the LO<sub>2</sub> tank is 17,500 cubic feet. Volume of the LH<sub>2</sub> tank is 41,500 cubic feet. They hold  $1.386 \times 10^6$  pounds of usable propellant at a mixture ratio of 7 to 1, including allowances for ullage and residual propellant.

Eight rocket engines of the fixed bell nozzle ( $\epsilon = 35$ ) type are gimbal mounted in three rows of three, three, and two. Each engine produces 400,000 pounds of thrust for takeoff at sea level. A thrust structure transfers the engine thrust from the gimbal trunnions to the liquid hydrogen tank wall. Four fanjet engines (5:1 bypass ratio) are mounted in pairs in nacelles on each side of the thrust structure. Each fanjet engine produces 27,000 pounds thrust for sea level takeoff. In the wing structure, 21,000 pounds of fuel is carried in cells.

4.2.2.2 Reaction Control System. The 14 RCS nozzles, burning gaseous hydrogen and oxygen, provide thrust for pitch, yaw, and roll control and for stage separation. The propellant is stored in six pairs of spherical tanks; two pairs are carried forward in the nose wheel compartment area, and four pairs are located in the thrust structure area. The nozzles are mounted in three groups of four nozzles each. One group, mounted in the space between the crew compartment and the forward end of the LO<sub>2</sub> tank in a cruciform pattern, provides thrust for pitch and yaw control and for stage separation. Two groups, one in each wing near the base of the fin, provide thrust for pitch and roll control and for stage separation. The two remaining nozzles, mounted on the thrust structure rear bulkhead, primarily provide thrust for yaw control.

4.2.2.3 Landing Gear. The main landing wheels of the tricycle type landing gear are located just aft of the landing center-of-gravity. Each main gear consists of two pairs of wheels in tandem, with the aft pair mounted on a trailing arm to help provide for a large angle-of-attack at touchdown without an extremely long shock strut. The main landing gear is mounted on the wing main beams, and it is retracted into the space in the wing-body fillets. The nose gear is situated in the bay between the LO<sub>2</sub> and LH<sub>2</sub> tanks. Bulkheads at each end of the intertank structure isolate the LO<sub>2</sub> tank from the LH<sub>2</sub> tank and provide hard points for mounting the nose gear and actuating mechanisms. Both main and nose gear retract by swinging forward to assure positive fail-safe extension.

4.2.2.4 Orbiter Attachments. The booster is attached to the orbiter at three points. One attachment strut, mounted on the intertank structure front bulkhead, retracts into the space between the LO<sub>2</sub> tank at the top of the fuselage. The strut and its supports are designed to resist loads normal to the vehicle centerline but to permit relative motion of the orbiter and booster in the axial direction. Two attachment struts are fastened to the upper edge of the thrust structure inboard of the inboard fanjet engines and approximately in the plane of the rocket engine gimbal mounts. Integrated with these two hard points are two launch-support pads. One of these struts is designed to resist loads along all three axes; the other strut resists axial and vertical loads, but permits relative movement of the orbiter and booster structures in the spanwise direction.

A third launch support pad is located on the wing trailing edge at the booster centerline.

4.2.2.5 Crew Compartment and Miscellaneous Systems Equipment. The crew compartment and life support systems equipment is located in the nose of the vehicle. A space of approximately 1000 cubic feet and structure for mounting additional vehicle system equipment exists in the intertank structure. It is accessible through the nose-wheel compartment.

#### 4.2.3 Orbiter (SKG 100969 and SKG 100869)

The Triamese orbiter general arrangement is similar to that of the Two-Stage system orbiter, except for certain additional features required for the Triamese launch vehicle.

The passenger entrance on the left-hand side connects via a passage to a door in the passenger module in the payload compartment. A swing-arm on the launch tower services this entrance. A redundant entrance is provided on the right-hand side.



#### 4.3 PILOT VISION CONCEPT (SKE 100969)

The pilot vision concept calls for providing the pilot a direct view of the approach zone and runway through a forward windshield. The windshield and pilot location geometry is configured to provide, at the high angles of attack associated with lifting body vehicles, landing vision comparable to that in conventional transport aircraft.

During the reentry phase, the windshield is covered by a variable geometry (droop) nose. The nose, in the up position, is configured to minimize reentry heating. (A reusable heat shield is used.) The nose in the down position allows the pilot an unobstructed straightahead view down 30 degrees from the vehicle horizontal reference point.

An oblique view of the nose side and top gives the pilot a visual pitch and yaw reference.

Since all vehicle aerodynamic flight phases involve relatively high angles of attack, the crew compartment horizontal reference plane is positioned 17 degrees nose down from the vehicle horizontal reference plane. This angle approximates the angle of attack for both subsonic and hypersonic L/D maximum. This arrangement maximizes the display space available between the pilot's knees and his line of vision over the instrument panel.

The windshield, of a V-shape, is composed of two large radius conical elements. The center of these elements coincides with the nose droop axis so that close clearances are maintained between the windshield and the aft upper end of the nose at all intermediate positions.

The use of intermediate positions provides the pilot adequate forward vision during cruise flight while minimizing the drag and pitching moment due to the nose droop.

Two side windows, aft of the windshield, are flush with the body lines. They are not covered during reentry.

Other visibility concepts are discussed in Section 11.

#### 4.4 PERSONNEL ESCAPE SYSTEMS

A hazardous condition may necessitate escape by means of any one or a combination of the following:

- Nose capsule escape system
- Ejection seats
- Inflated and uninflated slides
- Ladders
- Elevators
- Portable platforms
- Slide wire
- Slide pole

The selection of an optimum escape must be based on a thorough failure mode and reliability analysis of the complete launch vehicle. Some typical situations that would require escape abort are as follows:

- When a satisfactory landing site cannot be readied or when conditions make an attempted landing impractical
- Failure of an essential system after launch
- Failure of a booster system (explosion, fire, collapse)
- Crash landing of booster or orbiter
- On-pad abort

Escape requirements of the two recoverable vehicles are dissimilar. In the orbiter the passengers should not be expected to use such devices as ejection seats for emergency escape. On the other hand, the crewmen of the booster can be expected to use ejection devices.

Several methods of emergency escape, similar to those with conventional aircraft, include ejection seats, encapsulated ejection seats, and nose capsules. The choice of an escape method can come only from a thorough examination of the hazards, weight of the systems, the reliability of each system, the aerodynamic qualities of the vehicle,

and (equally important) the configuration of the vehicle. In addition, the abort capabilities of the total vehicles must be compared to emergency escape systems as a means of providing crew escape. A matrix presenting some of the critical aspects of the various escape concepts in relation to flight phases is presented in Table 4-1.

An important consideration is the advent of a booster explosion on the pad and during boost. On-the-pad explosion is generally critical because of the quantity of propellant on board. The characteristics of the explosion varies with the type of propellant and with the rate of mix of the fuel and oxidizer. Cryogenic systems generally produce the more severe explosion and with the highest overpressures. Selecting the method of escape from this type of hazard must be based in part on the time history of the size of the fire-ball and the overpressure generated.

The configuration of the vehicle eliminates some escape methods from consideration. Typical lifting body shapes, typified by the M-2 and HL-10 vehicles, are without a conventional fuselage; hence, nose capsules are not easily incorporated. Other body shapes considered for reentry are of the Dyna-Soar type, in which the fuselage can be distinguished. In this type, a nose capsule can be considered, especially if the cockpit is small as compared with the rest of the vehicle. The nose capsule would require complete control and maneuver capability in order to function during the high-altitude and near-orbit abort cases. It would require a large abort propulsion system to effect abort off the pad and through the maximum  $q$  phase and a parachute recovery system for terminal descent.

#### 4.4.1 Flight Escape

4.4.1.1 Approach. Consideration of parameters applied to the low earth orbital vehicle shows that the use of encapsulated seats is one valid approach. Escape by this means is divided into three logical modes:

- Abort Mode I

- Eject at up to 100,000 feet
  - Eject at below 100,000 feet following reentry

- Abort Mode II (100,000 to maximum altitude of boost phase)

- Terminate vehicle thrust
  - Separate from booster and perform retrograde burn if necessary
  - Eject from vehicle below 100,000 feet is necessary

- Abort Mode III (booster separation to orbit)
  - Terminate vehicle thrust
  - Perform reentry attitude and retrograde maneuvers
  - Reenter
  - Eject from vehicle below 100,000 feet if necessary

This system is of minimum weight, currently feasible, and simple; but escape is restricted by the flight envelope of the encapsulated ejection seats.

Another valid approach is a nose capsule escape system, with which escape may be accomplished as follows:

- Abort Mode I
  - Separate nose capsule between zero velocity and suborbital velocity (approximately 9100 feet per second)
- Abort Mode II (150,000 feet to maximum altitude of boost phase)
  - Terminate thrust
  - Separate from booster and perform retrograde burn if necessary
  - Remove nose capsule below 150,000 feet if necessary
- Abort Mode III (booster separation to orbit)
  - Terminate vehicle thrust
  - Perform reentry attitude and retrograde maneuvers
  - Reenter
  - Remove nose capsule below 150,000 feet if necessary

In addition to failure mode and reliability, the decision to eject an encapsulated seat or an entire nose or crew capsule is dependent on many other factors, including development costs and operational considerations. For instance, during development of the Space Shuttle, all crew members should have maximum feasible protection. Once the orbiter becomes operational, expanded crew and passenger payloads must rely on the basic vehicle to overcome in-flight difficulties. The booster crew will remain small after going operational, thus ejection systems may be appropriate. However, the booster crew must be concerned with optimizing the vehicle impact area and should have the opportunity to control the descent of the booster until the last moment. An encapsulated seat for all crew members of the booster and the orbiter during development and for the operational booster satisfies these needs.

Table 4-1

ESCAPE SYSTEM COMPARISON

Operational Parameters	Ejection Seats (Oxygen, Supply, No Pressure Suit)	Encapsulated Seat	Nose Capsule
Operational limitations in current state-of-the-art (limited by aerodynamic heating and human tolerance to deceleration)	Mach 4, max altitude of 50,000 ft	Mach 4, max altitude above 100,000 ft	Mach 4, max altitude of 150,000 ft (capsule must be capable of being controlled during all atmospheric and exoatmospheric flight phases)
Weight of system to implement escape	Ejection seat and parachute recovery system 260 lb per person	Encapsulated seat and parachute recovery system 450 lb to 1000 lb per person	1500-3500 lb per person; abort propulsion system weight dependent on time/distance history necessary to escape fire-ball (Apollo LES is 2/3 of CM weight.)
Launch abort (0 to 50,000 ft)	Applicable for storable propellants; not applicable for cryogenic propellants	Applicable for storable propellants; not always applicable for cryogenic propellants; requires specific case study	Applicable for either types of launch propellants
High-altitude abort (50,000 to 500,000 ft)	Not applicable	Applicable except altitude limited	Applicable except altitude limited
Orbital abort	Not applicable	Not applicable	Not applicable
Reentry abort	Not applicable	Not applicable	Not applicable
Landing abort	Applicable; ejection seats used to abort anytime during terminal flight phase	Applicable	Applicable if separation propulsion system is provided

4.4.1.2 Encapsulated Seat (SKJ 100369). Several seats have been developed for high-performance aircraft, but such seats would have to be modified to allow for the vertical launch condition. In this case, an upward thrust is provided by canting the rocket exhaust or ejection seat guide rails.

The encapsulated seat for the B-70 aircraft represents a fully developed system, which could be modified for use in the Space Shuttle.

There are two crew stations, side-by-side, in the XB-70A airplane. Each crewman is provided with an encapsulated seat, as shown in Fig. 4-1. Upon entering the seat, the crewman connects the on-point oxygen and communication lead and the torso-hip restraint harness at two fittings. Other than these devices, there is no tie to the occupant.

The major subsystems incorporated in the escape capsule are the rocket catapult, torso restraint, stabilization booms and parachutes, pressurization system, and recovery system. The seat is 20 inches wide at the hip and 21.25 inches wide at the elbows and shoulders. Figure 4-2 shows the overall installation dimensions, and Table 4-2 shows the weight breakdown of the capsule. To reduce fatigue during flight, arm rests are provided; and the seat may be reclined, electrically raised and lowered, and the under-thigh surfaces varied.

The seat occupant in normal flight (Fig. 4-3) sits well forward of the capsule shell and is able to perform flight duties unrestricted. Actuation of either of two control levers ballistically retracts the seat and crewman into the shell, closes the clamshell doors from top and bottom, and pressurizes the capsule. From this position, the pilot can monitor the instrument panel and control the airplane; or he may eject by squeezing one of two triggers at his side. The retracting-enclosing sequence may be performed alternately by hand and may be reversed to restore the crewman to his usual position.

Operation of either handgrip trigger jettisons the individual overhead hatch and, in sequence, ejects the capsule by firing the rocket-catapult, which produces an impulse of 4500 lb-sec. Within 11.0 second after ejection, a pair of cylindrical booms rotate and extend to a length of 9 feet from the capsule back, imparting medium- and high-speed aerodynamic stability to the capsule. For increased stability during low-speed

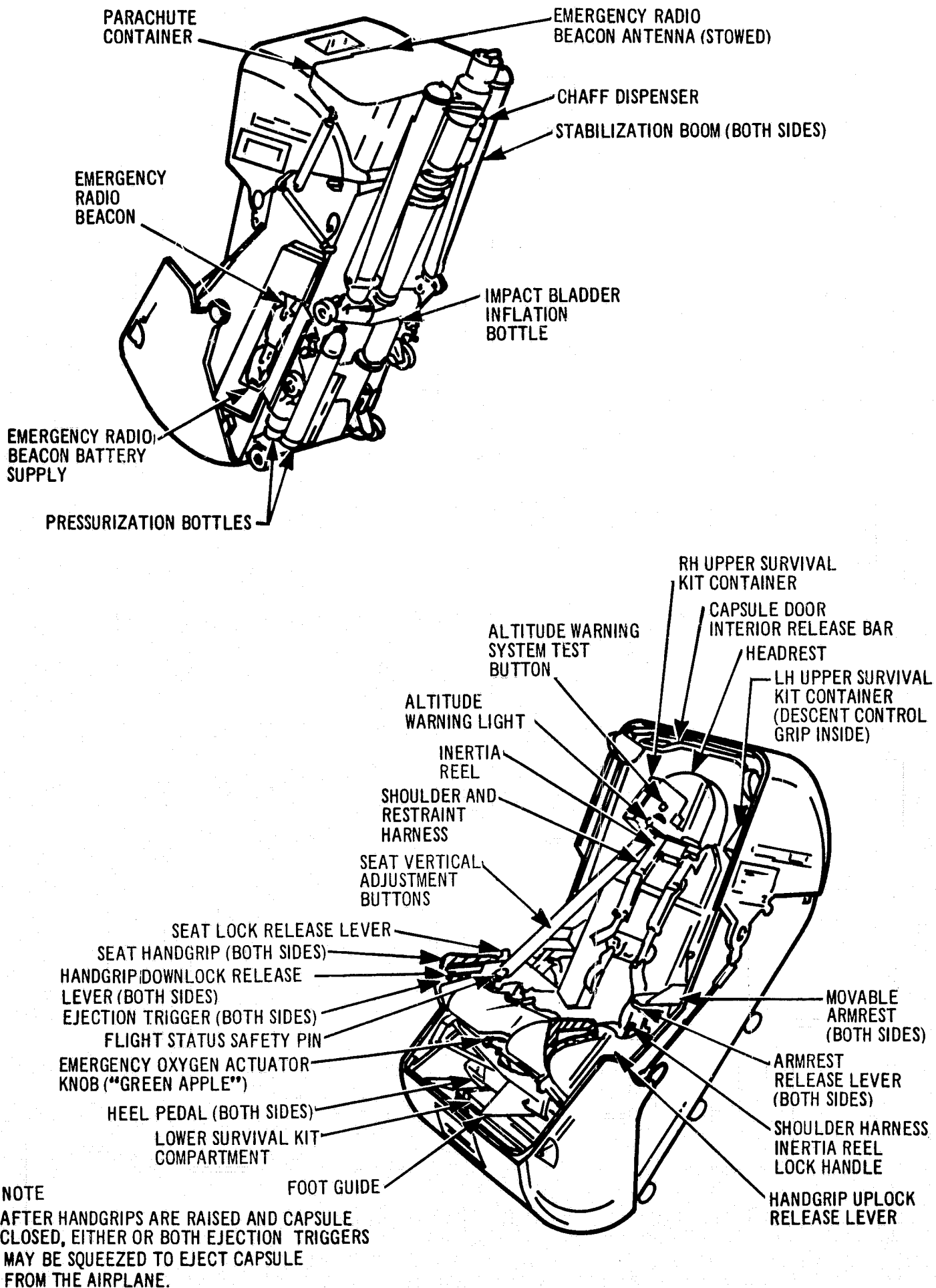


Fig. 4-1 North American B-70 Escape Capsule

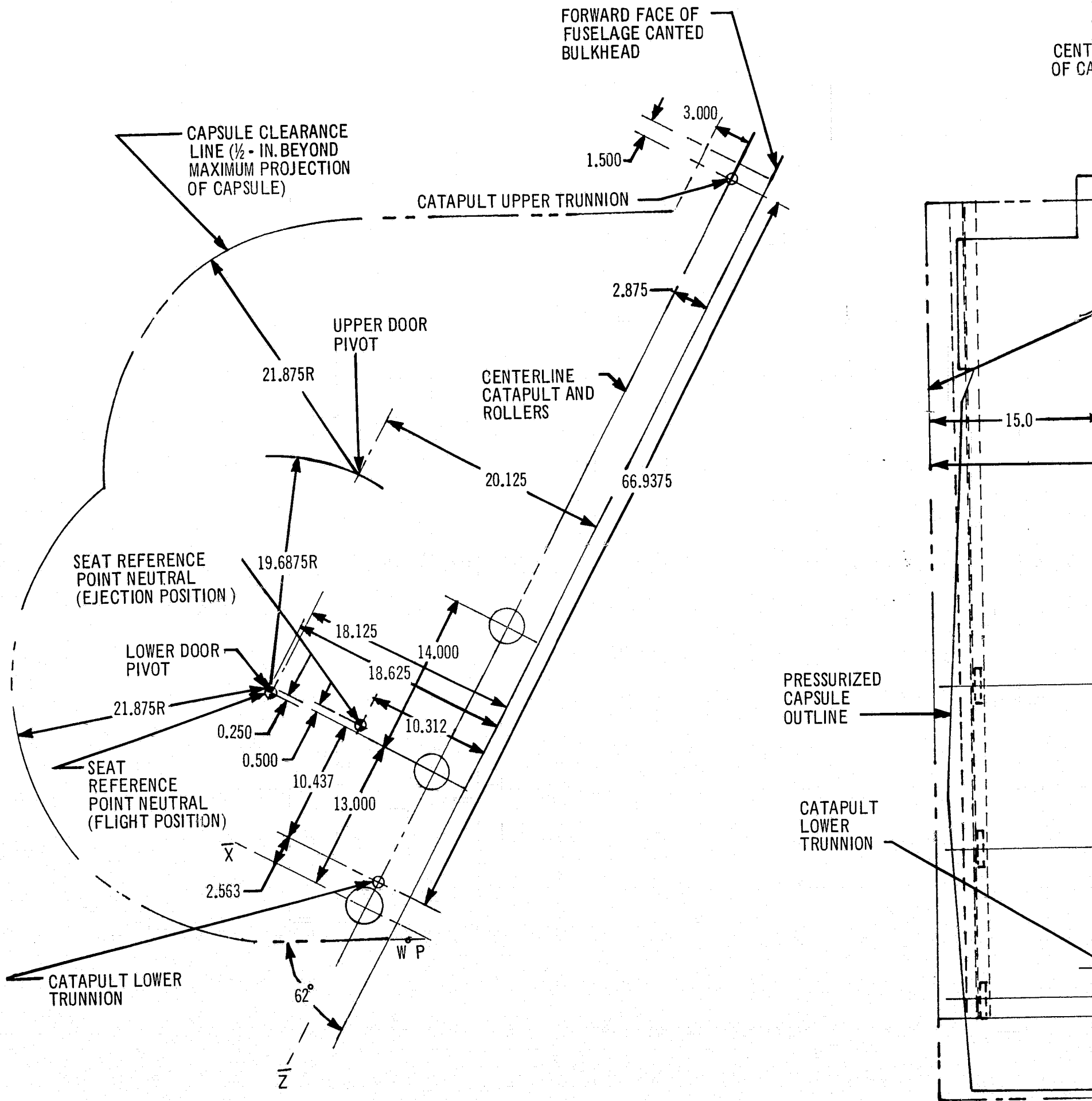


Fig. 4-2 North America

FOLDOUT FRAME /



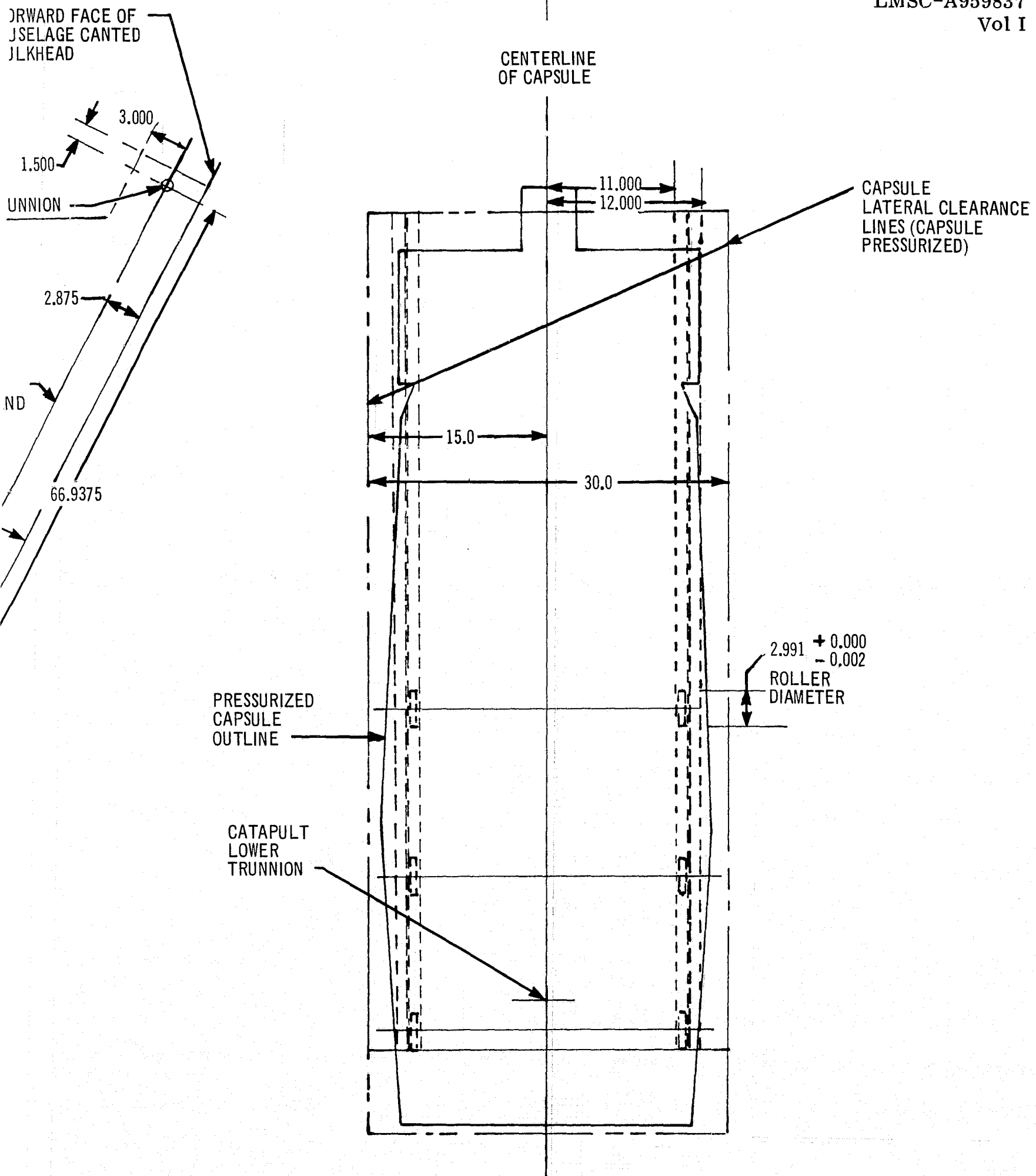


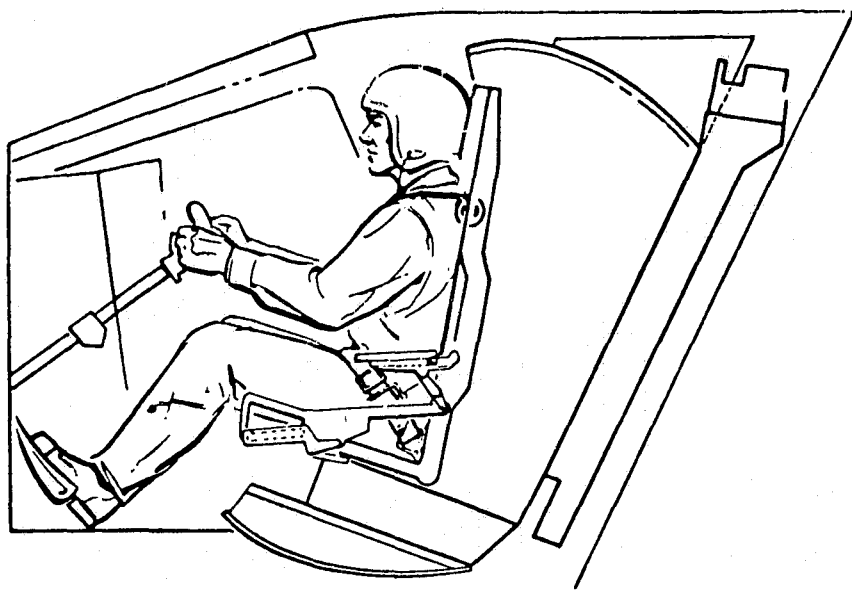
Fig. 4-2 North American B-70 Encapsulated Seat Installation Dimensions

Table 4-2

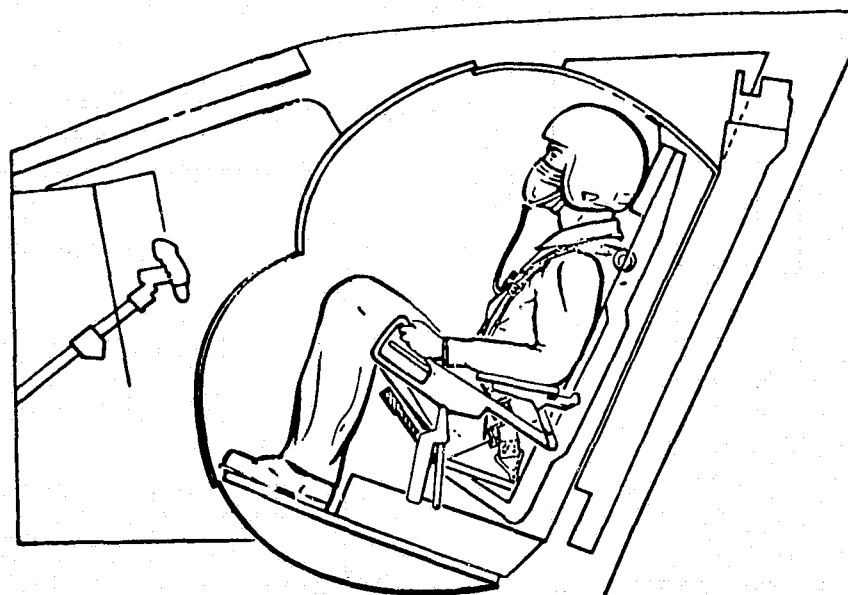
NORTH AMERICAN B-70 ENCAPSULATED SEAT WEIGHT BREAKDOWN

	<u>Weight (lb) Ejectable</u>	<u>Weight (lb) Nonejectable</u>
Capsule structure	208	
Seat	67	
Catapult inner tube and propellant	38	
Stabilization booms	102	
Recovery parachute installation (parachute = 31 pounds)	38	
Oxygen installation	35	
Impact attenuator installation	17	
Cartridge devices, hoses, and fittings	24	
Miscellaneous (capsule)	33	
Clothes and personnel equipment	12	
Survival gear	27	
Catapult outer tube		13
Ejection rails		36
Miscellaneous (airplane)		14
Ejectable weight	601	
Nonejectable weight		63
Total installed weight	664	
<u>Crewmember Weight (lb)</u>		
5 Percentile	134	
50 Percentile	162	
95 Percentile	200	

PRECEDING PAGE BLANK NOT FILMED.



NORMAL FLIGHT  
POSITION



RETRACTED EJECTION  
POSITION

Fig. 4-3 B-70 Seat Operation

ejections and for free-fall, a parachute deploys from each boom tip 1.5 seconds after extension. The main recovery parachute is deployed 1.9 seconds after ejection below 15,500 feet; if above 15,000 feet, the parachute withholds deployment until the capsule descends to this altitude. A radio homing beacon is actuated upon parachute deployment. To reduce opening loads and to ensure inflation, the 34.5-foot solid canopy with 10 percent extended skirt parachute is reefed for 2 seconds. A cautionary light illuminates within the capsule at 15,500 feet to inform the occupant that parachute opening altitude has been reached and deployment may be initiated manually, if necessary.

During descent, the capsule is in an upright attitude and contacts the ground or water in this position. One second after main parachute deployment, a bladder inflates from the bottom of the capsule to attenuate landing loads and, in conjunction with the stabilization booms, to bring the capsule to a rest position, affording rapid exit. The occupant may collapse the parachute to avoid dragging the capsule during high winds. Egress can be accomplished by raising the upper door or by explosively separating both doors.

All survival equipment is readily available to the seated occupant within the enclosed capsule. The equipment is stowed in two containers beside the crewman's head and in an underseat compartment. After water landings, the capsule floats stably in the supine position, allowing the crewman to scan the horizon and sky through the three capsule windows while awaiting rescue.

A complete developmental and qualification test program was accomplished on the capsule and the capsule subsystems. The complete systems was demonstrated in 32 ejection tests, in which escape conditions covering the complete XB-70A flight envelope were simulated. In these tests, 19 ejections were accomplished in flight, 11 from sleds, and 2 from a static ground position. Typical test trajectories demonstrating the system's capability are shown in Fig. 4-4.

4-30

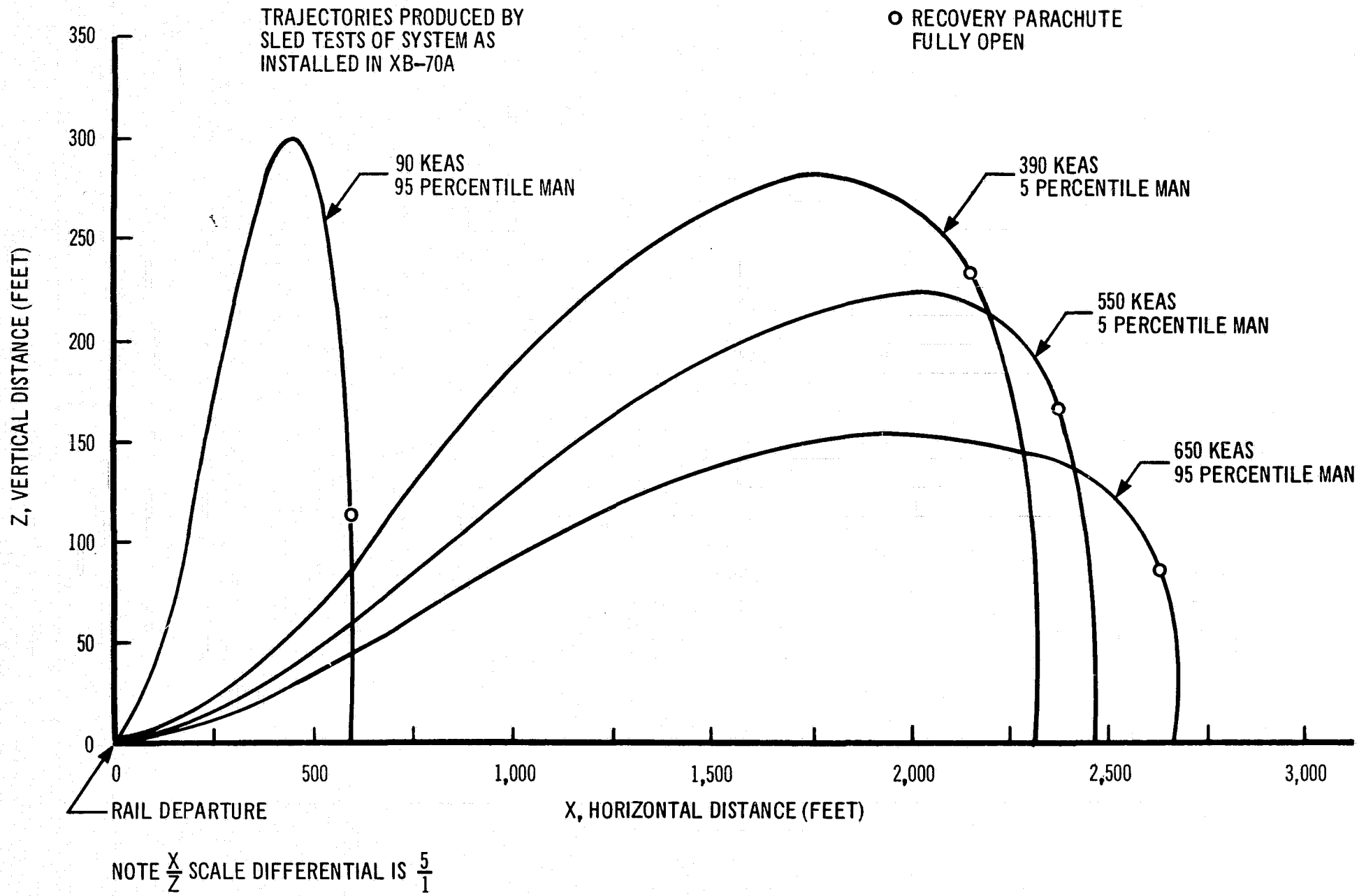


Fig. 4-4 B-70 Escape Capsule - Four Representative Trajectories

The event-time sequence history recorded during 93 KEAS tests was as follows:

Event	Seconds
Ejection initiation	0.0
Capsule first motion	0.022
Tripper actuation	0.145
Stabilization booms unlock	0.173
Upper roller tipoff	0.177
Catapult tube separation	0.195
Center roller tipoff	0.196
Lower roller tipoff	0.214
Stabilization booms fully rotated	0.227
Stabilization booms fully extended	0.264
Rocket catapult burnout	0.73
Stabilization boom parachute caps fired	1.83
Recovery parachute lid fired	2.27
Impact attenuator door jettisoned	3.56
Recovery parachute line stretch	3.70
Recovery parachute reefed open	5.47
Impact attenuator fully inflated	5.96
Recovery parachute disreefed	6.85
Recovery parachute fully open	7.98
Capsule touchdown	11.05

Capsule accelerations are moderated by aerodynamic characteristics, recovery parachute reefing, and by the gas-filled bag landing impact attenuator. The most severe conditions result in maximum force applications of 21 g seat-to-head and 15 g chest-to-back during ejection of a 5 percentile occupant at maximum indicated airspeed. Accelerations experienced during and immediately following capsule ejections during a low- and high-speed sled test are shown in Figs. 4-5 and 4-6. Since the ejected capsule trims aerodynamically at an angle close to the zero lift attitude, the variations in vertical accelerations are small with changes in air speed. During deployment and inflation of the recovery parachute, a maximum of approximately 11 g (at reefed open time) was recorded with force applications from seat-to-head predominating.

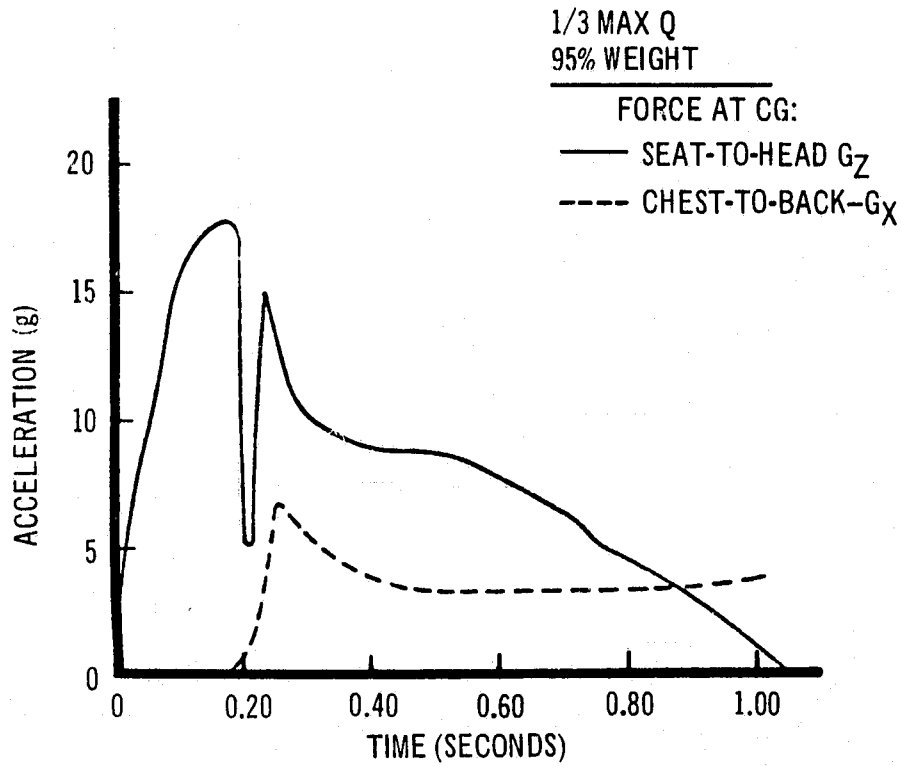


Fig. 4-5 Ejection Exit Histories - B-70 Escape Capsule Ejection Accelerations

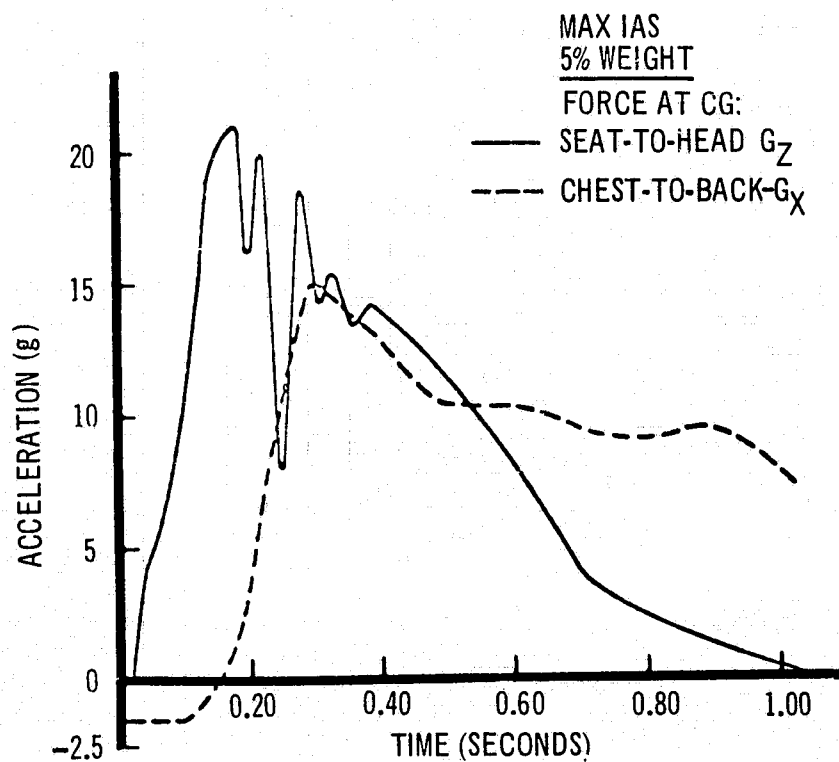


Fig. 4-6 Ejection Exit Histories - B-70 Escape Capsule Ejection Accelerations

Touchdown applied forces, recorded by instrumentation near the mass center-of-gravity during water entry, peak to 7 g seat-to-head and 4 g chest-to-back and laterally, while accelerations on drifting contact onto decomposed granite and vertical approach onto concrete reach maximums of 12 g seat-to-head and chest-to-back with 6 g laterally. Imposition of a 16-knot wind drift onto concrete raises maximum to 19 g seat-to-head and 9 g chest-to-back and laterally.

The encapsulated seat will provide safe escape throughout a speed range to supersonic.

#### 4.4.2 On-Pad Escape

The prelaunch to liftoff period represents one of the most demanding escape conditions. This is further complicated by the need to avoid any umbilical tower or even a personnel mast. Even if a personnel mast were permitted, the final configuration is intimately involved with the vehicle erection procedure.

In the escape version with a personnel mast, a vertical column is placed as near to the flyaway envelope as possible. The function of this column is solely to provide support to an inclined elevator truss. The elevator truss contains two cars, one stationed at the booster crew level and the other at the orbiter crew level. The inclined elevator truss provides for lateral displacement from the launch vehicle base as it descends. A subterranean sanctuary provides shelter in case of adverse ground level conditions. In addition, a 4-foot diameter tubular slide is provided for each crewman to use in case of elevator inadequacy. The slides discharge below ground level in the sanctuary room. If desired, a fan can blow air up the slide tube to provide ventilation or a braking effect.

The orbiter passengers are provided only with two slides. Repeated trips of an elevator car is deemed inadequate in an emergency, whereas a slide provides continuous means of escape. The distance from the passenger compartment to the elevator truss becomes excessive at lower elevations. Therefore the slides are located at the nearby vertical column. The two sanctuary rooms are connected below ground by an escape tunnel. Swing arms are hinged and actuated near the vertical column. If the personnel



mast were to be located in the alternate location, the swing arms would have to be L-shaped and be markedly longer.

The orbiter passenger would not be able to use the personnel mast, since a swing arm around the booster wing would be unwieldy. In this case, a portable slide would be implaced after vehicle erection. Other escape devices that would be used only if a personnel mast were present are slide wires and fireman's poles. Depending on the passenger payload configuration, a fireman's pole could be of value within the orbiter payload area to assist in vehicle egress.

If the personnel mast is not permitted, several alternates may be used. Encapsulated seats may be used by both booster and orbiter R&D crews. Inflated slides similar to those used in current airline practice could be deployed. It is feasible to have two side tunnels for the orbiter passengers. This tunnel, approximately 7 feet high by 4 feet wide, permits direct egress to the outside of the vehicle at an elevation of 59 feet above the pad. From here an inflated slide would be automatically deployed. Cherry pickers could be available for both crews. Even a helicopter with suspended net could be used. Development work has been done by some community safety groups on an uninflated tubular slide for tall buildings where the person's descent is slowed by internal friction on the tubes walls. As a last resort, a flexible ladder could be deployed.

#### 4.4.3 Post-Landing Escape (SKJ 100269)

The normal post-landing egress from the orbiter, where the vehicle has come to a stop away from ground facilities, is through a short internal tunnel, leading down through the personnel compartment to a stowable metal ladder. The ladder descends through the wheel well area to the ground. In case the vehicle has made a ditch landing, inflatable slides or flexible ladders can be deployed from the side egress tunnel (for passengers) or the normal entry hatch (for passengers and crewmen). Although the side egress tunnels are now oriented horizontally, their 4-foot height still permits rapid egress. The height above ground (10 to 12 ft) for a ditched vehicle is now to the point at which jumping is feasible. In the R&D versions, the encapsulated seat can be used by the crew.

The booster crew compartment is not accessible to the front wheel well; therefore, an inflated slide or flexible ladder deployed from the entry hatch is the preferred means of egress. The encapsulated seat is also available; and, in case of ditching, personnel could jump.

In addition to the basic problem of escape, survival after a satisfactory escape must be considered. Survival kits must contain food and clothing for the extremes of climate likely to be encountered. In the case of water landing, life rafts must be available for all the personnel. If encapsulated seats are provided, they are generally used as a seat cushion; but in a passenger vehicle, where individual ejection methods are not used, the location of survival gear becomes an important design problem. If this type of vehicle makes an emergency landing in water, it will be necessary to carry the survival gear and life rafts out of the vehicle before flooding occurs, necessitating an accessible storage area. On the other hand, a conventional arrangement where the raft and survival gear are automatically ejected and inflated from a compartment on the outside of the vehicle is more desirable if the environmental and structural conditions permit such a location. In either case, the crewman's path to the exit should be free of protruding objects and structure that may obstruct, strike, or snag the clothing of the escaping crew members.

#### 4.4.4 Orbital Escape

The temporary objective of orbital escape is to seek sanctuary from the hazard and then return to a safe environment. Several pressurized spaces may be used as sanctuary - the Space Station, the orbiter passageway, passenger compartment if any, or air lock. The next phase is to deorbit and return to earth. If the orbiter is unusable, a standby shuttle could effect a rescue.

One system studied by LMSC in 1968 could provide emergency orbital return capability. This system contains a minimum of components and complexity and makes maximum

possible use of available technology and hardware. Relatively simple manually controlled systems are used to provide high reliability and low cost. The overall system is divided into the following parts:

- Titan IIIB launch vehicle system
- Agena rendezvous and docking system
- Emergency escape system

In order to keep the emergency escape system simple, use is made of the Titan IIIB and Agena for launch, rendezvous, and docking of the escape system as a passive payload. Once the escape system is docked, the Agena is separated and used for other purposes or moved out of the Space Station orbit trajectory. The escape system hatch would be opened and the system checked out and stashed by the crewman, at which time it would be ready for emergency escape.

When used for escape, the crewmen would enter the system, secure the hatch, activate the environmental control and reaction (attitude) control system, and separate from the disabled vehicle by ignition of a pyro or V-band separation joint in the docking adapter. Separation action and pressure with the docking adapter would pulse the vehicle away from the station and impart a slow tumble of a few degrees per second. The artificial horizon and yaw indicator is a simple self-contained instrument containing a rate mode for use in the event of a tumble condition. The pilot aligns the vehicle to the earth's horizon by means of a sight and reticle on the hatch window, cages and uncages the artificial horizon indicator, and sets the earth geocentric rate potentiometer. Reentry time is verified by radio contact with the ground. The crewmen may loiter on orbit for as long as 9 or 12 hours while preparations are made for their recovery from the water and their orbit precession carries them into a select landing area. The pilot alone controls the vehicle attitude. He puts the escape vehicle into the proper attitude for retro propulsion by reference to the earth horizon or artificial horizon indicator and fires the retro rockets. After retro, the vehicle is oriented for atmospheric re-entry so that the system will have a minimum angle of attack. But if the vehicle enters the atmosphere backwards, the aerodynamic stability will right the system. At 400,000 feet, the pilot separates the retro module and reaction control system. At approximately 80,000 and Mach 2, the drogue chute is deployed and is later separated and a reefed main chute deployed. After water impact, the main chute is separated

and the system floats upright on the heat shield because of hydrodynamic single-point stability. The vehicle will right itself if inverted by wave action. If necessary, the crewmen can open the hatch and exit the escape vehicle. The battery supply and fan allow the crewmen to remain in the escape vehicle for at least 24 hours with the hatch secured.

The Phase A and B study requirements, which dictated the system configuration, encompass the Apollo Applications escape system requirements, as follows:

<u>Study Requirements</u>	<u>Apollo Applications Requirements</u>
100 - 300 nm orbit altitude	210 nm orbit altitude
28- to 90-degree orbit inclination	35 degrees
12-hour on-orbit loiter time	9 hour maximum
Water landing only	Same
24-hour minimum post-landing electrical capability	Same
Ballistic (zero life) aerodynamic reentry	Same
Single-point aerodynamic stability	Same
Single-point flotation stability	Same
One-, two-, or three-man optional escape crew	Same
Suited or unsuited ingress	Same
Suit removal capability	Same
Single-gas environmental control system	Same
Near-zero physiological angle	Same
5-year orbit storage life	9 month on-orbit life

The resulting three-man system configuration weight is 2400 pounds stored on orbit, and the size is 100 inches in diameter and 100 inches long. The nine-man system weight is approximately 5200 pounds, and the size is 143 inches in diameter and 143 inches long. The ablative heat shield is of a modified 80-degree conical shape of 1.00 to 0.25 inch thickness of silicon elastomer, contained in Fiberglas honeycomb cells. Attitude is determined by visual reference. A hand control operates the mono-propellant hydrazine reaction control system. Four 780-pound thrust, solid-propellant propulsion motors are fired sequentially for the three-man system to provide a

600 ft/sec retro velocity for reentry. Drogue and main chutes provide final descent velocity control. The basic capsule structure is of aluminum ring and skin construction.

#### 4.4.5 Recommendations

- Establish crew and passenger constraints, i. e. , maximum g loading temperature extremes, etc.
- Determine requirements for escape, i. e. , routes, speed of egress, volumes, etc.
- Conduct tradeoff of encapsulated seat versus nose capsule.
- Determine feasibility of reentering a nose capsule.
- Determine impulse requirements for on pad ejection.
- Acquire definitive information on state-of-the art escape systems.

#### 4.5 LAUNCH VEHICLE ATTACHMENT SYSTEM (SKB 101069)

The attachment scheme for the orbiter and the booster is basically of a three-point attachment concept. The two aft attachment points are rigid, while the forward point, floating (forward/aft), absorbs all forward/aft dimensional changes from the time of original mating on the ground to separation in flight. Built-in alignment capabilities are included at all attachment points for all three axes of the orbiter and the booster. This attachment concept permits two methods of separation:

- By simultaneous actuation of the release mechanisms at all three attachment points on the orbiter, perpendicular separation between orbiter and booster can be accomplished.
- A controlled rotational mode of separation is possible by sequencing the forward and aft release mechanisms.

##### 4.5.1 Orbiter - Forward Attachment

The forward attachment point in the orbiter is a double-latch arrangement located approximately 40 feet aft of the nose, just aft of the nose landing gear. Designed as a complete module, it can be operated, adjusted, and checked out prior to installation. The latch can then be installed and aligned, as a unit, without any further adjustment.

The forward latch half and aft latch half are opened or closed with two links actuated by hydraulic cylinders. The link from the booster can be latched and released by actuating either one or both of the actuators, giving redundancy of operation. In operating the latch, there is only a locking and unlocking action, free from exerting any forces tending to pull together or separate the orbiter and the booster.

##### 4.5.2 Orbiter - Aft Attachments

Aft attachment forks are mounted on the aft frame, 27 feet from the centerline of the orbiter (54 feet total). The fork fittings are adjustable in all three axes for final alignment during mating; they are retractable into the fuselage after separation.

#### 4.5.3 Booster - Forward Attachment

The forward attachment point in the booster is approximately 70 feet aft of the nose, on centerline, on top of the fuselage (lining up with the orbiter forward attachment point). The attachment link, stowed horizontally, pivots up and forward to engage with the latch in the orbiter. The link is hydraulically actuated for erection and retraction with free floating capability, between stops, so that the link can absorb the longitudinal differential lengths that occur from the time of original mate to separation.

#### 4.5.4 Booster - Aft Attachment

The aft attachment arm to the orbiter is a large V-frame mounted in the top of the nacelles, erected and rigidly held in place by drag links. The links are hydraulically actuated to extend and retract the V-frame. There are two V-frames symmetrically located (27 feet from the centerline of the booster) to line up with the two fork fittings on the aft end of the orbiter. A clam-shell type latch, located at the top (or end) of the V-frame, is designed to clamp and rigidly hold the pin, which extends through the fork fitting on the orbiter. The clam-shell type latch is pivoted on the aft end and when folded closed (forward), it is locked with two bolts. To release the orbiter's fork fitting, explosive nuts release the spring-loaded half of the clam-shell, which then rotates 90 degrees to permit separation. On the aft (or top) surface of the V-frame is attached insulation surface. When the V-frames are retracted into the top of the nacelles, the insulation is flush with the outer surface, thus eliminating the necessity for doors.

Internal retracting doors are used at the forward attachment points on both the orbiter and the booster. After separation, the self-sealing doors are extended into the closed position.

The two captive explosive bolts on each of the two aft attachment points on the booster are the only expendable items within the separation mechanism; they must be replaced after every separation.

An alternate location for the aft attachment location of the orbiter is lower and farther forward. The geometry is similar but with different attachment hinge arm locations on the booster. The forward attachment point remains the same, and the method of release is unchanged.



#### 4.6 PAYLOAD BAY DOOR CONCEPT (SKM 101569)

Two general concepts of cargo bay door design have been considered. One is a single door design actuated about a single hinge line, located parallel to and in the region of either of the bay longerons. The other is a pair of clam-shell type doors, each hinged parallel to the bay structure longerons.

The following ground rules appear to be appropriate at this time:

- The structural interface with door or doors must mate with any cargo bay structural cover that a wide and varied range of possible payloads may require. This implies an interchangeability feature for the payload bay interface. Present design plan is to incorporate interchangeability at this interface by a series of latches.
- Continuity of structure must be maintained across the payload bay span. This is done by adequate door structure and by adequate latching tiedowns along all edges of interface and at the centerline of vehicle, where two doors are used. Door hinges would not be structural in transferring or carrying loads across bay, but this would be capable of carrying door deployment loads only.
- The internal surface of door or doors must provide a radiator surface for cooling internal equipment. The door would be properly orientated for various rates of heat radiation. This implies a variable positioning of the door in open position to satisfy variable requirements. (Positioning would be automatically controlled.)
- Payload doors and accompanying mechanisms must be compatible with deployment/retrieval mechanisms now contemplated.

Latching has not been completely studied, but plans are to actuate door latches with a single mechanically synchronized actuation system. Such a design makes interchangeable payload structures quickly installable.

The outside of the door assembly is a replaceable heat shield, consisting of René 41 supported by René 41 flexible standoffs, which are mounted on a corrugated Fiberglas panel. The Fiberglas panel is attached to aluminum alloy substructure, consisting of frames and transversals, covered on the interior with special aluminum alloy paneling. This paneling serves as a radiator surface when doors are deployed.

It is planned that each door (where two are used) be actuated with a single hydraulic actuator with a manually actuated override. The opening sequence opens the left-hand door first. For varied radiator requirements in orbit, an automatic positioning mechanism for each door should be provided.

In the closed position, the substructure would be insulated from the doors to prevent heat shorts to the substructure.

It is planned to use necessary reinforcing corner structure as mounting bracketry for latches and door hinges.

The nominal clearance of 8 inches for theoretical payload clearance and deployment/retrieval mechanisms may be reduced in the future.

#### 4.7 ORBITER NOSE CAP CONCEPT (SKR 060969 and SKR 060669)

Reusable coated refractory metal nose cap studies have been conducted for a number of concepts, summarized in Table 4-3. Two basic design approaches were considered - one without redundancy (1 and 2) and one having a reliable redundant passive nose cap (3, 4, 5, and 6).

Employment of zircon insulation allows for a bonded attachment to the titanium substrate or redundant silicone elastomeric ablator, as in concept 1, illustrated in SKR 060969, and in concept 3, illustrated in SKR 060669. While the insulation composite of zircon and LI-1500 concepts 2 and 4 are lightest in weight, they entail mechanical attachment problems. Efficient design of a composite insulation, zircon/LI-1500, allows only for bonding of LI-1500 to the substrate or the ablator. Because of the high temperature at the zircon/LI-1500 interface, bonding agents cannot be employed, since decomposition of the organic constituents would occur. Differential expansion between zircon and LI-1500 requires a mechanical attachment technique that allows for a large differential expansion. (The outer layer of zircon is at the highest temperature and also has a thermal coefficient of expansion that is one order of magnitude greater than LI-1500.) The complexity of mechanical attachments for the composite insulation system more than offsets the weight advantage that may be achieved by employment of LI-1500.

The fail-safe concept (3) calls for a prime reradiative nose cap and a secondary (redundant) nose cap, capable of surviving a single entry if subjected to the entire aerodynamic heating environment. The insulation (zircon) system between the primary coated refractory metal nose cap and the silicone elastomeric ablator limits the ablator to temperatures sufficiently below the decomposition temperature for reuse. The most probable failure that could result in the prime nose cap would be a local failure in the coating undetected by preflight inspection. Oxidation of the metallic substrate would take place locally, and a hole would develop in the primary cap. The purpose of the redundant cap is to provide safe return of the vehicle from orbit in the event of such an unlikely failure.

Table 4-3

REUSABLE NOSE CAP DESIGN CONCEPTS

Concept	Refractory Metal	System Description		Substrate	Advantages	Disadvantages
		High-Temperature Insulation	Passive Redundant Nose Cap Material			
1	Tantalum or Tungsten	Zircon	None	Titanium	Lighweight Simple design	
2	Tantalum or Tungsten	Zircon/LI-15	None	Titanium	Lightweight	Insulation composite attachment problem
3	Tantalum or Tungsten	Zircon	Lightweight Silicone Elastomeric Ablator	Titanium	Fail-safe feature	Slight weight penalty for redundancy feature
4	Tantalum or Tungsten	Zircon/LI-15	Lightweight Silicone Elastomeric Ablator	Titanium	Fail-safe feature	Slight weight penalty for redundancy feature Insulation composite attachment problem
5	Tantalum or Tungsten	None	Beryllium (Structural Member Included)	None	Heat sink reduces maximum equilibrium operational temperatures	Heavy
6	Tantalum or Tungsten	None	Carbon/Carbon	None	Fail-safe feature	Complex attachment problems Redundant system Carbon oxidation affects reuse Heavy

Concept 5 (the coated tantalum, heat sink hybrid) is complex and heavy. The only advantage is that the equilibrium temperatures of the tantalum nose cap can be reduced by allowing a substantial portion of the convective heat load to radiate inward to the beryllium heat sink. Securing the heat sink, which retains substantial heat energy and maintains moderately high temperatures ( $1000^{\circ}\text{F}$ ) for a long period after landing, will result in a complex design, which could be justified only if the tantalum system temperature is critical with regard to either coating life or nose cap vehicle survival.

Concept 6 calls for a carbon/carbon redundant nose cap. While the carbon or graphite reinforced systems appear to be sturdy candidates, complex attachment problems are created because of their brittleness. They undergo oxidization at the anticipated operational temperature levels with the evolution of carbon dioxide. In addition, these material systems represent a significant weight penalty over the silicone elastomeric ablator. Fabrication of large size (6 ft diameter) and thick (5 in.) nose caps requires manufacturing development, which at best would lead to a graded density composite in depth, thus requiring considerable qualification and development testing. This system appears to present no distinct advantage and many design and manufacturing hazards. A marginal thermal stress situation exists, particularly in the stagnation region attributed to the thickness and type of thermal gradient in the material. For these reasons, the carbon/carbon redundant system is less attractive than the others described.

Both tungsten and tantalum were considered as the outer nose cap material in all the above concepts. Tantalum has inherently superior high-temperature properties in that it does not present a problem like that of tungsten because of embrittlement as a result of recrystallization after exposure at high temperature. Tantalum has satisfactory mechanical properties at high temperature and may be recycled in an entry environment. This makes it the preferred refractory metal candidate for reuse. The thin shell reradiative caps (oblate spheroid, ratio of semiminor to semimajor axes = 0.4) undergo some yielding at high temperature near the attachment region; however, the structural integrity of the system is satisfactory.

Since all refractories are subject to severe oxidation at high temperatures, the properties of applicable coating materials is of primary importance.

The reentry environment encountered by the Space Shuttle upper stage can be expected to produce a maximum temperature of  $2900^{\circ}\text{F}$  for an emittance of 0.8. Studies indicate that coated tantalum is compatible with these values. The data in this reference and recent test data indicate that, in the case of tantalum coated with R512C (Si-2OT: -10Mo), the emittance is greater than 0.8 and the coating life exceeds 12 entry cycles for a peak temperature of  $2900^{\circ}\text{F}$  and a stagnation pressure range ( $30 \leq P \leq 200$ -mm Hg). The effect of reduced pressure (corresponding to free stream pressure conditions between 0.025 and 1.0 mm Hg) results in a coating life of five entry cycles. In order to achieve a coating life on the inner surface of the nose cap consistent with that for the external surface, it may be necessary to maintain an air pressure of 10 mm Hg or greater on the inner surface by either a partially sealed gas purged reservoir or a sealed reservoir.

For a sealed system, the pressure would rise approximately nine fold from 10-mm Hg to 90-mm Hg (0.2 to 1.8 psi) during the heating period and therefore would not present any design difficulties. For a controlled pressure environment on the internal surface of the reradiative nose cap, the coating life may be increased by a factor of 4 or more as compared to an uncontrolled pressure environment based on the preliminary coating life data.

Improvement in maximum temperature capability of tantalum may be achieved by use of an experimental coating R515 (Hf-20Ta). This coating may afford better protection at low pressures, because it can be applied in a thicker coating than the silicide coatings. The temperature capability may be extended to  $3500^{\circ}\text{F}$ .

Tantalum is currently considered to have manufacturing advantages over tungsten. Presently tungsten spun items are limited to sizes of 30 inches in diameter because of presently available sheet stock widths. Similar limitations for tantalum do not exist for nose caps up to 6 feet in diameter or larger, presently being considered for the Space Shuttle. Screening tests conducted for four coated tungsten candidate systems (R516, R516B, R512, and R512I) did not indicate any significant high-temperature

advantage of coated tungsten over the single coated tantalum (R512C) system, based on coating life; therefore, the coated tantalum system is presently considered to be superior.

In summary, the large Two-Stage Space Shuttle concept has a large radius nose cap, resulting in relatively low equilibrium temperatures. This allows for the use of coated tantalum as the primary refractory metal nose cap material. Because of the distinct manufacturing advantages of tantalum over tungsten for large nose caps and the satisfactory mechanical properties at high temperature, the tantalum reradiative nose cap is considered to be the prime candidate refractory metal.

#### 4.8 ORBITER TANK SUPPORT CONCEPT (SKT 100969)

For the tank support system, Fiberglas and titanium materials were selected as the potential materials for strut and skirts, because of their high strength-to-weight ratio, as well as their low thermal conductivities.

As shown in views A and E, a network of eight struts in the forward end of the tank is used. The struts are arranged in four pairs around the perimeter of the tanks, and each strut is designed to withstand tensile load.

The forward LH<sub>2</sub> tank struts, as shown in view A, have a diameter of 3 inches and a nominal wall thickness of .065 inch for the orbit storage tanks. As shown in view E-E, the strut diameters are 2.50 inch and nominal wall thickness is .065 inch. Each strut is insulated with superinsulation.

As shown in view B, a network of eight struts in the aft end of the tank are arranged in four pairs around the perimeter of the tank dome. The struts are arranged in such a way that the longitudinal and vertical contraction could be achieved. A typical strut design consists of a continuous polar-wound epoxy resin-impregnated S-glass filament tube and titanium end fittings. Rod end bearings with a shank diameter of 1 inch have been selected on the basis of high load capacity and particular suitability for cryogenic use. Spherical bearings, incorporated in the rod ends, permit excursion of the strut assemblies during tank contraction. The strut attachment to the tank is achieved by means of titanium brackets and aluminum brackets to the spacecraft structure, as shown in views A and E.

A typical tank insulation for ascent storage is shown in section C-C. The insulation consists of .20 inch thick polyurethane foam and the vapor-barrier is on the outside.

A typical tank insulation for orbit storage is shown in section D-D. The insulation consists of 4.0 inch thick superinsulation made up of blankets and a mylar vapor barrier on the top of the insulation. On the outside of the vapor barrier is a netting of dacron, which considerably improves handling characteristics of the multilayer insulation blankets.



#### 4.9 BOOSTER THRUST STRUCTURE CONCEPT (SKQ 092969)

This a typical engine support system; station locations do not coincide with the base-line vehicle.

The design concept of engine thrust structure is defined for an 11-engine installation.

##### 4.9.1 Rocket Engine Installation

The rocket engine installation equipment is a gimbal system, mounted on a tube and beam space structure.

The welded space structure has joint fittings attaching to either forgings or built-up beams.

All loads are carried via tubes to built-up beams and to eight longerons on the fuselage and complemented by three longerons at the lower wing surface.

Access panels should be provided in the sides and upper portion of the fuselage.

##### 4.9.2 Turbofan Engine Installation

The turbofan engine mounting equipment consists of two primary supports at station 2845 and 2921 with diagonal truss bracing in the upper and lower regions.

Primary supports are forgings at station 2845 and 2921 with integral support positions for transferring engine loads and interfacing to fuselage side walls.

The entire engine can be installed in the fuselage by means of four tension bolts buttock line 160 on each side of the fuselage.

A welded truss is used at station 2845, and a bolted truss is used at station 2521.

All loads are carried via truss systems, while jet engine thrust loads are transferred to two forward/aft longerons at the fuselage side panels.

Access covers should be provided for the engine support system and fillets provided in the upper and lower portions of pod to fuselage region.

The engine pod concept should include removable panels for servicing.

#### 4.9.3 Wing to Engine Space Structure

The wing should be capable of joint interfacing to rocket and turbofan engine installations.

Mating joints at the aft portion of wing should be provided with three vertical fittings at stations 2698, 2845, and 2921, attaching to spars and/or wing chord ribs.

#### 4.10 BOOSTER PROPULSION SYSTEM CONCEPT (SKQ 101569)

This concept is for a 14-engine system. The cryogenic primary propulsion system consists of an oxidizer tank ( $\text{LO}_2$ ) in the forward portion of booster and a fuel tank ( $\text{LH}_2$ ), located in aft portion of the booster along with the plumbing lines and associated valves and mechanical components.

The  $\text{LO}_2$  fill line feeds from the left-hand aft end of the vehicle to the trunk line and then to the tank. The  $\text{LH}_2$  fill line feeds from the right-hand aft end of the vehicle directly to the tank.

The  $\text{LO}_2$  feeds directly to 10 engines from the left-hand side of the vehicle and the four pressurant engines feed from a Y in the same trunk line. Pressure/volume joints, along with associated sliding joints and gimbals, are in the feed lines. Separate  $\text{LH}_2$  lines feed to the four pressurant engines and to the 10 other engines. Pressure/volume joints and gimbals are in the feed lines.

The  $\text{LO}_2$  replenish line feeds from the left-hand aft end of the vehicle to the 10 engines then through a Y to manifold/feed to the four pressurant engines. The  $\text{LH}_2$  replenish line feeds from the right-hand aft end of the vehicle to manifold/feed to the 10 engines, then through a Y to manifold/feed to four pressurant engines.

The  $\text{LO}_2$  pressure line feeds from the forward end of the oxidizer tank on the left-hand side of the vehicle to manifold/feed to four pressurant engines. The  $\text{LH}_2$  vent line feeds from the right-hand aft end of the vehicle directly to the forward end of the tank and divides at a Y distribution to become a pressure line to the four pressurant engines.

The  $\text{LO}_2$  vent line feeds directly from the forward end of the oxidizer tank overboard to the left-hand side of the vehicle. The line is a part of the  $\text{LO}_2$  pressurization system, but divides for plumbing simplification.

## Section 5 PERFORMANCE AND FLIGHT MECHANICS

The configurations reported on in this section are the Two-Stage and dissimilar Triamese, for both 50,000-pound and 25,000-pound payload capacity. Primary emphasis is on the Two-Stage, 50,000 configuration. Sequential (tandem) burning is assumed for both configurations.

The various phases of flight covered in this section and where they may be found are illustrated in Fig. 5-1.

### 5.1 SYSTEM SIZING AND PARAMETRIC ANALYSIS

A launch vehicle sizing and sensitivity analysis was performed to accomplish the following:

- Examine parametrically design variables that have a major impact on the system, and select the values of those variables that tend to maximize performance or minimize cost.
- Investigate system sensitivity to certain vehicle parameters, and identify parameters that are critical to vehicle performance so that proper emphasis can be placed on them in the study.
- Study the effect of mission requirements on launch vehicle size in order to establish the mission parameters that have the greatest impact on launch system size.
- Define the capability of point-design vehicles at missions other than the design mission.

The primary emphasis in the sensitivity studies has been on the Two-Stage system, particularly the 50,000-pound payload vehicle (launch weight equal to 3.74 million pounds).

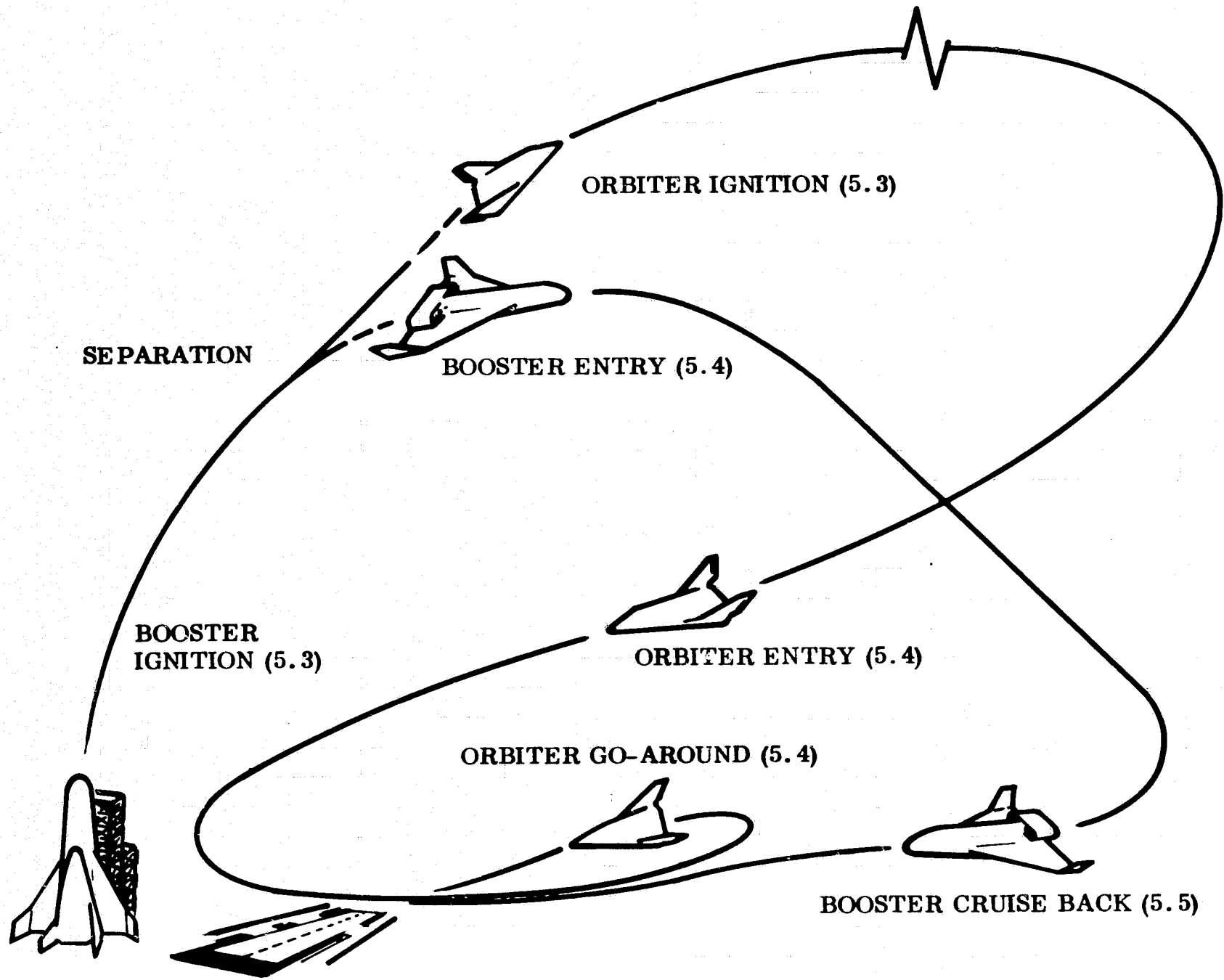


Fig. 5-1 Booster and Orbiter Trajectory Profile

Two methods were used to obtain sensitivities of the variable-size (rubberized) vehicle. The first method, a generalized technique used to optimize staging ratios of a two-stage system, was developed under the assumption of selected laws governing the behavior of inert weight with impulse propellant. This procedure is summarized in 5.1.1. The second procedure used to generate the remainder of the variable vehicle sensitivities involves use of the computer program MAGIC, described briefly in 5.1.2. Fixed vehicle sensitivities (for a point-design case, where the vehicle size has been fixed) are presented in 5.1.3.

### 5.1.1 General Performance Analyses

A generalized performance analysis of the Two-Stage system has been accomplished through use of basic performance parameters. This analysis, although based on relatively simple assumptions, models the Two-Stage system realistically and enables the effects of complex quantities to be evaluated in terms of simple parameters. The process is described below.

Given a linear weight scaling law for the booster and the orbiter of the form:

$$W_{I_i} = K_i + \left( \frac{1}{\eta_i} - 1 \right) W_{P_i} \quad \begin{array}{l} i = 1 \text{ booster} \\ i = 2 \text{ orbiter} \end{array}$$

The impulse propellant in the stage is denoted as  $W_{P_i}$ ; the inert weight of the stage is called  $W_{I_i}$ . The inert weight includes that of all dry weights, residuals and non-impulse expendables, and the crew, but not the discretionary payload for the orbiter or noseload for the booster. The propellant factor ( $\eta_i$ ) and inert constant ( $K_i$ ) are assumed to be constant for a given vehicle design. ( $K_2$  for the orbiter is a function of payload, however.) For a total ideal velocity and payload, the stages may be sized any number of ways. A certain combination of booster and orbiter propellants ( $W_{P1}$  and  $W_{P2}$ ) minimizes launch weight and still satisfies the mission requirements (payload and  $\Delta V$ ). The ideal staging velocity ( $\Delta V$  supplied by the booster) that results from these propellants is called the optimum ideal staging velocity. The less efficient a stage, either in propulsive efficiency (specific impulse) or in structural efficiency

(propellant factor  $\eta$  or inert constant  $k$ ), the less the velocity contributed by that stage should be to minimize launch weight. Figure 5-2 displays launch weight and optimum ideal staging velocity for a variety of orbiter and booster propellant factors, for both the 25,000-pound and the 50,000-pound payloads.

The relationship between  $\eta_i$  and  $\lambda'_i$ , the propellant fraction, is given below.

$$\eta_i = \frac{W_{P_i}}{W_{P_i} + W_{I_i} - k_i} \quad \text{propellant factor}$$

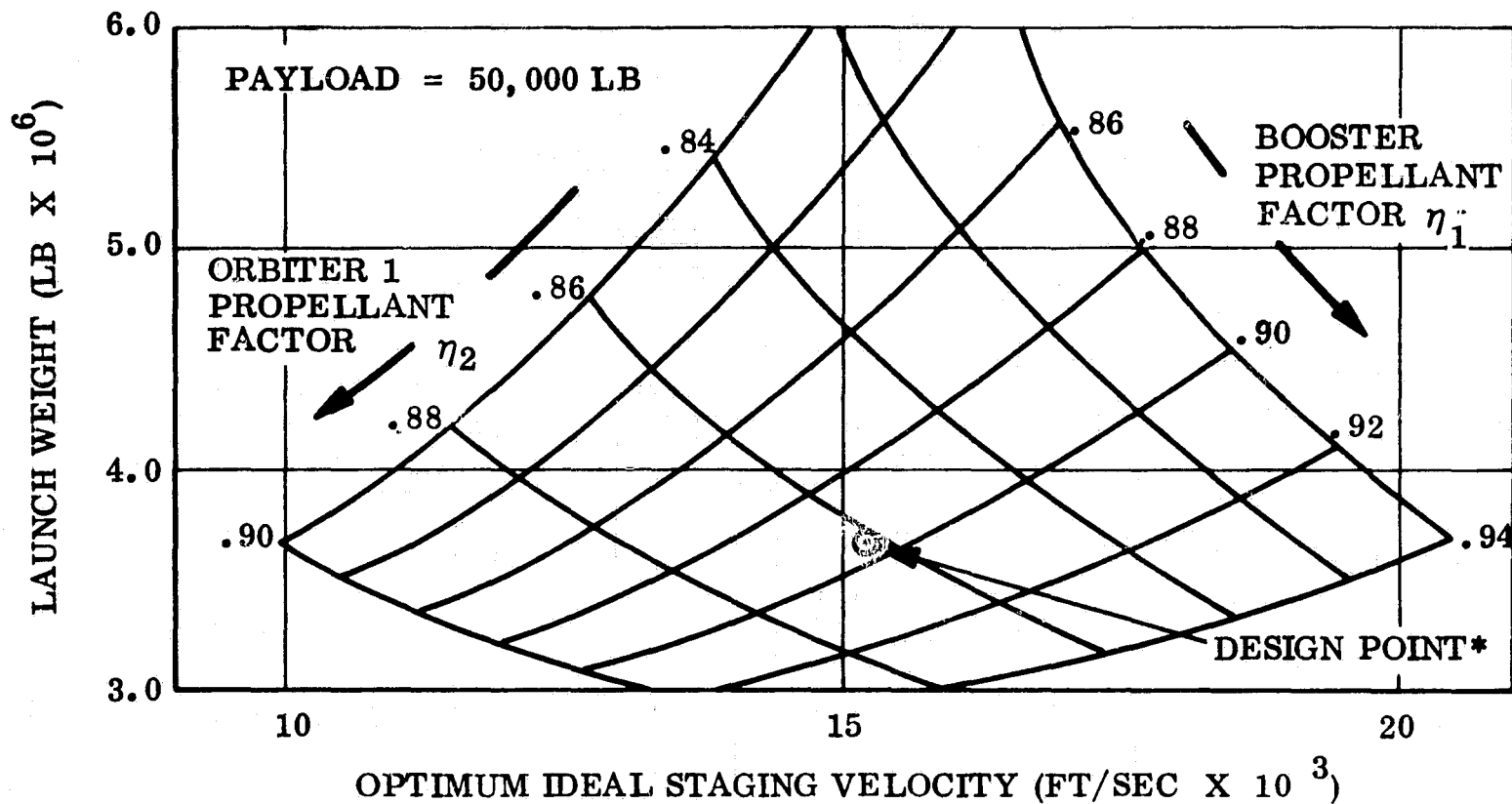
$$\lambda'_i = \frac{W_{P_i}}{W_{P_i} + W_{I_i}} = \frac{1}{\frac{1}{\eta_i} + \frac{k_i}{W_{P_i}}} \quad \text{propellant fraction}$$

For a given design (fixed shape but variable size),  $\eta_i$  and  $k_i$  are approximately constant; but  $\lambda'_i$  is a function of propellant. Assuming  $\eta_i$  and  $k_i$  to be fixed during vehicle growth is a less realistic assumption than assuming  $\lambda'_i$  to be fixed on the basis of studies performed with MAGIC. The  $\lambda'_i = \text{constant}$  is a special case of this more general model, where  $k_1 = k_2 = 0$  and  $\lambda'_i = \eta_i$ .  $\eta_i$  is always greater than  $\lambda'_i$ .

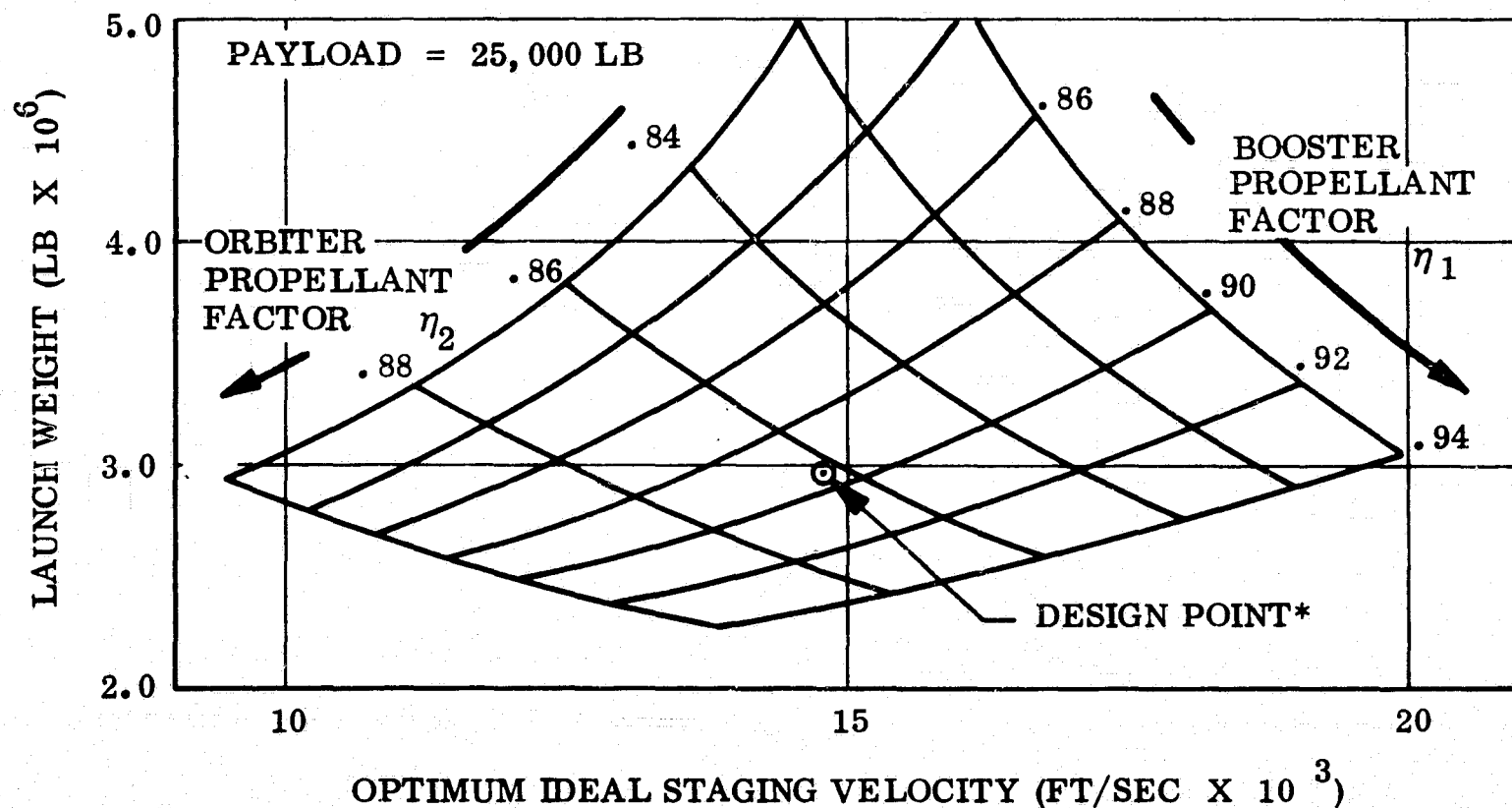
For the Two-Stage system, the following values were used:

Total ideal velocity = 32,422 ft/sec

Booster:		Orbiter:	
$k_1$	= 139,000 lb (50K)	$k_2$	= 107,000 lb (50K)
	= 139,000 lb (25K)		= 99,000 lb (25K)
$\eta_1$	= .895	$\eta_2$	= .862
$\lambda'_1$	= .850 (50K)	$\lambda'_2$	= .763 (50K)
	= .841 (25K)		= .745 (25K)
$I_{sp1}$	= 428.5 sec	$I_{sp2}$	= 454.2 sec



\*OPTIMUM POINT LAUNCH WEIGHT SLIGHTLY LOWER THAN BASELINE BECAUSE BASELINE STAGING VELOCITY IS NOT OPTIMUM



TWO-STAGE

Fig. 5-2 Effect of Propellant Factor on Launch Weight and Staging Velocity



The results of this analysis demonstrate the high sensitivity of launch weight and optimum staging velocity to propellant factor. On the other hand, the optimum staging velocity is not very sensitive to either payload or its equivalent, the orbiter inert constant ( $k_2$ ).

### 5.1.2 Variable-Vehicle Parametric and Sensitivity Analysis

The Two-Stage system was studied with the benefit of the computer program MAGIC, which sizes a launch vehicle (either Two-Stage or Triamese) on the basis of mission requirements and information available from studies in other technology areas (vehicle design, weights, structure, ascent performance, reentry and thermodynamics, aerodynamics, propulsion, etc.). A vehicle is first geometrically defined in the program (both orbiter and booster) and then weighed. Its performance capability is compared to that required. The size of one or both of the stages is then adjusted; and, through an iterative procedure, a launch system is developed to satisfy mission requirements down to subsystem level. MAGIC is a useful tool for launch vehicle definition, and it is continually being expanded and updated to reflect the latest studies being performed by the various disciplines involved in the system study.

The effect on system size of the following parameters was examined for this study:

- Thrust-to-weight ratio at launch
- Thrust-to-weight ratio of orbiter at separation
- Staging velocity
- Oxidizer/fuel ratio in booster and orbiter
- Payload weight and volume
- On-orbit  $\Delta V$
- Inert weight of booster and orbiter
- Propellant packaging factor in orbiter
- Specific impulse of booster and orbiter
- Orbiter cross range
- Go-around at landing
- Orbiter ignition at launch

For this study, both the orbiter and booster sizes change as the parameters are varied. Sensitivities are given in Table 5-1. Plots of various sensitivities are given in Figs. 5-3 through 5-8.

Table 5-1  
VARIABLE-SIZE VEHICLE SENSITIVITIES  
TWO-STAGE

Launch Weight Partial	50K Payload Vehicle	25K Payload Vehicle
Launch weight/inert weight of booster (lb/lb)*	4.73	4.86
Launch weight/inert weight of orbiter (lb/lb)*	27.0	29.0
Launch weight/specific impulse of booster (lb/sec)	-19,100	-10,800
Launch weight/specific impulse of orbiter (lb/sec)	-21,300	-14,600
Launch weight/payload weight (lb/lb)	28.0	30.1
Launch weight/payload volume (lb/ft <sup>3</sup> )	74.4	86.4
Launch weight/ideal velocity (lb/ft/sec)	550.	408.
Launch weight/orbiter cross range (lb/nm)	260.	248.
Launch weight/contingency (lb/%)	71,400	65,000
Launch weight due to elimination of go-around requirement (lb)	-501,000	-410,000
Launch weight due to 10% mass flow rate in orbiter during first stage (lb)	180,000	160,000

\*Does not include 10% contingency effect

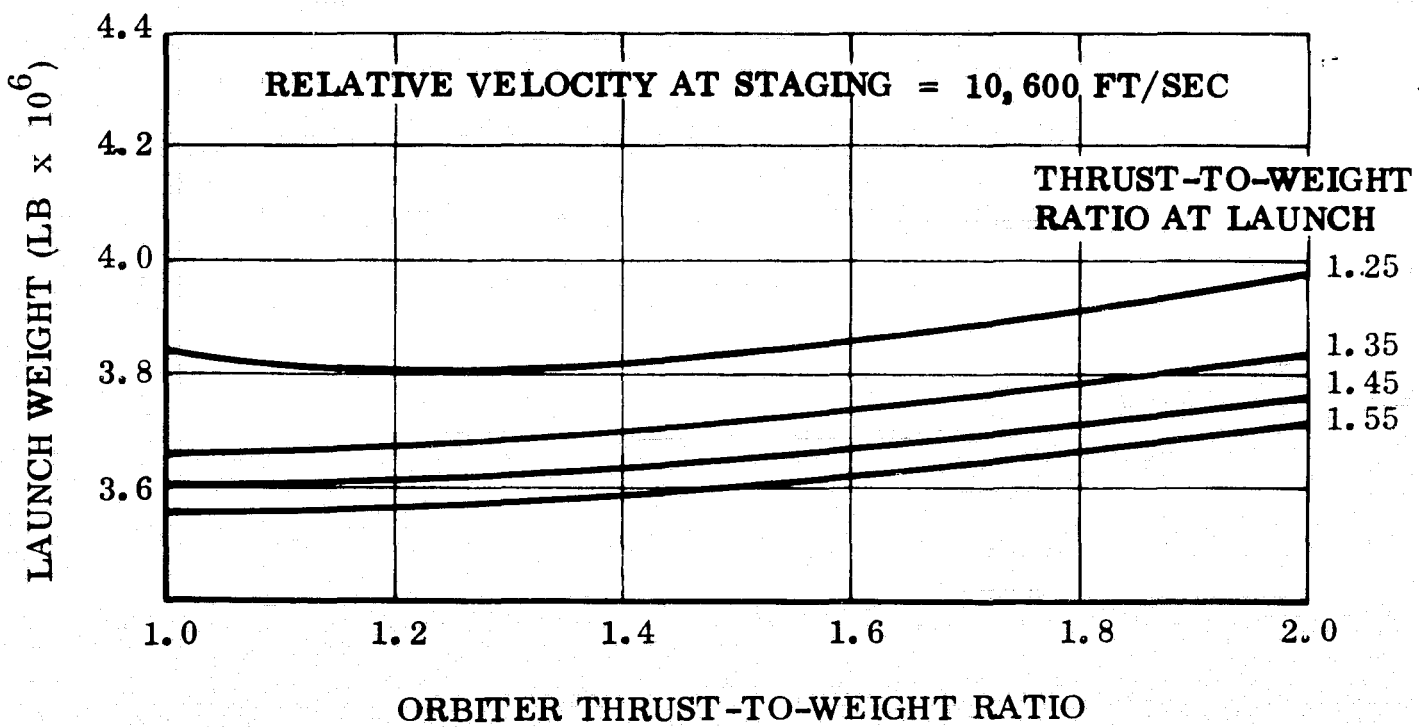
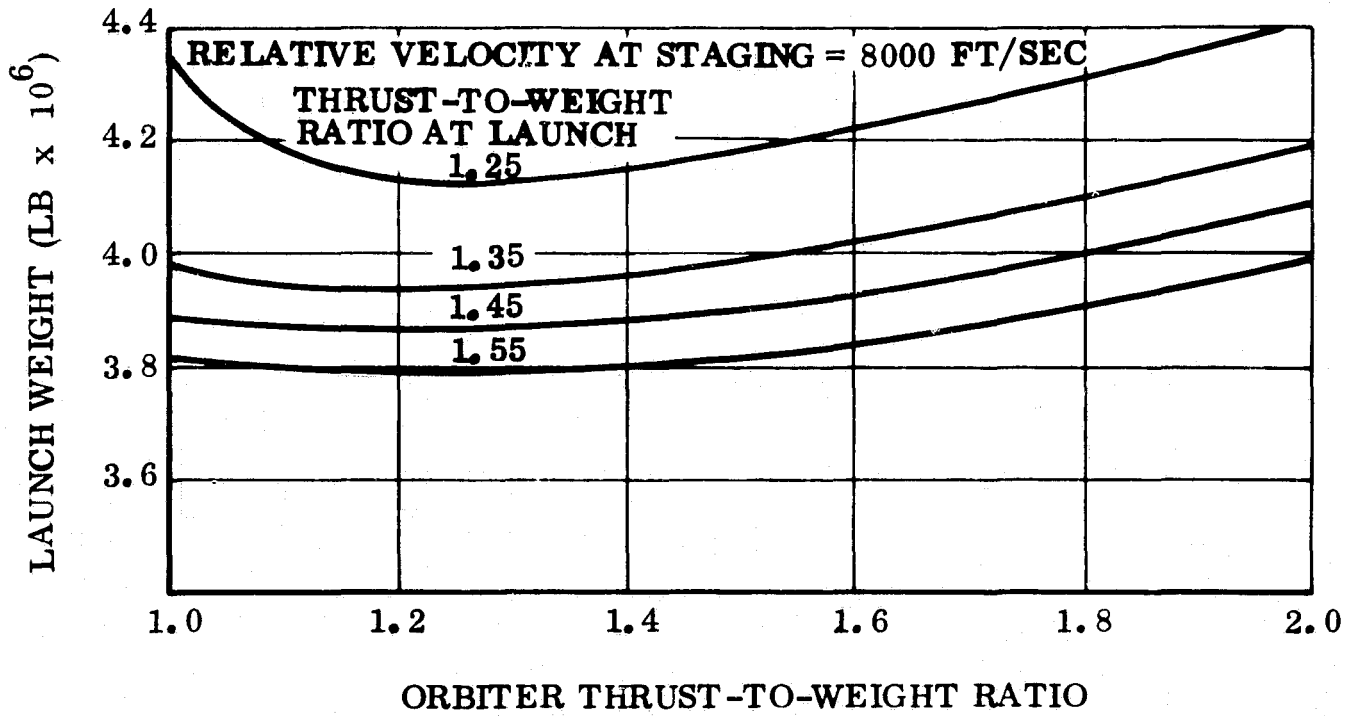


Fig. 5-3 Effect of Thrust-to-Weight Ratio

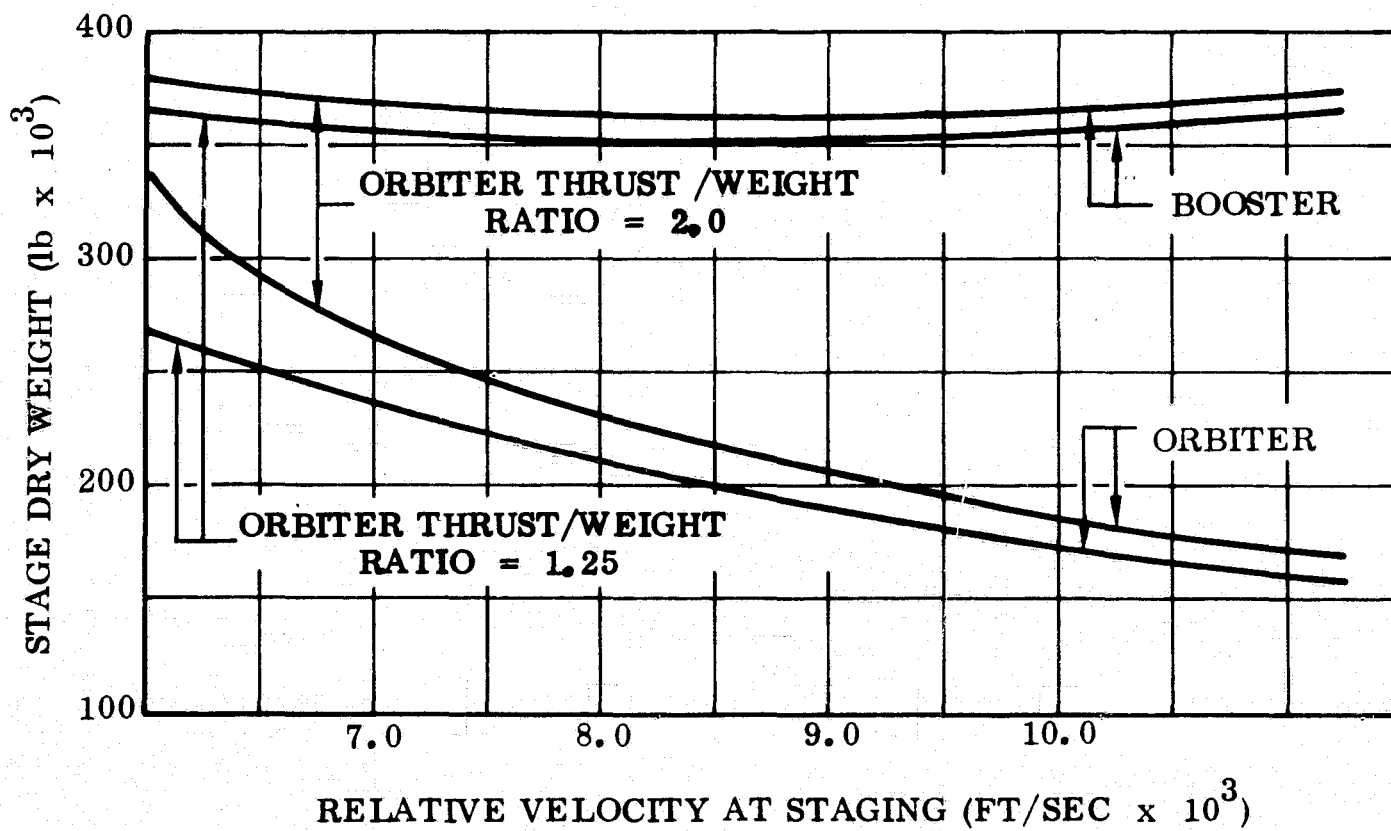
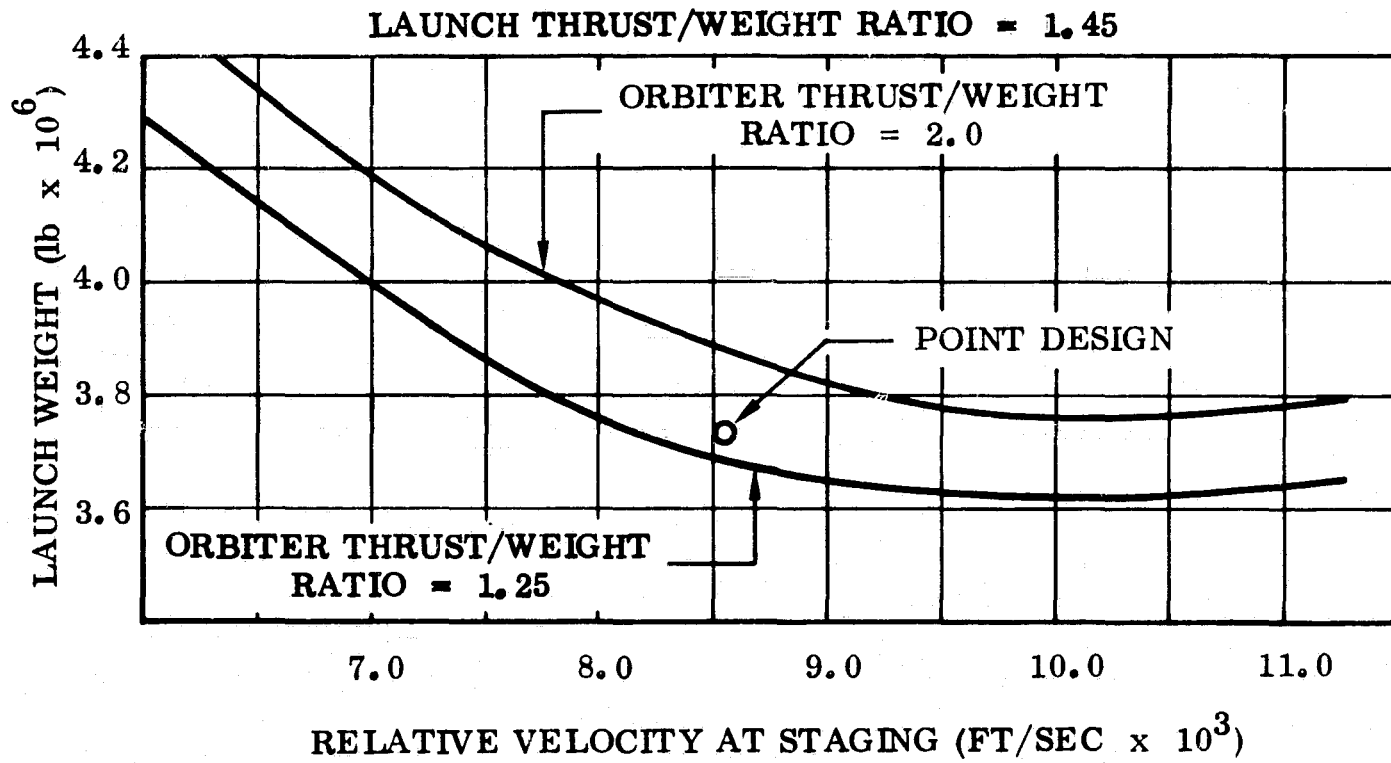
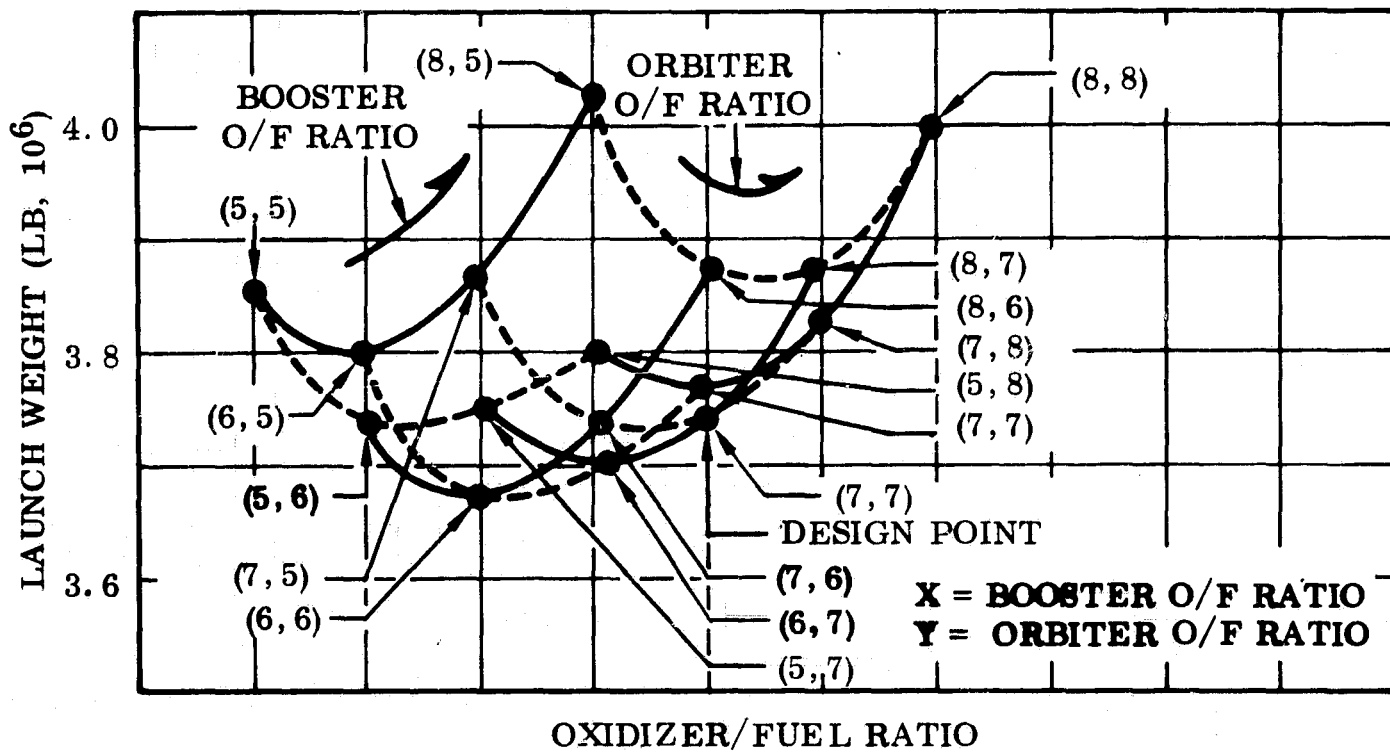


Fig. 5-4 Effect of Staging Velocity



————— CONSTANT O/F RATIO IN ORBITER  
 VARIABLE O/F RATIO IN BOOSTER  
 - - - - - CONSTANT O/F RATIO IN BOOSTER  
 VARIABLE O/F RATIO IN ORBITER

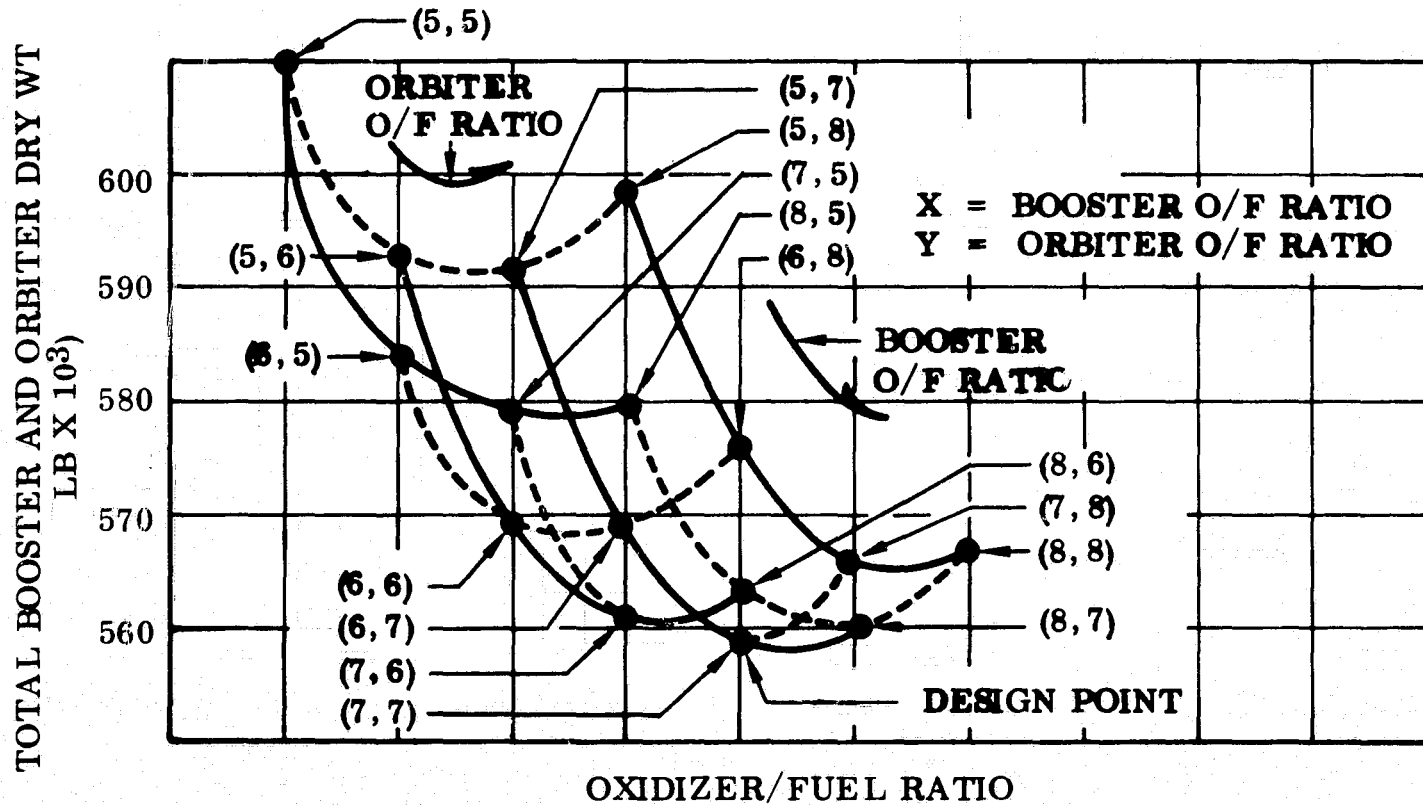


Fig. 5-5 Effect of Oxidizer-Fuel Ratio

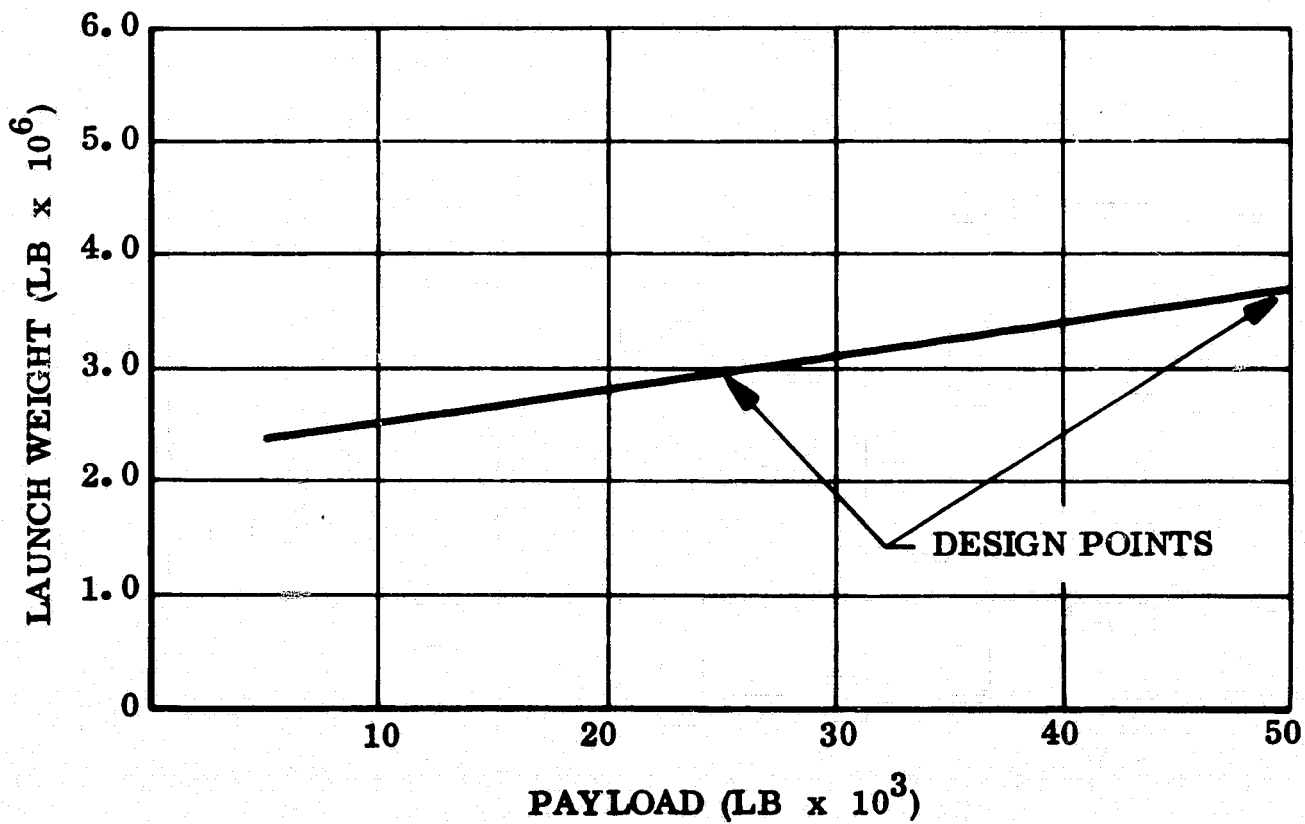
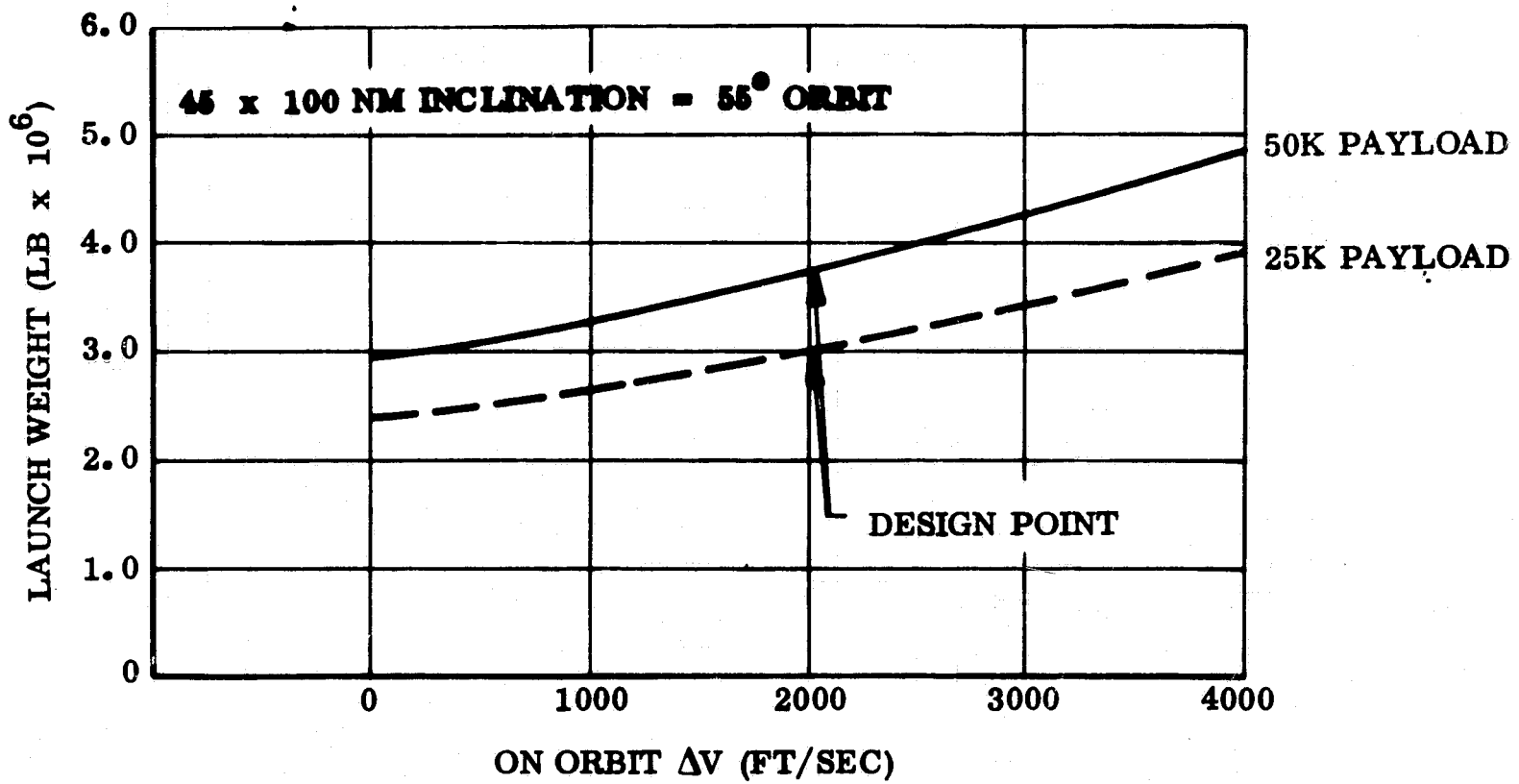


Fig. 5-6 Effect of Velocity and Payload

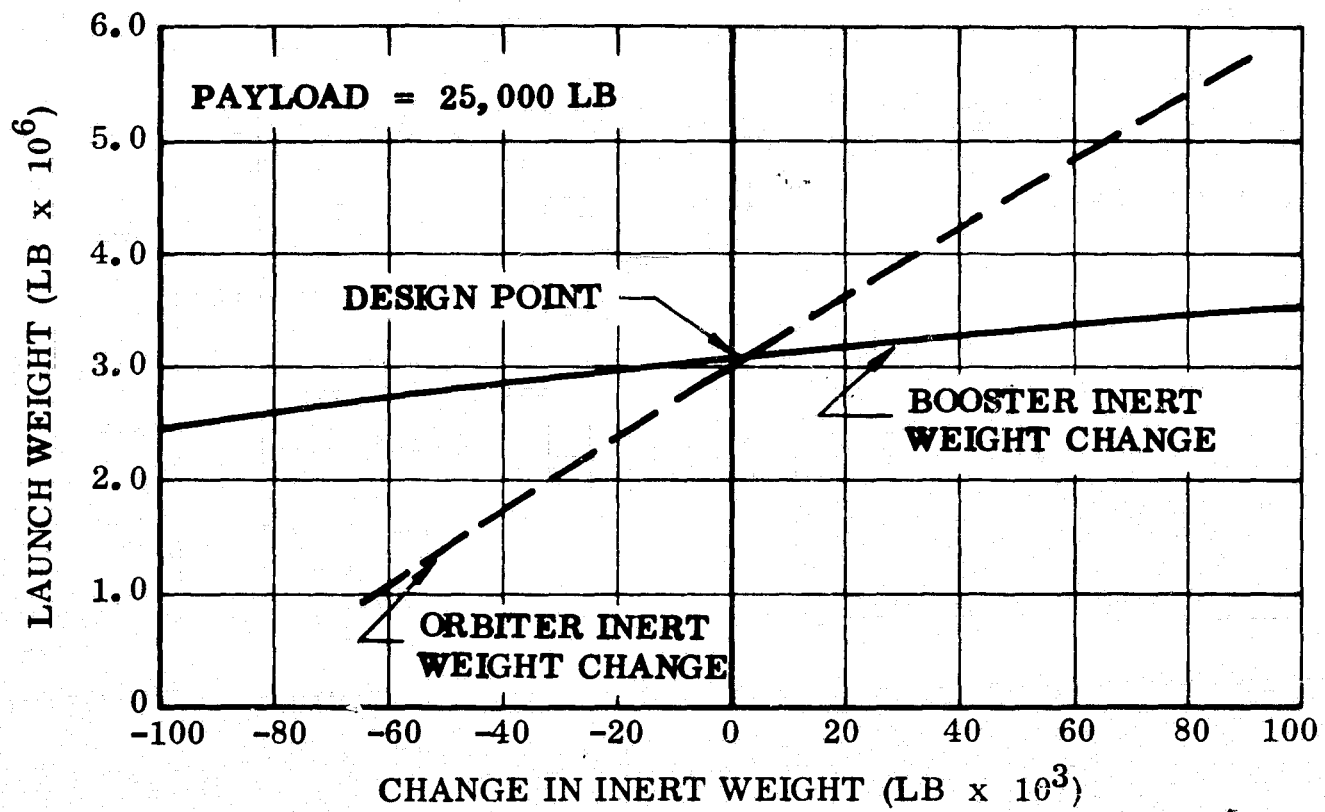
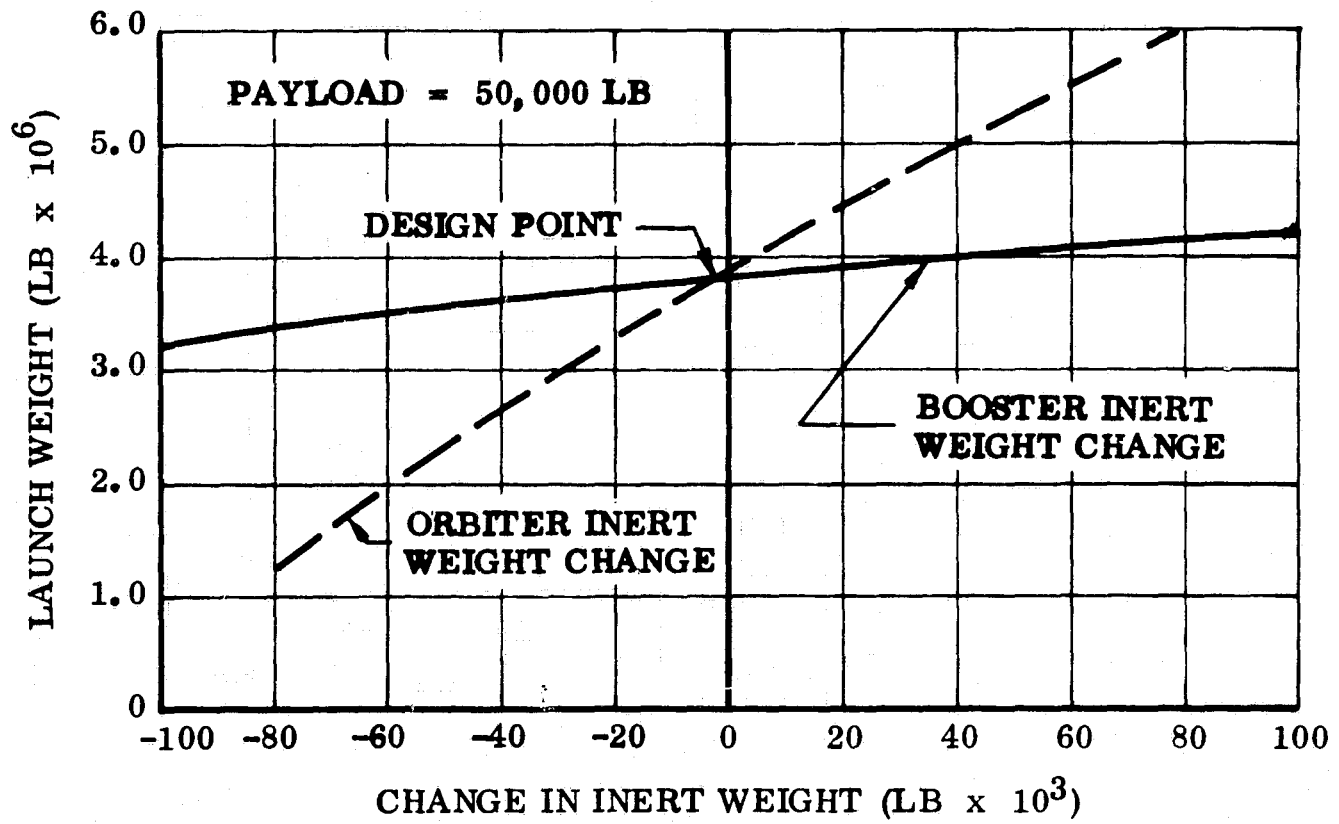
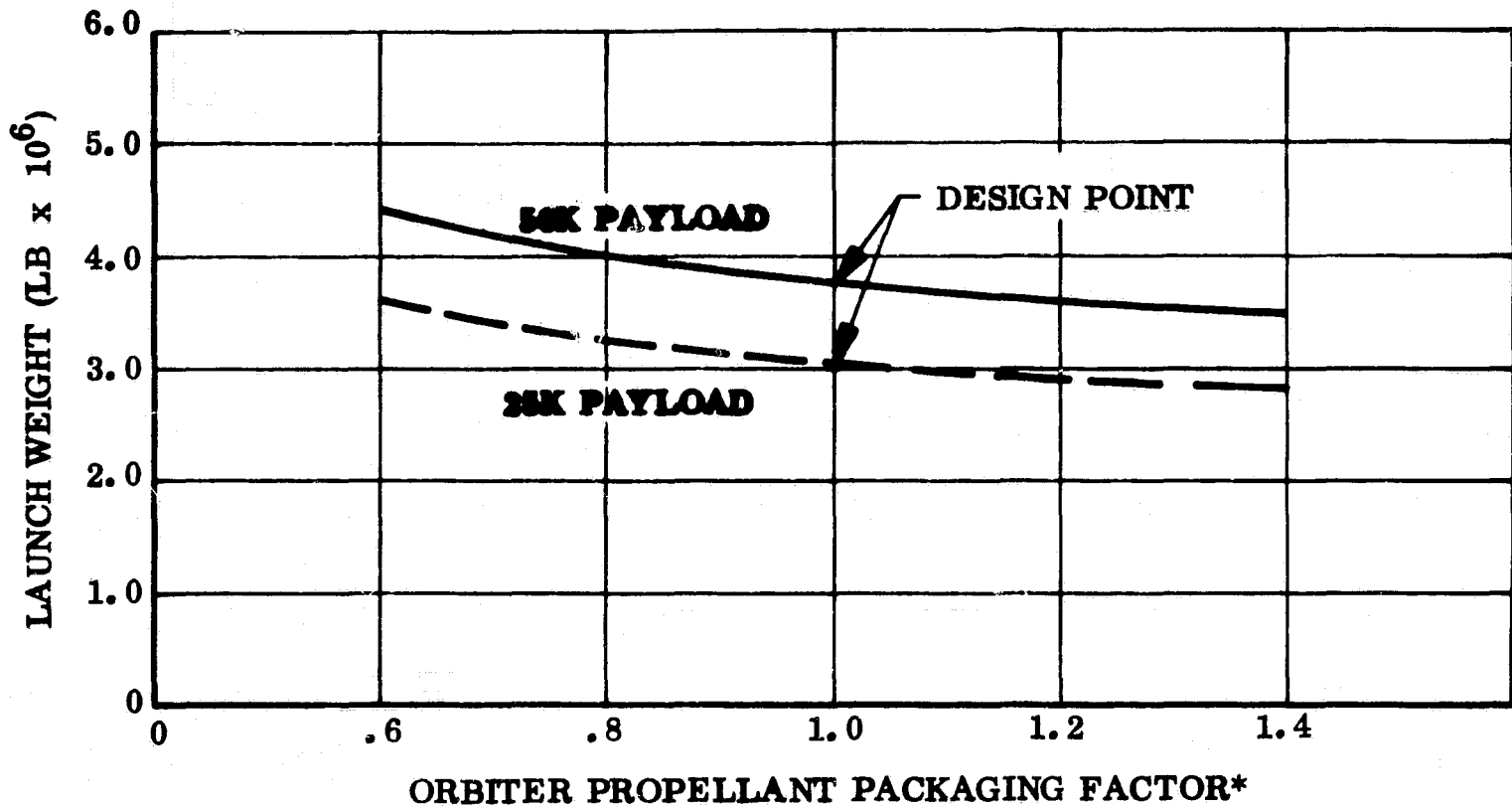


Fig. 5-7 Effect of Inert Weight



**\* DEFINED AS THE RATIO OF PROPELLANT IN ORBITER USING DIFFERENT TANKAGE DESIGN/PROPELLANT IN ORBITER USING PRESENT DESIGN**

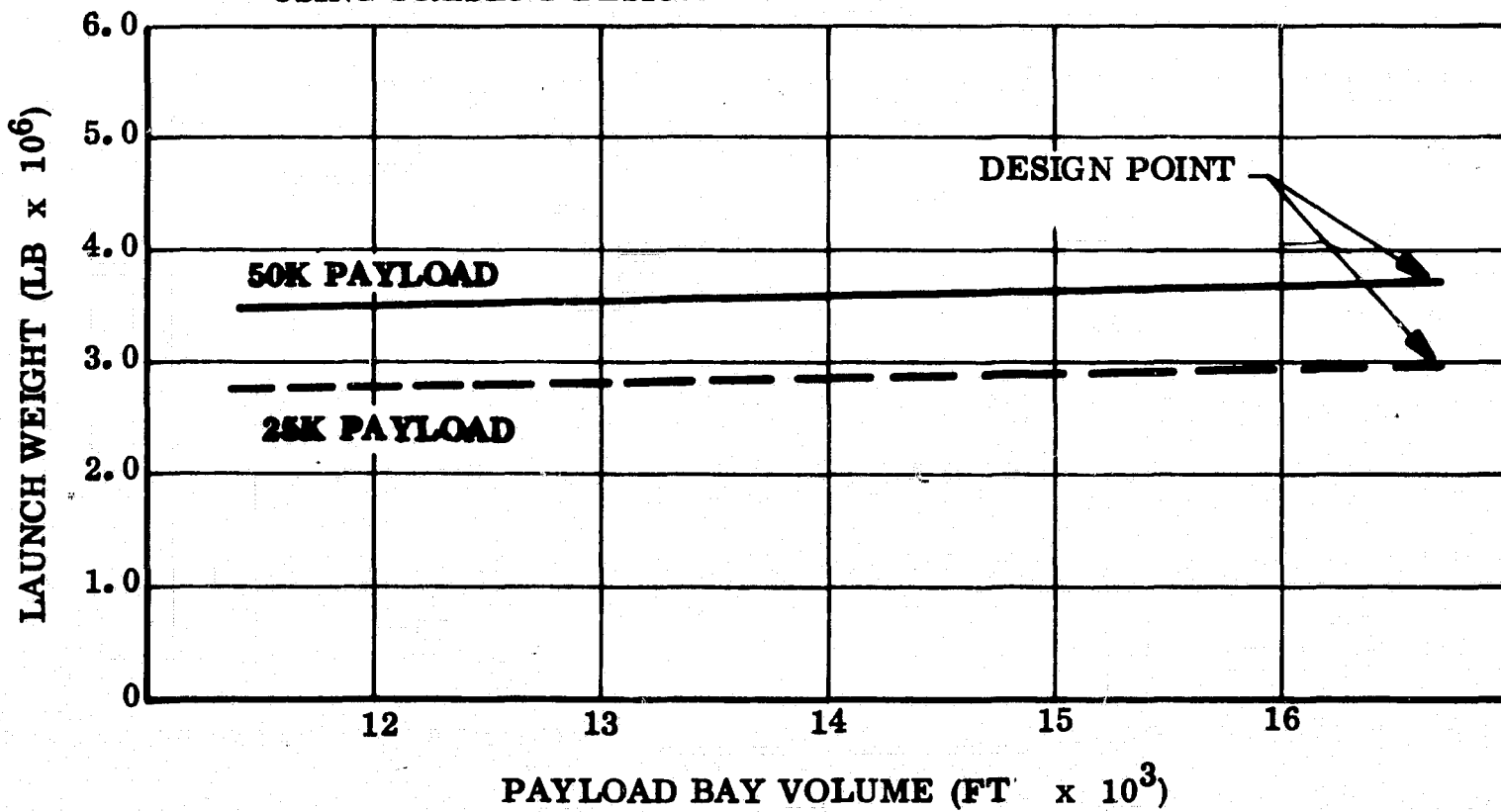


Fig. 5-8 Effect of Propellant Packaging and Payload Volume



5.1.2.1 Thrust-to-Weight Ratio. As the thrust-to-weight ratio (either at launch or at stage separation) increases, total ideal velocity required decreases as a result of reduced gravity and drag losses. Engine weight, as well as other weights dependent on engine weight, increases because more thrust is required. A tradeoff between  $\Delta V$  and inert weight is therefore called for. For the booster, a large reduction in required  $\Delta V$  can be obtained by designing for a high thrust-to-weight ratio, with only a relatively small penalty in launch weight due to the extra inert weight (because of the low sensitivity of launch weight to booster inert weight). The optimum launch thrust-to-weight ratio is in excess of 1.45; but, because of engine packaging considerations and dynamic pressure constraints, the baseline vehicle has been limited to a thrust-to-weight ratio of 1.45.

The impact of the thrust-to-weight ratio of the orbiter on launch weight involves criteria similar to those for the booster. For the orbiter, however, velocity gains due to high thrust-to-weight ratio are much smaller because of the small flight-path angle at stage ignition. In addition, the penalty for carrying additional inert weight is much greater. Therefore, the launch weight minimizes at a low, second-stage thrust-to-weight ratio, in the neighborhood of 1.1 to 1.3, depending on the velocity at staging. The recommendation, then, is for a relatively high thrust-to-weight ratio on the booster and a low thrust-to-weight ratio on the orbiter. Figure 5-3 presents these data for two different staging velocities and reflects the combined effect of thrust-to-weight ratio on ascent performance and vehicle weight.

5.1.2.2 Staging Velocity. The effect of staging velocity on launch vehicle size involves several tradeoffs. As staging velocity is increased, the booster gets larger, the orbiter smaller, and velocity losses get smaller (so the required  $\Delta V$  becomes less). The optimum staging velocity is sensitive to the particular vehicle designed and relative propellant packaging efficiency of the booster and the orbiter. For the type of configuration represented by the baseline vehicles, the optimum staging velocity is approximately 10,600 ft/sec (relative or aerodynamic velocity) or 15,400 ft/sec ideal velocity. The staging velocity chosen for the baseline vehicles is about 9000 ft/sec, somewhat less. This value, chosen primarily to provide a more desirable structural arrangement in the orbiter for accommodation of the large payload bay, involves little penalty from the optimum case, as shown in Fig. 5-4.

5.1.2.3 Oxidizer-Fuel Ratio. The effect of oxidizer fuel ratio on the launch weight and dry weights is shown in Fig. 5-5. The basic tradeoff involved is that for higher mixture ratios, the propulsive efficiency ( $I_{sp}$ ) is less but the structural efficiency ( $\eta$ ) is greater. Launch weight minimizes at about a 6:1 ratio in both the orbiter and the booster, but the total dry weight of the system (booster plus orbiter) minimizes at about 7:1 ratio (in both stages).

5.1.2.4 On-Orbit  $\Delta V$ . The effect on launch weight of changing the on-orbit  $\Delta V$  requirement is shown in Fig. 5-6. Launch weight is quite sensitive to this parameter. Reduction of the on-orbit  $\Delta V$  by 500 ft/sec decreases launch weight by 250,000 pound. It can also be seen that for the payload weights of interest, the magnitude of payload weight is a biasing effect and does not significantly affect the launch system sensitivity to velocity.

5.1.2.5 Payload Weight. The impact of payload weight is also shown in Fig. 5-6. In this case, as in all variable launch system studies, the data were developed under the assumption that ascent and return payload weights are equal.

5.1.2.6 Inert Weight. The sensitivity of launch weight to inert weight of both the booster and the orbiter is given in Fig. 5-7. For each extra pound of inert weight in the orbiter, the launch weight is increased approximately 30 pounds. As weight is added to the booster, a smaller sensitivity is evident, indicating a launch weight to inert weight ratio in the order of 5.

5.1.2.7 Propellant Storage Factor of the Orbiter. The propellant storage factor is a measure of the volumetric efficiency for packaging propellant. It is defined as the ratio of the propellant weight that might be stored to the propellant that is actually stored in the tanks called for in the baseline configuration; nominally it is 1. For values less than 1, the implication is that simpler tanks are used so that less propellant would be stored in the same volume. For values greater than 1, more complex tanks (such as lobed or pillow tanks) are required. As shown in Fig. 5-8, a value of .8, for example, implies that only 80 percent of the volume used in the present design would be used in the new design to obtain the new launch weight.

5.1.2.8 Payload Volume. The impact of payload volume is also shown in Fig. 5-8, since its influence on launch size is somewhat equivalent to propellant storage efficiency. As payload volume is reduced, propellant tanks are installed, enhancing the performance capability of the launch system. As shown in the figure, however, payload volume is not a significant parameter in terms of launch system size for the configuration under investigation.

### 5.1.3 Fixed Vehicle Sensitivities

To aid in the analysis of the launch system, fixed vehicle sensitivities have been generated. This has been done to aid analysis of multimission capability and to aid assessment of payload degradation due to off-nominal values of certain performance parameters. The sensitivities are listed in Table 5-2. Payload versus ideal velocity and orbit inclination are shown in Fig. 5-9. These sensitivities include the effect of velocity losses.

Table 5-2

#### FIXED VEHICLE SENSITIVITIES - TWO-STAGE

Payload Sensitivity Partial	50K Payload Vehicle	25K Payload Vehicle
Payload/inert weight of booster (lb/lb)	-.151	-.149
Payload/inert weight of orbiter (lb/lb)	-1.0	-1.0
Payload/propellant in booster (lb/lb)	.065	.062
Payload/propellant in orbiter (lb/lb)	.176	.183
Payload/specific impulse of booster (lb/sec)	720	569
Payload/specific impulse of orbiter (lb/sec)	908	712
Payload/launch thrust (lb/lb)	.0117	.0114
Payload/on-orbit (lb/ft/sec)	21.9	17.2

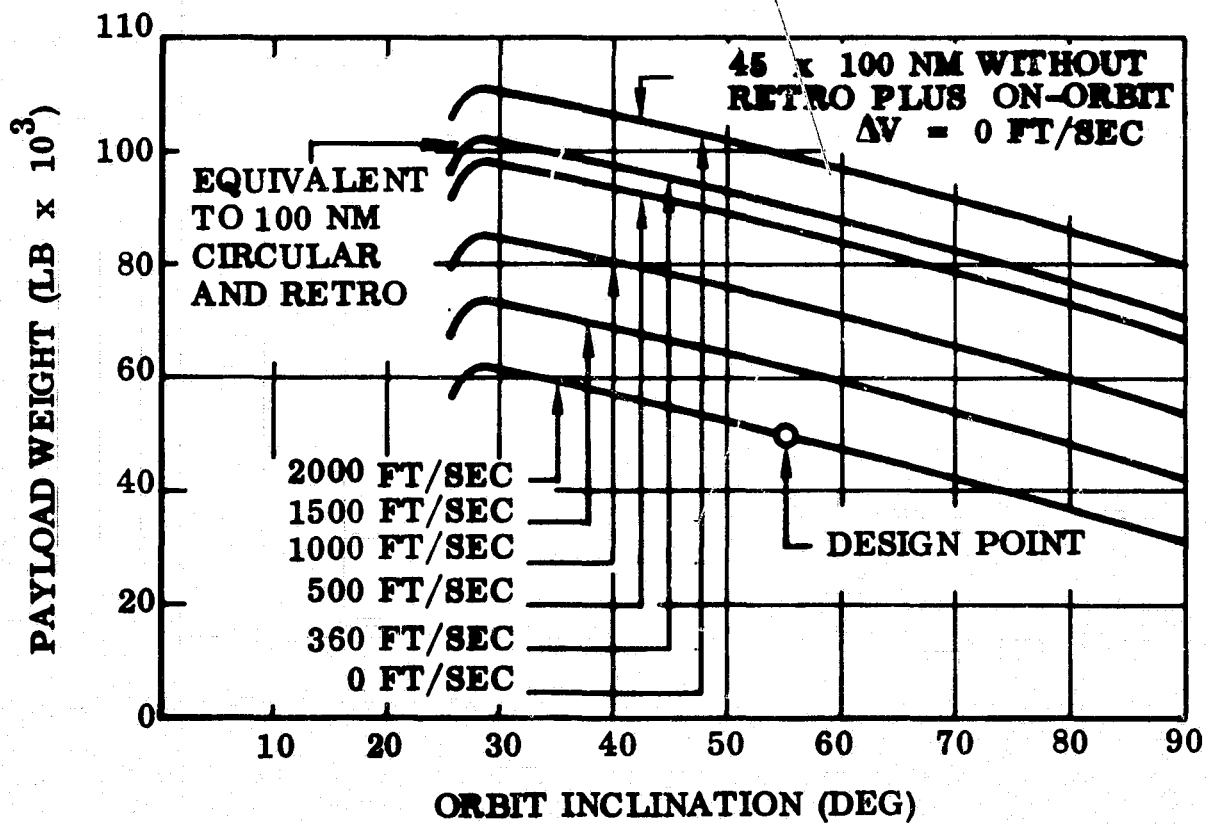
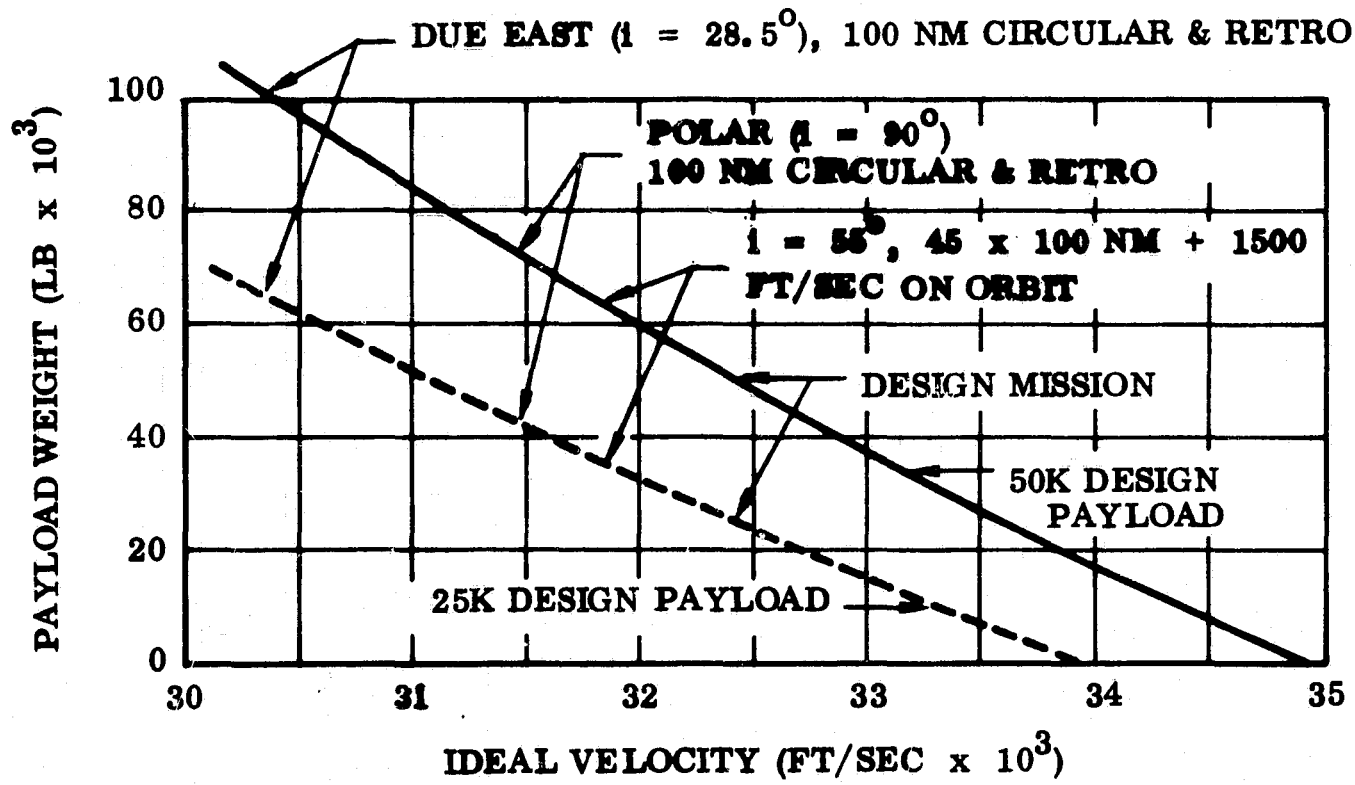


Fig. 5-9 Fixed Vehicle Payload-Velocity Characteristics

## 5.2 ASCENT TRAJECTORY ANALYSIS

An ascent trajectory analysis has been conducted for the following purposes:

- Examine system behavior for a wide range of vehicle parameters to assist in choosing design characteristics that maximize vehicle performance.
- Analyze the performance for alternate mission requirements, and investigate other ascent modes for the design mission.
- Provide a reference trajectory for use by other technology groups to aid in a vehicle design.

### 5.2.1 Trajectory Trades

A comprehensive study of ascent trajectories of Two-Stage configurations was performed for the purpose of assessing the mission velocity sensitivity to staging velocity, injection altitude, launch thrust/weight, second stage ignition thrust/weight, and final orbit inclination. Acceleration limits of 3 and 4 g were imposed, requiring continuous throttling capability in both stages. The orbit injection velocity tradeoff for four representative configurations designed to have different staging velocities is summarized in Fig. 5-10, from which the following conclusions can be drawn:

- The 30,400 fps is representative of the ideal injection velocity requirement for the current class of vehicles at 4 g. Although minimum velocity requirements occur with the higher acceleration levels (i.e., shorter total burn times), the impact of the correspondingly larger engine sizes must be included in an evaluation of minimum launch weight.
- The 3-g acceleration limit requires 20-60 fps additional velocity capability.
- The 1.25 launch thrust-to-weight ratio  $(T/W)_2$  and 28-degree inclination data repeat the velocity trends with  $(T/W)_2$ , implying that the sensitivity to staging velocity is predictable for alternate missions.
- Direct injection at 100 nm shows a different trend, favoring lower  $(T/W)_2$ 's. Optimum flight time conditions correspond to  $(T/W)_2 = 1.25$ , with a net additional velocity requirement of 300 fps (400 fps-100 fps circularization not required), increasing to 650 fps at  $(T/W)_2 = 2.0$ . The 3-g constraint requires an additional 70 fps.

Additional supporting studies (not documented in Fig. 5-10) have shown that:

- Velocity variations due to mixture ratio shifts (specific impulse effects) are equivalent to staging velocity shifts, since inert weight effects are negligible (less than 10 fps)
- Higher losses incurred by the Triamese require an additional 420 to 470 fps more than the Two-Stage for identical staging velocities
- Assuming a perigee injection at 45 nm is only marginally satisfactory because of post-injection drag forces potentially large enough to cause impact. Redefining perigee injection at 50 nm alleviates the problem for a minor velocity penalty (about 35 fps).

The effect of launch thrust/weight on the ascent velocity requirement, used for system sizing studies, is summarized in Fig. 5-11 for the 15,500-fps staging velocity configuration with a 4-g constraint. The effect of increasing launch (T/W) is one of reducing ascent velocity losses, achieved mainly through reduction in the gravity loss component. The ideal velocity requirements for various inclinations are also summarized in Fig. 5-11. The launch azimuth was not restricted and was varied as required to maximize the booster system performance.

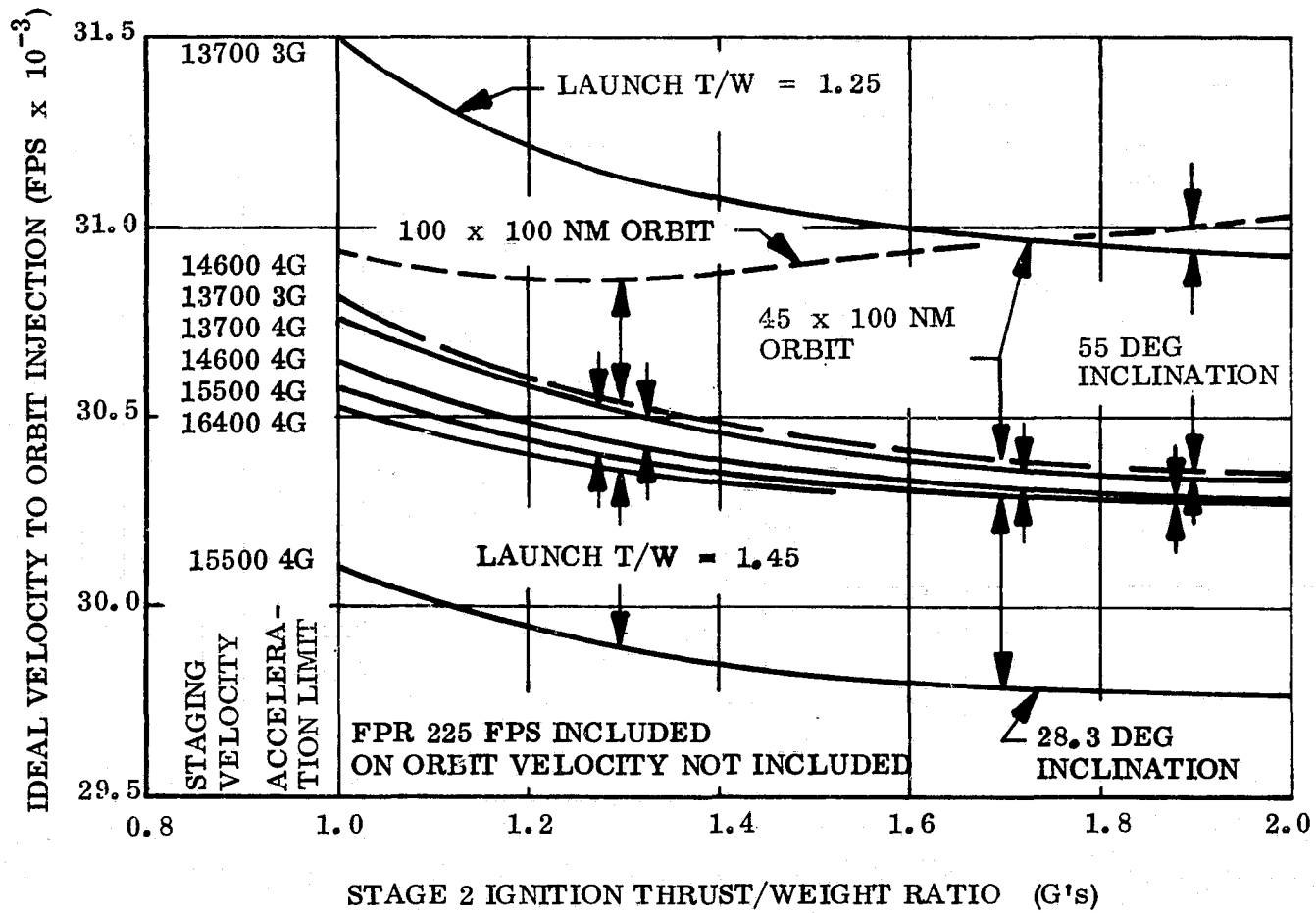


Fig. 5-10 Stage 2 Thrust-to-Weight Selection

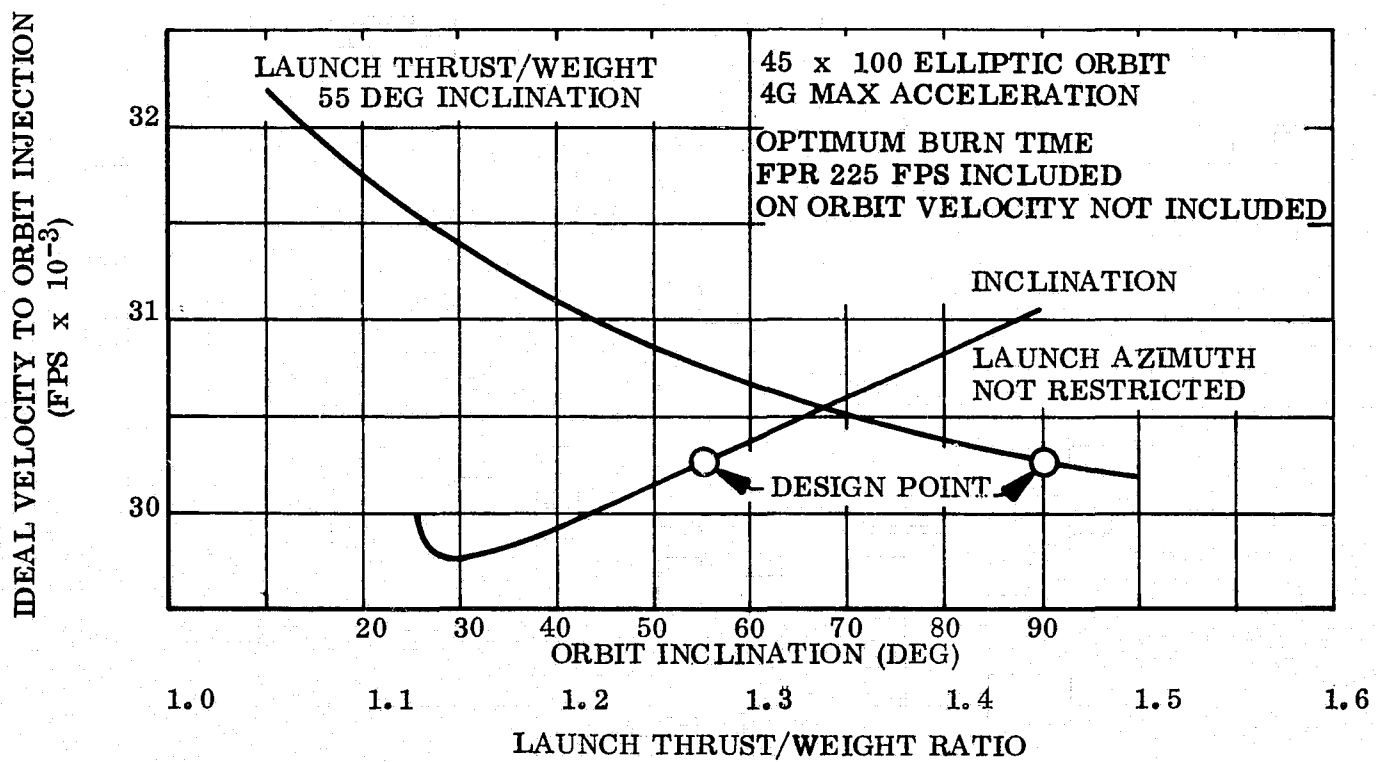


Fig. 5-11 Mission Velocity Sensitivity to Launch Thrust/Weight and Orbit Inclination

### 5.2.2 Reference Trajectories

The ascent trajectory profile studies have been conducted with the aid of the PRESTO digital computer program, in which a steepest descent optimization technique is used to define optimum thrust attitude guidance profiles. Initial representative ascent trajectories have been established for the Two-Stage and Triamese configurations. An ETR launch into a 55-degree inclination, 45 x 100 nm elliptic orbit is simulated. The launch T/W ratio was selected at 1.45; and second stage ignition T/W, at 1.20.

Figures 5-12 and 5-13 show the primary trajectory parameters versus flight time and define the reference ascent profiles. Acceleration constraints of 3 and 4 g are shown for the Two-Stage and 3 g for the Triamese. The profiles are representative of ballistic flight for the first 130 seconds of burn. At this point, where the dynamic pressure is less than 100 lb/ft<sup>2</sup>, optimum thrust attitude programming is initiated. These ascent profiles are terminated at perigee injection into a 45 x 100 nm transfer orbit.

Reference trajectories are necessary for guidance, dynamics, ascent heating, and reentry analyses. A comparison of the profile histories generated for various sensitivity trades shows only minor differences, except for peak dynamic pressure, which directly reflects the launch T/W. Thus analyses based on these data should produce essentially valid results for an extremely wide variety of missions and vehicle configurations.

For the Two-Stage and Triamese configurations, respective dynamic pressures of 558 and 540 psf are encountered during first-stage burn, and first/second-stage separation occurs above 170,000 (221,000) feet altitude with a dynamic pressure of less than 40 (11) psf. Staging velocity is about 9300 (9910) fps at less than a 13 (11) degree flight path angle.

### 5.3 REENTRY MANEUVER TRAJECTORY ANALYSIS

The reentry maneuver trajectory analysis was performed with a LMSC 5DOF point mass computer program, which was specifically developed for analyzing lifting reentry and guidance problems and techniques.



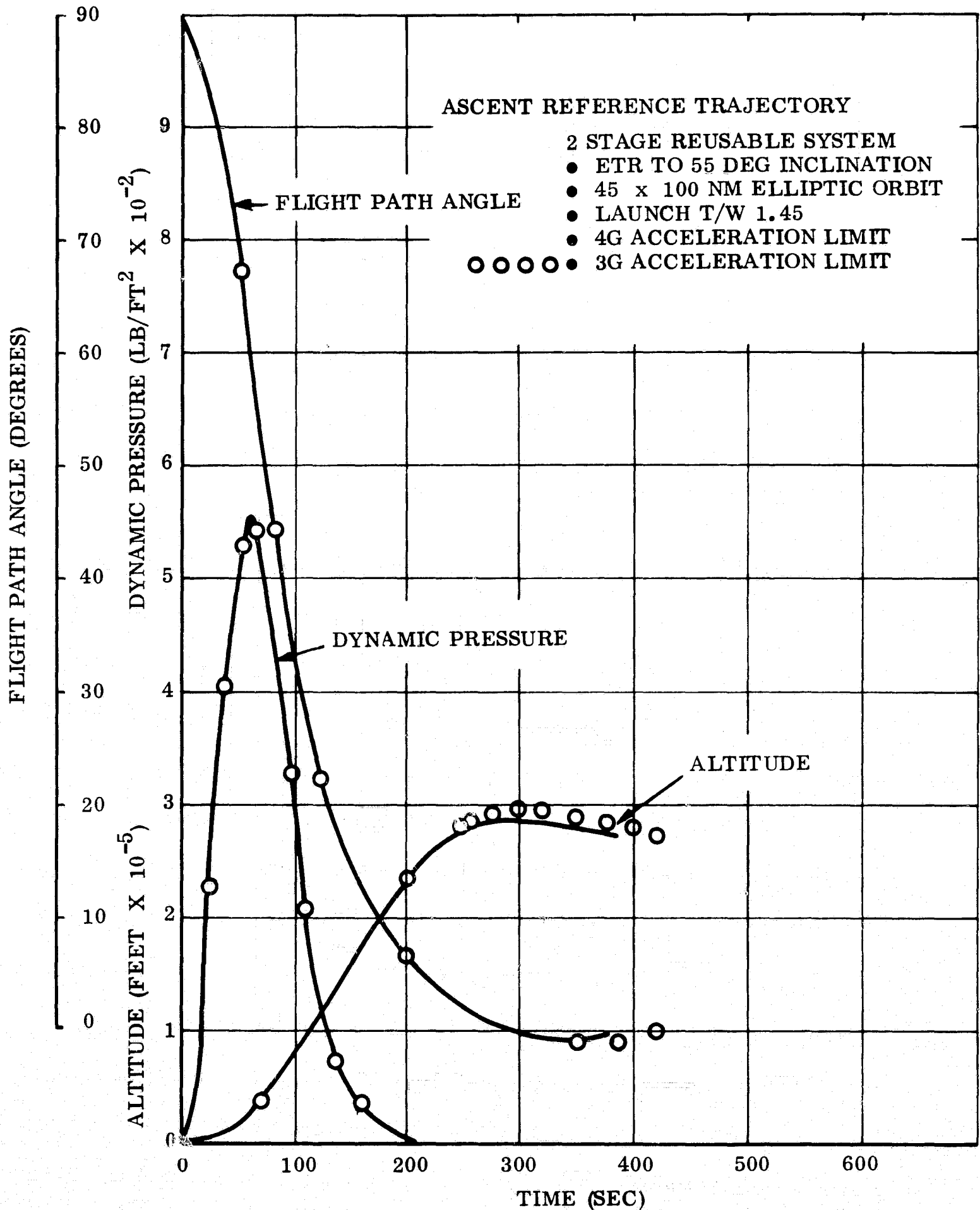


Fig. 5-12a Ascent Trajectory Profile - Two-Stage Configuration

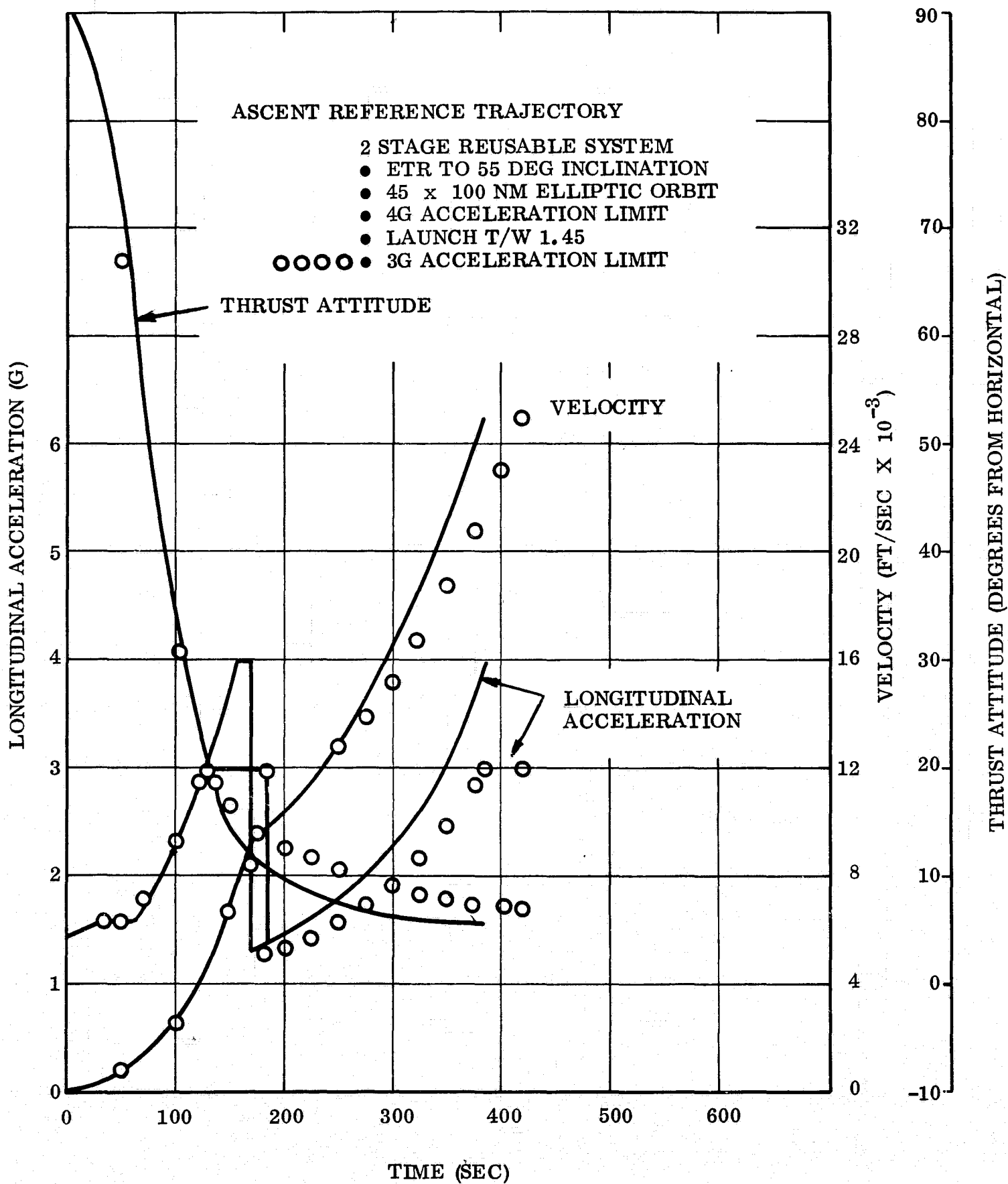


Fig. 5-12b Ascent Trajectory Profile - Two-Stage Configuration

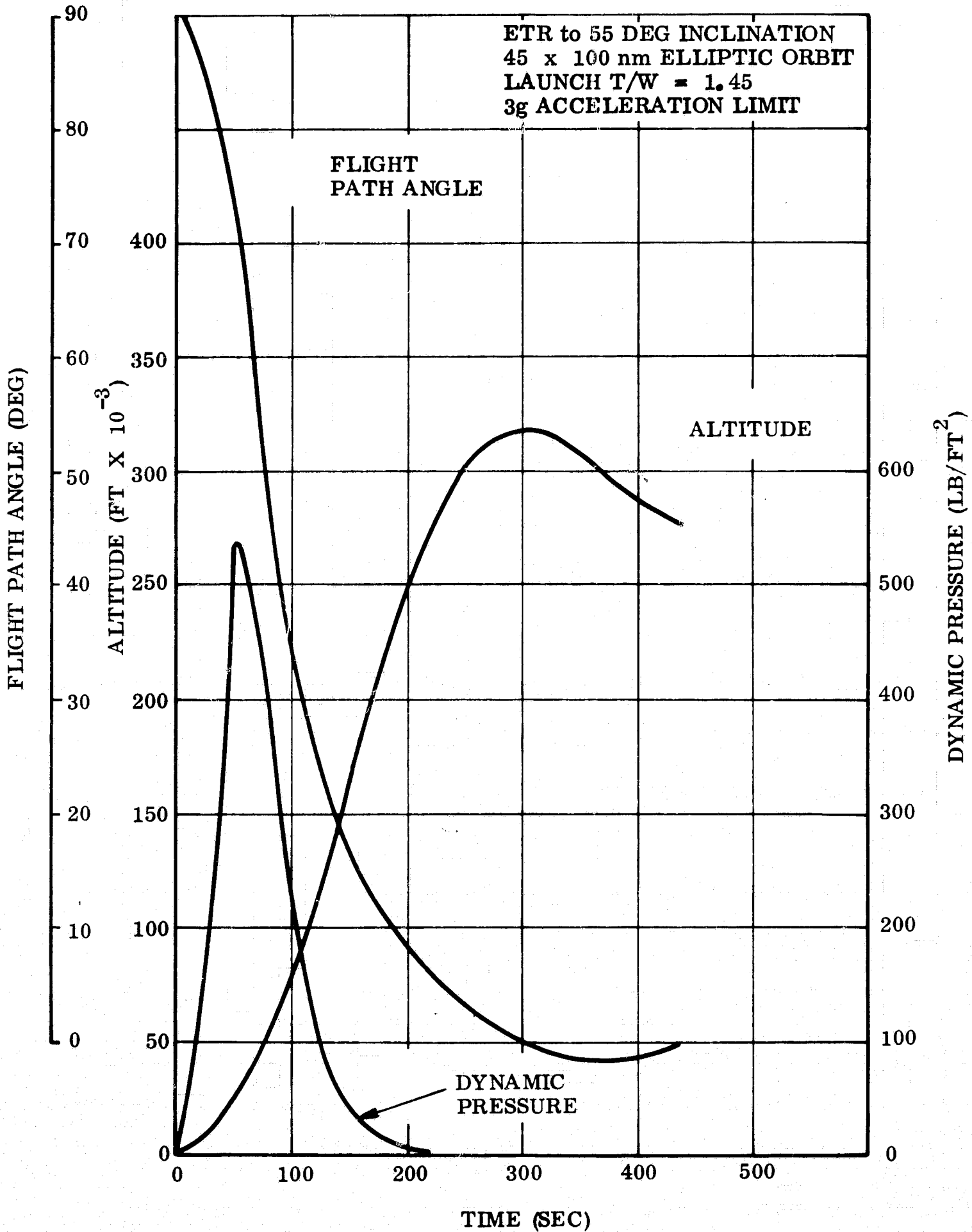


Fig. 5-13a Ascent Trajectory Profile - Triamese Configuration

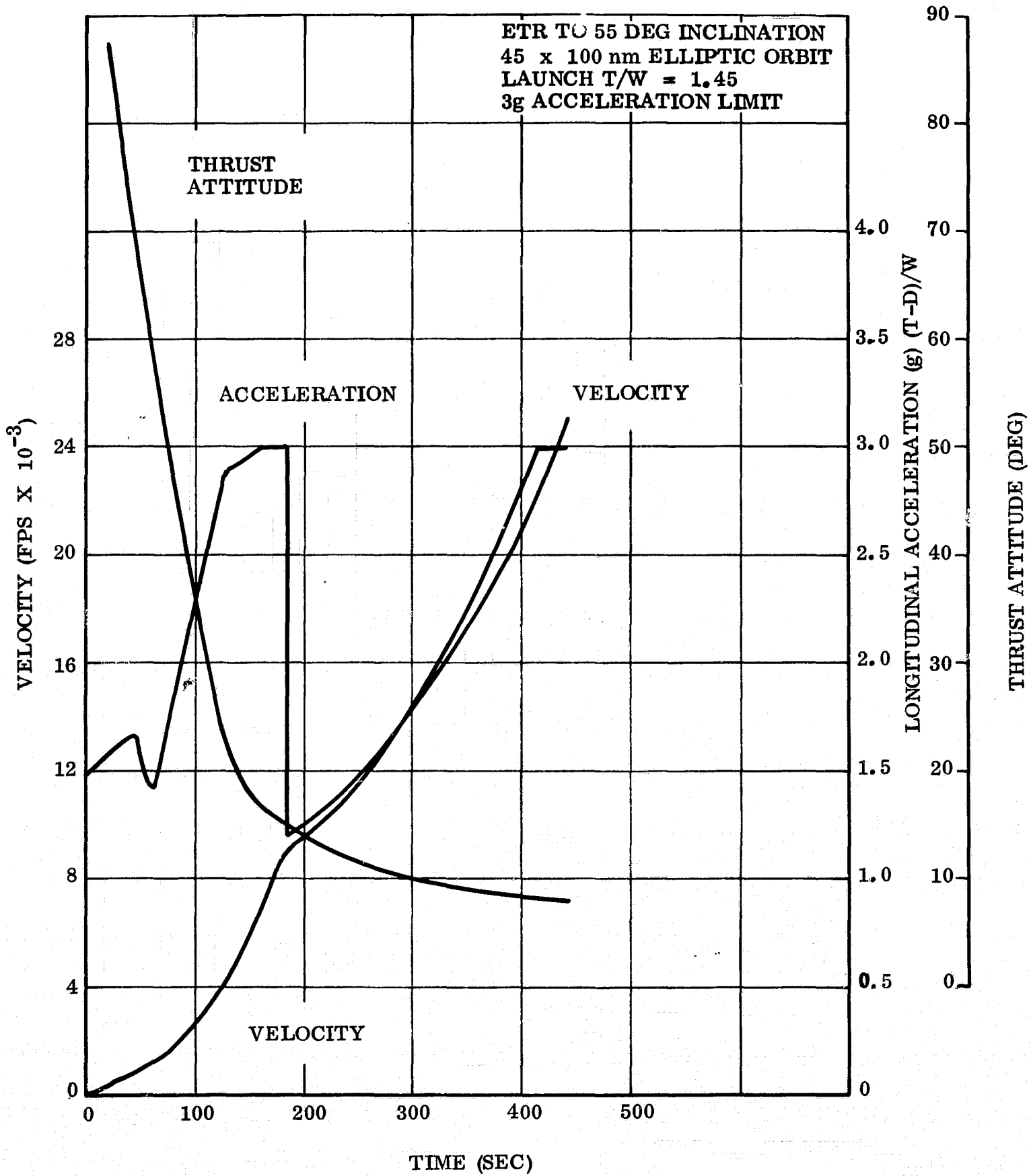


Fig. 5-13b Ascent Trajectory Profile - Triamese Configuration

Past studies indicate that to satisfy thermal protection system requirements for minimum surface temperature and total heating and to maximize cross-range, reentry should be initiated with the vehicle at a high angle of attack ( $\alpha_v = 55$  deg) for  $C_{L_{\max}}$  to be held through pullup. Afterwards, bank angle and  $\alpha_v$  can be modulated downward to selected values determined for the critical heating/temperature region. During the subsequent terminal glide phase,  $\alpha_v$  must be modulated downward again to 15 degrees for  $(L/D)_{\max}$  for maximum cross-range maneuvering capability. This mode of operation was used for both the booster and the orbiter return/reentry trajectory analyses.

### 5.3.1 Vehicle Aerodynamic Characteristics

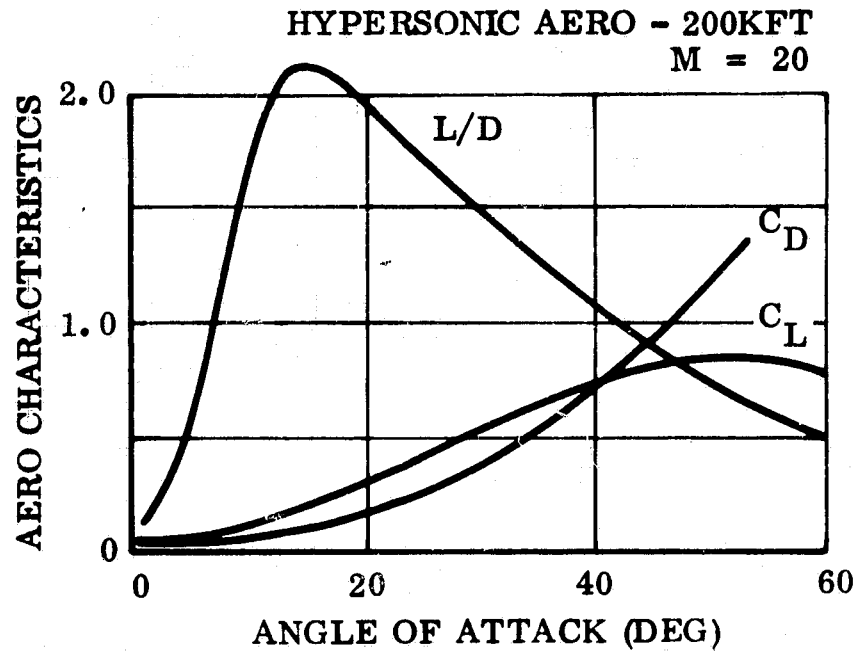
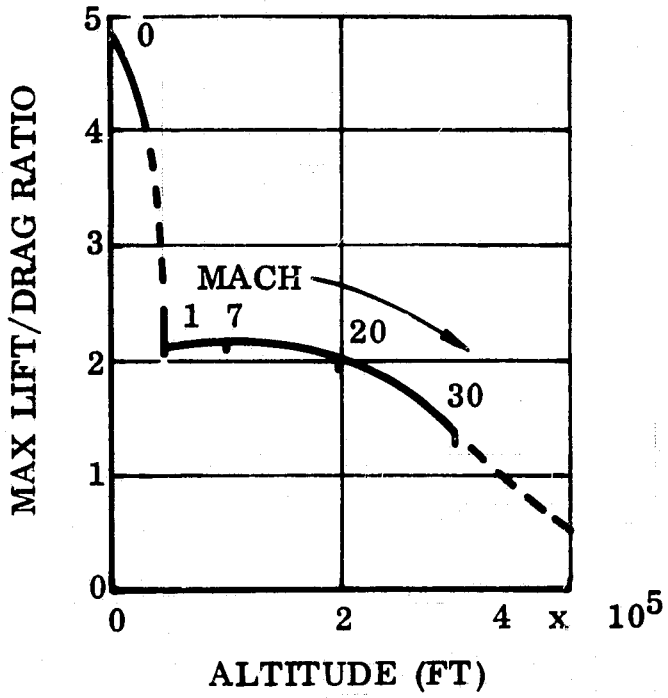
For this analysis, the geometry and wing loading of the LMSC Triamese and Two-Stage reusable vehicles were essentially identical; therefore, the vehicle aerodynamic force coefficients and characteristics shown in Fig. 5-14 were used for studies of both configurations. The aerodynamic force coefficients include increments due to hypersonic viscous effects.

### 5.3.2 Booster Return Analysis

The combined ascent/return trajectory profiles for a typical reusable Space Shuttle are shown in Fig. 5-15. The two staging points are for the LMSC Triamese at 221,000 feet and the Two-Stage at 170,000 feet altitude. Following orbiter staging, the booster reenters and returns to a lower altitude, where cruise-back operations are initiated. Constraints on the return trajectory include maximum load limitations, temperature limits, and range from final landing site.

Constraints imposed on the return trajectory included a 4-g load limit and a maximum lower surface temperature of 1600°F. Booster flight sequence after staging included trim at  $C_{L_{\max}}$  ( $\alpha_v = 55$  deg) with a bank angle ( $\chi$ ) to sustain equilibrium glide after pullup until  $\chi = 45$  degrees. Bank angle was then fixed until a heading change from 180 to 200 degrees was accomplished. Angle of attack was modulated from 55 to 22 degrees in the supersonic flight regime to preclude overly steep descent angles and to ensure that assumed stability limits were not exceeded. Final descent to cruise-back altitude (20,000 ft) was at subsonic  $(L/D)_{\max}$ .

2ND STAGE ORBITER



FIRST STAGE BOOSTER

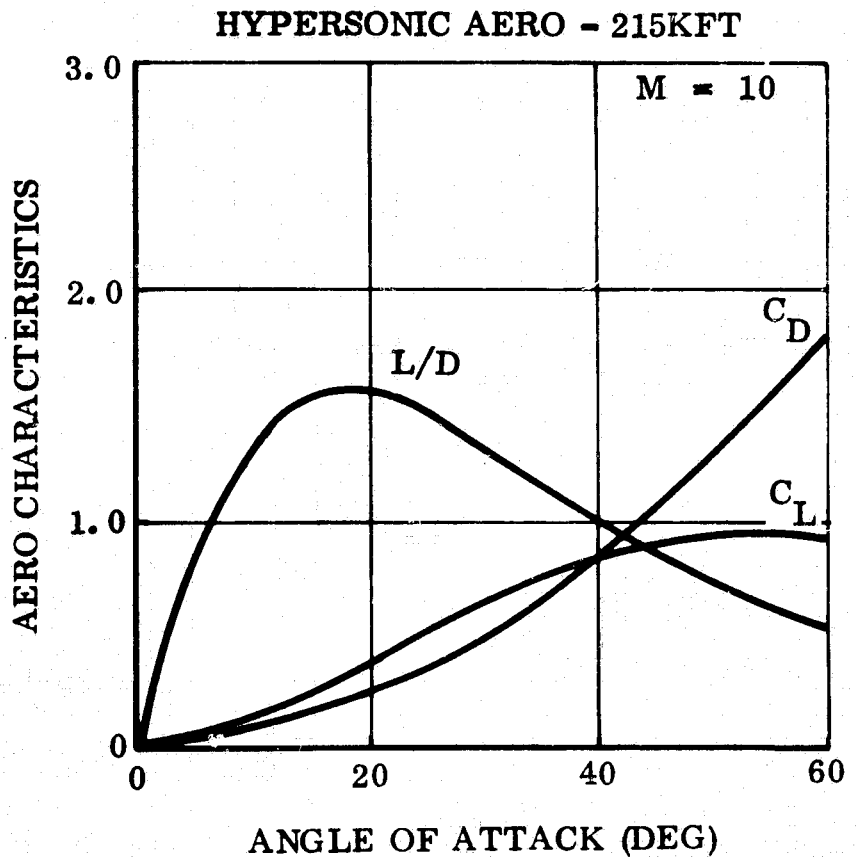
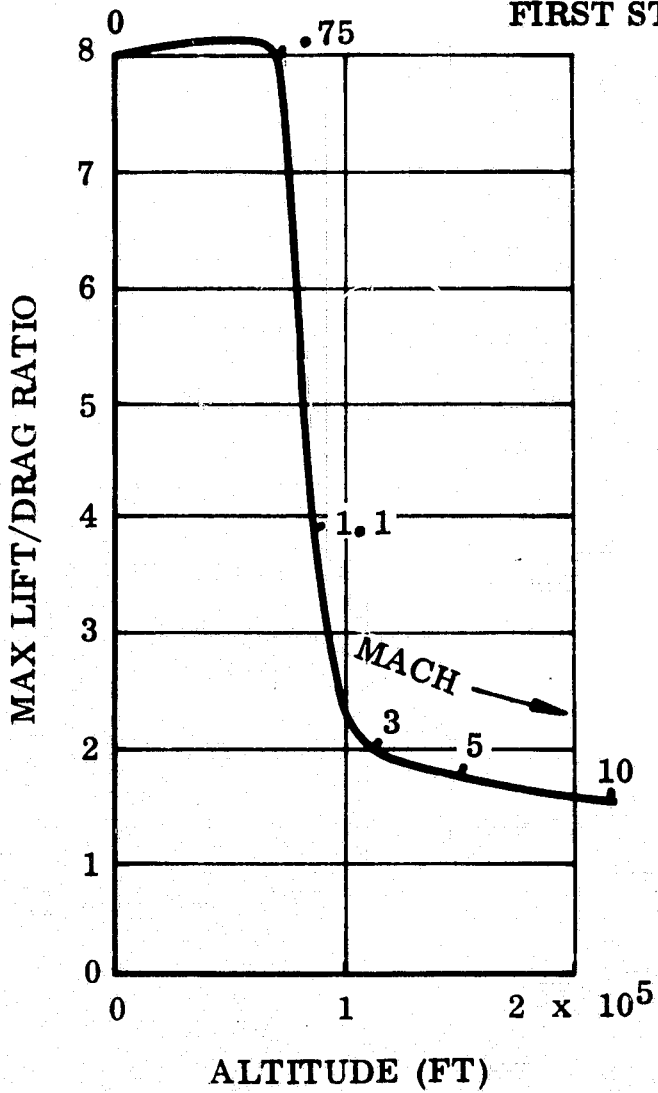


Fig. 5-14 Vehicle Aerodynamics

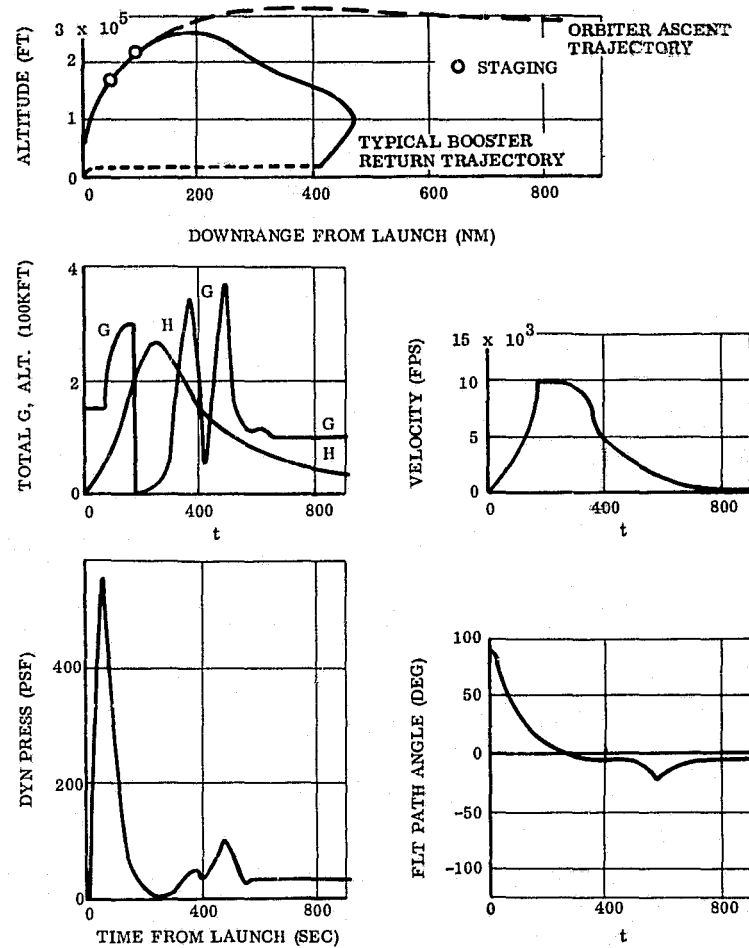


Fig. 5-15 Booster Ascent/Return History

Final range from the launch point is about 425 nm, as shown in Fig. 5-15. This range will change if staging conditions or other bank angles are assumed during the turn maneuver.

Histories of various trajectory parameters shown in Fig. 5-15 indicate maximum acceleration loads during descent will be about 3.6 g's. The two load peaks shown represent conditions at initial booster pullout and when angle of attack is reduced for supersonic flight. Maximum descent angle is about 23 degree, as illustrated by the flight path angle history.

### 5.3.3 Orbiter Ascent/Reentry Profiles

The ascent trajectory characteristics for the combined booster/orbiter and the orbiter injection history are shown in Fig. 5-16, in which the curves show the variation of flight path angle ( $\gamma$ ), velocity ( $V$ ), longitudinal load factor ( $g$ ), and dynamic pressure ( $\bar{q}$ ) as a function of time.

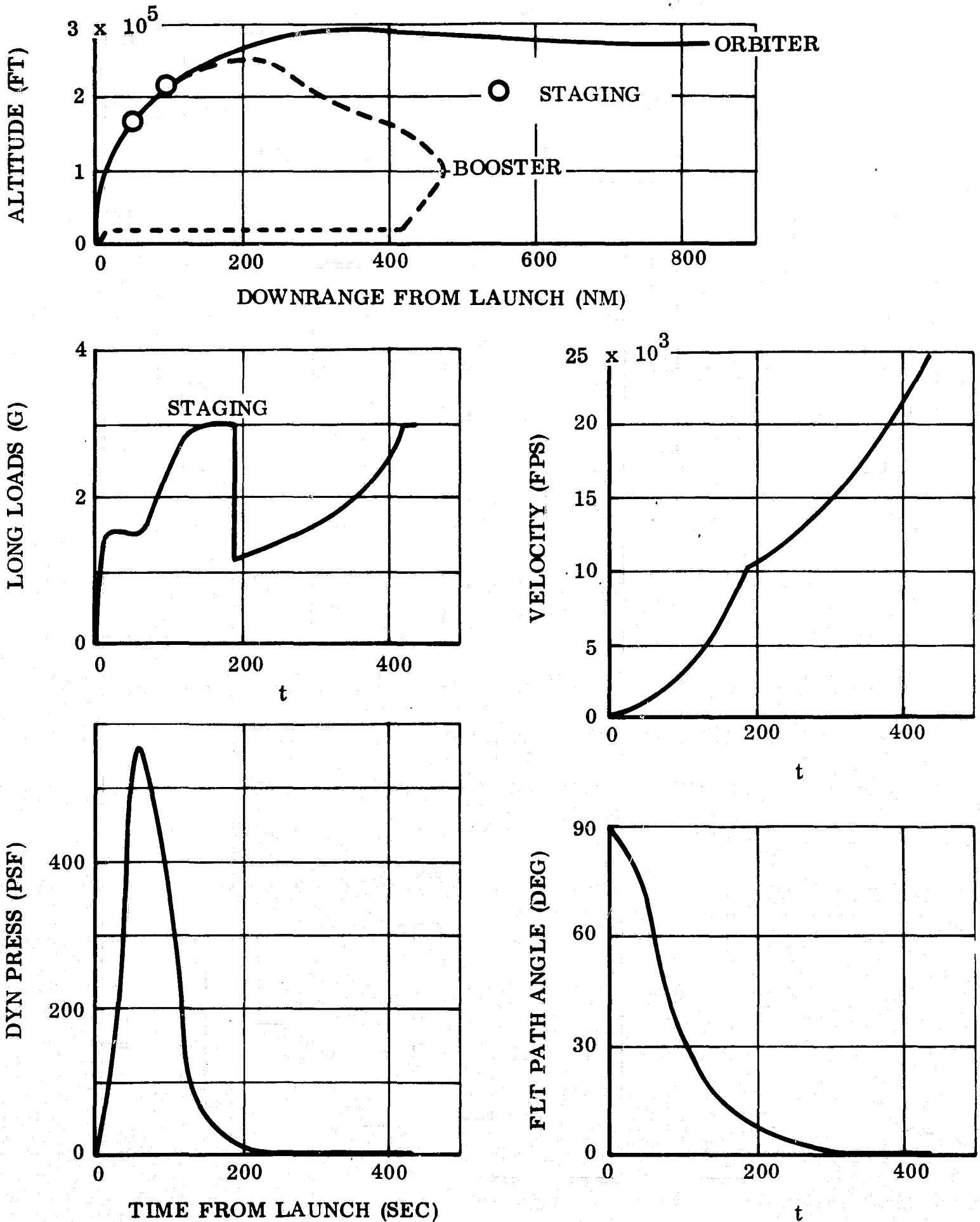


Fig. 5-16 Booster Ascent/Injection History



Typical reentry trajectory curves from retro at 100 and 270 nm altitude down to 20,000 foot altitude are summarized in Figs. 5-17 and 5-18. Reentry parameters during terminal glide are quite similar for both altitudes, except for down-range differences.

#### 5.3.4 Retro and Reentry Parameters

In the interest of minimizing retro propellant requirements and reentry pullup heat rates (also g loads), the effects of orbit altitude on retrovelocity ( $V_R$ ) and reentry flight path angle (FPA) were investigated. The results, which are plotted in Fig. 5-19 (a and b), show that minimum retrovelocity is required at the shallow reentry FPA. Also, pullup stagnation heat rate and, implicitly, heat shield weight are minimum at the shallow reentry FPA. Superimposing the maximum equilibrium glide heat rate values represented by a dashed line on the curve (a) yields the desired approximate reentry FPA for each orbital altitude. Curve (b) shows that a minimum retrovelocity of 262 ft/sec applied 180 degrees to the flight direction ( $\theta_{VR} = 180$  degrees, which is near-minimum deboost impulse for the range of reentry FPA considered) will, for a 100 nm circular orbit, attain the desired reentry FPA of  $-1.0$  degree at 400,000 foot altitude. Similarly, a retrovelocity of 434 ft/sec will produce a reentry FPA of  $-1.5$  degree at 400,000 foot altitude for a 270 nm circular orbit.

Reentry FPAs less than equilibrium glide values were arbitrarily excluded to avoid oversensitivity to deboost and guidance errors. FPA and corresponding retrovelocities can be selected for each altitude mission from these curves.

The additional reentry parameters at 400,000 foot altitude, such as reentry velocity ( $V_E$ ) and range angle ( $\theta_{RG}$ ), and the vehicle mass ratio ( $R$ ) are shown as a function of orbit altitude and reentry FPA in Fig. 5-19 (c and d).

#### 5.3.5 Vehicle Lower Surface Minimum Peak Temperature Concept

Current rationale indicates that reentry trajectories should be flown not at maximum design temperature but at the minimum peak temperature that could be expected at a judiciously selected point along the reentry trajectory. At this point, the vehicle

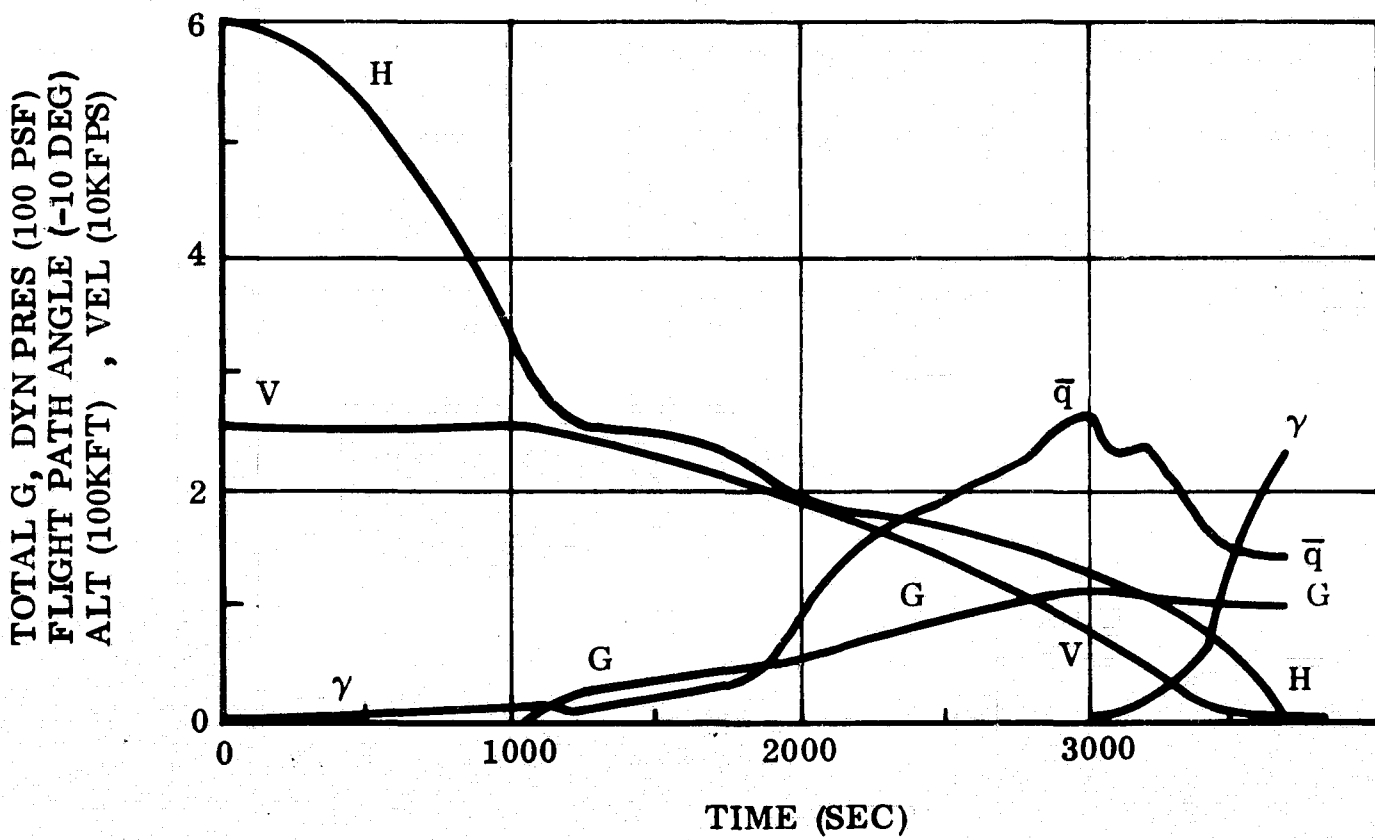
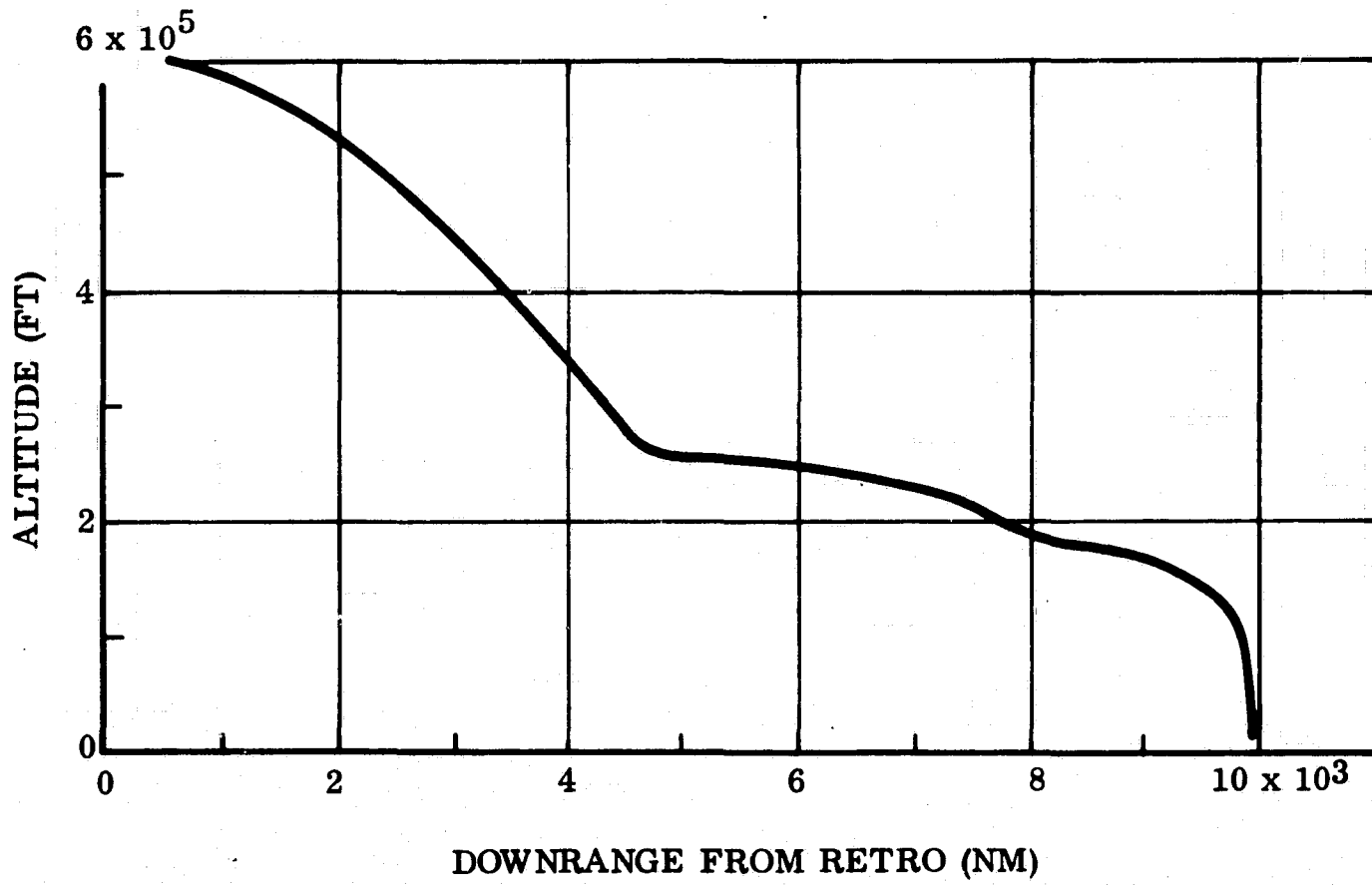


Fig. 5-17 Orbiter Reentry History - 100 nm

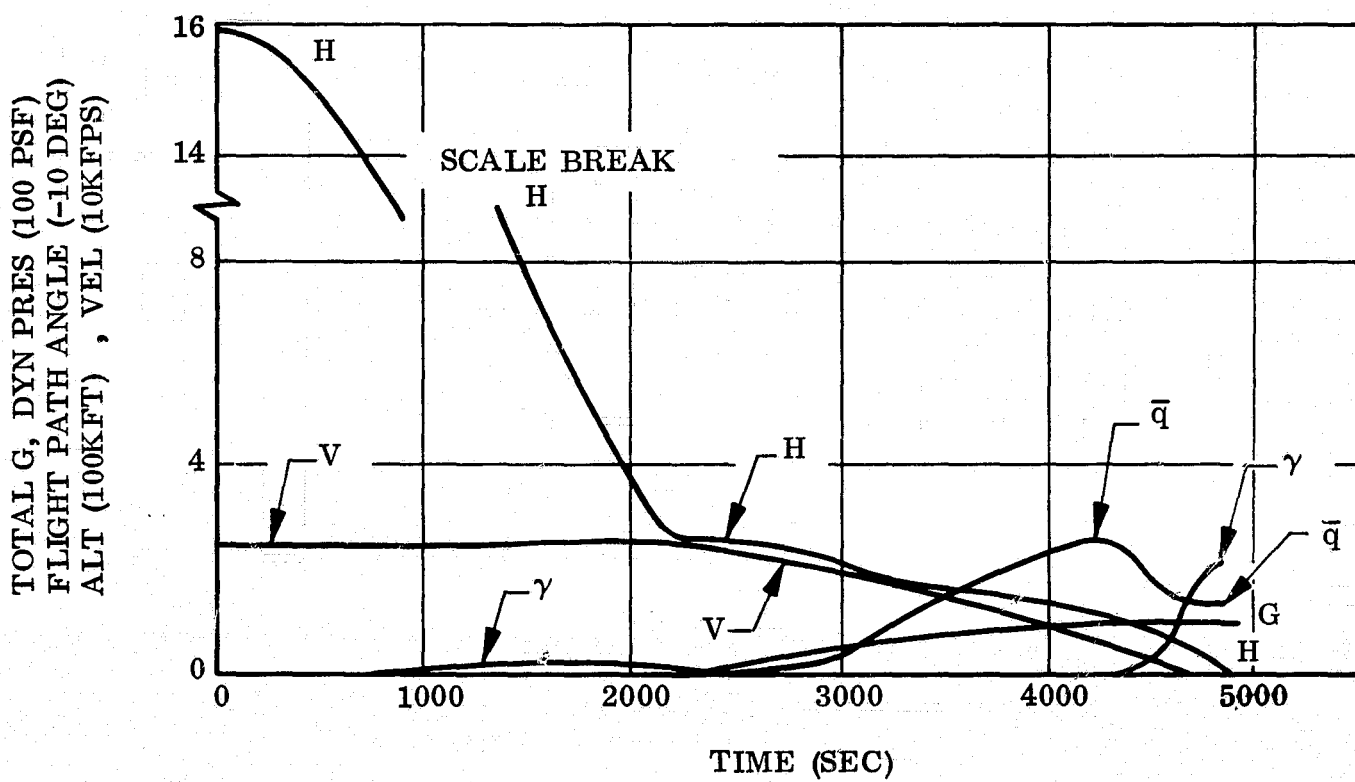
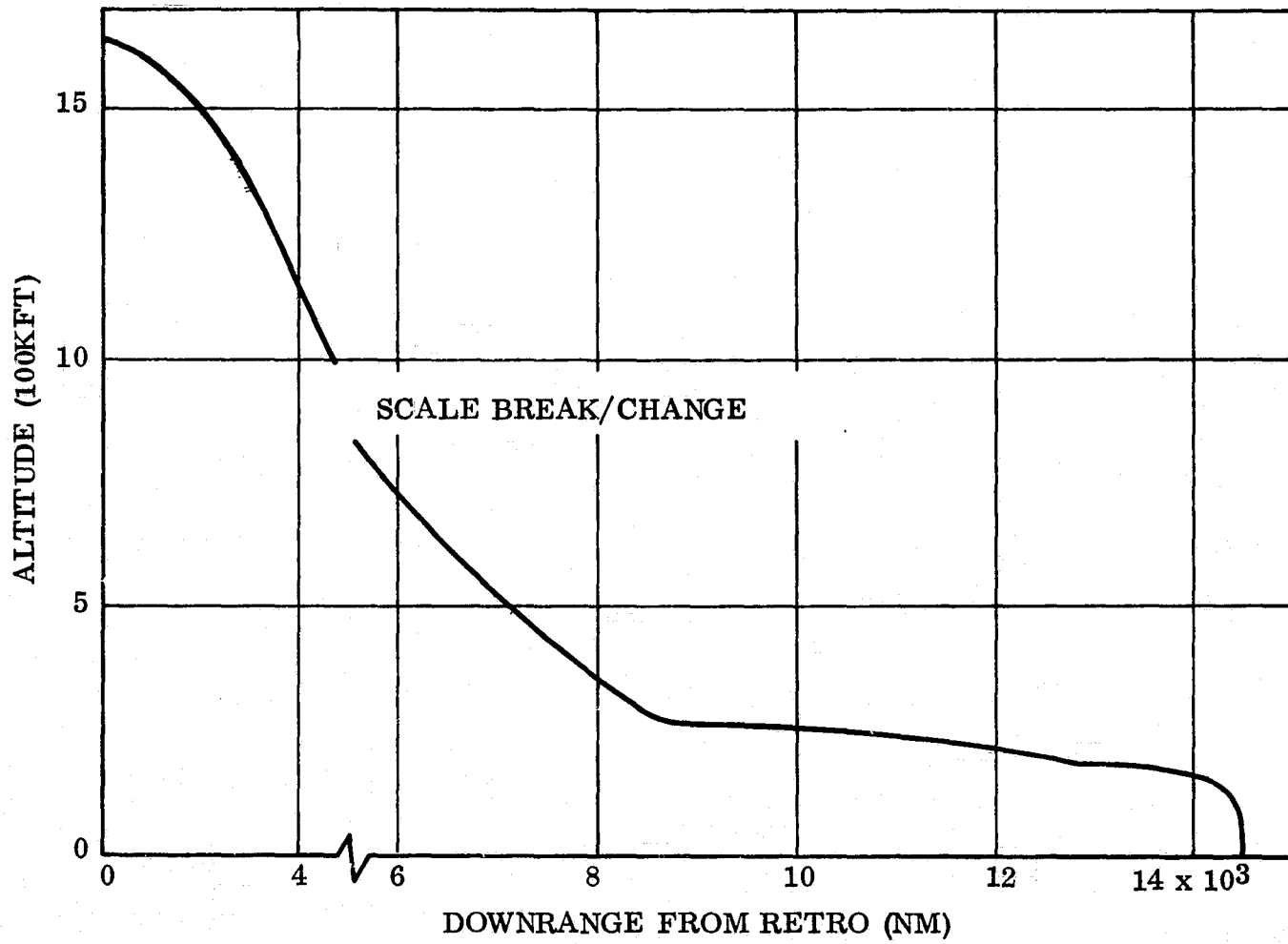


Fig. 5-18 Orbiter Reentry History - 270 nm

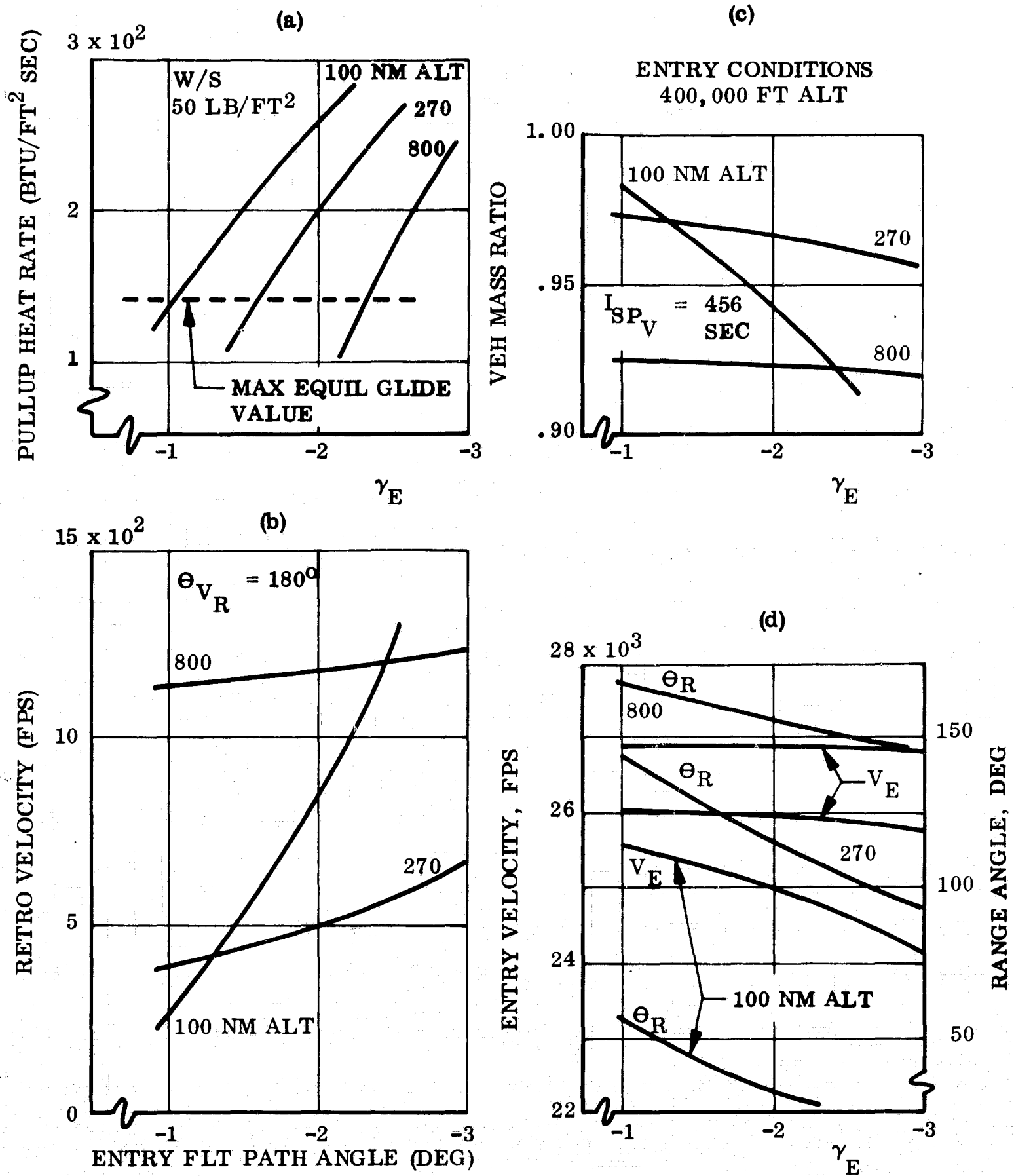


Fig. 5-19 Retro and Reentry Parameters

lower surface minimum peak temperature profile, as developed from Rho-Mu turbulent flow theory, is coincident with the unbanked equilibrium glide profile; in other words, the altitude distance/corridor margin between the two profiles is zero. By design, other trajectory points have some greater positive altitude corridor margin. This altitude increment then represents a region whereby vehicle maneuvers via angle of attack and/or bank angle modulation can be made primarily to fly at reduced temperatures on the vehicle lower surface and also to maximize cross-range maneuvering capability.

5.3.5.1 Reentry Heating Boundaries. Minimum flight altitude/velocity profiles based on lower surface temperature limits of 2100, 2200, 2300, and 2500<sup>o</sup>F were used for this analysis. These temperature profile curves, which are based on radiation equilibrium conditions, are used to establish the entry corridor available for maneuvering. The configuration assumed to generate the minimum altitude/velocity profiles is a slab delta wing with 78 degrees sweep angle.

The calculations exclude the first 5 feet aft of the stagnation point, where use of a material with higher temperature capability is assumed. At the higher velocities, the altitude limits are determined by laminar heating at the start of the lower surface heat shield ( $x = 5$  ft). At lower velocities, the altitude limits are determined by turbulent heating at the location of boundary layer transition on the forward ramp. The heating boundaries are calculated as a function of forward ramp local angle of attack ( $\alpha_L$ ), which is equal to vehicle angle of attack plus 6 degrees for both orbiter configurations.

Because of geometric and planform loading similarities, the LMSC Triamese and Two-Stage vehicles have identical entry thermal environments. Consequently, entry heating analyses, which have been based on the Two-Stage orbiter, are also applicable to the Triamese orbiter.

5.3.5.2 Altitude Corridor Margin. The curves shown in Fig. 5-20 (a) are typical of the equilibrium glide trajectories (EGT) for wing loadings (W/S) from 40 through 80 lb/ft<sup>2</sup> and lower surface temperature profiles from 2100 to 2500<sup>o</sup>F, all as functions of altitude, velocity, and vehicle angle of attack. The positive altitude displacement at any given  $\alpha_v$  of the EGT above any temperature profile represents positive altitude corridor margin ( $\Delta H$ ).

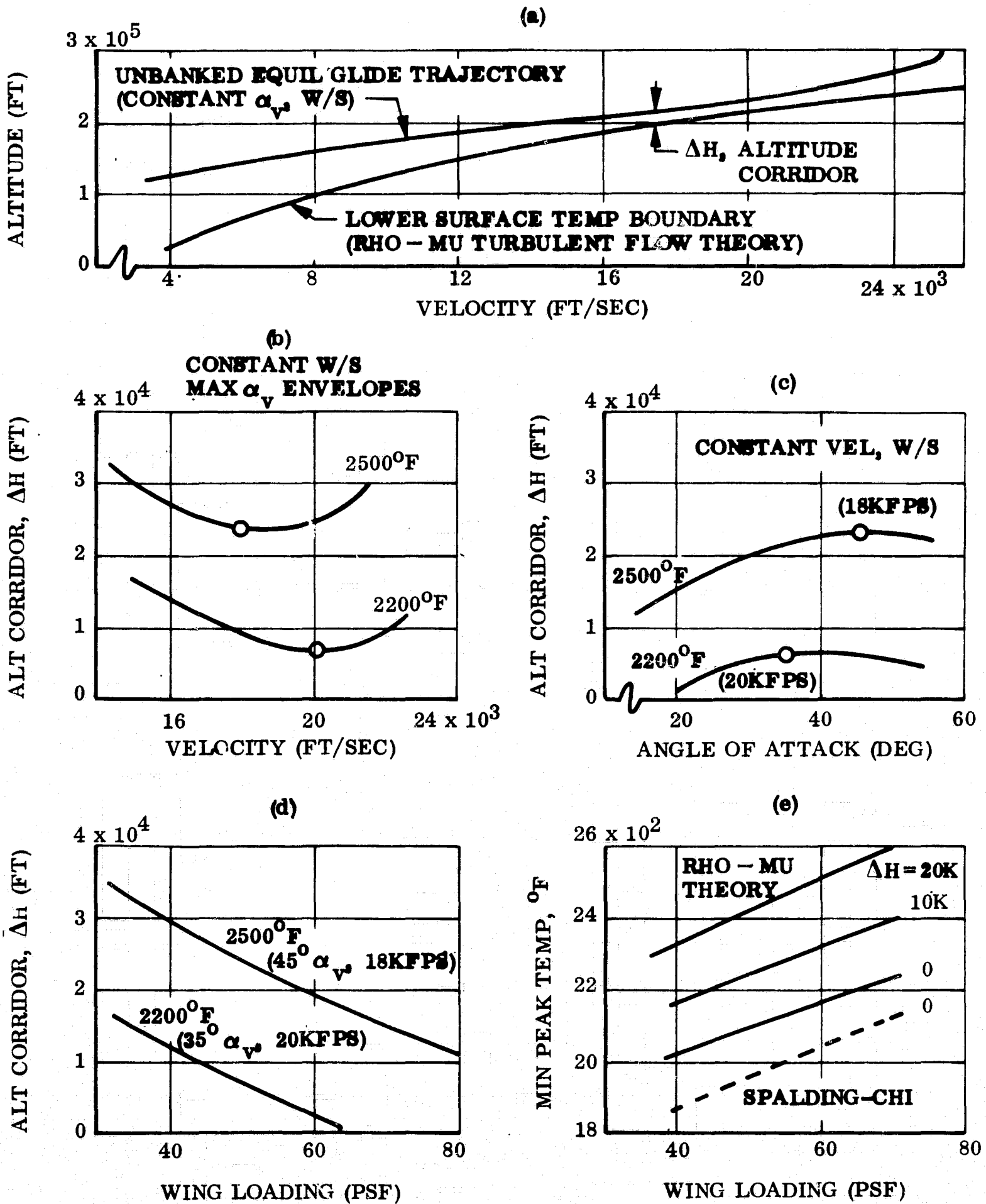


Fig. 5-20 Reentry Minimum Peak Temperature Concept

The  $\Delta H$  for selected temperature profiles were plotted in Fig. 5-20 (b) as a function of velocity for constant W/S. In turn, the value of  $\Delta H$  within the temperature profile bucket was cross plotted as a function of  $\alpha_v$ , as shown in the curves of Fig. 3-20 (c). For a temperature of 2500<sup>o</sup>F, the minimum value of  $\Delta H$  was selected from the (b) curves at a velocity of 18K ft/sec; for 2200<sup>o</sup>F,  $\Delta H$  was selected at 20K ft/sec.

The  $\Delta H$  for the selected  $\alpha_v$  and velocity was taken from Fig. 5-20 (c) and cross plotted as shown in (d) as a function of W/S. Further cross plotting in (e) yields  $\Delta H$  as a function of lower surface minimum peak temperature ( $T_{min}$ ) and W/S. Several important points may be drawn from the curves of Fig. 5-20 (e). First, for a heat shield temperature limit of 2100<sup>o</sup>F, the vehicle wing loading cannot exceed 50 lb/ft<sup>2</sup>, whereas at 2200<sup>o</sup>F, wing loadings up to approximately 65 lb/ft<sup>2</sup> can be used. In other words, changing the heat shield allowable temperature by only 100<sup>o</sup>F permits the wing loading to be increased by about 15 lb/ft<sup>2</sup>. Second, higher wing loadings are desirable because of their association with shorter vehicle lengths and reduced launch weights, in contrast to low wing loading vehicles.

The value of  $T_{min}$  for any W/S can be determined from the  $\Delta H = 0$  curve. For a value of W/S = 50 lb/ft<sup>2</sup>,  $T_{min} = 2100^{\circ}\text{F}$  (Rho-Mu turbulent flow theory). By comparison, Spalding-Chi theory yields  $T_{min} = 1970^{\circ}\text{F}$  for W/S = 50. The value of  $T_{min}$  associated with various values of  $\Delta H$  and W/S can be readily determined from the curves of Fig. 5-20 (e).

5.3.5.3 Cross-Range Maneuver Capability. The curves of Fig. 5-20(e) were cross plotted and appear as the upper curves of Fig. 5-21 to show the relationship between  $\Delta H$  and  $T_{min}$  for various values of W/S.

A variety of trajectory cases were computed and the resulting cross-range values plotted as shown in the lower curves of Fig. 5-21 as a function of  $T_{min}$  and W/S. Since these cases represent the use of a variety of conditions, the cross-range values are not necessarily maximum; they will be subject to revision upward as optimization programs for minimum peak temperature, angle of attack and bank angle modulation, and maximum cross-range maneuvering capability are developed.

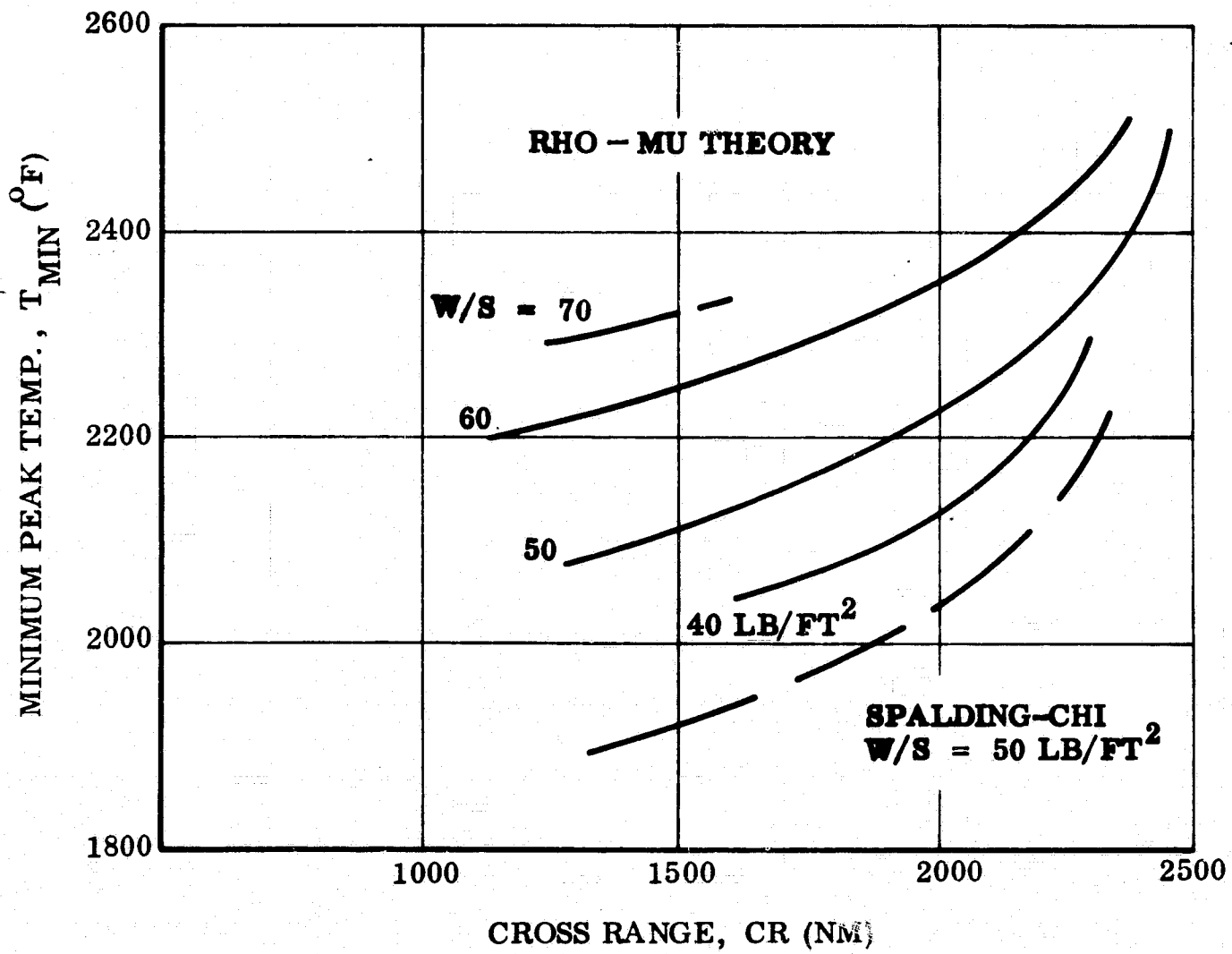
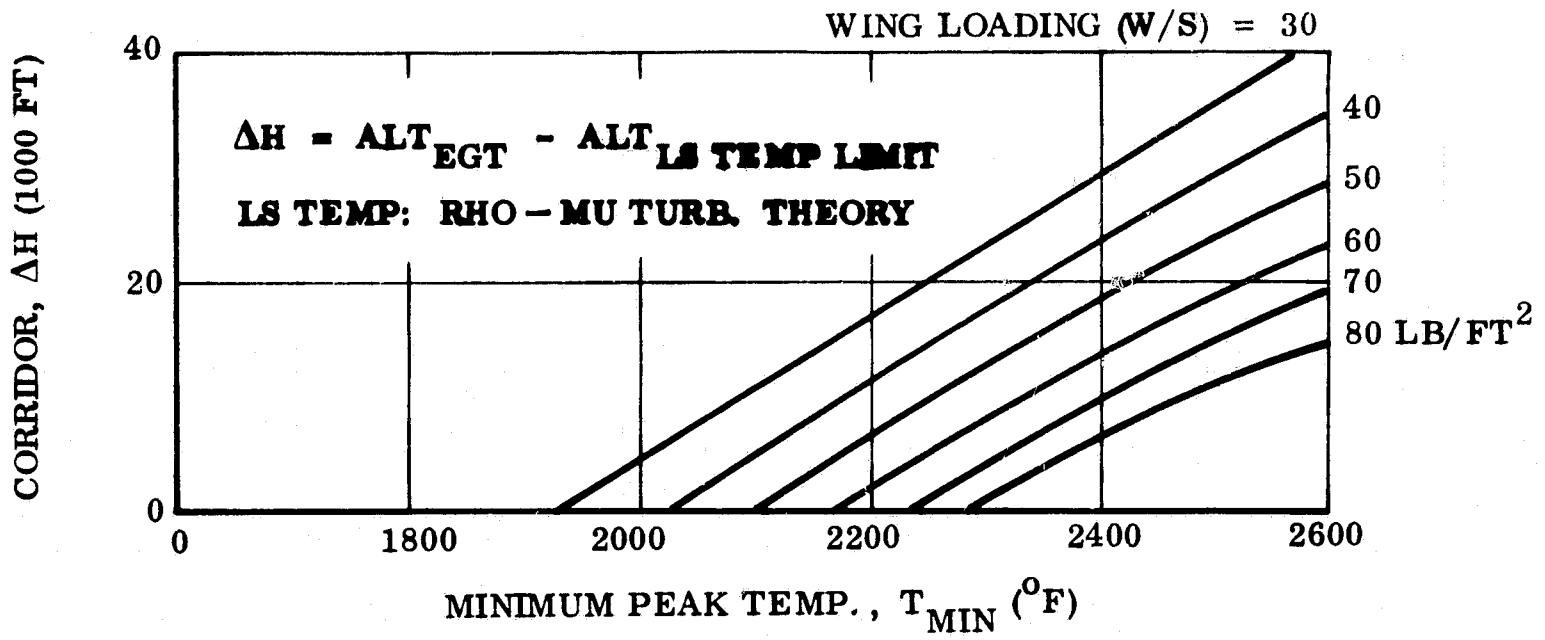


Fig. 5-21 Cross Range as a Function of Minimum Peak Temperature and Wing Loading



Again, a comparison of the Rho-Mu and Spalding-Chi values at a W/S of 50 lb/ft<sup>2</sup> can readily be made to evaluate the effects of turbulent flow theory on temperature/heating predictions.

### 5.3.6 Reentry Trajectory Maneuver Analysis

The data and curves just presented indicate that the orbiter ideally could reenter at a minimum peak temperature of 2100° F for a W/S of 50 lb/ft<sup>2</sup> – ideally, that is, if the assumed initial conditions, atmospheric and earth models, guidance and navigation techniques, and trajectory temperature profiles were perfectly predictable to allow a realtime flight with zero altitude margin.

Realistically, errors or uncertainties in each of these operational modes will affect the altitude corridor/margin and, consequently, the reentry trajectory. This means that flight simulations must be performed at temperatures greater than the ideal minimum of 2100° F to insure altitude margin. Therefore, temperatures of 2200 and 2500° F, which are the design temperatures for the thermal protection system materials of TD-NiCr and LI-1500, respectively, were selected for study.

The 100 nm orbit altitude reentry trajectory data are shown in Figs. 5-22 and 5-23 for 2200° F and 2500° F, respectively. Whereas the curves for 2200° F are reasonably smooth, the velocity-altitude profile for 2500° F shows definite phugoid-type motion, beginning at 15,000 ft/sec. This, in turn, initiates abrupt  $\bar{q}$  and  $g$  oscillations.

The 270 nm orbit altitude reentry trajectory data are shown in Figs. 5-24 and 5-25 for 2200° F and 2500° F, respectively. Again, the prime difference between the two trajectories (with range neglected) lies in the  $\bar{q}$  and  $g$  histories. For the same temperature profile, the data/curves for 100- and 270-nm initial orbit altitude appear to be quite similar.

The range results of the orbiter reentry trajectory maneuvering studies are plotted in Fig. 5-26 as typical footprints for 20,000 foot termination altitude. Because of its higher initial orbit altitude, the 270 nm orbit footprint has the greater down-range distance. The cross-range values for each altitude are essentially the same, partly because of the thermal restraints and vehicle attitude/modulation similarities.

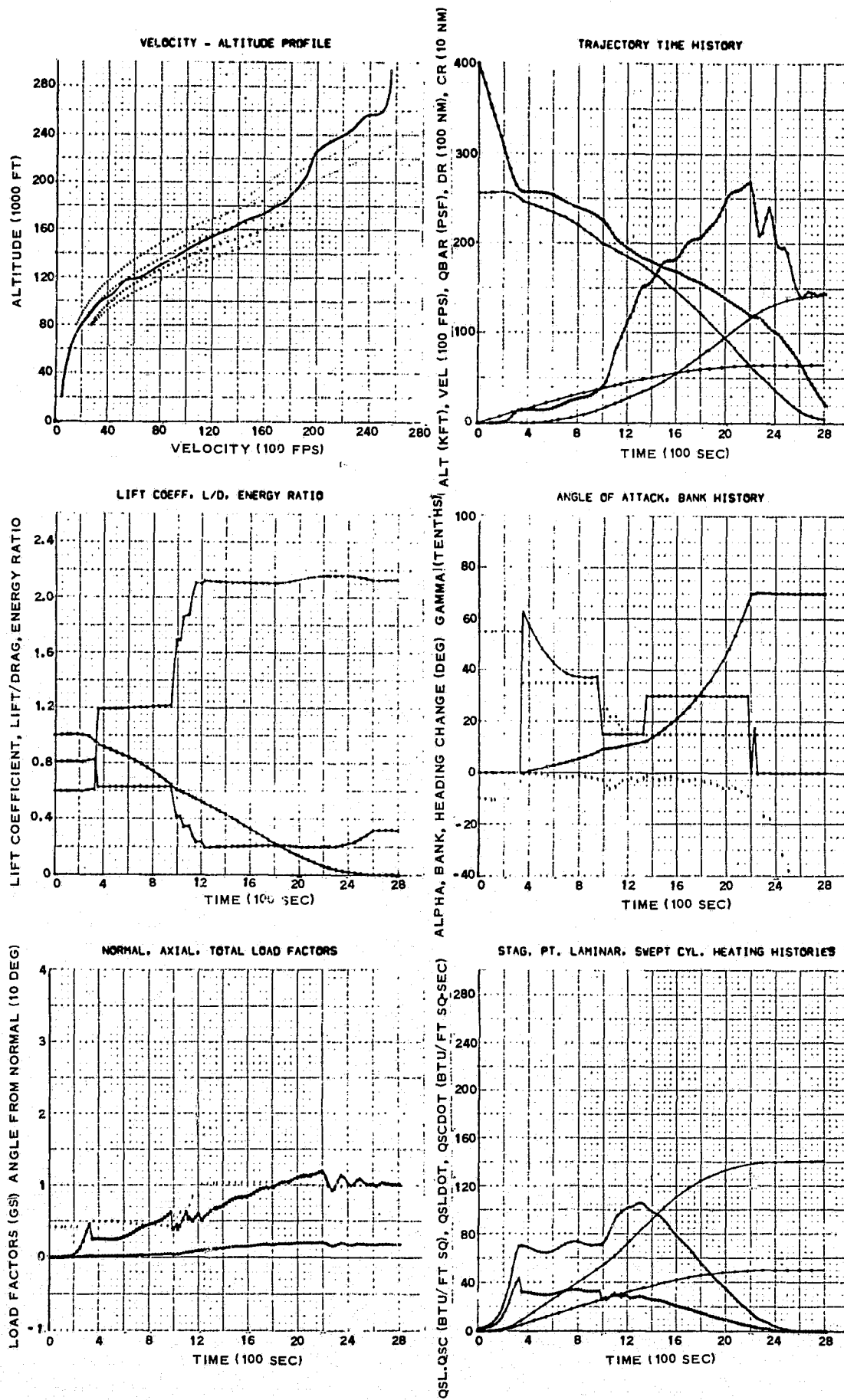


Fig. 5-22 100-nm Reentry Trajectory for 2200°F Profile

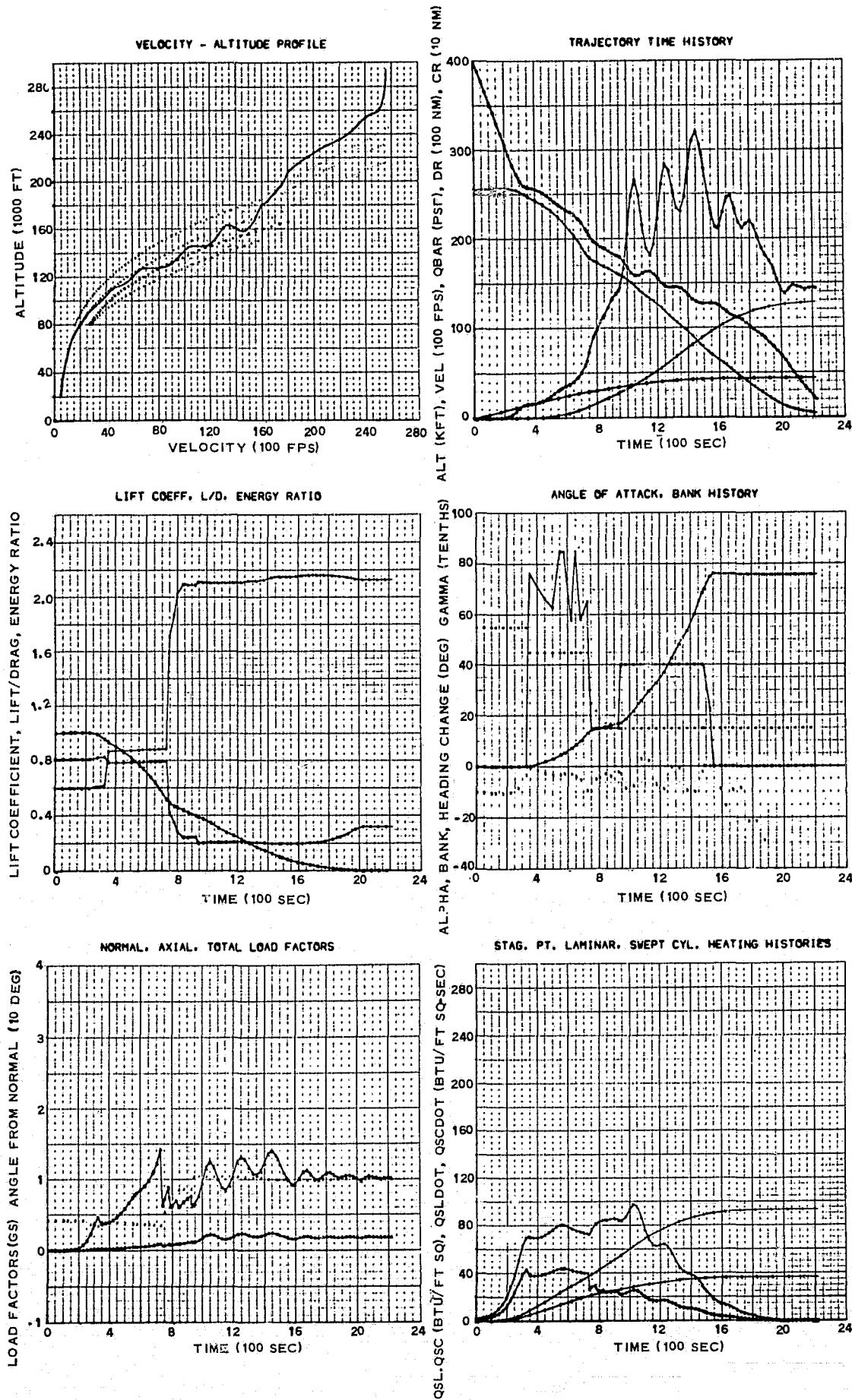


Fig. 5-23 100-nm Reentry Trajectory for 2500° F Profile

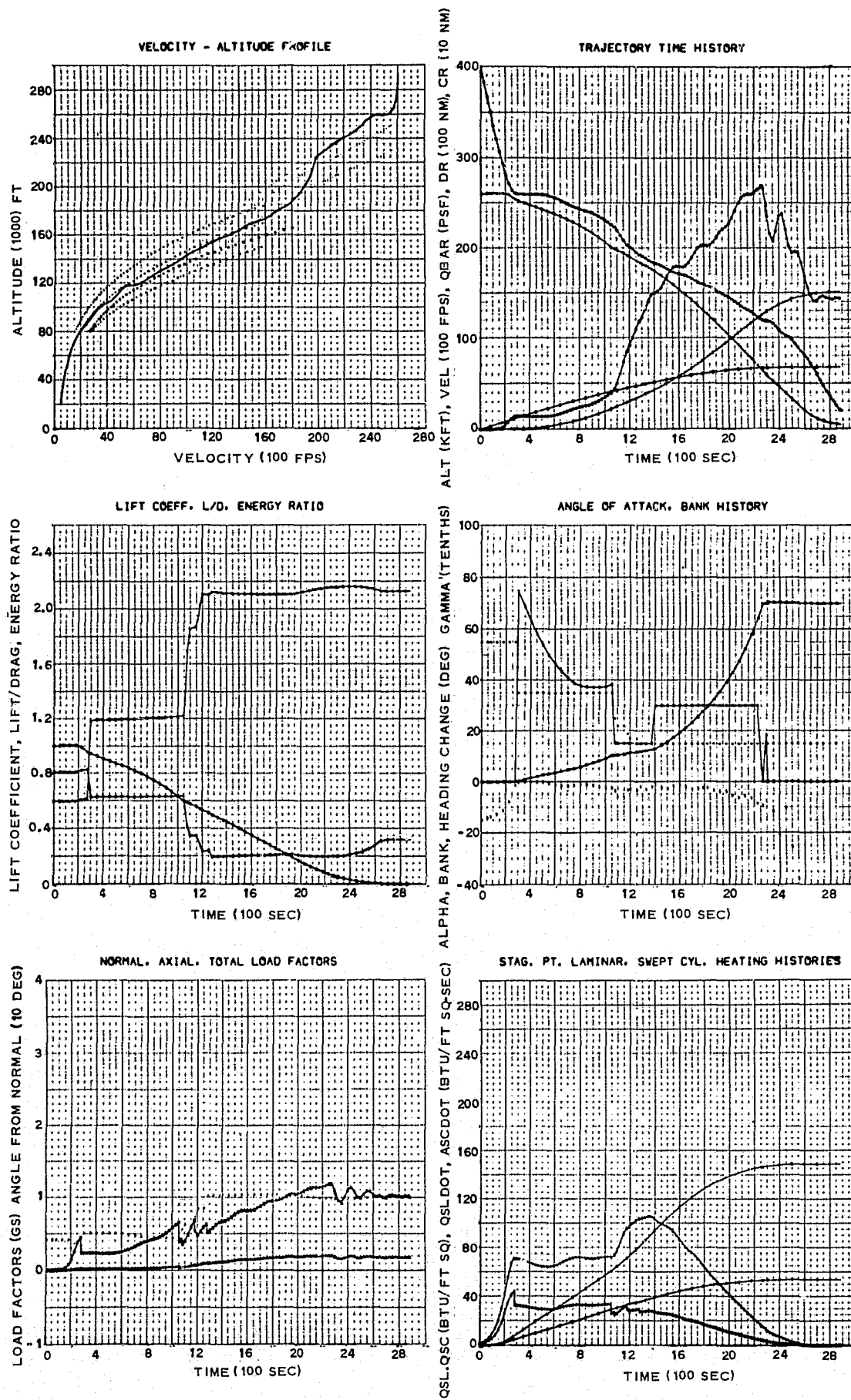


Fig. 5-24 270-nm Reentry Trajectory for 2200<sup>o</sup>F Profile

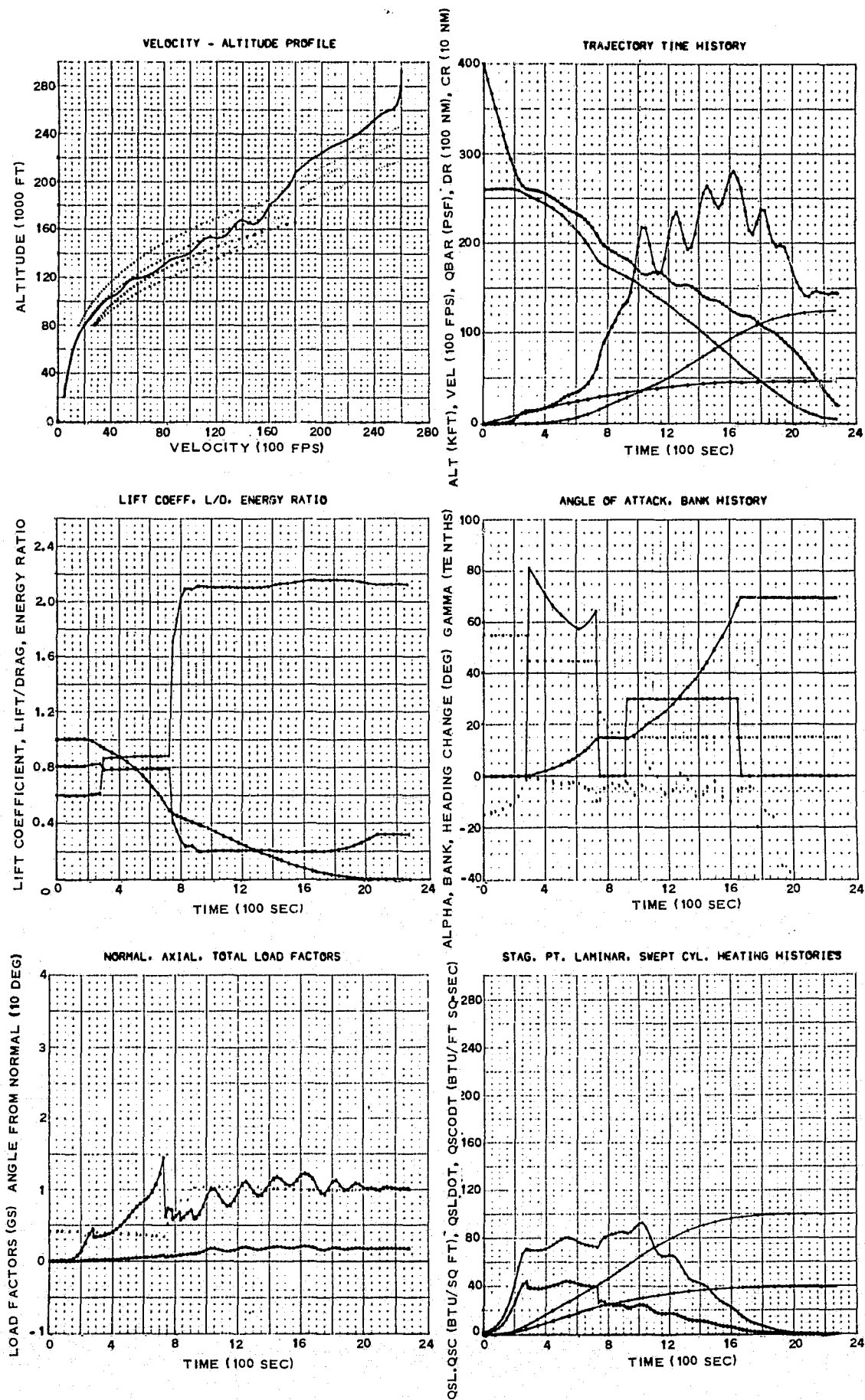


Fig. 5-25 270-nm Reentry Trajectory for 2500<sup>o</sup>F Profile

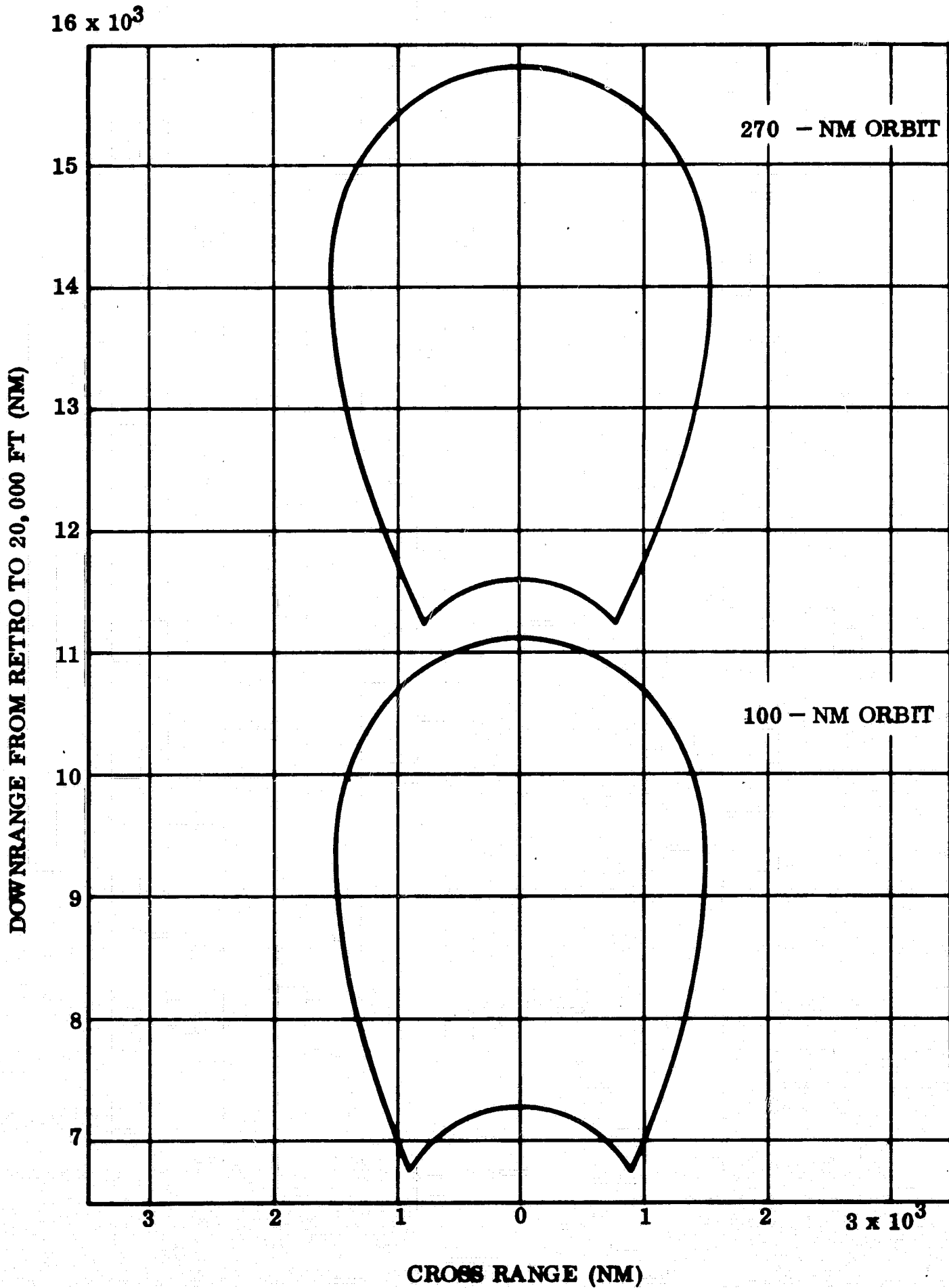


Fig. 5-26 Orbiter Reentry Footprints

### 5.3.7 Reentry Maneuver Trajectory Conclusions

A limited evaluation of the various trajectory reentry/attitude modulations support the operational mode of initial reentry at high angle of attack for  $C_{L_{max}}$  through pullup, a gradual reduction in both  $\alpha_v$  and bank angle thereafter, and a further decrease in  $\alpha_v$  to the value for  $(L/D)_{max}$  for the terminal glide phase of the trajectory.

The booster return-to-base range can be reduced from the 425 nm value if the staging altitude is decreased or the ascent trajectory steepened. Additional reentry attitude modulation optimization could afford improvements in range reduction.

Although firing the retro rocket horizontally aft requires only the simplest guidance, certain missions could possibly require some restraint on the down-range distance. If this arises, other retro angles with appropriate increases in retro velocity/propellant can be used to decrease down range. Reentry conditions, as well as maneuvering capability, will be affected.

The vehicle lower surface minimum peak temperature concept provides a very useful tool for establishing thermal protection system materials requirements. With consideration of various sources of altitude error, such as guidance and control, initial entry conditions, atmospheric dispersions plus required tolerance for uncertainties, and required tolerance for uncertainties in aerodynamic heating prediction, an altitude margin of about 20,000 feet is probably required for realtime operations.

These considerations lead to the conclusion that a lower surface heat shield temperature capability of about 2500<sup>o</sup>F is most desirable to allow flexibility in wing loading and also altitude margin. As shown earlier, the requirement for large cross-range drives toward either low wing loadings or high heat shield temperature capabilities.

The reentry maneuvering trajectories presented in this report were selected as representative of the wide variety of mission profiles available that meet established ground rules and requirements while providing reasonable altitude corridor/margin.

## 5.4 JET ENGINE SYSTEM STUDIES

It has been the purpose of this study to investigate and assess the implications of requirements leading to the selection of a jet engine system. Of main concern were the following primary modes of operation:

- Cruise back of the booster
- Go-around capability for the booster and orbiter
- Ferry performance

A fourth mode, which is applicable to the orbiter only, is the minimum requirement of instant L/D. This particular mode has been studied for purposes of comparison.

The primary objective has been to accommodate the requirements of the modes of operation and to study parameters leading to the minimization of the jet system weight. Parameters available in the selection of jet engine systems are the unique characteristics displayed by the low and high bypass ratio turbofan, as well as the lift engine. Considerations of engine weight and specific fuel consumption, coupled with the variational effects of the performance delivered with altitude and Mach number, must be combined with the operational time. In addition, the final jet system size and operating condition is further influenced by the vehicle weight and aerodynamic properties.

These considerations have been studied, as documented in the following paragraphs.

### 5.4.1 Cruise-Back Performance for the Booster Vehicle

The study of the cruise-back operation is one in which engine class selection, operating altitude, and Mach number are combined to determine the minimum jet system weight. As brought out in 5.3, the summation of booster ascent and entry range is in the order of 400 nm. The operational time of cruise back is therefore in the order of 1-1/2 to 2 hours and, as shown in Fig. 5-27, the minimum jet engine system weight is provided by a high bypass ratio turbofan engine. While the figure is representative of sea level operation, similar results were obtained for higher cruise altitudes.



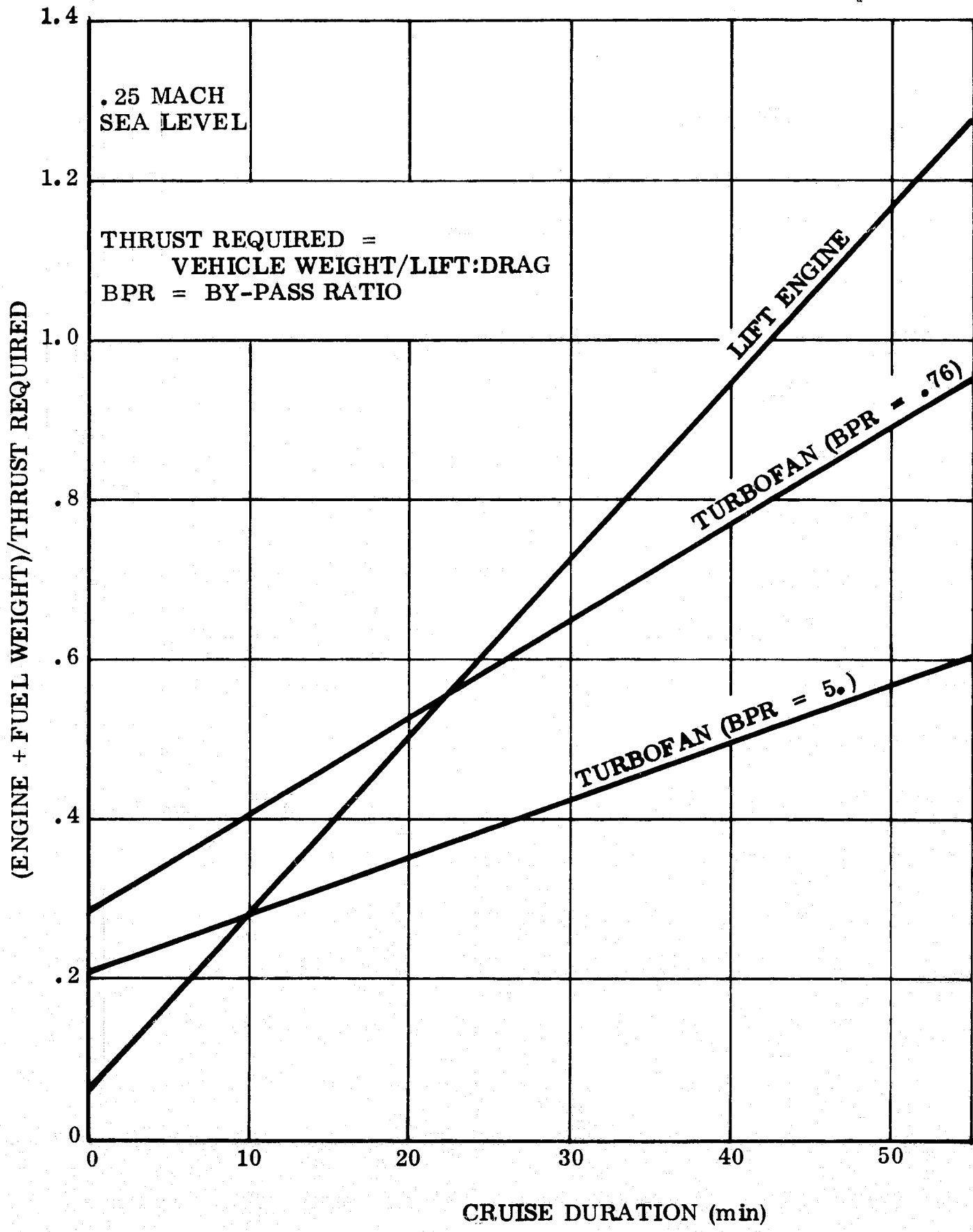


Fig. 5-27 Cruise System Weight

With the trimmed booster aerodynamics shown in Vol III, a study was made to minimize the system weight of the booster vehicle for a cruise-back range of 400 nm. As shown in Fig. 5-28, minimum fuel weight for cruise back occurs when the booster is operating at the highest possible altitude, 40,000 feet. This is also the highest altitude at which the engines selected can be started. However, at these high altitudes, engine performance is poor and more thrust is required. This correspondingly means heavier and larger engines, resulting in increased engine installed weight, as shown in Fig. 5-29. With the effects of fuel and engine weight combined, it can be seen from Fig. 5-30 that economical cruise-back performance (minimum system weight) occurs when the booster is cruising at altitudes under 20,000 feet. Figure 5-30 indicates that the altitude for minimum system weight lies between sea level and 20,000 feet and that the booster is operation at a lift coefficient near but on the front side of the booster's L/D maximum. To determine the fuel and system weights for cruise-back ranges other than 400 nm, the incremental fuel and range curve shown in Fig. 5-31 can be used to determine the fuel reduction or addition to cruise ranges other than 400 nm.

The effect of vehicle aerodynamics on the cruise-back range is shown in Fig. 5-32. It was assumed that the L/D ratio of the booster can be increased 10 percent by raising the lift 10 percent or by reducing the vehicle drag 10 percent. From Fig. 5-32 it can be seen that the reduction in drag results in a direct increase in range. However, the increase in lift results in a small increase in range at the lower angle of attack and a much higher increase in range at the higher angle of attack, because at lower angles of attack, the vehicle is operating along the flat part of the drag curve, where changes in the coefficient are small. However, at the higher angles of attack, the vehicle is operating on the drag curve, where there is a definite slope and an increase in lift results in large reduction in vehicle drag. Thus, as indicated in Fig. 5-32, the most advantageous way of increasing booster cruise coefficient back range is by reducing the vehicle drag rather than trying to increase lift coefficient.

BOOSTER EMPTY WEIGHT = 350,000 lb  
REFERENCE AREA = 12,000 ft<sup>2</sup>

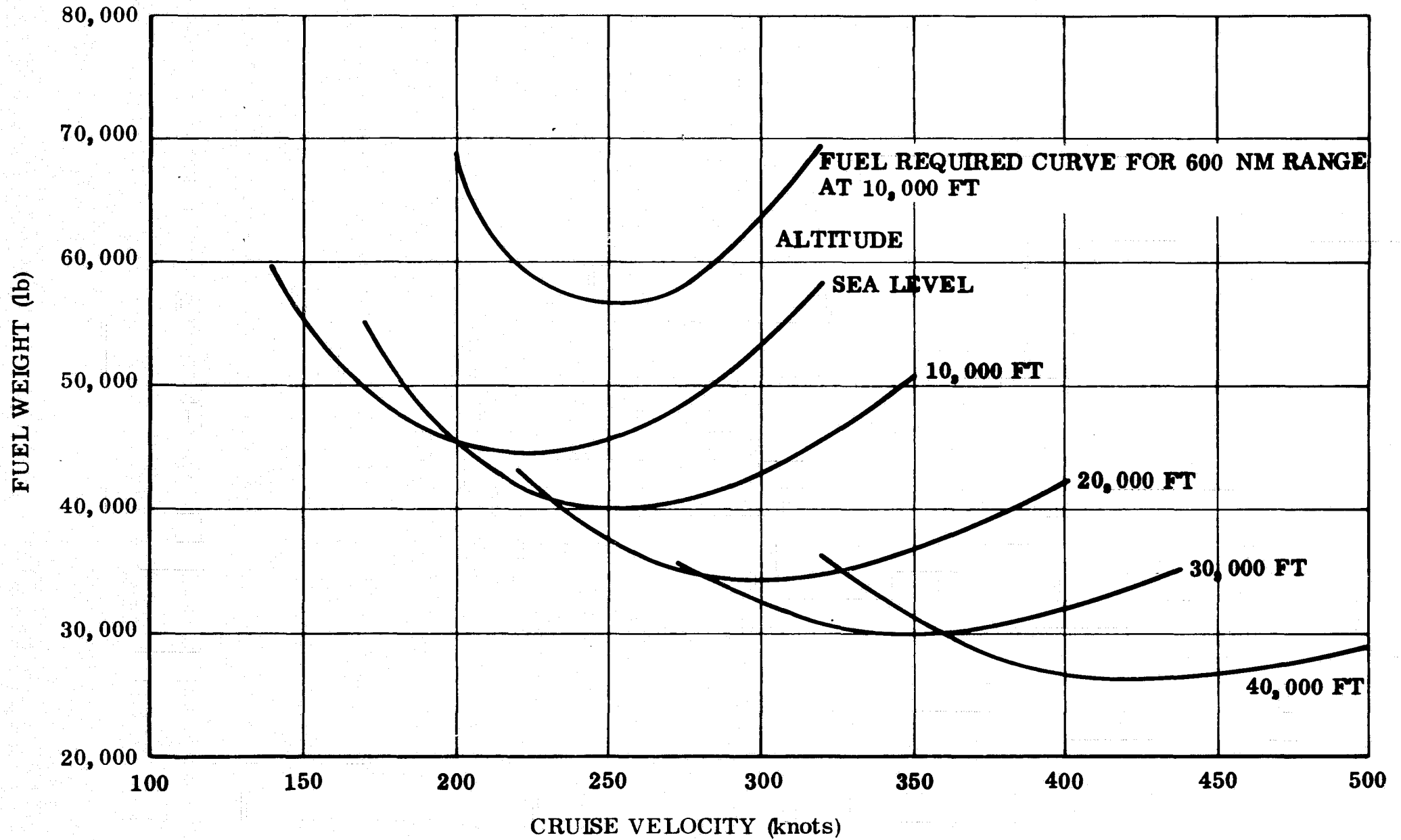


Fig. 5-28 Fuel Required for Booster Vehicle to Cruise 400 nm at Altitude

BOOSTER VEHICLE EMPTY WEIGHT = 350,000 lb  
REFERENCE AREA = 12,000 ft<sup>2</sup>

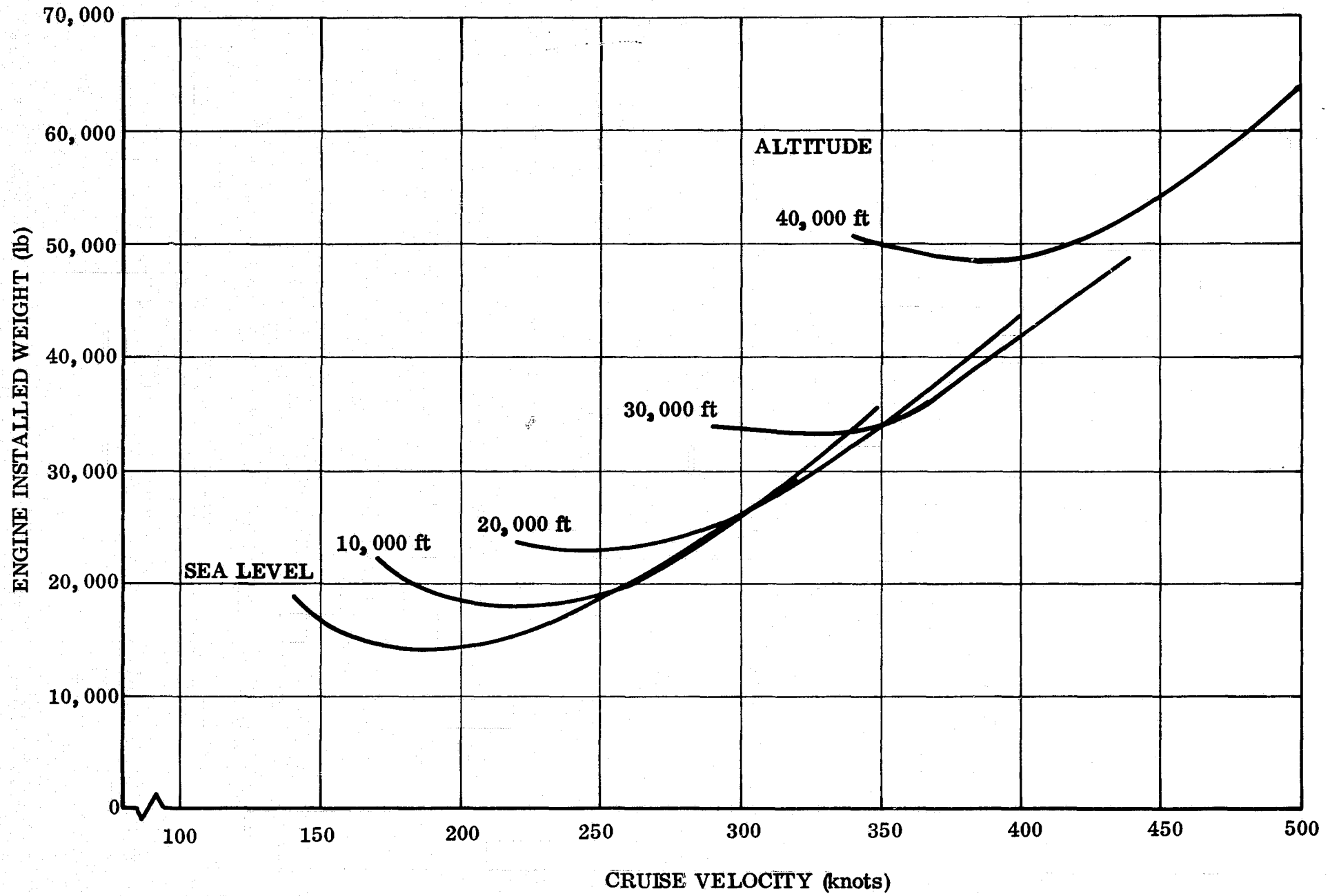


Fig. 5-29 Engine Installed Weight vs Cruise Velocity for Booster to Cruise 400 nm at Altitude

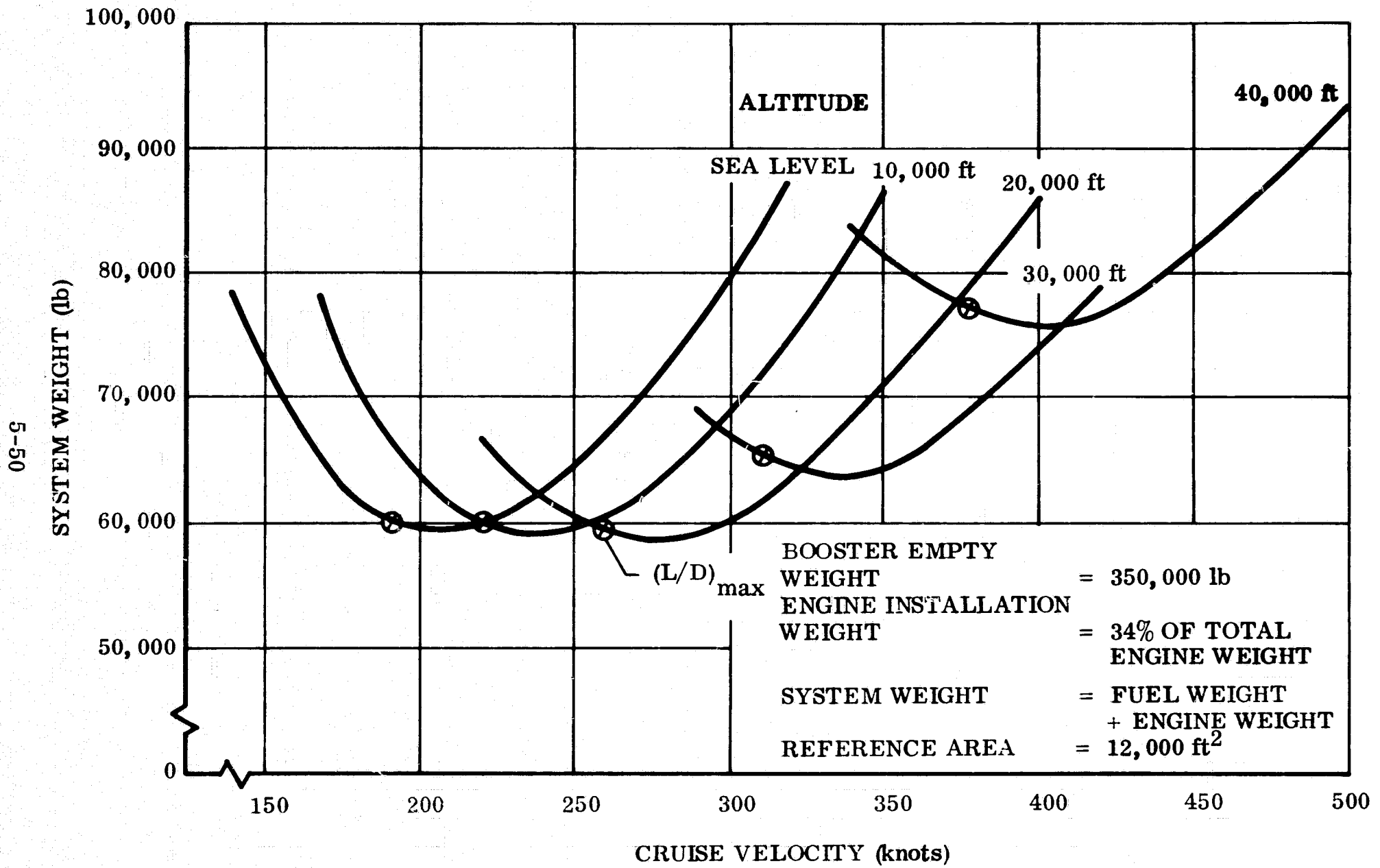


Fig. 5-30 System Weight for Booster to Cruise 400 nm at Altitude

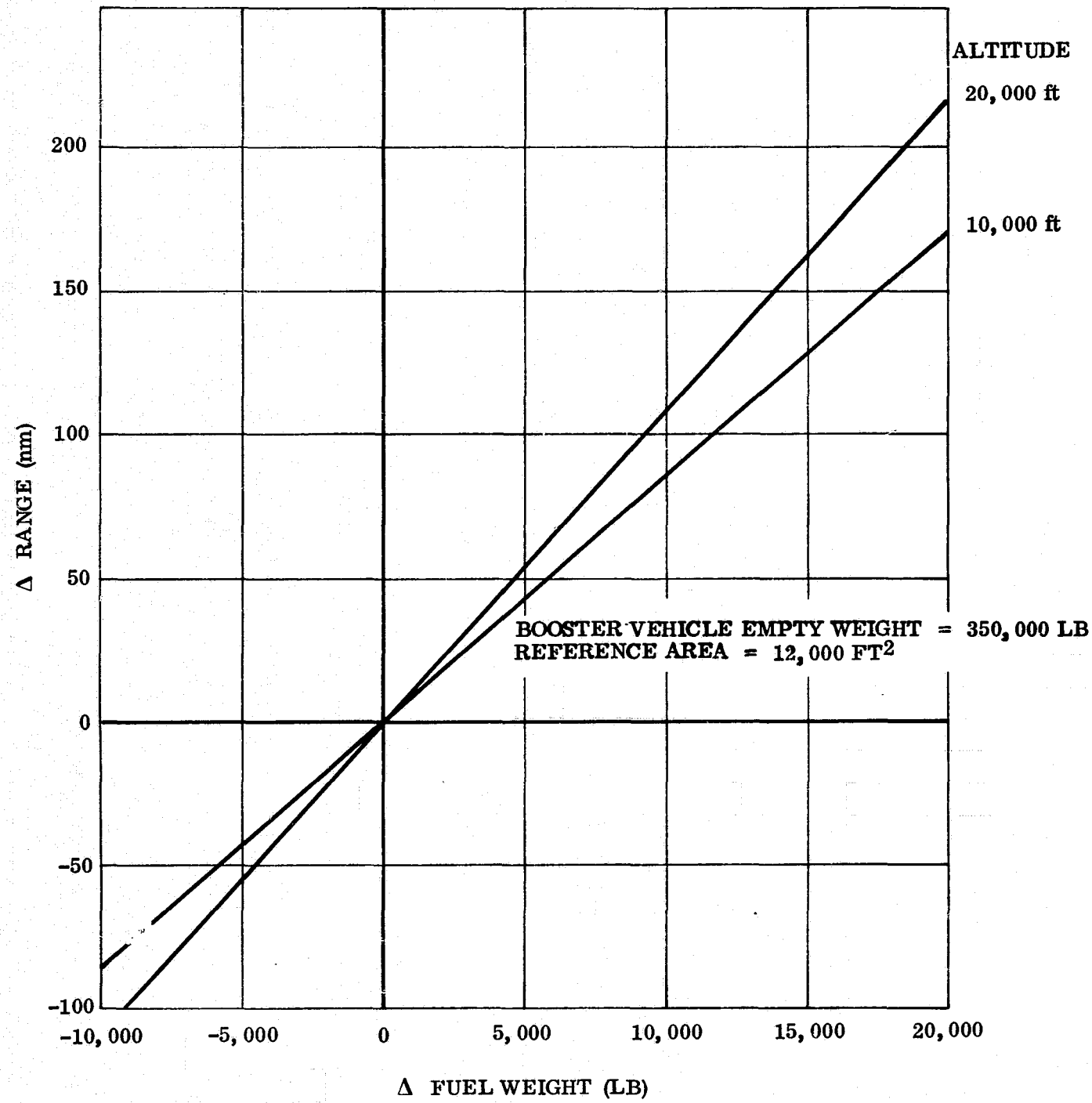


Fig. 5-31 Additional Fuel Required for Incremental Increases in Cruise-Back Range for Booster Vehicle

BOOSTER EMPTY WEIGHT = 350,000 LB  
FUEL WEIGHT = 40,000 LB  
ALTITUDE = 10,000 LB

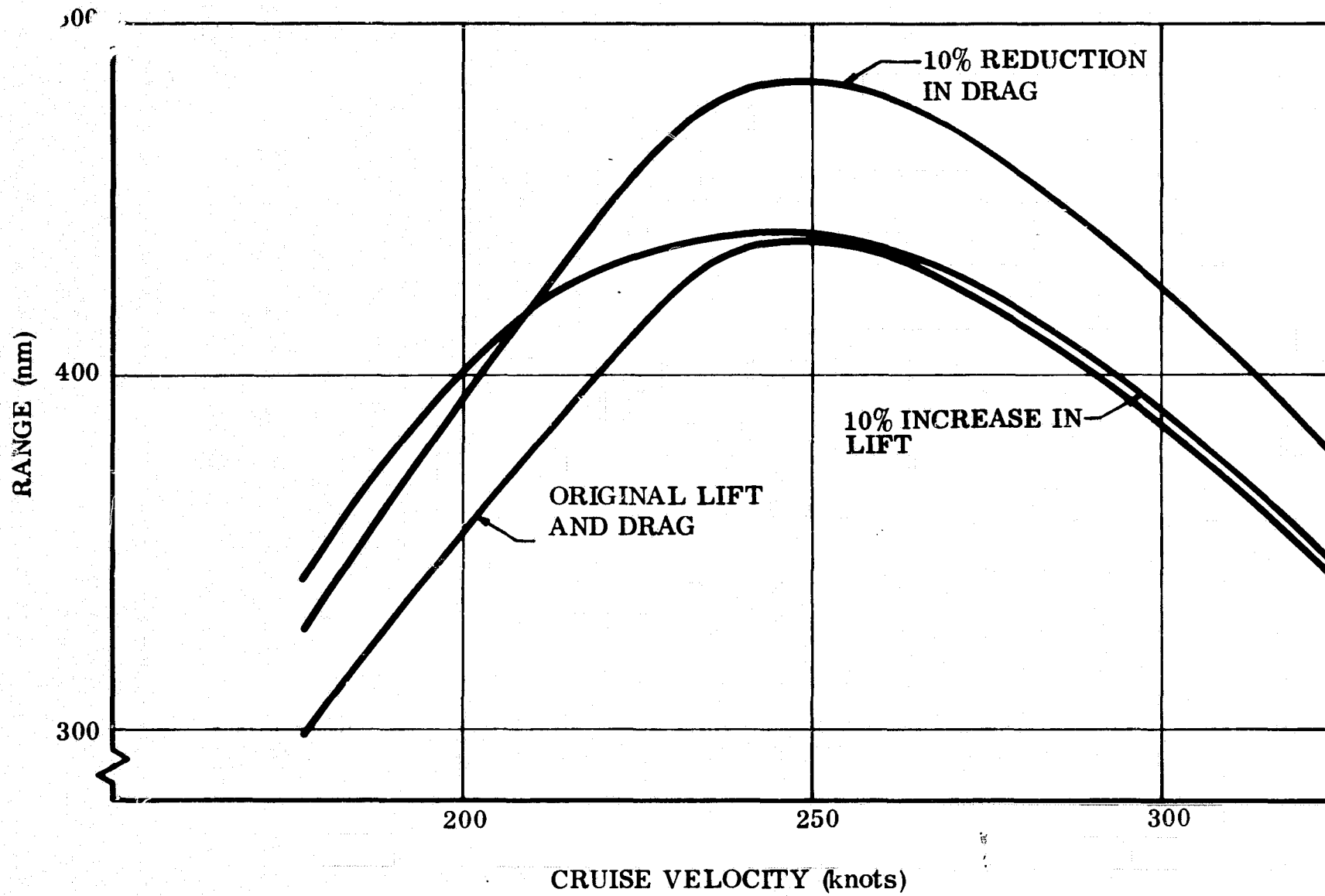


Fig. 5-32 Effect of Varying Vehicle Aerodynamics on Range Capability of Booster

#### 5.4.2 Approach and Landing Performance

The trajectory dynamics and performance characteristics of the booster and the orbiter for horizontal landing have been studied, as discussed in Volume III, Section 5.1, of this report.

The orbiter approach and landing pattern established enables either a normal power-on landing or an emergency dead-stick landing in event of failure of the jet engines to start. As shown in Fig. 5-33, as the orbiter glides toward the landing field, an engine start sequence is initiated at 40,000-foot altitude. A decision-key point is established at 25,000 feet. If the engines have started by this time, a 360-degree spiral turn is made, leading to a standard aircraft final approach and landing pattern. If the engines have not started at decision key, a straight-in-gliding approach is made and landing is accomplished in the same manner as at NASA-FRC (Edwards) with the X-15, M2-F2, X-24, and HL-10.

Orbiter touchdown speed with a powered approach is 160 knots; and with an unpowered approach, 168 knots. Both speeds are sufficiently low to meet NASA safety criteria and to enable operation on 10,000-foot runways.

The booster will necessarily be approaching the landing field with jet engines running and therefore will not require dead-stick landing capability. Booster landing patterns are expected to be similar to those of present jet transport aircraft. The low booster wing loading results in a touchdown speed of only 128 knots.

A standard go-around pattern has been established, (as shown in Fig. 5-34); and jet thrust and fuel requirements have been identified. The go-around maneuver is expected to be similar to that for present large aircraft.

#### 5.4.3 Ferry Mission

A comprehensive analysis of the ferry missions of the orbiter and the booster is reported in Volume III. Contained in this section is a brief summary of the ferry study to permit comparison of the effects of criteria on jet system size.



5-54

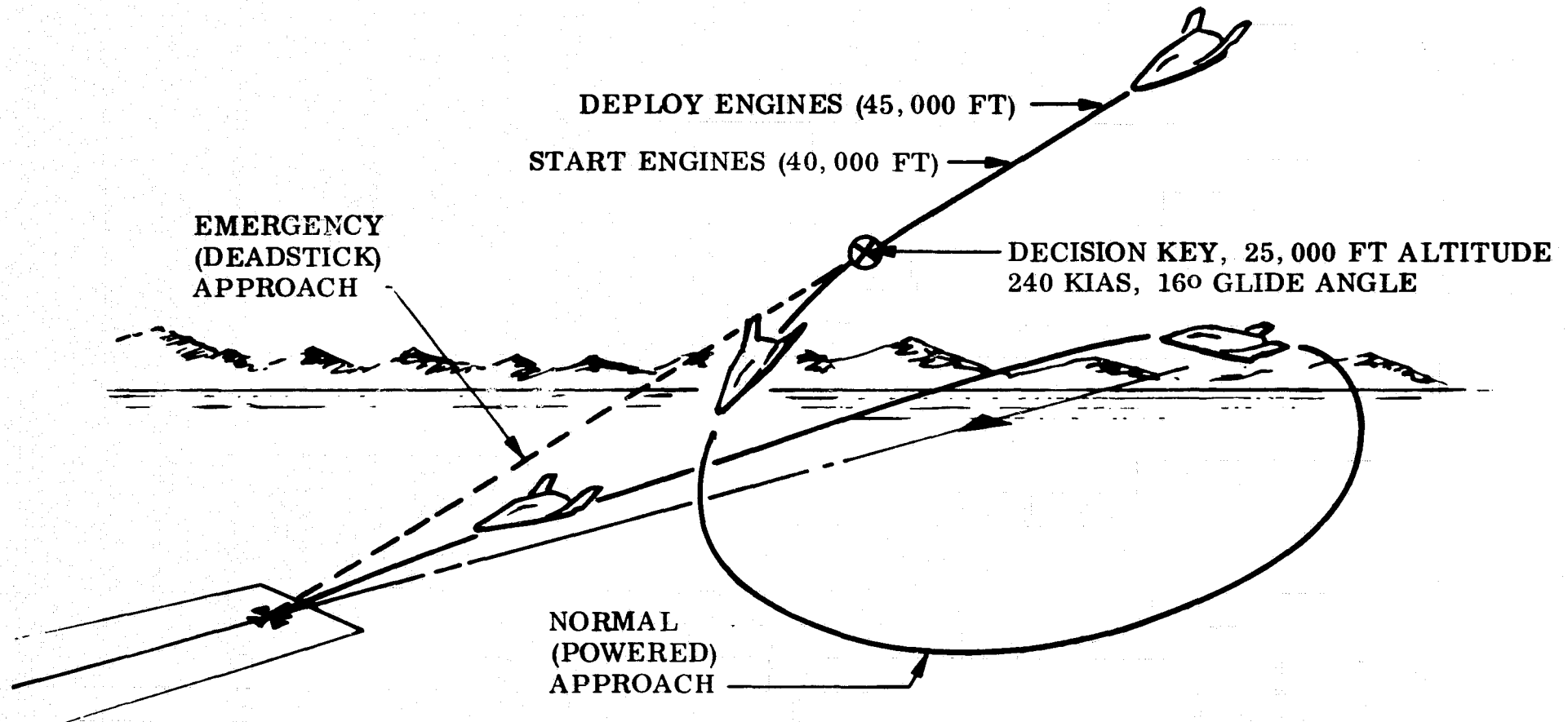
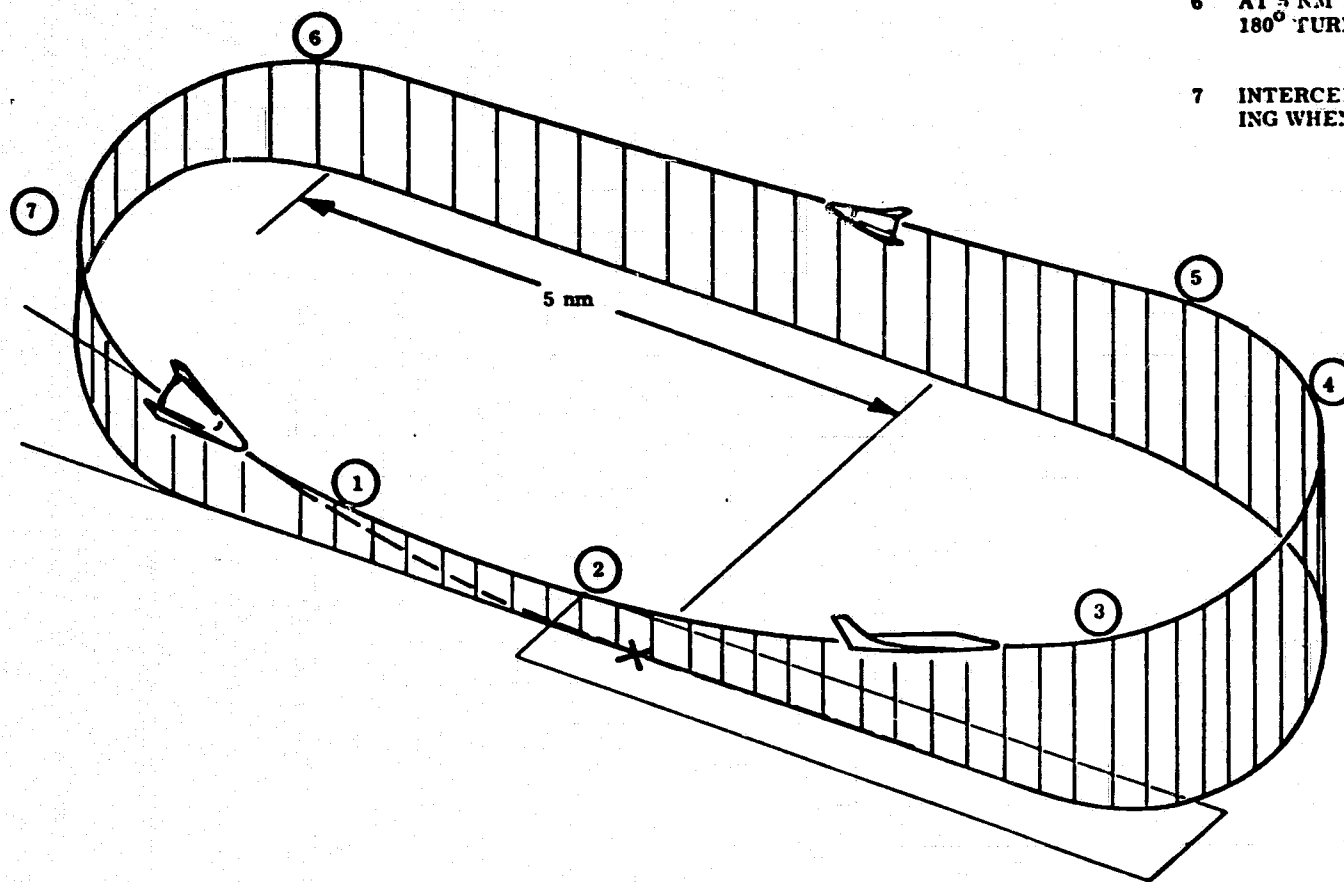


Fig. 5-33 Typical Orbiter Approach



- 1 INCREASE THRUST AND INITIATE PULLUP
- 2 ESTABLISH MAX CLIMB AT MAX L/D
- 3 AT 1000 FT ALTITUDE, INITIATE 180° TURN AND INCREASE AIRSPEED TO 110% V L/D MAX
- 4 AT 2000 FT ALTITUDE, ESTABLISH LEVEL FLIGHT AT V = 110% V APPROACH
- 5 ROLL OUT OF TURN AT 180° POINT, ESTABLISH DOWNWIND LEG
- 6 AT 5 NM FROM TOUCHDOWN POINT INITIATE 180° TURN TO FINAL APPROACH
- 7 INTERCEPT GLIDE SLOPE AND RUNWAY BEARING WHEN APPROPRIATE

Fig. 5-34 Go-Around Profile

The ferry mission consists of the vehicle accomplishing a takeoff, climb-to-altitude, cruise, descent, and landing. Figure 5-35 summarizes the fuel requirements associated with ferry range, vehicle weight, and cruise altitude and includes an assessment for takeoff, climb, and descent. Four 40,000-pound thrust engines were assumed in this study with the size dictated mainly by takeoff and climb requirements. The engine size influence on fuel requirements has been determined to be of secondary significance. The satisfaction of ferry requirements is accomplished therefore with a much larger jet system than was evidenced for go-around or cruise back. Should ferrying become a requirement, it is recommended that a strap on system be considered.

#### 5.4.4 Jet System Comparisons

A study of subsonic performance has been accomplished in the sense of satisfying each mode of operation through separate analyses. A comparison of the operational modes is contained in Table 5-3, reflecting the approach used and the jet system weight (fuel plus installed engine weight) required if those modes were imposed on an orbiter vehicle.

In the case of instant aerodynamic improvement (L/D), the short operation time (in the order of 6 minutes) supports the selection of the jet engine system based primarily on engine installed weight, with specific fuel consumption being of secondary importance. The lift fan engine, which shows both the lightest weight and thrust degradation with velocity, is therefore the selected system for instant L/D. For go-around, marked improvement in specific fuel consumption of a high bypass ratio turbofan makes it the best candidate. This situation, of course, holds for the cruise and ferry modes.

It is interesting to note that the engine required for go-around corresponds in size to that which would be used for cruise. The additional system weight between the two operational modes is therefore due to the propellant requirements. In the ferry mode, takeoff field length in the presence of an engine out increases significantly the engine size requirements. Additional fuel for takeoff and climb to cruise altitude is of secondary importance.

4-40,000 lb THRUST ENGINES  
 ORBITER/TWO STAGE  
 ENGINE WEIGHT =  $\frac{4 \times 40,000 \times 1.34}{6.5} = 32,984.6 \text{ lb}$

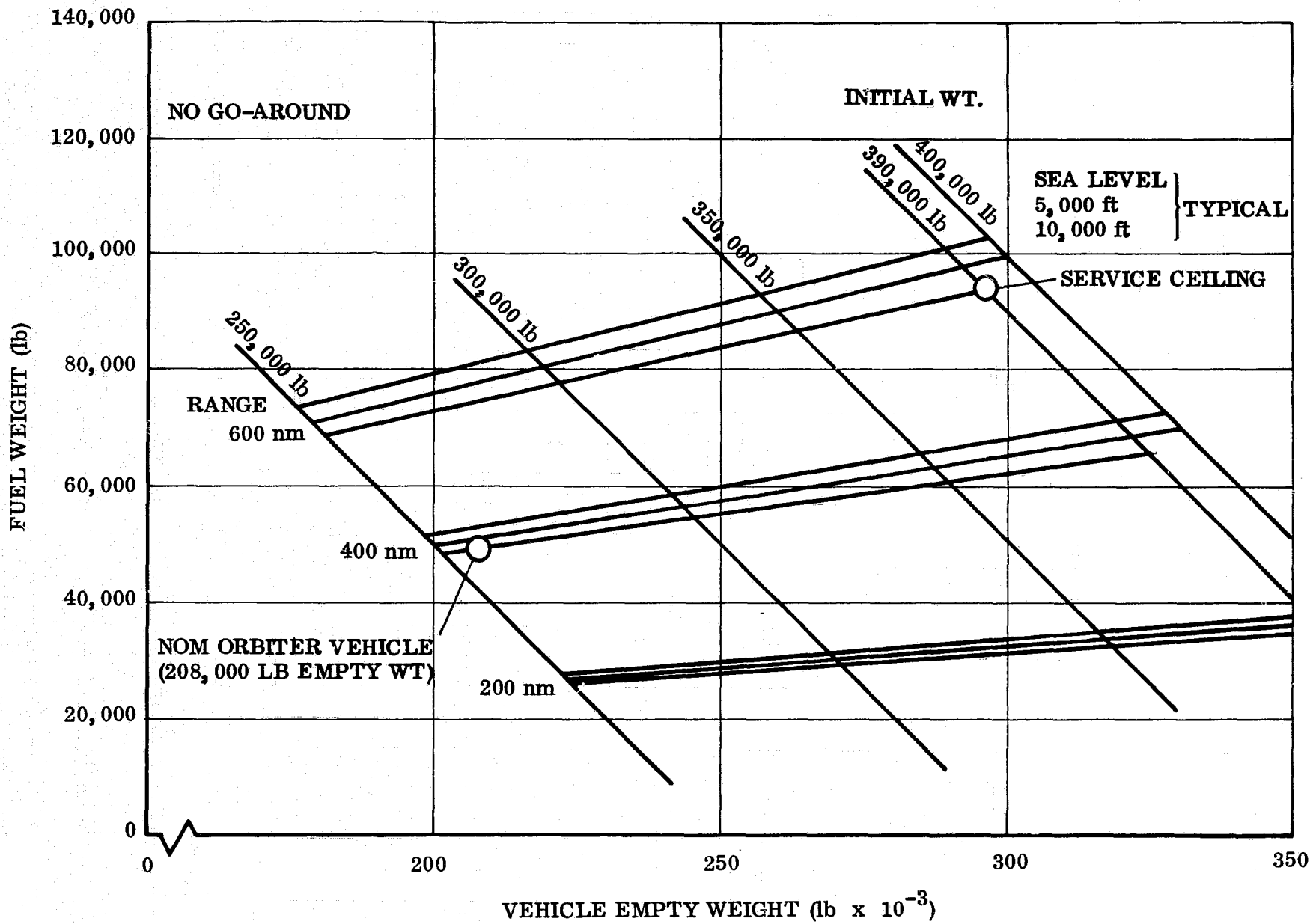


Fig. 5-35 Fuel Required for Ferry Mission of Orbiter at Various Altitude and Initial Weight

It can be seen in Table 5-3 that the final selection of the operational requirement will severely impact the size of the launch system.

Table 5-3  
EFFECT OF JET SYSTEM CRITERIA

	Instant L/D	Go- Around	Cruise 400 nm	Ferry 400 nm
Power setting	Takeoff	Takeoff	Max cont	Takeoff
Operating altitude - feet	Sea level	3,000	1,000	Sea level
Selected engine	Lift fan	Turbofan	Turbofan	Turbofan
Number - takeoff static rating - lb	4 - 10,000	4 - 25,000	4 - 25,000	4 - 40,000
Installed engine weight - lb	3,200	20,600	20,600	33,000
Fuel - lb	4,700	6,000	46,200	49,000
Total system weight - lb	7,900	26,000	66,800	82,000

Section 6  
**AERODYNAMICS**

Aerodynamic characteristics are presented for the orbiter, the return booster, the composite two-stage, and the composite Triamese configurations shown in Figs. 6-1 through 6-4. The orbiter and the return booster, which are used in combination to form the composite Two-Stage and Triamese launch configurations, are sized in each case to meet the mission requirements of the particular composite configuration. The design payload is 50K lb in all cases.

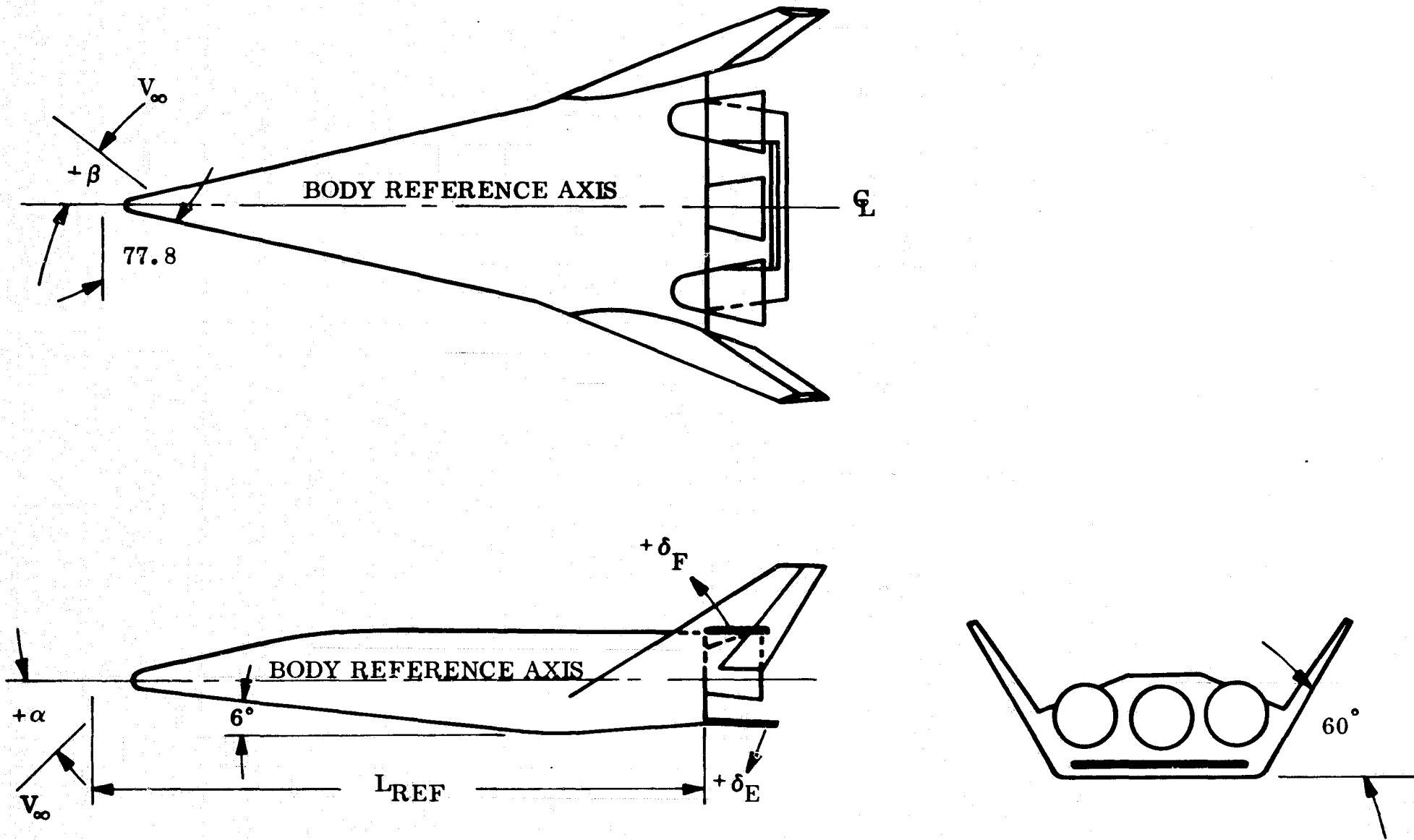


Fig. 6-1 Spacecraft General Arrangement

6-3

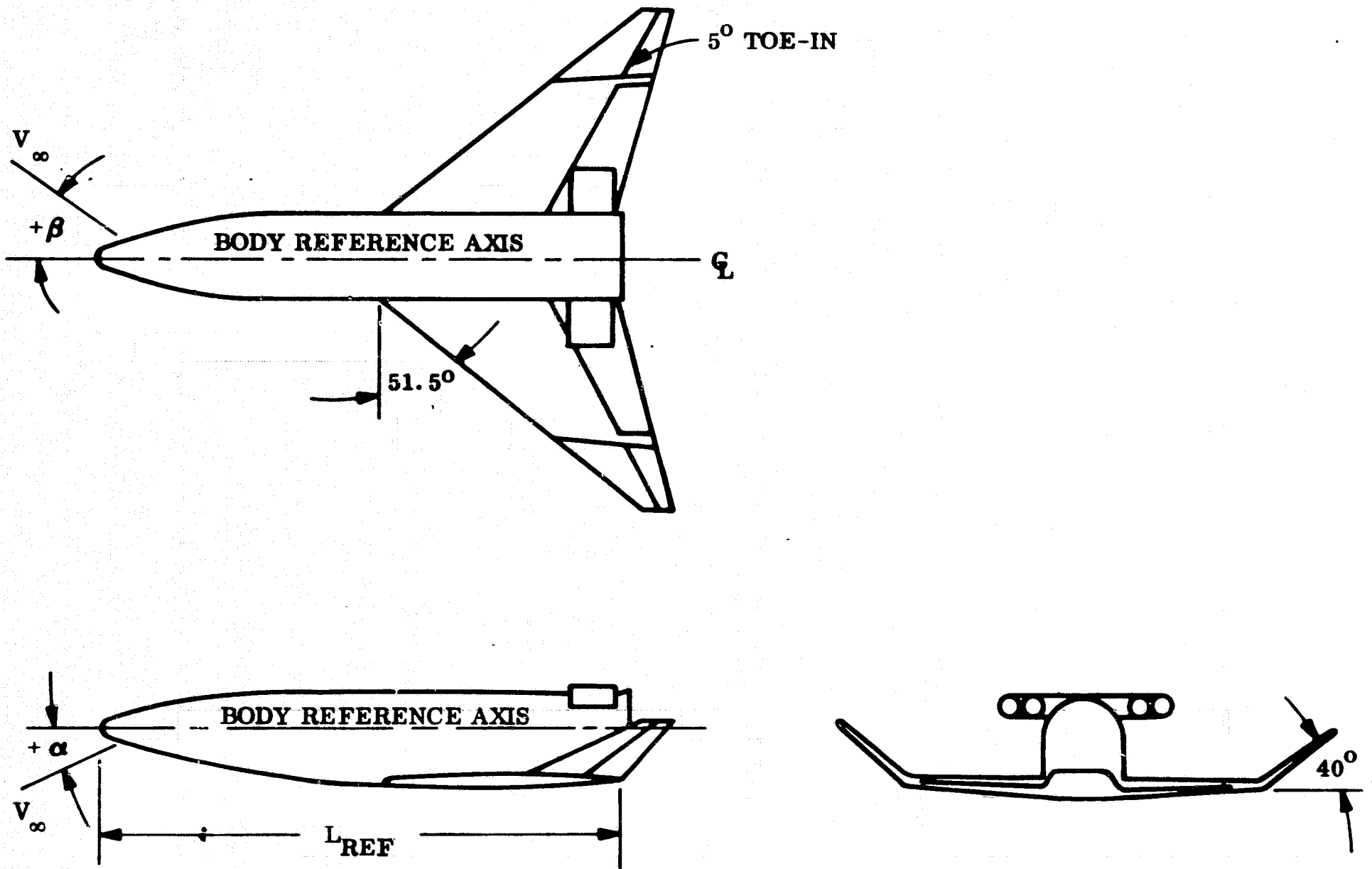


Fig. 6-2 Return Booster General Arrangement



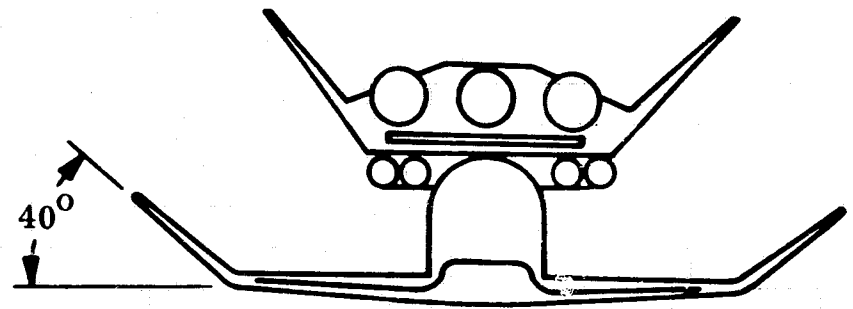
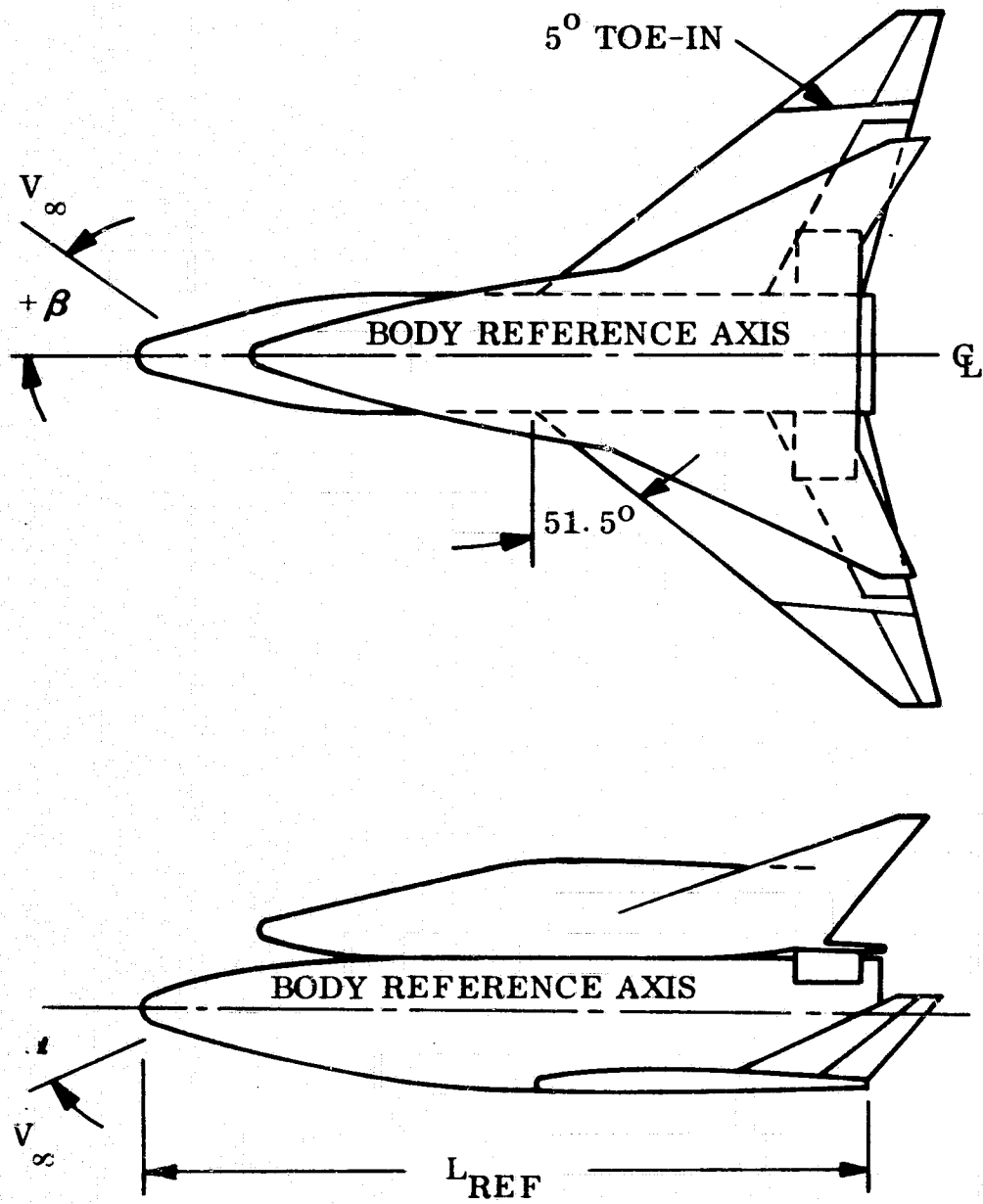
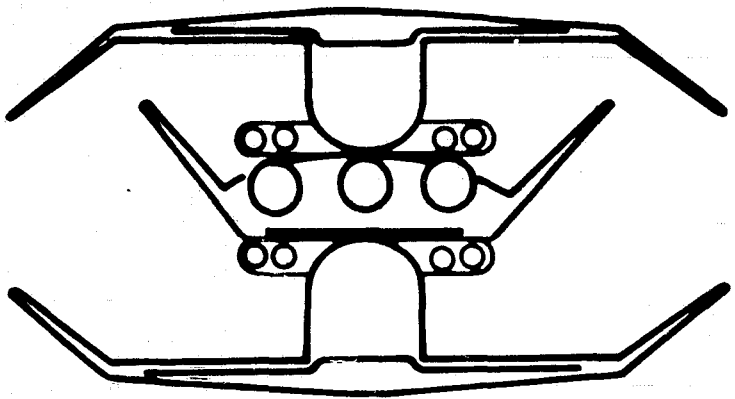
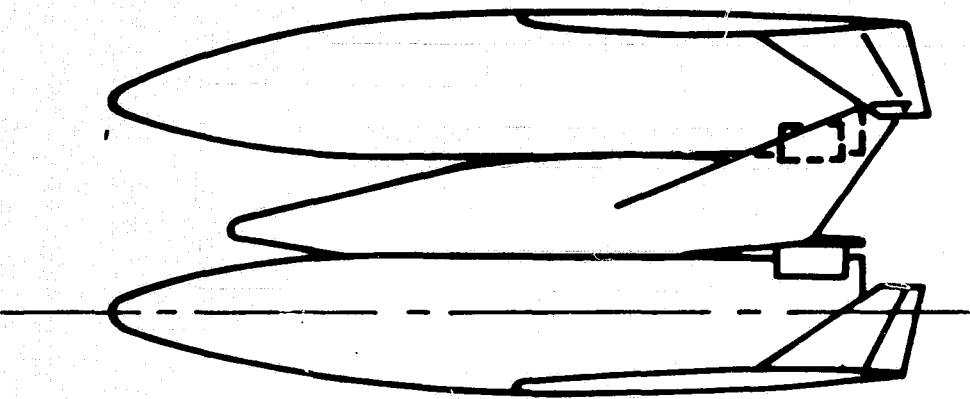
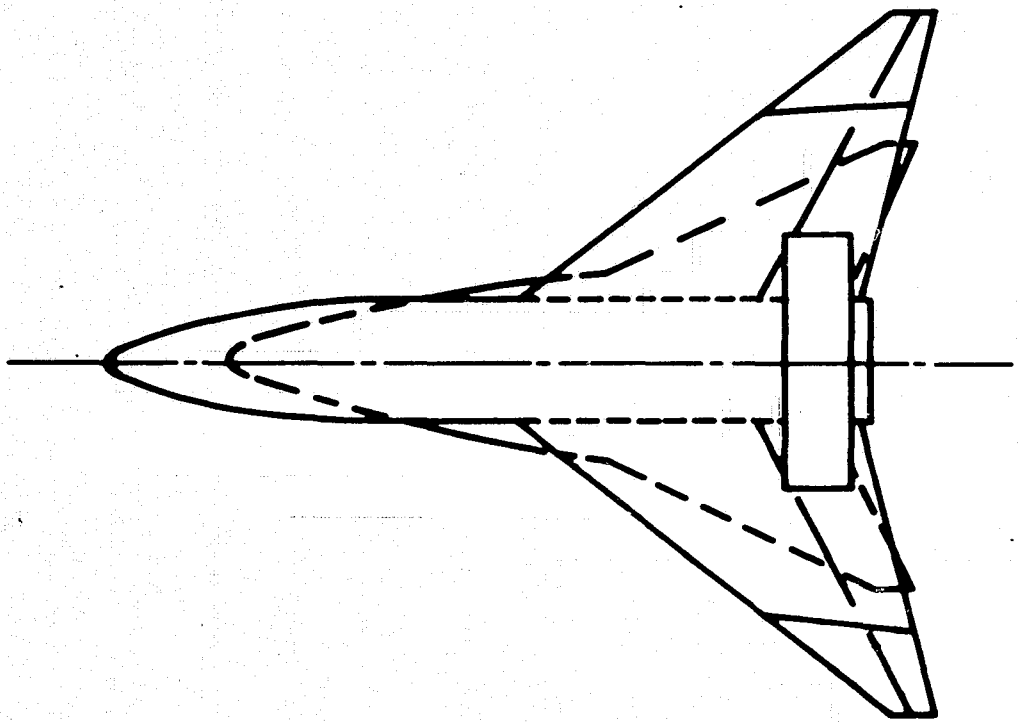


Fig. 6-3 Two-Stage Composite Launch Vehicle General Arrangement



6-5

Fig. 6-4 Triamese Composite Launch Vehicle General Arrangement

Data for the orbiter are based on results of wind tunnel tests and hypersonic predictions made with the aid of an arbitrary body computer program. These data include trimmed subsonic through hypersonic coefficients as well as longitudinal and directional stability characteristics.

The aerodynamic data for the return booster are based on low-speed wind tunnel results for a similar configuration and analytical prediction techniques. Longitudinal trim capability and longitudinal and directional stability characteristics are presented for subsonic ( $M_\infty = 0.2$ ) and hypersonic ( $M_\infty = 10.0$ ) velocities.

Linear aerodynamic coefficients ( $C_{N\alpha}$  and  $C_{A0}$ ) are presented as a function of Mach number for the composite Two-Stage and Triamese launch vehicles. These characteristics have been estimated between Mach 0 and Mach 10.0 for use in trajectory simulation.

Terms are defined as follows, with values given for 50K payload systems:

$A_{Base}$	Base area ~ ft <sup>2</sup>	
$A_{REF}$	Reference area	
	<u>Two-Stage</u>	
	Orbiter	( 5,720 ft <sup>2</sup> )
	Return booster	(12,000 ft <sup>2</sup> )
	Composite launch	(12,000 ft <sup>2</sup> )
	<u>Triamese</u>	
	Orbiter	( 5,720 ft <sup>2</sup> )
	Return booster	( 9,160 ft <sup>2</sup> )
	Composite launch	( 9,160 ft <sup>2</sup> )
$L_{REF}$	Reference length	
	<u>Two-Stage</u>	
	Orbiter	(164 ft)
	Return booster	(206 ft)
	Composite launch	(206 ft)

Triamese

Orbiter (164 ft)  
Return booster (180 ft)  
Composite launch (180 ft)

$C_{A_0}$	Axial force coefficient at zero lift = $\frac{\text{Force}}{q_\infty A_{\text{ref}}}$
$C_N$	Normal force coefficient = $\frac{\text{Force}}{q_\infty A_{\text{ref}}}$
$C_{N_\alpha}$	Normal force coefficient slope ~ per degree
$C_m$	Pitching moment coefficient = $\frac{\text{Moment}}{q_\infty A_{\text{ref}} L_{\text{ref}}}$
$C_l$	Rolling moment coefficient = $\frac{\text{Moment}}{q_\infty A_{\text{ref}} L_{\text{ref}}}$
$C_{l_\beta}$	Rolling moment derivative
$C_n$	Yawing moment coefficient = $\frac{\text{Moment}}{q_\infty A_{\text{ref}} L_{\text{ref}}}$
$C_{n_\beta}$	Yawing moment derivative
$C_{n_{\beta D}}$	Dynamic yawing moment derivative = $C_{n_\beta} - C_{l_\beta} \left( \frac{I_z}{I_x} \right) \sin \alpha$
$M_\infty$	Freestream Mach number
$q_\infty$	Freestream dynamic pressure
mrp	Moment reference point
H	Altitude ~ feet
L/D	Lift-to-drag ratio
$\alpha$	Angle-of-attack ~ degrees
$\beta$	Angle-of-sideslip ~ degrees, positive nose lift
$\delta_E$	Elevon deflection angle ~ degrees, positive trailing edge down
$I_x, I_z$	Moments of inertia

## 6.1 ORBITER CHARACTERISTICS

The aerodynamic force and moment characteristics for the orbiter were determined from a combination of wind-tunnel results; extrapolated wind-tunnel results; and high-speed studies, in which the results of a hypersonic arbitrary body computer routine were used. In general, the subsonic Mach number data are directly related to wind-tunnel results, whereas the high-speed data are a combination of the aforementioned computer analyses and experimental results.

The orbiter, shown in Fig. 6-1, consists of a modified delta planform, configured for efficient use of volume along with acceptable aerodynamic characteristics at all Mach numbers. Forward cross-sections, which are basically triangular, are designed to be shadowed behind the leading edge at a preselected hypersonic attitude. Aft cross-sections are rolled out 30 degrees from the vertical, providing an additional benefit in pitch and yaw stability. The basic body has been cambered to provide favorable trim characteristics for all Mach numbers. Side fins have been added to provide acceptable hypersonic directional and longitudinal stability. Elevons are installed to provide pitch trim over the entire Mach number regime.

Aerodynamic data as a function of angle of attack are presented in Fig. 6-5 for Mach numbers of 0.24 and 20. The maximum trimmed lift-to-drag ratios are seen to be 4.7 at Mach 0.24 and 2.0 at Mach 20.0 for normal force coefficients of 0.42 and 0.24, respectively. The vehicle is stable in pitch at all trim angles of attack at Mach 0.24 and Mach 20.0, as shown. A stable vehicle in yaw is indicated by the dynamic yaw stability parameter at all angles of attack at Mach 0.24 and at angles of attack greater than 10 degrees at Mach 20.

The longitudinal stability characteristics for the Mach number regime are shown in Fig. 6-6. A trimmable vehicle throughout the Mach number regime is shown with no transonic pitch-up noted for the anticipated normal force coefficient range.

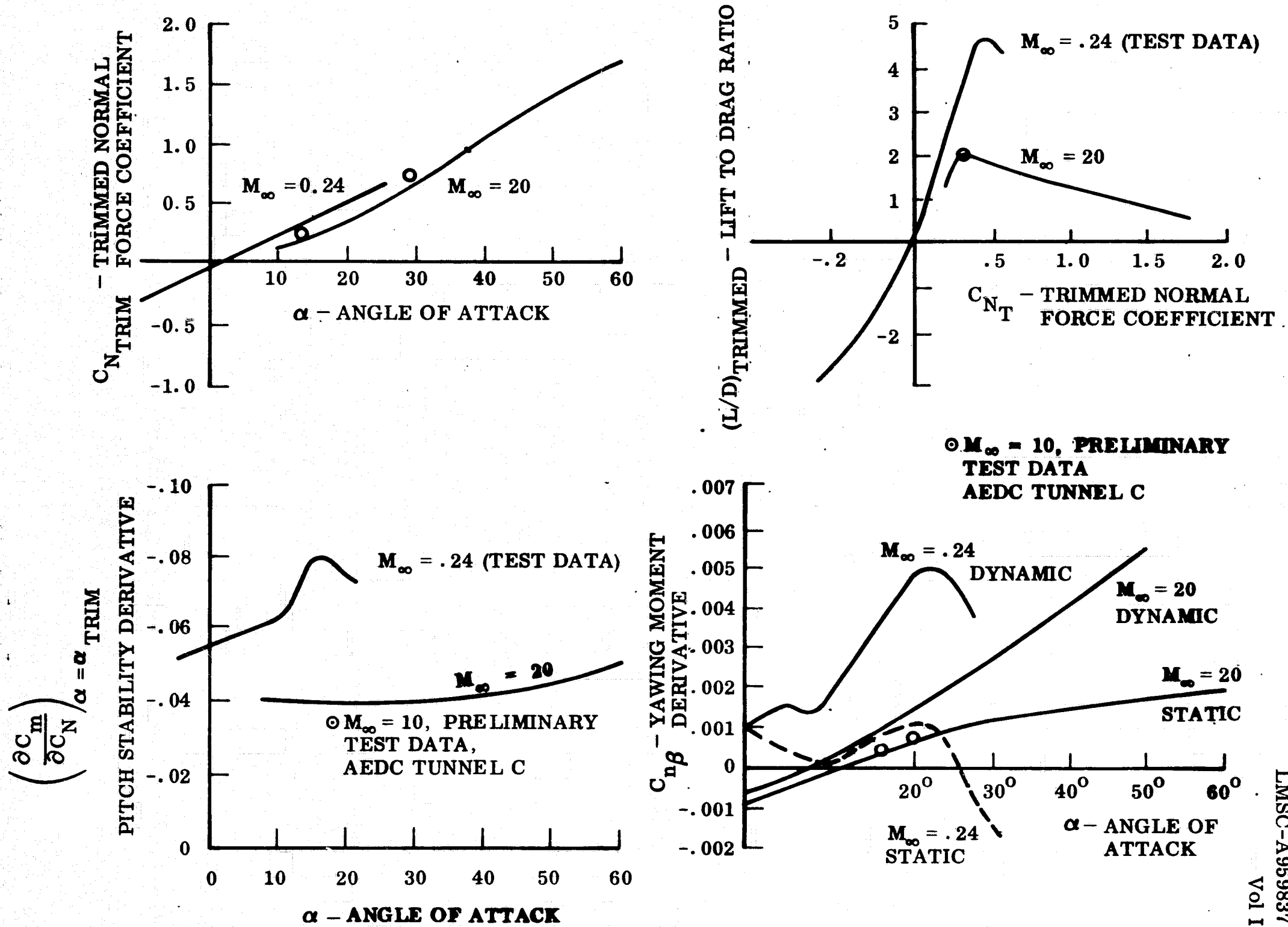


Fig. 6-5 Orbiter Aerodynamic Trim Characteristics - Subsonic and Hypersonic

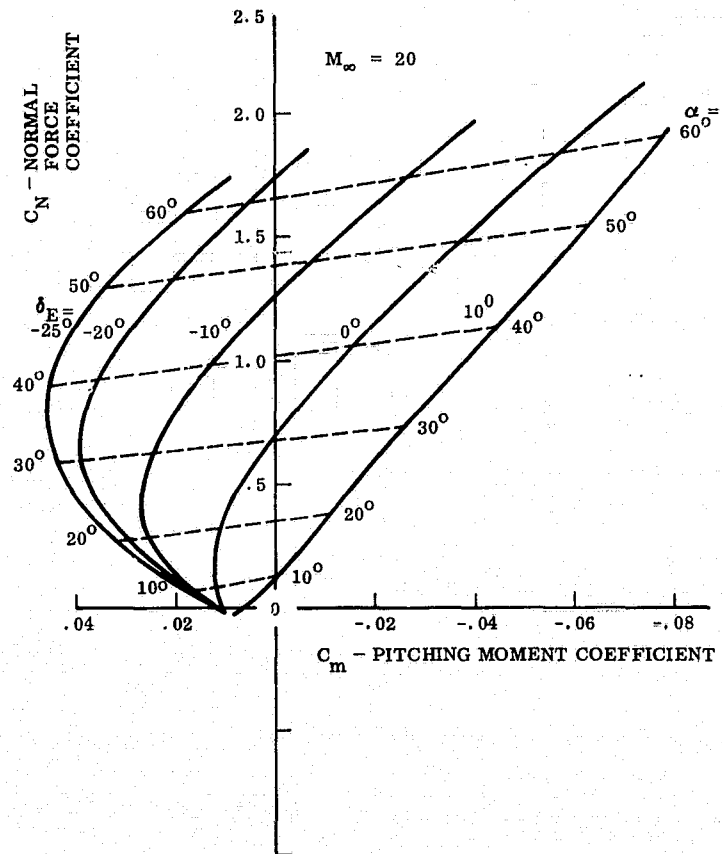
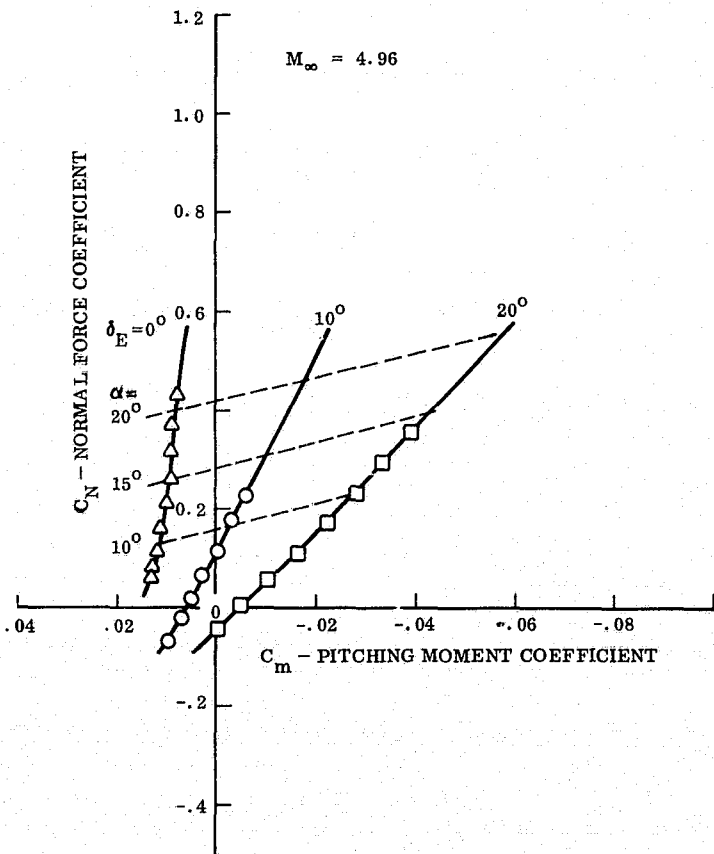
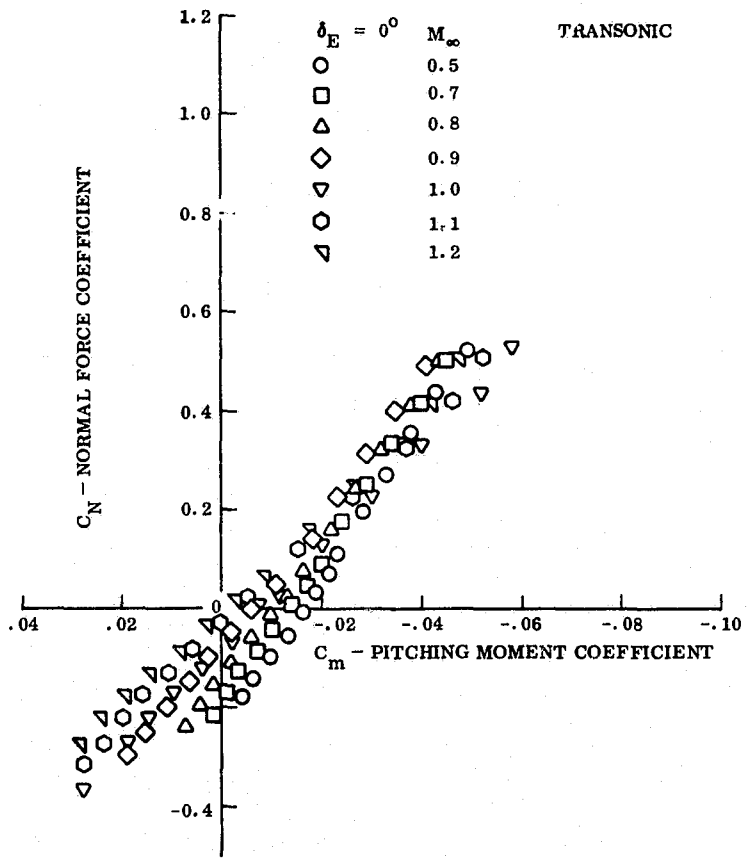
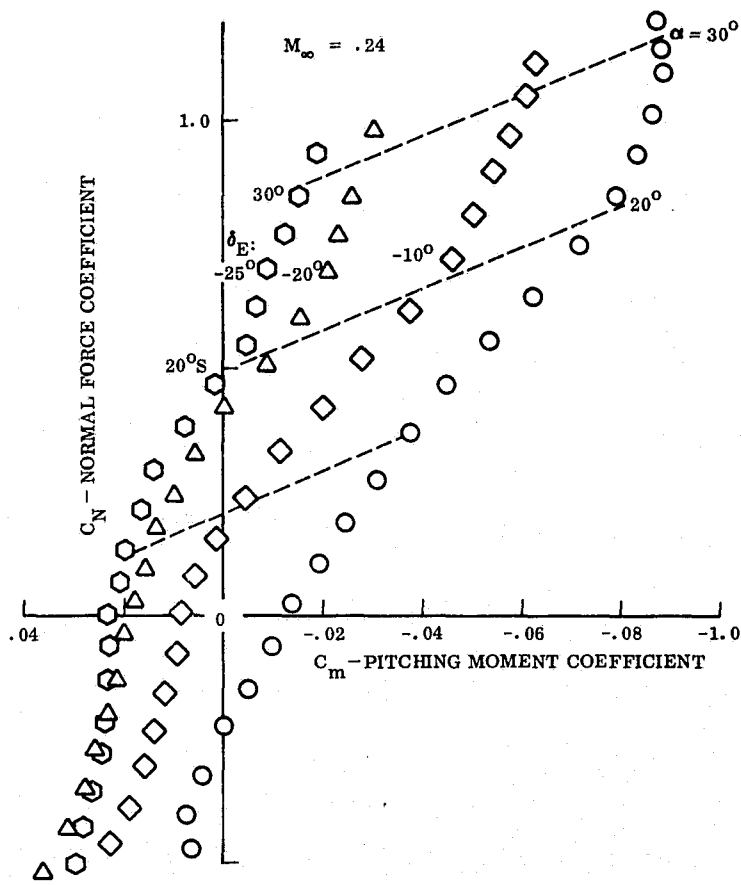


Fig. 6-6 Orbiter Longitudinal Stability Characteristics

The variation of vehicle aerodynamic characteristics with Mach number is summarized in Figs. 6-7 and 6-8. The trimmed normal force variation with Mach number shown in Fig. 6-7 for  $\delta_E = +10^\circ$  to  $-25^\circ$  indicates that a wide range of trimmed vehicle attitudes can be attained. Full-scale maximum trimmed lift to drag ratio variation with attitude is shown in Fig. 6-7 for a typical Mach number-altitude variation. As previously noted, the maximum trimmed lift-to-drag ratio varies from 4.7 at subsonic Mach numbers to 2.0 at hypersonic Mach numbers. Stable pitch trim at  $L/D_{\max}$  is attained throughout the flight regime. The normal force slope and zero lift axial force variation with Mach number is shown in Fig. 6-8. The rolling and yawing moment derivation variation with Mach number indicates a stable vehicle in roll and yaw for the Mach number regime.

## 6.2 RETURN BOOSTER CHARACTERISTICS

The aerodynamic force and moment characteristics were determined from low-speed wind tunnel results for a similar configuration as well as data predicted by use of the USAF Datcom, RAS Data Sheets, and a hypersonic arbitrary body computer routine.

The booster, shown in Fig. 6-2, consists of a fuselage, configured to provide the required volume efficiently, and a 51.5-degree sweep clipped-arrow wing. The wing is located aft on the fuselage with a surface area and planform selected to provide the required lift and stability throughout the Mach number regime. Partial span elevons are installed to provide trim and pitch control throughout the Mach number range encountered. The wing tips are rolled up to provide adequate lateral and directional stability. Rudders are installed on the trailing edge of the rolled up wing tips to provide yaw control.

Return booster aerodynamic data as a function of angle of attack are presented in Fig. 6-9 for Mach numbers of 0.20 and 10.0. The maximum untrimmed lift-to-drag ratio - 8.1 at Mach 0.2 and 1.5 at Mach 10.0 - occurs at angles of attack of 5.5 and 21.5 degrees, respectively. The maximum subsonic lift-to-drag ratio of 8.1 will provide efficient subsonic cruise capability, while the hypersonic value of 1.5 is sufficient to meet the high-speed requirements. The dynamic yaw stability parameter shown in Fig. 6-9 indicates yaw stability at all angles of attack for Mach 0.2 and at angles of greater than 10.0 degrees for Mach 10.0. A stable vehicle in roll is indicated at Mach 0.2 and 10.0.



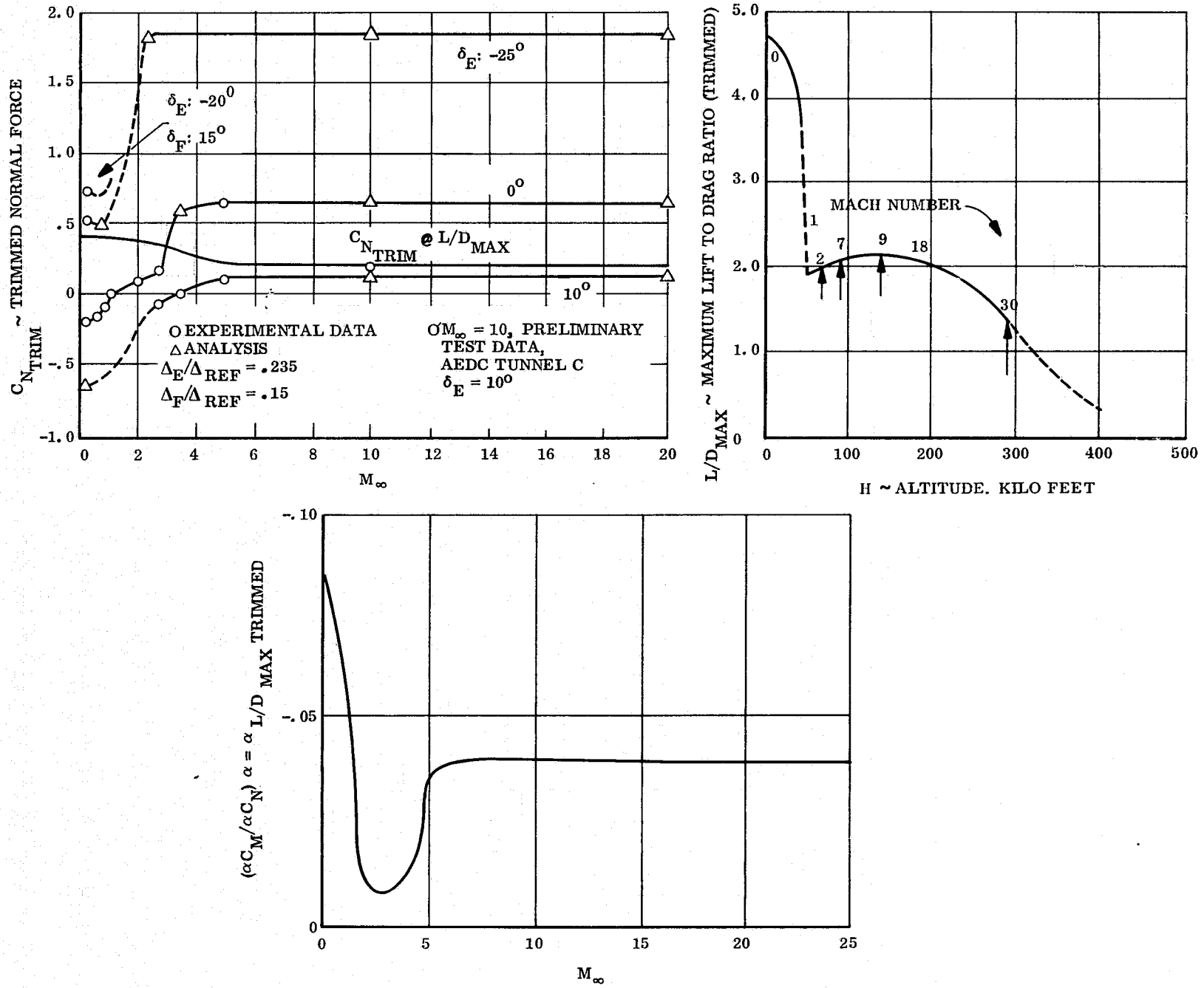
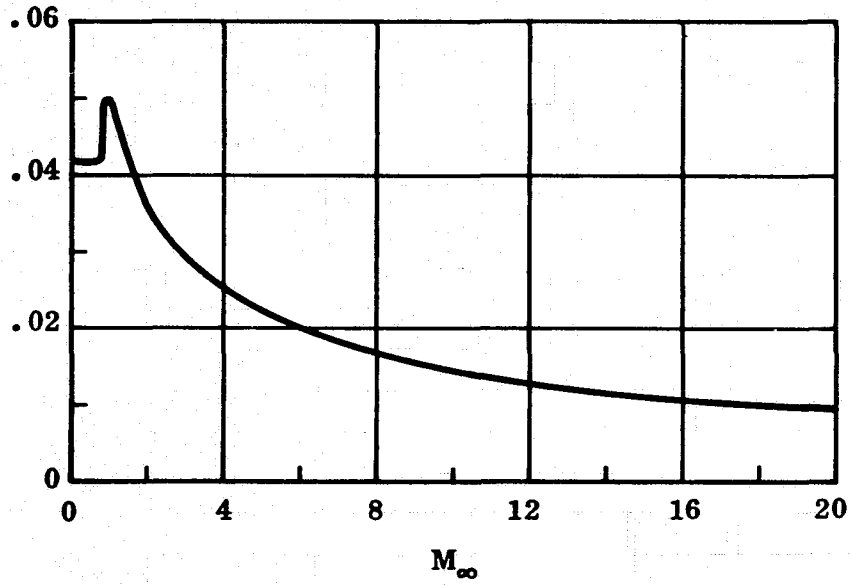


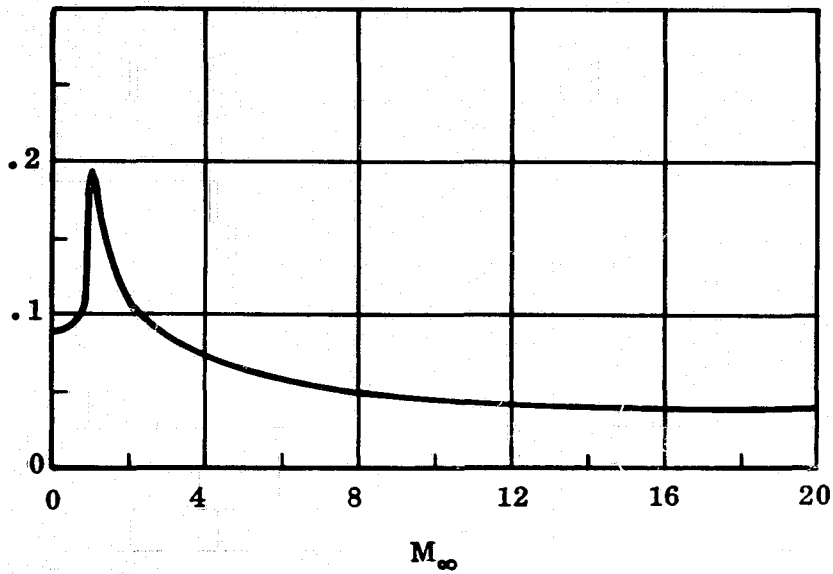
Fig. 6-7 Orbiter Trim Characteristics as a Function of Mach Number

6-13

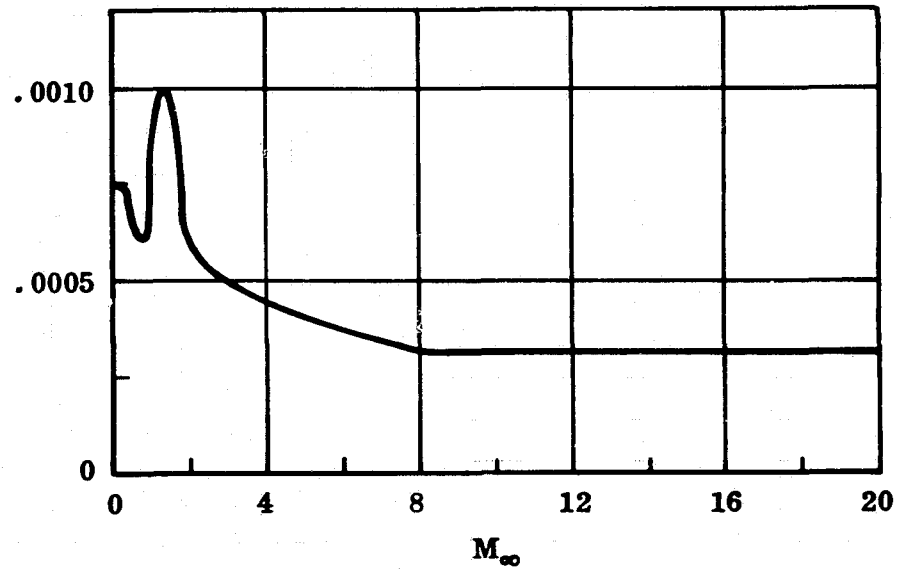
$C_{N\alpha}$  ~ NORMAL FORCE COEFFICIENT SLOPE



$C_{A_0}$  ~ ZERO LIFT AXIAL FORCE COEFFICIENT



$C_{n\beta} @ \alpha_{L/D MAX}$



$C_{L\beta} @ \alpha_{L/D MAX}$

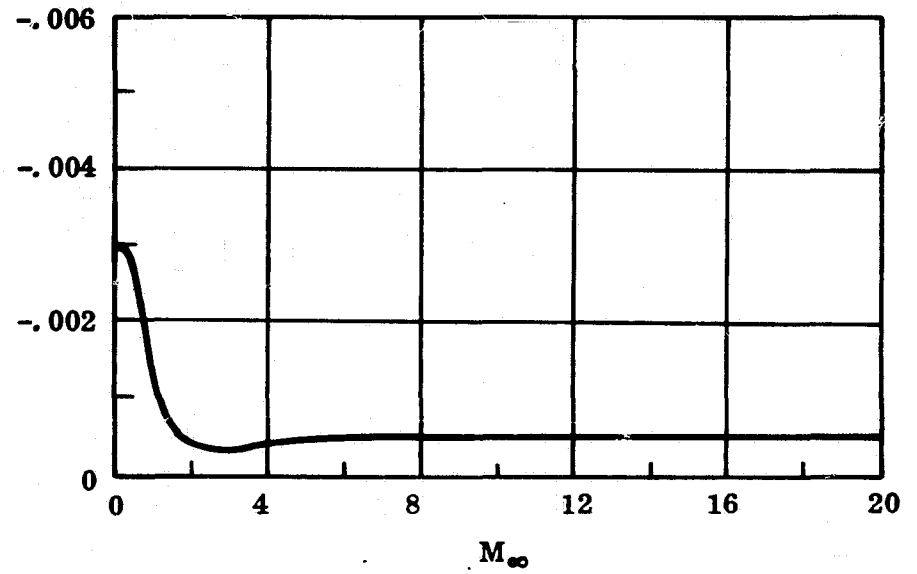


Fig. 6-8 Orbiter Aerodynamic Characteristics as a Function of Mach Number

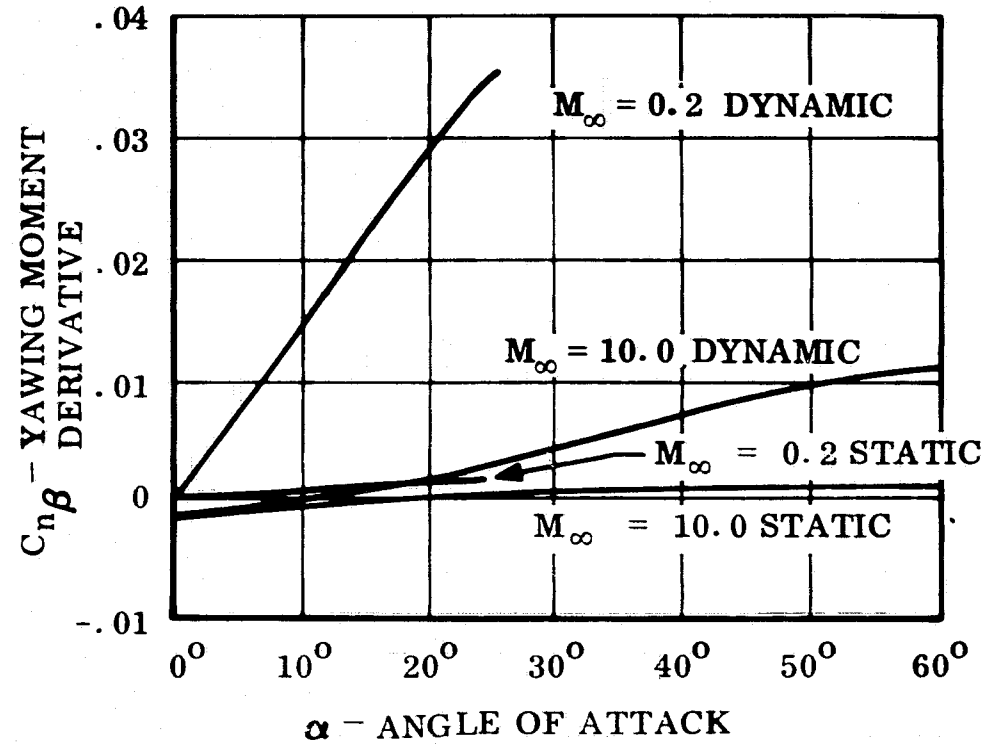
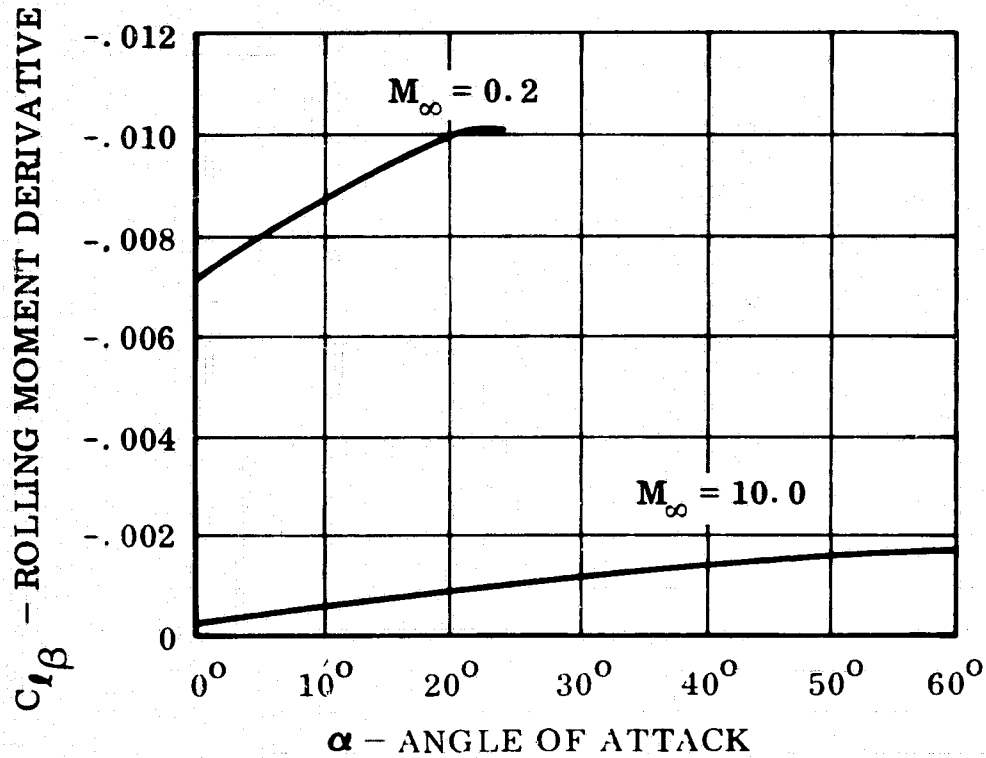
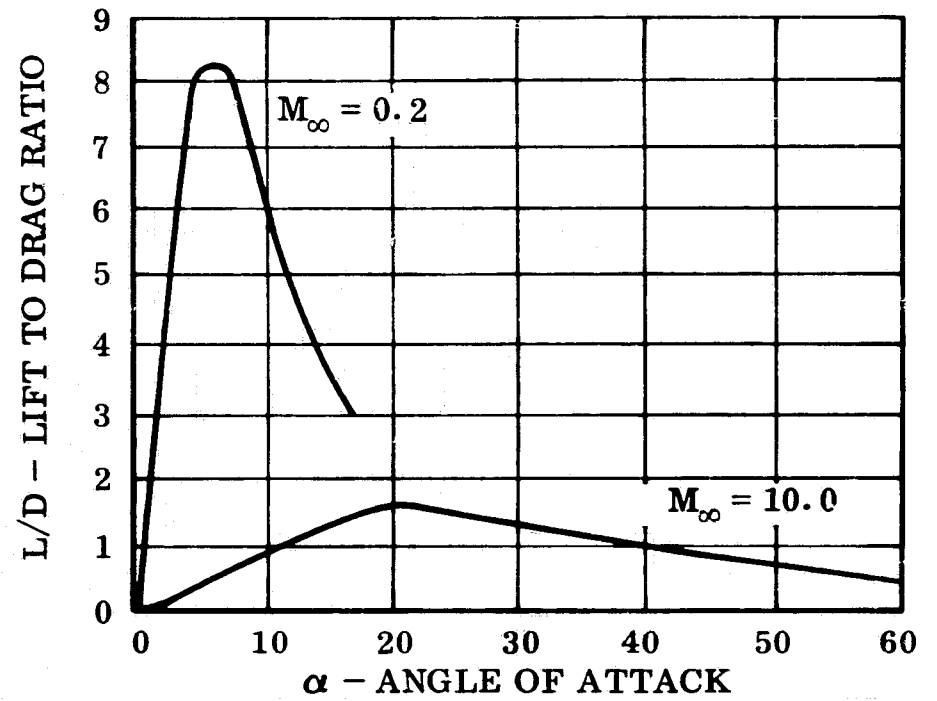
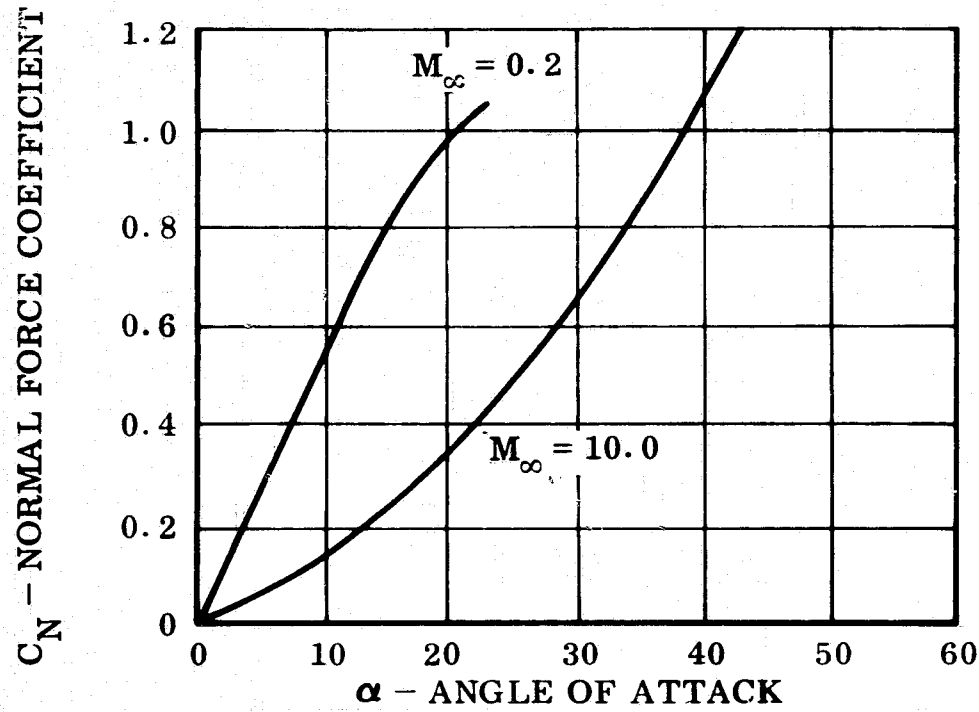


Fig. 6-9 Return Booster Aerodynamic Characteristics as Function of Angle of Attack (Subsonic and Hypersonic)

The longitudinal stability data presented in Fig. 6-10 show a stable configuration for all angles of attack at Mach 0.2 and trim capability with small values of elevon deflection. The stability data for Mach 10.0 presented in Fig. 6-10 show that for the proposed entry attitude of 60 degrees angle of attack, the configuration is trimmed with zero elevon deflection. Trim capability is available to zero degrees angle of attack with elevon deflections of 15 degrees or less. The configuration at Mach 10.0 is stable to neutrally stable in pitch at trim angles of attack above 15 degrees.

The variation of normal force coefficient slope and zero lift axial force coefficient with Mach number are shown in Fig. 6-11. The axial force coefficient remains at a high relative level for increasing supersonic Mach numbers because of the effect of the blunt nose of the fuselage and the flat face of the nonoperating jet engines. The maximum lift-to-drag ratio is shown in Fig. 6-11 as a function of Mach number for an altitude-Mach number variation expected for a nominal descent trajectory. The lift-to-drag ratio varies from 8.1 to 1.5 over the subsonic to hypersonic Mach number range.

Longitudinal stability and trim characteristics have been shown in Fig. 6-10 for Mach numbers of 0.2 and 10.0. The wing planform and elevon selected are expected to provide a stable and trimmable transition from the 60-degree hypersonic entry to the subsonic cruise mode. No undesirable transonic trim changes are anticipated.

### 6.3 COMPOSITE LAUNCH VEHICLE CHARACTERISTICS

The Two-Stage composite launch vehicle, shown in Fig. 6-3, consists of a combination of a return booster and an orbiter. The Triamese composite launch vehicle, shown in Fig. 6-4, consists of a combination of two return boosters and one orbiter. For both the Two-Stage and Triamese launch configurations, the individual stages are sized according to the mission requirements for the particular composite configuration.

Normal force coefficient slope and zero lift axial force coefficient for the Two-Stage and Triamese composite launch vehicles are presented in Fig. 6-12 as a function of Mach number. These data represent best available estimates and are intended primarily for use in trajectory simulation.

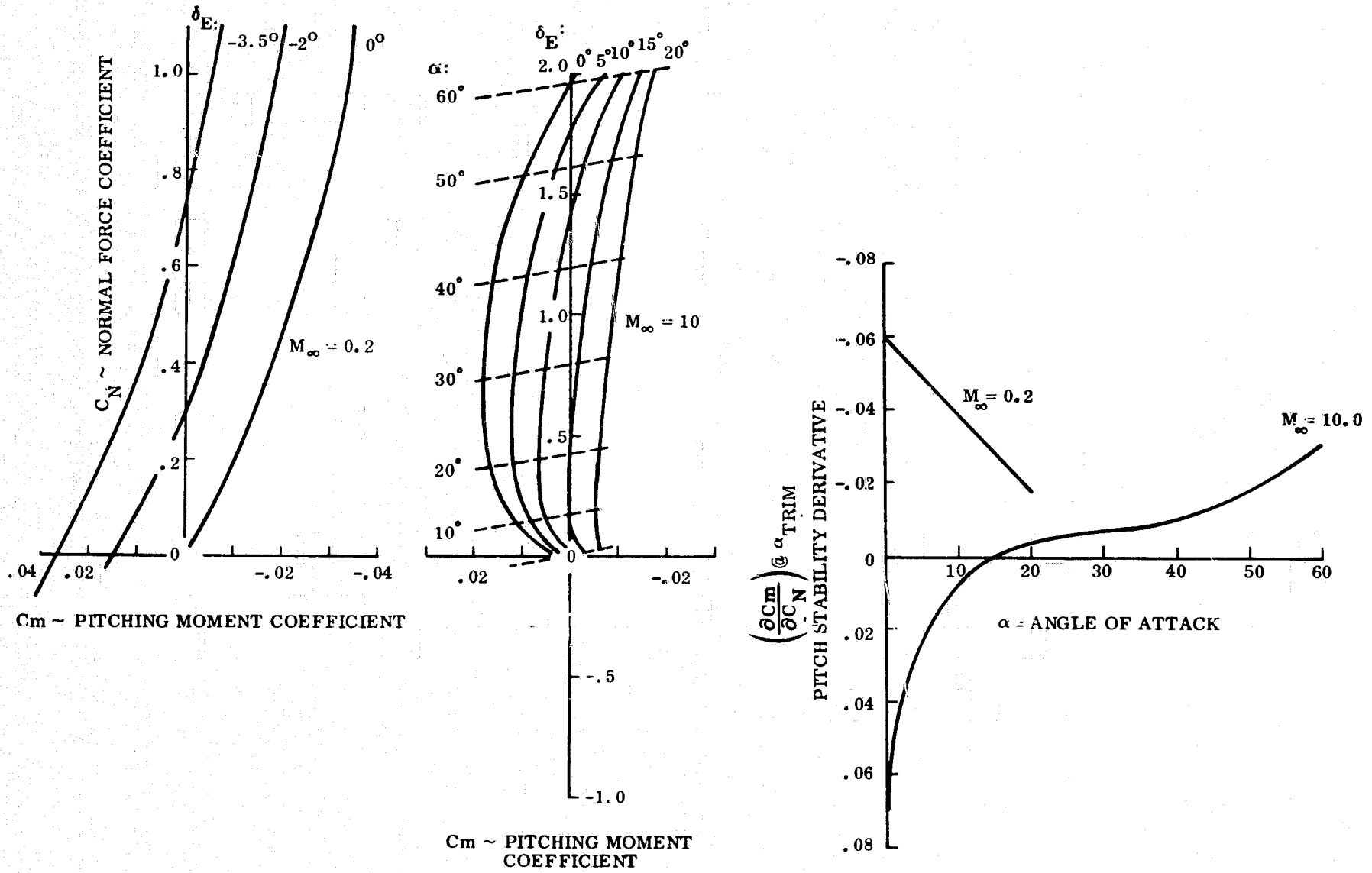


Fig. 6-10 Return Booster Longitudinal Stability Characteristics (Subsonic and Hypersonic)

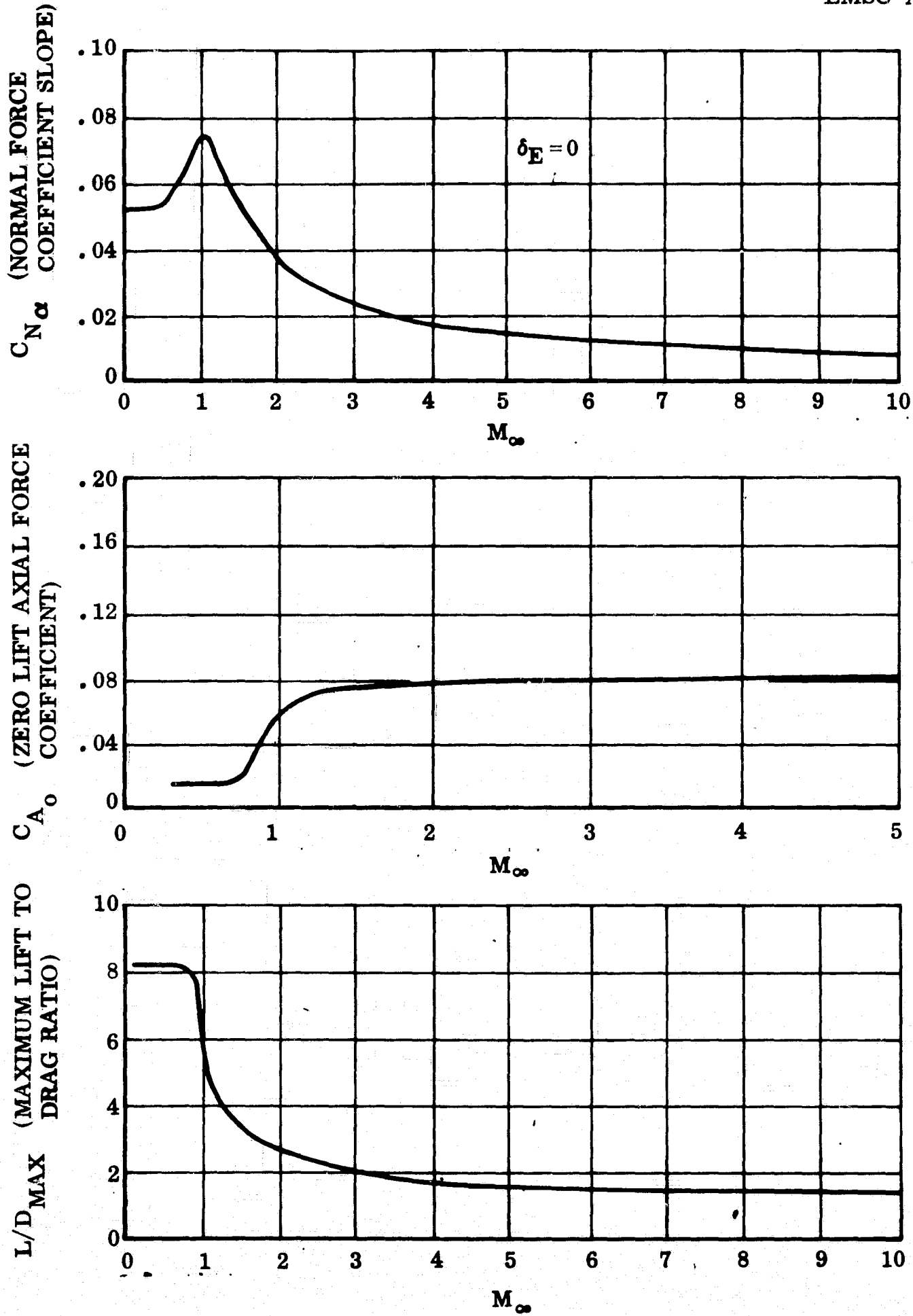


Fig. 6-11 Return Booster Aerodynamic Characteristics as Function of Mach Number

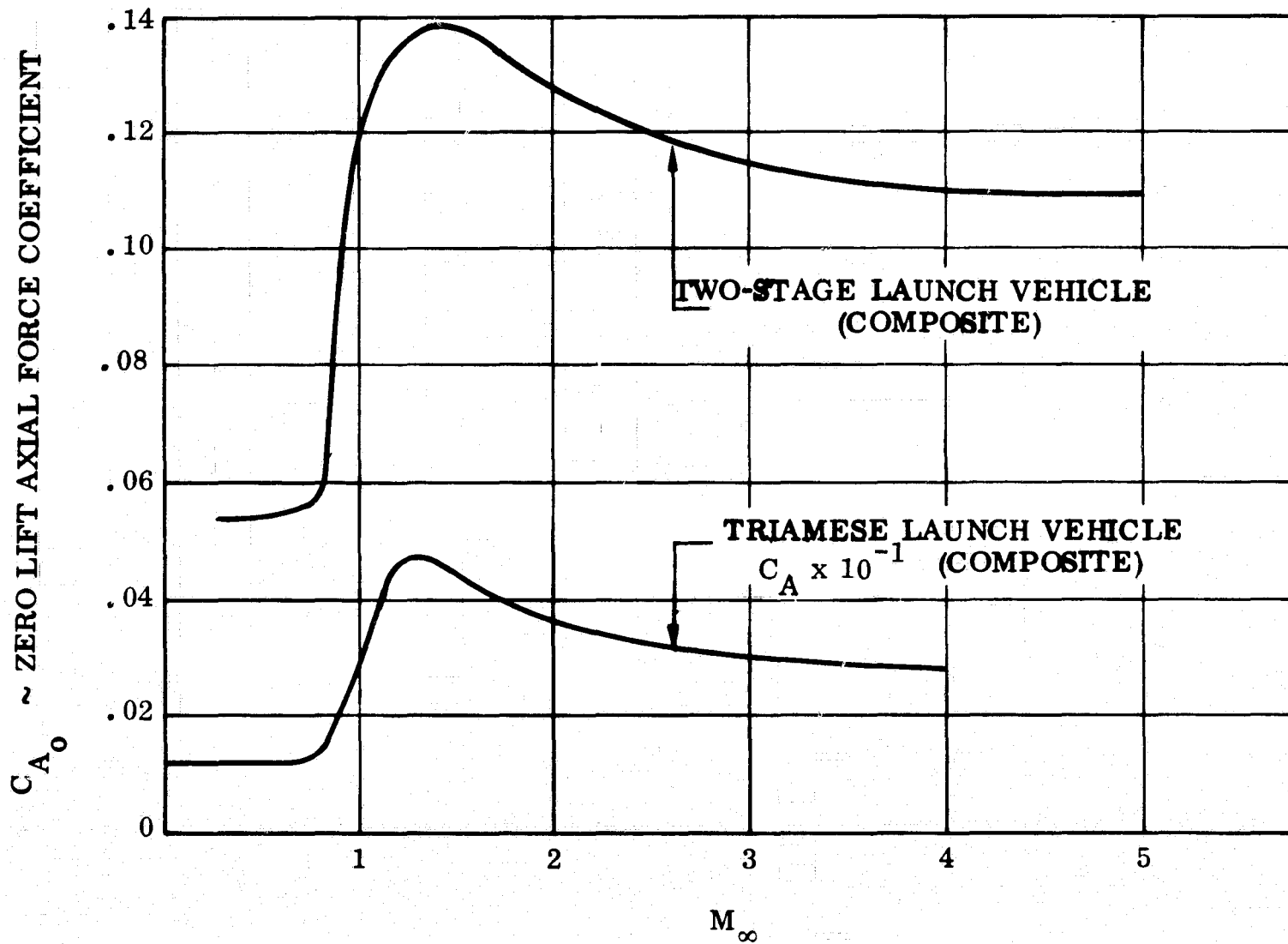
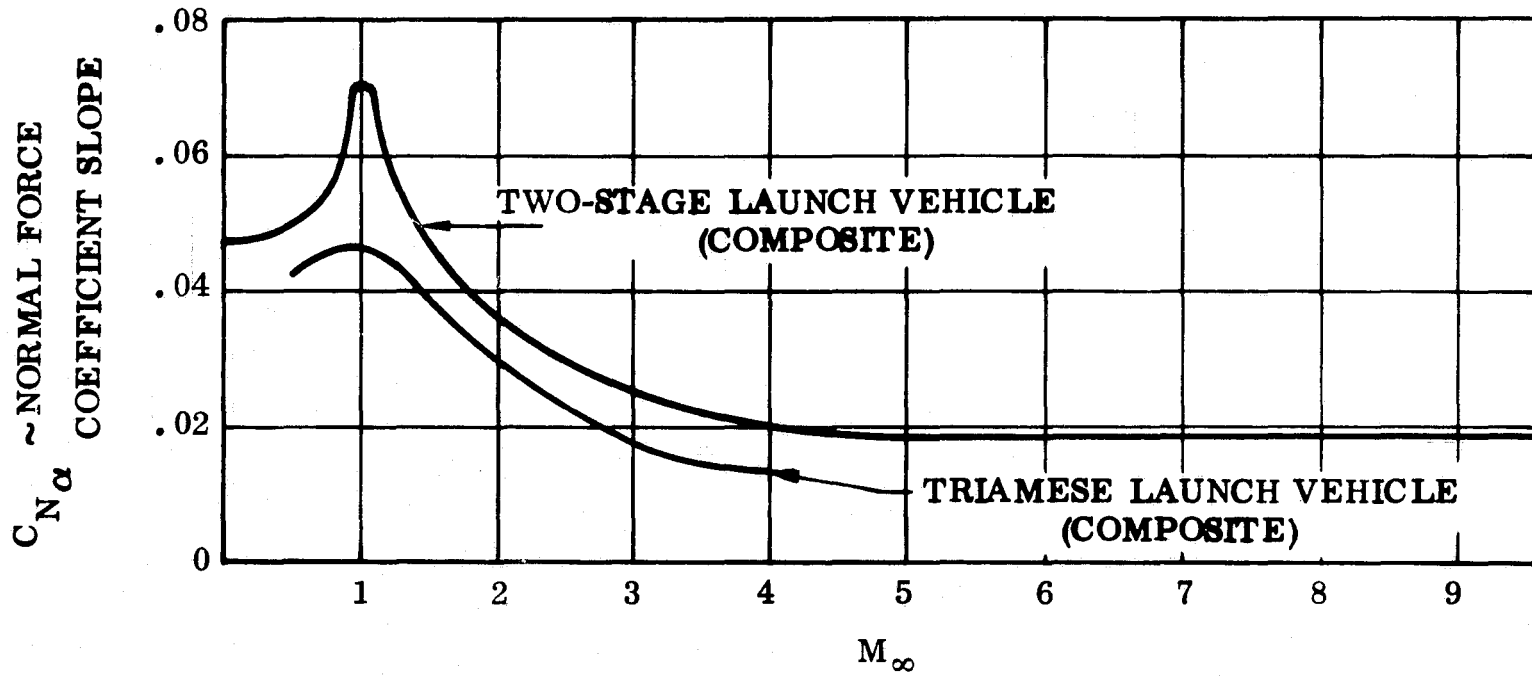


Fig. 6-12 Triamese and Two-Stage Composite Vehicles - Aerodynamic Characteristics vs Mach Number

Section 7

AEROTHERMODYNAMICS

Ascent, reentry, and base heating thermal environments and plume effects during separation for the baseline vehicles are discussed in this section. More detail on reentry heating and thermal protection is given in Volume III.

7.1 ASCENT THERMAL ENVIRONMENT

The thermal environment for the Two-Stage and Triamese boosters is based on the trajectory shown in Fig. 7-1. Staging of the orbiter element occurs at 10,500 ft/sec at an altitude of 235,000 feet. The booster continues along a ballistic flight path after staging and enters at an angle of attack of 55 degrees to minimize the cruise time back to the launch site.

Radiation equilibrium temperature histories for the booster wing are presented in Fig. 7-2. The maximum temperature on the leading edge varies from 1350°F at the root chord to 1500°F at the tip chord. Maximum temperatures on the wing are 1400°F on the lower surface and 620°F on the upper surface.

Temperature histories for selected locations on the fuselage are presented in Figs. 7-3 and 7-4. The maximum temperature on the booster fuselage is 1480°F at the nose cap. The maximum temperatures on the lower surface of the fuselage, about 1300°F, occur during reentry at a velocity of about 8500 ft/sec.

According to an estimate of the effect of impingement of the orbiter bow shock on the booster upper fuselage and upper wing, using an interference heat transfer coefficient of five times the undisturbed value would increase the maximum temperature on the booster upper fuselage from about 600°F to 1100°F. The assumed interference heating factor was based on wind tunnel data for a wedge-generated shock impinging on a circular cylinder. Wind tunnel tests will be required to establish a more accurate value for the Space Shuttle launch configuration.



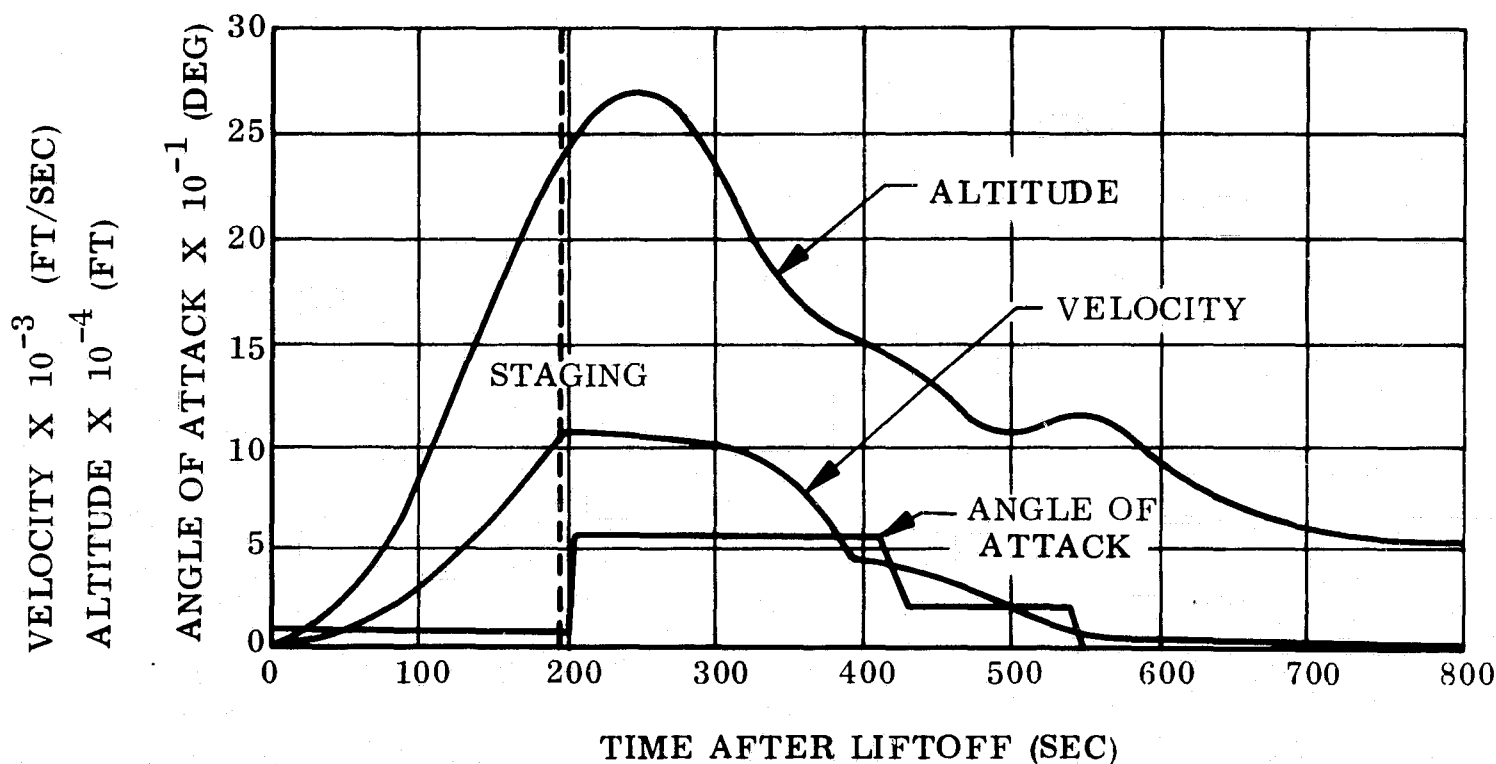


Fig. 7-1 Triamese and Two-Stage Booster Trajectory

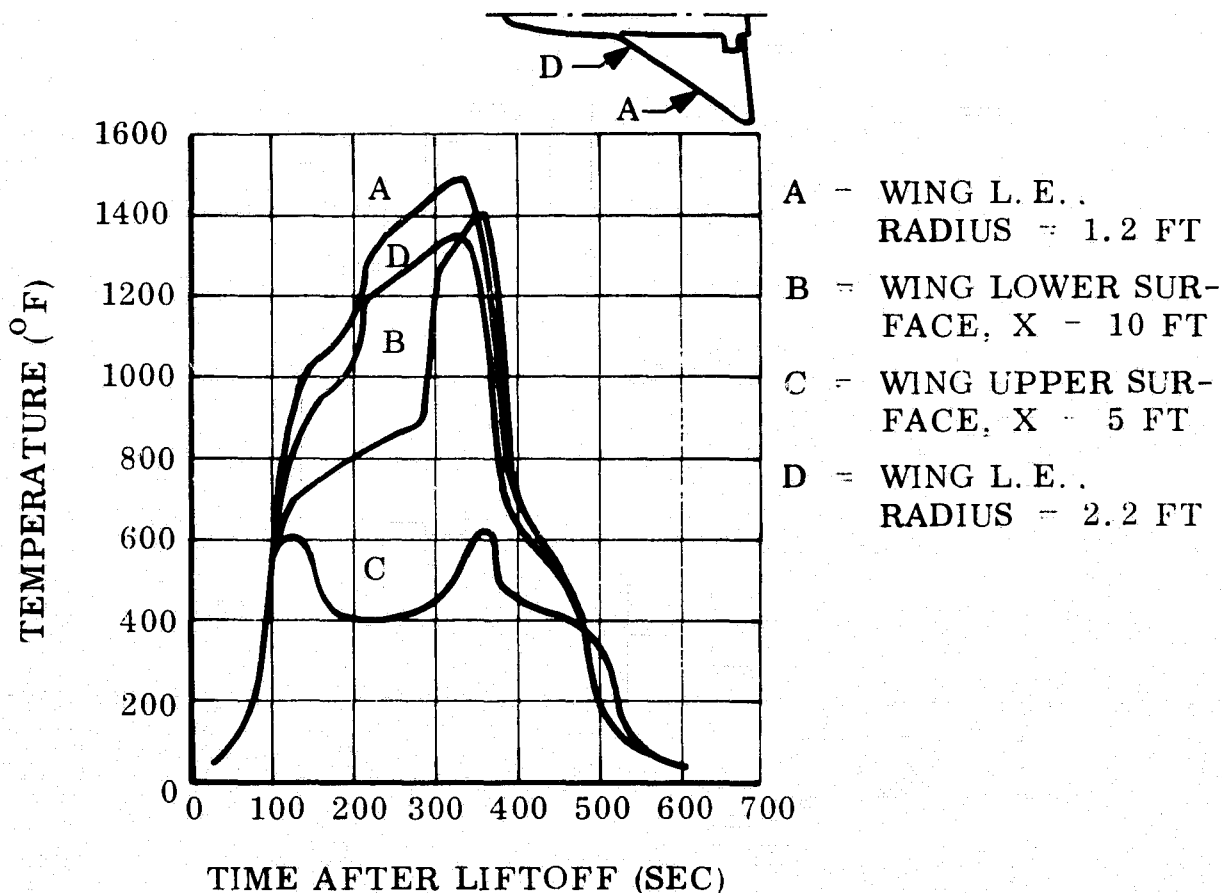


Fig. 7-2 Typical Temperature Histories on Triamese and Two-Stage Booster Wing

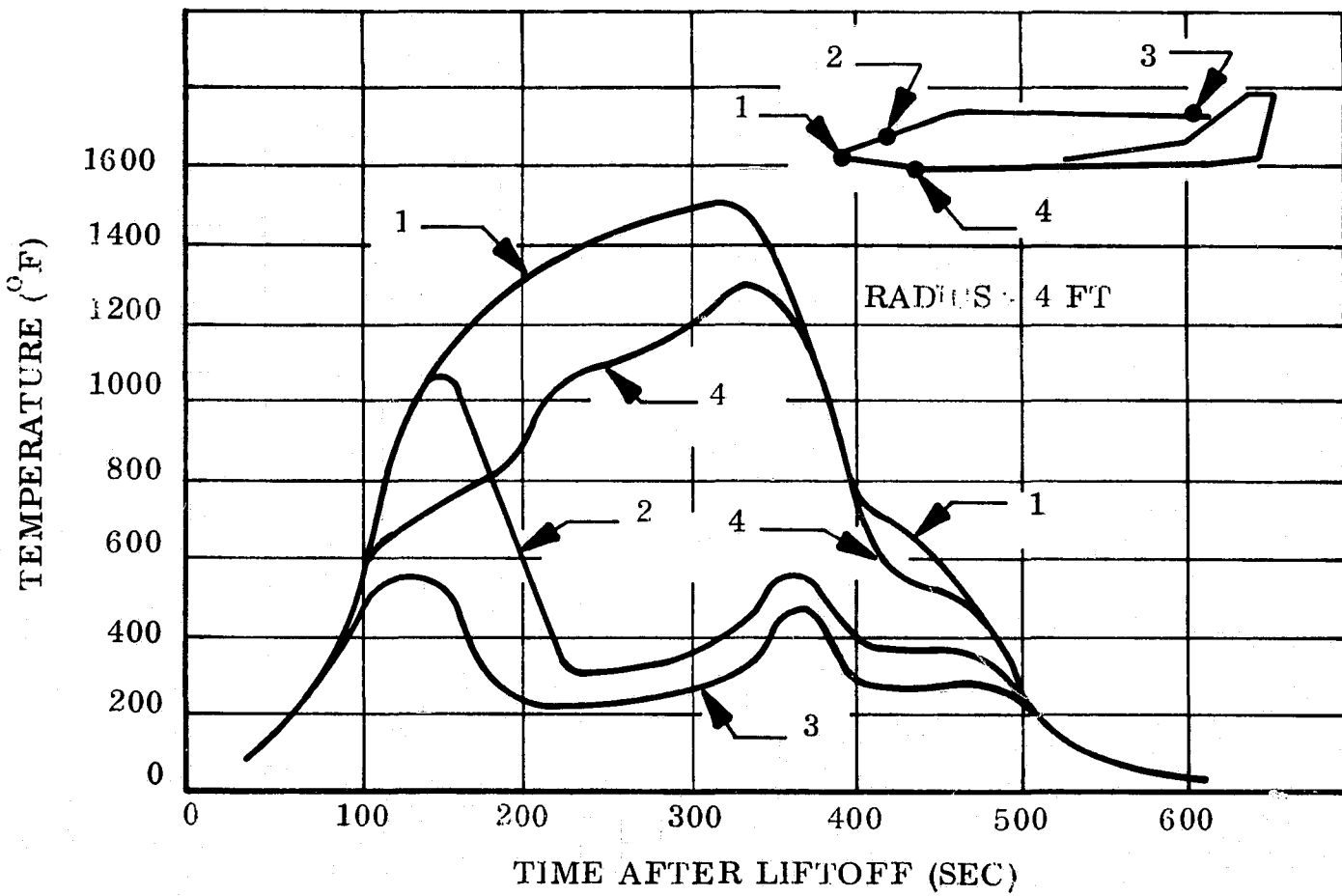


Fig. 7-3 Typical Temperature Histories on Triamese and Two-Stage Booster Fuselage

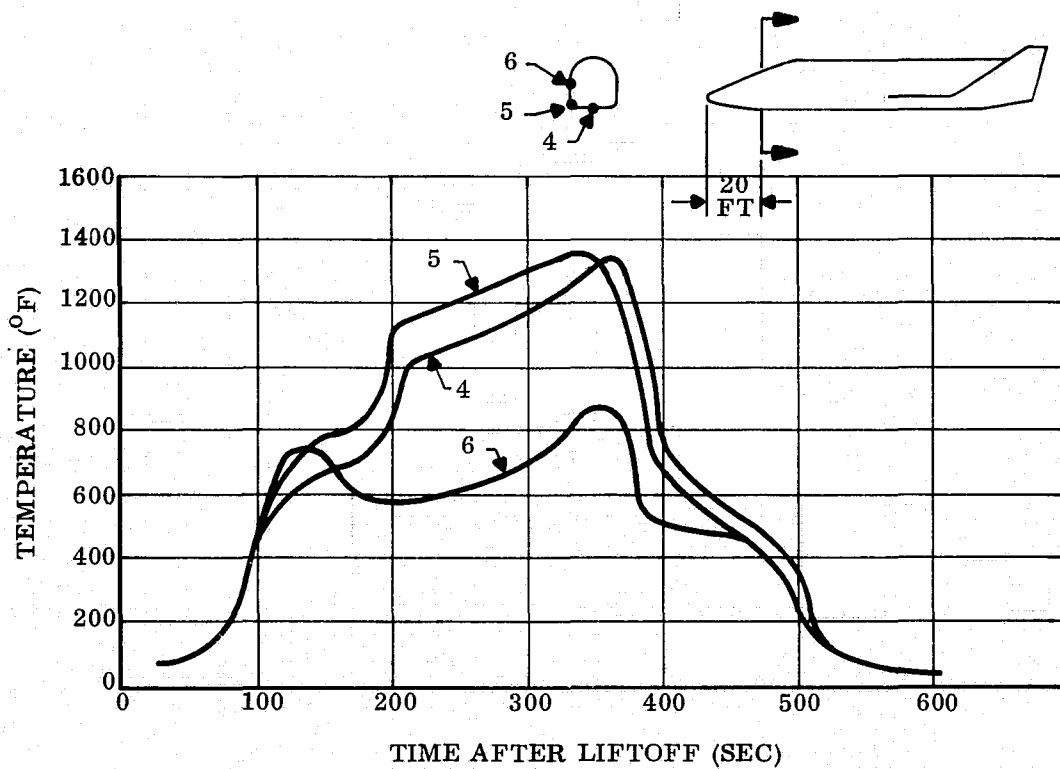


Fig. 7-4 Typical Temperature Histories on Triamese and Two-Stage Booster Fuselage

The results of a preliminary separation analysis presented in Section 7.4 indicate that the temperatures resulting from impingement of the orbiter plume on the booster are within the capability of the proposed upper surface heat shield materials (René 41 for windward surfaces and titanium for leeward surfaces).

## 7.2 REENTRY HEATING AND THERMAL PROTECTION

A parametric study of reentry heating and thermal protection concepts has been conducted on the basis of the LMSC orbiter. This configuration, which is representative of both the Two-Stage and the Triamese systems, is characterized by a flat bottom, constant leading edge sweep, delta wing lifting body. An oblate ellipsoidal nose cap is used to minimize stagnation point heating levels.

Reentry temperature-time histories are shown in Figs. 7-5 through 7-8 for various orbiter locations. These curves are based on an entry trajectory generated for a wing loading of  $50 \text{ lb/ft}^2$ , initial entry angle of  $-1$  degree, constant angle of attack of  $25$  degrees, and peak lower surface temperature of  $2200^\circ\text{F}$ . The resulting aerodynamic cross range is  $1606 \text{ nm}$ .

Figure 7-5 shows temperature histories for the nose stagnation point and the fin and body leading edge stagnation lines. The nose cap is ellipsoidal with semimajor axis of  $3$  feet and semiminor axis of  $1.5$  feet. The peak stagnation point temperature is  $2730^\circ\text{F}$ . Peak temperatures on the fin and body leading edges are  $2200^\circ\text{F}$  and  $2070^\circ\text{F}$ , respectively. Lower centerline temperature histories at  $25$ ,  $50$ ,  $75$ , and  $100$  percent chord are shown in Fig. 7-6. Peak temperatures are  $2120$ ,  $2190$ ,  $1890$ , and  $1730^\circ\text{F}$ , respectively. The change in slope of the temperature histories reflects the assumption of gradual boundary layer transition, starting at a local Reynolds number of  $1$  million and ending at  $2$  million. Figure 7-7 shows temperature histories at four upper surface locations. A sketch of the vehicle cross-section is included to show the locations analyzed. Peak upper surface temperatures range from  $600$  to  $1000^\circ\text{F}$ .

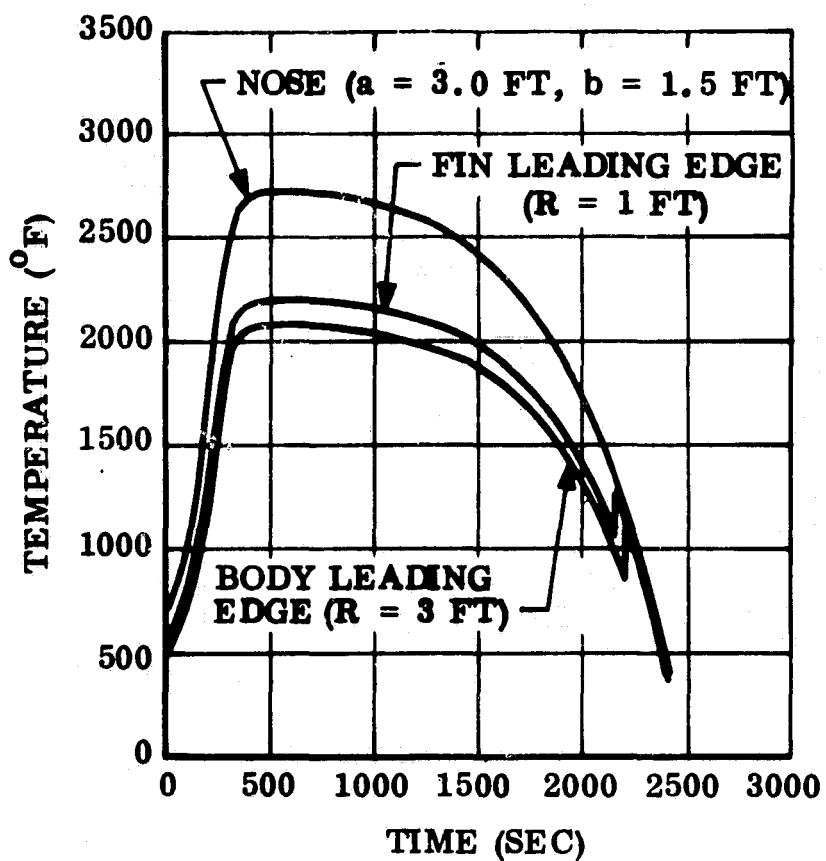


Fig. 7-5 Nose and Leading Edge Temperature Histories for Entry at  $\alpha = 25$  Deg

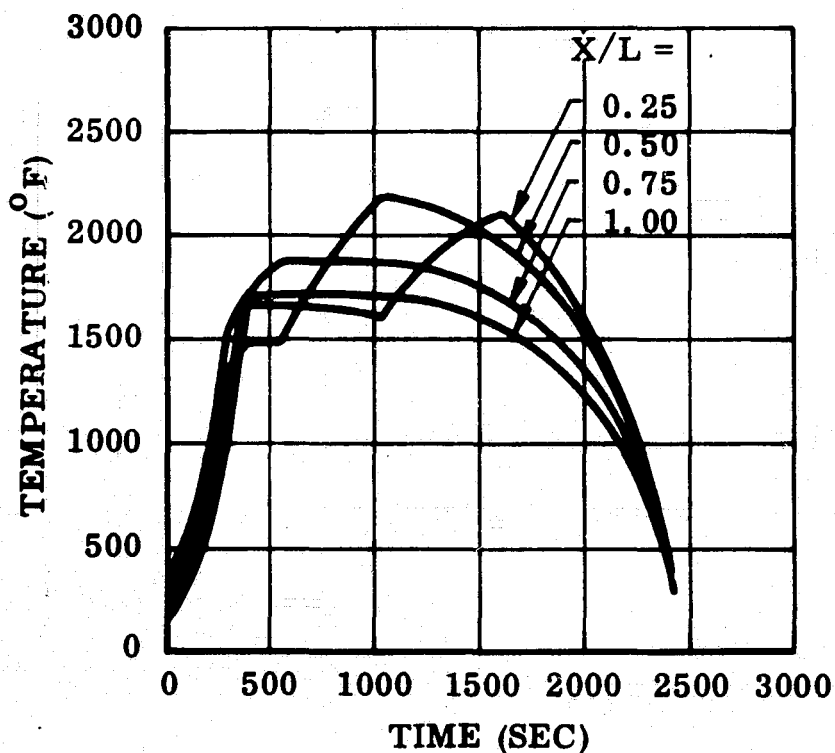


Fig. 7-6 Lower Centerline Temperature Histories for Entry at  $\alpha = 25$  Deg

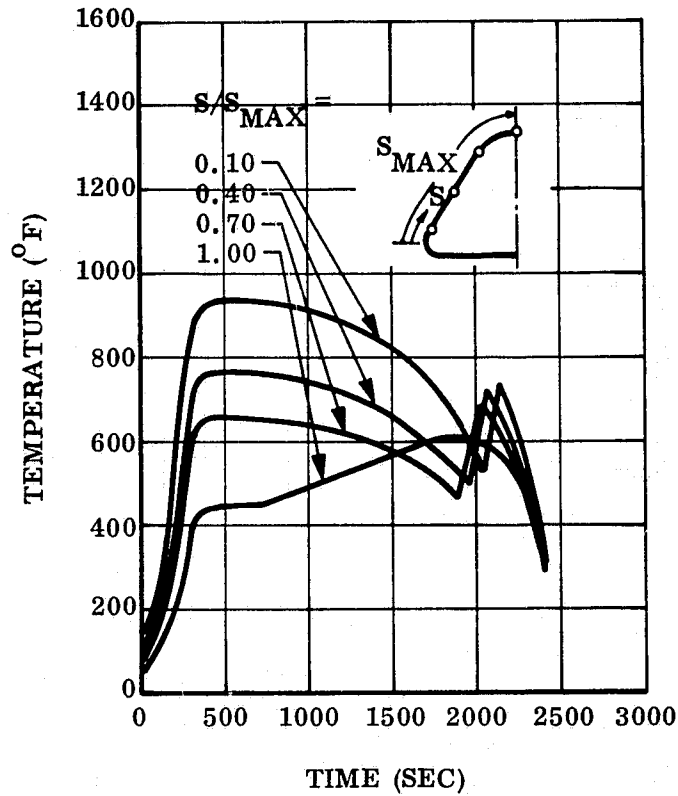


Fig. 7-7 Upper Surface Temperature Histories at 50 Percent Chord for Entry at  $\alpha = 25$  Deg

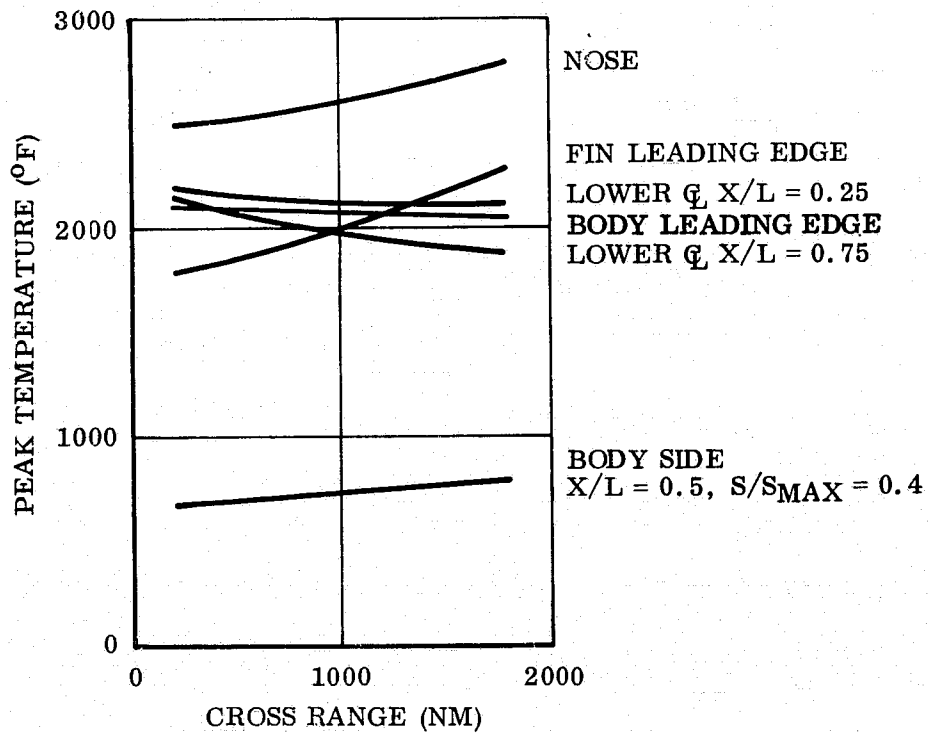


Fig. 7-8 Effect of Cross Range on Peak Surface Temperatures

Additional heating analyses have been performed for 35 and 45 degree angle-of-attack entry trajectories. These trajectories are also temperature constrained, with bank angle modulated to maintain a constant lower surface maximum temperature of 2200°F during periods of high heating. The resulting crossrange is 460 nm for  $\alpha = 45$  degrees and 840 nm for  $\alpha = 35$  degrees. Figure 7-8 shows the effect of crossrange on peak surface temperature at six vehicle locations, based on calculations for the three trajectories. Entering at large angle of attack (which increases with decrease in crossrange) results in a reduction in peak temperature for the nose cap, the fin leading edge, and all upper surface locations. The body leading edge and most lower surface locations experience an increase in peak temperature as the angle of attack is increased although the peak temperature is 2200°F for all three trajectories.

Table 7-1 shows the percentage of orbiter surface area that experiences various peak temperature levels for crossranges of zero, 500, 1000, and 1500 nm. These data were generated by using the three constant angle-of-attack entry trajectories discussed above. With the exception of the nose cap, all surfaces experience temperatures between 500 and 2200°F.

Table 7-1

PERCENTAGE OF ORBITER SURFACE AREA FOR VARIOUS TEMPERATURE RANGES

Temperature Range (°F)	Crossrange (nm)			
	0	500	1000	1500
Below 200	0	0	0	0
200 to 500	0	0	0	0
500 to 800	34	33	33	32
800 to 1500	11	12	13	13
1500 to 2000	25	27	28	30
2000 to 2200	30	28	26	25
2200 to 2500	0.3	0.4	0.4	0.4
2500 to 3000	0	0.1	0.1	0.1
Over 3000	0	0	0	0

The thermal environment associated with the orbiter unbanked reentry at  $C_{L \text{ MAX}}$  ( $\alpha = 55^\circ$ ) has also been evaluated. This trajectory involves a reentry time of 1950 seconds from 400,000 feet to touchdown, as compared to 3150 seconds for the 25-degree angle-of-attack trajectory, which generates 1606-nm crossrange. Temperature histories for the nose cap and leading edge are shown in Fig. 7-9. Peak temperatures of  $2400^\circ\text{F}$  and  $2225^\circ\text{F}$  are experienced by the nose cap and leading edge, respectively. To constrain the maximum temperature on the lower surface to  $2200^\circ\text{F}$  the first 12 feet of the vehicle requires a heat shield material capable of withstanding temperatures from  $2200^\circ\text{F}$  to  $2400^\circ\text{F}$ . Figure 7-10 shows temperature histories for five lower surface locations. The abrupt increases in temperature indicate transition from laminar to turbulent flow; for entry at  $C_{L \text{ MAX}}$ , peak temperatures usually result from laminar heating.

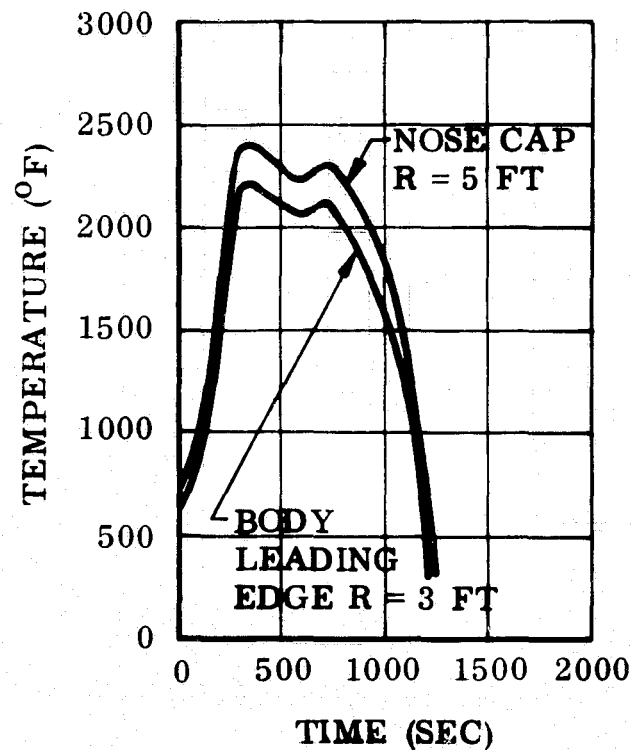


Fig. 7-9 Nose and Leading Edge Temperature Histories for Entry at  $\alpha = 55$  Deg

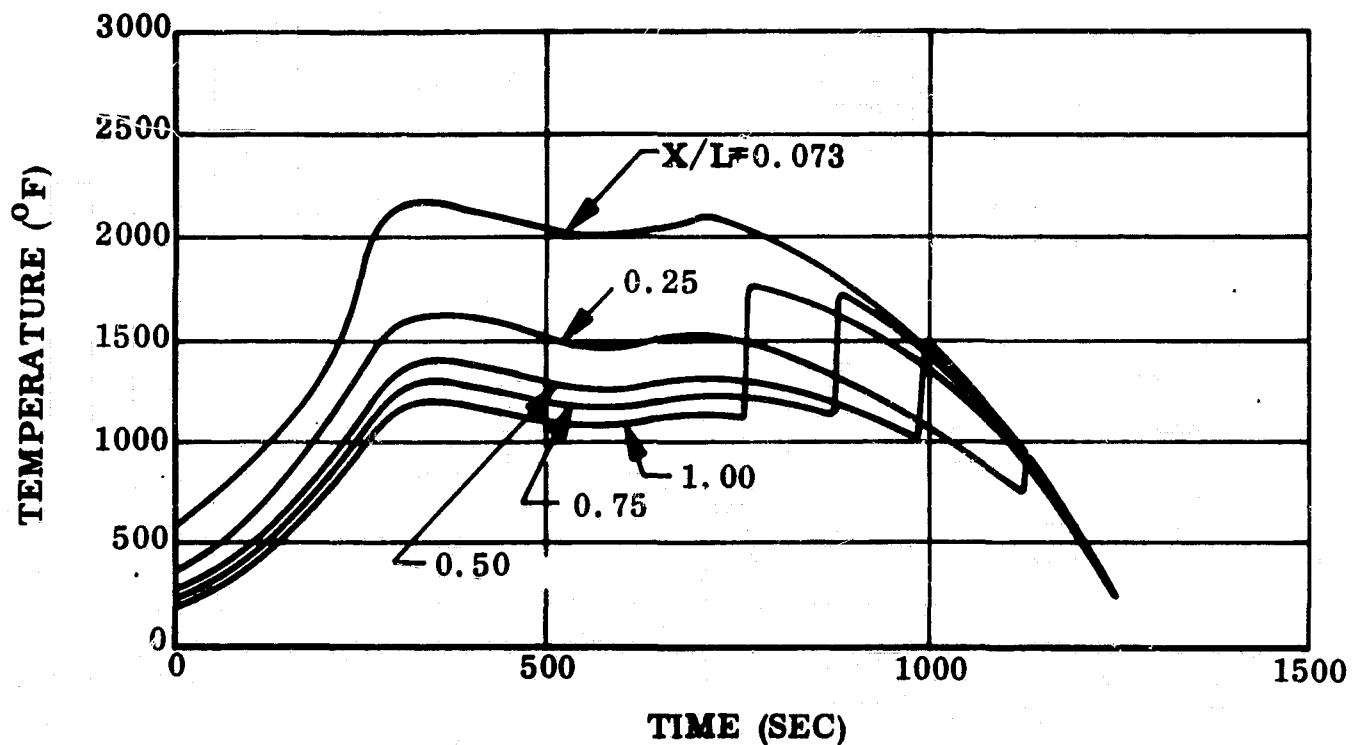


Fig. 7-10 Lower Centerline Temperature Histories for Entry at  $\alpha = 55$  Deg

### 7.3 BASE HEATING ENVIRONMENT AND CANDIDATE MATERIAL SYSTEMS

#### 7.3.1 Heating Environment

The thermal environment in a base region involving a multiengine cluster is relatively severe because of the combined convection and radiation (primarily from exhaust gases) as a result of nozzle plume interaction. Considerable flight data have been accumulated from Fleet Ballistic Missiles, Minuteman, and Saturn. For example, an empirical correlation of a considerable quantity of Fleet Ballistic Missile data for four-nozzle clusters has been obtained to predict the base heating environment.\* This method has been applied to Minuteman and Saturn with

\*"An Empirical Correlation of Polaris Base Heating Data," by D. M. Tellep and Y. Kawamura, LMSC-801511, March 20, 1962.



equal success; therefore, it represents a suitable method for a first estimate of the heat transfer when the major contribution to the total heat is a result of reverse flow into the base region from nozzle interaction without combustion. The estimated peak heating environments are presented in Table 7-2 for the candidate booster and orbiter configurations. The gas temperature near the base shield surface is on the order of  $3250^{\circ}\text{R}$ , 50 percent of the chamber temperature. Therefore, the actual convective heat transfer to the heat shield surface and flame curtains will be significantly less than those presented in Table 7-2 for a cold wall temperature of  $70^{\circ}\text{F}$ . Estimates of the combustion effect on the total heat transfer to the base heat shield, which constitutes an engine compartment protective cover, were made on the basis of S-I and S-IV data. (An analysis should be made to establish an upper limit value of the hydrogen burning contribution to the base heat transfer during the entire ascent phase.)

Regions of external air flow separation at the rear of the vehicle cause recirculation of hydrogen from the base region (for an oxidizer/fuel ratio of 7:1), with resultant localized burning and associated radiative heat transfer. For asymmetrical vehicles (mated booster and orbiter), large separated regions could exist between the booster and the orbiter, particularly at angles of attack. The extent of this region will be defined from wind tunnel tests, and depending on the estimated combustion contributed heat rate levels, reconfiguring may be required to minimize this effect. The amount of free hydrogen in the nozzle exhaust is essentially identical for both the bell-type and the Aerospike engines.

### 7.3.2 Candidate Material Systems

Candidate material systems that may be used for the booster base heat shield and flexible flame curtains are presented in Tables 7-3 and 7-4. A promising state-of-the-art system consists of a rigid heat shield of silicone elastomer in an open-celled honeycomb of phenolic fiberglass, supported by a reinforced phenolic Fiberglass honeycomb structure. The flame curtains are composed of a flexible silicone elastomer, reinforced by silica fibers and covered on both surfaces with silica cloth covers. They are attached between the rigid heat shield and movable nozzles, similar to that for the S-I vehicle. The corresponding typical heat protective material and compartment structure section weight are presented for both bell-type and the Aerospike engine systems in Figs. 7-11 and 7-12.

Table 7-2

BASE HEAT SHIELD\* PEAK HEAT RATE LEVELS

BELL NOZZLE CONFIGURATION							
	Number of Engines	Nominal Sea Level Thrust, Klb	Expansion Ratio	Location Measured From Nozzle Exit Plane, in.	Convective Heat Rate Btu/ft <sup>2</sup> sec Cold Wall (T <sub>w</sub> = 70°F)	Combustion Effect on Base Environment Btu/ft <sup>2</sup> sec**	Total Heat Btu/ft <sup>2</sup> sec
BOOSTER	13	400	35/1	68	10	10-30	20-40
ORBITER	3	400	150/1	208	<2.5	Small	<5
AEROSPIKE NOZZLE CONFIGURATION							
BOOSTER	7	800	—	32	100	10-30	110-130
ORBITER	3	400	—	32	10-20	Small	10-20

\*Base heat shield or engine compartment enclosure.  
 \*\*Preliminary estimates, based on S-I and S-IV data.

Table 7-3

## BASE HEAT SHIELD CONCEPTS

	Maximum Use Temperature, °F	Working Maximum Heat Rate Level, Btu/ft <sup>2</sup> sec
Reusable Candidate Material Systems		
Stainless steel - Fiberglas insulation	1400	5
Haynes 25 - Fiberglas insulation	1800	10
TD-NiCr - Fiberglas insulation	2200	20
Rigid lightweight silica insulation (LI-1500)	2500	30
Columbium/disilicide coating - silica insulation	2500	30
Tantalum/disilicide coating - zircon insulation	3000	60
Regeneratively cooled liquid hydrogen	-	150+
Nonreusable Candidate Material Systems		
Open-faced honeycomb-cells, filled with lightweight silicone elastomer*		125 ( $\rho = 25 \text{ lb/ft}^3$ )
		200 ( $\rho = 55 \text{ lb/ft}^3$ )
Silicone elastomer reinforced with silica cloth or rigid silica matrix*		125 ( $\rho = 25 \text{ lb/ft}^3$ )
Refrasil phenolic or carbon phenolic		200 and up

\*Substrate - phenolic Fiberglas

Table 7-4

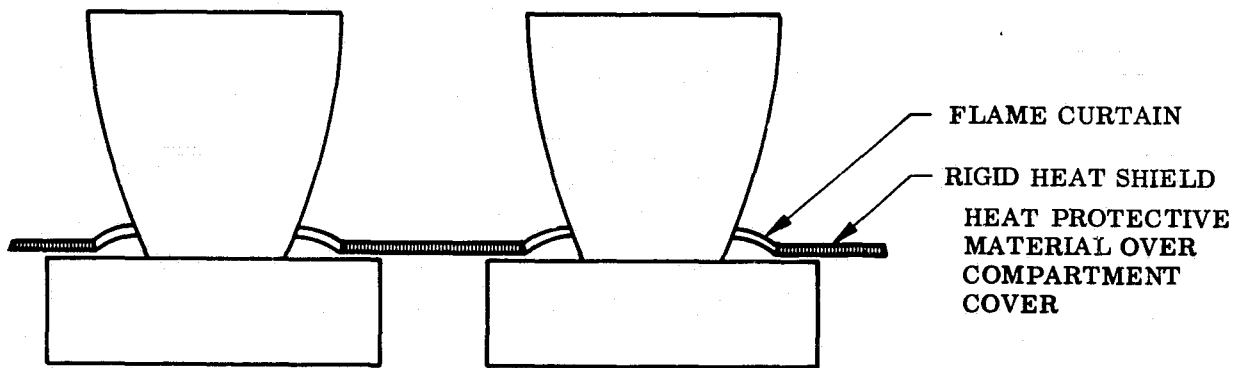
FLAME CURTAIN HEAT PROTECTION CONCEPTS

	Maximum Use Temperature, °F	Maximum Use Heat Rate, Btu/ft <sup>2</sup> sec
Silicone elastomer, reinforced with silica fibers or cloth and sandwiched between Fiberglas cloth		125-200
Flexible metallic (accordion like) structure	< 3000	< 60
Metallic shingle system	< 3000	< 60

In addition to these systems, a variety of refractory metallic (reradiative), high-temperature insulative materials, regeneratively cooled liquid hydrogen, and ablative materials may be used for the base heat shield, as outlined in Table 7-3. Each of these systems will be considered for application in the base region, dependent on the localized heating environment and upon weight and cost of the protective system.

Candidate systems for flame curtains are quite limited because of the requirement for flexibility. In addition to the flexible reinforced silicone elastomer, flexible metallic (accordion like) structures and metallic shingle systems are potential candidates for further consideration.

Table 7-2 shows that the compromise bell configuration base shield environment is expected to be less than 40 Btu/ft<sup>2</sup> sec, which allows for application of reusable shields of coated tantalum or a regeneratively cooled liquid hydrogen heat exchanger of Haynes 25 metallic shield. Because of the high heating environment, 130 Btu/ft<sup>2</sup> sec, the reusable heat shield candidate for the optimum Aerospike configuration may be limited to a regeneratively cooled liquid hydrogen heat exchanger shield.



TYPICAL SECTION WEIGHTS

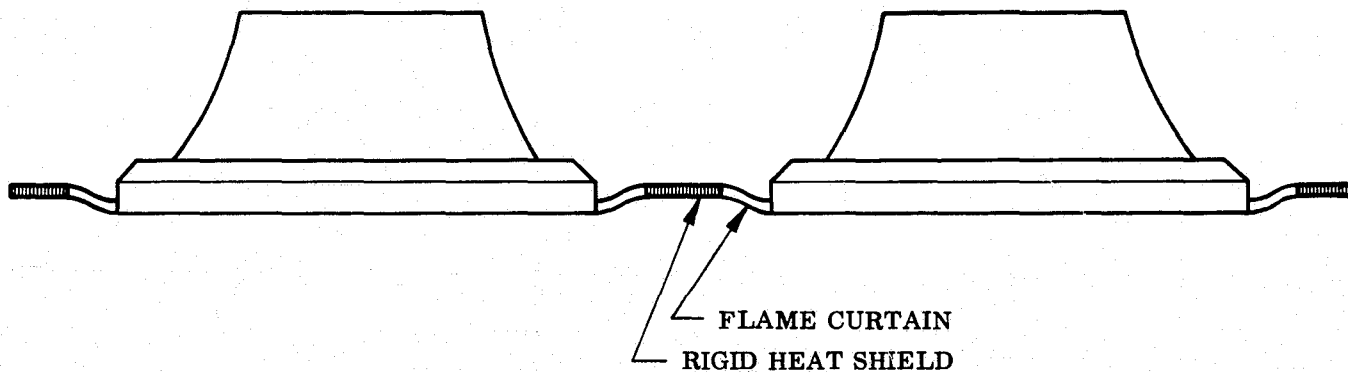
HEAT SHIELD

- HEAT PROTECTIVE MATERIAL - SILICONE ELASTOMER/  
PHENOLIC FIBERGLAS HONEYCOMB. 2.0 LB/FT<sup>2</sup>
- REINFORCED PHENOLIC FIBERGLAS HONEYCOMB STRUCTURE 2.0 LB/FT<sup>2</sup>

FLAME CURTAIN

- FLEXIBLE HEAT PROTECTIVE MATERIAL - REINFORCED  
SILICONE ELASTOMER WITH SILICA CLOTH COVERS 1.0 LB/FT<sup>2</sup>

Fig. 7-11 Typical Booster Base Heat Shield - Bell System



TYPICAL SECTION WEIGHTS

HEAT SHIELD

- HEAT PROTECTIVE MATERIAL - SILICONE ELASTOMER/  
PHENOLIC FIBERGLAS HONEYCOMB. 4.0 LB/FT<sup>2</sup>
- REINFORCED PHENOLIC FIBERGLAS HONEYCOMB  
STRUCTURE 2.0 LB/FT<sup>2</sup>

FLAME CURTAIN

- FLEXIBLE HEAT PROTECTIVE MATERIAL - REINFORCED  
SILICONE ELASTOMER WITH SILICA CLOTH COVERS 4.0 LB/FT<sup>2</sup>

Fig. 7-12 Typical Booster Base Heat Shield - Aerospike System

The most severe heating rate on the orbiter heat shield occurs during ascent. For the bell nozzle configuration, the maximum heating rate during orbiter engine operation is less than 5 Btu/ft<sup>2</sup> sec (combined convective and radiative heating neglecting combustion); therefore, this potentially allows for consideration of all the reusable candidates of Table 7-3. However, localized combustion in the orbiter base region during the booster burning with or without simultaneous low-level thrusting of the orbiter (10 percent of full thrust) could result in a substantially higher heating rate environment and restrict the number of reusable candidate systems. The combined level of convective and radiative heating for the Aerospike configuration results in a more severe heating environment than for the bell nozzle configuration and further restricts the candidate material systems to those capable of surviving in environments in which the heating rate exceeds 20 Btu/ft<sup>2</sup> sec when combustion is significant. The insulation required to protect the substructure from heat conduction is sized in all cases by the long heating period during entry.

#### 7.4 ORBITER PLUME EFFECTS DURING SEPARATION

Evaluation of the effect of the orbiter engine exhaust plumes on the convective heat transfer to the booster as the orbiter exhaust sweeps over the booster during the separation maneuver shows that the heating environment has a negligible impact on the booster thermal protection system.

The booster nose (stagnation point) and fuselage heating rate and heat flux histories presented in Figs. 7-13 and 7-14 were calculated for initial vertical separations of zero, 50, and 200 feet between the orbiter and the booster prior to dethrottle of the booster. For this parametric study, the initial vertical separation was assumed to occur by a separation device that provides only vertical parallel movement of the booster relative to the orbiter without relative axial motion.

The addition of the plume heating to the aerodynamic heating load during ascent results in a peak forward fuselage temperature of less than 1600°F (allowable for René 41). Where titanium is employed (as on booster leeward surfaces), the available heat capacity limits temperature increases resulting from plume heating to less than 600°F, which is the allowable reuse temperature for titanium.

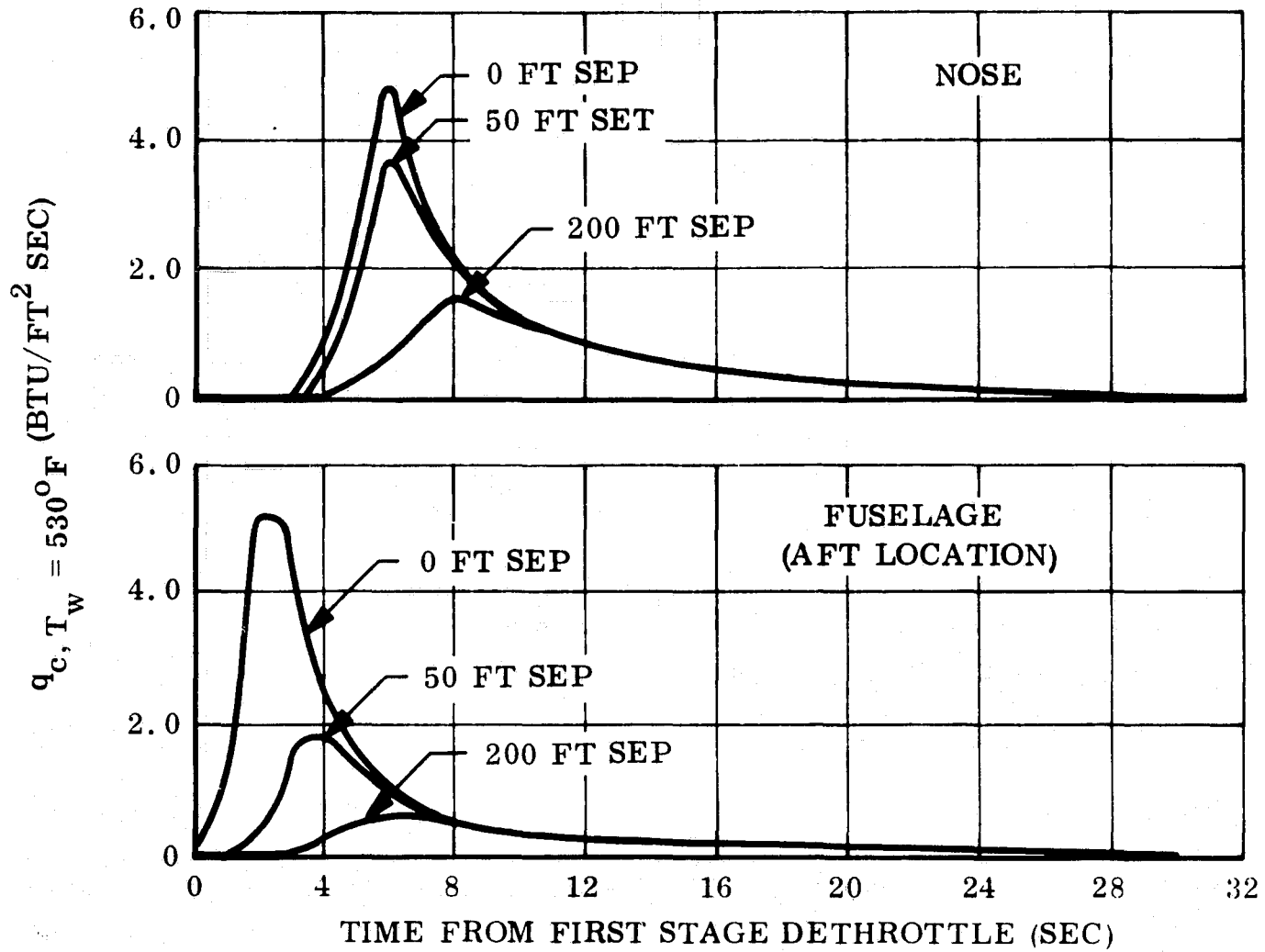


Fig. 7-13 Convective Heat Rates to Booster Stage From Orbiter Bell Engine Exhaust

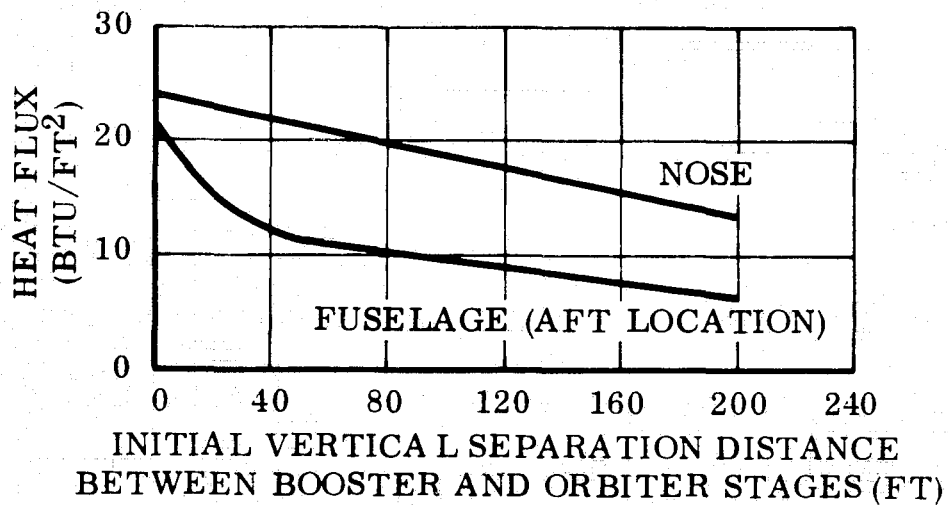


Fig. 7-14 Convective Heat Flux to Booster Stage From Orbiter Bell Engine

For separation systems in which the flow could impinge on either the booster or orbiter vehicles from hot gas, liquid, or solid propellant rocket devices, the additional localized heating from these plumes should be accounted for in future designs.



**Section 8**  
**STRUCTURES AND MATERIALS**

Structural design criteria and the thermal load environment data were used to select candidate materials for the preliminary weight estimates. The results of an evaluation of candidate thermal-structural concepts and materials were used to define the structural arrangements.

**8.1 DESIGN CRITERIA AND LOADING REQUIREMENTS**

The structure must survive the critical loading conditions and associated environments over the specified number of missions with a minimum refurbishment and in a manner that does not reduce the probability of mission success. Consideration should be given to the cumulative deteriorating effect of repeated exposure to critical environmental conditions such as temperature, creep, and fatigue.

Nonflight conditions and environment should be treated in a manner that will minimize influence on the structural design.

The following ultimate factors of safety have been established:

- General structure                      1.5
- Pressurized compartments        2.0

Documents serving as guidelines for establishing the structural design criteria include the following:

NASA-SP 8000 Series	Design Criteria
NASA-TM-X-53328	Terrestrial Environment (Climatic) Criteria Guidelines for Use in Space Vehicle Development, 1 May 1966
MIL-A-8860 (ASG)	General Specification for Airplane Strength and Rigidity, 18 May 1960

MIL-A-8861 (ASG)	Airplane Strength and Rigidity, Flight Loads, 18 May 1960
MIL-A-8862 (ASG)	Airplane Strength and Rigidity, Landplane Landing and Ground Handling Loads, 18 May 1960
MIL-A-8865 (ASG)	Airplane Strength and Rigidity, Miscellaneous Loads, 18 May 1960
MIL-A-8866 (ASG)	Airplane Strength and Rigidity, Reliability Requirements, Repeated Loads and Fatigue, 18 May 1960
MIL-M-855A	Missiles, Guided: Design and Construction, General Specifications for, 6 October 1960
MIL-HDBK-5A	Metallic Materials and Elements for Aerospace Vehicle Structures, 8 February 1966

#### 8.1.1 Loads and Structural Dynamics Criteria

Forseeable factors that can influence the structural design include vibration, shock, acoustics, buffeting, flutter and aeroelastic effects, and quasistatic and dynamic loads.

Landing and ground handling criteria are as follows:

- Hoisting – The vehicle is hoisted only in the dry weight configuration. The hoisting load factor is 1.5.
- Taxiing – For taxiing, the vehicle weight is the dry weight plus payload plus jet engine propellant weight. Taxi load factor is  $N_z = 2.0$ .
- Turning – The turning weight is the taxi weight. The side load factor is  $N_y = 0.4$ .
- Landing – The landing weight is the taxi weight less half of the weight of the jet engine propellants. Landing sinking speed is 9 feet per second. The aerodynamic lift is equal to the landing weight, and the maximum load transmitted through the landing gear is assumed to be two times vehicle weight.
- Ground winds – The vehicle structural loads with the propellant tanks full or empty, pressurized or unpressurized, is induced by the 99 percent probability ground winds and gusts defined in NASA TM-X-53328. The effects of vortex shedding, stand misalignment, launcher and launch vehicle flexibility, and the interaction of winds with adjacent structures must be considered.

Flight criteria follow:

- Ascent – The ascent trajectory must be tailored so that the maximum longitudinal load factor will be  $N_x = 4.0$  for cargo missions and  $N_x = 3.0$  for missions with passengers aboard. The effects of winds and gusts must be included and oriented in the most adverse direction. For preliminary design loads determination, it is assumed that the autopilot will limit the maximum angle of attack to 5 degrees in the presence of 95 percent worst month or 99 percent mean annual MSFC winds. Engine-out conditions must be considered.
- Separation and staging – Loads arising from staging, thrust transients, and control forces acting during separation must be determined. The effects of gimbal offsets and aerodynamic forces, if applicable, should be included.
- Orbital flight – During the orbital phase, maneuvers are required to effect orbit changes, rendezvous, and docking. Loads must be determined for each of these modes, including the possible interaction and coupling between control systems and vehicle structural modes. The structural implications resulting from payload deployment and cargo transfer requirements should be investigated.
- Atmospheric reentry – The reentry trajectory should be tailored to minimize the surface temperatures of the vehicle. Maximum accelerations should be limited to 2 g's.
- Maneuvers – For low-speed flight, the maximum design maneuvering load factor is limited to 2.5. Velocity is limited to 250 knots from sea level to 25,000 feet and Mach 0.6 above 25,000 feet. The weight configuration is for entry weight.
- Vertical gust – For low-speed flight, the design vertical gust velocity is 50 feet per second at the limited level flight speed. At velocities up to 1.6 times stall velocity, the design vertical gust velocity is 66 feet per second.

Since the abort, or early separation, criteria constitute a mandatory requirement for manned craft, a detailed investigation of this mode must be performed. Early separation loads should be considered, and propellant expulsion to reduce the landing weight should be investigated.

### 8.1.2 Loading Requirement

Preliminary design loading distributions have been determined during the concept design phase so that values of structural loading can be ascertained, critical load paths established, and primary structural elements sized. While not all possible loading conditions have been fully analyzed at this point in the design development,

the loads presented should constitute an adequate definition of the vehicle loading environment for preliminary sizing purposes. The structural design criteria sections and vehicle performance parameters form the basis for establishing these design loads.

8.1.2.1 Two-Stage Vehicle Loads. Loading distributions shown are typical of loads developed for various two-stage vehicle configurations analyzed during the design development phase. Conditions for which loading distributions have been evaluated are as follows:

- Ground wind loading conditions resulting from the combined vehicle configuration erected on the launch pad
- Maximum airload bending condition (maximum  $a q$ ) occurring during ascent phase of flight
- Booster stage burnout condition
- Landing approach condition (subsonic maneuver) resulting from a 2.5-g low-altitude maneuver
- Landing condition based on a sinking speed of 9 feet per second
- Taxi condition with the 2.0 g loading required by MIL-A-8862

Load distributions for these conditions, presented in Figs. 8-1 through 8-11, are for the alternate separation system concept. A summary of design load factors and including other ascent and reentry flight loading events is presented in Table 8-1.

8.1.2.2 Triamese Vehicle Loads. Preliminary loading distributions have been established for the conditions of maximum airload bending, landing, and taxi for a typical Triamese vehicle configuration analyzed during the design development phase.

A summary of design load factors used for the Triamese vehicle system load studies is shown in Table 8-2.

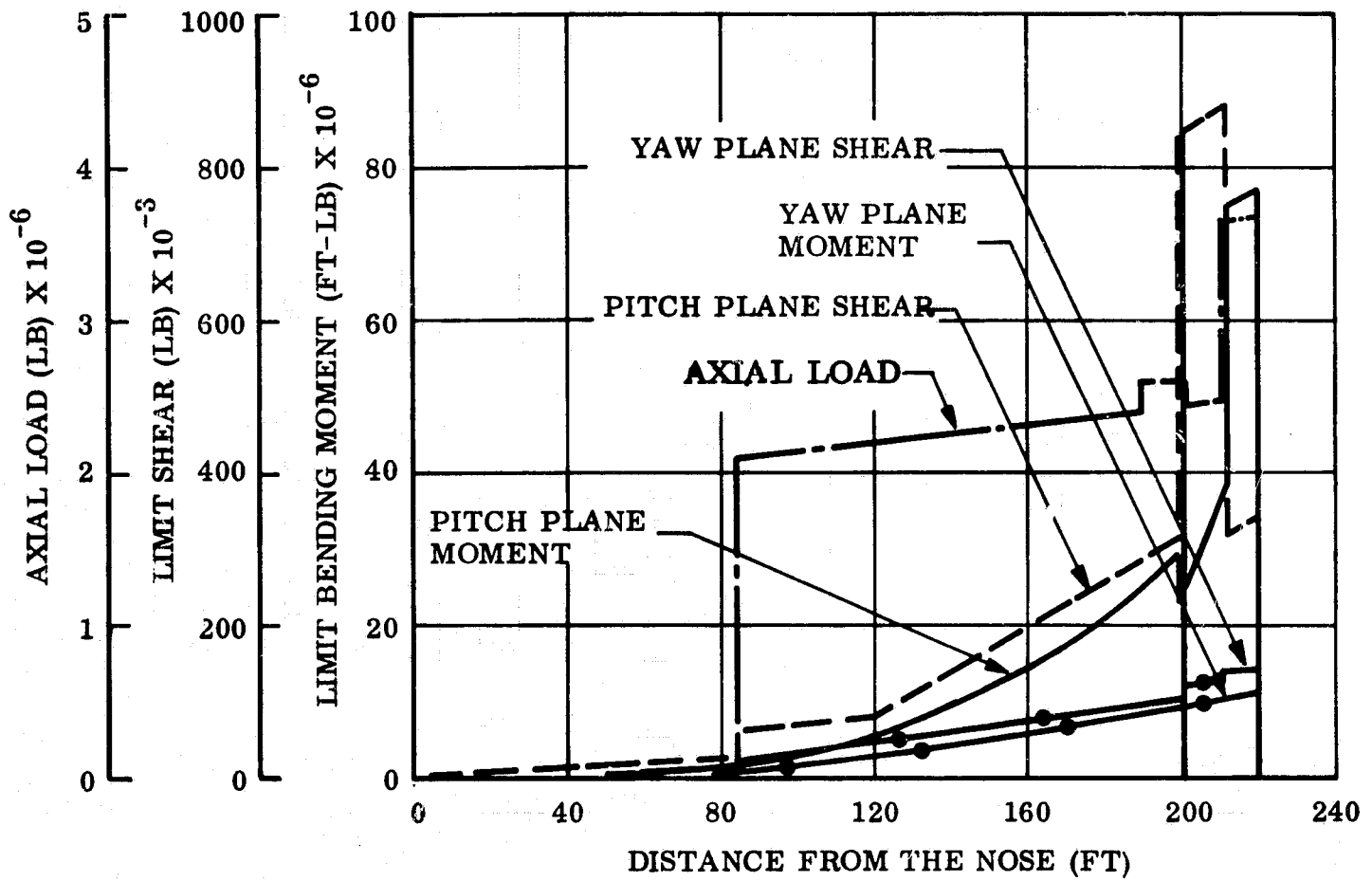


Fig. 8-1 Two-Stage Booster Vehicle Ground Winds Loading Distribution

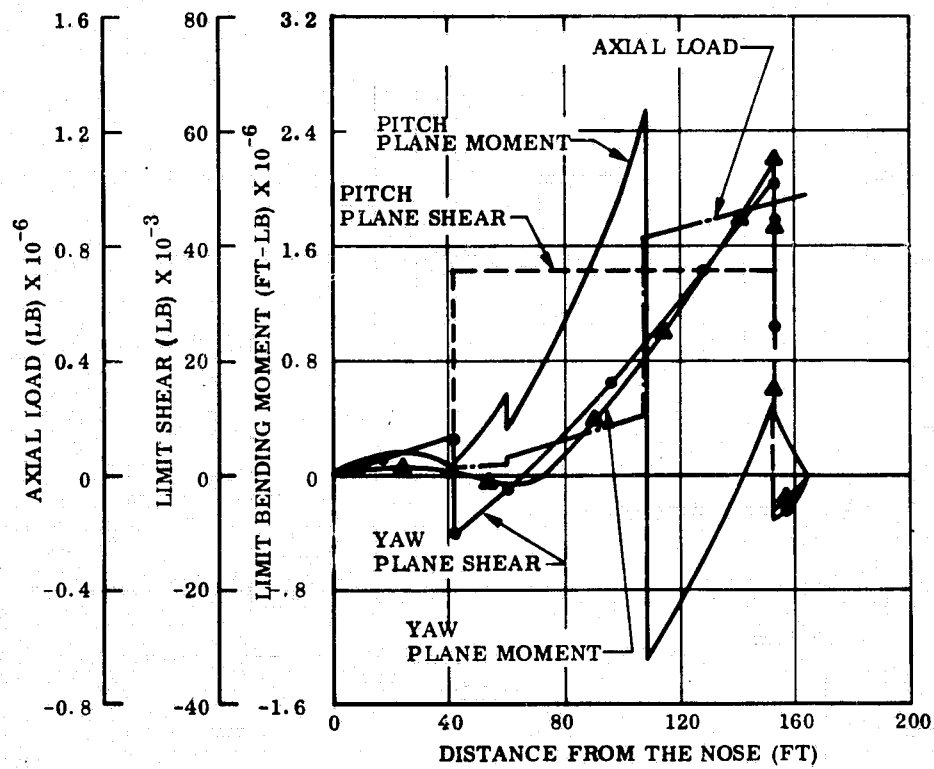


Fig. 8-2 Two-Stage Orbiter Vehicle Ground Winds Loading Distribution

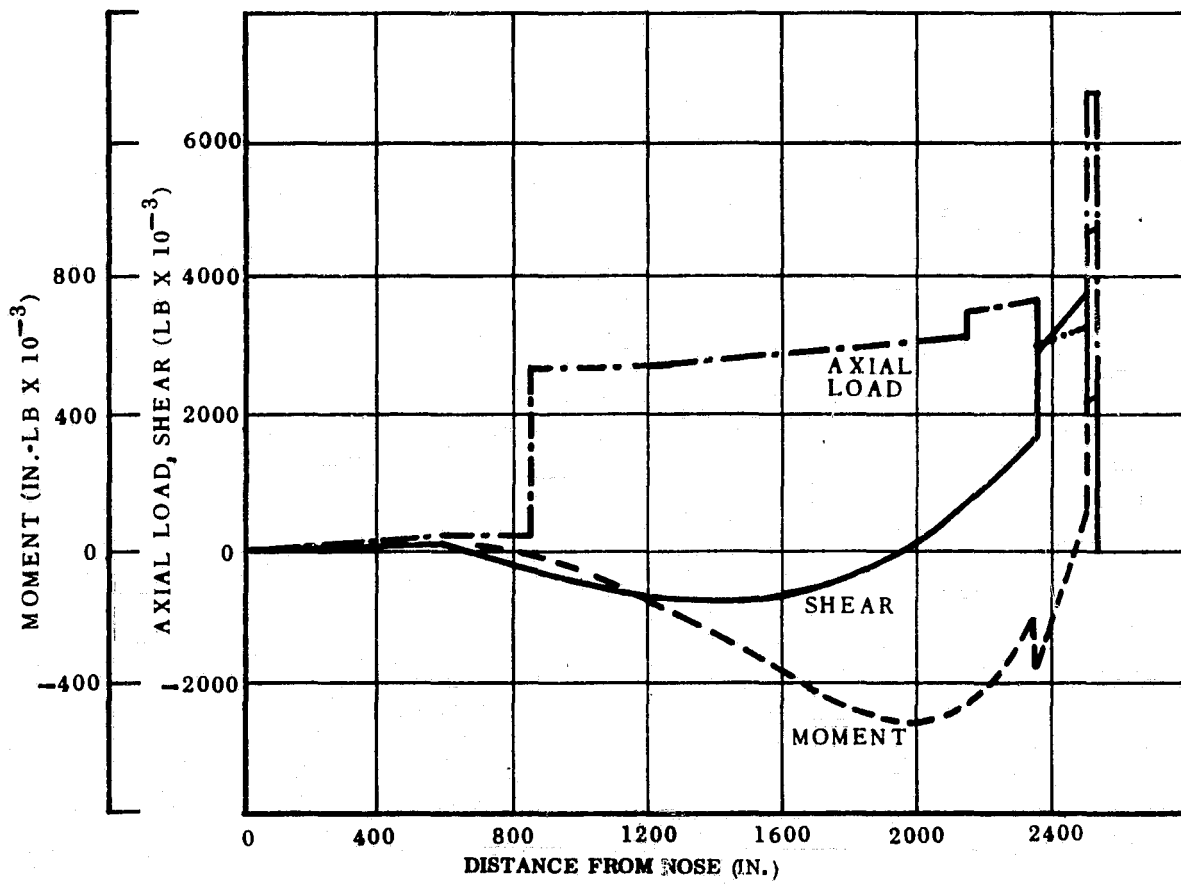


Fig. 8-3 Two-Stage Booster Vehicle Launch Phase Loads (max  $\alpha q$  Condition)

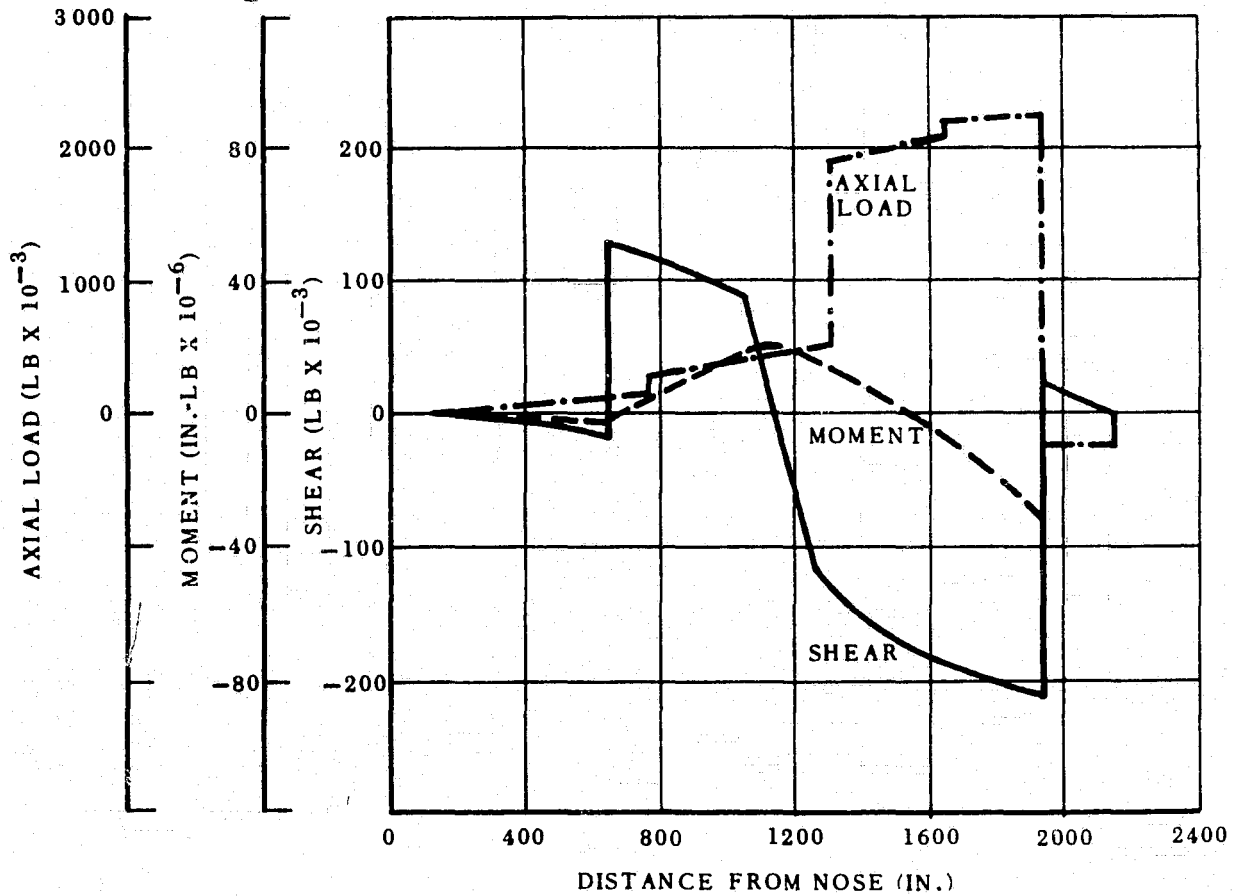


Fig. 8-4 Two-Stage Orbiter Vehicle Launch Phase Loads (max  $\alpha q$  Condition)

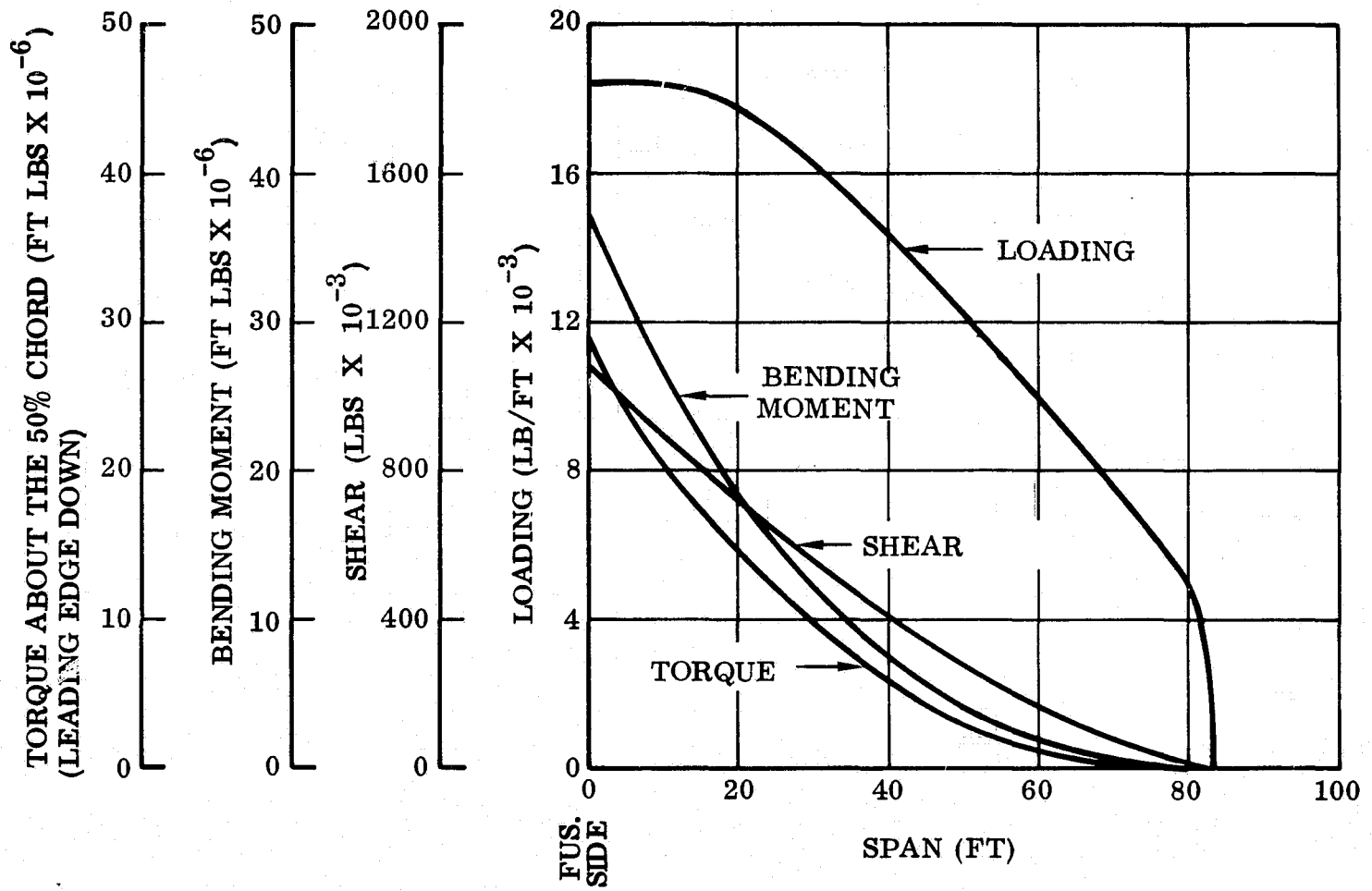


Fig. 8-5 Two-Stage Booster Vehicle Maximum Wing Spanwise Bending Moments (max  $a_q$  Loading Condition)

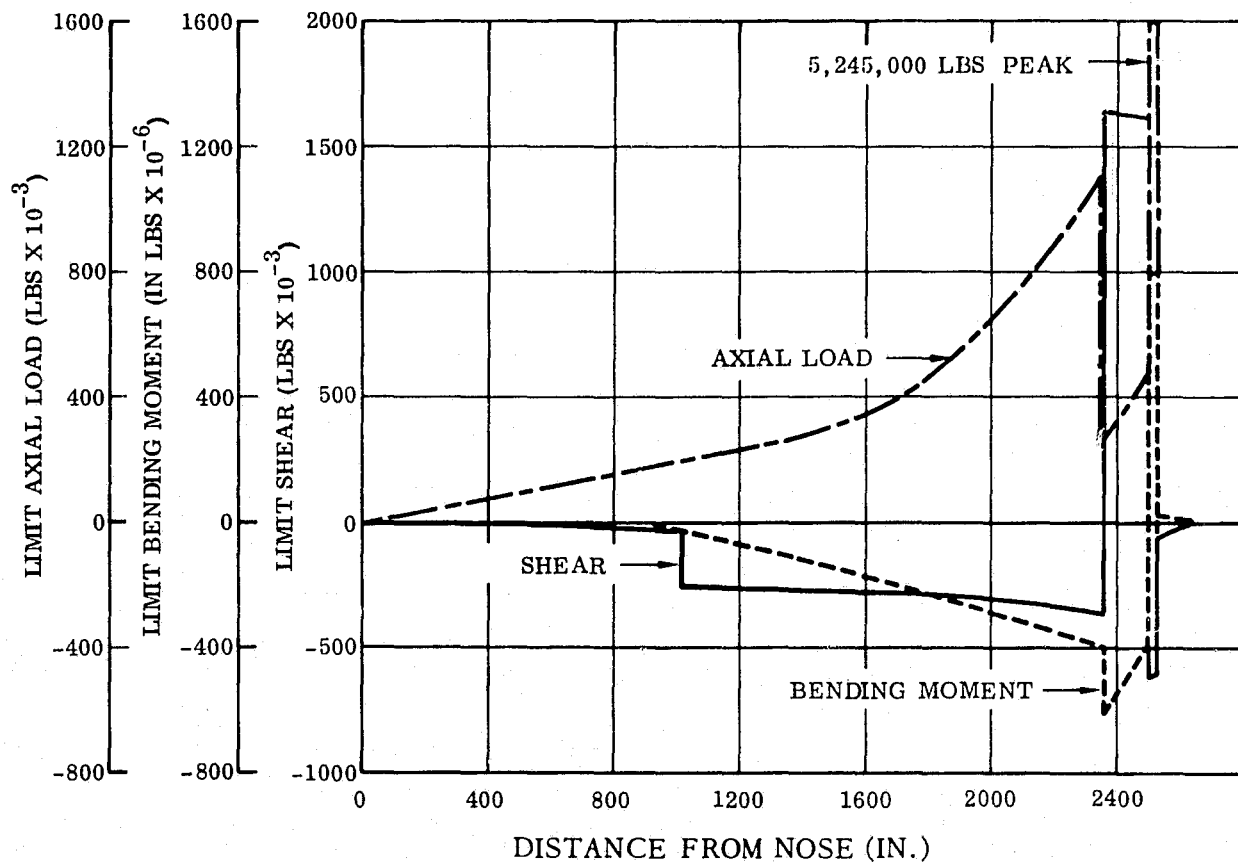


Fig. 8-6 Two-Stage Booster Vehicle Loads for Maximum Axial Load Factor at Burnout

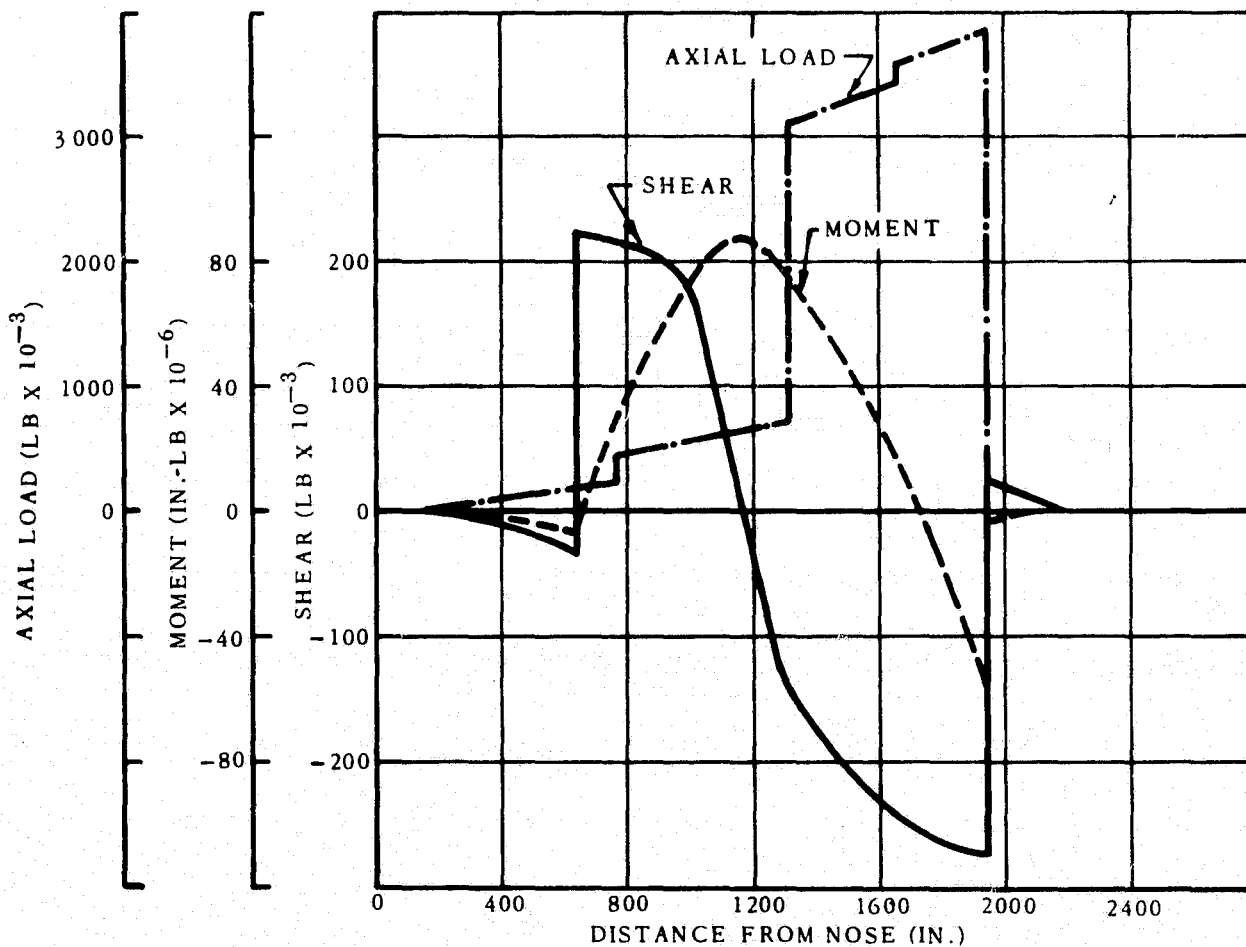


Fig. 8-7 Two-Stage Orbiter Vehicle Loads for Maximum Axial Load Factor at Burnout



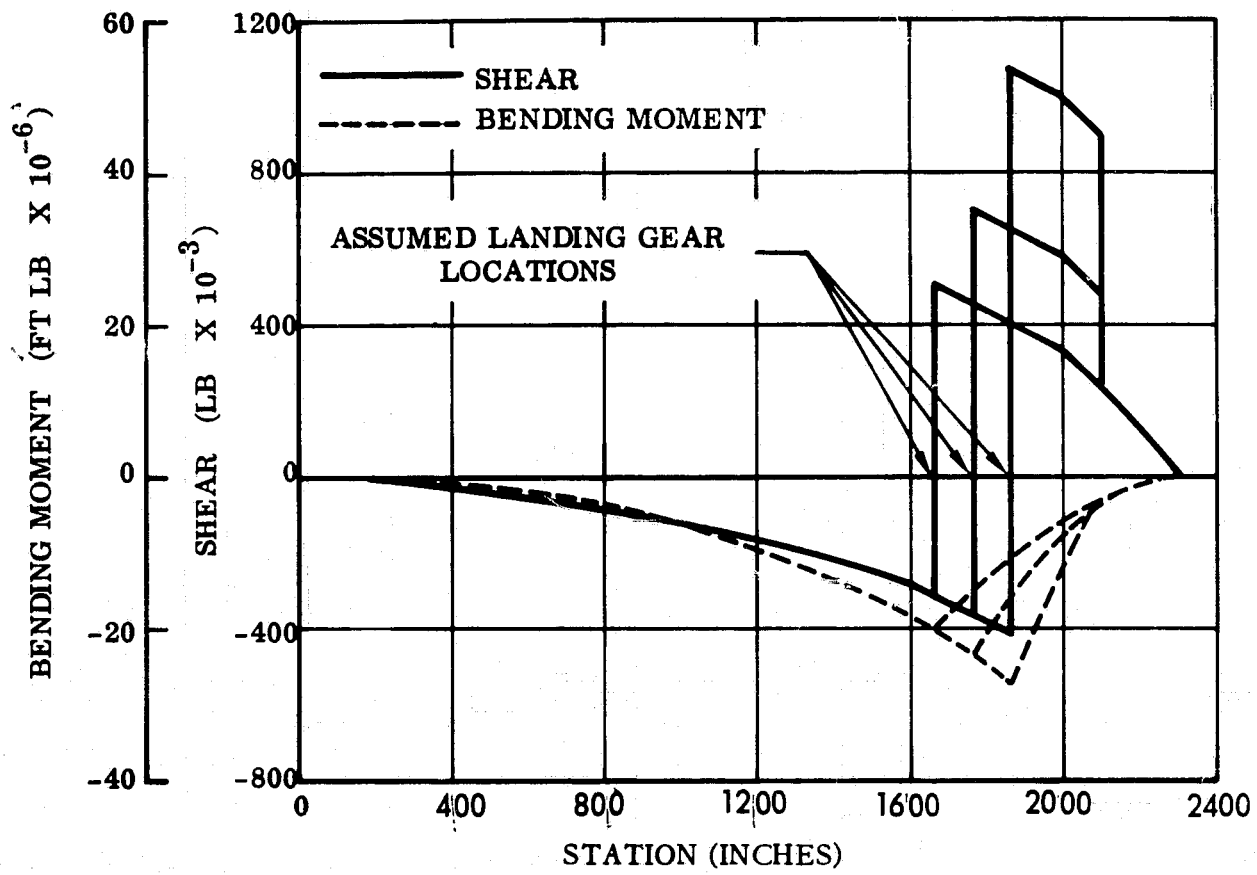


Fig. 8-8 Two-Stage Booster Vehicle Landing Condition Loads

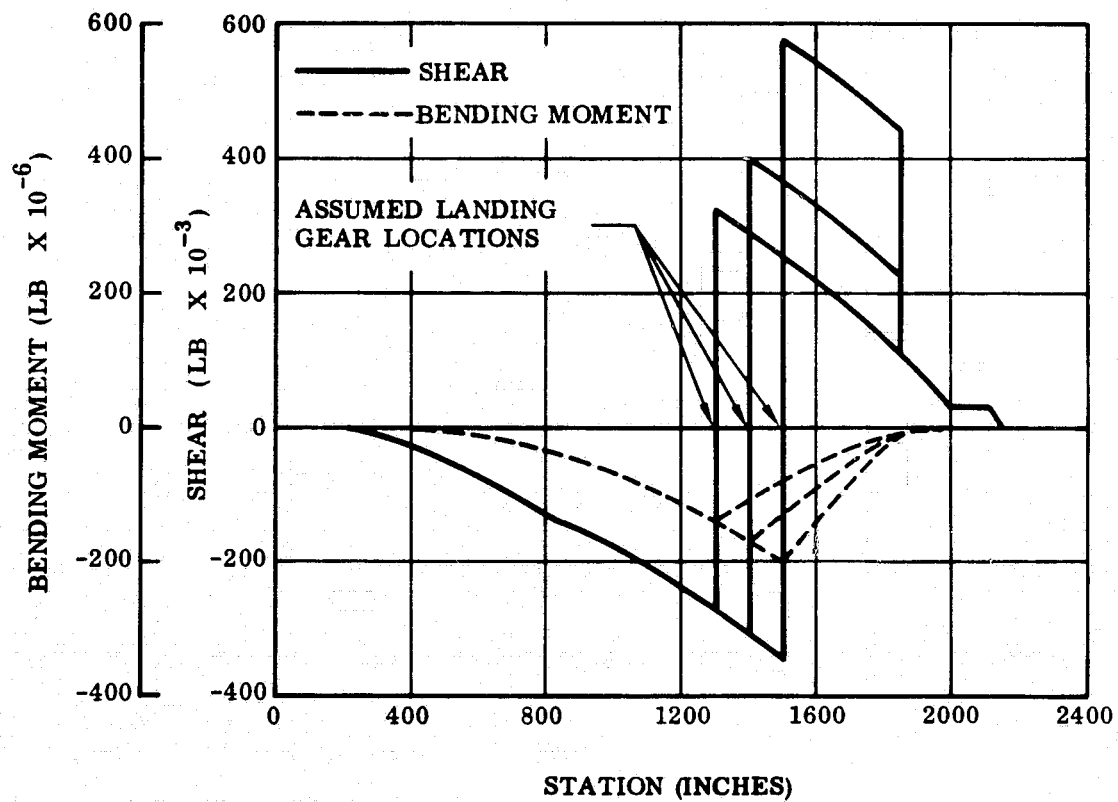


Fig. 8-9 Two-Stage Orbiter Vehicle Landing Condition Loads

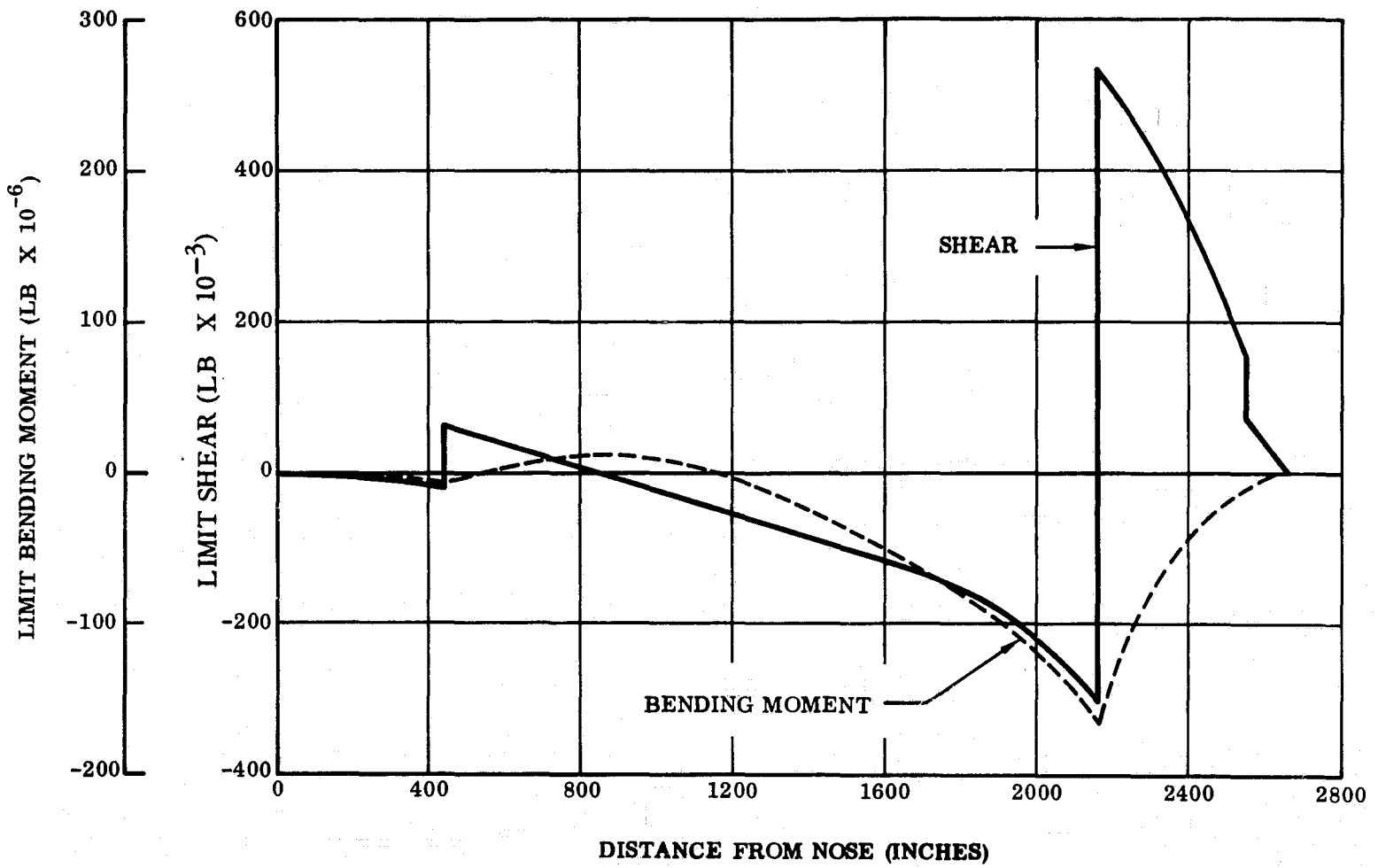


Fig. 8-10 Two-Stage Booster Vehicle Taxi Condition Loads

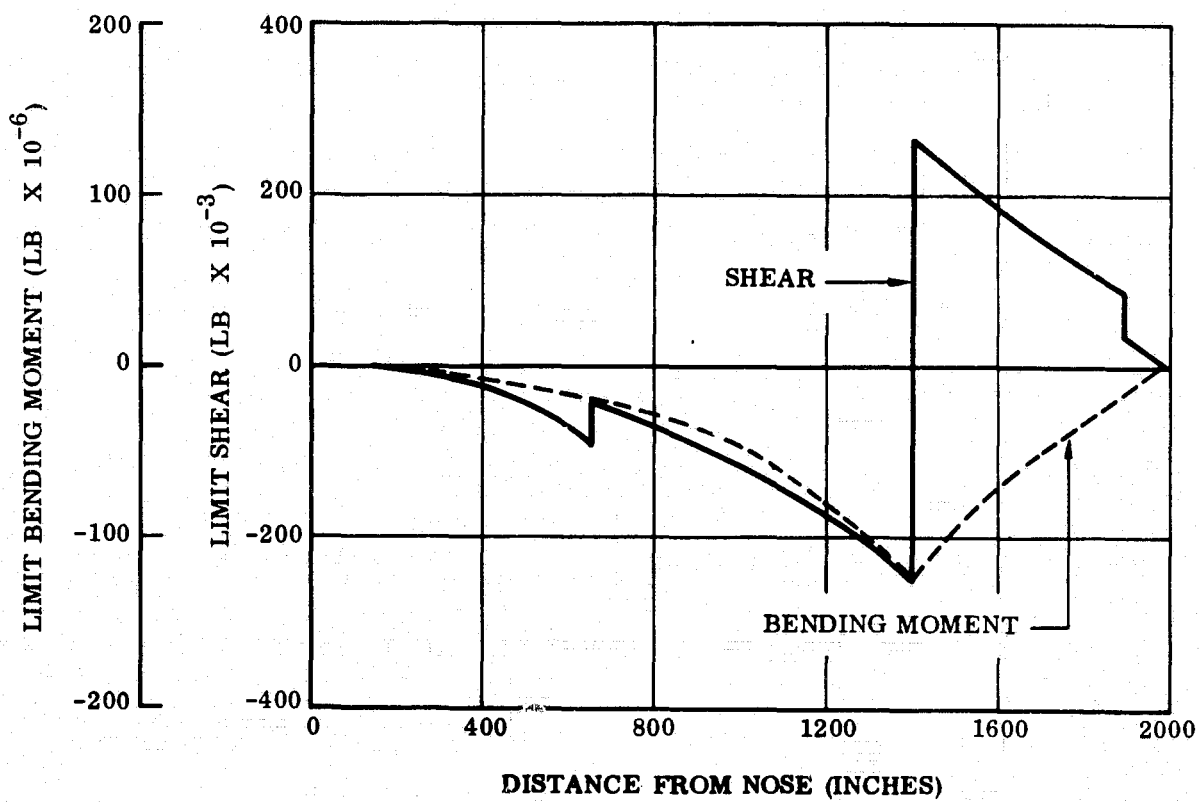


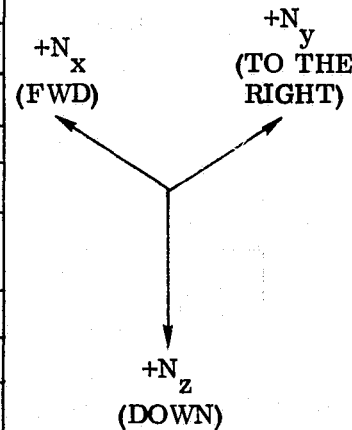
Fig. 8-11 Two-Stage Orbiter Vehicle Taxi Condition Loads

Table 8-1

TWO-STAGE VEHICLE - DESIGN LOAD FACTORS

Loading Condition	Booster Vehicle			Orbiter Vehicle			
	$N_x$	$N_y$	$N_z$	$N_x$	$N_y$	$N_z$	
Ground Handling	±2.0 in Any Direction						
Launch Phase	Liftoff	+1.8***	±0.3	±0.3	+1.8***	±0.3	±0.3
	Maximum $\alpha q$	+1.7	±0.3	±.75	+1.7	±0.3	±.75
	Stage Burnout	+4.0*	±0.3	±0.3	+4.0*	±0.3	±0.3
Orbit Phase	-	-	-	**	**	**	
Reentry	4.0 max vector sum			2.0 max vector sum			
Landing Approach (Subsonic Maneuver)	-2.0	±1.0	+0.5 -2.5	-2.0	±1.0	+0.5 -2.5	
Landing	-1.0	±0.7	-2.0	-1.0	±0.7	-2.0	
Taxi	-	-	-2.0	-	-	-2.0	
Abort	To be determined						

SIGN CONVENTION FOR LOAD FACTORS



All load factors shown in g's (acceleration units)

\*For cargo missions only. Limited to 3.0 g's for mission with passengers aboard.

\*\*Accels not critical for major structure.

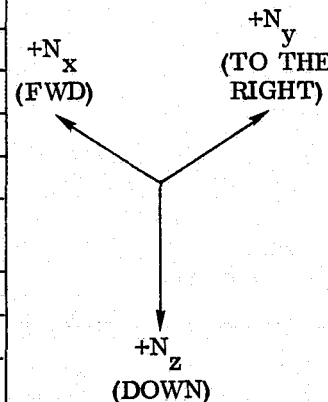
\*\*\*Includes emergency rating factor (1.25 x nominal thrust)

Table 8-2

TRIAMESE VEHICLE - DESIGN LOAD FACTORS

Loading Condition	Booster Vehicle			Orbiter Vehicle			
	$N_x$	$N_y$	$N_z$	$N_x$	$N_y$	$N_z$	
Ground Handling	±2.0 in Any Direction						
Launch Phase	Liftoff	+1.8***	±0.3	±0.3	+1.8***	±0.3	±0.3
	Maximum $\alpha q$	+1.7	±0.3	±0.5	+1.7	±0.3	±0.5
	Stage Burnout	+4.0*	±0.3	±0.3	+4.0*	±0.3	±0.3
Orbit Phase	-	-	-	**	**	**	
Reentry	4.0 max vector sum			2.0 max vector sum			
Landing Approach (Subsonic Maneuver)	-2.0	±1.0	+0.5 -2.5	-2.0	±1.0	+0.5 -2.5	
Landing	-1.0	±0.7	-2.0	-1.0	±0.7	-2.0	
Taxi	-	-	-2.0	-	-	-2.0	
Abort	To be determined						

SIGN CONVENTION FOR LOAD FACTORS



All load factors shown in g's (acceleration units)

\*For cargo missions only. Limited to 3.0 g's for mission with passengers aboard.

\*\*Accels not critical for major structure.

\*\*\*Includes emergency rating factor (1.25 x nominal thrust)

## 8.2 MATERIALS

The Lockheed concept calls for a state-of-the-art aluminum or titanium primary load-carrying structure, shielded from the thermal environment by interchangeable heat shields of three types:

- LI-1500\* lightweight rigid insulation
- Metallic with insulation
- Ablative

Current weight estimates are based on either LI-1500 or metallic heat shields, since the weight values are competitive for these two systems. The metallic materials considered attractive are summarized in Table 8-3. As indicated, TD-NiCr is being considered for applications to 2200°F. While TD-NiCr has a short time capability to 2400°F, Cb-752 will be considered for ranges from 2200 to 2500°F for prolonged-temperature designs.

Merit indices were devised to relate materials to various design characteristics and to provide an efficient index for materials comparison. Considered in preparation of these indexes were factors listed below:

- Structural stability during cycling exposure  $\rho/E_c^{1/2}$
- Fabricability
- Physical properties ( $\alpha K C \rho$  and emissivity)
- Mechanical properties ( $Ftu/\rho$ ,  $Fcy/\rho$ , and creep)
- $t_m$  - material practical minimum gage thickness
- Oxidation characteristics
- Metallurgical stability during cyclic environment

---

\*During the past several years the Lockheed Materials Sciences Laboratory has been working on material systems applicable to reentry vehicles. One of the major developmental efforts has been on an advanced, reusable, rigidized, lightweight insulation heat shield for application to lifting reentry vehicle designated as LI-1500 (a lightweight insulation, weighing approximately 12 to 15 lb/ft<sup>3</sup>). This material system is an all-silica system, consisting of randomly oriented quartz fibers inorganically bonded and sintered at high temperatures. It has a surface temperature capability in excess of 2500°F for long periods of time without surface melting or material removal. It is being considered for application over the major portion of a lifting reentry vehicle in the areas in which the heating rate is 40 Btu/ft<sup>2</sup>-sec or less.

An example of the first factor, structural stability, is shown in Fig. 8-12, in which the weight advantage of the composite materials is noted. The lower the factor,  $\rho/E^{1/2}$ , the lighter the structural weight. For stability critical primary structure, graphite-composite structure may offer up to 40 percent weight savings. Projected costs of graphite-composite systems for the Space Shuttle time phase make this material attractive for further consideration.

A similar chart, Fig. 8-13, shows the stability index of heat shield materials, with René 41 having some advantage in the below 1800° range. Also, it can be welded (with careful attention) and is quite reusable for the mission life considered.

TD-NiCr can be used to 2200°F (short times to 2400°F) without oxidation-protection coatings. However, this material does have its disadvantages, such as low welding allowables and low strength at 2200°F. But minimum weight heat shield concepts can be designed by using mechanical fasteners and unique panel configurations. However, this material requires further evaluation before final selection.

Columbium (Cb-752) with an oxidation-protection coating (R512E) is a candidate for application from 2000°F to 2500°F. While recent coating tests have shown many hours of life at 2500°F, Cb-752 may be limited to approximately 50 reentry cycles with a maximum temperature of 2500°F due to creep deflection. This material requires further evaluation for application to the Space Shuttle. Other columbium materials with higher creep strengths must be investigated.

Ta-10w alloy with an oxidation-protection coating (R512c), for nose cap application, has been evaluated in a plasma-arc facility for 37 6-minute cycles (3.7 hours) at 2800°F without failure.

Table 8-3  
MATERIALS AND PREDICTED TEMPERATURES

**Two-Stage**

Surface	Orbiter			Booster		
	Forward	Center	Aft	Forward	Center	Aft
Body Upper Heat Shield	700 to 1100 Rene' 41	600 to 1000 Rene' 41	500 to 1000 Rene' 41	1100 Rene' 41	650 Ti	500 Ti
Body Lower Heat Shield	2000 to 2200 TD-NiCr	2000 to 2200 TD-NiCr	1800 to 2000 TD-NiCr	1200 Rene' 41	1000 Rene' 41	800 Rene' 41
Nose	2750 Ta-10W	-	-	1450 Rene' 41	-	-
Fin Leading Edge	-	-	2200 TD-NiCr	-	-	1650 Rene' 41
Wing/Body Leading Edge	-	2080 TD-NiCr	2080 TD-NiCr	-	1650 Rene' 41	1650 Rene' 41
Wing Upper Heat Shield	-	-	-	650 Ti	600 Ti	550 Ti
Wing Lower Heat Shield	-	-	-	1250 Rene' 41	1200 Rene' 41	1100 Rene' 41
Primary Structure-Tanks	← 150° F, 2219-T87 Aluminum →					

**Triamese**

Surface	Orbiter			Booster		
	Forward	Center	Aft	Forward	Center	Aft
Body Upper Heat Shield	700 to 1100 Rene' 41	600 to 1000 Rene' 41	500 to 1000 Rene' 41	1100 Rene' 41	650 Ti	500 Ti
Body Lower Heat Shield	2000 to 2200 TD-NiCr	2000 to 2200 TD-NiCr	1800 to 2000 TD-NiCr	1250 Rene' 41	1200 Rene' 41	1100 Rene' 41
Nose	2750 Ta-10W	-	-	1450 Rene' 41	-	-
Fin Leading Edge	-	-	2200 TD-NiCr	-	-	1650 Rene' 41
Wing/Body Leading Edge	-	2080 TD-NiCr	2080 TD-NiCr	-	1650 Rene' 41	1650 Rene' 41
Wing Upper Heat Shield	-	-	-	650 Ti	600 Ti	550 Ti
Wing Lower Heat Shield	-	-	-	1250 Rene' 41	1200 Rene' 41	1100 Rene' 41
Primary Structure-Tanks	← 150° F, 2219-T87 Aluminum →					

- Note: 1. Cb-752, 2200° F to 2500° F (if required)  
2. LI-1500 is interchangeable for heat shields  
3. Ablator - backup heat shield

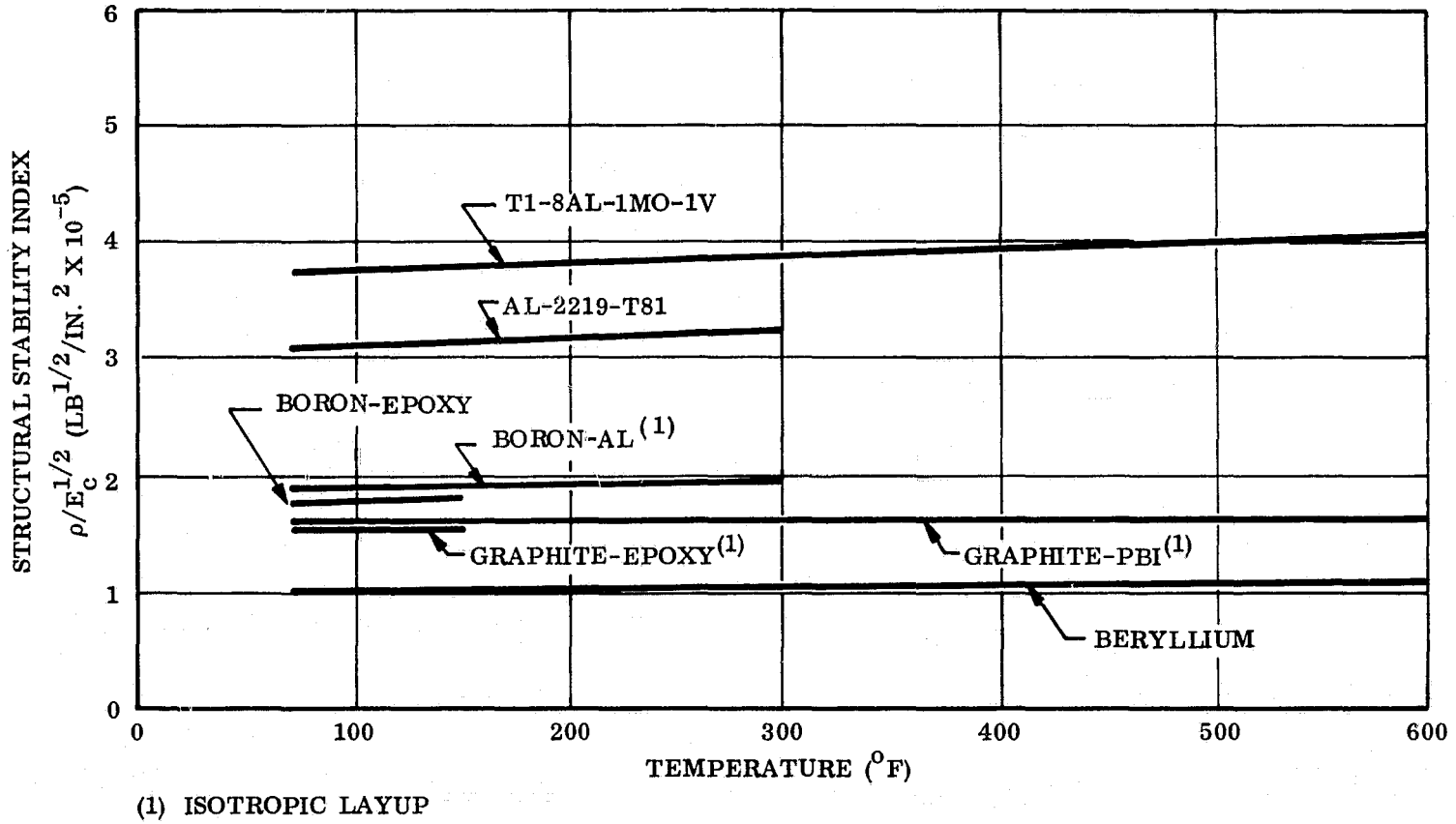


Fig. 8-12 Structural Stability vs Temperature of Various Materials

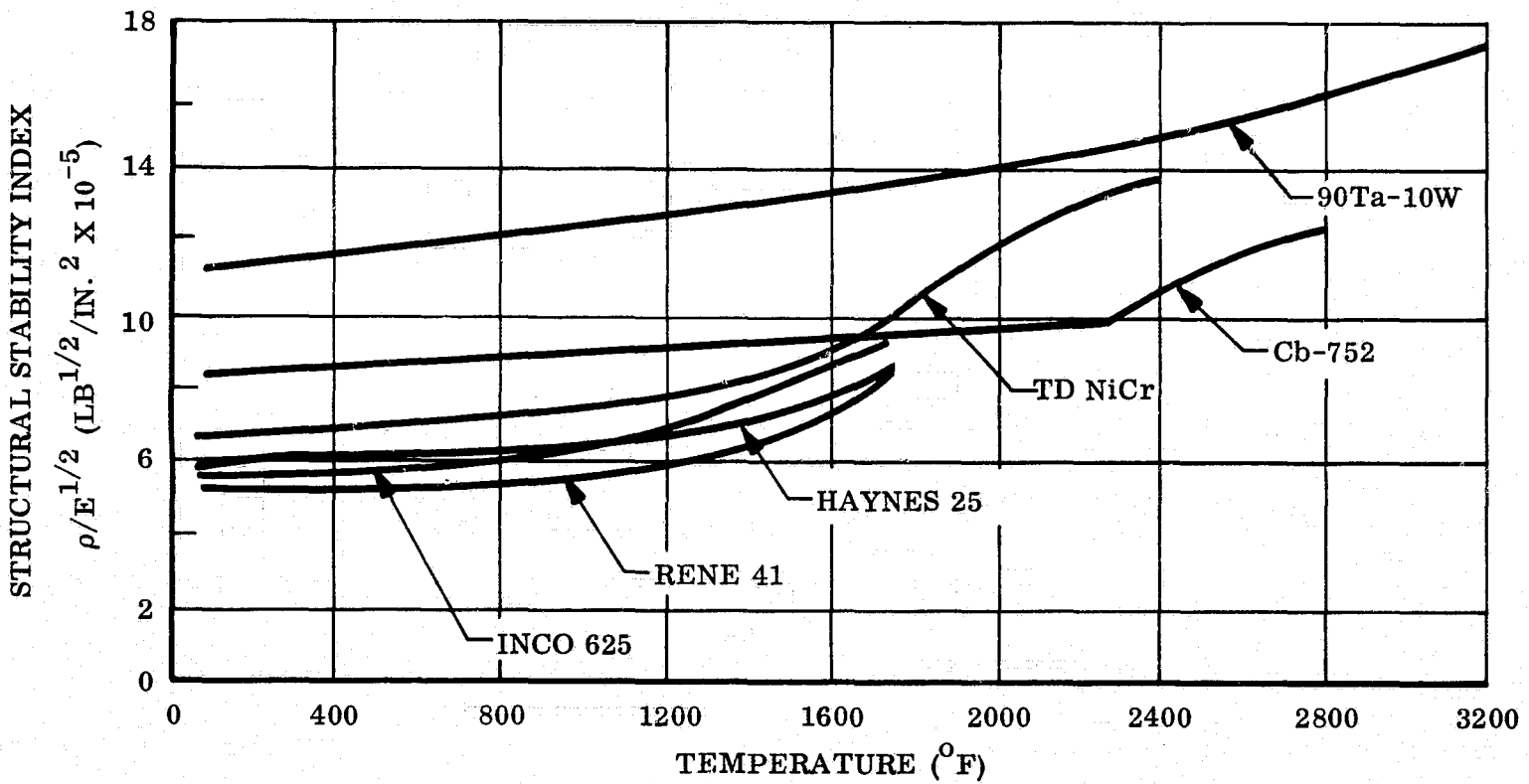


Fig. 8-13 Structural Stability Comparison of High-Temperature Heat Shield Materials

### 8.3 THERMAL STRUCTURAL CONCEPTS

The heat shield approaches are indicated in Fig. 8-14 for the orbiter. Both metallic and rigid insulation (LI-1500) are shown; the rigid heat shield is interchangeable with the ablative system.

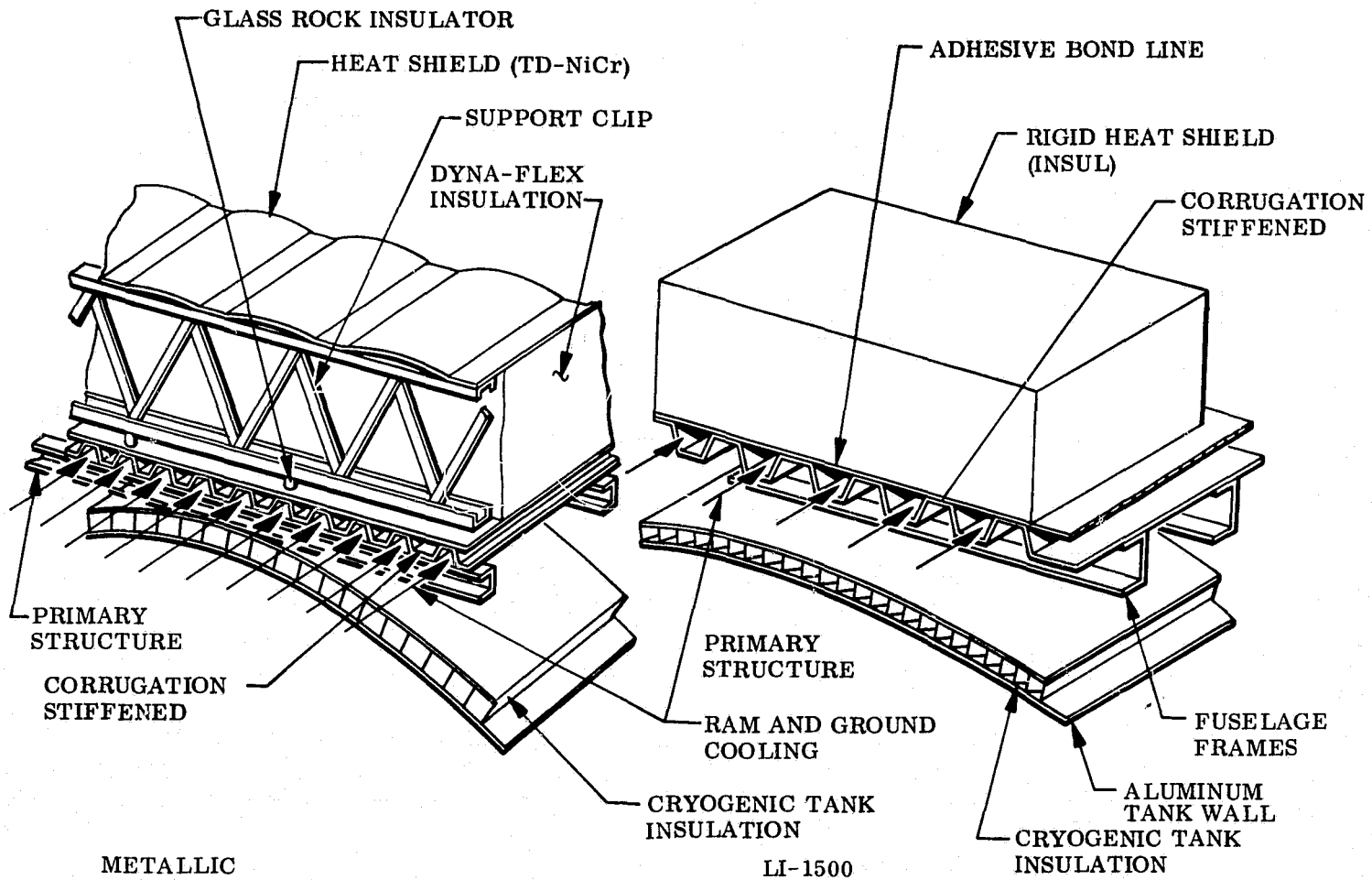


Fig. 8-14 Orbiter Heat-Shield Approaches



The use of interchangeable thermal protection systems entail minimum development risks. During early vehicle flights, good temperature data are needed; this indicates the use of a radiative (nonablative) heat shield. Existing metallic heat shield materials or LI-1500 can be used for early test flights. However, if temperatures are higher than anticipated for the fully operational flights, ablators are available for use on local areas of the vehicle. The various heat shields can be made interchangeable without greatly affecting the aluminum primary structure. The preferred metallic heat shield is a large corrugated panel mounted with a multiple clip arrangement through a glass rock insulator to the primary aluminum structure. Corrugation amplitude is one-tenth the corrugation pitch, with a flat provided between corrugation arcs to enable attachment of the continuous support clip. Mechanical fasteners and resistance spot welding are used to attach the TD-NiCr and Rene'41 corrugated heat shields.

Blanket-type insulation (dynaflex and microquartz) is packaged between the corrugation shield and the structural panel.

The LI-1500 material system shown in Fig. 8-14 is being considered as the outer surface thermal protection system for the vehicles in areas where the temperatures are 2500<sup>0</sup>F or less. The LI-1500 material protects the primary load-carrying structure and is subjected only to its own inertial loads and to air loads. The LI-1500 panels are bonded to the primary structural panels. Since the LI-1500 material has a very low thermal coefficient expansion, minimum external expansion joint are necessary.

The temperature ranges and metallic heat shield materials are shown in Fig. 8-15 with percentage of surface area plotted against temperature for both booster and orbiter. Titanium and Rene'41, are used over 99 percent of the surface area of the booster and over 52 percent of the surface area of the orbiter.

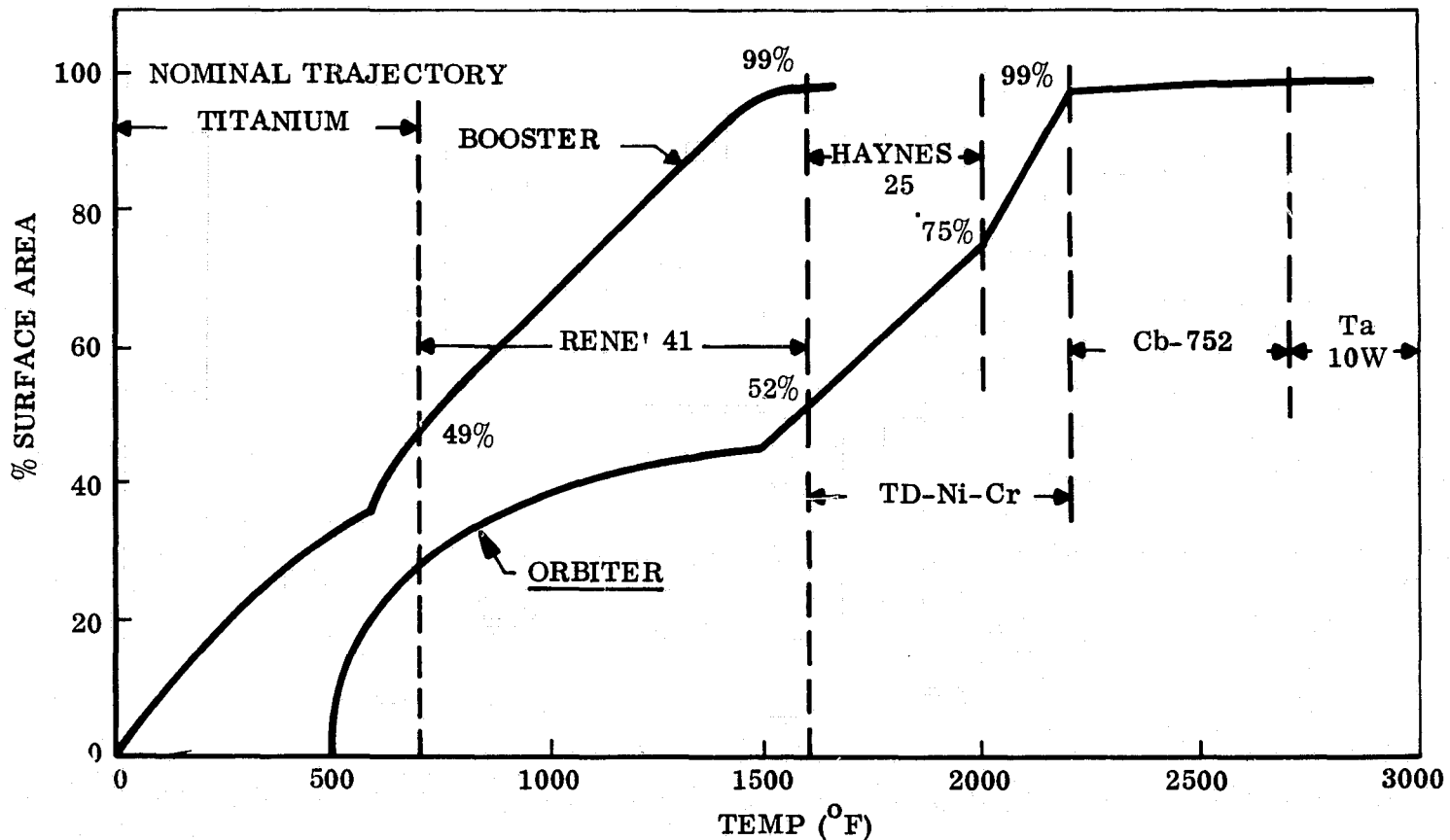


Fig. 8-15 Temperature Ranges and Heat-Shield Materials

Initially, various thermal protection systems employing both passive and active systems were studied. Passive systems provide sufficient thermal insulation to limit the maximum structure temperature to an acceptable value. The following passive system concepts were evaluated:

- Felt-like high-temperature insulations, such as dynaflex and microquartz in conjunction with metallic heat shields
- LI-1500
- A fiberglass-reinforced silicone elastomeric ablator ( $\rho = 20 \text{ lb/ft}^3$ )

The LI-1500 and metallic heat shield concept were also evaluated in conjunction with a closed-loop active cooling system. In all cases, orbiter internal structure was assumed to have a design maximum temperature of  $150^\circ\text{F}$ . Heating calculations were based on the L/D of the spacecraft and maximum cross-range entry trajectory.

Because of the large potential saving in insulation weight, two approaches to alleviate the effects of post-touchdown heating were considered. One is to cool during low-speed flight with either ram air cooling or engine-bleed air; the other is to use a ground cooling system after landing. Analysis indicates that the use of ram air and ground cooling reduces the required LI-1500 thickness from greater than 5 inches to approximately 3 inches at the maximum heating lower surface location.

Shown in Fig. 8-16 are comparisons of the candidate thermal protection system weights (exclusive of the structure weight common to all systems). The ablator weight is based on an assumed 20 lb/ft<sup>3</sup> partial depth ablator with a bond-line temperature of 600°F. A 12-lb/ft<sup>3</sup> rigid insulator is used between the ablator and the structure.

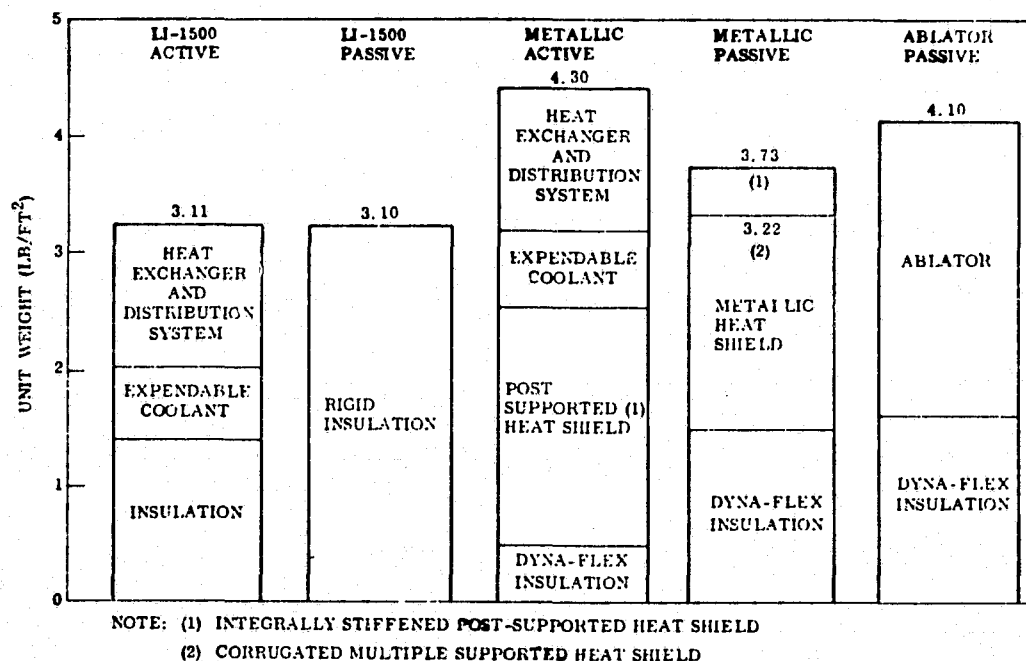


Fig. 8-16 Thermal Protection System Comparison (Orbiter)

The 3.22 lb/ft<sup>2</sup> weight for the corrugated heat shield compares favorably with the 3.10 lb/ft<sup>2</sup> for the LI-1500 rigid insulation. These values are for the hottest point at the lower centerline of the vehicle.

## 8.4 VEHICLE STRUCTURAL ARRANGEMENT

The leading structural arrangements and materials presently being considered are as follows:

- Booster

Heat shielding: lower surface -Rene'41 or LI-1500  
upper surface: Rene'41 and titanium or LI-1500

Load-carrying structure: fuselage, aluminum; wing, titanium or aluminum

Load-carrying tanks: (fuselage)

- Orbiter

Heat shielding: upper surface (Rene'41 or LI-1500; ablator, backup)

lower surface (TD-NiCr or LI-1500; ablator, backup)

Load-carrying structure: aluminum

Nonload-carrying tanks

### 8.4.1 Orbiter

The orbiter structural configuration has a wedge planform shape with a triangular cross-section for the required lifting body characteristics. The body is basically of corrugated stiffened panel construction, with intermediate supporting frames of aluminum construction to sustain the critical flight and landing loads. Figure 8-17 indicates primary thrust longeron load paths. A preliminary weight trade study for the corrugated panel construction applicable to the lower fuselage structure is shown in Fig. 8-18, in which the present all-aluminum baseline design is compared to that of aluminum skins with beryllium frame; all beryllium construction, graphite/epoxy skins with aluminum frame; and graphite/epoxy skins with beryllium frame. The figure shows that a significant weight reduction may be achieved by using materials other than aluminum. For the predicted ultimate loading intensity of  $N_x = 3000$  lb/in. at the fuselage midbody lower surface, the geometric proportions of the other materials are well within the manufacturing limitations. Since 1 pound of inert

orbiter weight is worth 30 pounds of liftoff weight, it is recommended that these alternate materials be given serious consideration as a replacement for the baseline aluminum construction.

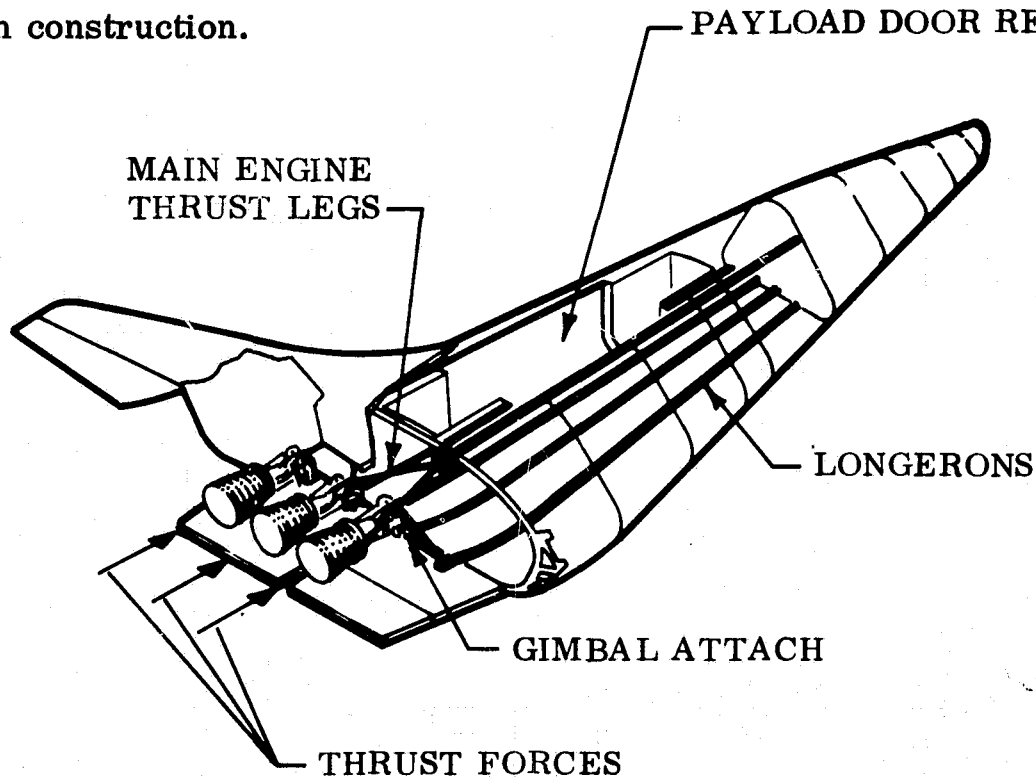


Fig. 8-17 Orbiter Primary Load Paths

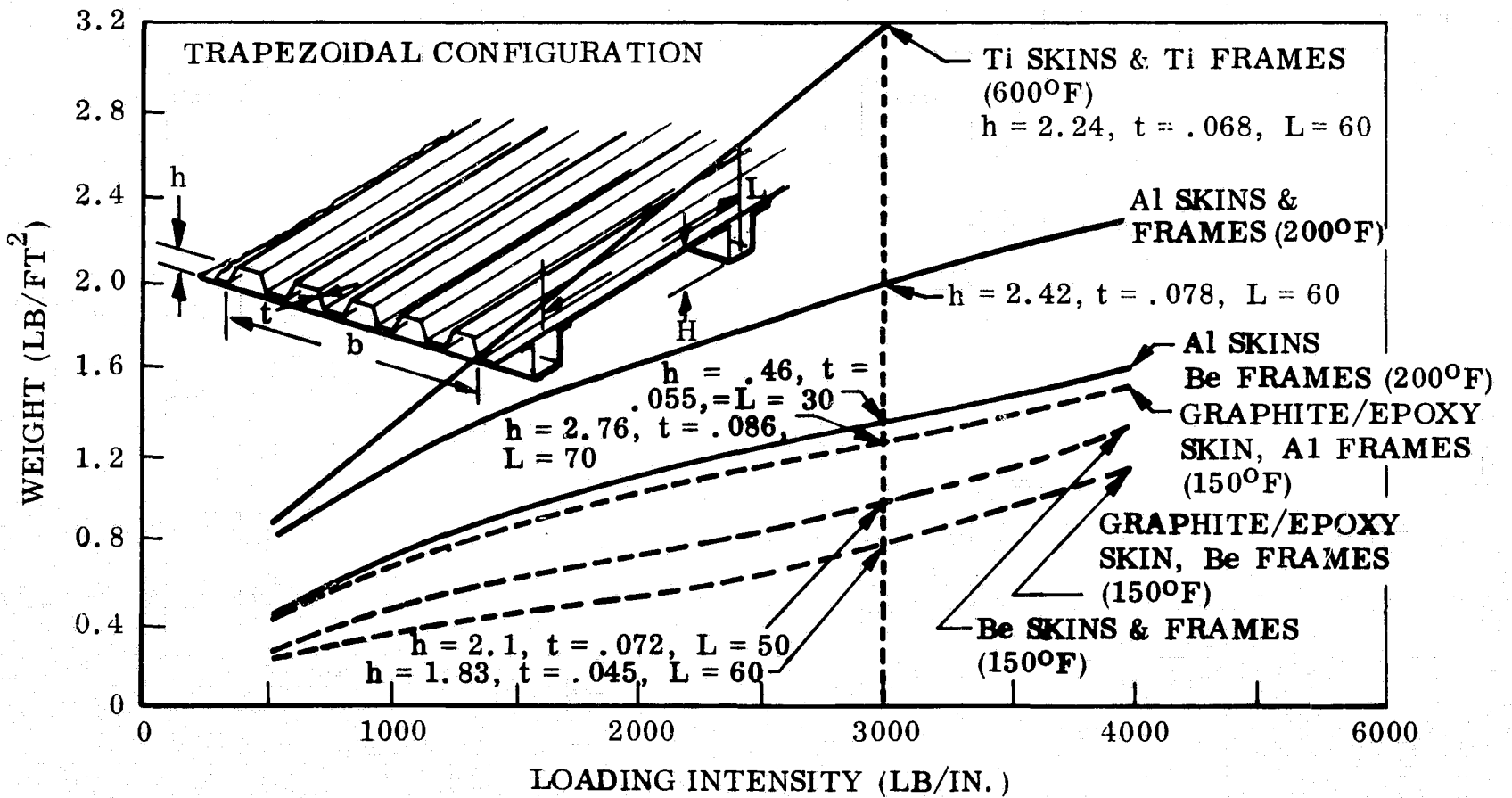


Fig. 8-18 Variation of Orbiter Primary Structure Weights

The aluminum propellant tanks are nonintegral to the fuselage structure and are designed by membrane stresses caused by the internal ullage and hydrostatic pressure. A weight trade study for the large forward LH<sub>2</sub> (2219-T87) propellant tanks to that of 6A1-4V titanium alloy indicated that weight savings of 15 percent could be achieved by the use of this titanium alloy, with a negligible weight savings available for the smaller LH<sub>2</sub> tanks. The conclusion is based on a minimum gage restraint of .030 for the titanium construction. The nose section of the fuselage is designed to withstand the collapse pressure and the body bending loads induced during the max  $\alpha$ q flight condition. Since the body bending loads are relatively small over this region, light-gage skins are used primarily to react the pressure loads to the closely spaced stringers and supporting frames.

With the present planform design, based on the nonintegral tank concept, cylindrical and conical shaped LH<sub>2</sub> and LO<sub>2</sub> tanks are used to achieve high-volumetric efficiency. Support of the propellant tanks to the primary fuselage structure is accommodated by circumferentially located tension link supports connected to the dome closure rings. These discrete support points reduce the heat flux to the primary shell and minimize the thermal stresses in the tank structure. The concentrated longitudinal forces induced in the fuselage structure are reacted out by longitudinal members and subsequent shear transfer in the skin.

#### 8.4.2 Booster

The booster load paths are indicated in Fig. 8-19, with fuselage tankage considered as primary load-carrying structure. This tankage is designed for dual roles – first, as a pressure vessel (storing fuel or oxidizer) and, second, a spacecraft fuselage (reaction to loads imposed from various flight and ground conditions, including support of the orbiter vehicle).

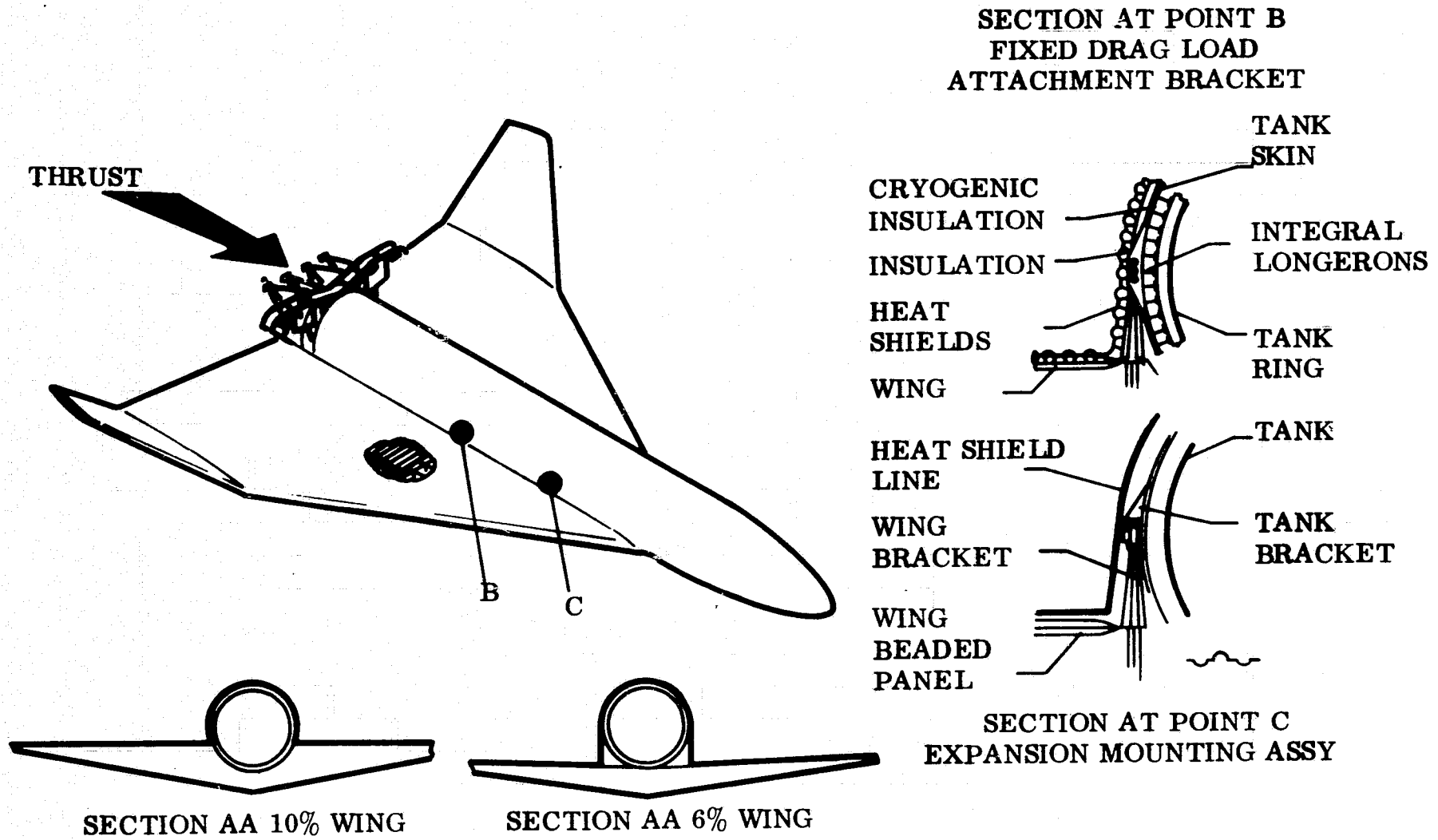


Fig. 8-19 Booster Load Paths

In order to consider damage-tolerance (fail-safe) criteria, full pressurization is considered active only for the primary ascent boost load condition, at which time maximum dynamic pressure and thrust occur. Should a loss of internal pressure occur within a portion of the tankage, engine malfunction will follow. For abort modes and maneuver landing, taxi, and ferrying modes, zero gage pressurization is assumed for design; i. e., the fuselage shell structure must be capable of sustaining loads without aid from internal pressure.

The booster comprises three basic structures, of which a wing box and a cylindrical fuselage housing  $\text{LO}_2$  and  $\text{LH}_2$  propellant are similar to corresponding components of conventional aircraft. The third is the engine thrust structure. The fuel tankage (in the fuselage) is designed as primary load-carrying structure to minimize vehicle weight. The  $\text{LO}_2$  tank, located in the forward section, is tied structurally to the  $\text{LH}_2$  tank by a conventional missile interstage ring-stringer stiffened shell.

The  $\text{LO}_2$  tank is designed principally for a combination of internal ullage and hydrostatic pressure. The shell thickness is tailored to meet the linear varying pressure requirements. Intermediate rings are added to the shell to provide the necessary stiffness required for the additional flight and ground load conditions. The  $\text{LH}_2$  tank is designed for a combination of internal pressure, body bending, and axial boost loads. Since hydrostatic pressure is small in comparison to ullage pressure, the maximum design pressure for determination of shell wall thickness is established from the maximum (absolute) ullage pressure requirements. Transverse rings and longitudinal stiffeners are added to the shell to provide the necessary stiffness for the additional flight and ground load conditions.

Both the  $\text{LO}_2$  and  $\text{LH}_2$  tanks have fusion-welded elliptical domes, which are built up from gore sections and a spherical cap. The walls of the tanks are fabricated from rolled-extruded and machined integrally stiffened planks. Y rings are used at the dome-cylinder junction to permit mechanical fastener attachment of the adjacent structure. At the aft-skirt section, the engine thrust structure supports fourteen 400,000 pound thrust engines and four turbojet engines. In addition to reacting the booster thrust loads and flight thrust loads, provision is made for interstage (shear and radial load) attachment of the orbiter vehicle. Additional radial load attach structure for the



orbiter is located in the forward booster  $\text{LO}_2/\text{LH}_2$  intrastage structure. The thrust structure is a combination of a space frame assembly (to gather up the numerous engines) and a double-bridged plate girder to react the orbiter inertia loads during boost and to distribute the engine thrust loads to a conical stiffened shell aft skirt.

The basic problem in the design of this complex structure is to react the large concentrated loads introduced by the orbiter, as well as the concentrated engine thrust loads, and redistribute them to the  $\text{LH}_2$  tank as uniformly as possible. The booster  $\text{LO}_2/\text{LH}_2$  intrastage structure, which connects the  $\text{LH}_2$  tank, is merely an extension of the  $\text{LH}_2$  ring-stringer stiffened shell, except that mechanical fasteners can be used to attach the shell to the Y-ring stub skirts of the tanks. In addition to the miscellaneous equipment stored within this area of the booster, provisions for the nose landing gear are located here. Access doors are provided where necessary.

The wing is a single delta, multispar and rib-box type, assembled from built-up extruded shapes and integrally stiffened cover sheets. Propellant storage is accomplished elsewhere, allowing a dry wing design. The main landing gear will be housed within the center wing section. The major structural problem is the design of the attachment of the hot wing to a cold fuselage. Extreme relative displacements take place between the hydrogen filled fuselage (at a temperature of  $-420^\circ\text{F}$ ) and a wing at a temperature of  $100^\circ\text{F}$ ). To permit the fuselage to contract freely (approximately 10 inches), a simple statically determinate trussed frame is extended vertically from the wing root rib to the fuselage at five discrete transverse frame locations. Of the five spanwise shear ties, only the middle tie resists chordwise shear. The remaining four permit the fuselage to move longitudinally relative to the wing chord by providing a captive-roller support design.

Several prime material candidates for the fuselage and wing have been under consideration. For the  $\text{LO}_2$  tank, two materials evaluated were 2219-T87 aluminum and 9Ni-4Co-.25C steel. For the  $\text{LH}_2$  tank, 6A1-4V titanium was also considered. (It exhibited good service experience in cryogenic applications.) The following weight comparisons resulted:

Item	Mass Thickness, pounds per square feet		
	Aluminum	Steel	Titanium
LO <sub>2</sub> tank	4.41	3.87	-
LH <sub>2</sub> tank	4.60	3.68	3.06

These study results reveal that 2219-T87 aluminum may be heavier than high-strength steel and titanium alloys. The main reason is that weldable aluminum alloys do not result in high strength-to-weight efficiencies, as do the typical aircraft alloys, such as the 2024 and 7075 series. More detail studies are required to confirm this trend and evaluate related disciplines, i.e., producibility, cost, etc.

Comparison of wing weight results may reflect the opposite conclusion; i.e., aluminum may be lighter than titanium. The main reason is that full advantage of titanium compressive properties may not be realized. While studies of C-5A structures have confirmed this conclusion, further detail design studies of titanium are warranted for Space Shuttle applications. Aluminum is also attractive since the critical design condition occurs at room temperature during the ascent max  $\alpha q$  condition.

Section 9  
PROPULSION

The Space Shuttle propulsion requirements are fulfilled by three systems -- primary, reaction control, and subsonic cruise. Propulsion requirements for the Two-Stage vehicle configurations and in a Triamese vehicle configuration have been identified in terms of thrust level and impulse propellant in Table 9-1.

Table 9-1

ENGINE AND PROPELLANT REQUIREMENTS

Vehicle \ Payload		50,000 lb		25,000 lb	
		Booster	Orbiter	Booster	Orbiter
Two Stage	Thrust	13-400 k (SL)	3-470 k (Vac)	11-400 k (SL)	3-470 k (Vac)
	Impulse Propellants	2,344,297 lb	705,571 lb	1,924,126 lb	553,709 lb
Triamese	Thrust	8-400 k (SL)	3-470 k (Vac)	7-400 k (SL)	3-470 k (Vac)
	Impulse Propellants	1,386,199 lb Each Booster	709,523 lb	1,155,946 lb Each Booster	555,730 lb

The primary propulsion systems of the booster and the orbiter use high-performance rocket engines having commonality in turbomachinery and in combustion chamber sizing. The booster engines operate at maximum thrust until the maximum acceleration limit (3-g or 4-g) is reached; they are continuously throttled thereafter to sustain the maximum acceleration until the stage-separation altitude is reached. After staging, the three orbiter engines are operated at maximum thrust until the vehicle acceleration limits are reached. They are continuously throttled thereafter to sustain the limiting acceleration until orbit injection is attained. After staging, the booster follows a ballistic flight path and reenters with aerodynamic braking. It is powered by subsonic cruise turbojets during a portion of the return flight to the launch base.

The orbiter, after performing its mission, is braked out of orbit by operation of its rocket engines. It then reenters the atmosphere and returns to the launch base in the same manner as does the booster.

Descriptions, design and performance requirements, and operational considerations for each of the separate propulsion systems are presented in the following paragraphs.

## 9.1 PRIMARY PROPULSION SYSTEM

The primary propulsion systems for each stage of both vehicle configurations have been examined with the consideration that either the bell-type or the aerospike oxygen/hydrogen engine might be used. The selected approaches and subsystem applications are based on maximum application of existing cryogenic propulsion system technology and hardware. However, in some instances, subsystems selected are somewhat more advanced than current systems. Also basic to the approaches are anticipated improvements in the state-of-the-art over the next several years.

### 9.1.1 Overall Propulsion System Configurations

The vehicle configurations of the Two-Stage and Triamese systems, presented in Section 3, Configuration Summary, and Section 4, Vehicle Design, are shown with bell-type engine installations, although LMSC has examined the various tradeoffs associated with the aerospike engine as well as the bell type. A summary of these studies is presented in Volume III, Section 2. Results related to the booster indicate that:

- On the Two-Stage booster, use of the 35:1 bell-type engine results in somewhat more performance than use of the 100:1 bell-type engine, indicating a trend toward the use of the lower expansion ratio bell-type engine.
- The base area of a Two-Stage booster employing a 35:1 bell-type engine must be enlarged to approximately twice its area to provide for interchangeability with an aerospike engine of the same thrust, giving better overall vehicle performance.
- In terms of Two-Stage booster base area, the equivalent area between 35:1 bell-type engines and aerospike engines is essentially achieved by replacing two bell-type engines with one aerospike engine of twice the thrust.

- For Two-Stage booster base areas designed for aerospike engines, there is an overall increase in booster performance with increasing specific impulse (or increasing area ratio), which is a result of increasing the engine diameter at a fixed thrust. (This is the converse of the trend for bell-type engines as previously discussed.)
- Plumbing, thrust structure, and other aspects of the booster designs are of relatively minor consequence in designing for either the bell-type engine or the aerospike engine.

The general result of these studies related to the orbiter indicate that it appears possible to design an orbiter that could use either a bell-type engine or an aerospike engine at the same thrust with relatively minor modification to the designs. An additional fairing appears to be necessary for protection of the nozzle of the bell-type engine (retracted positions) during entry and landing phases.

#### 9.1.2 Two-Stage Propulsion System Configuration

9.1.2.1 Booster. The booster is designed with cylindrical load bearing propellant tanks integrated into the fuselage structure. The LOX tank (located forward) and the fuel tank (aft) together occupy most of the fuselage volume. LOX flows from the tank via a single line to a manifold, located just forward of the engines. The manifold distributes the flow to each of the engines. The fuel is distributed directly from the tank sump to each engine via individual lines.

Tank surfaces adjacent to the outer mold line of the vehicle support the vehicle skin with a standoff structure having a high thermal resistance. The propellant tank insulations are discussed in Section 9.1.7.

The booster propellant systems are not required to store propellants for extended periods; so, as in the case of any cryogenic booster, providing sufficient net positive suction pressure is the major consideration. The propellant tanks will be pressurized prior to engine start; and pressurization during engine operation will be provided by heated engine bleed, as shown in Fig. 9-1. The pressurization system is discussed in Section 9.1.6.

9-4

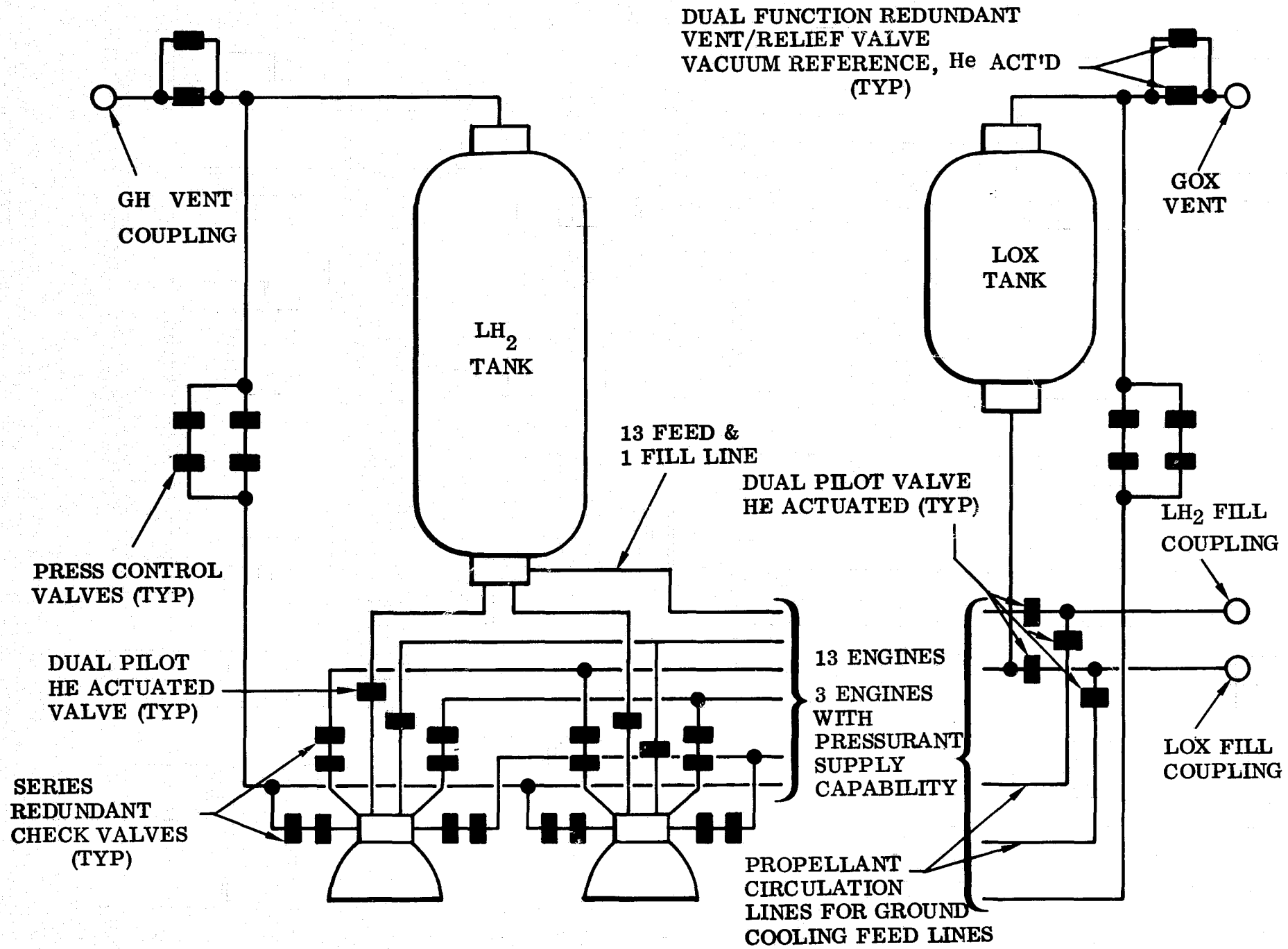


Fig. 9-1 Typical Booster Schematic

9.1.2.2 Orbiter. The orbiter propulsion system has multiple oxidizer and fuel tanks. In the current configurations, the tanks are of simple-geometry, nonload-bearing design. The propellants required for ascent are separated from the propellants required for orbital transfer, maneuvering, and retro. This allows the ascent tanks to be designed in such a manner that prolonged propellant storage is not necessary. The tanks containing the orbit transfer, maneuver, and retro propellants, which may be slightly oversized, serve as sump tanks, receiving the flow from the ascent tanks in a series/parallel feedline configuration. This procedure assures that all of the liquid propellants are drained from the ascent tanks. The tanks containing the orbit transfer, maneuver, and retro propellants are designed for storage of cryogenic propellants for extended periods of time. The orbiter propulsion system, shown schematically in Figs. 9-2 and 9-3 is based on the assumption that the orbital maneuvers will be accomplished by low thrusts with the main engines,

### 9.1.3 Triamese Configuration

The design of the primary propulsion system for the Triamese configuration is essentially the same as that of the Two-Stage configuration. The booster is similar to and follows the same design concepts used in the design of the booster of the Two-Stage vehicle. Also, the Triamese orbiter is very similar in design to that of the Two-Stage orbiter.

### 9.1.4 Reusable Propellant Tankage

The fill cycles and pressurization cycles to which the propellant tanks are subjected are relatively insignificant in their effect on the tankage reusability. This is, of course, based on the assumption that the tanks and related structure are designed so as to prevent over stressing from these effects. The major problem with tank reusability is the sustained pressure loading to which the tanks are subjected in their multimission applications.

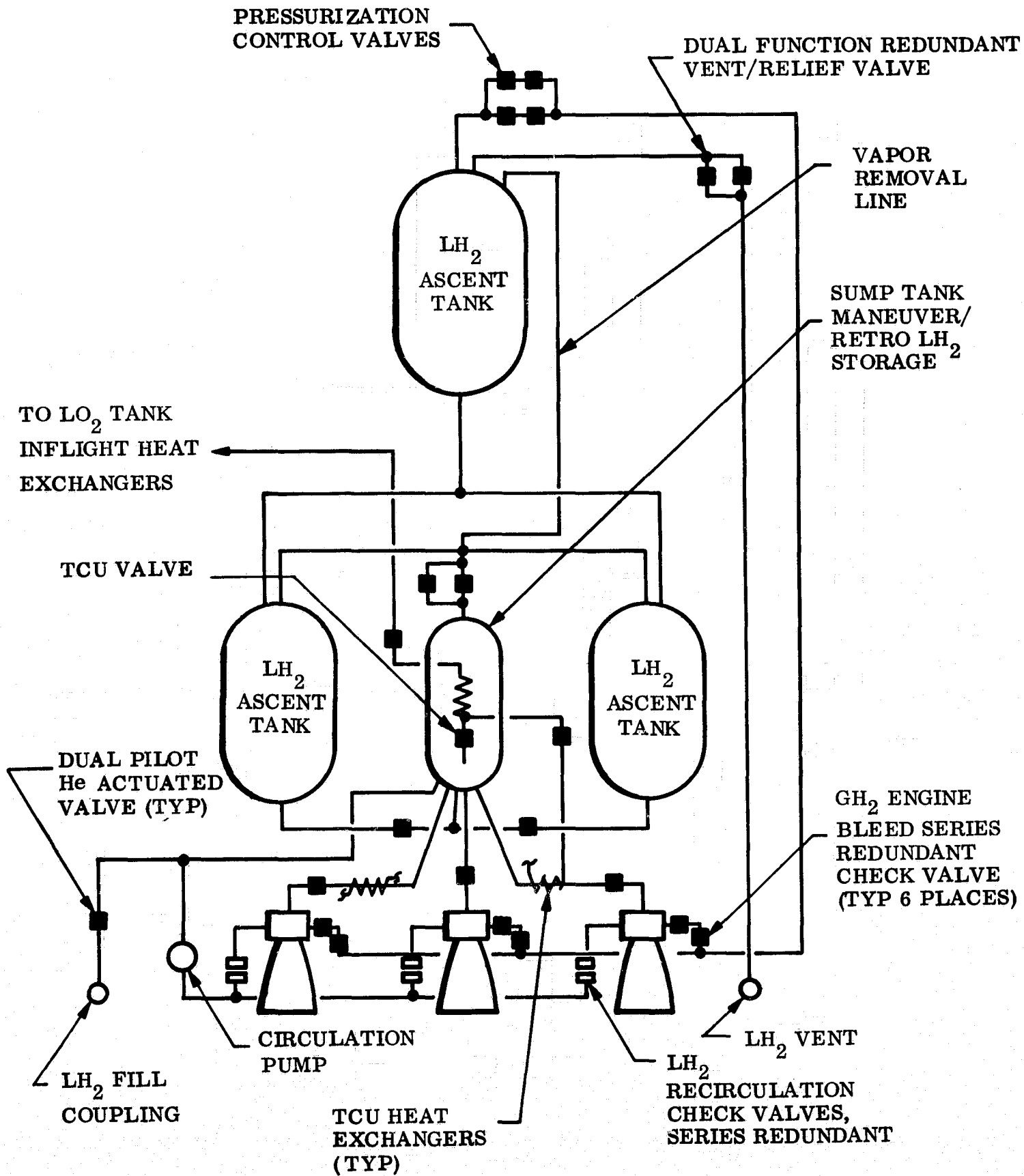


Fig. 9-2 Orbiter LH<sub>2</sub> Propulsion Fluid Schematic



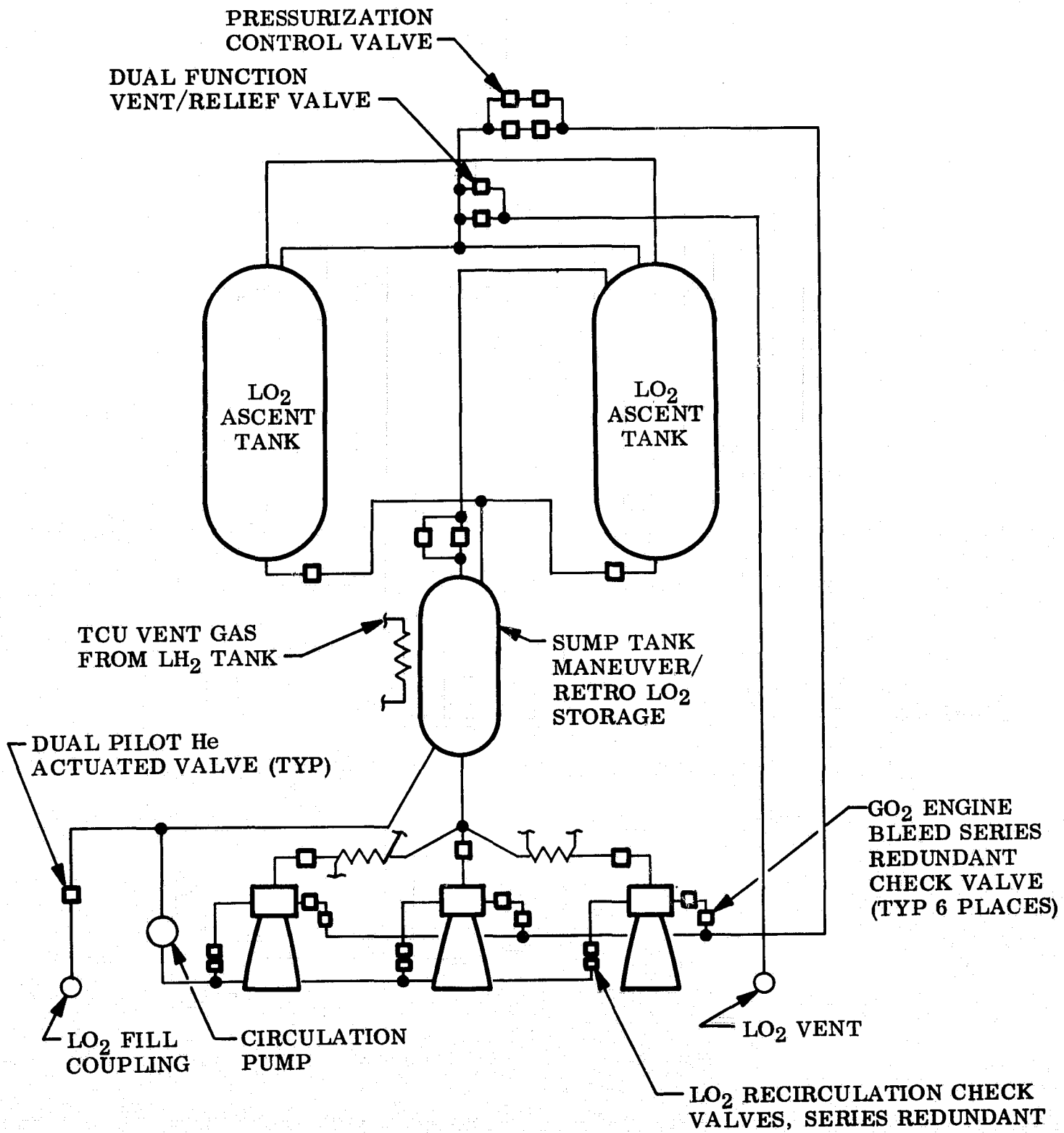


Fig. 9-3 Orbiter LO<sub>2</sub> Propulsion Fluid Schematic

The design allowables for reusable tankage for the Space Shuttle must be based on consideration of the threshold stress intensity factors of the tank materials. This is related to the maximum flaw sizes established as being acceptable in the materials under cryogenic conditions and sustained pressure loading. As indicated in the technology recommendations in Volume II, there are presently insufficient data to establish accurately the design allowables; so additional experimental programs are required.

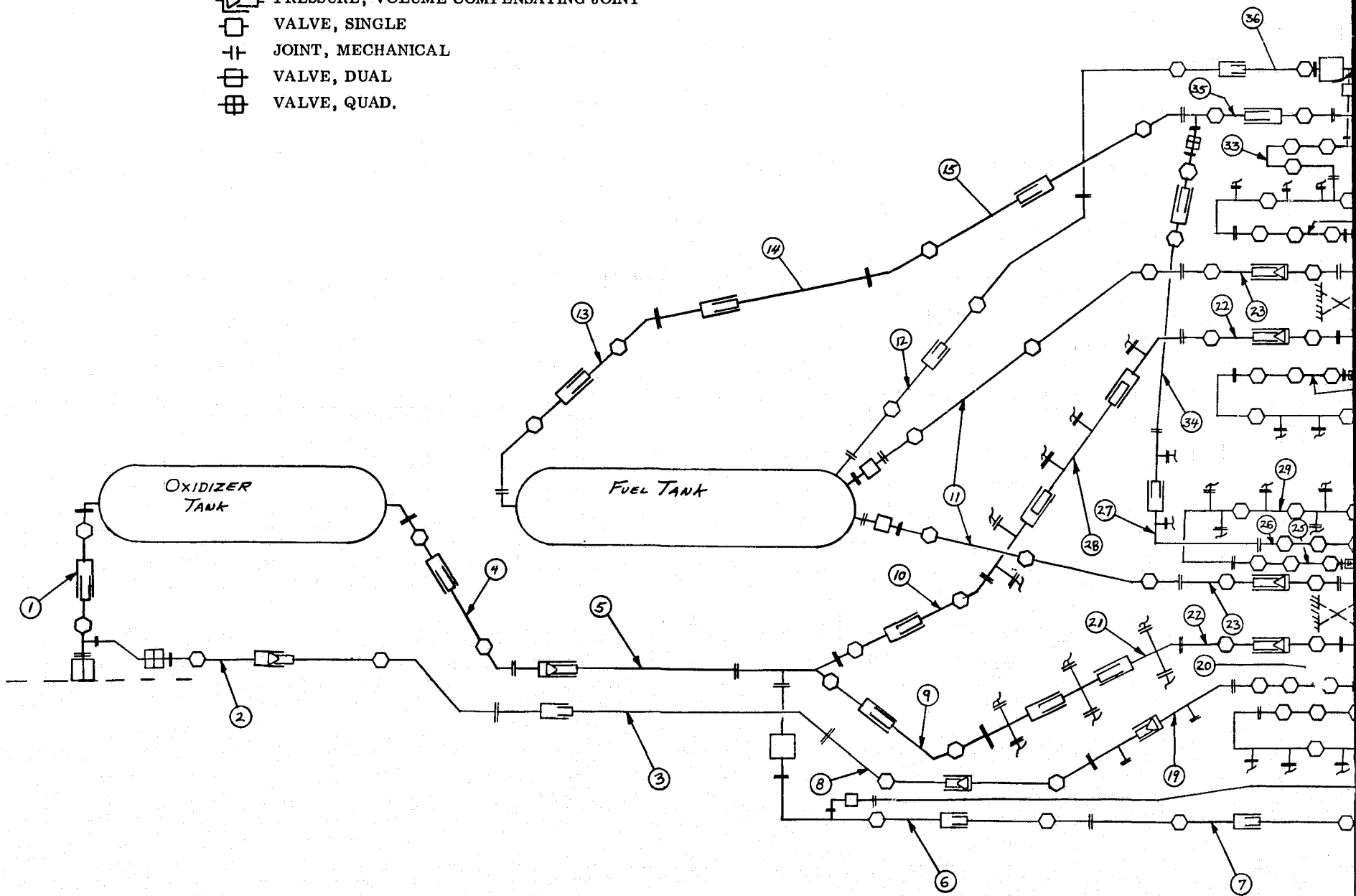
Low heat leak tank supports will be required for the orbital transfer, maneuver, and retro propellant tanks in the orbiter, since these must store propellants for extended periods of time. Fiberglass or titanium support struts appear to be satisfactory for this application.

#### 9.1.5 Propulsion System Plumbing Design and Operation

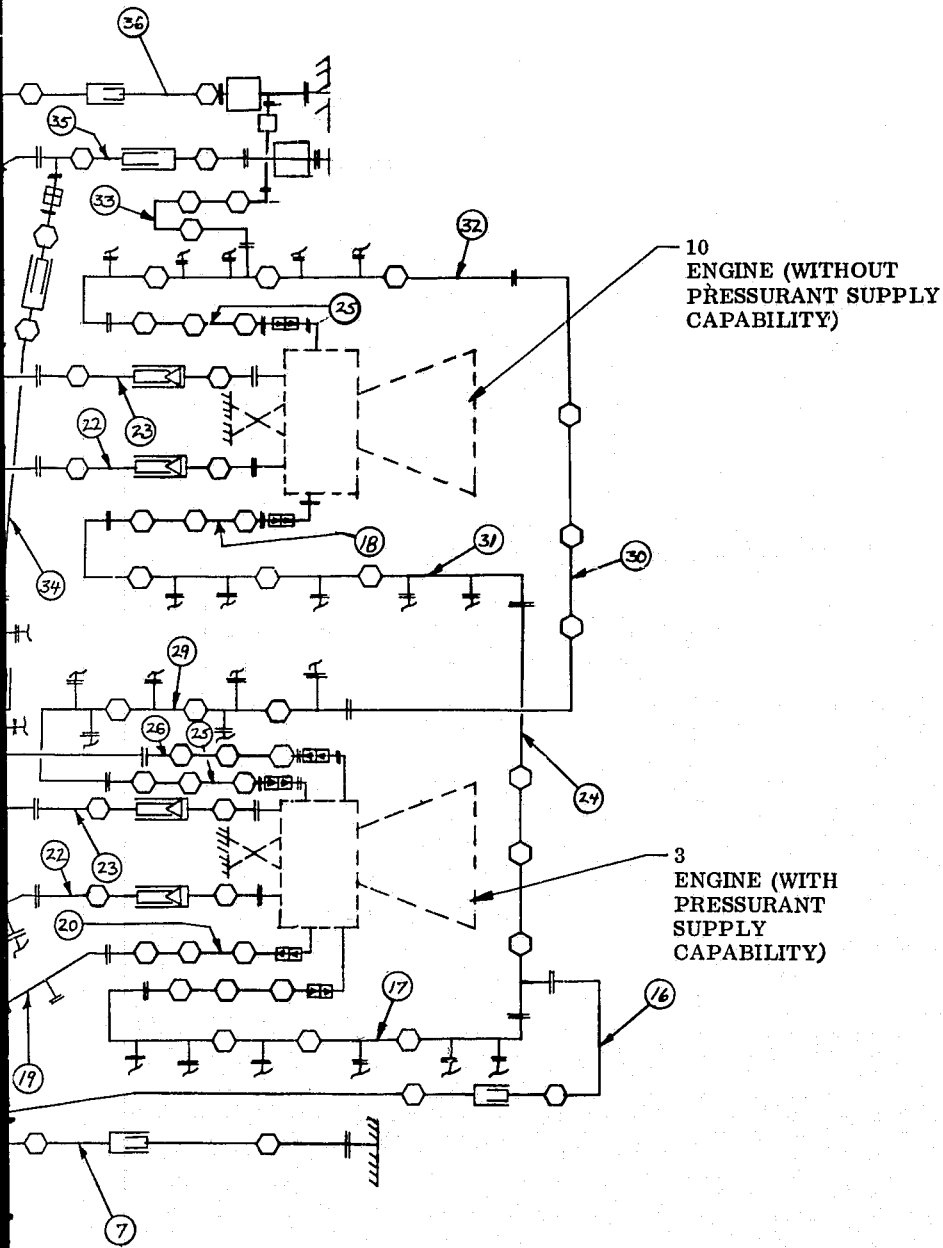
In plumbing designs formulated for the booster and the orbiter, maximum use is made of Saturn technology and approaches.

9.1.5.1 Booster Plumbing Description and Operation. In the booster, a single 22-1/2-inch diameter line carries the propellant from the  $\text{LO}_2$  tank in the forward portion of the vehicle to the distribution manifold in the aft end of the stage. Feeder lines of 7-1/2 inches in diameter distribute the flow to each of the engines. The  $\text{LH}_2$  is distributed to the engines by individual lines from the fuel tank in the aft portion of the vehicle. Gimbal motion is taken care of by pressure volume compensators in both  $\text{LO}_2$  and  $\text{LH}_2$  lines. In segments of the line supported structurally against axial force due to internal line pressure, simple bellows joints capable of linear displacement are used to take care of thermal expansion/contraction from the line temperatures changes. A set of three bellows type gimbal joints is used to take care of thermal expansion/contraction where structural support against internal line pressure reaction may not be available, such as at bends. Flexures used for thermal expansion/contraction provide a secondary function of also taking up linear and angular variations due to manufacturing tolerances. The booster plumbing is shown in Fig. 9-4.

- GIMBAL JOINT
- ▭ SLIDING JOINT
- ▭ PRESSURE, VOLUME COMPENSATING JOINT
- VALVE, SINGLE
- ⊕ JOINT, MECHANICAL
- ▭ VALVE, DUAL
- ⊕ VALVE, QUAD.



FOLDOUT FRAME 7



Item No.	Nomenclature	Diameter and Length	Line Makeup					
			Gimbal Joints	Sliding Joints	Press Vol Comp. Joints	No. of Flanges	Operating Press psia	No. Lines/Vehicle
1	Lox Vent Line	8" x 13'	2	1	-	3	35	1
2	Lox Pressurization Line, Fwd	6" x 15'	2	1	-	2	500	1
3	Lox Press. Line, Long	6" x 190'	-	1	-	2	500	1
4	Lox Trunk Line, Fwd	22" x 13'	2	1	-	2	130	1
5	Lox Trunk Line, Long	22" x 100'	-	1	-	2	130	1
6	Lox Fill Line, Fwd	8" x 15'	2	1	-	2	130	1
7	Lox Fill Line, Aft	8" x 15'	2	1	-	3	130	1
8	Lox Press. Line, Fwd	6" x 10'	2	1	-	2	500	1
9	Lox Manifold Feed Line, Long	15" x 25'	2	1	-	4	330	1
10	Lox Manifold Feed Line, Short	15" x 16'	2	1	-	2	330	1
11	Fuel Feed Line, Fwd	8" x 20'	3	-	-	2	35	13
12	Fuel Fill Line, Fwd	8" x 20'	2	1	-	2	35	1
13	Fuel Vent Line, Fwd	12" x 13'	2	1	-	2	35	1
14	Fuel Vent Line, Long	12" x 100'	-	1	-	2	35	1
15	Fuel Vent Line, Mid	12" x 20'	2	1	-	2	35	1
16	Lox Replenish Line	2" x 20'	2	1	-	2	330	1
17	Lox Replenish Manifold	2" x 30'	3	-	-	8	330	1
18	Lox Replenish Manifold Feed	2" x 5'	3	-	-	2	330	13
19	Lox Press. Manifold	6" x 19'	-	1	-	4	500	1
20	Lox Press. Line, Engine	3" x 15'	3	-	-	2	500	3
21	Lox Feed Manifold	15" x 30'	-	2	-	8	330	1
22	Lox Feed Line,	8" x 14'	2	-	1	2	330	13
23	Fuel Feed Line, Engine	8" x 14'	2	-	1	2	35	13
24	Lox Replenish Manifold Feed	2" x 20'	3	-	-	2	330	1
25	Fuel Replenish Line, Engine	2" x 5'	3	-	-	2	35	13
26	Fuel Press. Line, Engine	3" x 15'	3	-	-	2	500	3
27	Fuel Press. Manifold	6" x 19'	-	1	-	4	500	1
28	Lox Feed Manifold	15" x 30'	-	2	-	7	330	1
29	Fuel Replenish Manifold	2" x 30'	3	-	-	8	35	1
30	Fuel Replenish Manifold Feed	2" x 20'	3	-	-	2	35	1
31	Lox Replenish Manifold	2" x 30'	3	-	-	7	330	1
32	Fuel Replenish Manifold	2" x 30'	3	-	-	8	35	1
33	Fuel Replenish Manifold Feed	2" x 20'	3	-	-	2	35	1
34	Fuel Press Line Aft	6" x 30'	2	1	-	2	500	1
35	Fuel Vent Line, Aft	12" x 15'	2	1	-	3	35	1
36	Fuel Fill Line, Aft	8" x 15'	2	1	-	-	35	1

Fig. 9-4 Cryogenic Schematic, Booster, Two-Stage Primary Propulsion (Preliminary)

Maintaining the propellants at the proper conditions in the lines in the reference booster configuration is by the flow of replenishment propellant selectively through the feed lines. After propellant loading, replenishment propellant is pumped into the tanks via the propellant circulation lines, the engine pumps, and the feed lines. (The redundant series check valves prevent reverse flow into the propellant circulation lines upon engine start as the pump discharge pressure builds up.) This method is marginal, since the amount of required replenishment propellant is dependent on the boiloff loss rate. An alternate approach is to provide for recirculation by pump through the feed lines and back into the tanks.

The vent and pressurization lines are connected to the umbilicals at the aft base of the vehicle. In both oxidizer and fuel vent circuits, dual-function redundant valves are used. Each valve is designed with a single helium-powered actuator, controlled by a small solenoid valve pilot and a vacuum referenced relief valve pilot. During liquid hydrogen loading, the valve is opened by the solenoid pilot for force passage of vent gas to the ground support equipment that maintains emergency control over fill rate and vent backpressure to avoid tank over pressurization. Tank pressure is monitored by the ground support equipment. The relief valve function is an emergency measure in that the ground system maintains ground hold pressure and relief of pressure is not expected in a normal flight. Helium prepressurization is provided prior to engine start to provide necessary NPSP.

A similar system is provided for the oxidizer system. The direct venting of the oxygen to the atmosphere is not considered to be desirable at this time. If it is possible to provide adequate separation between hydrogen lines and the oxygen vents, direct venting may be adopted. Helium prepressurization is provided prior to engine start.

9.1.5.2 Orbiter Plumbing Description and Operation. Because of the vehicle design constraint to locate the payload at the spacecraft center of gravity, propellant tanks have to be packaged in the remaining available space; and this necessitates multiple tanks. Consideration had to be given to solving filling, draining, and venting problems associated with multiple tanks.

Liquid Hydrogen System Description and Operation. The four fuel tanks are arranged with the large axially located forward tank draining into the two side-by-side aft tanks. These two tanks are coupled in parallel to the tank containing the orbital transfer, maneuver, and retro propellant, which forms the series link to the terminal lines feeding the engines. The plumbing diagram is shown in Fig. 9-5. With this tank arrangement, the propellant required for ascent is stored in the large forward and side-by-side aft tanks. No valving separates these tanks; and the tanks have minimum insulation, consistent with the short propellant storage time requirement. The propellant for on-orbit maneuver and retro propulsion is stored in the small sump tank, which is insulated with super insulation, consistent with the requirement for storage of propellant from 7 to 30 days.

The fill system consists primarily of a fill line from the aft end of the vehicle to the orbit storage tank. All of the LH<sub>2</sub> tanks are filled simultaneously through the single fill line. An initial slow flow will be used to chill the aft ascent tanks and the orbital storage tank. After adequate chilling and initial loading at slow fill, the valves in the vapor removal line are closed and fast fill is started. When the forward tank is almost full, flow is reduced to slow fill and the valves in the vapor removal lines are opened, allowing vapors to vent off from the orbital storage and aft ascent tanks so that venting allows these tanks to become essentially full. Prior to engine start, the tanks are pressurized to suppress boiling and produce NPSP. Any vapor formed will be removed by the vapor removal lines, and liquid will flow down the intertank lines.

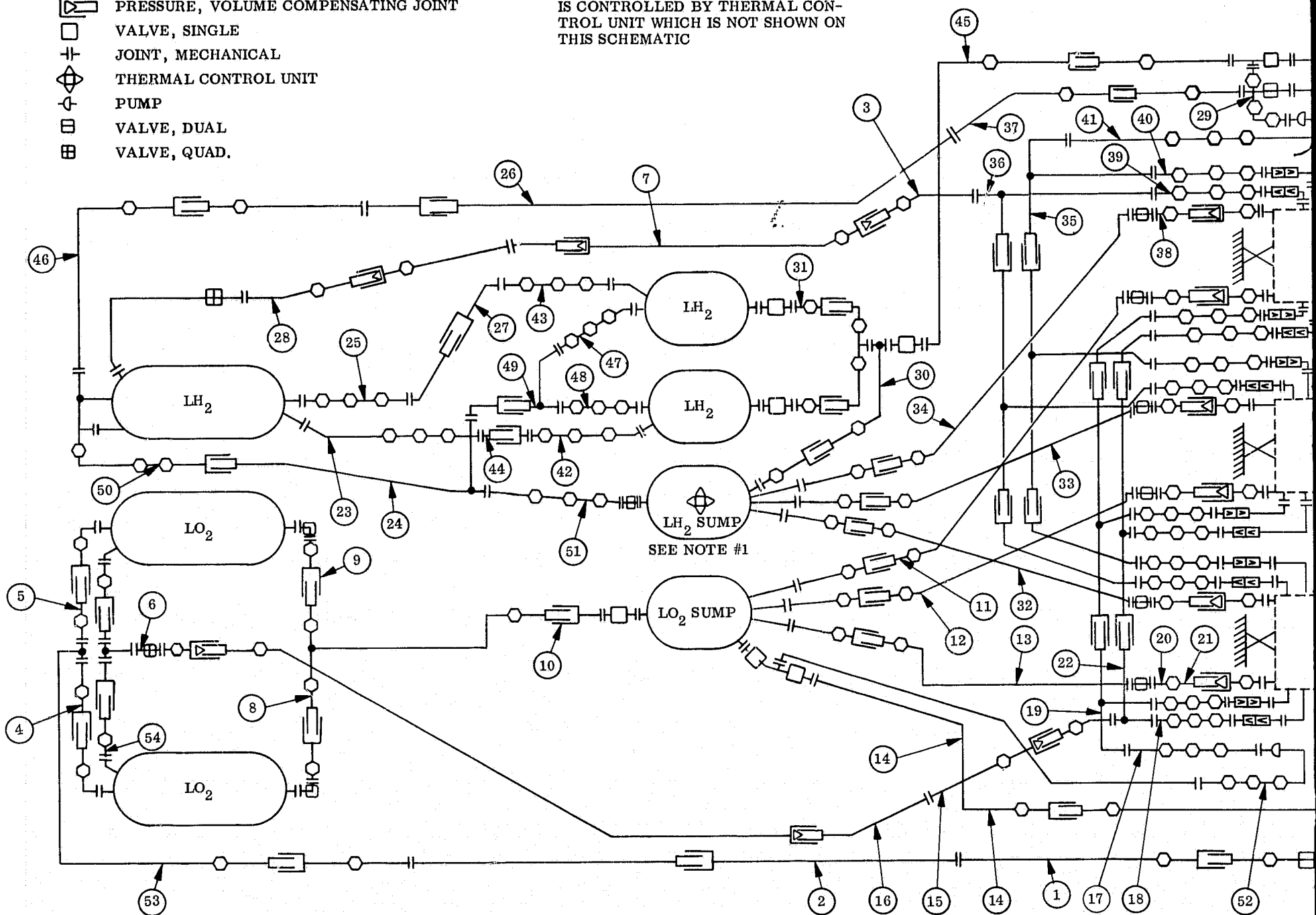
The nonisolation feed line concept employed affords the following advantages:

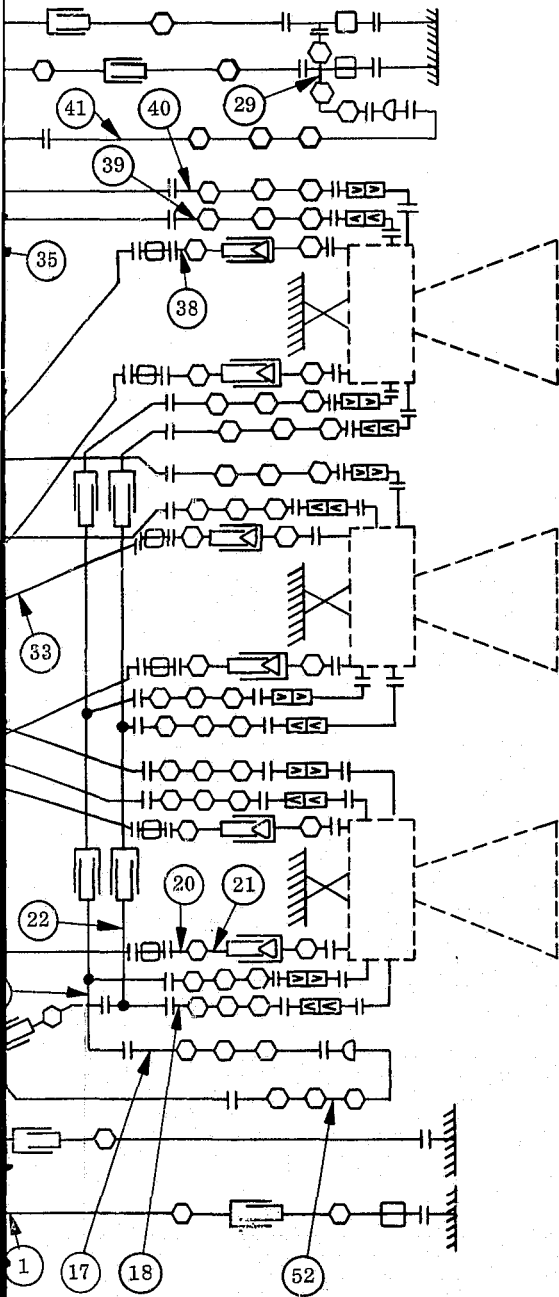
- Reduced feedline weight and elimination of isolation valves
- Reliance on one pressurization line, with attendant reduction of valves
- Elimination of switching of flow from the forward tank to aft tank during burn

- GIMBAL JOINT
- ▭ SLIDING JOINT
- ▭ (with diagonal line) PRESSURE, VOLUME COMPENSATING JOINT
- VALVE, SINGLE
- ⊥ JOINT, MECHANICAL
- ⊕ THERMAL CONTROL UNIT
- ⊖ PUMP
- ▭ (with horizontal lines) VALVE, DUAL
- ▭ (with vertical lines) VALVE, QUAD.

NOTE #1

IN ORBIT VENTING OF BOTH SUMPS IS CONTROLLED BY THERMAL CONTROL UNIT WHICH IS NOT SHOWN ON THIS SCHEMATIC





Item No.	Nomenclature	Diameter and Length	Line Makeup					No. Lines/Vehicle
			Gimbal Joints	Sliding Joints	Press Vol Comp. Joints	No. of Flanges	Operating Press psia	
1	Lox Vent Line, Aft	5" x 42"	2	1	-	2	35	1
2	Lox Vent Line, Long	5" x 60"	-	1	-	2	35	1
3	Fuel Press. Line Aft	3" x 40'	2	1	-	2	500	1
4	Lox Vent Line, Interconnect	4" x 13'	2	1	-	2	35	1
5	Lox Vent Line, Interconnect	4" x 13'	2	1	-	2	35	1
6	Lox Press. Line, Fwd	3" x 7'	2	1	-	3	500	1
7	Fuel Press. Line, Long	3" x 60'	-	1	-	2	500	1
8	Lox Feed Line, Le.	10" x 25'	2	1	-	2	116	1
9	Lox Feed Line, Right	10" x 25'	2	1	-	2	116	1
10	Lox Feed Line, Fwd	14" x 6'	2	1	-	3	116	1
11	Lox Feed Line, Eng. #1	8" x 20'	2	1	-	2	165	1
12	Lox Feed Line, Eng. #2	8" x 6'	2	1	-	2	165	1
13	Lox Feed Line, Eng. #3	8" x 20'	2	1	-	3	165	1
14	Lox Fill Line	4" x 34'	2	1	-	2	195	1
15	Lox Press. Line, Aft	3" x 40'	2	1	-	2	500	1
16	Lox Press. Line, Long	3" x 60'	2	1	-	2	500	1
17	Lox Replenishing Line, Aft	1" x 34'	3	-	-	2	195	1
18	Lox Press. Line, Gimbal	2" x 6'	3	-	-	2	500	3
19	Lox Replen. Manifold	3" x 32'	-	2	-	4	165	1
20	Lox Feed Line, Gimbal	1" x 6'	3	-	-	2	165	3
21	Lox Press. Manifold	8" x 6'	2	-	1	2	165	3
22	Lox Press. Manifold	3" x 32'	-	2	-	4	500	1
23	Fuel Feed Line	10" x 22'	3	-	-	2	35	1
24	Sump Vent Line, Ground	3" x 56'	3	-	-	3	35	1
25	Fuel Vent Line	10" x 22'	3	-	-	2	35	1
26	Fuel Vent Line, Long	6" x 60'	-	1	-	2	35	1
27	Fuel Feed Line, Long	10" x 60'	-	1	-	2	35	1
28	Fuel Press Line, Fwd	3" x 20'	2	1	-	2	500	1
29	Fuel Circulation Line	1" x 10'	3	-	-	2	35	1
30	Fuel Feed Line, Sump	10" x 39'	2	1	-	3	35	1
31	Fuel Interconnect Line	10" x 40'	4	2	-	3	35	1
32	Fuel Feed Line, Eng. #3	8" x 20'	2	1	-	2	35	1
33	Fuel Feed Line, Eng. #2	8" x 6'	2	1	-	2	35	1
34	Fuel Feed Line, Eng. #1	8" x 20'	2	1	-	2	35	1
35	Fuel Replen. Manifold	1" x 32'	-	2	-	4	35	1
36	Fuel Press Manifold	3" x 32'	-	2	-	4	500	1
37	Fuel Vent Line, Aft	6" x 42'	2	1	-	3	35	1
38	Fuel Feed Line, Gimbal	8" x 6'	2	-	1	2	35	1
39	Fuel Press Line, Gimbal	2" x 6'	3	-	-	2	500	1
40	Fuel Replen. Line, Gimbal	1" x 6'	3	-	-	2	35	1
41	Fuel Replen. Line, Aft	1" x 34'	3	-	-	2	35	1
42	Fuel Feed Line	10" x 18'	3	-	-	2	35	1
43	Fuel Feed Line	10" x 18'	3	-	-	2	35	1
44	Fuel Feed Line, Long	10" x 60'	-	1	-	2	35	1
45	Fuel Fill Line	4" x 34'	2	1	-	2	35	1
46	Fuel Vent Line Fwd	6" x 12'	2	1	-	2	35	1
47	Fuel Vent Line, Grnd, Aft	3" x 20'	3	-	-	2	35	1
48	Fuel Vent Line, Grnd, Aft	3" x 20'	3	-	-	2	35	1
49	Fuel Vent Line, Grnd, Fwd	6" x 10'	-	1	-	3	35	1
50	Fuel Vent Line, Fwd	6" x 15'	3	-	-	2	35	1
51	Fuel Vent Line, Aft	3" x 15'	3	-	-	2	35	1
52	Lox Circulation Line	1" x 30'	3	-	-	2	195	1
53	Lox Vent Line, Fwd	5" x 30'	2	1	-	3	35	1
54	Lox Press. Line, Tank	3" x 13'	2	1	-	2	500	2

Fig. 9-5 Cryogenic Schematic, Orbiter, Primary Propulsion (Preliminary)



At ignition, propellant will flow from the forward tank to the aft tanks, through the orbital storage tank, and to the engines. Depletion of the tanks will also follow that order. However, as each tank is drained, all of the liquid propellant will be drained with no residuals remaining. Complete scavenging of the intertank lines is assured by sizing the sump tank to contain some of the ascent propellant. The intertank line shutoff valves are closed by propellant sensors in both lines. This assures that when one aft tank depletes before the other, it can be isolated by closing the proper valve. The shutoff valves incorporate dual redundant pilot valves to give fail safe reliability.

Two vent systems are provided in the orbiter - one for normal inflight vent and the other for emergency in-flight vent and ground venting. The in-flight vent, designated TCV in Fig. 9-5, operates by cooling the tank contents. Cooling is accomplished by extracting a portion of the liquid hydrogen, expanding and subcooling it in a throttling process, running it through an in-tank heat exchanger, and feed line heat exchangers, and finally venting it overboard. The ground/ascent/emergency vent design approach is the same as that called for in the booster design previously described.

Recirculation maintains propellant temperature in the feed lines at a temperature approaching bulk propellant temperature. It is required to assure proper propellant conditions at the pump inlet during ascent on the booster if sequential burn is employed.

Vacuum jacketed lines are used in conjunction with forced flow, and a pump is installed at the fill line to provide forced flow. Propellant is drawn from the sump tank through the feed line, forced through a distribution manifold to the engine pumps, and returned to the orbital storage tank via the feedlines. Dual, series-redundant check valves are placed in each engine branch of the manifold to prevent backflow as the pump pressures build up at engine start.

Liquid Oxygen System Description and Operation. The LO<sub>2</sub> systems are very similar to the hydrogen system, with only a few noteworthy differences. The basic configuration differs in that there are only two ascent propellant tanks. These both feed into the sump tank, as in the hydrogen system. Figure 9-5 shows the corresponding plumbing diagram.

The fill system operational procedure will be similar to the LH<sub>2</sub> side. The ground vent, pressurization, feed, and recirculation systems are quite similar to the LH<sub>2</sub> systems and need not be discussed further here.

#### 9.1.6 Pressurization

The pressurization for oxidizer and fuel of both stages is by propellant vapors bled at 600°R from the engines during ascent. Prepressurization, if required, is supplied a ground or by an onboard source. Pressurant trapped in depleted propellant tanks is used for on-orbit operation.

In the booster, three engines are plumbed to the pressurization system, with a capability of any two engines to supply all of the pressurant for the stage. In the orbiter, all engines are plumbed into the pressurization system, with either capable of supplying all of the pressurant for the stage. Redundant check valves, located at the pressurant outlet of each engine, provide for engine-out or for malfunction in the pressurant supply systems of a single engine on each stage.

The pressure is regulated by on/off operation of a quad cluster of normally closed valves for each propellant in both the booster and the orbiter.

Ullage pressure is sensed by transducers mounted at the ullage end of each tank. The pressure sensors are coupled in closed loop to their respective valve clusters. In addition, redundant sensors are coupled through a voting circuit capable of overriding pressure sensing circuits in the event of malfunction or out-of-tolerance operation.

After the ascent phase, the propulsion impulse requirements are small and a single engine operating at 10 percent thrust is adequate to meet even the largest on-orbit impulse requirement (retro at 500 ft/sec) within a burn time of 2 minutes. With pump chill-down requirements for operating the engines at 10 percent thrust still somewhat in doubt, the assumption was made, for purposes of analysis, that the engine pumps would be chilled down by unpumped idle mode operation over 10 seconds,

after which the engine would operate at 10 percent thrust. The pump inlet pressure for unpumped idle mode operation was assumed to be 20 psia for the oxidizer and 25 psia for the fuel. This pressure would give an unpumped idle mode thrust of approximately 800 pounds thrust per engine (based on recent Pratt & Whitney data).

Based on the on-orbit starting sequence indicated above, adequate on-orbit pressurization is considered to be available for both oxidizer and fuel from residual  $\text{GH}_2$  and  $\text{GO}_2$  trapped in the empty ascent tanks. This is evident from the fact that the volume of the on-orbit propellants, which are contained in the orbital storage tanks, is only 6 percent of the total orbiter propellant volume.

An evaluation was made of the effect of varying NPSP on both the  $\text{LO}_2$  and  $\text{LH}_2$  systems on stage and vehicle system weight. The approach was to optimize feed line sizes for the reference conditions selected and then to determine the slope of NPSP versus stage weight. The results are presented in Table 9-2. As may be seen, an improvement in the liquid hydrogen NPSP can result in significant weight savings.

Table 9-2

## STAGE AND VEHICLE WEIGHT VS PUMP NPSP

	Stage Wt (lb) per 1 psi NPSP	Vehicle Wt (lb) per 1 psi NPSP
Booster $\text{LOX}$	126	690
Booster $\text{LH}_2$	600	3300
Spacecraft $\text{LOX}$	57	1880
Spacecraft $\text{LH}_2$	265	8745

## 9.1.7 Cryogenic Thermal Protection

The insulation for the booster tanks is required only to prevent liquefaction of air and excessive icing and to prevent excessive vapor pressure rise from affecting NPSP. A foam-type of insulation may be employed for this purpose. Since internal foam insulations cannot be used on the liquid oxygen tanks and may produce contamination problems in the liquid hydrogen tanks, external insulation is necessary.

The ascent tanks for the orbiter, used during ascent only, require only a foam-type insulation. The tank containing the orbital transfer, maneuvering, and retro propellant must be insulated with high-performance multilayer insulation. This insulation must be purged during ground hold with helium, which is vented to produce a vacuum during ascent. Reentry with the insulation in a vacuum would result in crushing and atmospheric contamination (icing, vapor, particles, etc). Therefore, the recommended insulation would be refilled with helium during reentry by maintaining a slightly positive pressure in the purge bag.

#### 9.1.8 Propellant Utilization

Variations in temperature, in engine pumping ratio caused by pump inlet variations and engine control variables, in propellant loading, and in propellant heating are all capable of producing unpredictable deviations between the ratio of propellant loaded and nominal engine propellant mixture ratio. In order to maximize the utilization of propellant, the engine mixture ratio is computer controlled in response to propellant gaging data so that the consumption ratio always matches the ratio of effective impulse propellant remaining on board.

The gaging method tentatively selected consists of a capacitor gage for primary sensing plus a minimum number of resistance-type point sensors to establish calibration levels and to serve as a minimum capability redundant system. While this gaging system is limited to measuring propellant quantity only under acceleration, its capability to measure within 0.5 percent accuracy has been established. During orbital operation, the effectiveness of the system is a function of the frequency of readings permitted by maneuvers that orient the propellants.

#### 9.2 REACTION CONTROL SYSTEM

The selected reaction control systems for the booster and the orbiter are oxygen/hydrogen integrated reaction control systems, which use propellants from the main propellant tanks. The integrated reaction control system provides the following:

- Flexibility in use of propellants
- Elimination of redundant propellant tankage

- Lower system weight
- Less prelaunch activity
- Lower system volume requirements

One possible disadvantage of the integrated reaction control system is that it operates at a mixture ratio of 4, rather than the engine mixture ratio of 6 or 7.

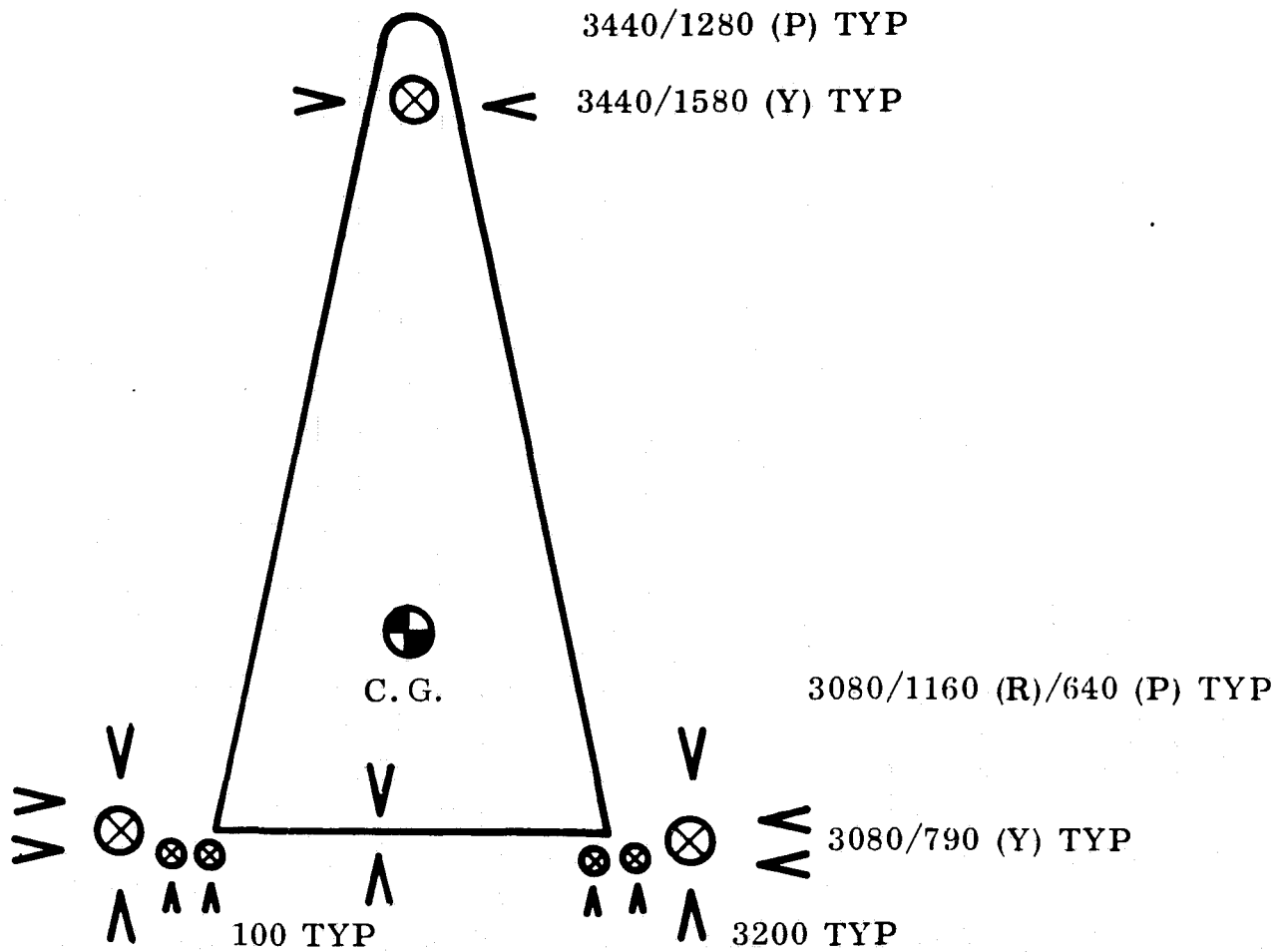
The propellants will be supplied to the thrusters in a gaseous condition, approximately 350 to 440°R and 400 psia. The gas/gas approach was selected because of the pulsing and short operating requirements of the thrusters. The integrated reaction control system consists of the following major components:

- Propellant collection devices or methods to allow propellants to be taken from the main tanks
- Pumping devices to raise the pressure of the propellants
- Liquid/gas conversion and temperature conditioning heat exchangers
- Gas accumulators
- Thrusters

#### 9.2.1 Thruster Selection and Locations

The reaction control system thrusters provide capability in the pulse mode for limit cycling and in the steady-state mode for attitude maneuvers and translations. The required thrust levels and the requirements establishing these are presented in Figs. 9-6 and 9-7. For the orbiter limit cycling operations, small thrusters (100 pounds thrust) are pulsed individually or in pairs. The smaller impulse bits of these thrusters minimize propellant consumption on the orbiter. For attitude maneuvers and translation, the large throttlable thrusters (3500 pounds maximum thrust) are employed as required. The larger thrusters are sized by the acceleration requirements.

Since the minimum impulse bit of the large thrusters is estimated to be over 60 lb-sec, an appreciable propellant saving can be accomplished through the use of the 100-pound thrusters with minimum impulse bits of approximately 10 lb-sec. This orbiter propellant saving would make installation of the smaller thrusters economical for even the shortest missions.



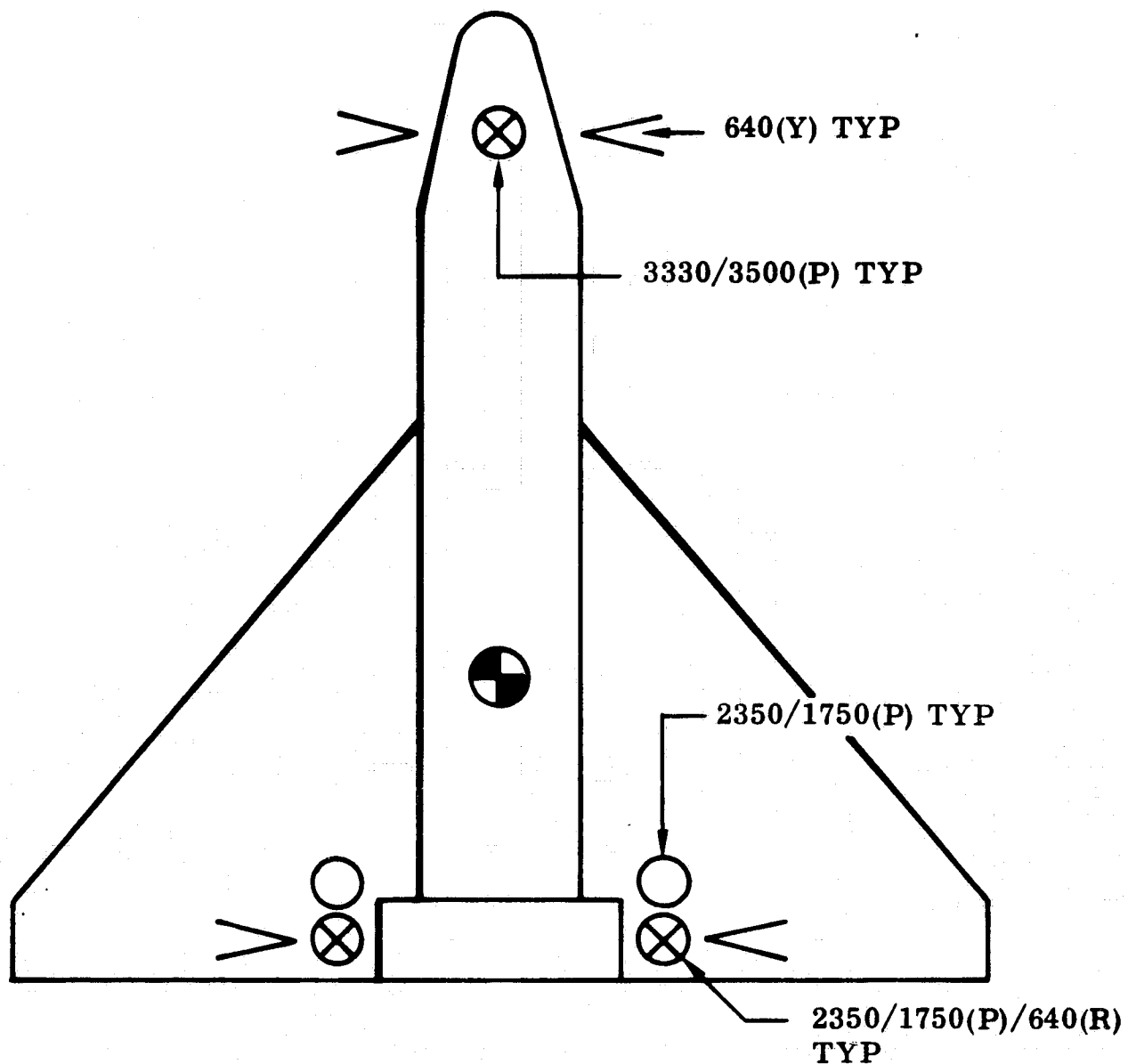
REQUIREMENTS

- TRANSLATION  $\Delta V$  = 142 FT/SEC  
ACCELERATION = 1 FT/SEC<sup>2</sup> (ABOUT ALL AXES)
- MANEUVER ACCELERATION = 1 DEG/SEC<sup>2</sup> (ABOUT ALL AXES)  
RATE = 1 DEG/SEC (ABOUT ALL AXES)
- DEADBANDS COARSE: ±5.0 DEG, ±0.5 DEG/SEC, 166 HR  
FINE: ±0.5 DEG, ±0.5 DEG/SEC, 2 HR

APPROXIMATE VALUES

	ROLL	PITCH	YAW
MOMENT OF INERTIA (SLUG-FT <sup>2</sup> )	4.0 X 10 <sup>6</sup>	10.8 X 10 <sup>6</sup>	13.4 X 10 <sup>6</sup>
LEVER ARMS C.G./G <sub>L</sub> TO THRUSTERS	30 FT - RIGHT AND LEFT	95 FT - FORWARD 53 FT - AFT	95 FT - FORWARD 53 FT - AFT

Fig. 9-6 Typical Thrust Levels, Orbiter



**REQUIREMENTS**

SEPARATION  $\Delta V$  = 10 FT/SEC  
 SEPARATION ACCELERATION = 1 FT/SEC<sup>2</sup> DOWN ONLY  
 MANEUVER RATE = 39 DEG IN 30 SEC, PITCH ONLY  
 DEADBANDS =  $\pm 5.0$  DEG,  $\pm 0.5$  DEG/SEC

**APPROXIMATE VALUES**

	ROLL	PITCH	YAW
MOMENT OF INERTIA (SLUG - FT <sup>2</sup> )	$5.9 \times 10^6$	$55.3 \times 10^6$	$55.8 \times 10^6$
LEVER ARM CG/G TO THRUSTERS	49 FT - RIGHT AND LEFT	148 FT - FORWARD 52 FT - AFT	148 FT - FORWARD 52 FT - AFT

Fig. 9-7 Typical Thrust Levels, Two-Stage Booster

The attitude maneuver and translation requirements of the orbiter result in thrust levels that are best fulfilled by a common thruster that has a 5.5:1 throttling ratio. The difference in thrust level results from the ratio of lever arms and the requirement that a pure translational force be imparted to the vehicle.

The thruster arrangements and operational modes are presented in Figs. 9-8 and 9-9. The orbiter has 30 nozzles - 18 thrusters of 3500-pound thrust and 12 thrusters of 100-pound thrust. The twelve 100-pound thrust limit cycling thrusters afford complete redundancy for a single malfunction. The high thrust level thrusters should have series-parallel propellant valves to satisfy the single-malfunction, fail-operational criteria. The only single malfunction that would prevent satisfaction of the criteria would be a sticking throttle valve. Completely satisfying the criteria would require an additional 10 large thrusters on the orbiter.

On the orbiter, all of the aft-mounted thrusters are on extendable structure and are retracted for reentry. All of these thrusters except the forward firing units, can be operated in the retracted position. The thrusters in the forward end of the orbiter are covered by the nose cap during reentry.

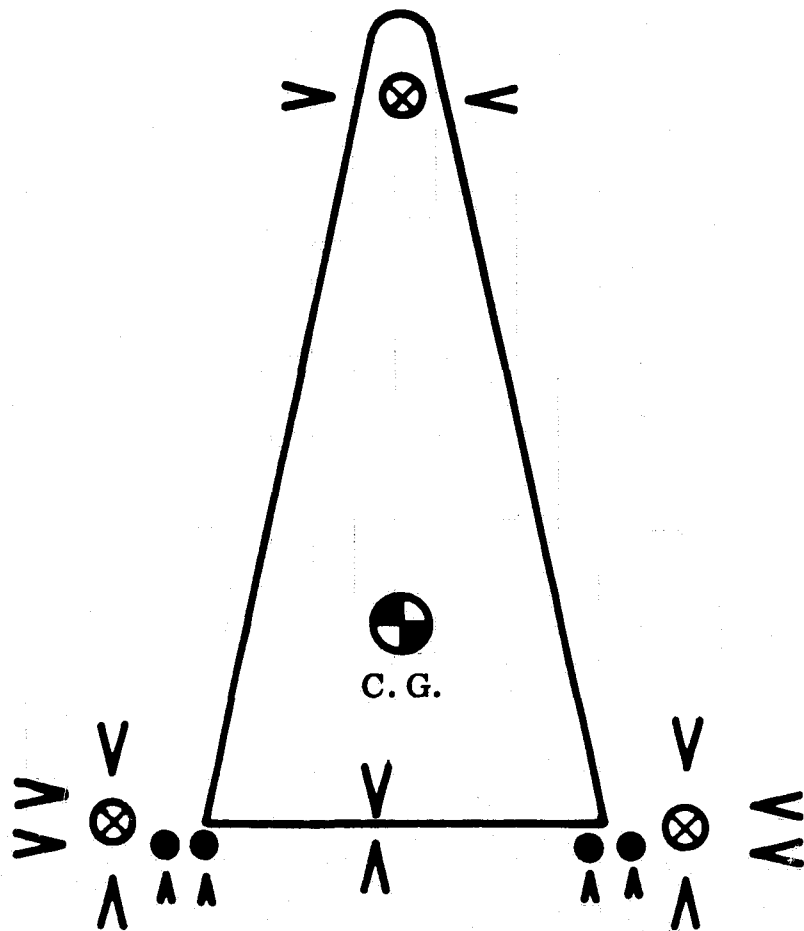
The thrusters on the booster are of the same design as the attitude maneuver/translation thrusters for the orbiter except that the nozzle area ratios would be 20:1 instead of 30:1. This results in a thrust chamber assembly that is approximately 5 inches shorter.

The reaction control system performance characteristics are summarized in Table 9-3.

### 9.2.2 Propellant Feed and Conditioning System

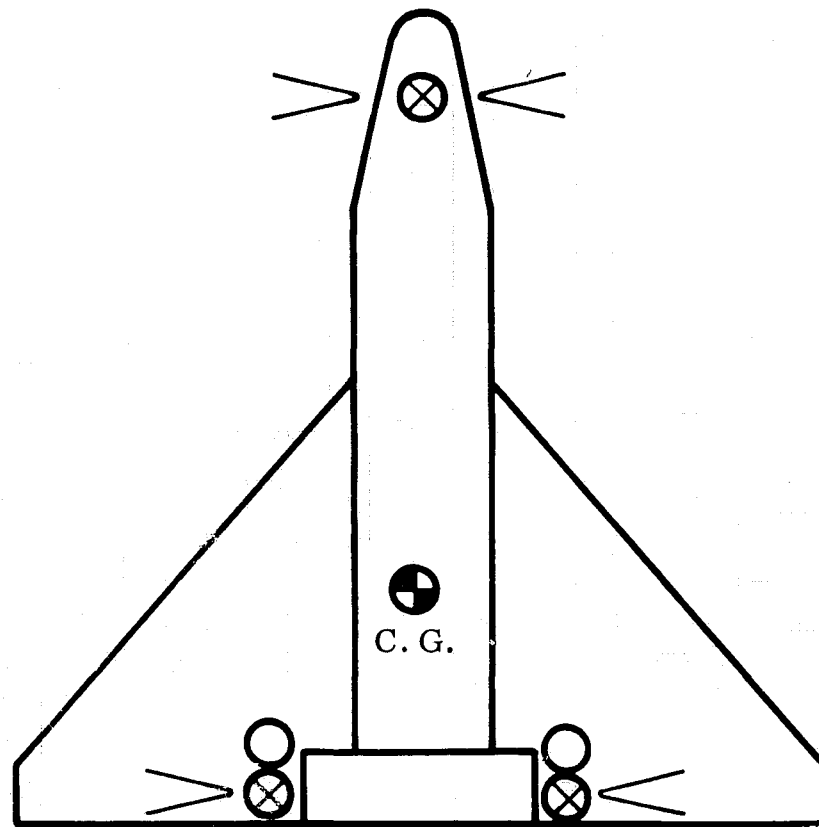
Propellant feed and conditions systems for the reaction control systems have been examined in considerable detail. The selected approaches provide practical and workable systems.





	ACTIVE THRUSTERS				NORMAL OPERATION TOTAL
	L-REAR	R-REAR	C-REAR	FORE	
<b>LIMIT CYCLE</b>					
PITCH	-	-	-	2	2
ROLL	-	2	-	-	2
YAW	-	-	-	1	1
<b>ATTITUDE MANEUVERS</b>					
PITCH	1	1	-	1	3
ROLL	1	1	-	-	2
YAW - RIGHT	-	1	-	1	2
YAW - LEFT	1	-	-	1	2
<b>TRANSLATE</b>					
RIGHT	2	-	-	1	3
LEFT	-	2	-	1	3
FORE & AFT	1	1	1	-	3
UP & DOWN	1	1	-	1	3

Fig. 9-8 RCS Thruster Arrangement and Operational Mode, Orbiter



	ACTIVE THRUSTERS				NORMAL OPERATION TOTAL
	L-REAR	R-REAR	C-REAR	FORE	
LIMIT CYCLE					
PITCH	-	-	-	1	1
ROLL	-	2	-	-	2
YAW	-	-	-	1	1
ATTITUDE MANEUVERS					
PITCH	1	1	-	1	3
ROLL	1	1	-	-	2
YAW - RIGHT	-	1	-	1	2
YAW - LEFT	1	-	-	1	2
TRANSLATE					
RIGHT	1	-	-	1	2
LEFT	-	1	-	1	2
UP	1	1	-	1	3
DOWN	1	1	1	1	4

Fig. 9-9 RCS Thruster Arrangement and Operational Mode, Booster

Table 9-3

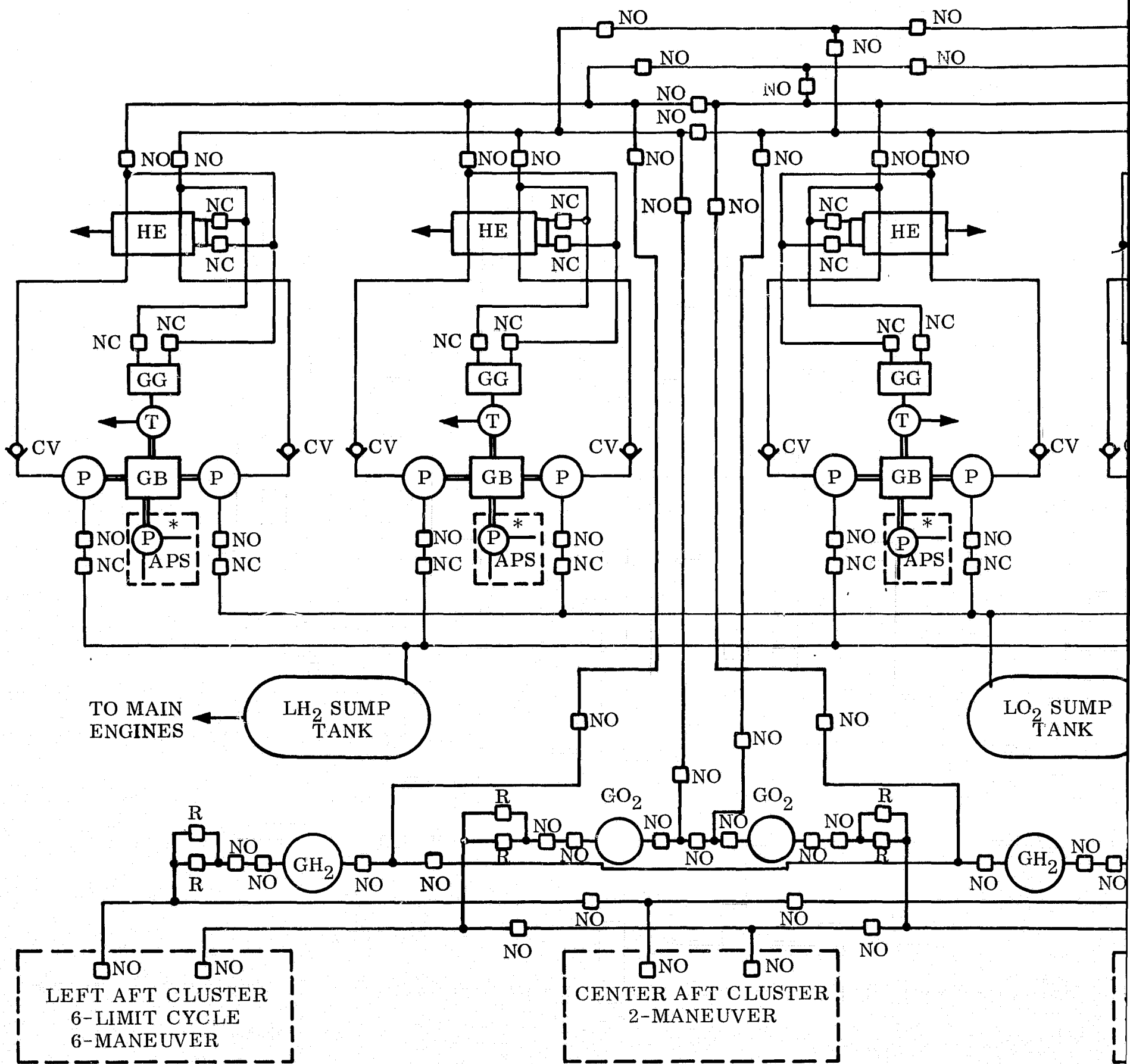
RCS PERFORMANCE CHARACTERISTICS

	Orbiter		Booster
	Limit Cycle	Maneuvering/ Translation	
Thrust (lb)	100	3500/640	3360/640
Specific Impulse (sec)			
Steady state	410	420	414
Pulsing	336	—	300
Minimum Impulse Bit (lb-sec)	10-12	—	120
Mixture ratio	4.0	4.0	4.0
Chamber pressure (psia)	250	250	250
Thruster area ratio	40:1	30:1	20:1
Thruster weight (lb)	10	67.5	65
Thruster length (in.)	10	33	28
Thruster diameter (in.)	4	16	15
Propellant feed pressure (psia)	400	400	400
Propellants	GO <sub>2</sub> /GH <sub>2</sub>	GO <sub>2</sub> /GH <sub>2</sub>	GO <sub>2</sub> /GH <sub>2</sub>

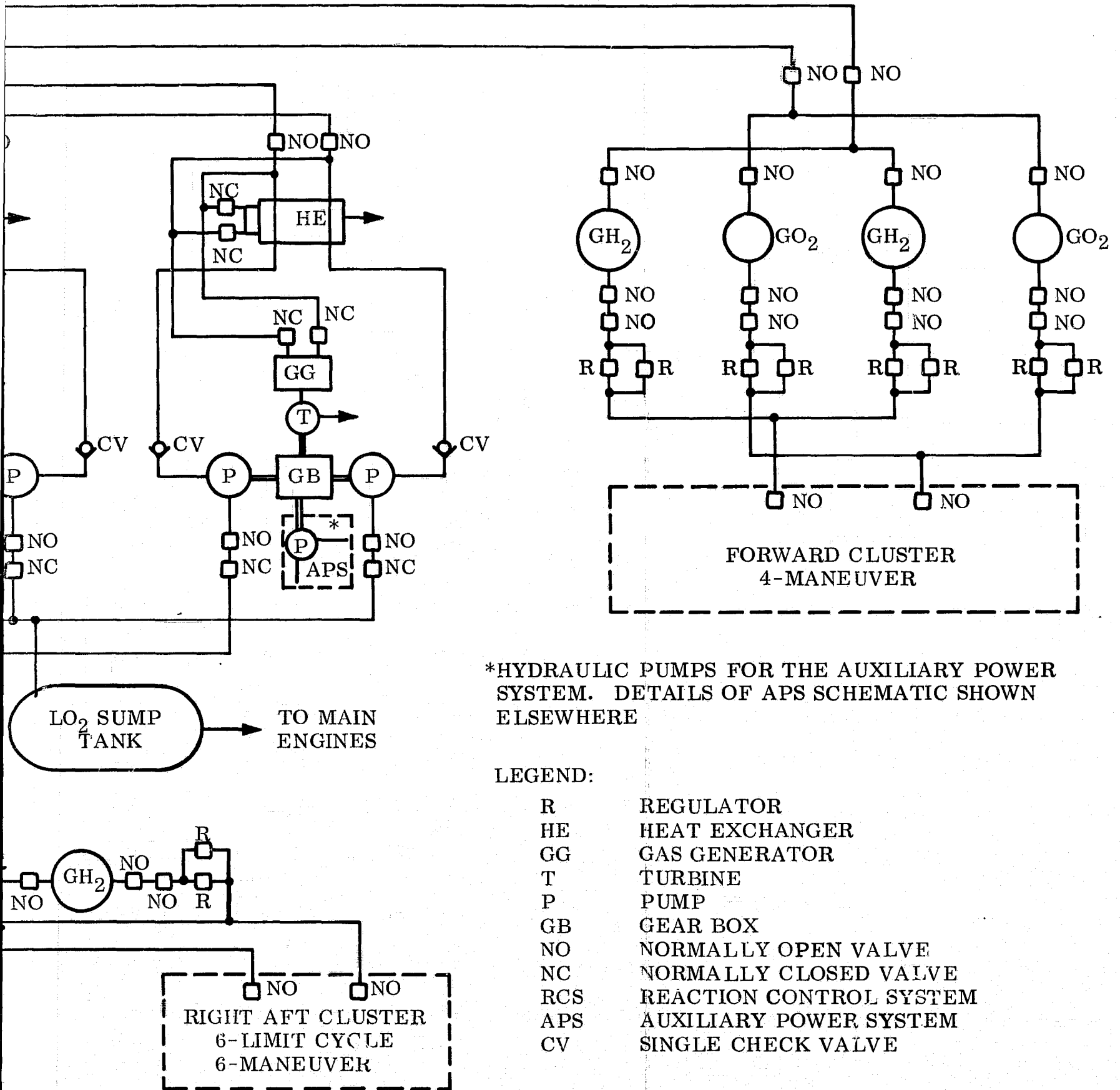
9.2.2.1 Orbiter Vehicle Propellant System. The selected system for the orbiter is shown in Fig. 9-10, and the system description is presented in Table 9-4. As indicated, the power for the pump has been integrated with auxiliary power units and hydraulic pumps, discussed in Section 9.4.

Each of the hydrogen accumulator tanks, 5 feet in diameter, has a capacity of 53 cubic feet. The oxygen tanks are 3 feet in diameter, each having a capacity of 10 cubic feet.

Considerable redundancy is provided in the system.



FOLDOUT FRAME /



\*HYDRAULIC PUMPS FOR THE AUXILIARY POWER SYSTEM. DETAILS OF APS SCHEMATIC SHOWN ELSEWHERE

Fig. 9-10 Integrated RCS/APS Propellant Feed and Conditioning Schematic, Orbiter

FOLDOUT FRAME 2

Table 9-4

DESCRIPTION OF THE ORBITER PROPELLANT SYSTEM

Components	Application
Liquid Hydrogen and Liquid Oxygen Pumps (4 of each)	Increase the pressure of the liquid propellants from the orbital storage tanks to the pressure of the accumulators (500 to 1000 psia)
Gear Boxes (4)	Distribute the power from the turbines to the propellant pumps or to the hydraulic pumps
Turbines (APU) (4)	Operate on the gases from the gas generators to produce the power to drive the pumps
Gas Generators (4)	Operate at a mixture ratio of 1:1 to produce gases to run the turbines at approximately 1500°F
Heat Exchanger/Vaporizer	Convert the propellants from the liquid phase to the gaseous phase and adjust the temperature to 350 to 400°R (The burner operates at a mixture ratio of 4:1 and a temperature of approximately 4800°F.)
Check Valves (8)	Prevent backflow of propellants in the pumps
GH <sub>2</sub> Accumulator Tanks (4)	Store gaseous hydrogen at high pressure and at a temperature of 350 to 400°R for use by the engines when the pumps are inactive (Four are used for redundancy if one fails. Two are located in the forward region and two in the aft region.)
GO <sub>2</sub> Accumulator Tanks (4)	Same as GH <sub>2</sub> accumulator
Regulators (16)	Reduce pressure of propellants in accumulator tanks to the operating pressure of the engines (The regulators are parallel redundant.)
Normally Closed Valves Located at Heat Exchanger (8)	Control the flow of GH <sub>2</sub> and GO <sub>2</sub> to the combustion chamber of the heat exchanger

Table 9-4 (Cont.)

Components	Application
Normally Closed Valves Located at Gas Generator (8)	Control the flow of propellants to the combustion chamber of the gas generator
Normally Closed Valves Located Upstream of Propellant Pumps (8)	Control the flow of liquid propellants to the pump inlets
Normally Open Valves – Gaseous Failure Only (64)	Isolate component failures
Normally Open Valves (Liquid) Failure Only (8)	Isolate component failure

9.2.2.2 Booster Propellant System. The propellant system for the booster vehicle reaction control differs substantially from that of the orbiter vehicle. The system is separate in that the propellants are not taken from the main propellant tanks, but are stored in the gaseous state at approximately 360°R. The maximum tank pressures are 1500 psia and the pressures are allowed to drop to a minimum of 500 psia. The thrusters operate at 400 psia. The booster system is presented schematically in Fig. 9-11.

The propellant tankage consists of six 5-foot diameter gaseous hydrogen tanks and six 3-foot diameter gaseous oxygen tanks. To minimize tank development, these tanks were chosen to be the same size as the booster vehicle tanks.

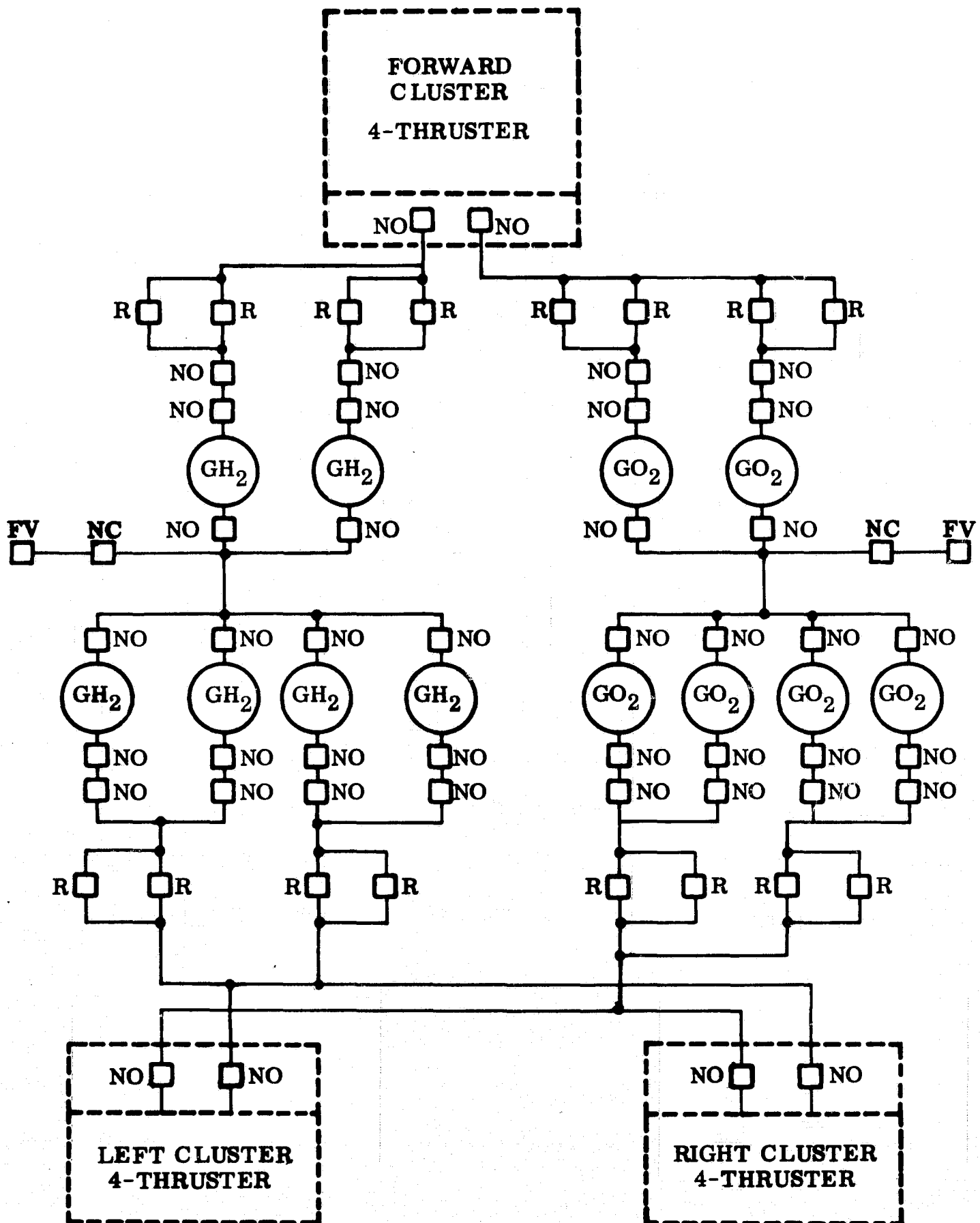


Fig. 9-11 RCS Schematic, Booster



### 9.3 SUBSONIC CRUISE PROPULSION SYSTEM

For the orbiter, the subsonic cruise propulsion system provides the thrust required for powered approach, go-around, and ferry. For the booster, the system provides thrust for fly-back, powered approach, go-around, and ferry.

During the reentry glide of the orbiter at a predetermined altitude and Mach number, the engines are deployed and started. The slope of the glide path is altered to decrease the rate of descent. The system is designed for providing for one go-around, if required, followed by a powered approach and landing.

The sequence of events affecting the subsonic cruise propulsion for the booster is the return to base mission mode, whereby, after separation, the booster follows a ballistic trajectory coupled with a turn to head back to the landing site and, at a predetermined altitude and Mach number, the engines are ignited. The booster then cruises back to the landing site for a normal powered approach and landing.

For the orbiter and the booster, the ferry mission mode consists of thrusting for takeoff and climb, cruise, go-around (if required), powered approach, and landing.

#### 9.3.1 Engine Selection Considerations

The selection of the subsonic cruise propulsion system is strongly dependent on the planned flight profile. The cruise altitude and the time allowed for climb to this altitude in go-around and ferrying are very important considerations. The requirements, based on a cruise altitude of 10,000 feet, are listed in Table 9-5.

A general comparison and relative positions of various engines are presented in Fig. 9-12. The absolute values of the weights are not complete in that fuel storage, installation, and other related factors are not included. However, the information presented indicates a trend.

Table 9-5

SUBSONIC CRUISE PROPULSION SYSTEM REQUIREMENTS

Parameter	Orbiter	Booster
Number of engines	4	4
Engine thrust level (sea-level static) (lb)	21,750	33,750
Total thrust (sea-level static) (lb)	87,000	135,000
Intended use (standing, ferry)	Both	Both
Subsonic cruise for cross-range capability	15 min plus go-around	-

While the information in Fig. 9-12 indicates that lift type engines are very attractive, the engines produced to date of this type are of relatively small thrust. Advancement to a thrust level on the order of 40,000 to 50,000 pounds is considered to be a major step. Therefore, the turbofan engine has been selected as possibly being the most attractive candidate engine type at this time.

9.3.2 Subsonic Cruise Propulsion Systems

Four high by-pass ratio turbofan engines, installed in the orbiter to provide the required thrust, are submerged within the vehicle during the boost and orbit phase of the mission, deployed during the entry glide mission phase, and operated during the remainder of the mission. In addition to providing thrust, the engines incorporate power takeoffs to run auxiliary equipment, such as hydraulic and electrical power generators. These auxiliary power generators are used during the ferry mode and may be used as a backup during the entry mission phase.

Four high by-pass ratio turbofan engines, installed in the booster to provide the required thrust, are installed in nacelles at the rear of the vehicle and need not be deployed for operation. However, a protective housing may be necessary at the inlet and exhaust duct to protect the engine during the boost and reentry phases. In

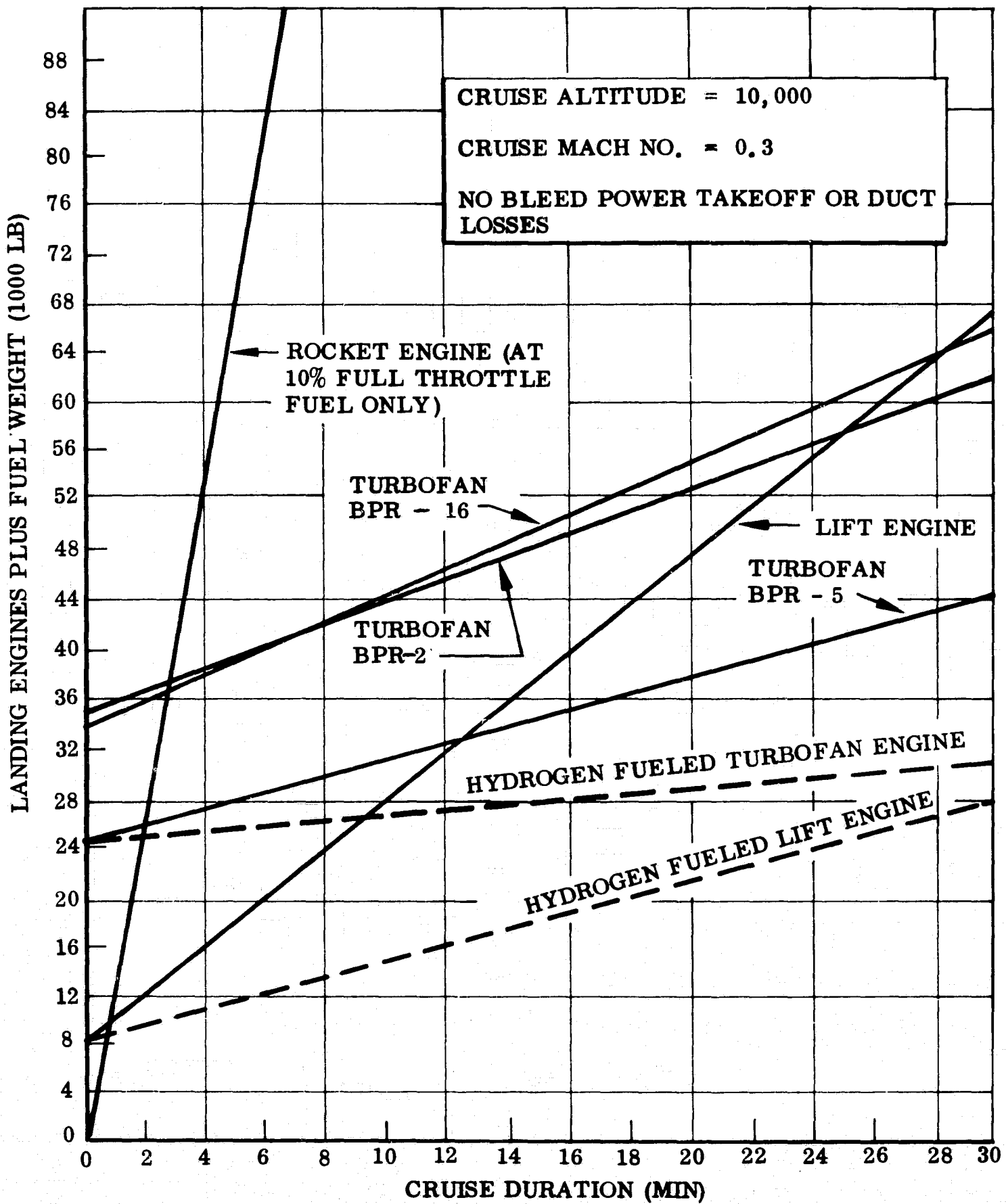


Fig. 9-12 Comparison of Engine Types

addition to providing thrust, the engines incorporate power takeoffs to run auxiliary equipment, such as hydraulic and electric power generators. These power generators are used during the ferry mode and the return-to-launch-base mode.

### 9.3.3 Propellant Storage and Feed System

Propellant storage and feed hardware consists of the fuel tanks, boost pumps, control components, and associated fuel lines from the tanks to the engines. The configuration shown in Fig. 9-13 consists of two tanks for powered approach and go-around for both the orbiter and the booster. The system will be used to ferry the orbiter back from the landing base to the launch base. Because more fuel is required for the ferry mission than for the reentry cruise mission, additional fuel and associated tankage, pumps, lines, etc., are stored in the payload compartment and connected through connectors mounted in the payload compartment walls. The fuel tanks for the booster, sized to provide sufficient fuel for flyback, may be adequate for the ferry requirement.

With the vehicle in the horizontal attitude, fuel is loaded under pressure through the disconnect (1) into Tanks A and B. Tank A will fill first because of the increased line pressure drop going to Tank B. When the fill indicator (2) is activated, shutoff valve (3) is closed; and filling of Tank B is completed when the fill indicator (4) is activated. A total flow gage of the ground fuel-transfer system will provide assurance that the proper amount of fuel is loaded. The vent float valves (5), which are horizontally functional, are above the level of the fuel; so the vents are open to atmosphere. De-fueling can be accomplished in the reverse direction by gravity.

During ascent and at all other times when jet engine use is not required, the ram air shutoff valve (6) is closed. At 40,000-foot altitude, the aneroid valve (7) closes automatically. The tanks are then sealed at a pressure less than 3 psia. The aneroid valve contains a relief feature in the event tank pressures rise above some predetermined level.

The ram air shutoff valve (6) is opened at or immediately before jet engine ignition. The boost pumps (8) supply fuel to the jet engines. One boost pump has the capacity to supply two engines. A second pump in each tank is added for redundancy and to

TO ENGINES

### EQUIPMENT LIST

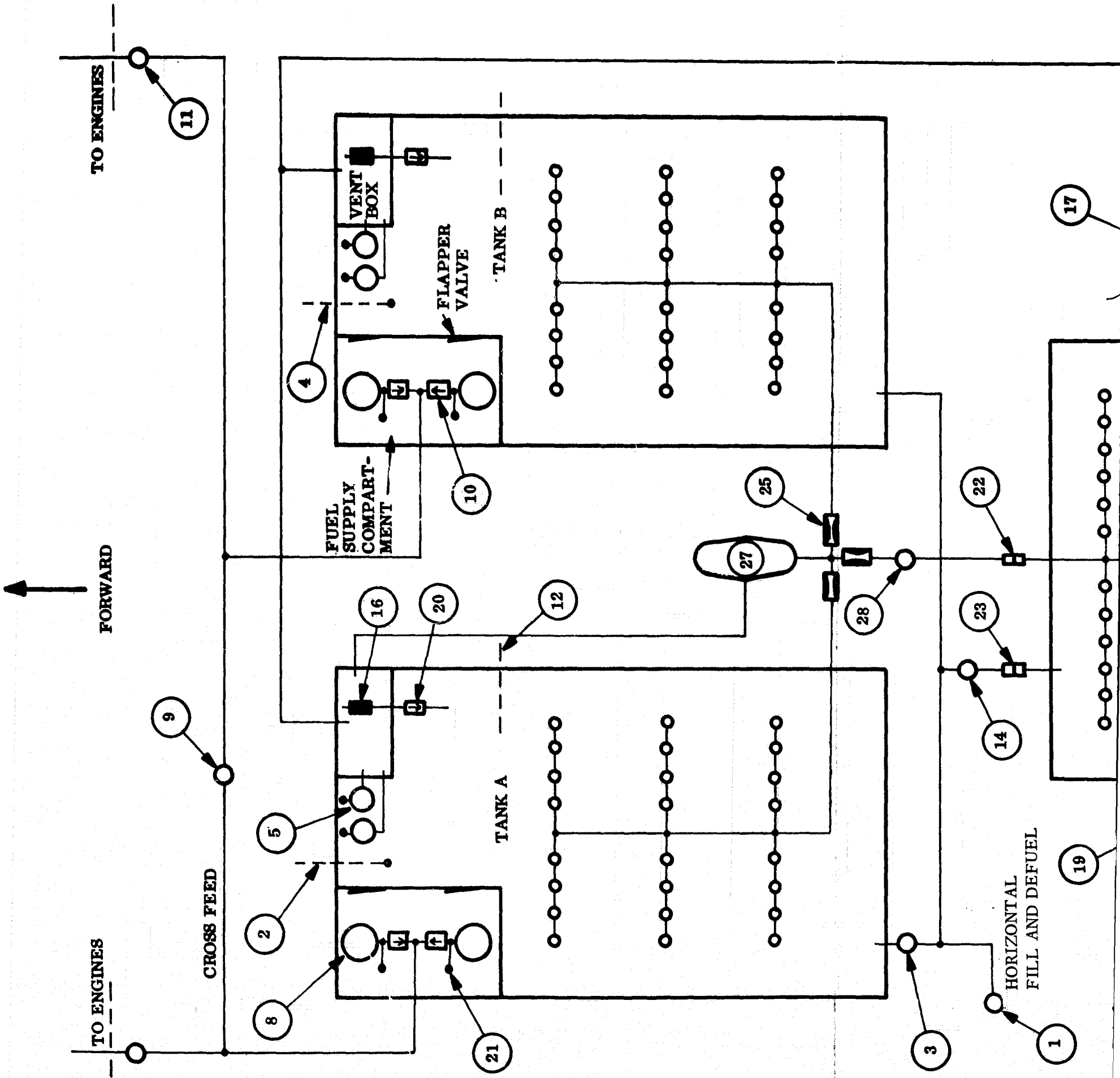
Item No.	Quantity Required	Nomenclature
1	1	Disconnect - fill and drain
2	1	Gage - fill indicator
3	1	Valve - shutoff, fueling
4	1	Gage - fill indicator
5	4	Valve - float, vent
6	1	Valve - shutoff, ram air
7	1	Valve - aneroid, vent
8	4	Pump - boost
9	1	Valve - shutoff, crossfeed
10	4	Valve - check, fuel supply
11	2	Valve - shutoff, engine
12	2	Gage - fuel quantity
13	1	Valve - disconnect
14	1	Valve - shutoff, interconnect
15	1	Valve - disconnect, defuel
16	2	Pump - scavenge, vent box
17	1	Valve - shutoff, pneumatic
18	1	Valve - check, pneumatic
19	1	Gage - fuel quantity, auxiliary tank
20	2	Valve - check, scavenge
21	4	Switch - pressure, boost pump
22	1	Coupling - interconnect
23	1	Coupling - interconnect
24	1	Coupling - interconnect
25	3	Valve - flow limiting, N <sub>2</sub> gas
26	1	Flame Arrester
27	1	Generator - N <sub>2</sub> gas
28	1	Valve - shutoff, isolation



FORWARD

TO ENGINES

BOLDDOUT FRAME



TO ENGINES

FORWARD

TO ENGINES

CROSS FEED

FUEL SUPPLY COMPONENT

VENT BOX

FLAPPER VALVE

TANK A

TANK B

HORIZONTAL FILL AND DEFUEL

FOLDOUT FRAME

2

FOLDOUT FRAME

11

4

10

16

20

12

2

8

21

25

27

28

22

23

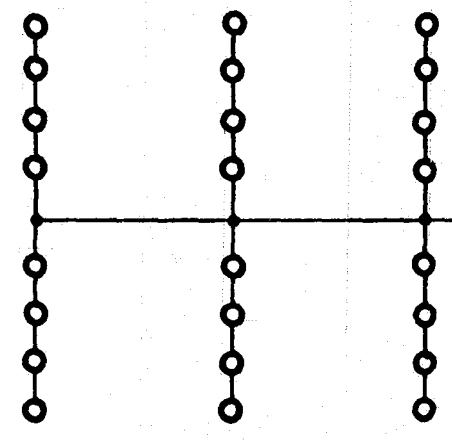
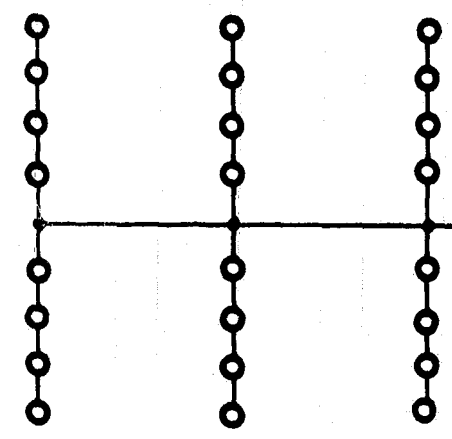
14

17

19

1

3



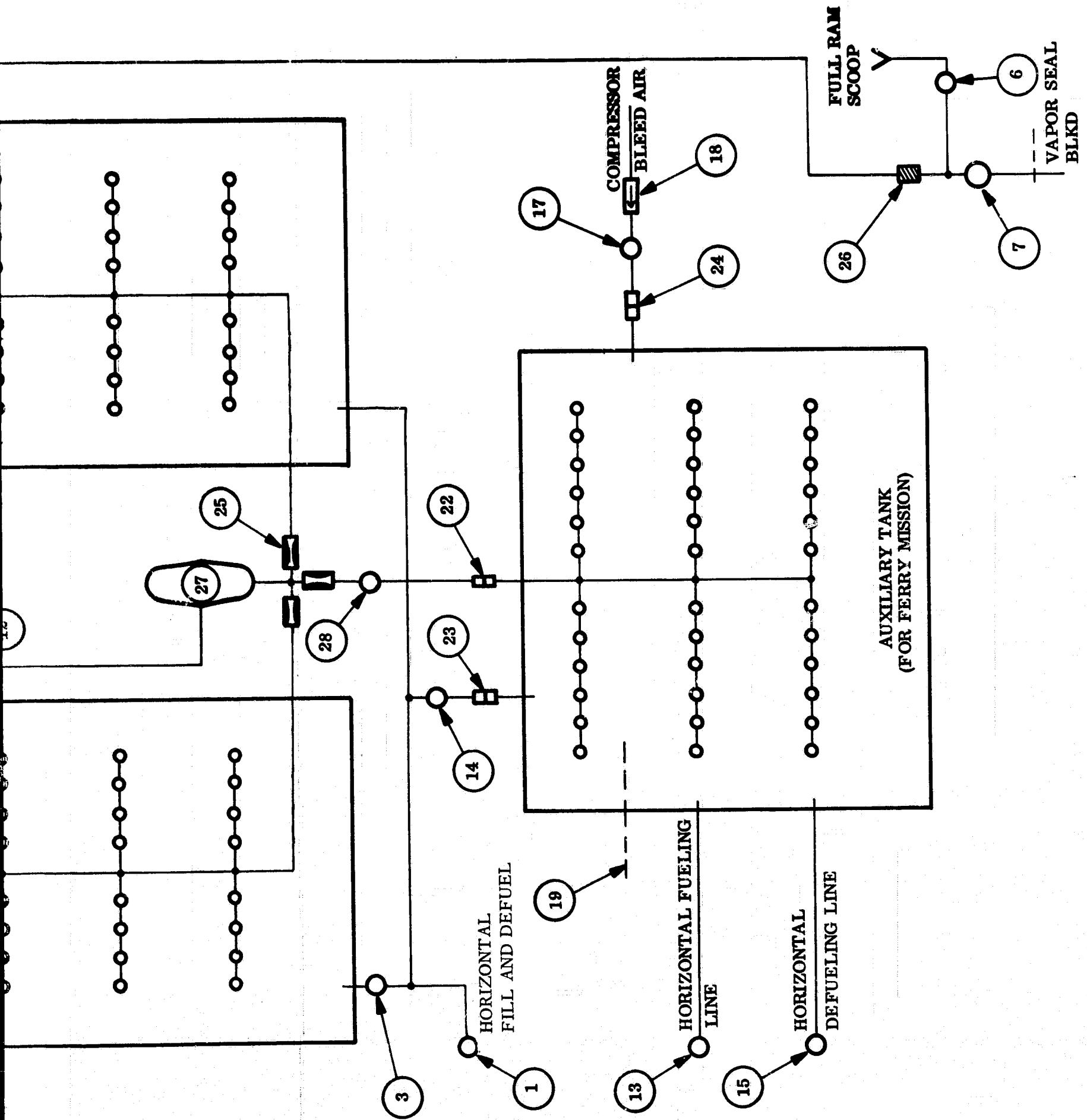


Fig. 9-13 SCPS Fuel Storage and Feed - Schematic

FOLDOUT FRAME

PRECEDING PAGE BLANK NOT FILMED.

FOLDOUT FRAME ?

permit operation of all engines from one tank. The electrical power supply for each pump in each tank comes from a separate bus. Either tank can supply fuel to all engines by opening the crossfeed shutoff valve (9). Reverse flow into an inoperative pair of pumps is prevented by the fuel supply check valves (10). The engine shutoff valves (11) are open during engine operation. Fuel availability is monitored with the fuel quantity gage (12), which will probably be the new type resistance-gage system.

For ferrying, an auxiliary tank is installed in the orbiter cargo compartment. Fuel is loaded by gravity through the auxiliary tank fuel-fill connect (13) with the vehicle in the horizontal attitude; that is, fuel is loaded in essentially the same way that an automobile is fueled. Tanks A and B are gravity filled when the tank interconnect shutoff valve (14) is opened.

If the auxiliary tank is located lower than Tanks A and B, the following procedure may be used:

- Fill the auxiliary tank.
- Close the fill interconnect (13).
- Pressurize the auxiliary tank.
- Fill Tanks A and B.
- Top off the auxiliary tank.

The vent float valves (5), which prevent Tanks A and B from overflowing, have a relief feature to prevent overpressurization.

Defueling is accomplished by gravity from all tanks. It is directed from Tanks A and B through disconnect (1) and from the auxiliary tank through disconnect (15). The scavenge pumps (16) are used for draining the vent box compartments.

The auxiliary tank is pressurized through shutoff valve (17) from the jet engine compressor (stage X) bleed air. The auxiliary tank empties while maintaining the filled Tanks A and B. The check valve (18) prevents any possibility of vapor or liquid reverse flow to the engine compressor. Auxiliary tank fuel is monitored with the fuel quantity gage (19).



Vernier control of vehicle balance was not considered. For primary mission descent, the change due to uneven feed from Tanks A and B will be negligible. Location, shape, and size of the auxiliary tank must be designed to provide satisfactory balance during the ferry flight. More than one auxiliary tank may be required for satisfactory balance control if a single tank creates problems.

Fuel jettisoning was not included in this first design. It is assumed that safe landing may be accomplished when Tanks A and B are full. Rapid jettisoning of auxiliary tank fuel may be accomplished by teeing off from the auxiliary tank defueling line.

## 9.4 AUXILIARY POWER/HYDRAULIC SYSTEM

The auxiliary power system on each element of both the Two-Stage and Triamese vehicles provides power to meet short-term peak demands not efficiently met by the electrical power system. On the orbital element of each concept, the principal short-term demands are the requirements for hydraulic power to actuate aerodynamic control surfaces during reentry and landing. High requirements are caused by the need for high-rate actuation of the control surfaces. Additional hydraulic power may be required as primary or backup supply for extending and starting the subsonic propulsion engines and for extending the landing gear. Provision for generating electrical power can also be provided.

### 9.4.1 System Description

The system is based on the use of auxiliary power units in three phases of the missions:

- Shaft power from the rocket engines is employed to drive hydraulic pumps at any time that the rocket engines are operating.
- Power is available from the jet engines during the times that they are operating.
- Oxygen/hydrogen auxiliary power units are in the reentry phase when other sources of power are not available.

The auxiliary power/hydraulic system for the orbiter is illustrated in Fig. 9-14.

### 9.4.2 Prelaunch Functions

Preflight checkout operations, general housekeeping, and prelaunch system conditioning will require hydraulic system pressurization, performed with the electric motor pump in the standby flight control hydraulic system. The checkout operations should include system leak checks and verification of functional response of engine gimbal actuators and control surface actuators.

9-42

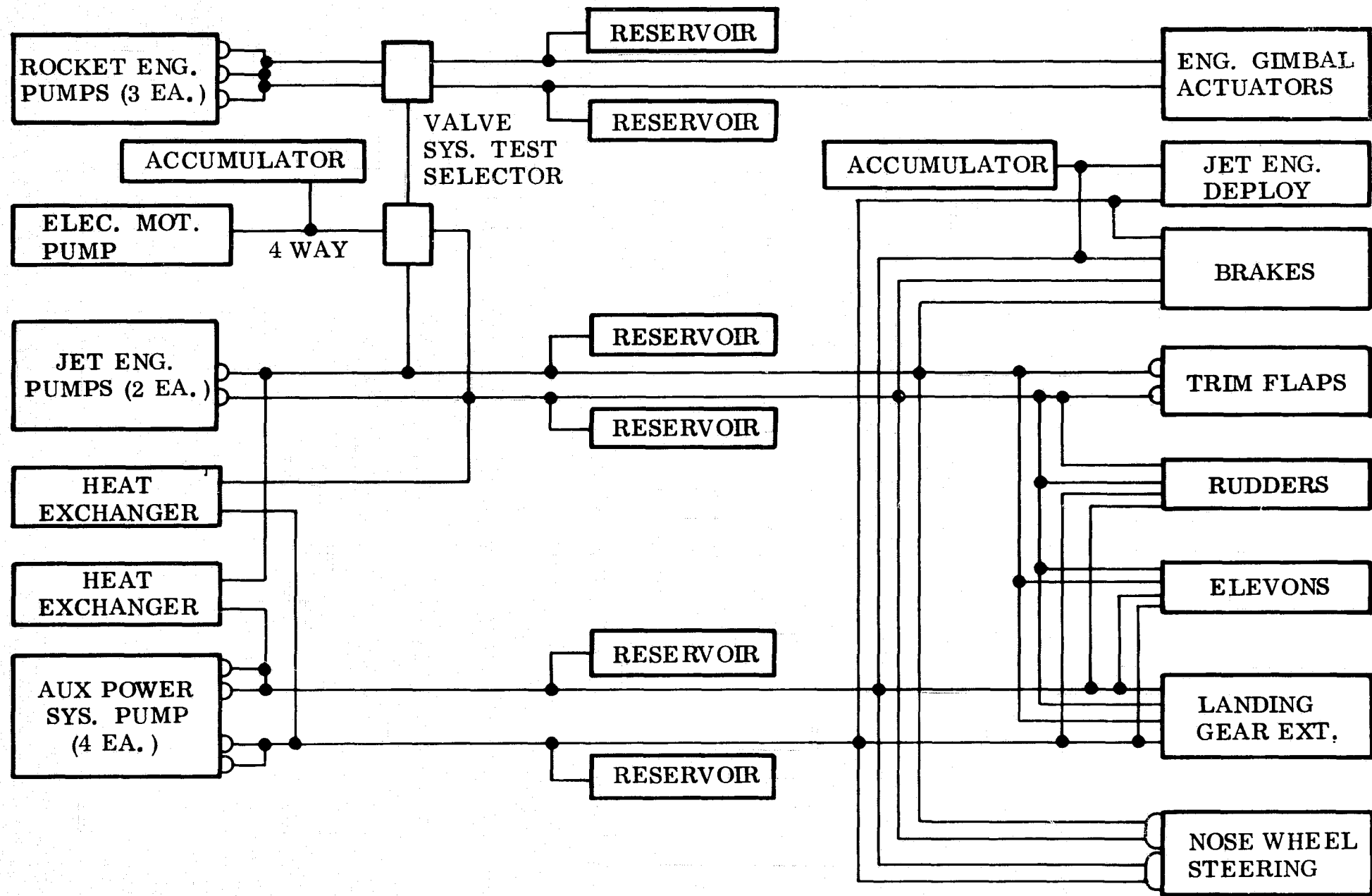


Fig. 9-14 Auxiliary Power/Hydraulic System

#### 9.4.3 Ascent and Orbital Engine Operation

Firing of the main rocket engines will supply power to the hydraulic pumps of the rocket engine gimbal system. These pumps are of the constant-pressure variable volume type, functioning in parallel at partial capacity. Tandem rocket engine actuators have mechanical feedback to assure better servo-loop accuracy and a null position if the electrical input signal is lost or removed.

In the event of loss of these systems, the gimbal actuators can be pressurized from the flight control system by switching in the system test selector valve. During launch and orbit operations, the flight control surfaces are faired and snubbed by the hydraulic actuators. This is an automatic characteristic of the actuator design which does not require system pressurization. The trim flap system is a hydraulically powered mechanical screw jack system, which will remain in whatever position it is placed.

#### 9.4.4 Orbit Functions (Engines Not Operating)

There are no defined requirements for auxiliary power supply system usage during orbit. Minor housekeeping requirements would be supplied by the accumulator and the electrical motor pump. Should a major work load be desired, the flight control auxiliary power unit pump(s) could be started to support main rocket engine operation in the unpumped idle mode for maneuvering or retro action. The flight control system could also be used to move the rocket engines away from the flap in preparation for reentry and to retract the rocket engine nozzle extensions. Actuators will stay in their last position after hydraulic pressure has been removed.

#### 9.4.5 Reentry Functions

The reaction control system will provide attitude control during reentry until the atmosphere becomes dense enough to make the control surfaces effective. The auxiliary power system would be powered at the beginning of reentry operation, but until the control surfaces develop loads the pump would supply full system pressure with minimum stroke. After the reaction control system is shutdown, the attitude control is

maintained by the control surfaces throughout the remainder of the flight. Auxiliary power system drive hydraulic pumps supply pressure actuators for the elevons and hydraulic screw jacks for the flaps. The flight control hydraulic system also has check valves in each of the pump high-pressure lines to prevent back flowing a nonoperating pump, a heat exchanger for sustained operation, and an accumulator reservoir. Should the primary hydraulic system fail, a secondary system comes on the line when the pressure to the actuators drops below a predetermined point, thereby signaling failure mode activity.

#### 9.4.6 Turbojet Engine Flight Mode Functions

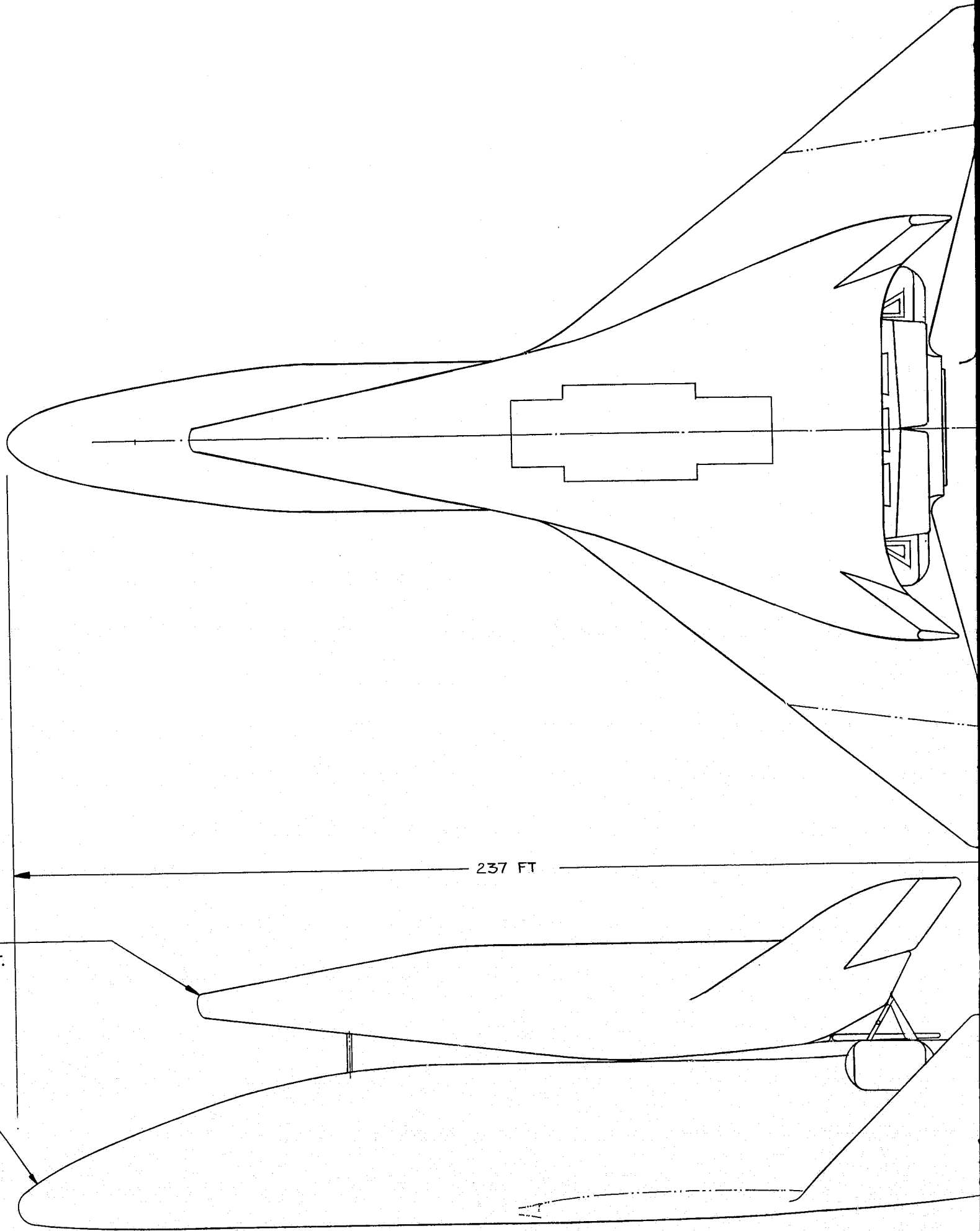
The primary extend engine system consists of a hydraulic actuator, charged with auxiliary power system hydraulic pressure. When the normally closed valve is opened, hydraulic pressure is transmitted to the extend engine actuators, driving them to the full-extend position. The secondary extend engine hydraulic system obtains pressure from the drive pumps (primary hydraulic flight control system). The normally closed valve is opened to the extend engine actuator and the normally open by-pass valve is closed. This directs flight control hydraulic system pressure to the extend engine actuator, which has two pistons on the same shaft. One piston is fed by the secondary hydraulic system, and the second piston is fed by the flight control hydraulic system. When the second piston is not in use, oil is by-passed by one side of the piston to the other through the normally open valve. In the event of failure resulting in loss of fuel to the auxiliary power units, an accumulator is provided to ensure the capability of fanjet extension.

Power for the hydraulic system can be taken from the airbreathing engines. This is desirable to satisfy reliability design requirements, and it is the preferred mode of operation for extended subsonic flight. During reentry flight, the auxiliary system would furnish hydraulic power. The air-breathing-engine-supplied hydraulics would be standby power thereby avoiding unnecessary switching.

Landing activities require hydraulic power for control surfaces, landing gear extensions, nose wheel steering, and wheel braking. Power is normally obtained from the auxiliary power units or from the fanjet engines. The accumulators and electric motor pump can be configured to provide these functions.

APPENDIX A  
DRAWINGS

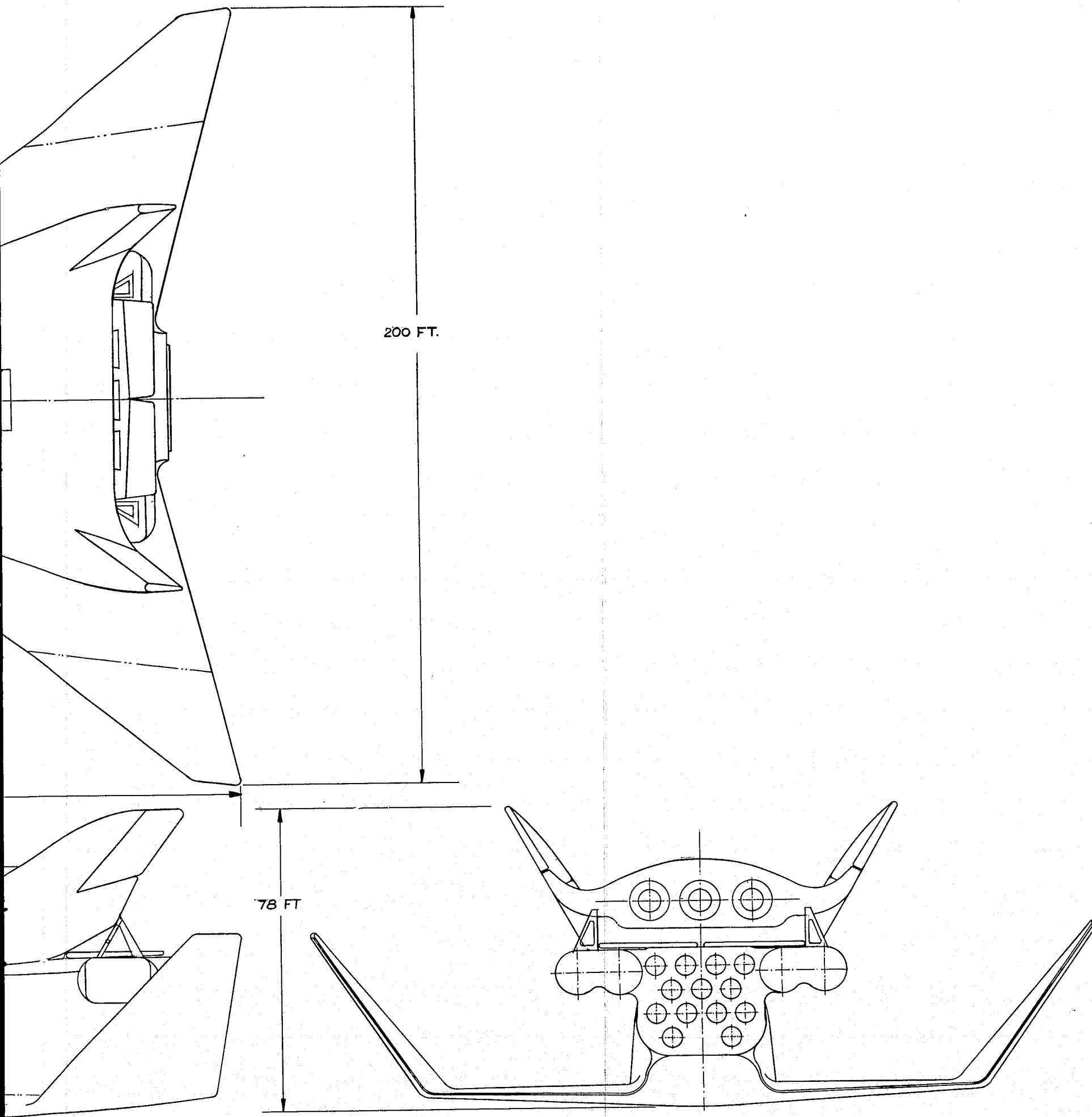
<u>Drawing</u>	<u>Drawing Number</u>	<u>Page Number</u>
Launch Vehicle General Arrangement	SKS 101069	A-1
Booster General Arrangement	SKS 100969	A-2
Booster Inboard Profile	SKS 1001169	A-3
Booster Structural Arrangement	SKX 100269	A-4
Booster Main Propellant Lines	SKD 101569	A-5
Orbiter General Arrangement	SKS 100769	A-6
Orbiter Inboard Profile	SKS 100869	A-7
Orbiter Structural Arrangement	SKW 101069	A-8
Orbiter Main Propellant Lines	SKB 101569	A-9
Launch Vehicle General Arrangement	SKD 100969	A-10
Booster General Arrangement	SKG 100769	A-11
Booster Inboard Profile	SKG 100369	A-12
Orbiter General Arrangement	SKG 100969	A-13
Orbiter Inboard Profile	SKG 100869	A-14
Pilot Vision Study (Spacecraft)	SKE 100969	A-15
Personnel Escape System Concept	SKJ 100169	A-16
Personnel Escape System Concept	SKJ 100269	A-17
Personnel Escape System Concept	SKJ 100369	A-18
Launch Vehicle Attachment System	SKB 101069	A-19
Payload Door Concept	SKM 10156	A-20
Orbiter Nosecap Concept	SKR 060969	A-21
Nosecap Concept	SKR 060699	A-22
Orbiter Tank Support Concept	SKT 100969	A-23
Launch Vehicle Two-Stage - 25 K Payload	SKJ 101669	A-24
Launch Vehicle - 25 K Payload	SKJ 101769	A-25
Booster Thrust Structure	SKQ 092969	A-26
Booster Propulsion System	SKQ 101569	A-27



ORBITER  
REF: SKS 100769 - GEN. ARR'MT.  
SKS 100869 - INBOARD

BOOSTER  
REF: SKS 100969 - GEN. ARR'MT.  
SKS 101169 - INBOARD

WOLDOUT

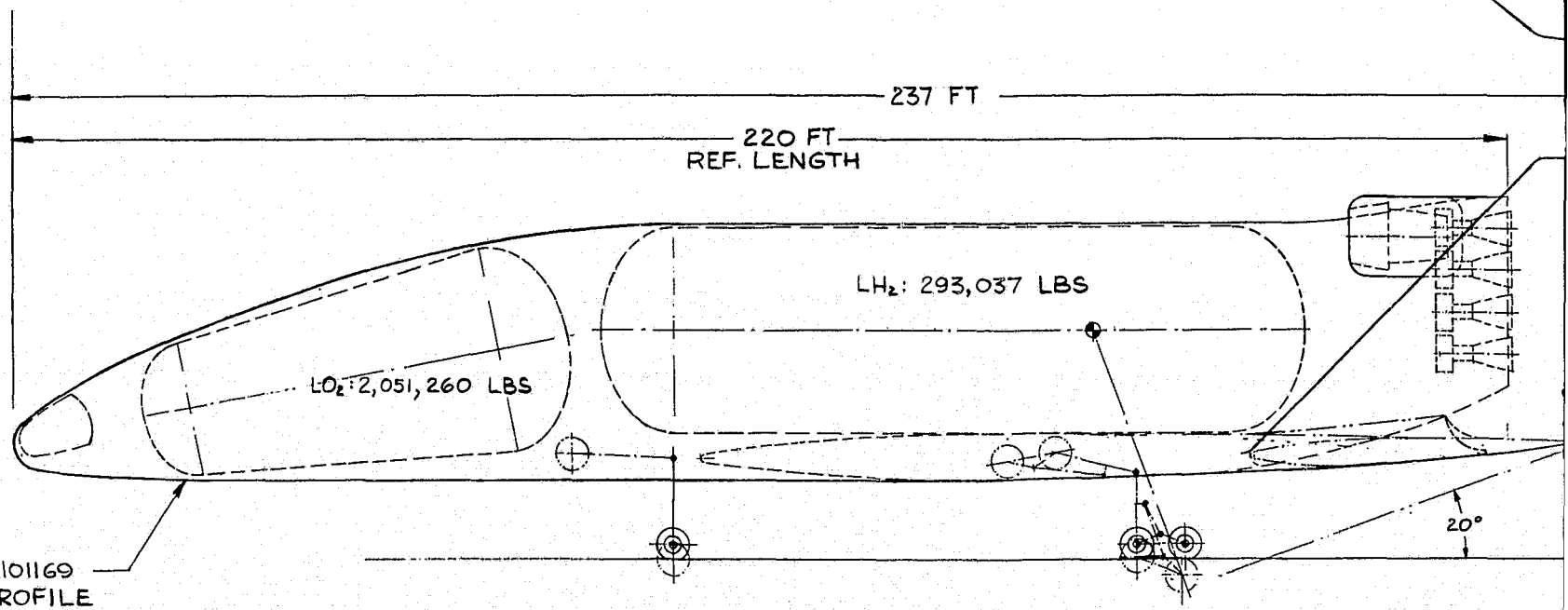
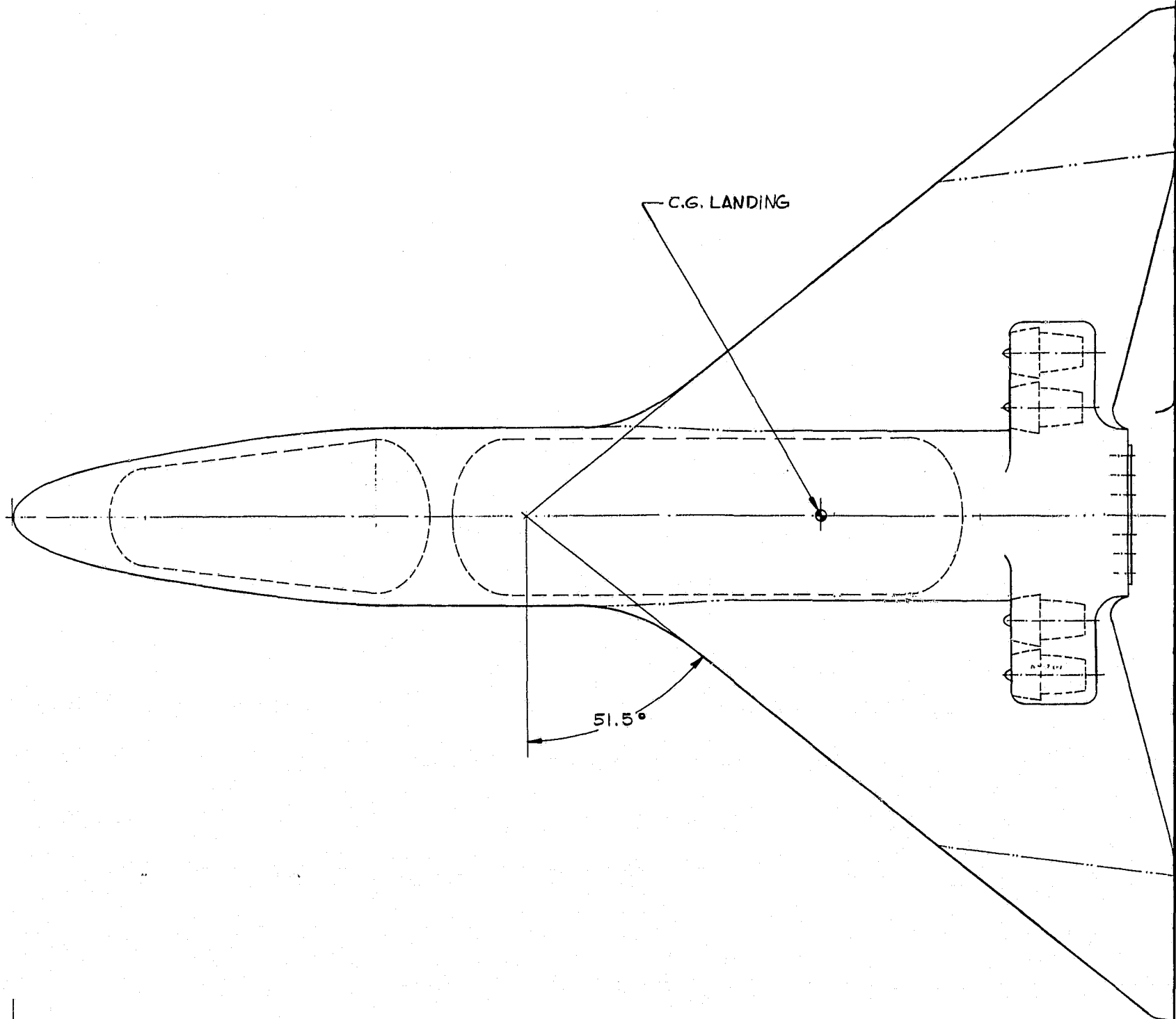


FOLDOUT FRAME 2

DATE	Oct 10, 1969	LOCKHEED MISSILES & SPACE COMPANY	
DR	H. Schmidt	A GROUP DIVISION OF LOCKHEED AIRCRAFT CORPORATION SUNNYVALE, CALIFORNIA	
APPD		LAUNCH VEHICLE	
ENGR		2 STAGE SYSTEM - 50 K P/L	
CHK		GENERAL ARRANGEMENT	
APPD		SIZE CODE IDENT	DRAWING NO.
APPD			SKS 101069
		SCALE 1/120	SHEET 1 OF 1

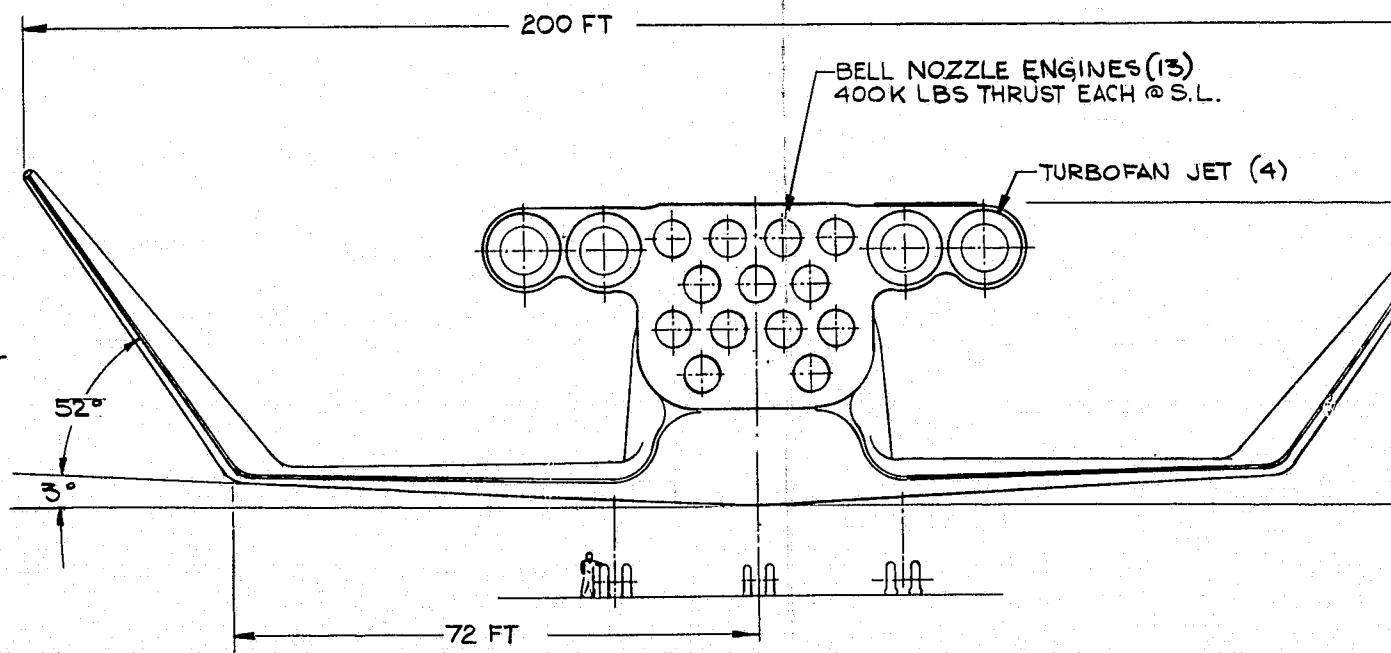
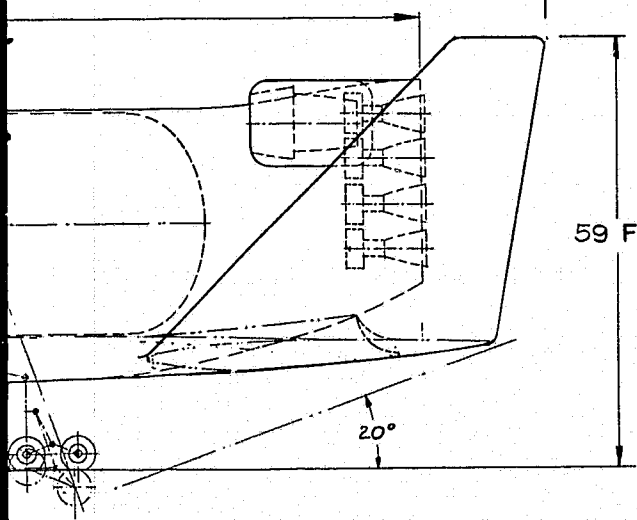
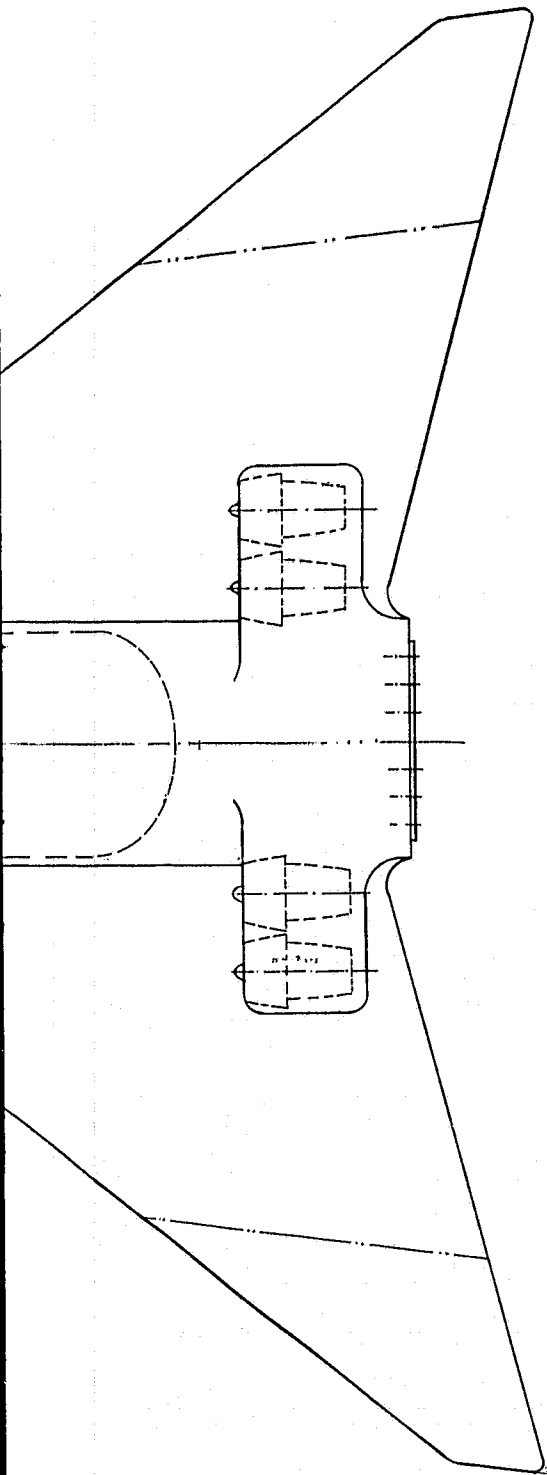
A-1





REF.: DWG. SKS 101169  
INBOARD PROFILE  
# DWG. SKD 101569  
PROP. LINES

FOLDOUT FRAME 1



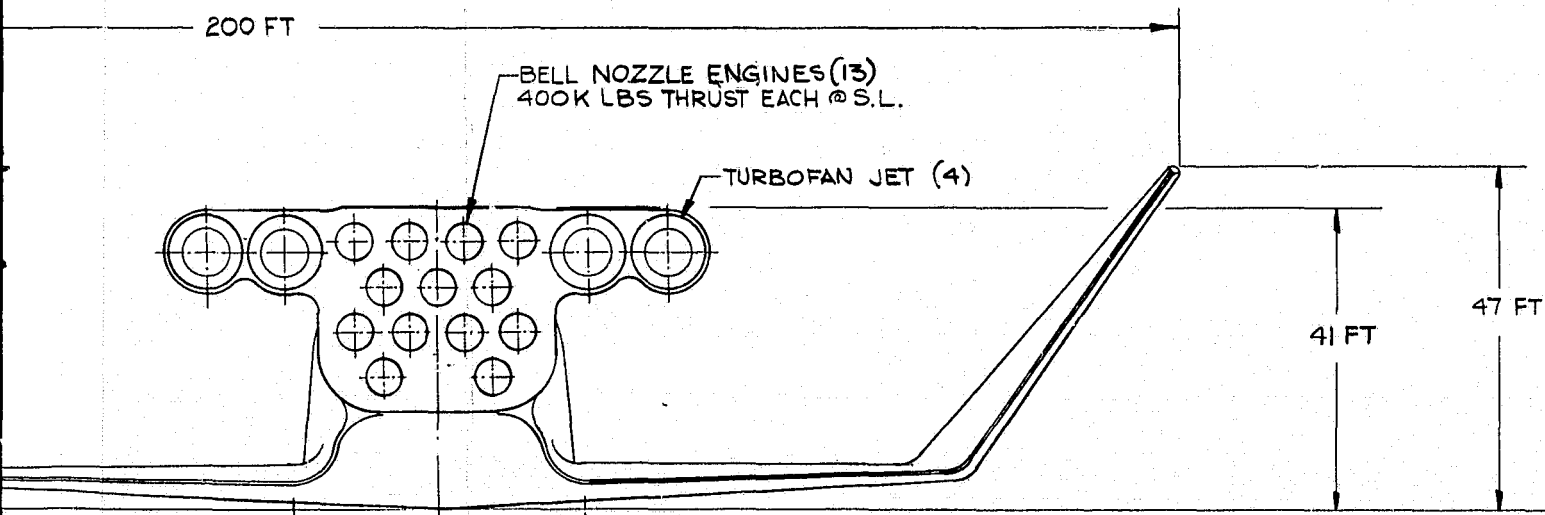
BELL NOZZLE ENGINES (13)  
400K LBS THRUST EACH @ S.L.

TURBOFAN JET (4)

0 5 10 20 30 40 FT  
SCALE

FOLDOUT FRAME 2

FOLDOUT



BELL NOZZLE ENGINES (13)  
400K LBS THRUST EACH @ S.L.

TURBOFAN JET (4)

41 FT

47 FT

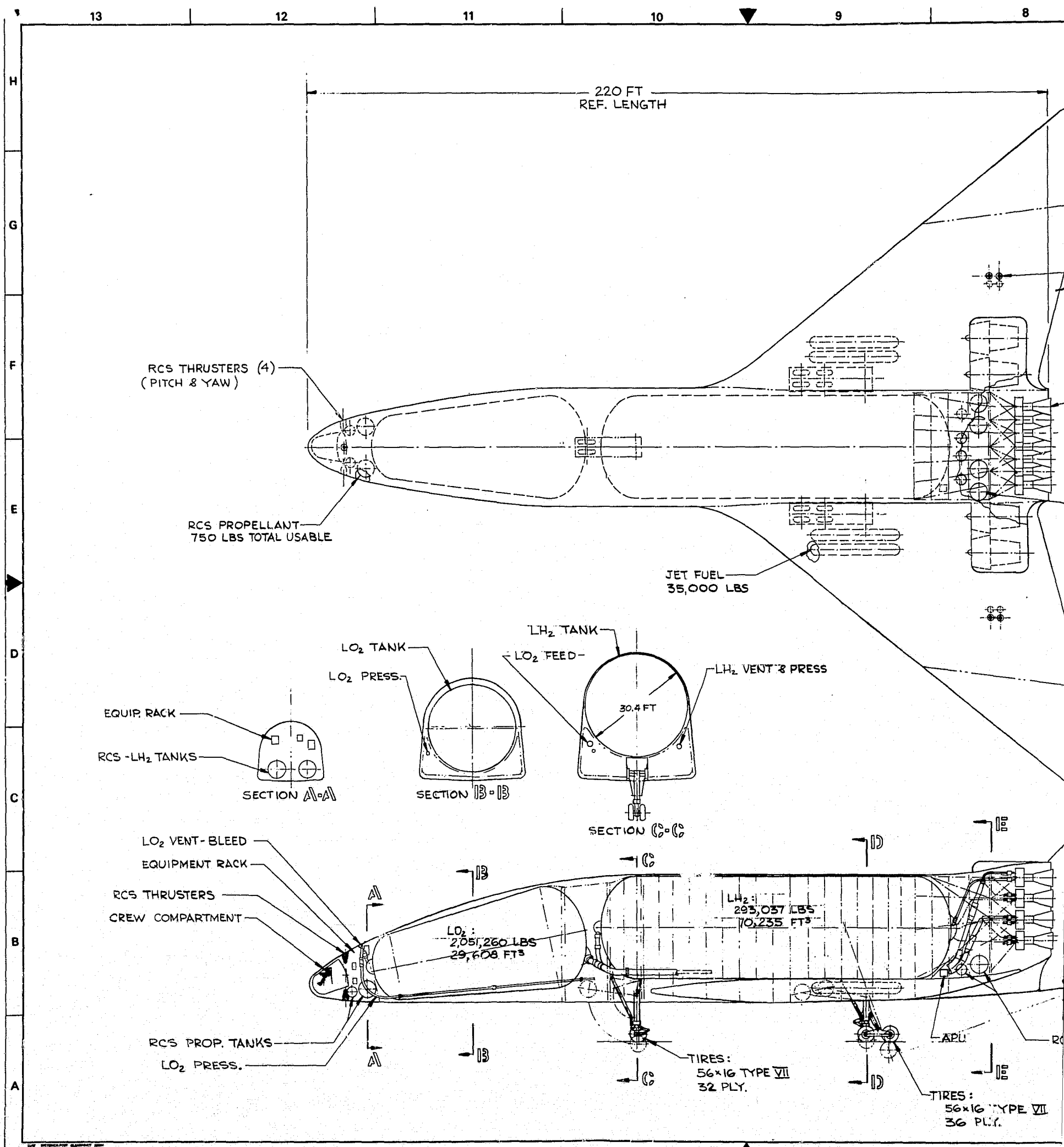
72 FT

0 5 10 20 30 40 FT  
SCALE

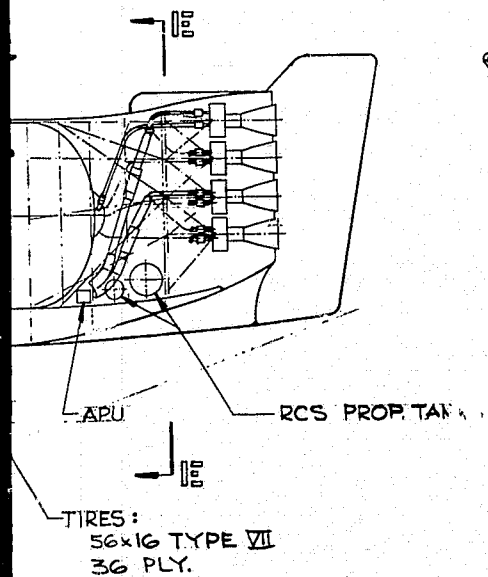
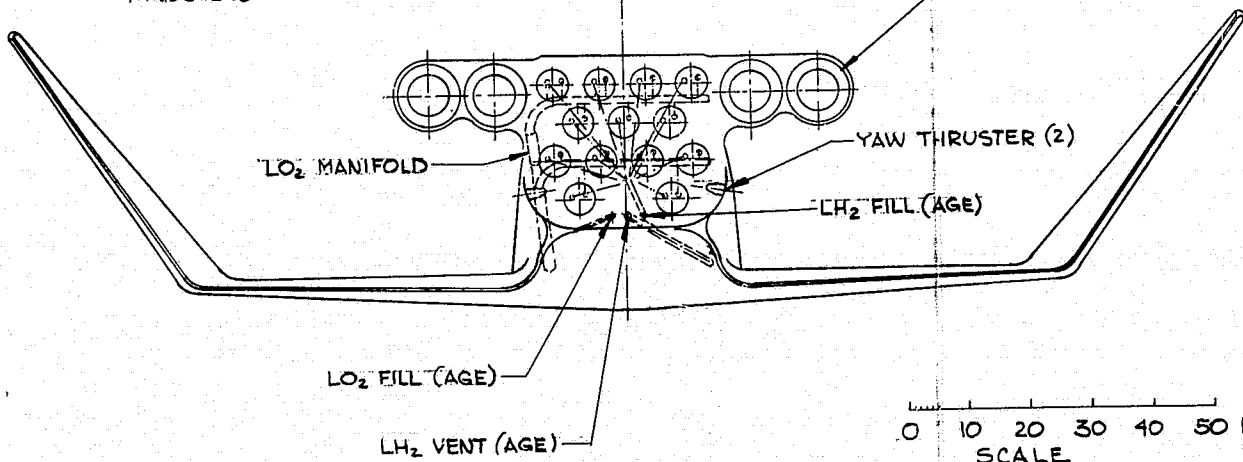
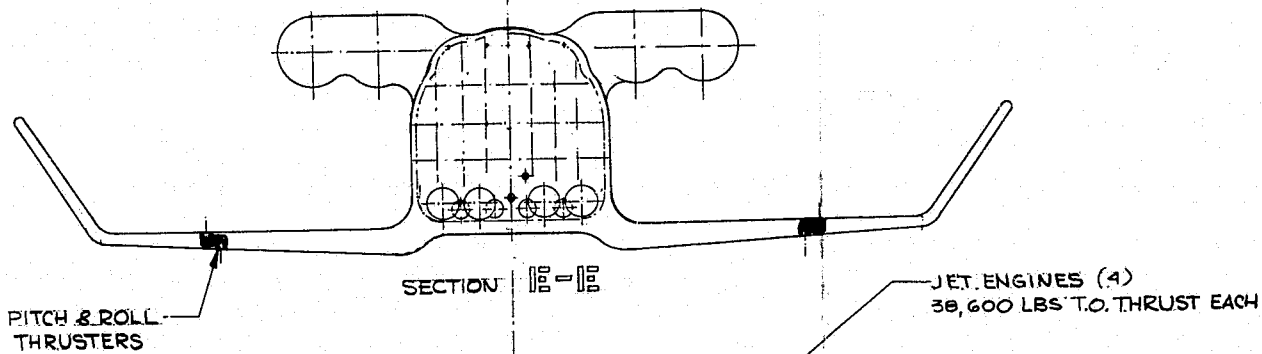
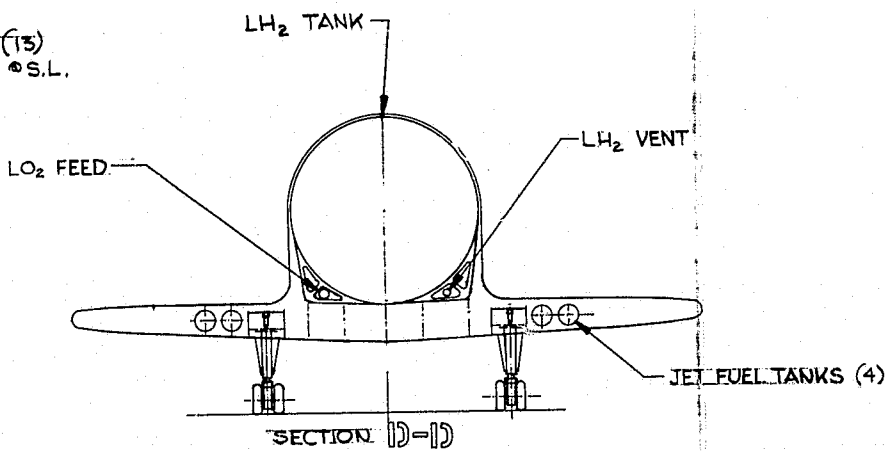
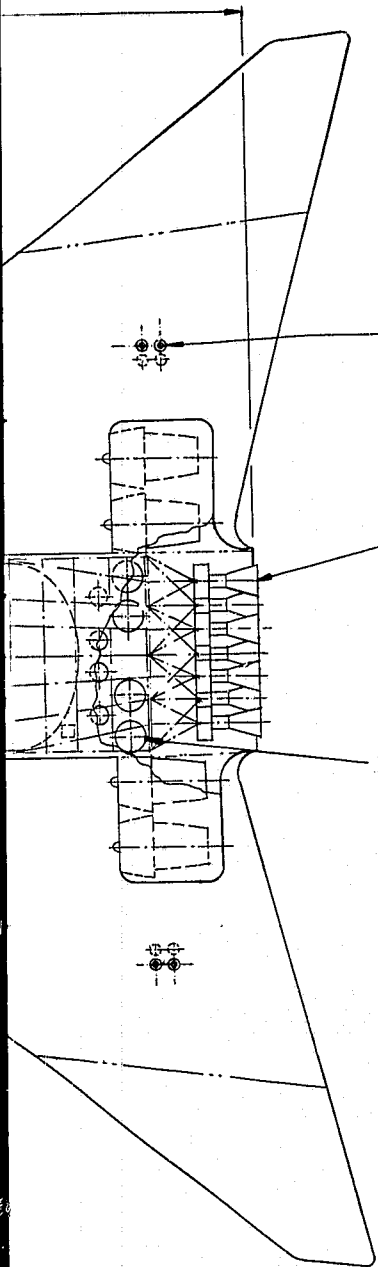
DATE	Oct. 9, 1969	LOCKHEED MISSILES & SPACE COMPANY	
DR	H. Schmidt	A GROUP DIVISION OF LOCKHEED AIRCRAFT CORPORATION SUNNYVALE, CALIFORNIA	
APPD		BOOSTER	
ENGRG		2 STAGE SYSTEM - 50 K P/L	
CHK		GENERAL ARRANGEMENT	
APPD		SIZE CODE IDENT	DRAWING NO.
APPD			SKS 100969
		SCALE 1/120	SHEET 1 OF 1

FOLDOUT FRAME 3

A-2



FOLDOUT FRAME 1



0 10 20 30 40 50 FT  
SCALE

NOTES

DRAWING NUMBER	REV	SH

INTERPRET DWG PER	
QTY REQD	
NEXT ASSY APPLICATION	USED O
FORM LMSC 15	

**FOLDOUT FRAME 2**

FOLDOUT

5

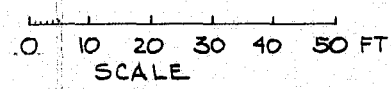
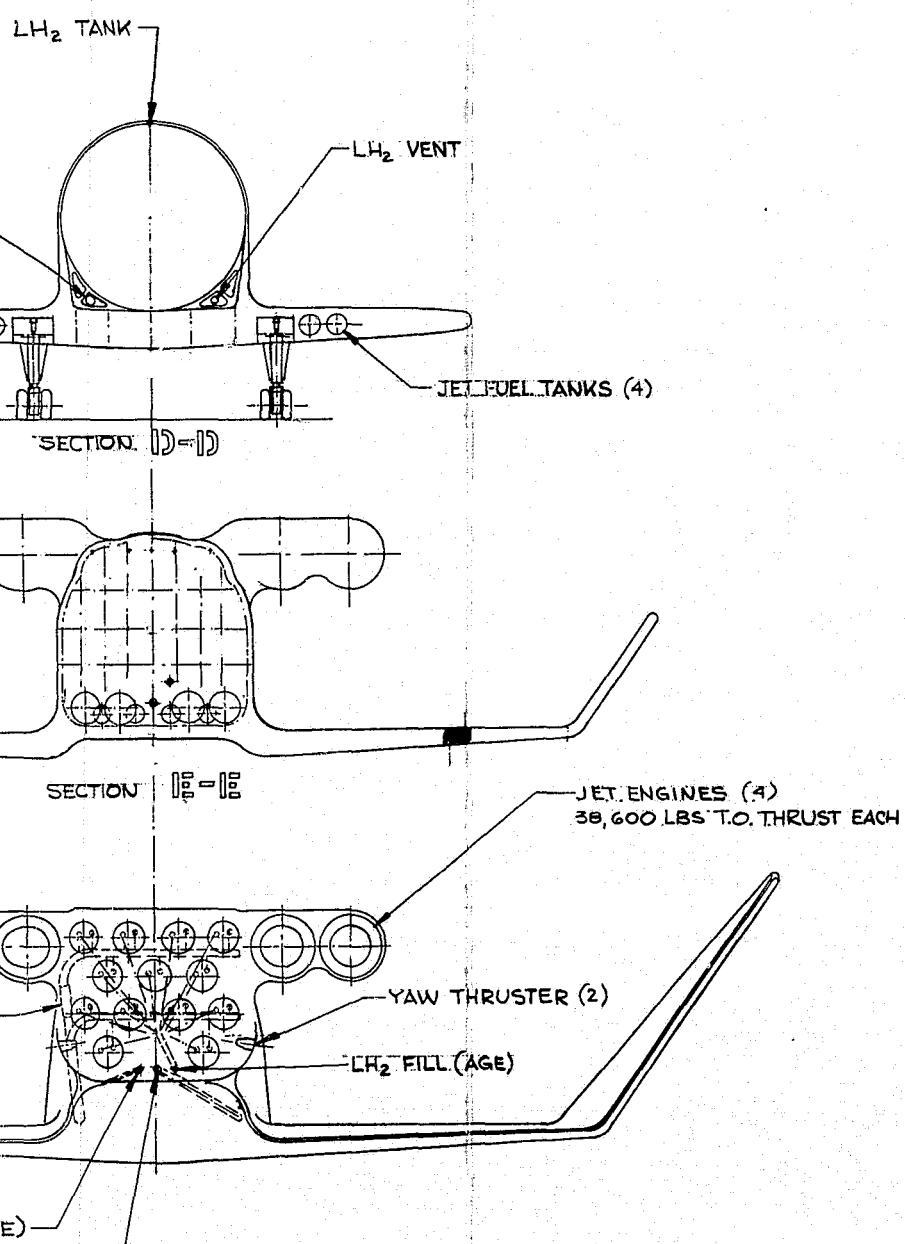
4

3

2

1

LIMITED CALENDAR LIFE	LIMITED OPERATING LIFE	REVISIONS		DATE	APPD
		ZONE/CTR	DESCRIPTION		



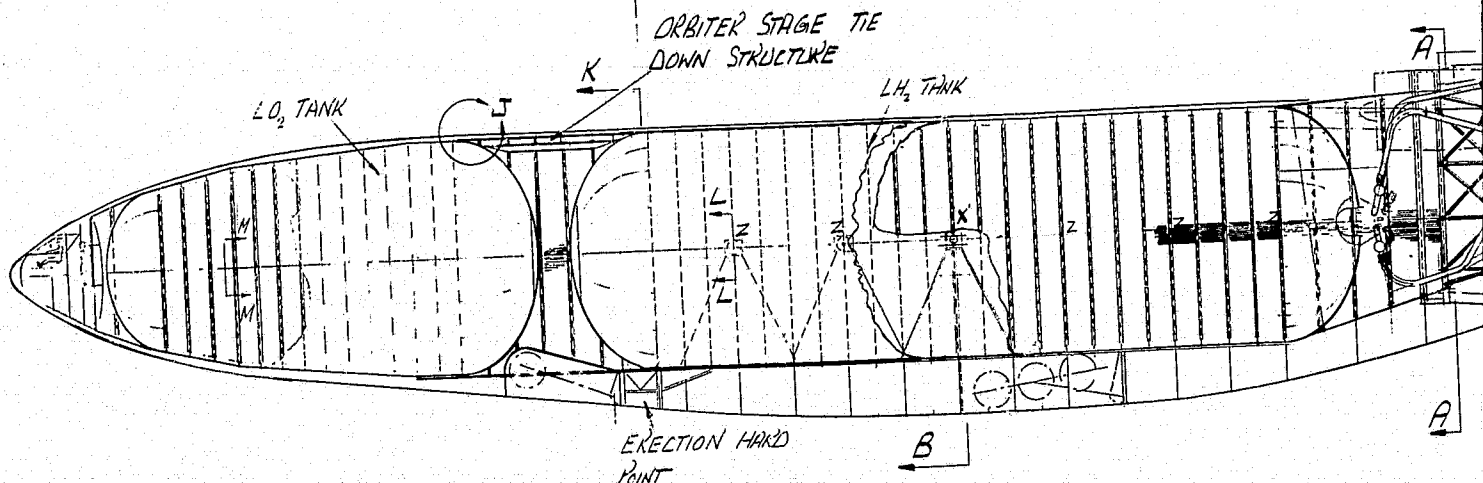
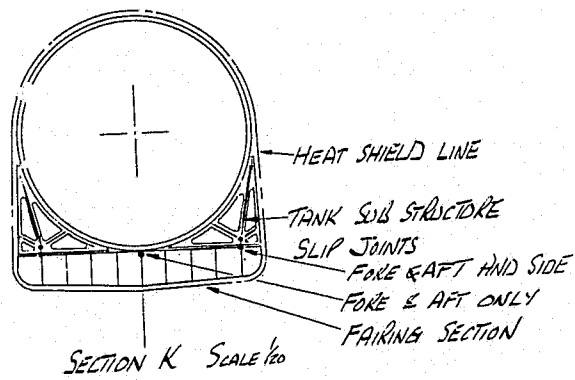
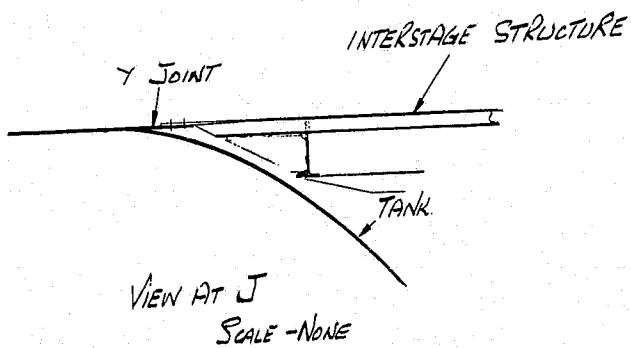
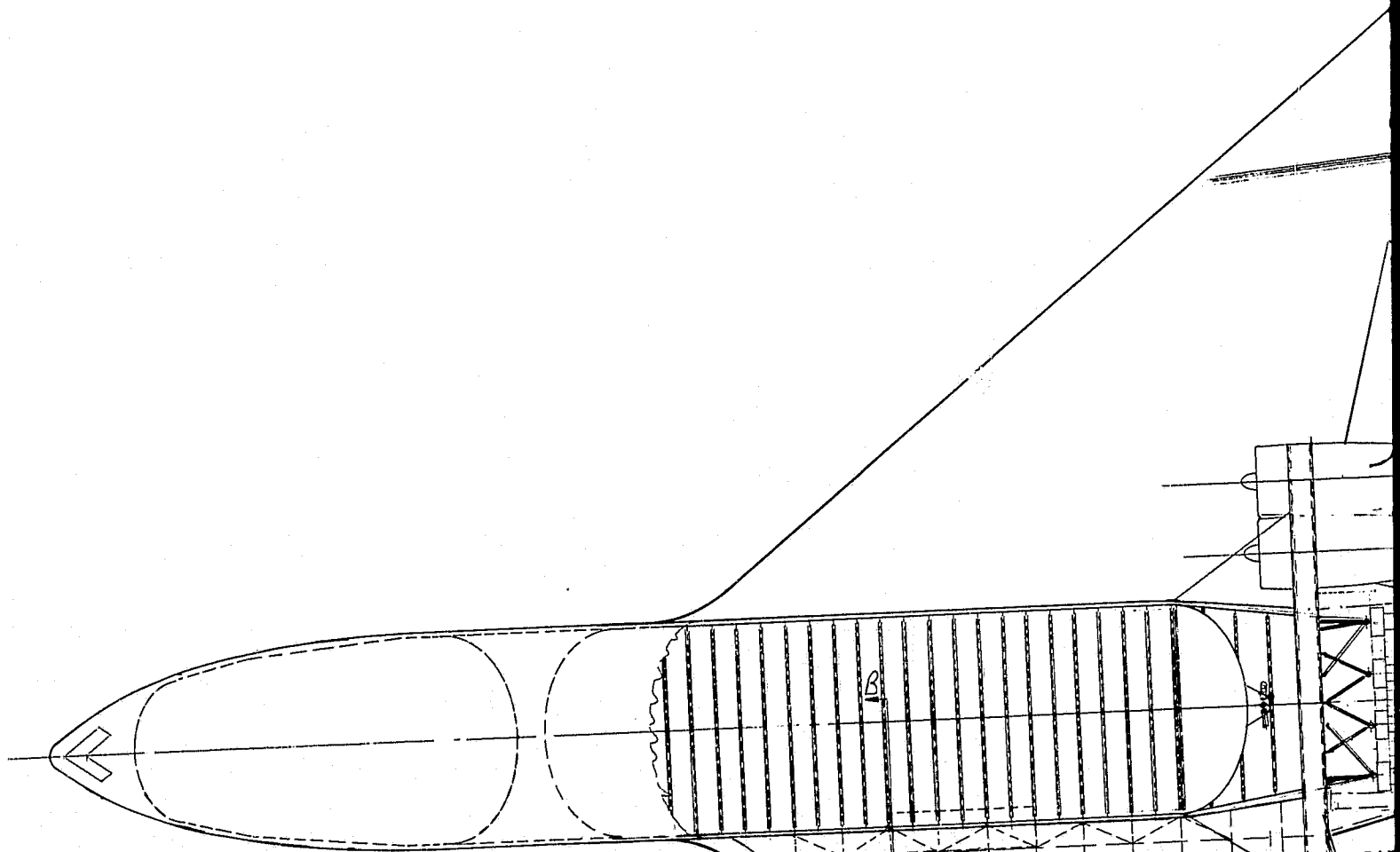
NOTES

QTY RECD	CODE IDENT	PART OR IDENTIFYING NO.	NOMENCLATURE OR DESCRIPTION	MATERIAL DESCRIPTION OR NOTE	MATERIAL SPECIFICATION	ZON	ITEM NO.
PARTS LIST							
INTERPRET DWG PER			UNLESS OTHERWISE SPECIFIED DIM. ARE IN INCHES. TOLERANCES ON: FRACTIONS = ± 1/16. DECIMALS: .X = ± .1 .XX = ± .03 .XXX = ± .010 ANGLES = ± 2 DEG		DATE Oct 14 1969 DR #2 Schmidt		LOCKHEED MISSILES & SPACE COMPANY A GROUP DIVISION OF LOCKHEED AIRCRAFT CORPORATION SUNNYVALE, CALIFORNIA
NEXT ASSY USED ON APPLICATION			CONTR CCA/CEI		APPD ENGRG CHK APPD		SIZE CODE IDENT DRAWING NO. REV J SKS 101169 1
					SCALE 1/120		SHEET 1 of 1

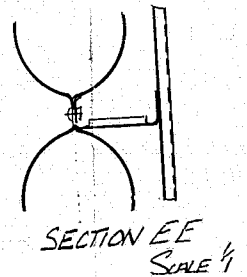
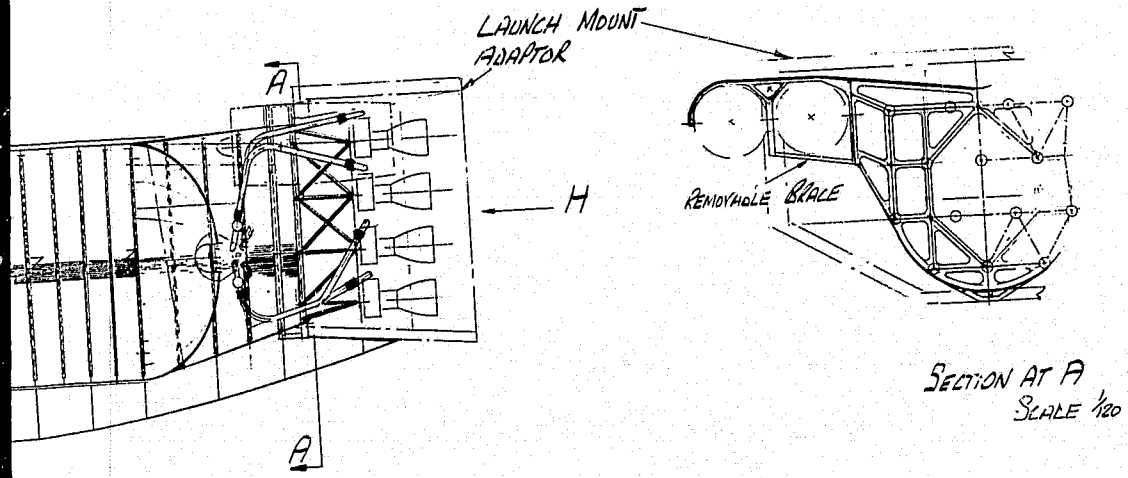
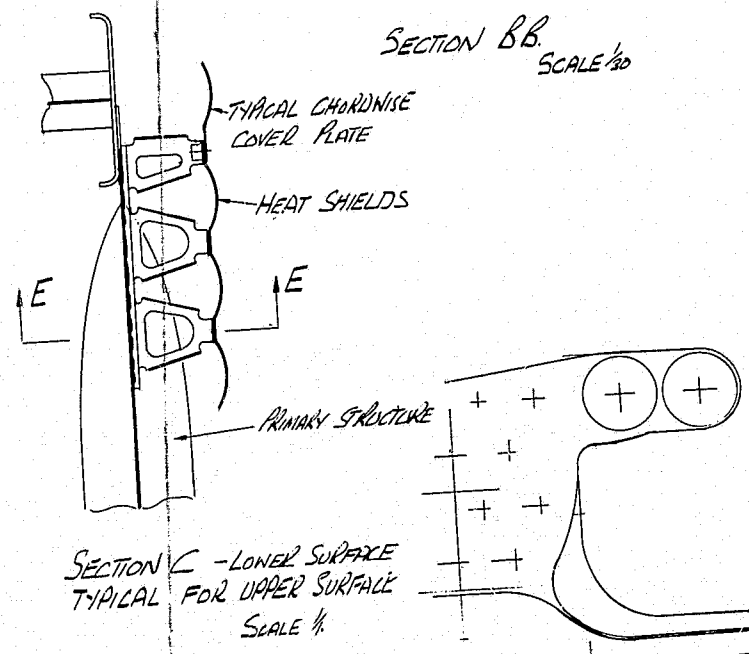
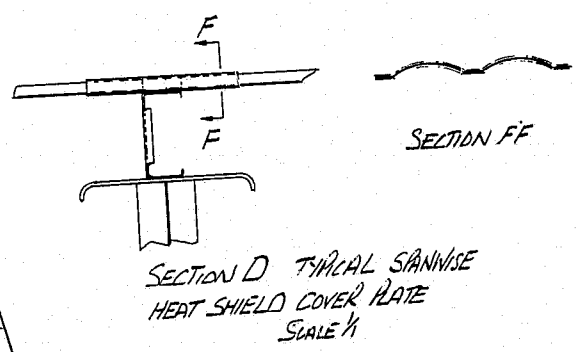
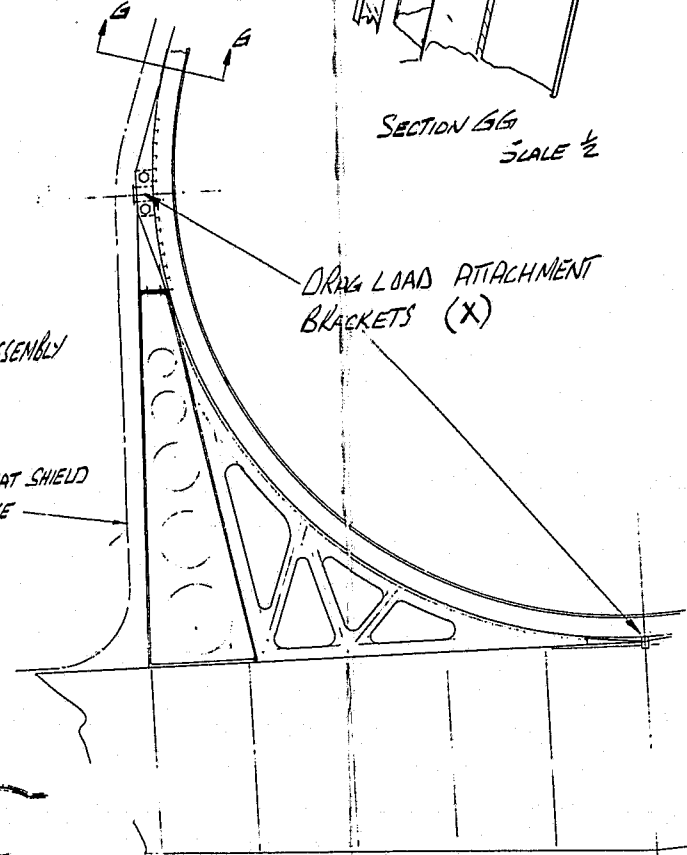
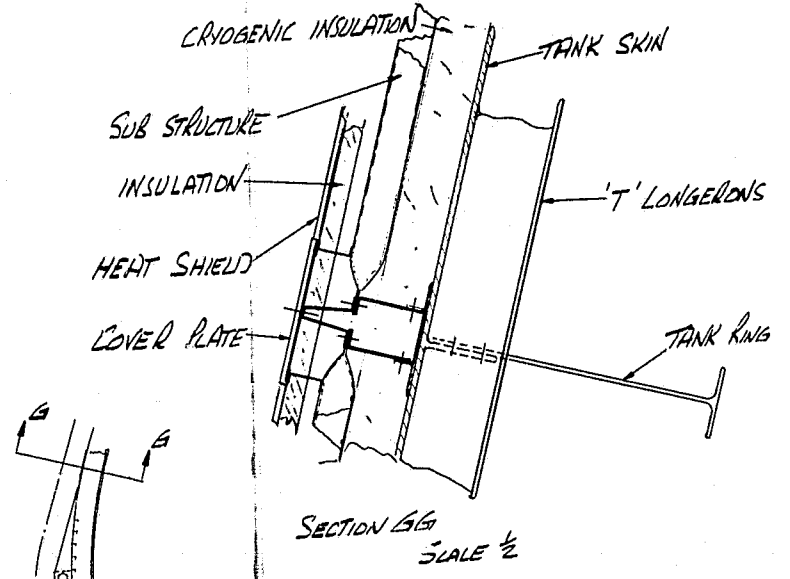
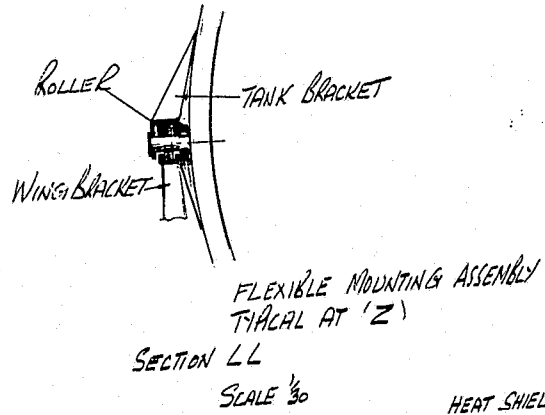
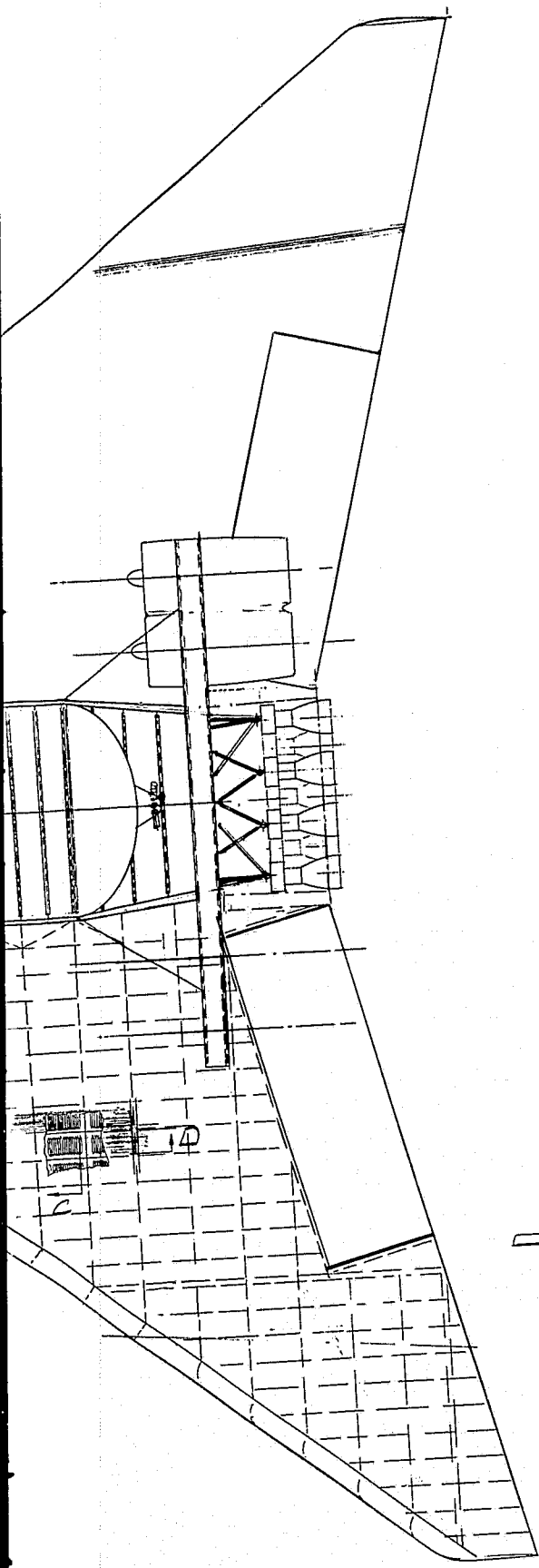
BOOSTER  
2 STAGE SYSTEM - 50K P/L  
INBOARD PROFILE

A-3

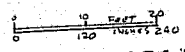
FOLDOUT FRAME ?



FOLDOUT FRAME

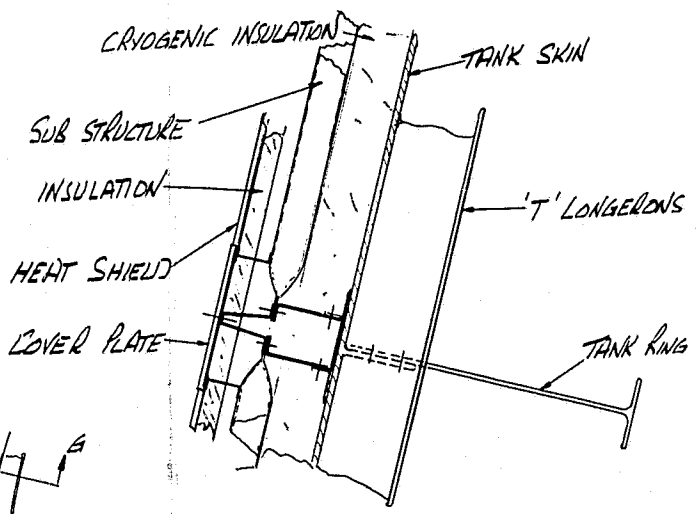


FOLDOUT FRAME 2

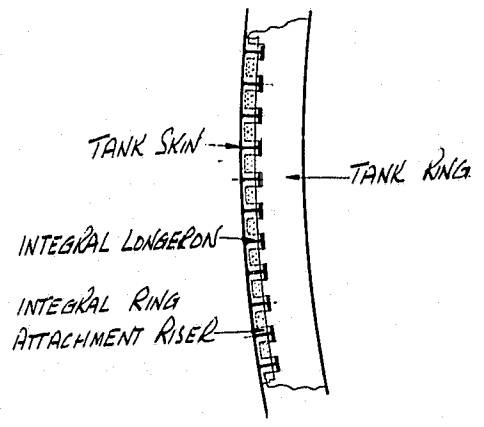


FOLDOUT

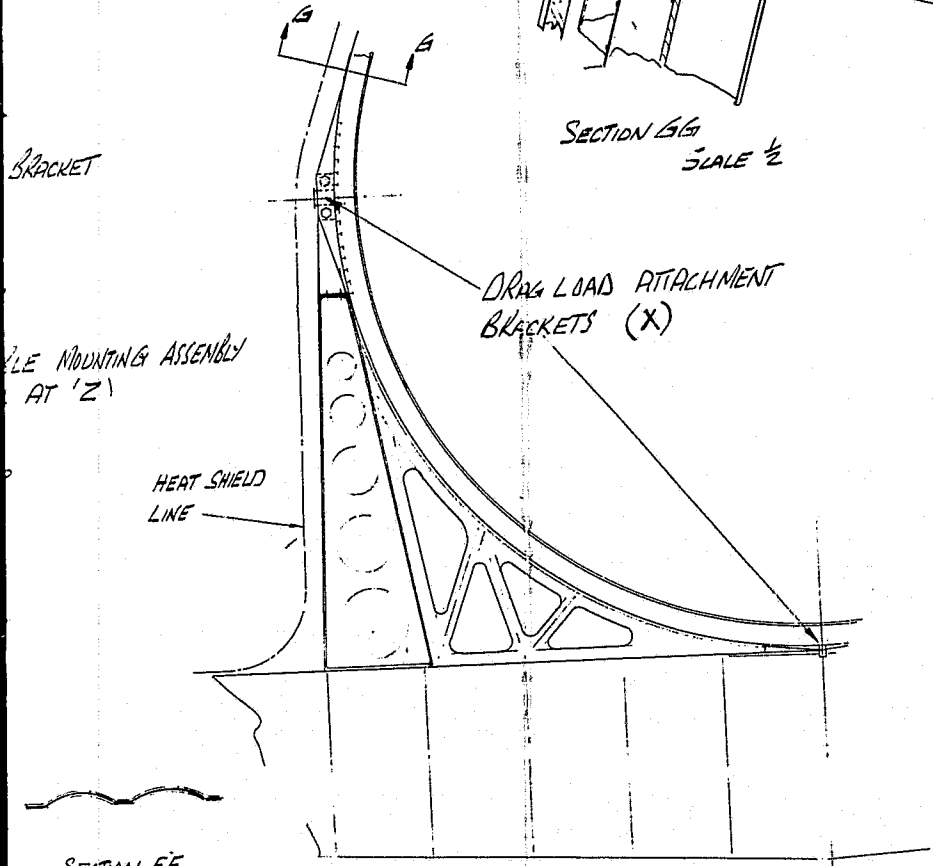




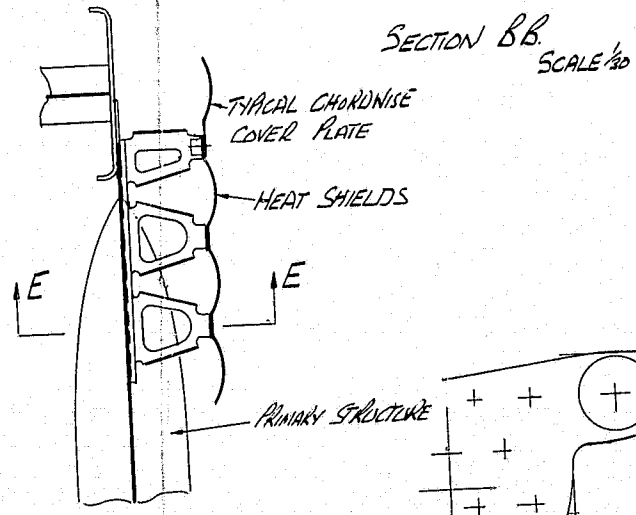
SECTION GG  
SCALE 1/2



SECTION MM  
SCALE 1/10  
TANK CONSTRUCTION

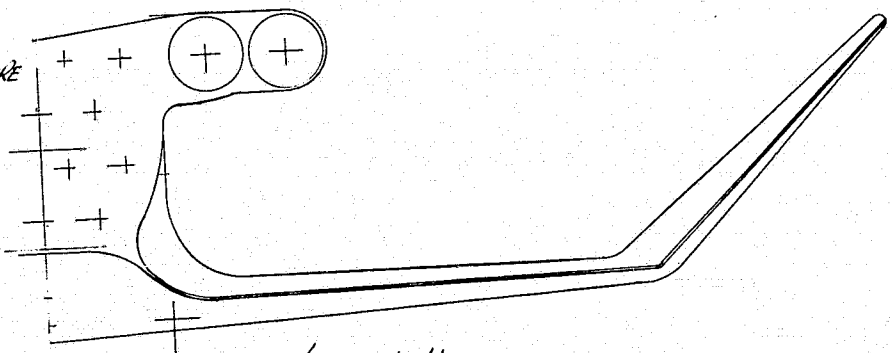


SECTION FF



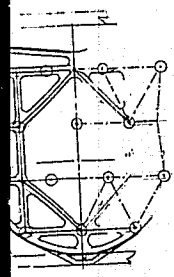
SECTION BB  
SCALE 1/20

SECTION C - LOWER SURFACE  
TYPICAL FOR UPPER SURFACE  
SCALE 1/4

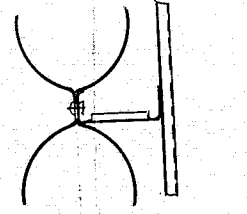


VIEW ON H

SPANWISE PLATE

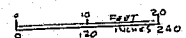


SECTION AT A  
SCALE 1/20



SECTION EE  
SCALE 1/4

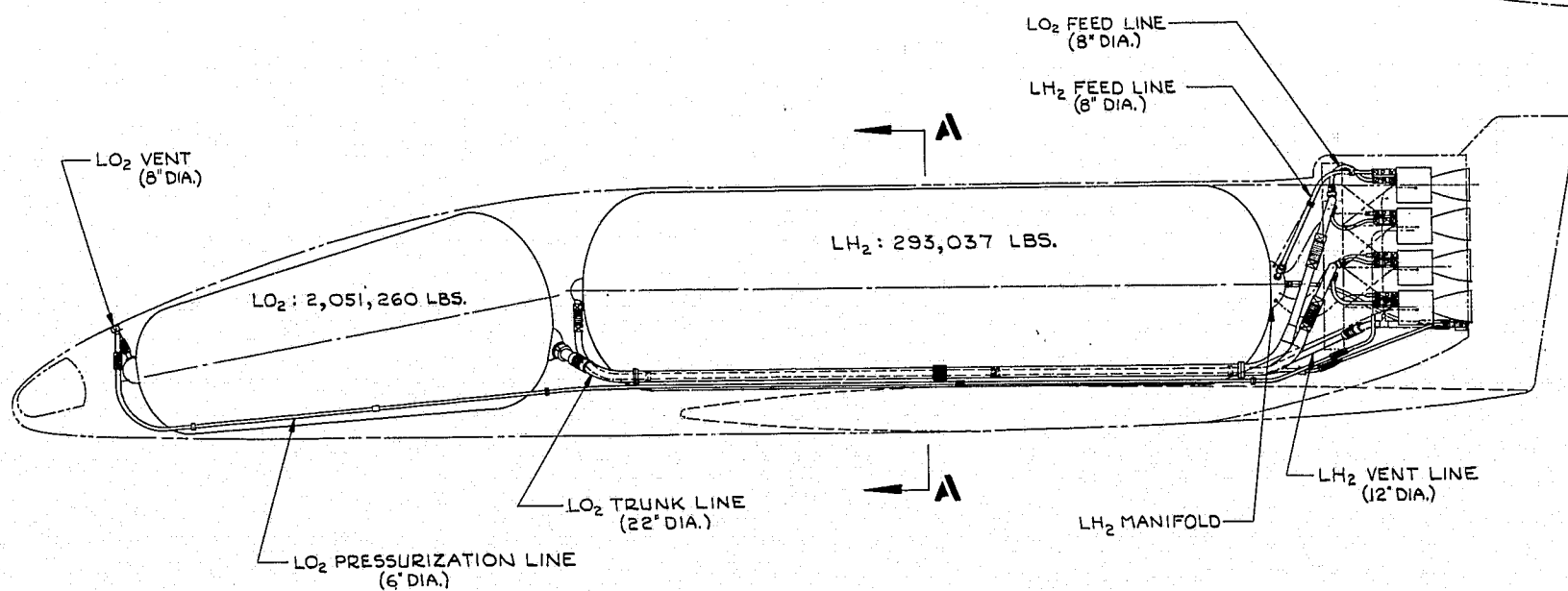
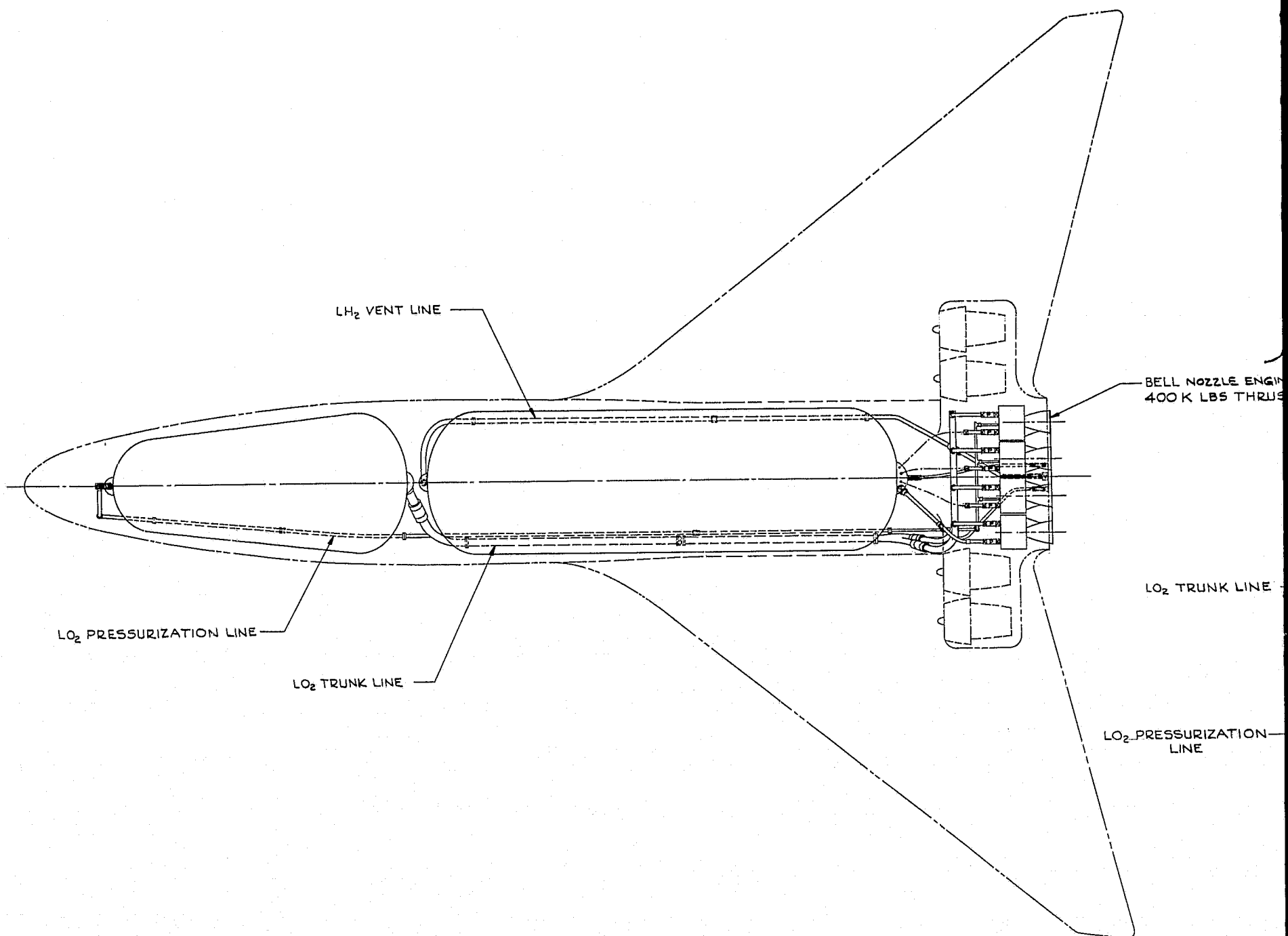
2



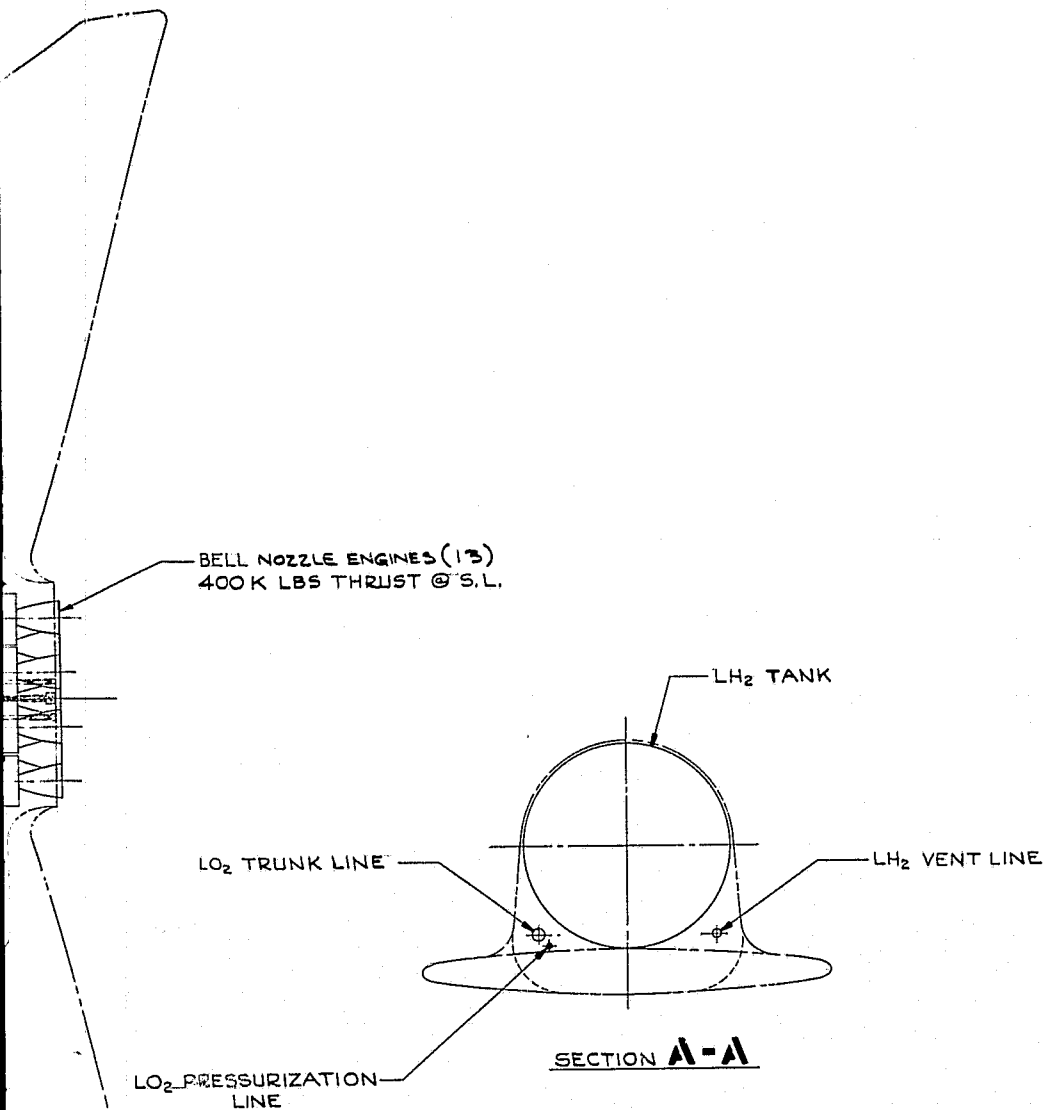
FOLDOUT FRAME

DATE	OCT 2 69	LOCKHEED MISSILES & SPACE COMPANY		
DR	BEVAN	A GROUP DIVISION OF LOCKHEED AIRCRAFT CORPORATION		
APPD		SUNNYVALE, CALIFORNIA		
APPD		STRUCTURE - BOOSTER		
ENGRG		TWO STAGE SYSTEM		
CHK		SIZE	CODE IDENT	DRAWING NO.
APPD				SKX 100269
APPD		SCALE	NOTED	SHEET

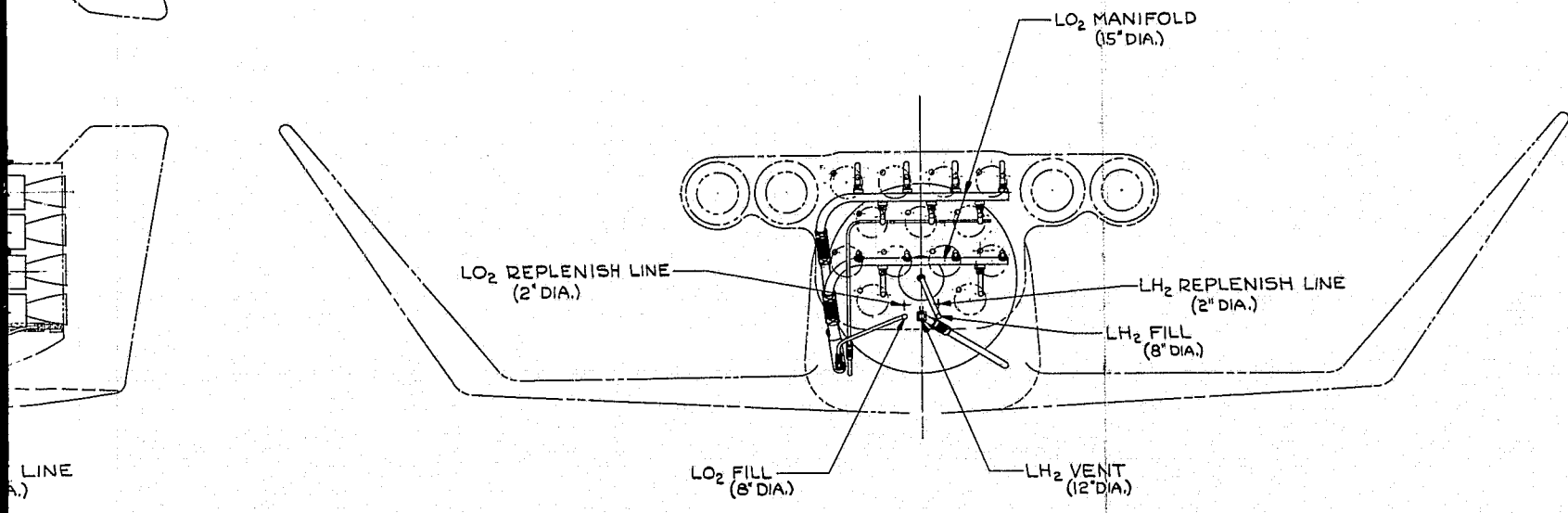
A-4



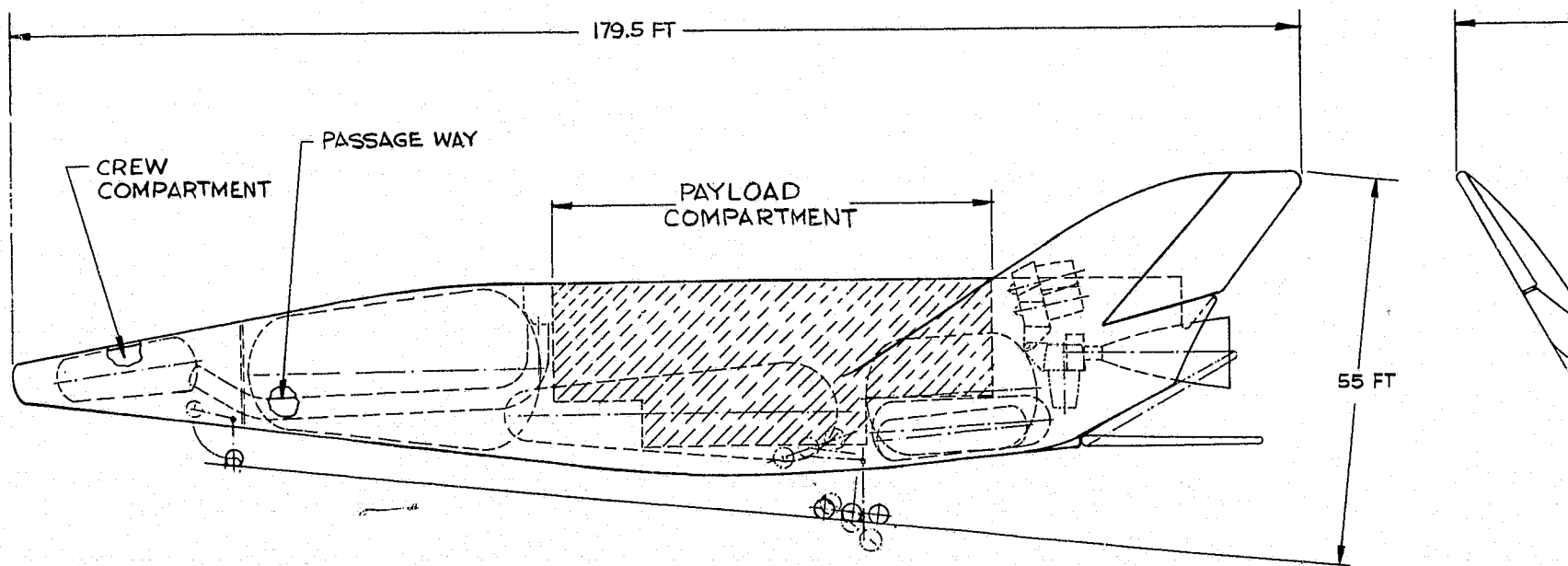
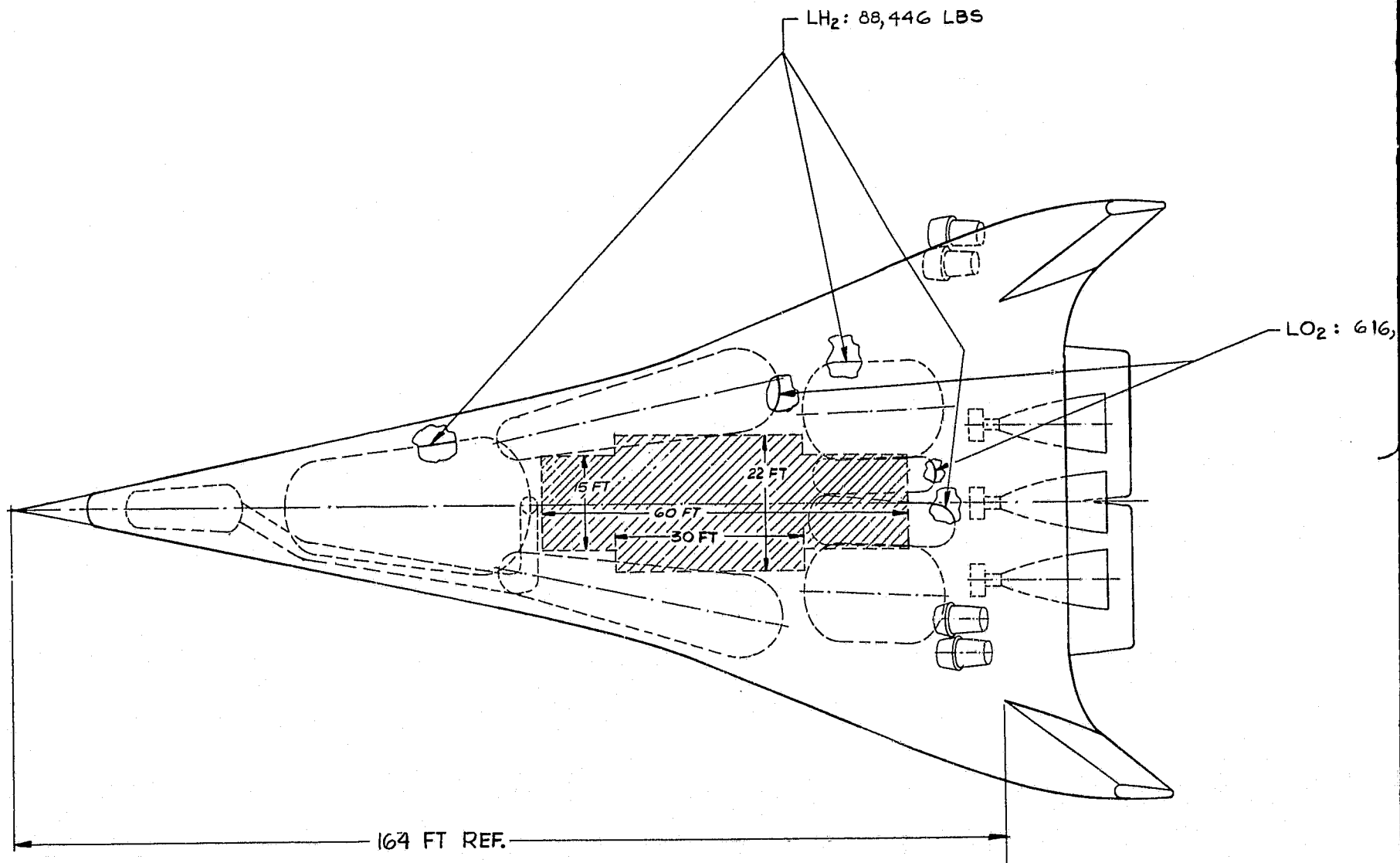
**FOLDOUT FRAME** /



- SYMBOLS
- ☒ GIMBAL JOINT
  - ▨ SLIDING OR EXPANSION JOINT
  - ∇ VALVE
  - P PRESSURE, VOLUME COMPENSATING JOINT
  - ▤ MECHANICAL JOINT

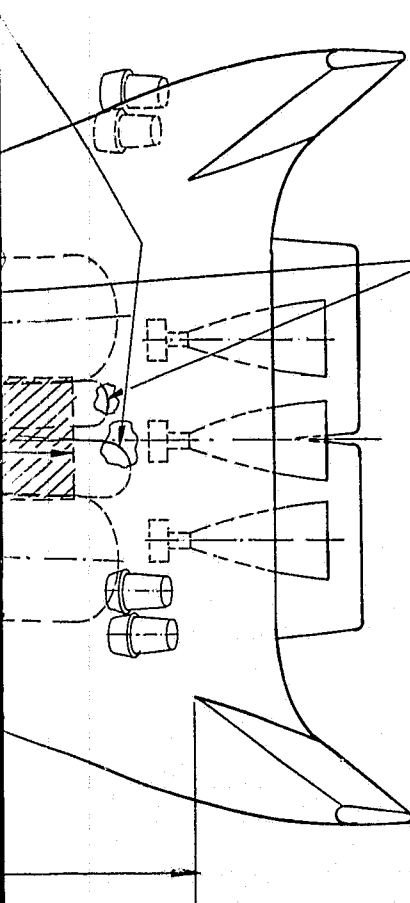


DATE	15 OCT. 1968	LOCKHEED MISSILES & SPACE COMPANY	
DR	D.B. SMITH	A GROUP DIVISION OF LOCKHEED AIRCRAFT CORPORATION	
		SUNNYVALE, CALIFORNIA	
APPD		BOOSTER -	
ENGRG		2-STAGE SYSTEM	
CHK		MAIN PROPELLANT LINES	
APPD	SIZE	CODE IDENT	DRAWING NO.
APPD			SKD101569
	SCALE 1/120		SHEET

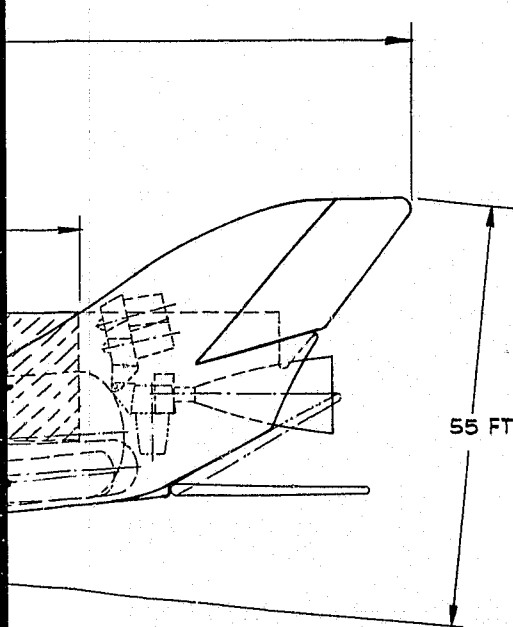


FOLDOUT FRAME /

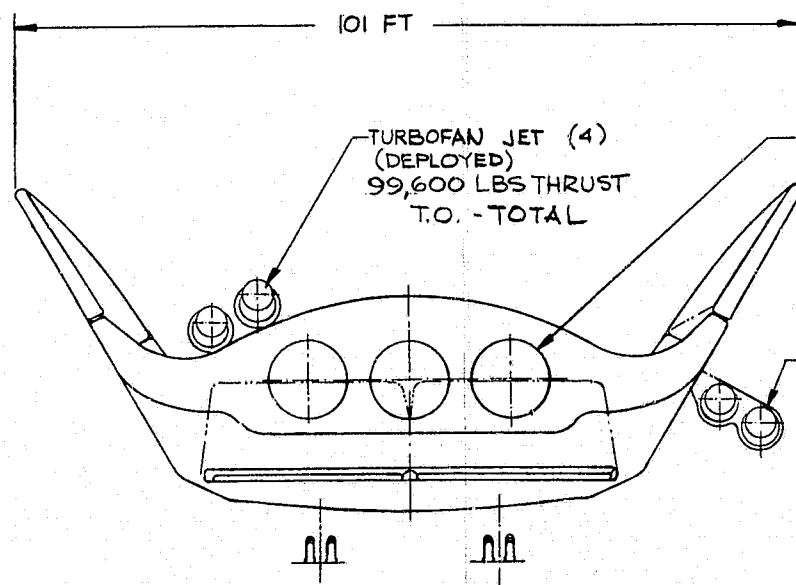
88,446 LBS



LO<sub>2</sub> : 616,592 LBS



55 FT



101 FT

TURBOFAN JET (4)  
(DEPLOYED)  
99,600 LBS THRUST  
T.O. - TOTAL

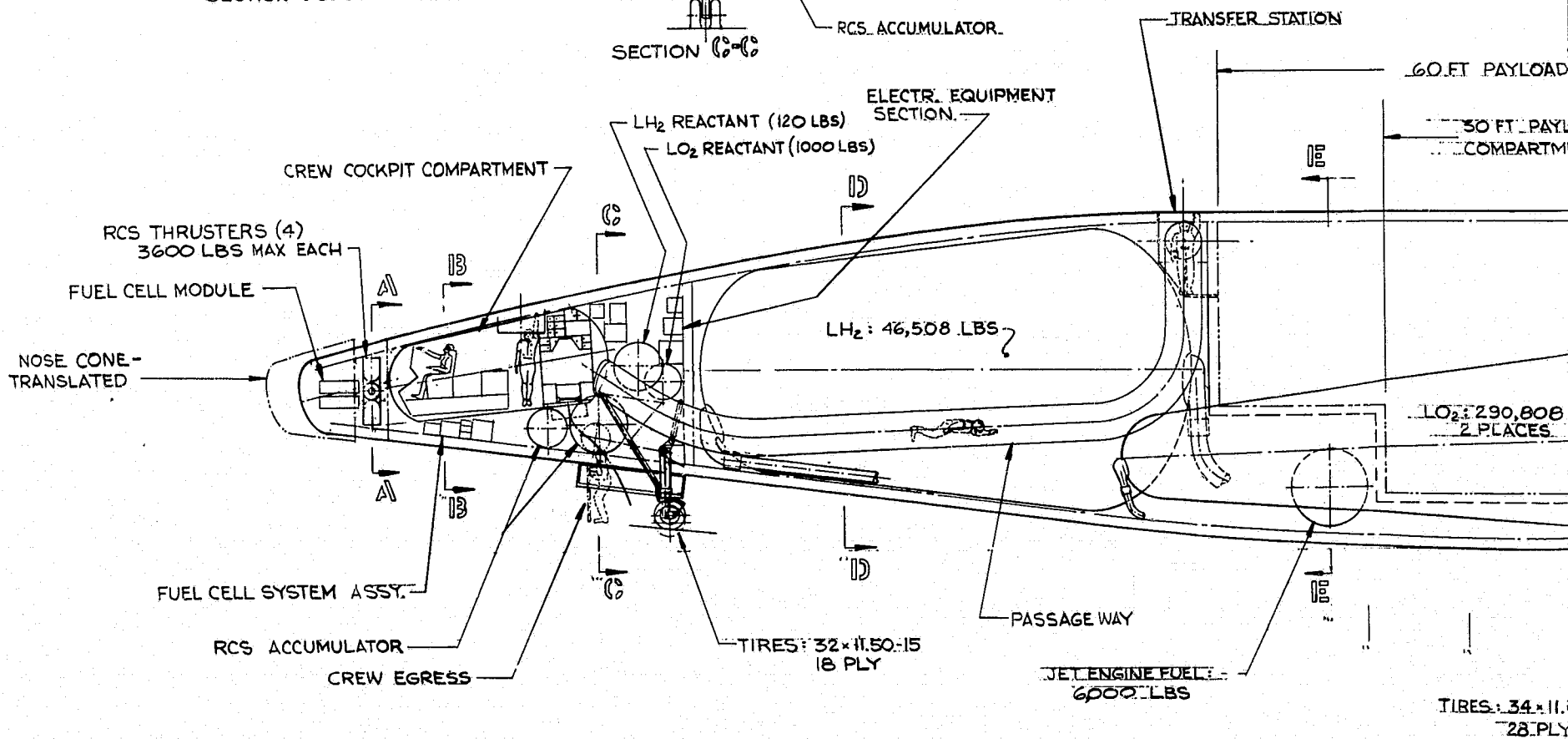
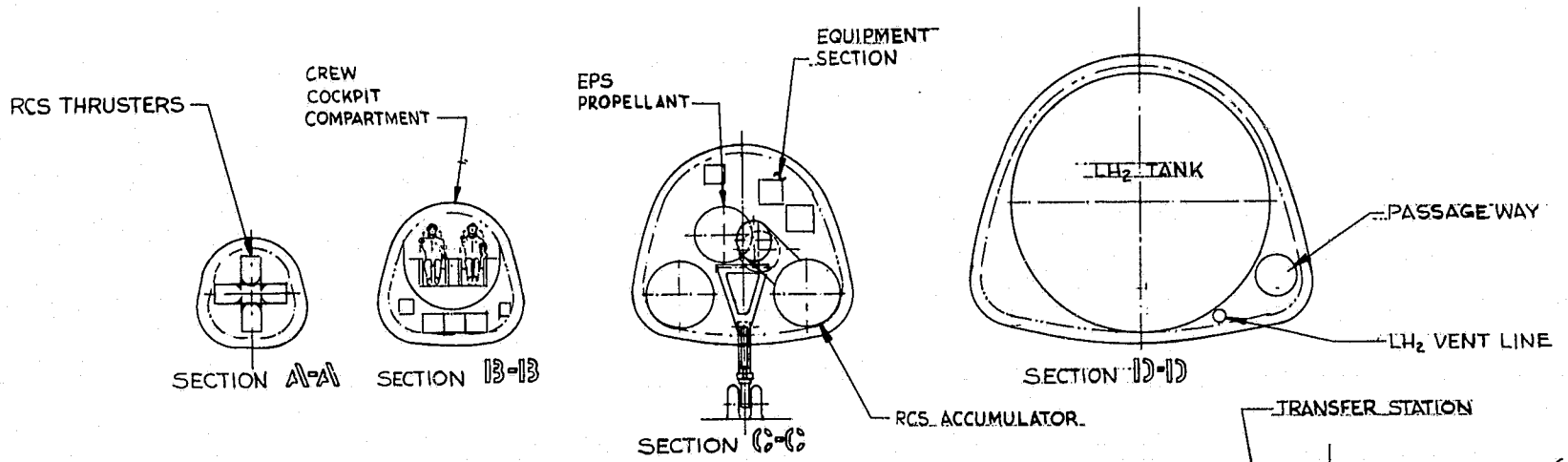
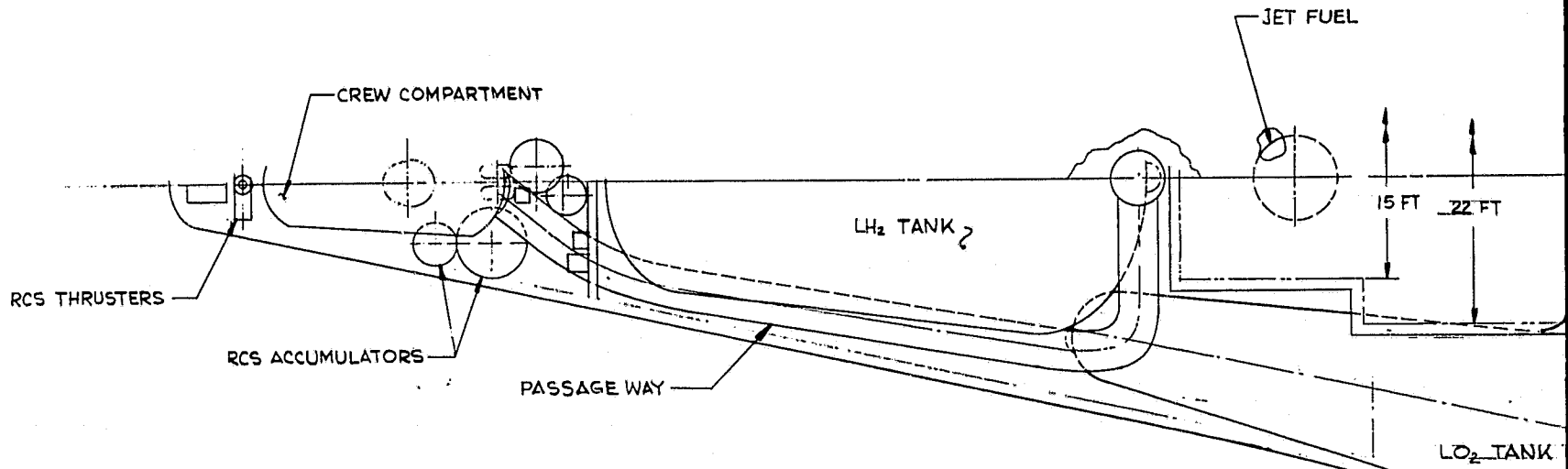
BELL NOZZLE ENGINES (3)  
400 K LBS THRUST EACH @ S.L.

TURBOFAN JET - ALTERNATE  
POSITION (DEPLOYED)

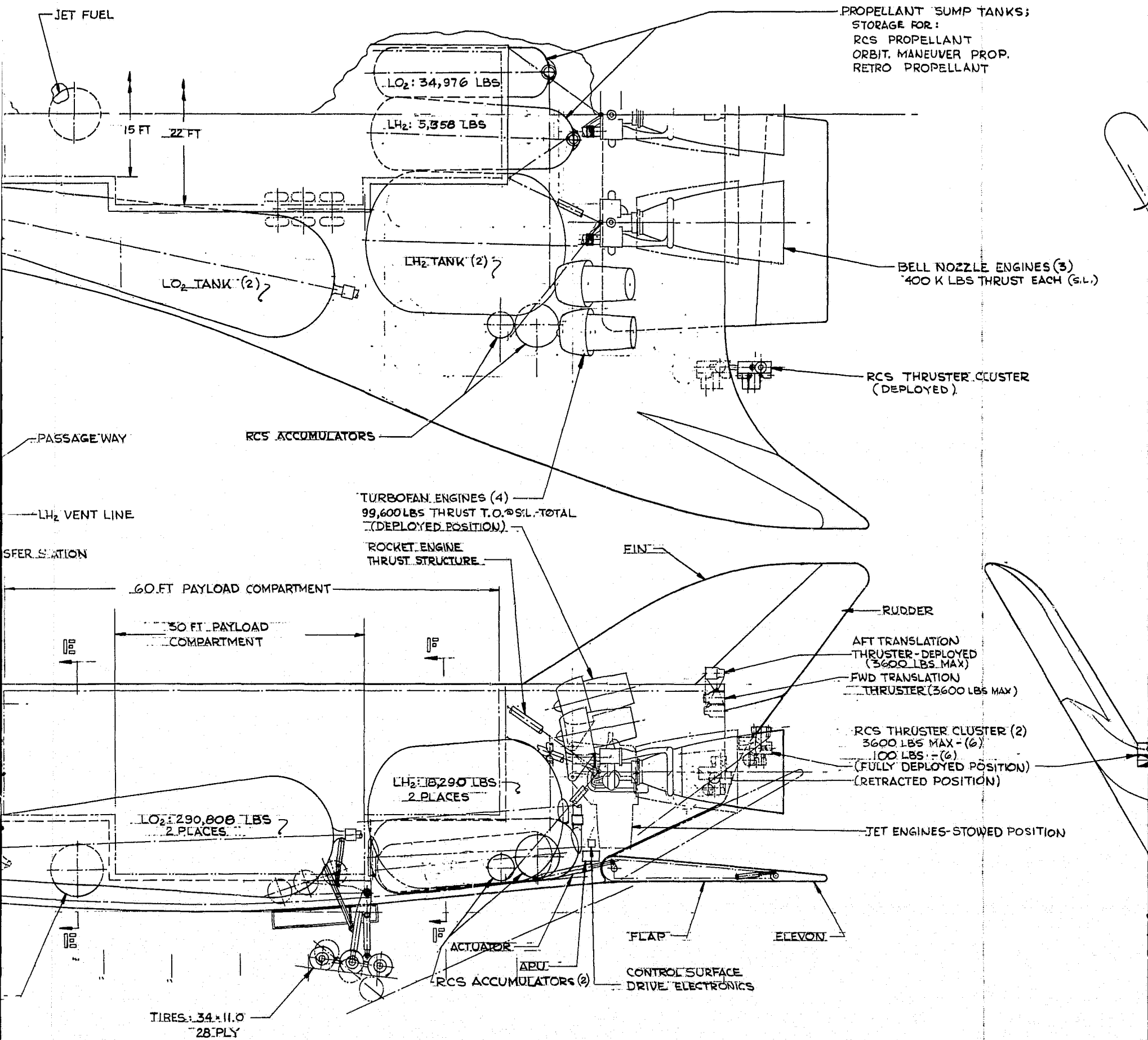
DATE Oct 9, 1965	LOCKHEED MISSILES & SPACE COMPANY		
DR H. Schmidt	A GROUP DIVISION OF LOCKHEED AIRCRAFT CORPORATION		
APPD	SUNNYVALE, CALIFORNIA		
APPD	ORBITER		
ENGRG	2 STAGE SYSTEM - 50 K P/L		
CHK	GENERAL ARRANGEMENT		
APPD	SIZE	CODE IDENT	DRAWING NO. REV
APPD			-SKS 100769 -
	SCALE 1/120		SHEET 1 OF 1

A-6

FOLDOUT FRAME

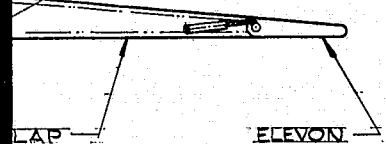
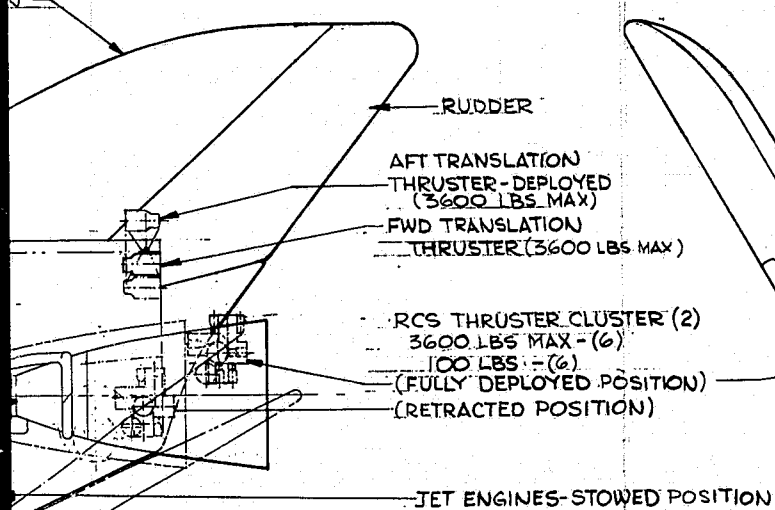
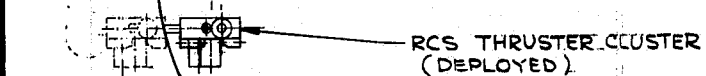
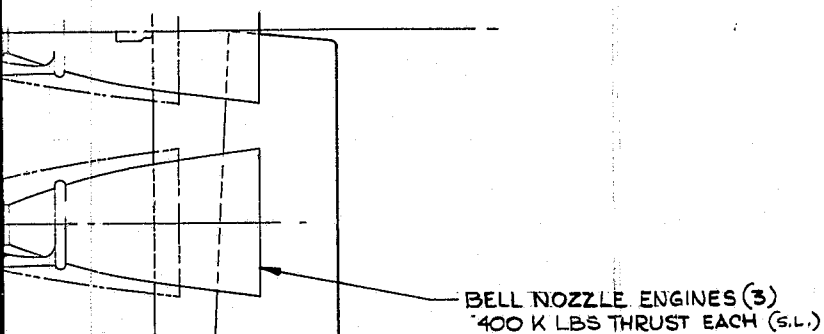


FOLDOUT FRAME 1

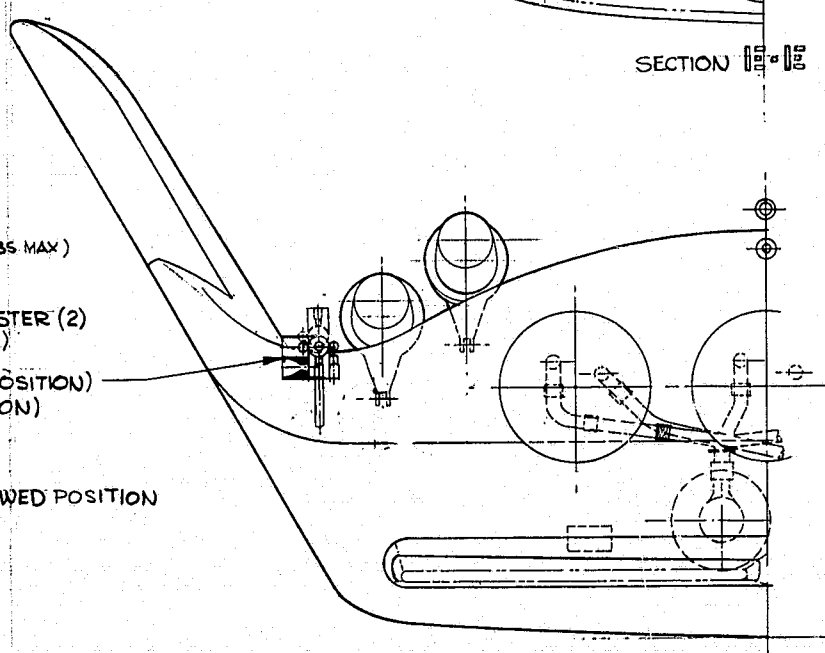
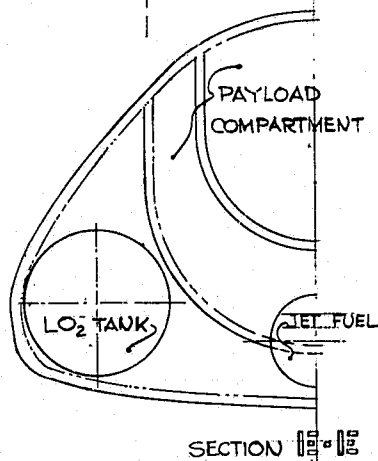
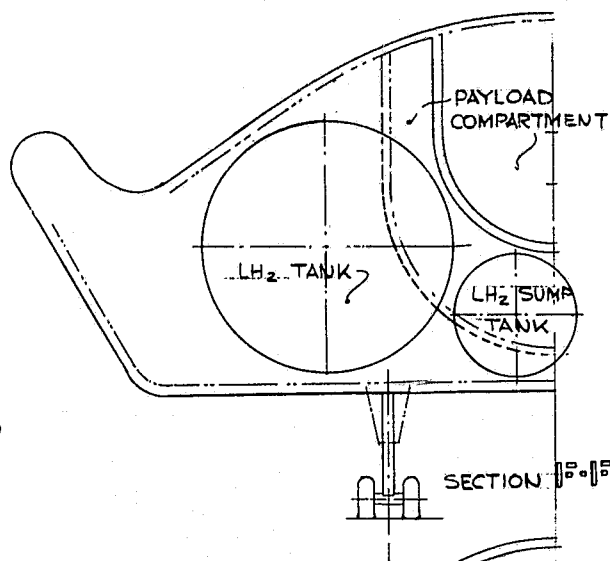


FOLDOUT FRAME 2

PROPELLANT SUMP TANKS;  
STORAGE FOR:  
RCS PROPELLANT  
ORBIT. MANEUVER PROP.  
RETRO PROPELLANT



CONTROL SURFACE  
DRIVE ELECTRONICS



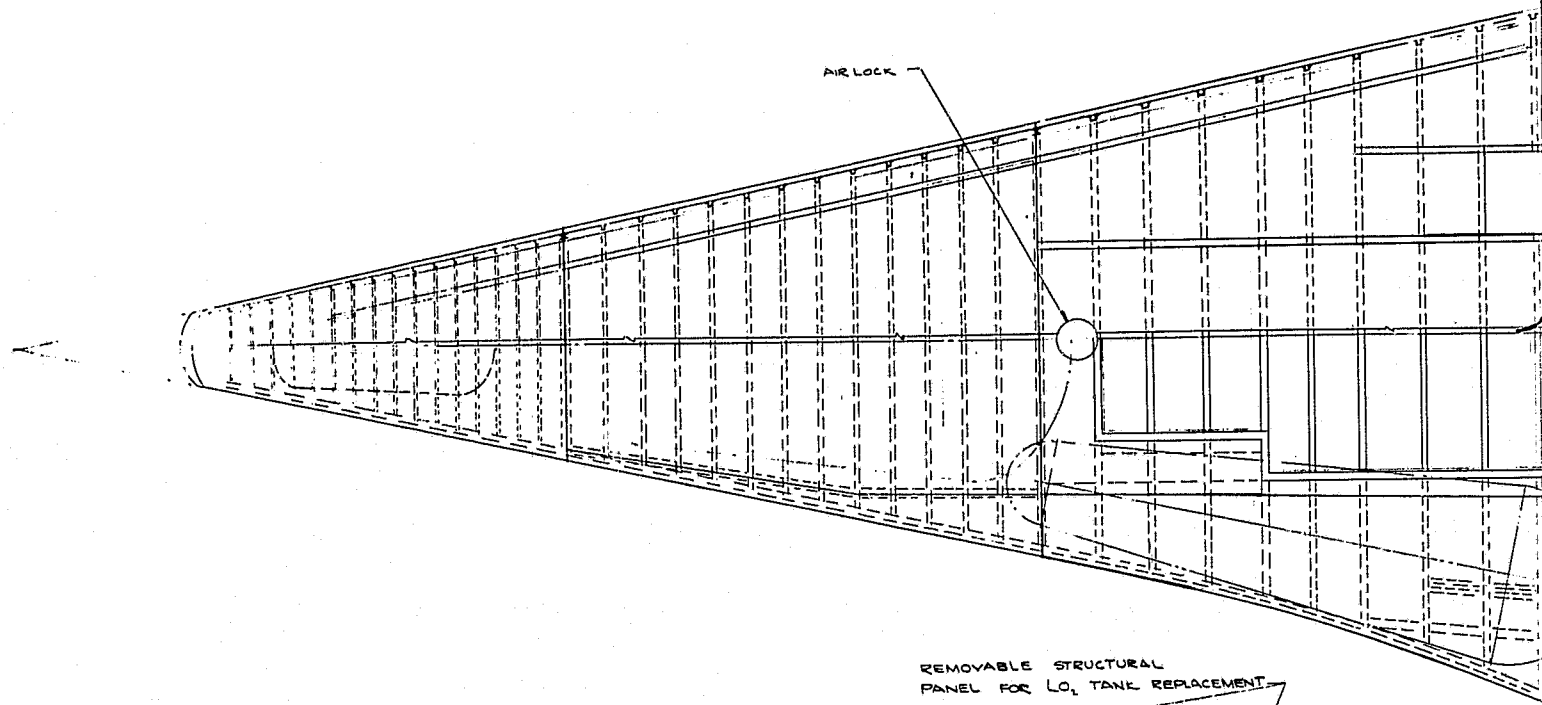
DATE	Oct 9, 1969	LOCKHEED MISSILES & SPACE COMPANY	
DR	H. Schmitt	A GROUP DIVISION OF LOCKHEED AIRCRAFT CORPORATION	
		SUNNYVALE, CALIFORNIA	
APPD		ORBITER	
ENGRG		2-STAGE SYSTEM, 50K P/L	
CHK		~ INBOARD PROFILE ~	
APPD		SIZE CODE IDENT	DRAWING NO.
APPD		SCALE 1/50	SKS 100869
			REV
			SHEET 1 OF 1

A-7

FOLDOUT FRAME 2

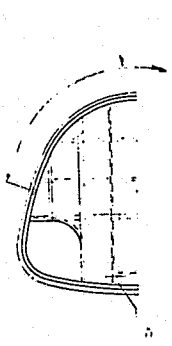
FOLDOUT FRAME 3



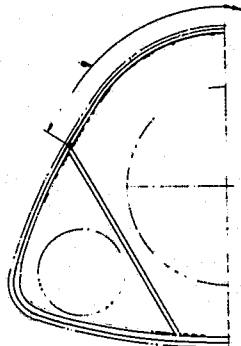


REMOVABLE STRUCTURAL  
PANEL FOR  $LH_2$  TANK  
REPLACEMENT

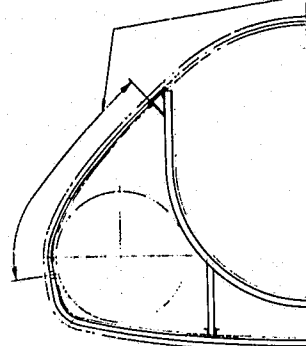
REMOVABLE STRUCTURAL  
PANEL FOR  $LO_2$  TANK REPLACEMENT



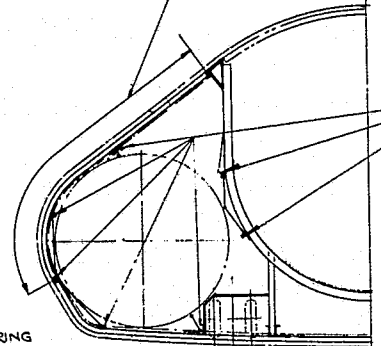
SECT A-A



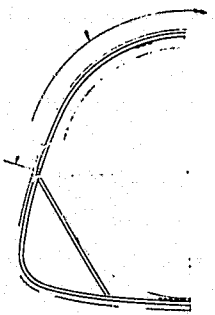
SECT C-C



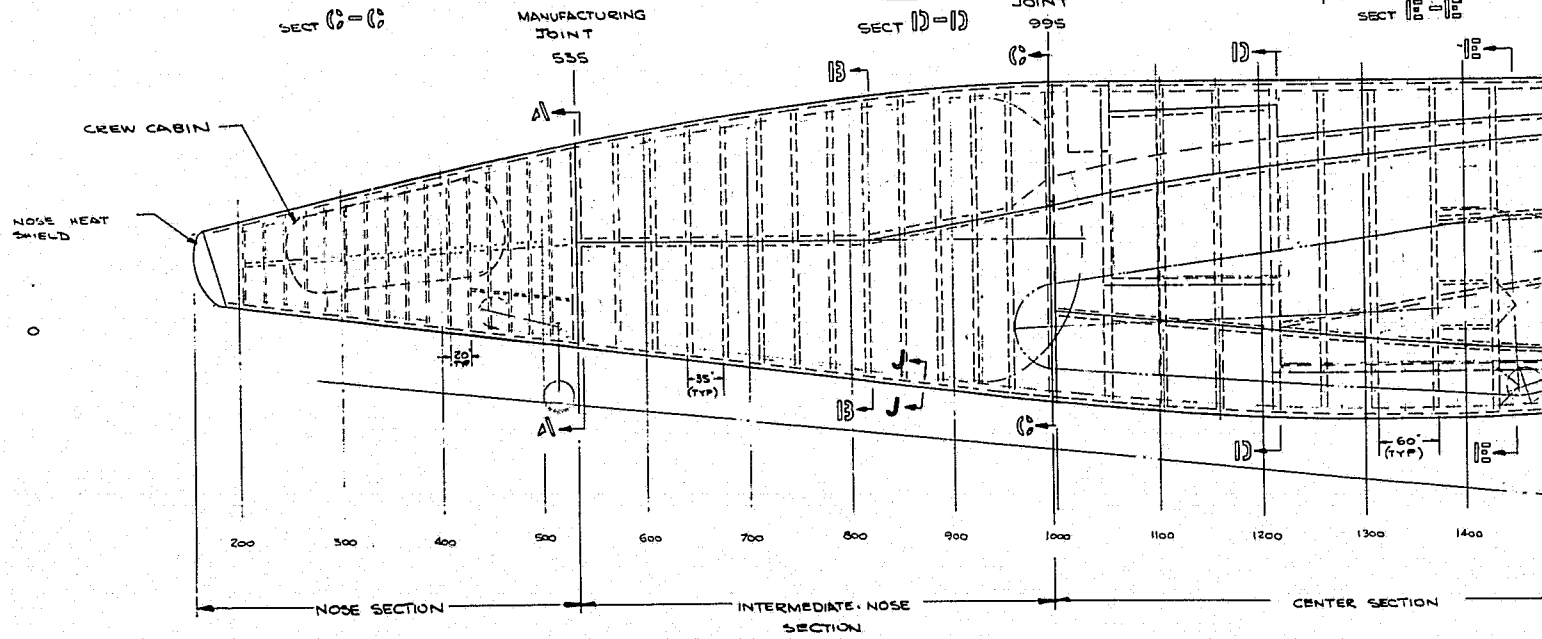
SECT D-D



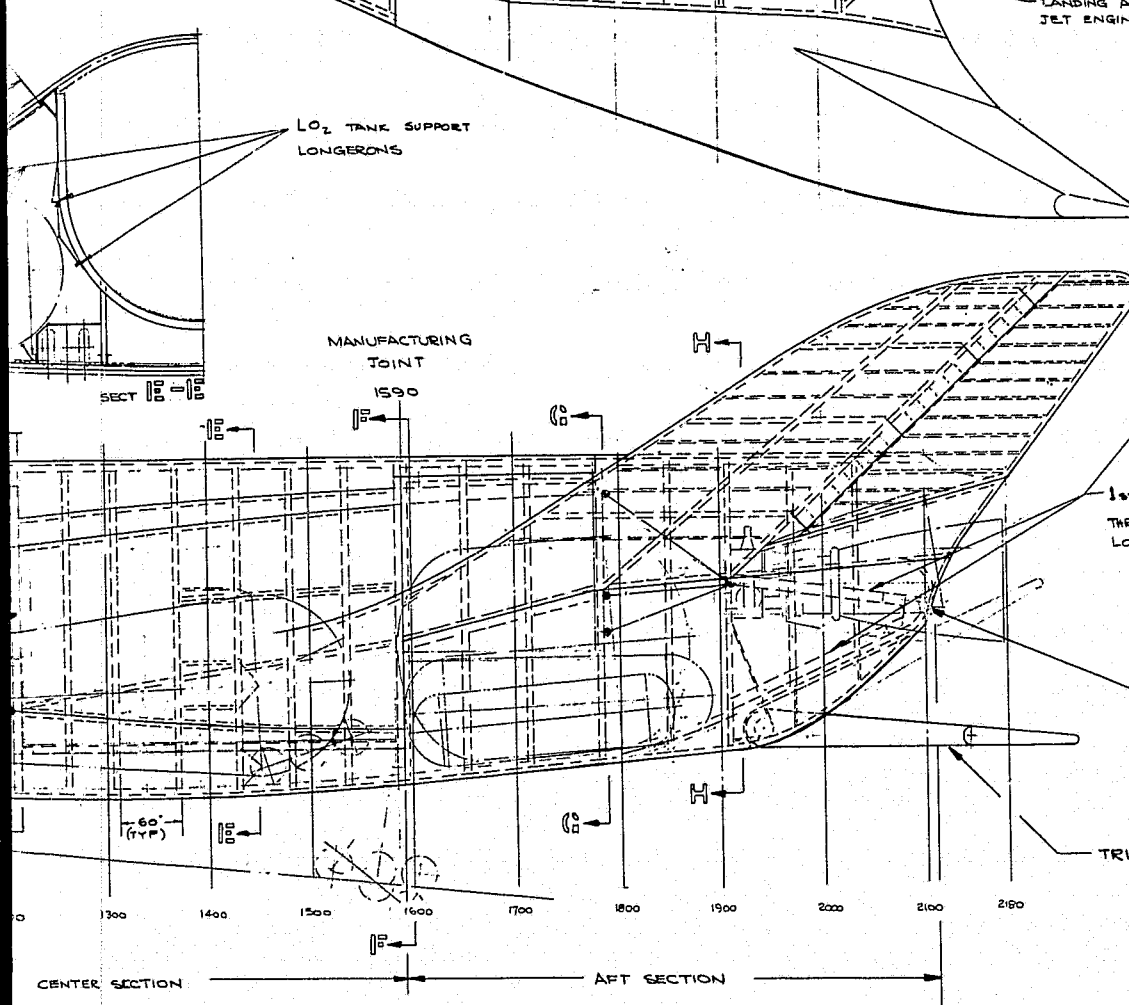
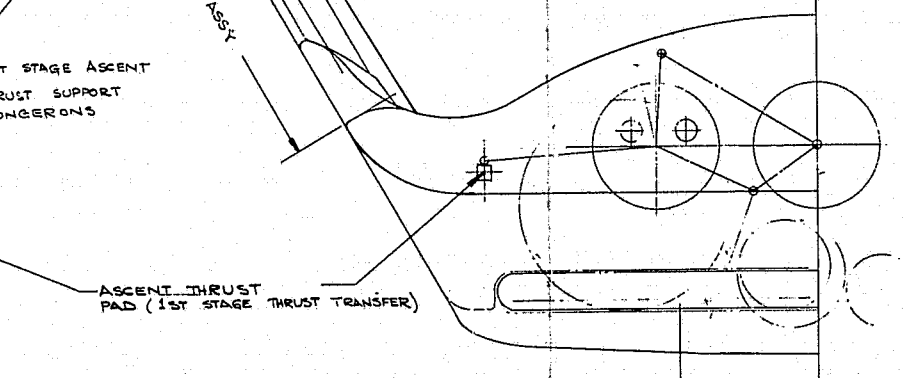
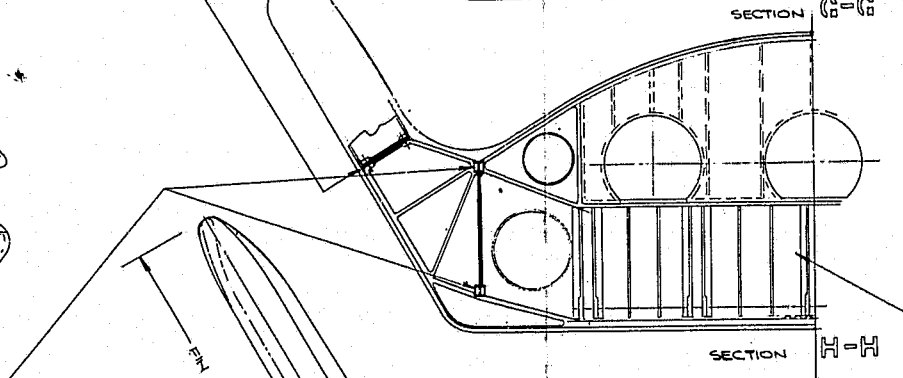
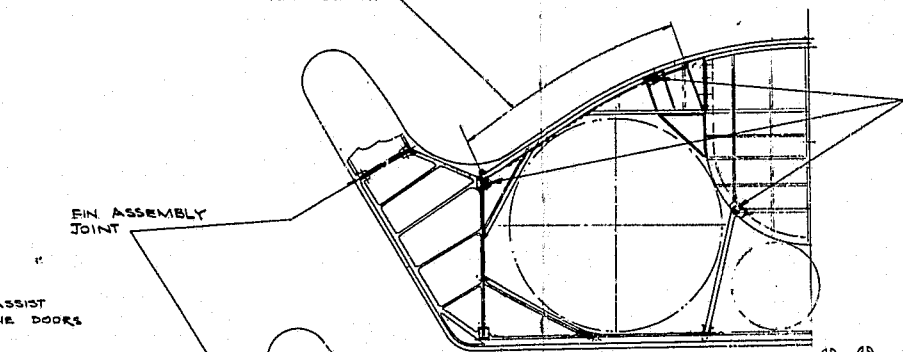
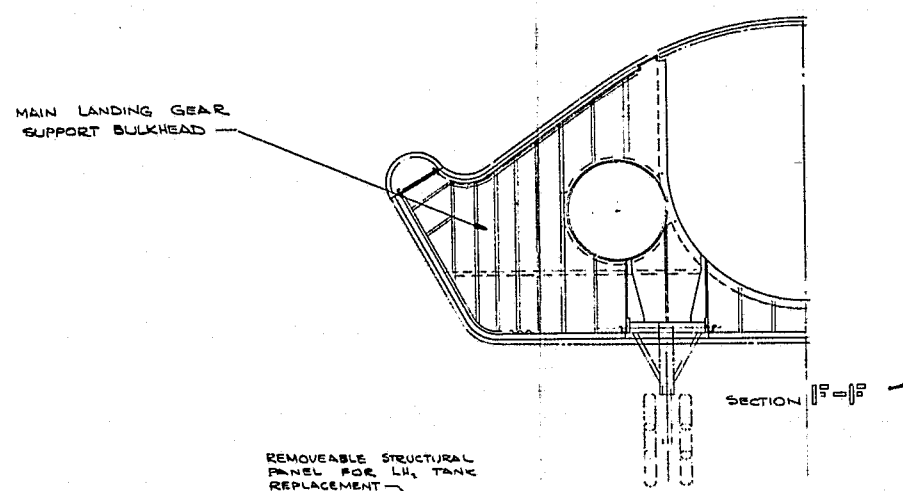
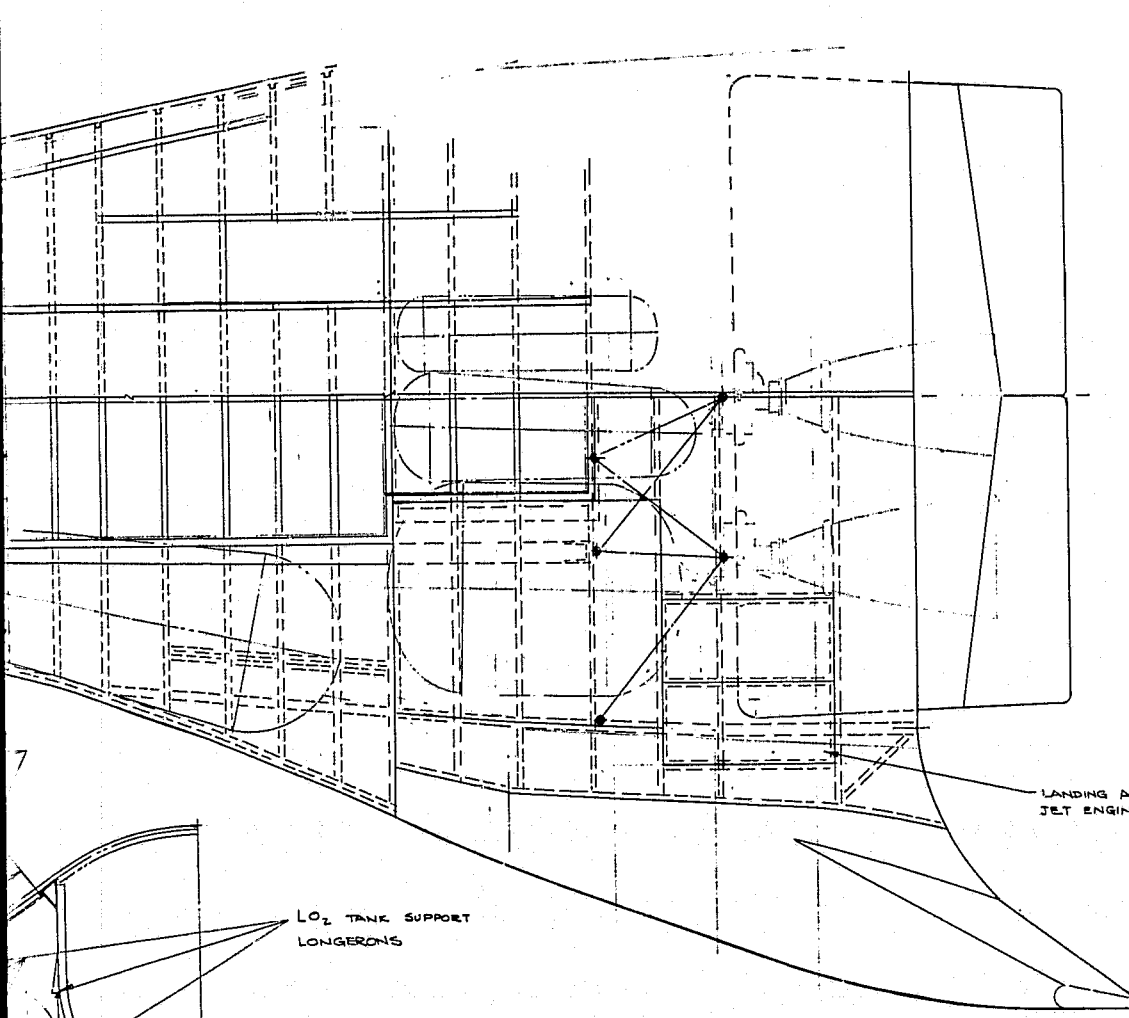
SECT E-E

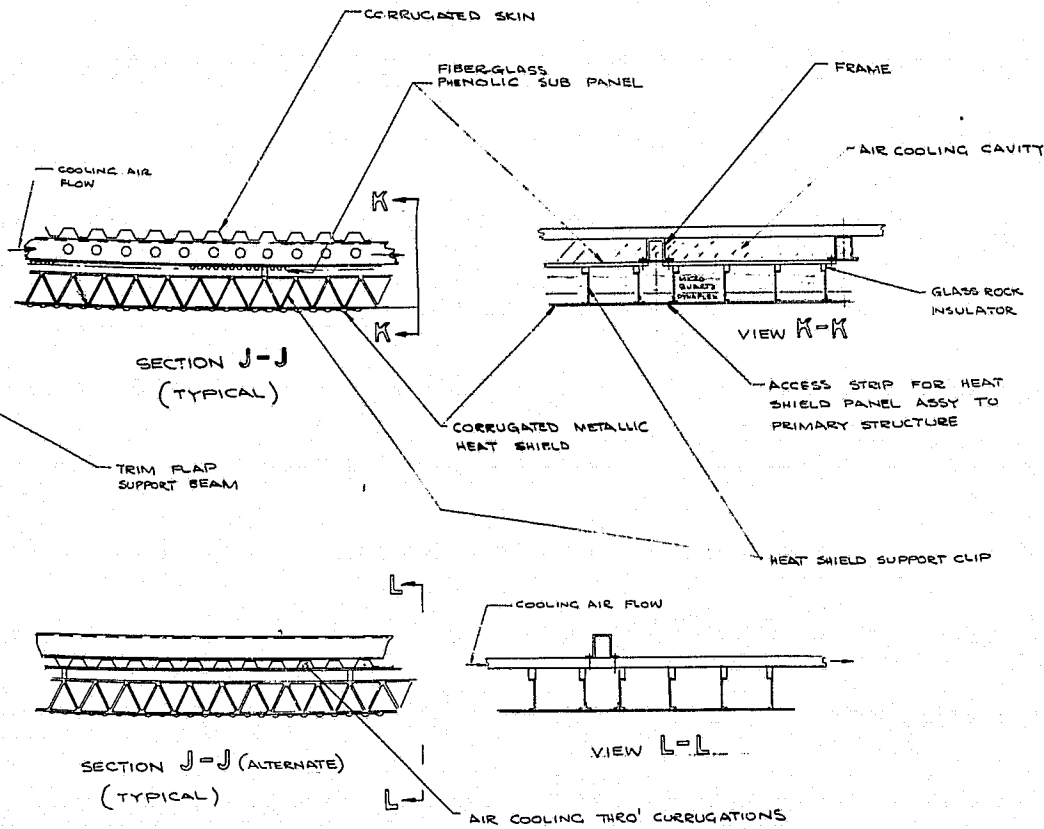
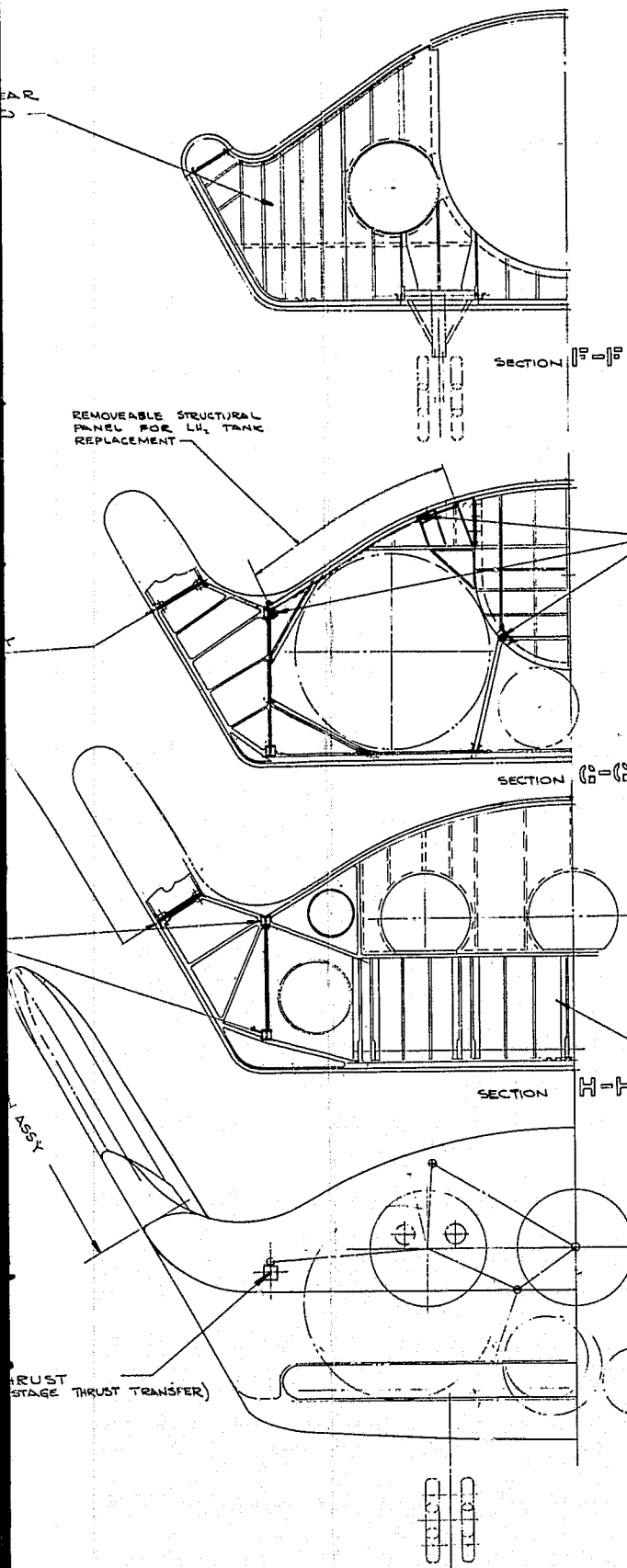


SECT B-B



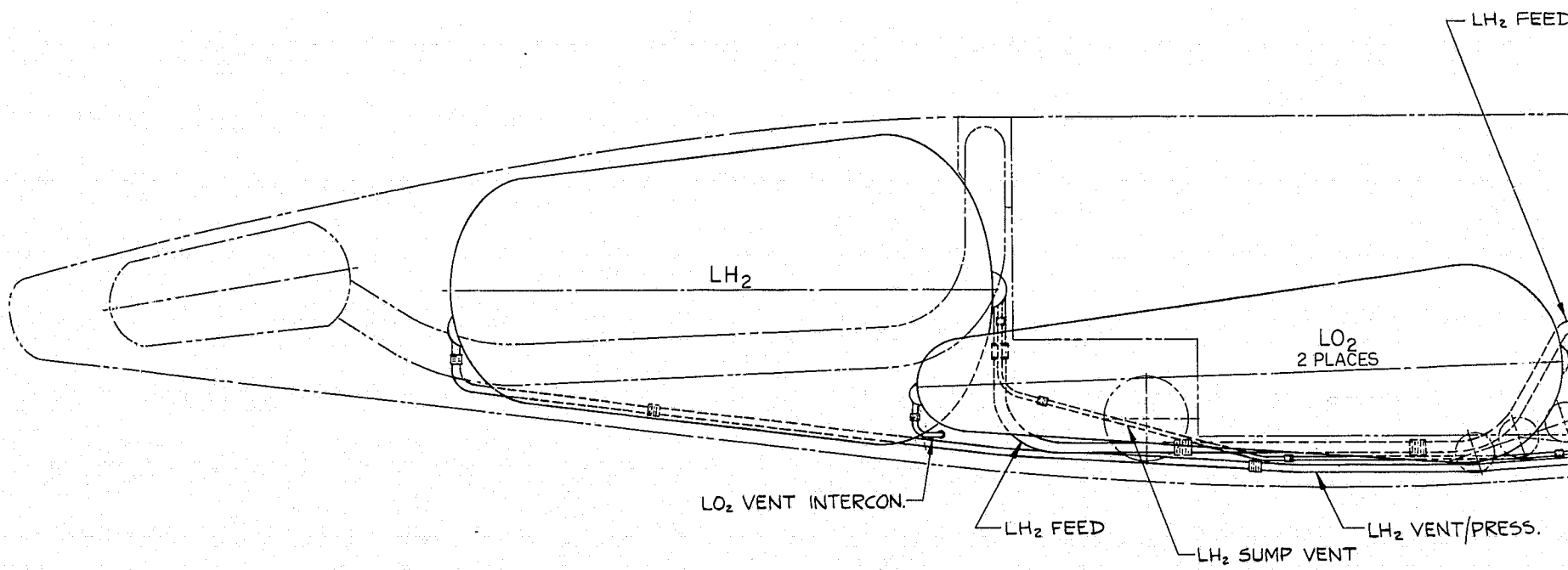
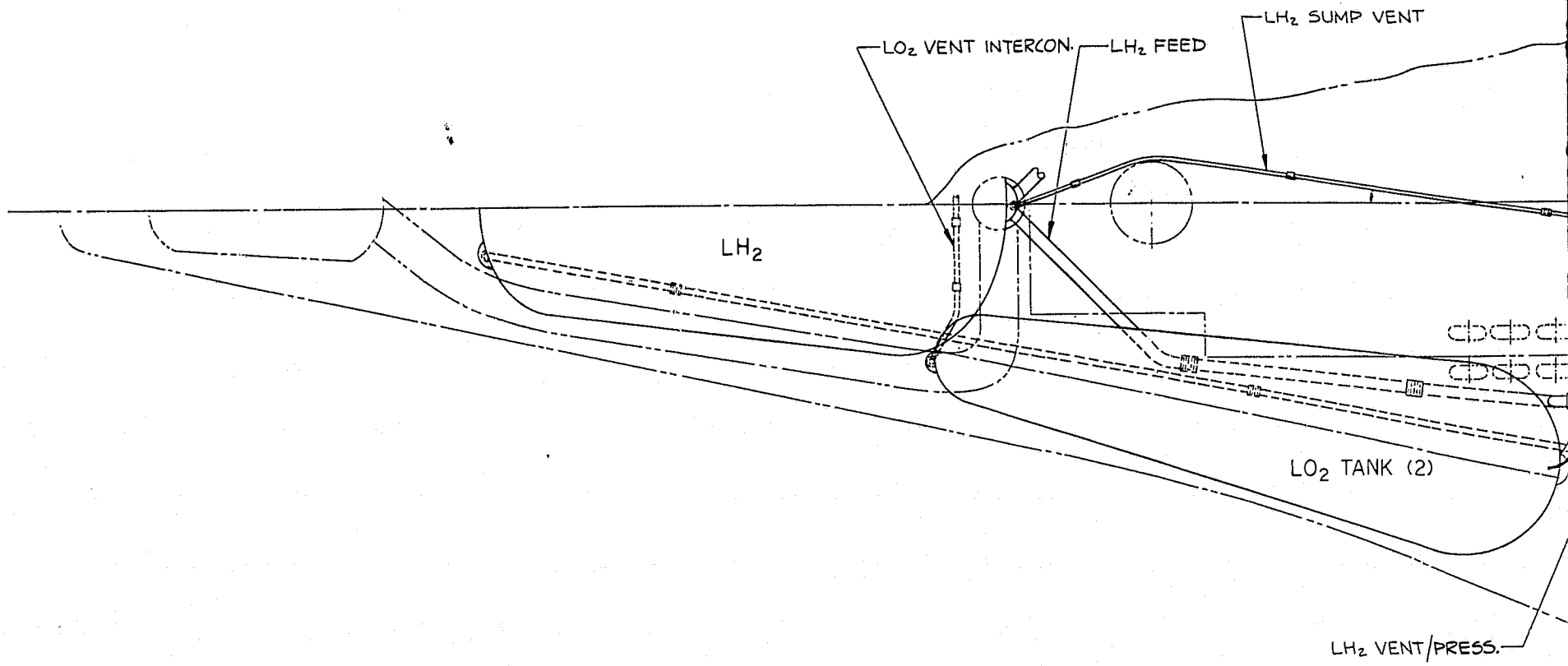
**FOLDOUT FRAME**



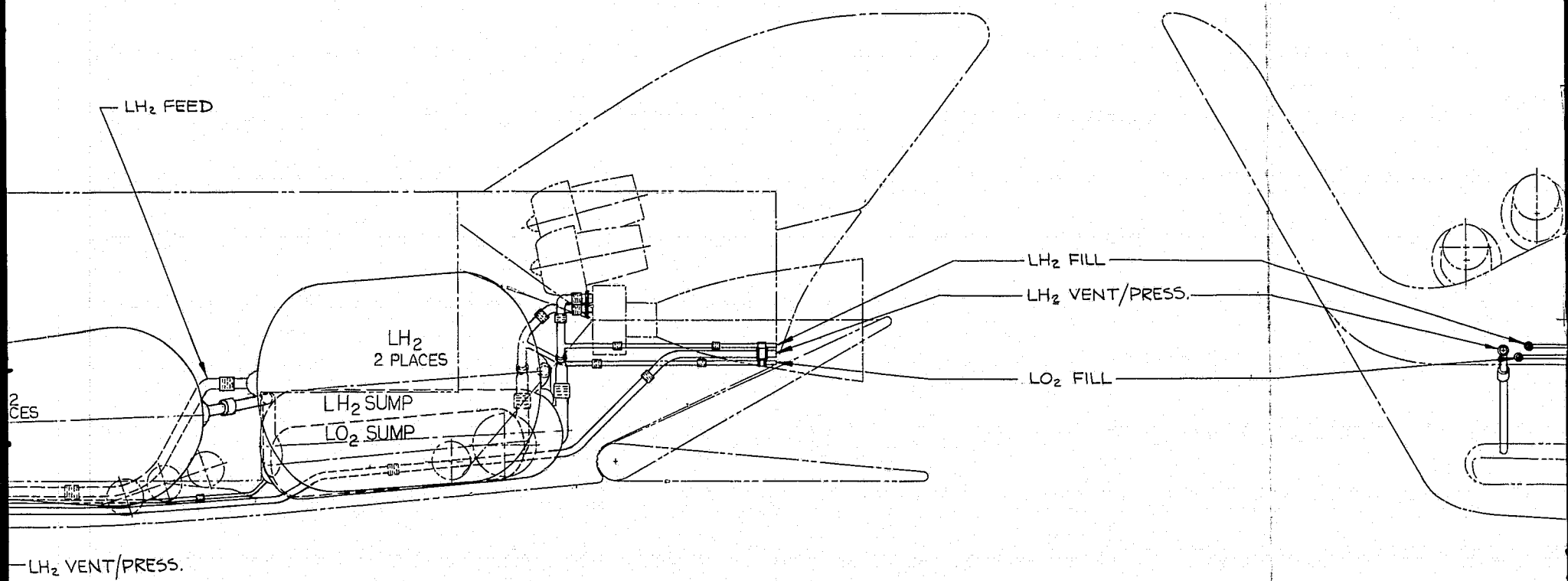
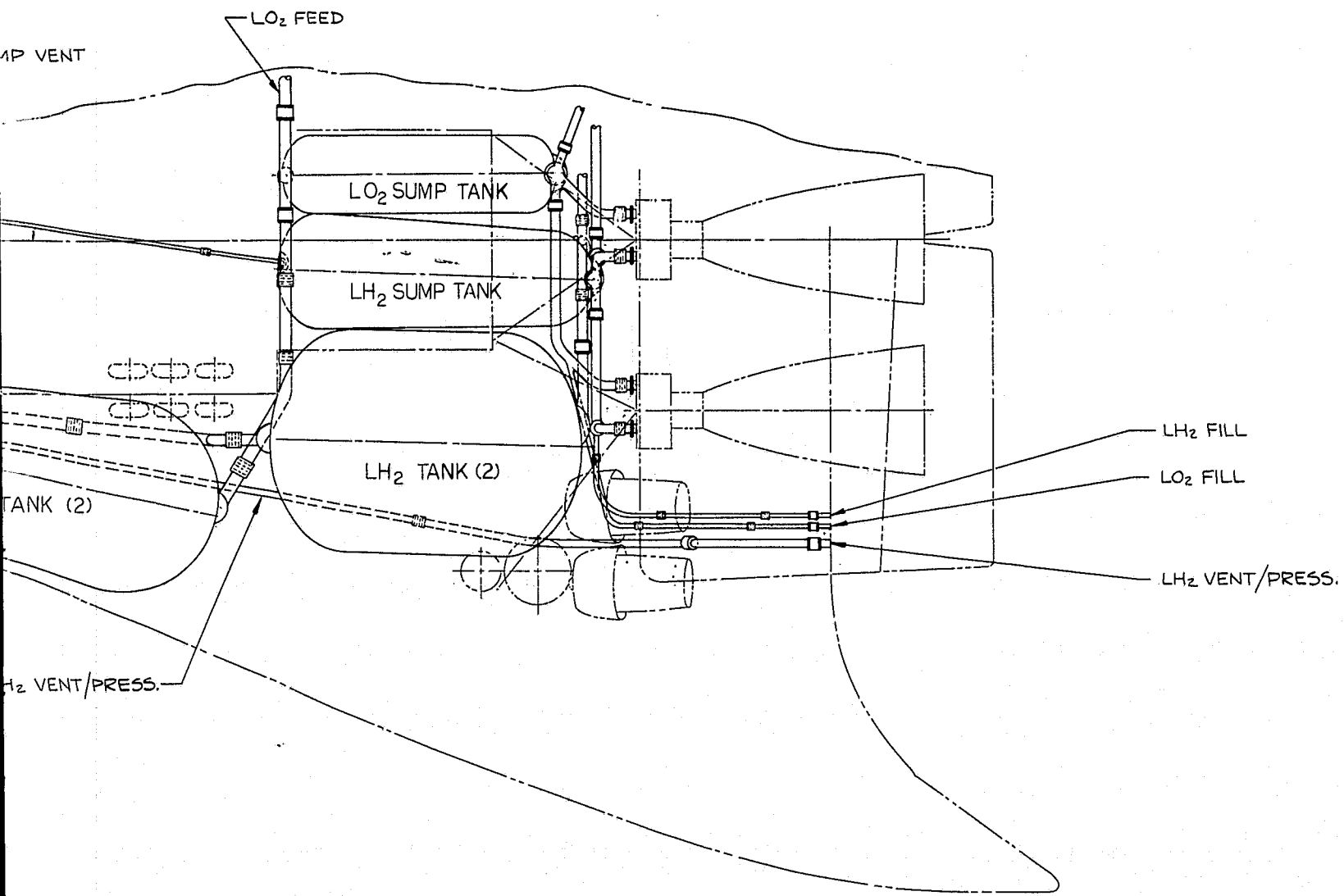


DATE 10-10-69	LOCKHEED MISSILES & SPACE COMPANY	
DR AM WEST	A GROUP DIVISION OF LOCKHEED AIRCRAFT CORPORATION	
APPD	SUNNYVALE, CALIFORNIA	
APPD	ORBITER STRUCTURAL	
ENGRG	ARRANGEMENT	
CHK	2 STAGE SYSTEM	
APPD	SIZE CODE IDENT	DRAWING NO. REV
APPD	SCALE 1/8"	SKW101069 .1
		SHEET

A-8



FOLDOUT FRAME 1



FOLDOUT FRAME 2

LH<sub>2</sub> FILL

LO<sub>2</sub> FILL

LH<sub>2</sub> VENT/PRESS.

LH<sub>2</sub> ENGINE FEED (TYP)

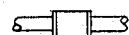
LO<sub>2</sub> ENGINE FEED (TYP)

LH<sub>2</sub> FILL

LH<sub>2</sub> VENT/PRESS.

LO<sub>2</sub> FILL

LEGEND:

 VALVE

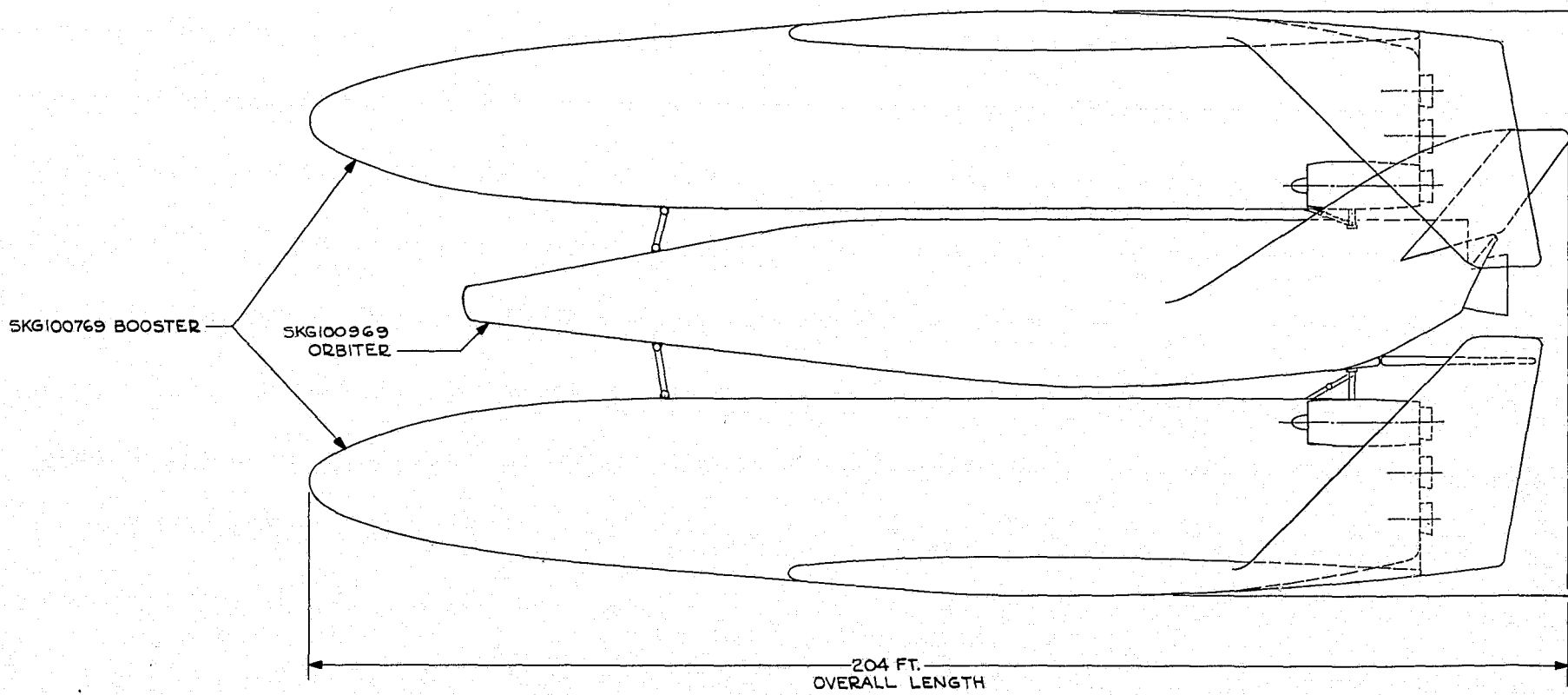
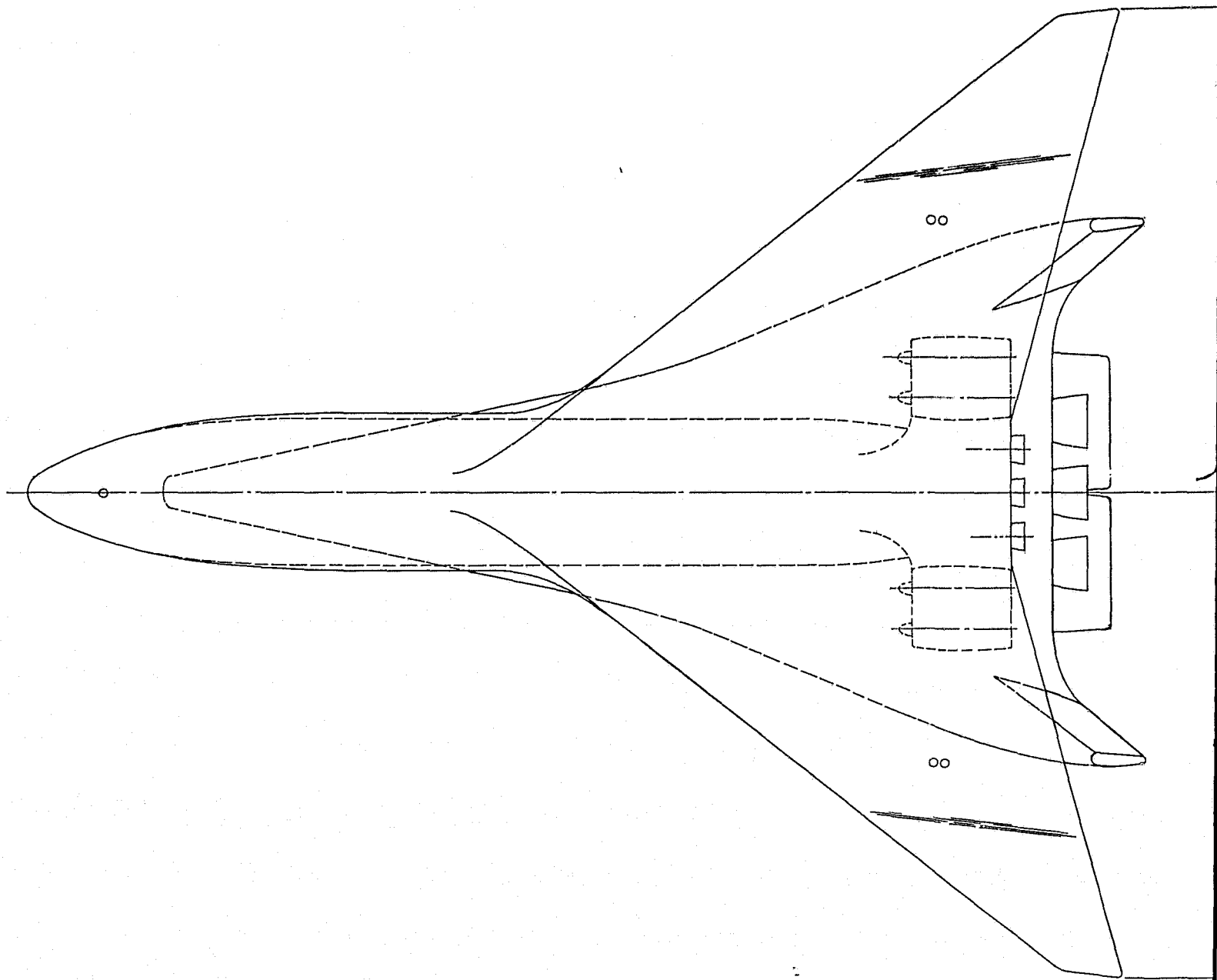
 GIMBAL JOINT

JTY REQD	CODE IDENT	PART OR IDENTIFYING NO.	NOMENCLATURE OR DESCRIPTION	MATERIAL DESCRIPTION OR NOTE	MATERIAL SPECIFICATION	ZONE	ITEM NO.
PARTS LIST							
INTERPRET DWG PER	UNLESS OTHERWISE SPECIFIED DIM. ARE IN INCHES. TOLERANCES ON:		DATE OCT 15, 69	LOCKHEED MISSILES & SPACE COMPANY			
	FRACTIONS = ± 1/16		DR B Rudin	A GROUP DIVISION OF LOCKHEED AIRCRAFT CORPORATION			
	DECIMALS: .X = ± .1		APPD	SUNNYVALE, CALIFORNIA			
	.XX = ± .03		APPD	ORBITER 2 STAGE SYSTEM MAIN PROPELLANT LINES			
	.XXX = ± .010		ENGRG				
	ANGLES = ± 2 DEG		CHK	SIZE	CODE IDENT	DRAWING NO.	REV
NEXT ASSY	USED ON	CONTR	APPD			SKB 101569	
APPLICATION		CCA/CEI	APPD	SCALE 1/50			SHEET 1 OF 1

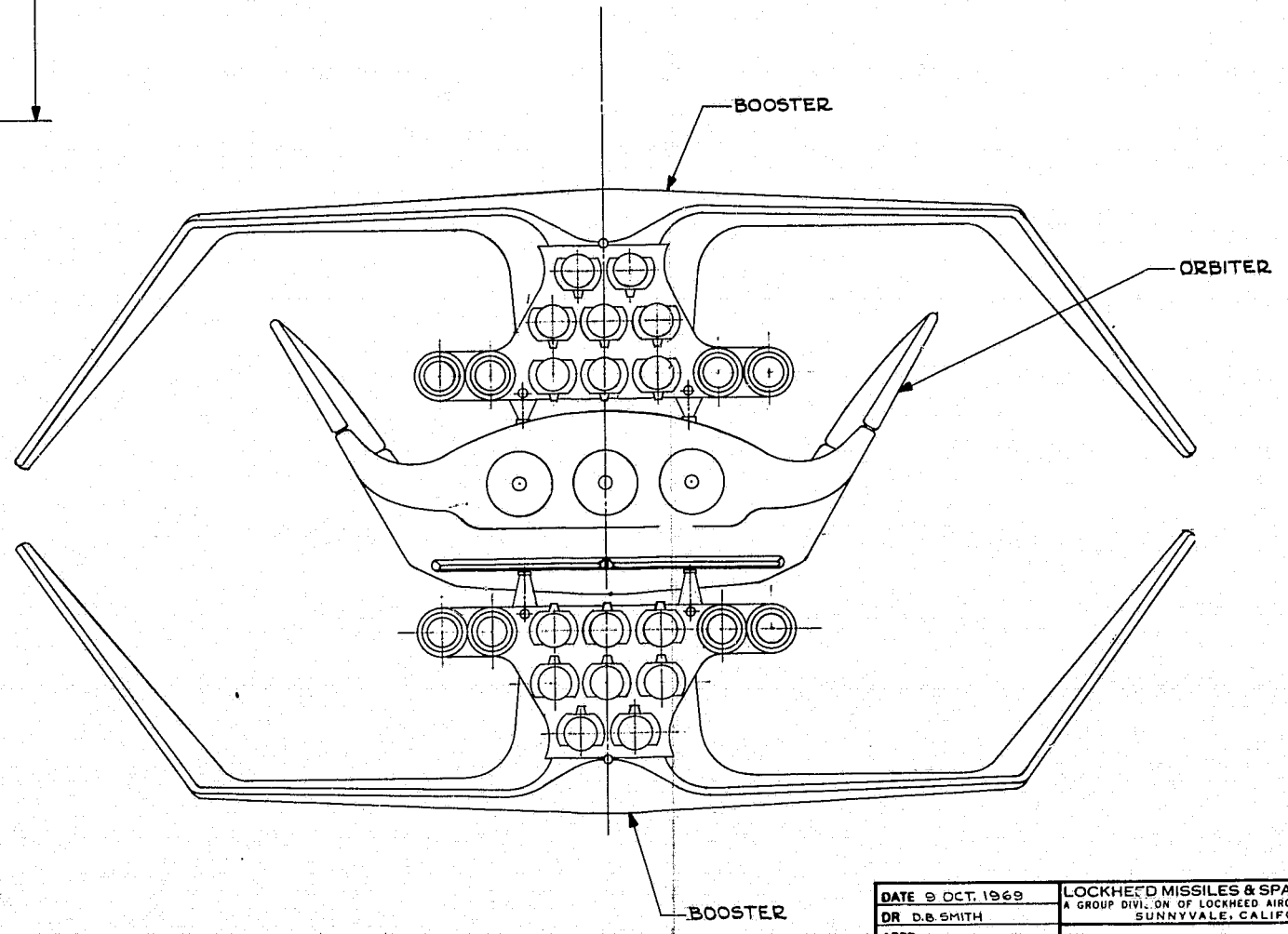
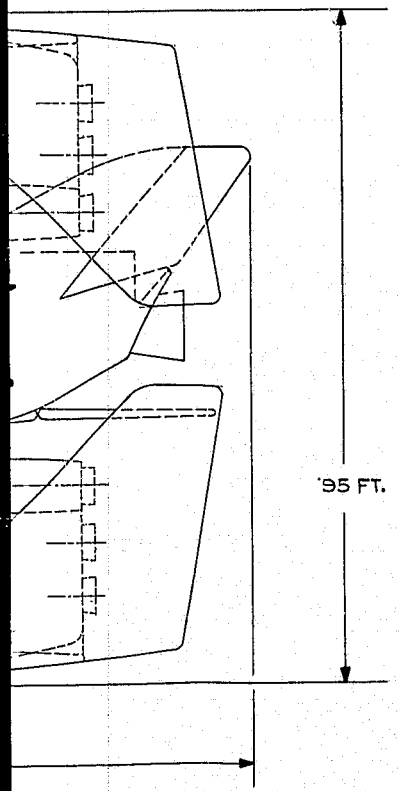
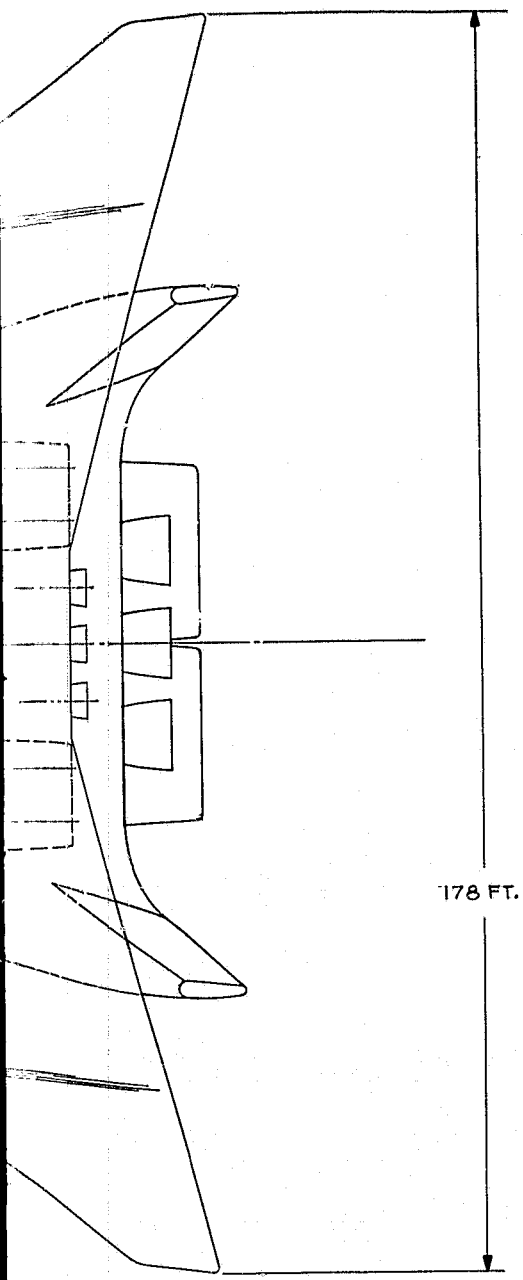
2

1-9

FOLDOUT FRAME 3



FOLDOUT FRAME 1



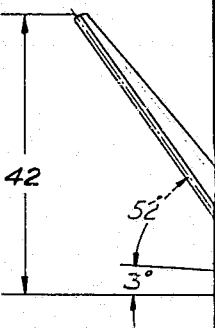
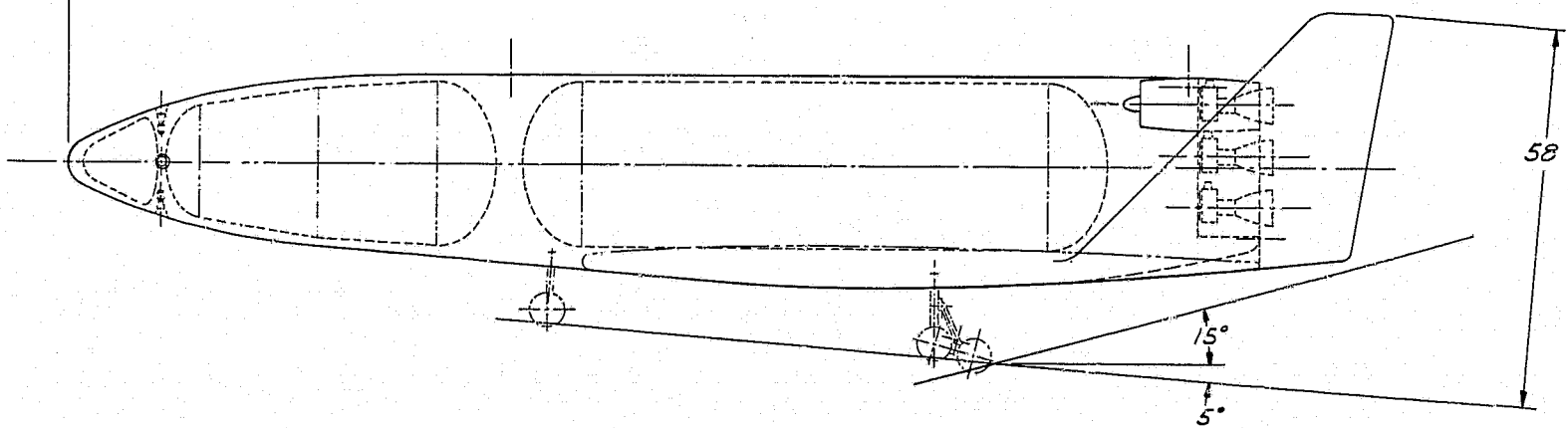
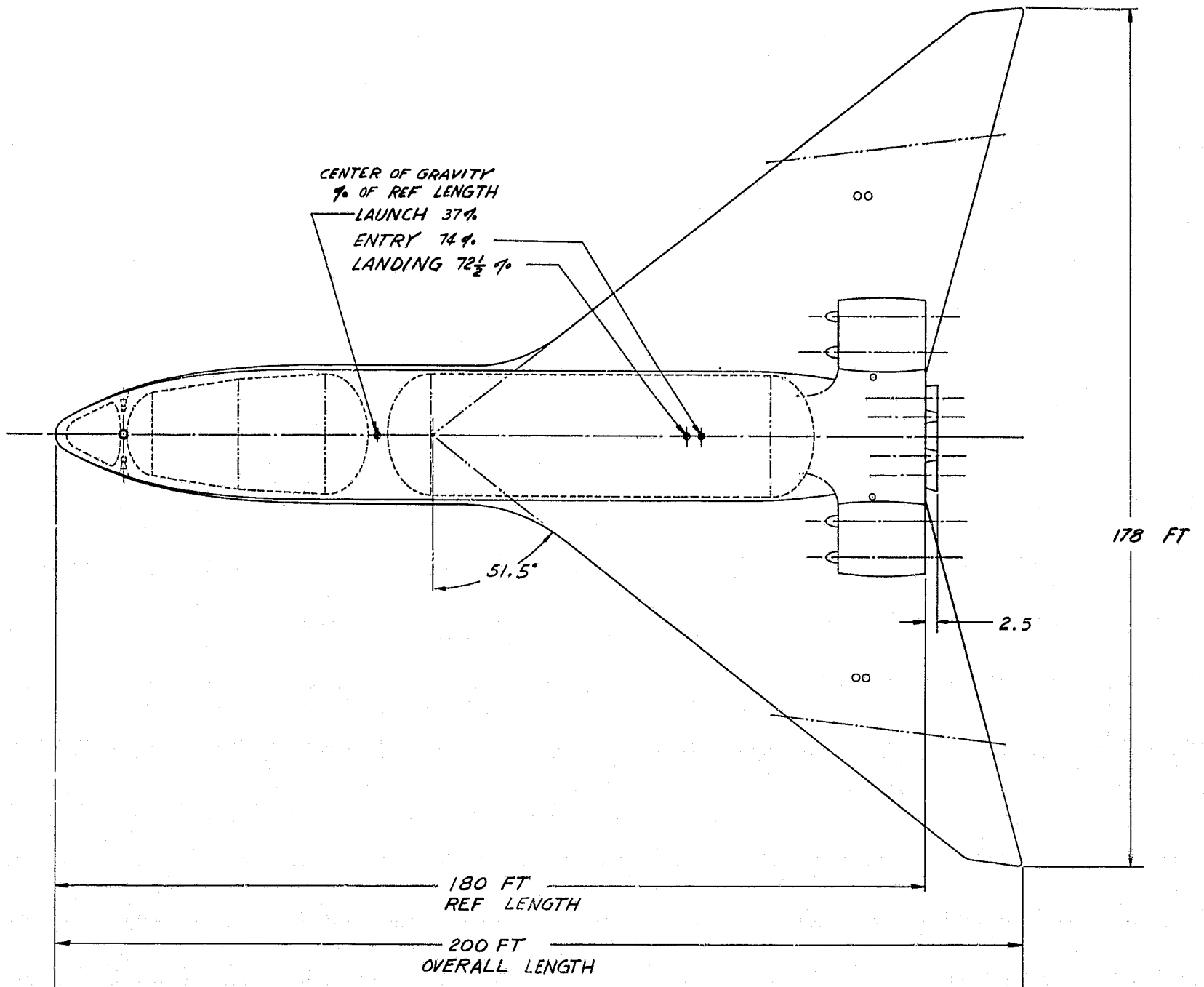
0 5 10 20 30 40 50  
SCALE ~ FT.

DATE 9 OCT. 1969	LOCKHEED MISSILES & SPACE COMPANY	
DR D.B. SMITH	A GROUP DIV. OF LOCKHEED AIRCRAFT CORPORATION	
APPD	SUNNYVALE, CALIFORNIA	
ENGRG	LAUNCH VEHICLE - DISSIMILAR	
CHK	TRIAMESE, 50K PAYLOAD	
APPD	SIZE CODE IDENT	DRAWING NO. SKD100969
APPD	SCALE 1/120TH	REV -
		SHEET

FOLDOUT FRAME 2

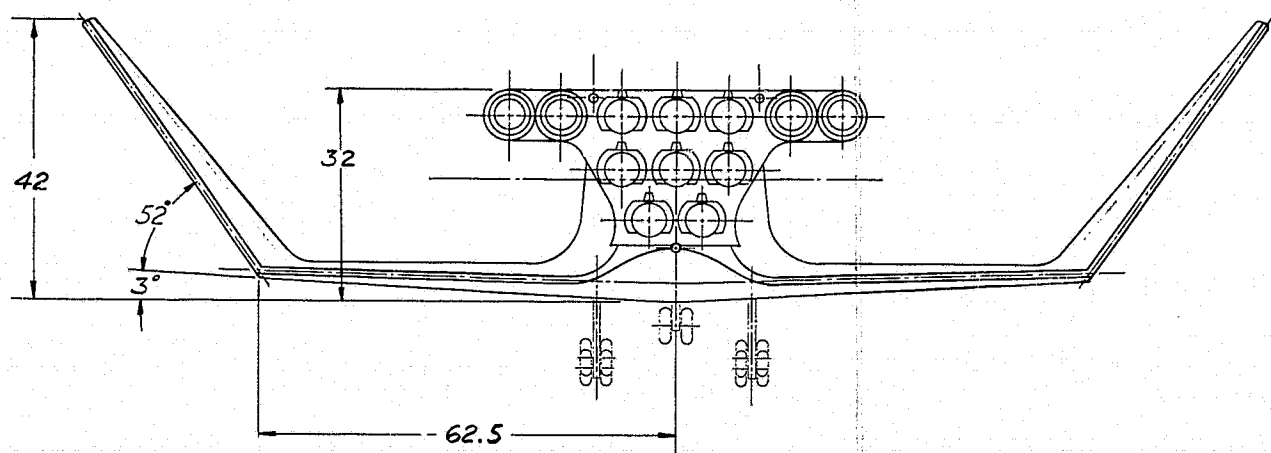
A-10





FOLDOUT FRAME

178 FT

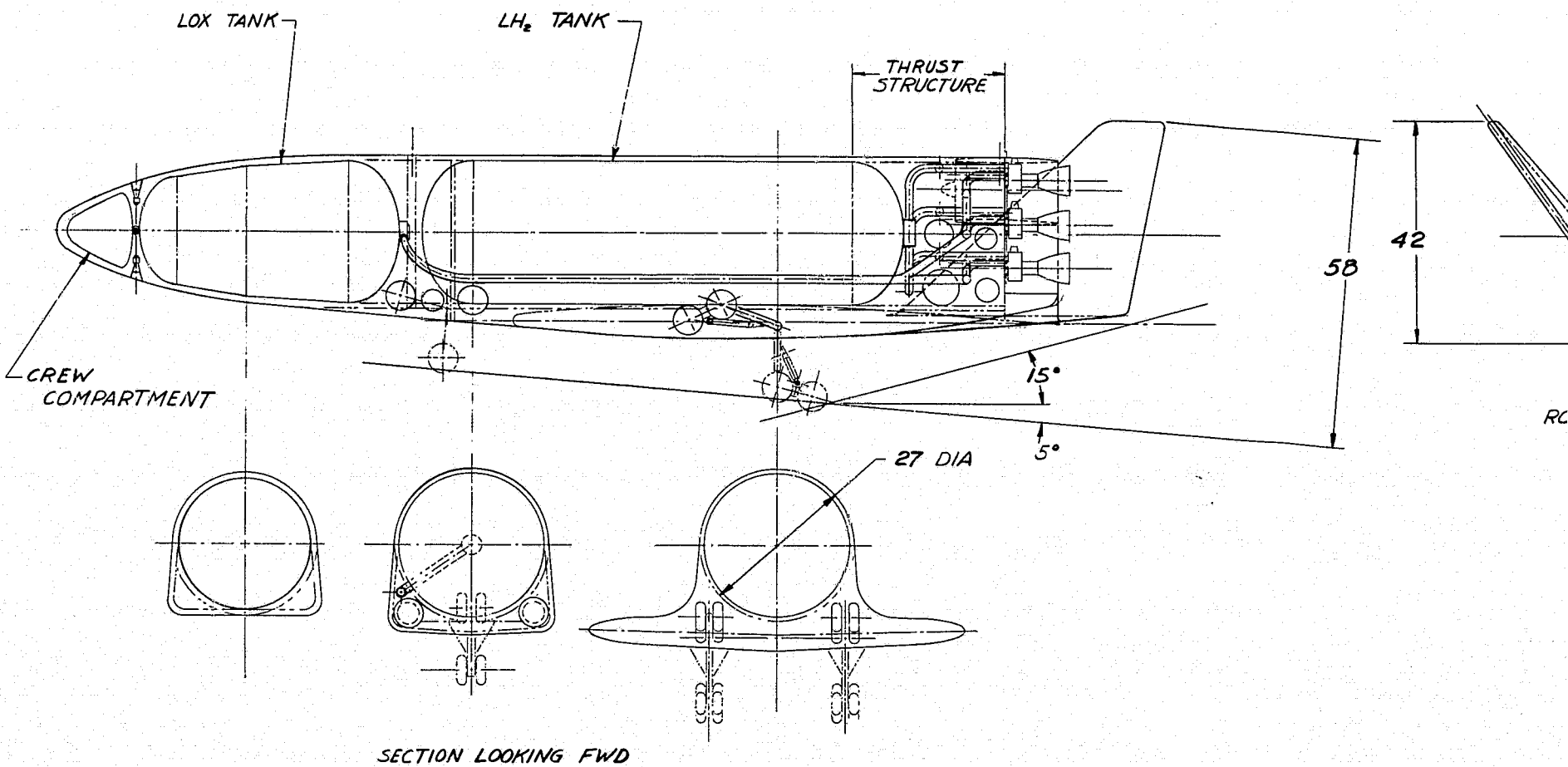
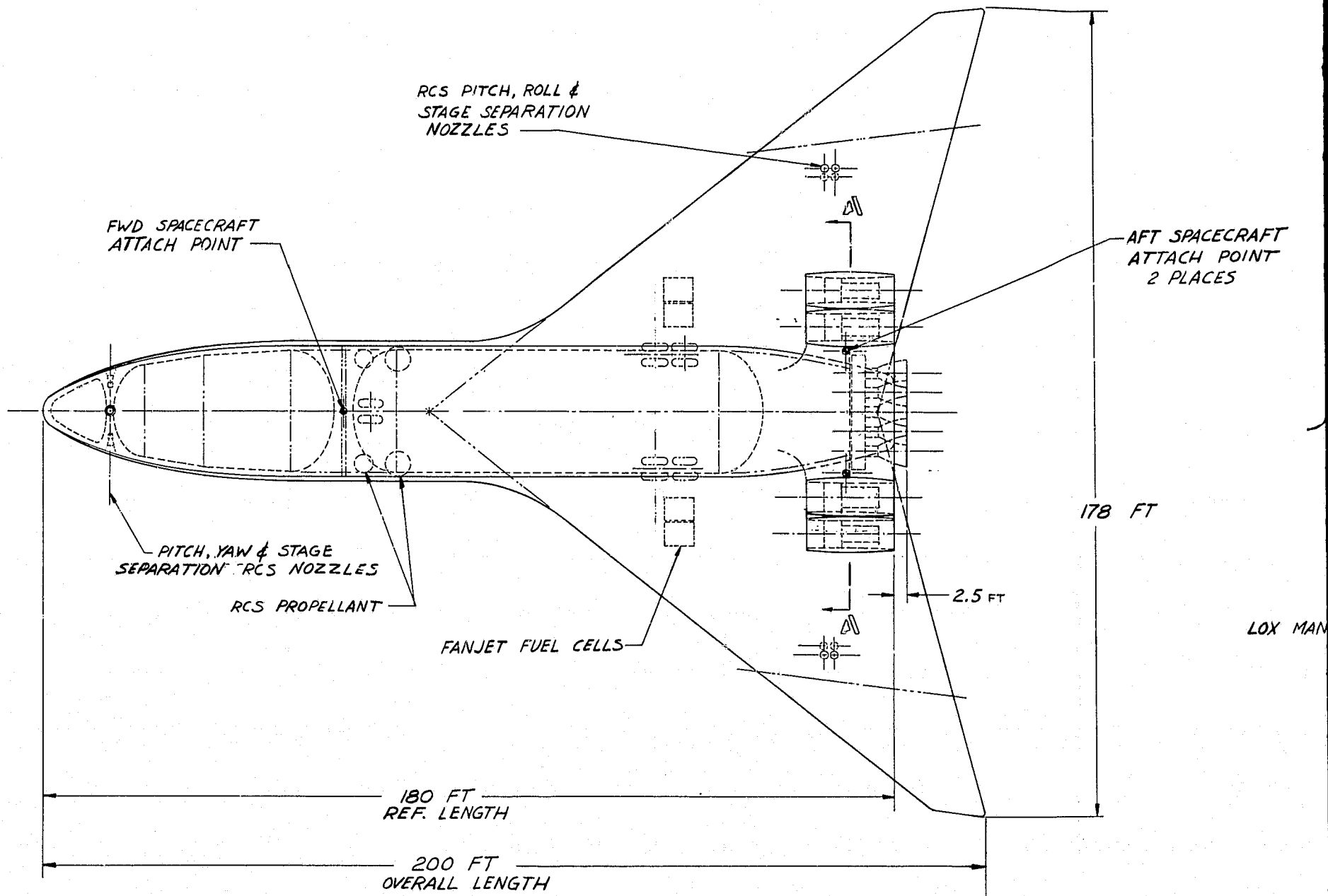


0 5 10 20 30 40 50  
SCALE ~ FT

DATE	10-7-68	LOCKHEED MISSILES & SPACE COMPANY	
DR	M.G.	A GROUP DIVISION OF LOCKHEED AIRCRAFT CORPORATION	
APPD		SUNNYVALE, CALIFORNIA	
APPD		BOOSTER, DISSIMILAR	
ENGRG		TRIAMESE - 50 K PAYLOAD	
CHK		GENERAL ARRANGEMENT	
APPD		SIZE	DRAWING NO.
APPD		SCALE 1:120	SKG100769
			REV
			SHEET

FOLDOUT FRAME 2

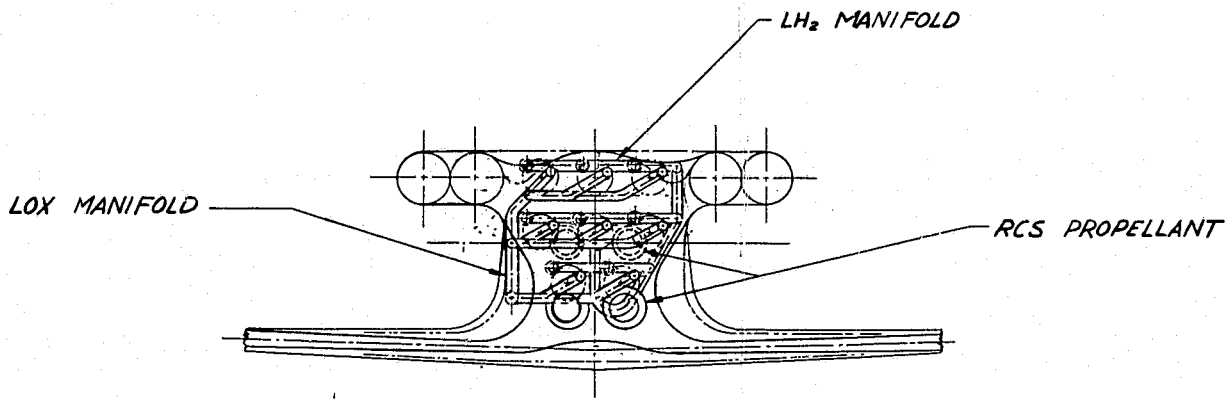
A-11



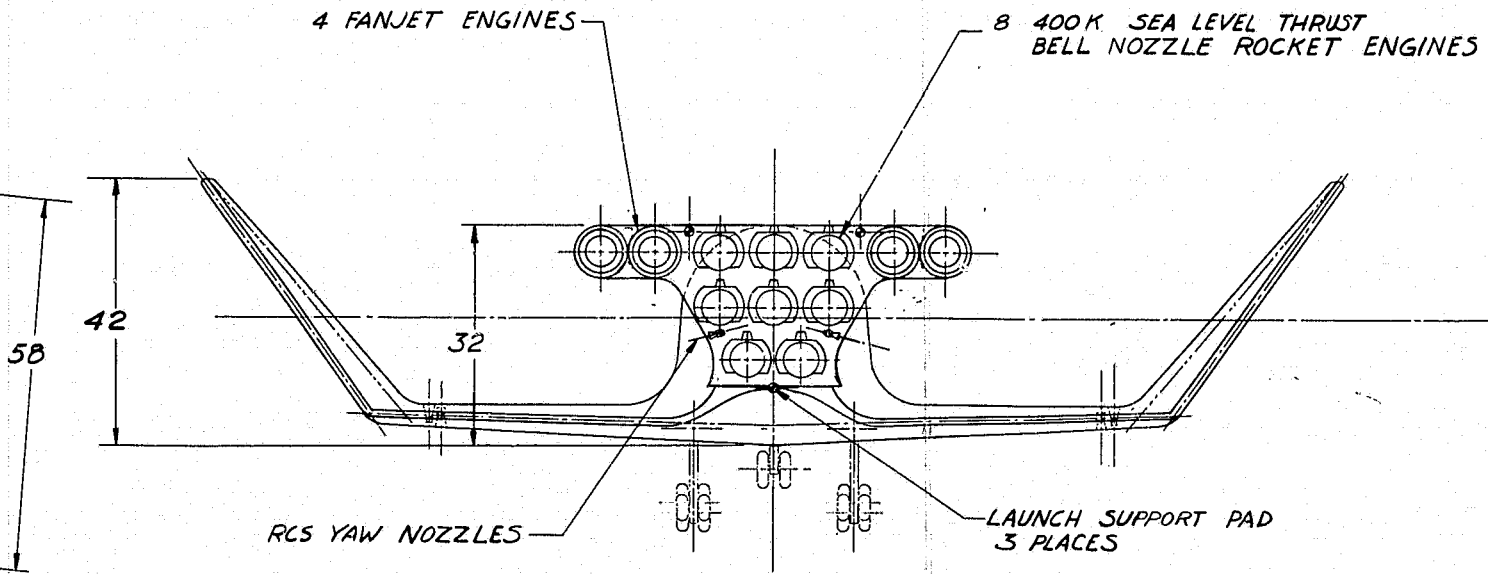
FOLDOUT FRAME 1

AFT SPACECRAFT  
ATTACH POINT  
2 PLACES

178 FT



SECTION A-A

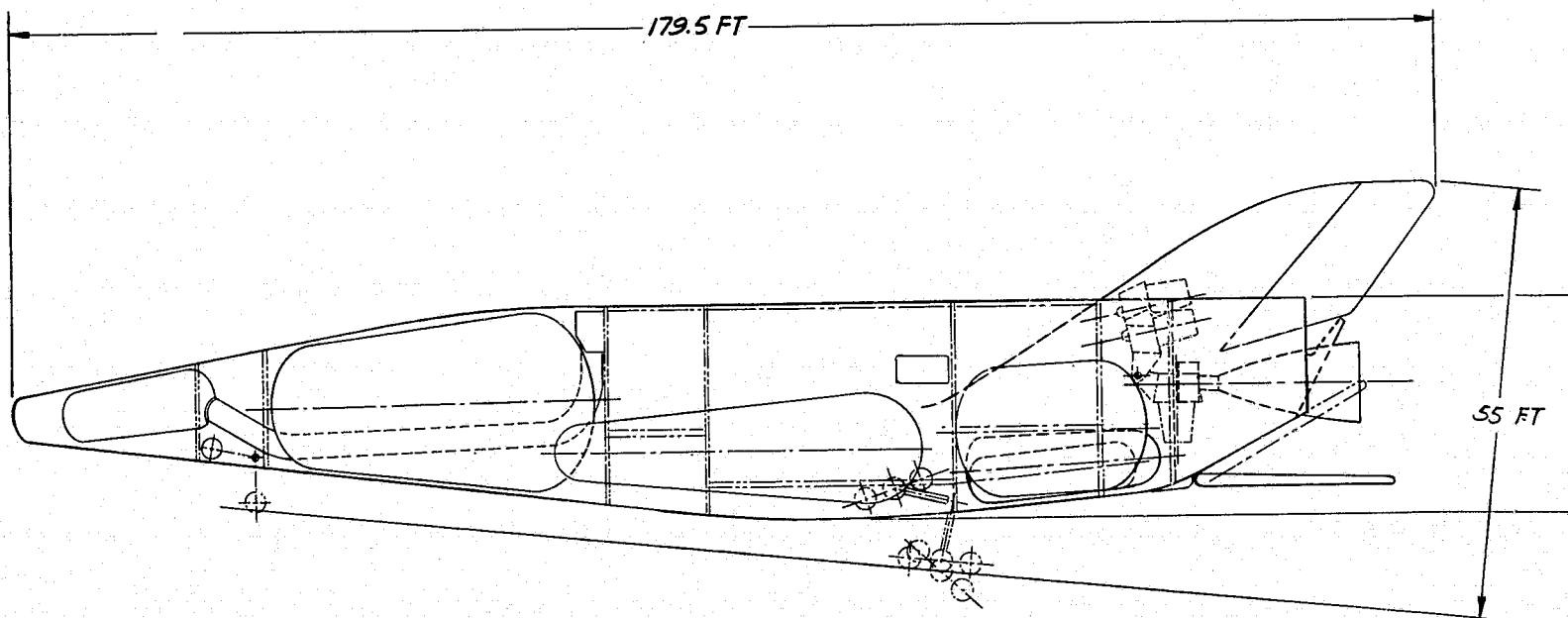
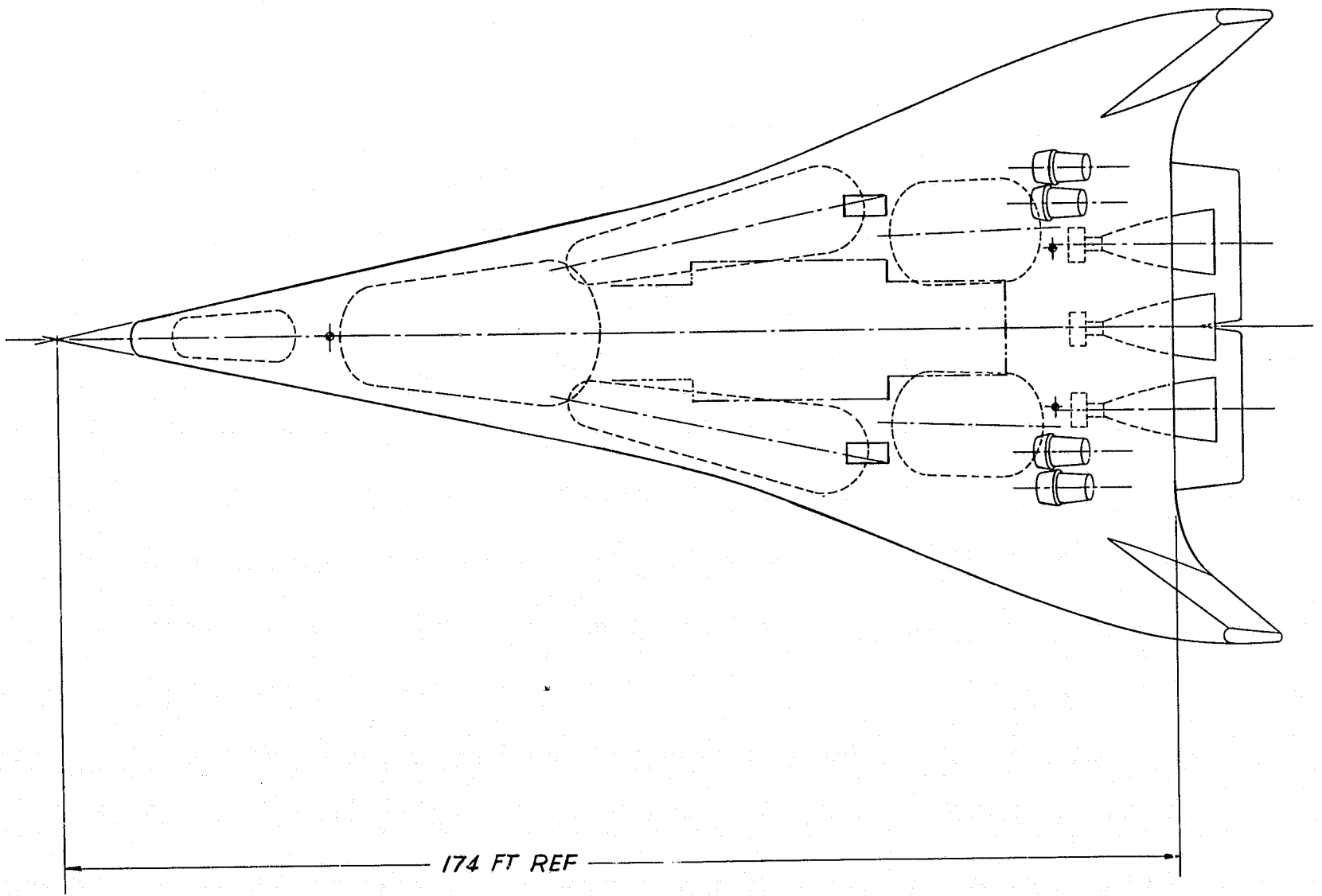


0 5 10 20 30 40 50  
SCALE - FT

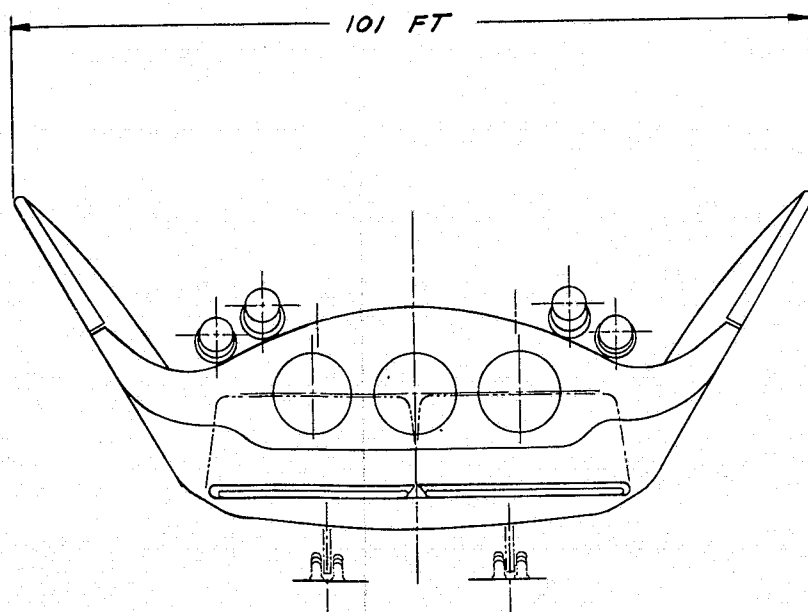
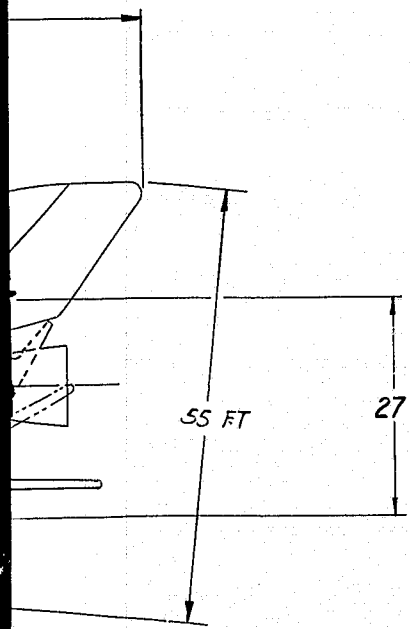
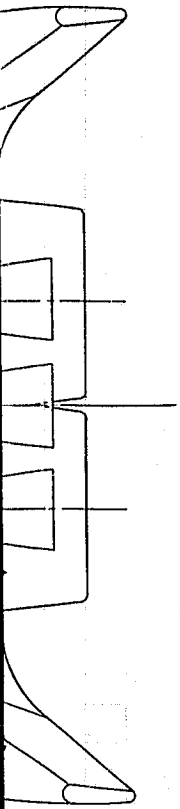
DATE	10-3-69	LOCKHEED MISSILES & SPACE COMPANY	
DR	MG	A GROUP DIVISION OF LOCKHEED AIRCRAFT CORPORATION SUNNYVALE, CALIFORNIA	
APPD		BOOSTER, DISSIMILAR TRIAMESE, 50 K PAYLOAD	
ENGRG		INBOARD PROFILE	
CHK		SIZE CODE IDENT	DRAWING NO.
A*PD			SKG100369
APPD		SCALE 1:120	SHEET

FOLDOUT FRAME 2

A-12



FOLDOUT FRAME |

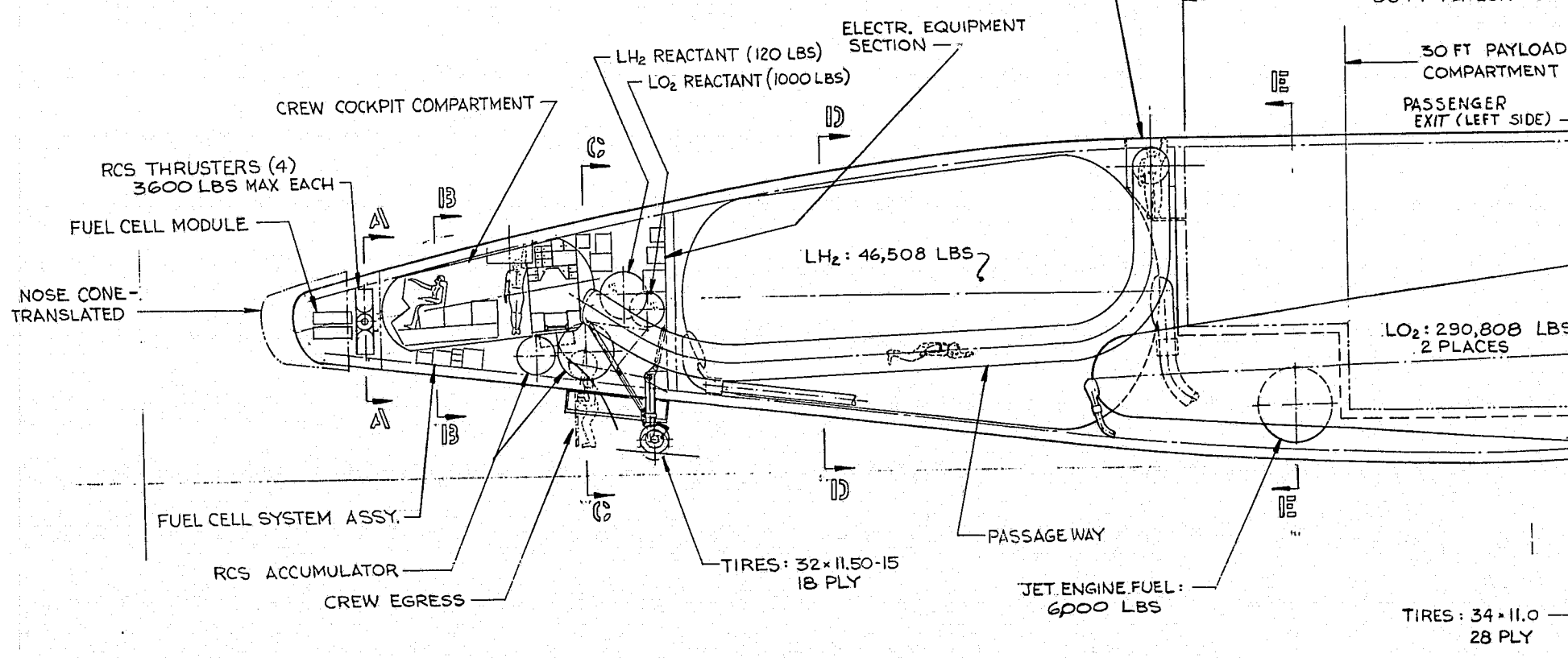
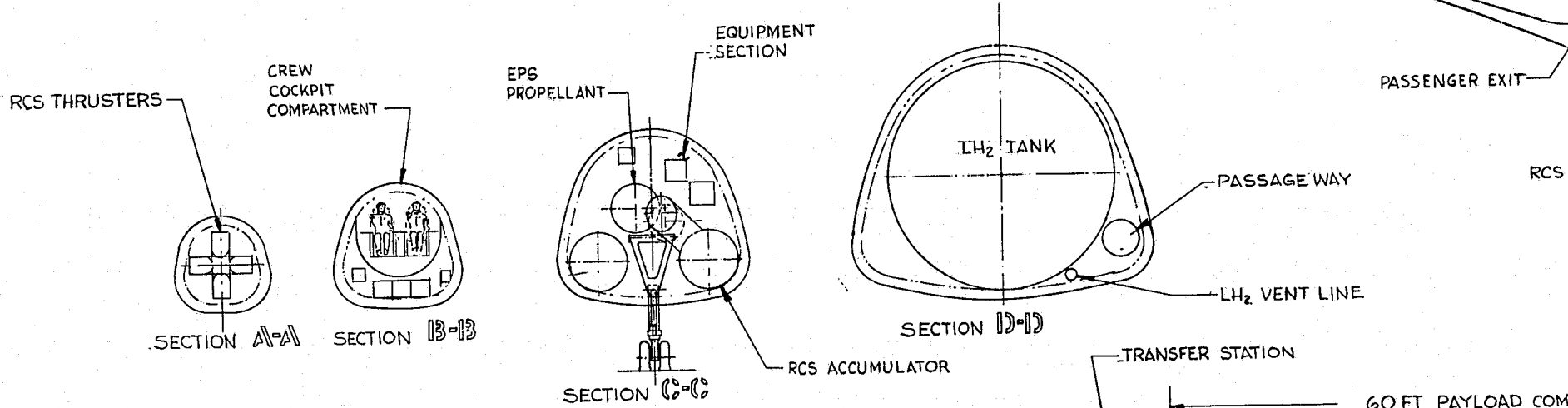
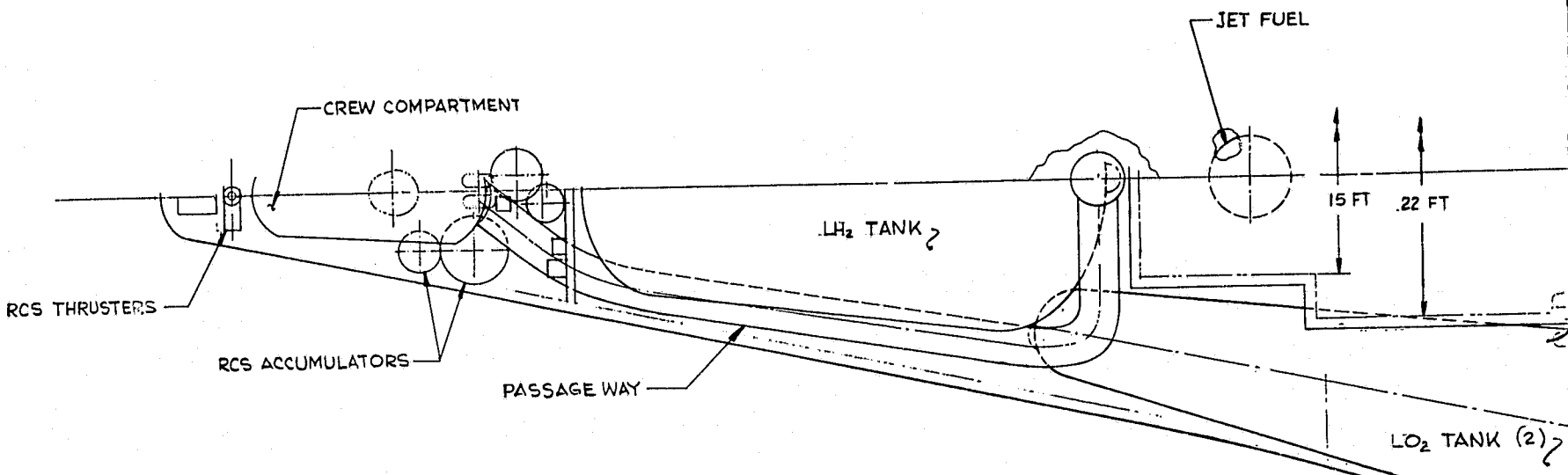


DATE	10-9-69	LOCKHEED MISSILES & SPACE COMPANY	
DR	MG	A GROUP DIVISION OF LOCKHEED AIRCRAFT CORPORATION	
APPD		SUNNYVALE, CALIFORNIA	
APPD		ORBITER, DISSIMILAR	
ENGRG		TRIAMESE, 50K PAYLOAD-	
CHK		GENERAL ARRANGEMENT	
APPD		SIZE	CODE IDENT
APPD			DRAWING NO.
			SKG100969
		SCALE 1:120	SHEET

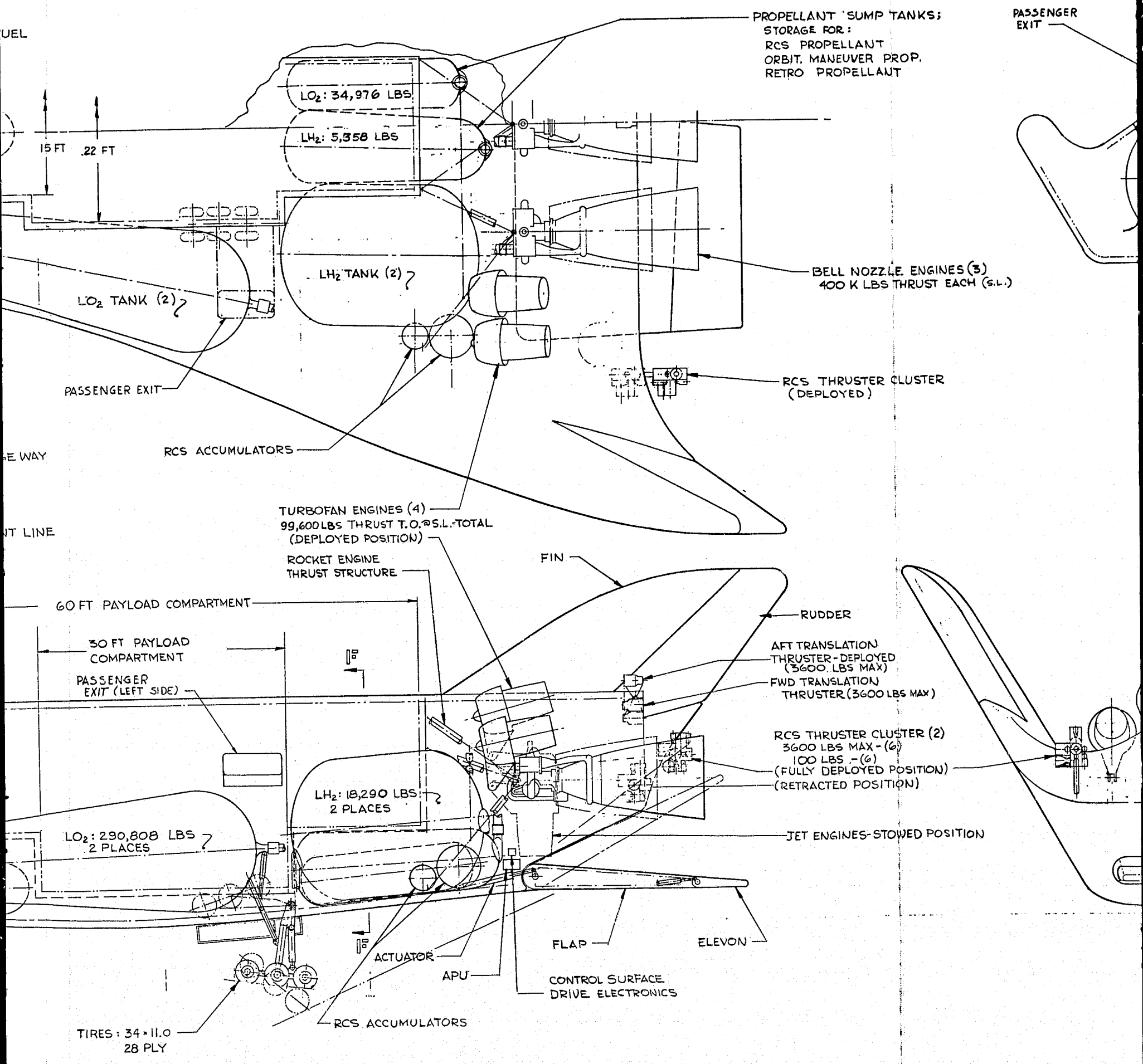
A-13

FOLDOUT FRAME

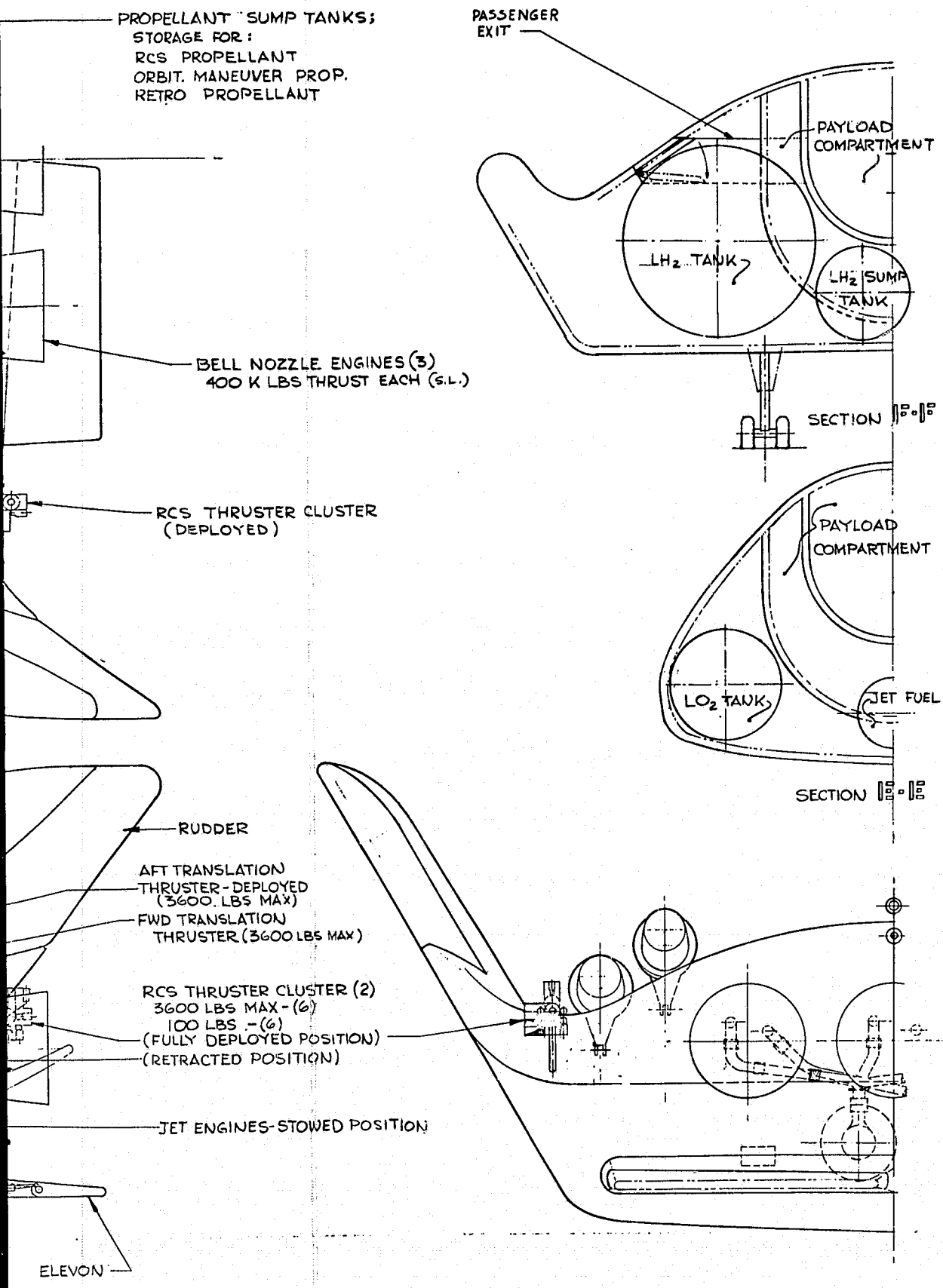
2



**FOLDOUT FR**







A-14

DATE	Oct 3, 1969	LOCKHEED MISSILES & SPACE COMPANY	
DR	MG	A GROUP DIVISION OF LOCKHEED AIRCRAFT CORPORATION SUNNYVALE, CALIFORNIA	
APPD		ORBITER, DISSIMILAR	
APPD		TRIASESE, 50K P/L	
ENGRG		~ INBOARD PROFILE ~	
CHK			
APPD		SIZE CODE IDENT	DRAWING NO. REV
APPD			SKG 100869
		SCALE 1/2"	SHEET 1 OF 1

FRAME 2

FOLDOUT FRAME 3

**VIEW C-C**  
(NOSE RAISED)

PICTURE PLANE

**VIEW B-B**  
(NOSE DROPPED)

BL 19.5

CT

B1

HORIZON ( $\alpha = 17^\circ$ )

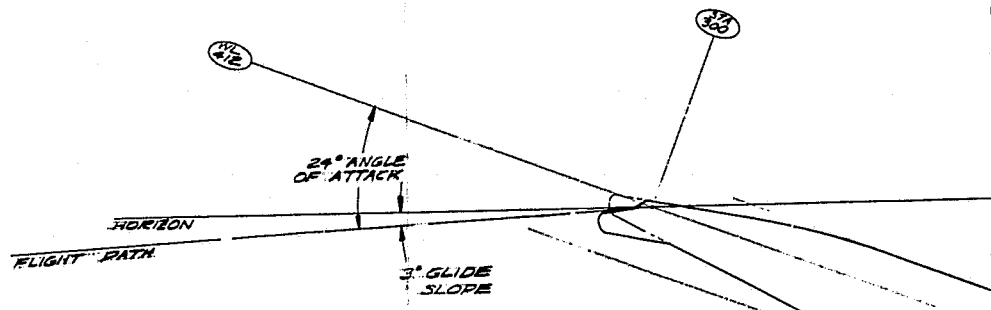
HORIZON ( $\alpha = 24^\circ$ )

**FOLDOUT FRAME**

TOUCHDOWN POINT @ 1/2 MI.  
300 FT. x 10,000 FT. RUNWAY  
TOUCHDOWN POINT 950 FT.  
PAST END. GLIDE SLOPE = 3°

PICTURE PLANE PROJECTION  
PILOT'S FORWARD VIEW  
(NOSE DROPPED)

NEW C.G.  
(SEE RAISED)



LANDING ATTITUDE  
1/240 SCALE

PILOT'S EYE  
NOMINAL  
POSITION

A

B

C

17° (APPROX  
2.5° FOR CLIMB)

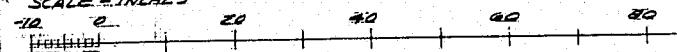
STA 312

STA 329

STA 300

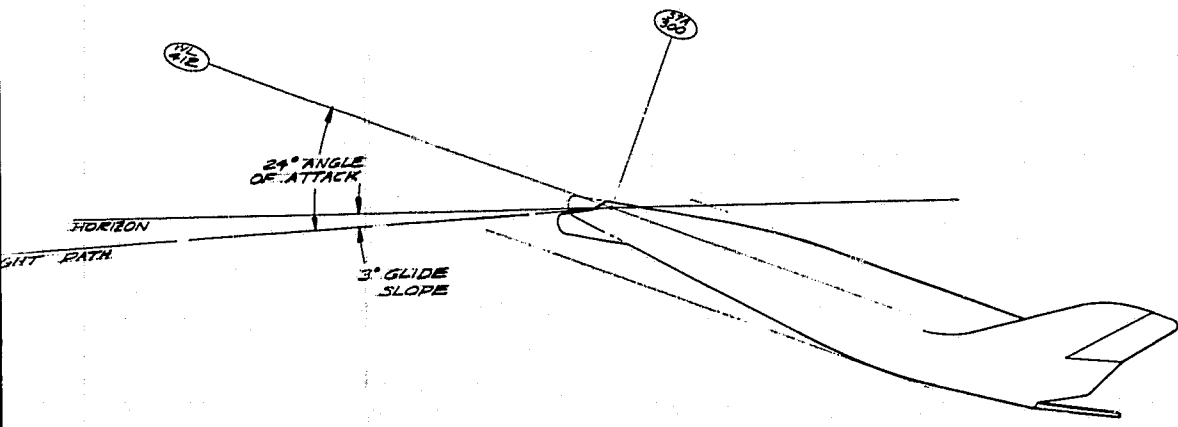
STA 322

SCALE - INCHES

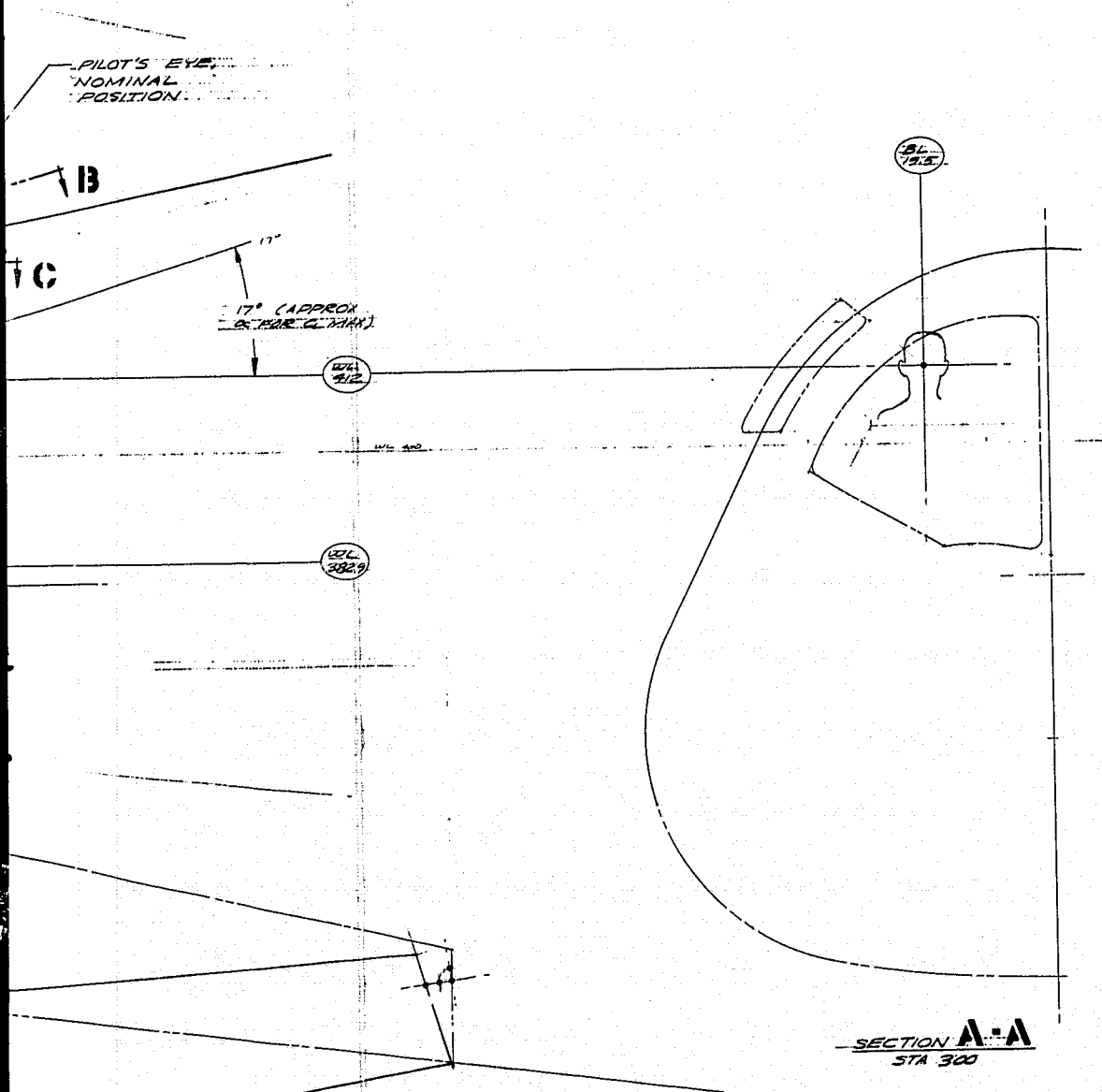


A FOLDOUT FIGURE 2

FOLDOUT



LANDING ATTITUDE  
1/200 SCALE



SECTION A-A  
STA 300

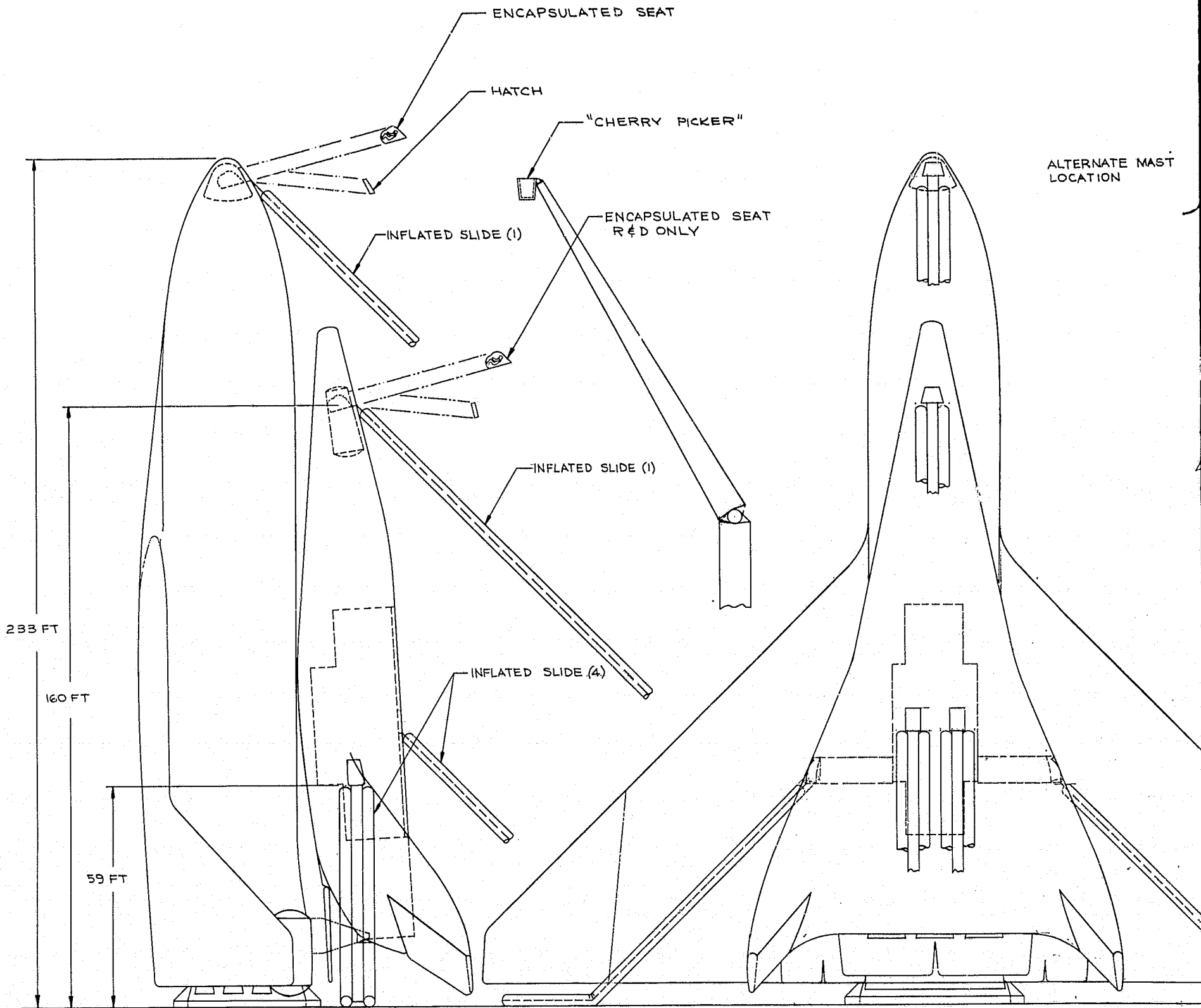
DATE	9 OCT 1969	LOCKHEED MISSILES & SPACE COMPANY A GROUP DIVISION OF LOCKHEED AIRCRAFT CORPORATION SUNNYVALE, CALIFORNIA	
DR	BERWINE		
APPD		PILOT VISION STUDY	
ENGRG		2 STAGE SYSTEM ORBITER	
CHK		DROOP NOSE	
APPD		SIZE CODE IDENT	DRAWING NO.
APPD		J	SKE-100969
		SCALE 1/10	SHEET 1 OF 1

2

FOLDOUT FRAME

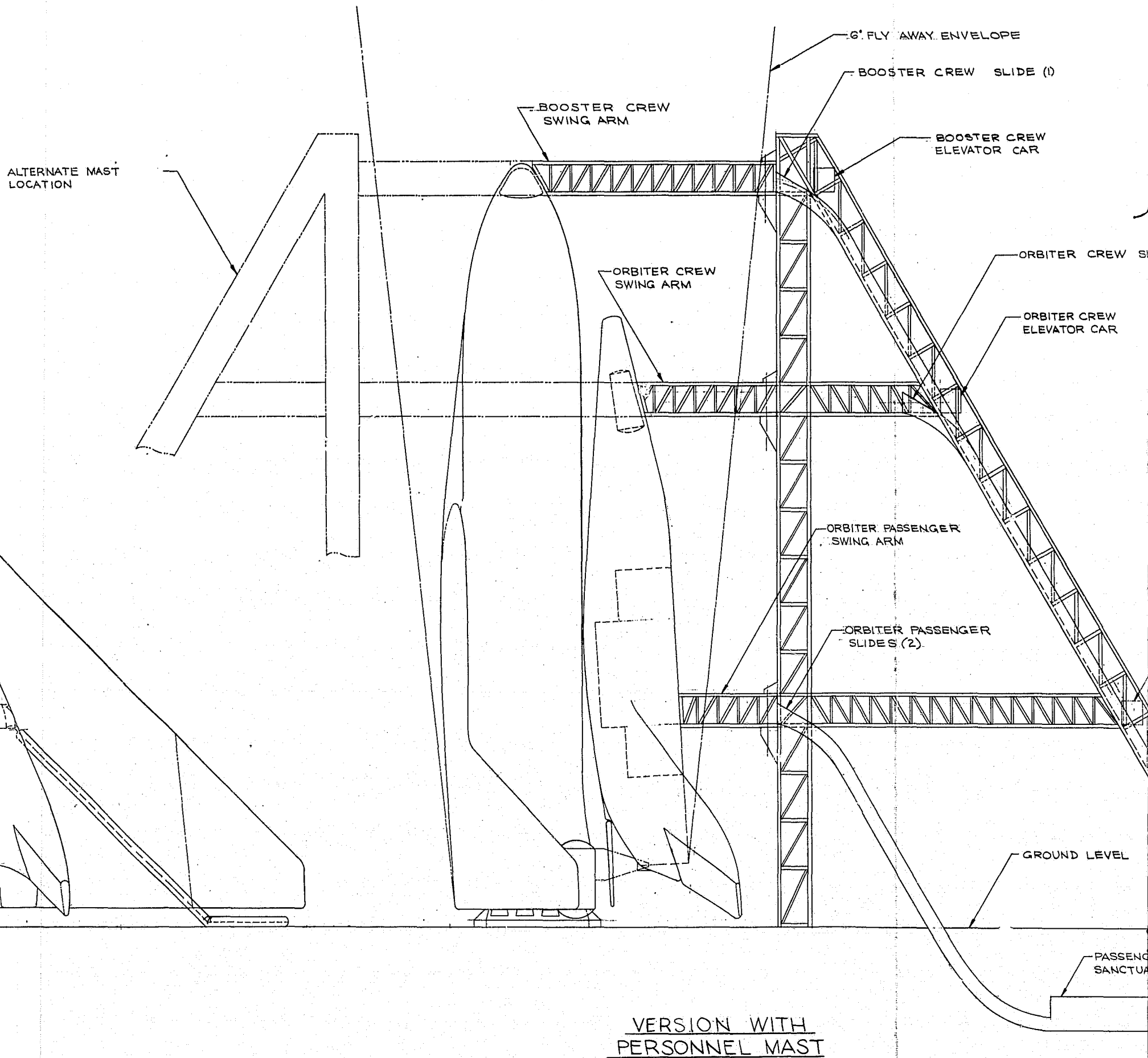
3

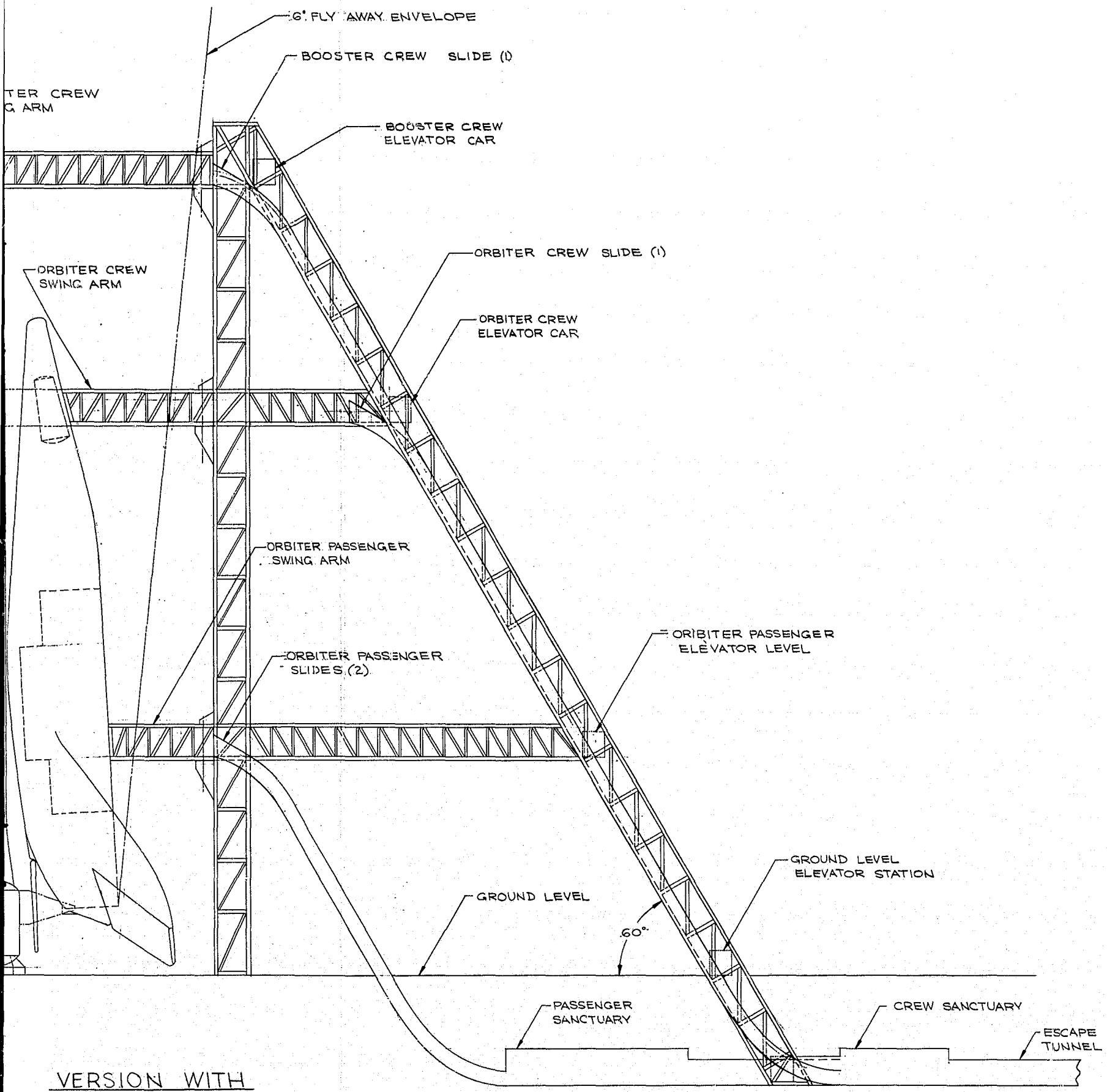
A-15



VERSION WITHOUT PERSONNEL MAST

FOLDOUT FRAME /





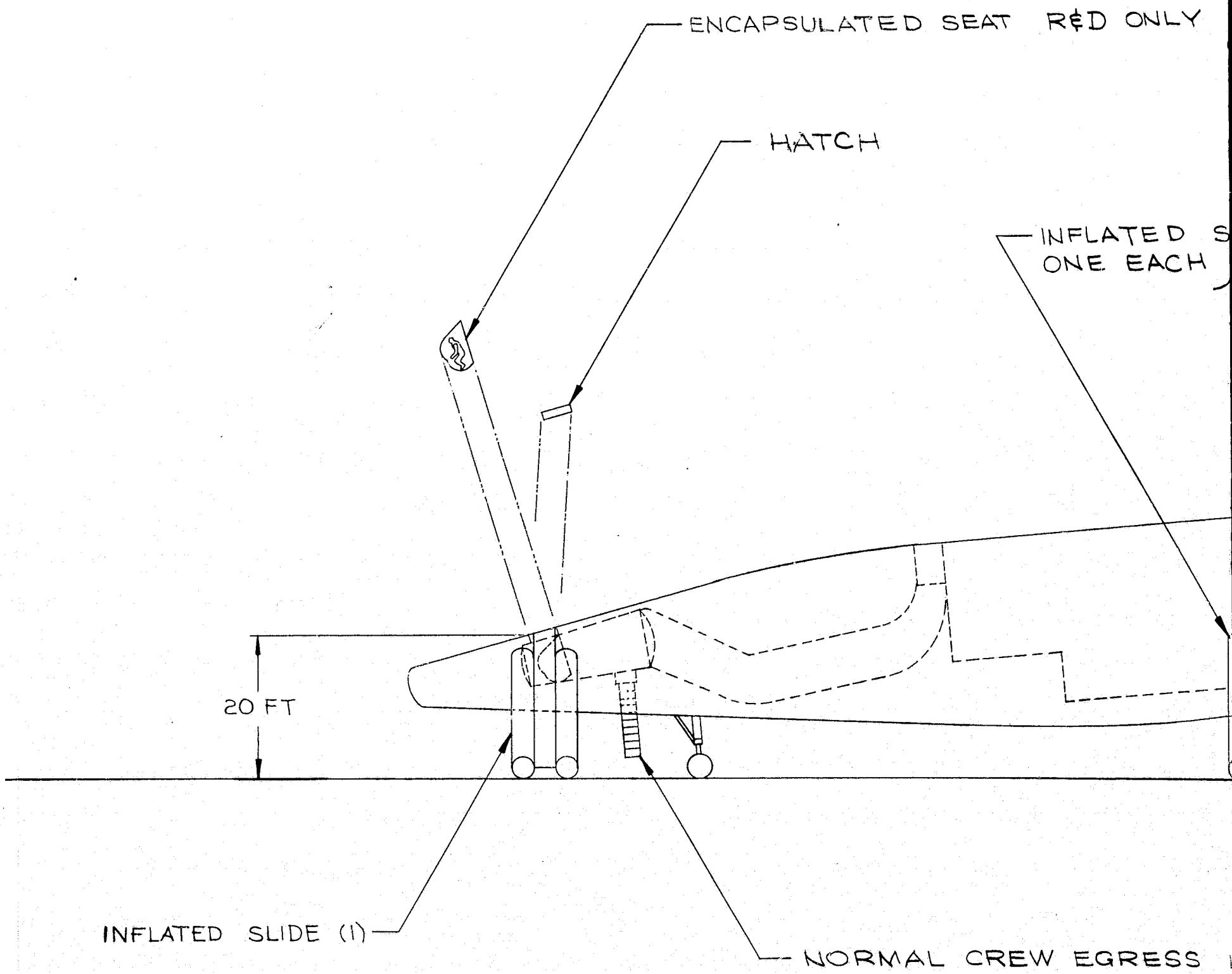
VERSION WITH PERSONNEL MAST

A-16

2-STAGE LAUNCH  
 PERS. ESCAPE PROVISIONS  
 1/20 SKJ 100169

2

FOLDOUT FRAME 3



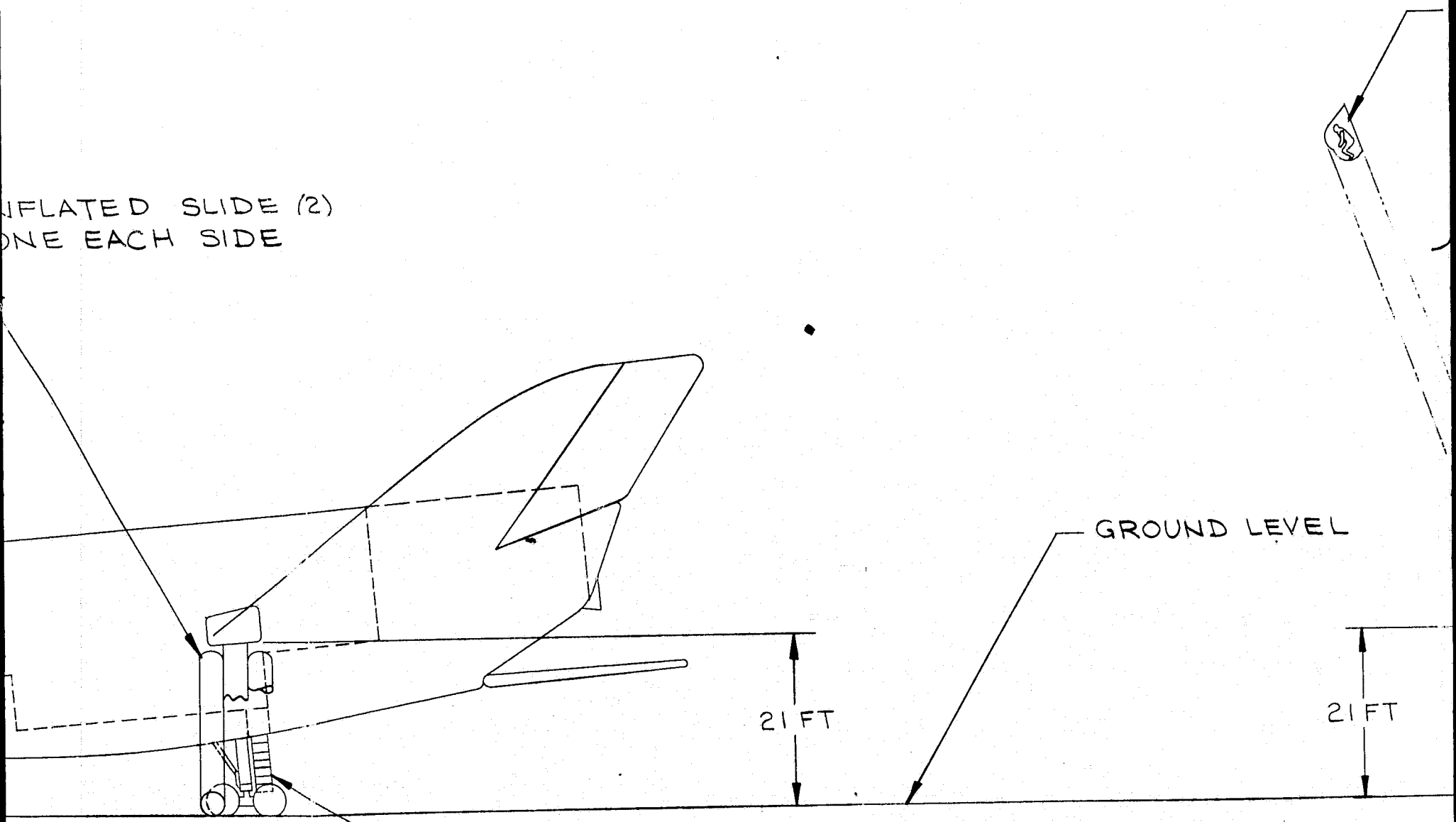
ORBITER

FOLDOUT FRAME



RED ONLY

INFLATED SLIDE (2)  
ONE EACH SIDE



GROUND LEVEL

21 FT

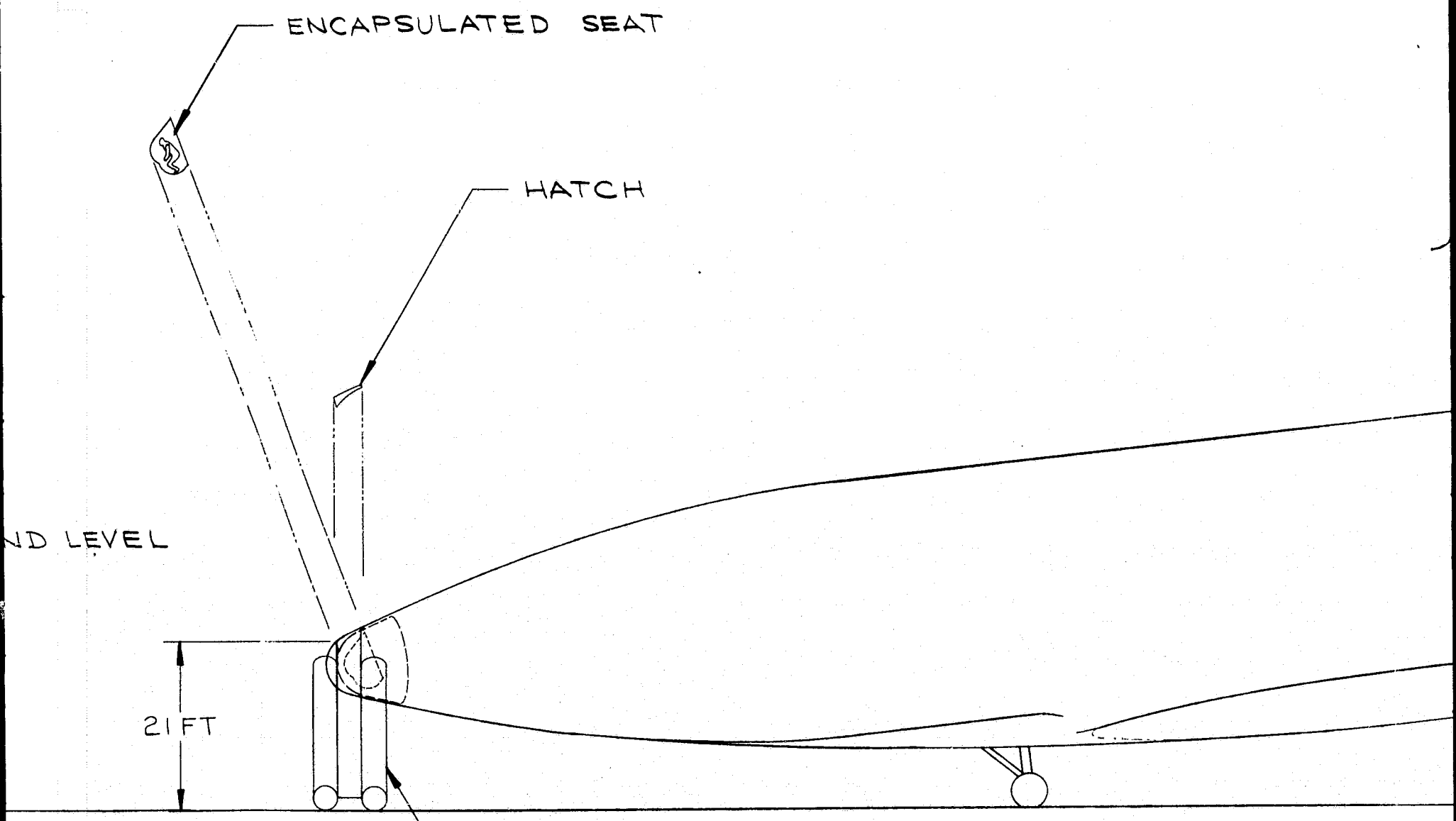
21 FT

EGRESS LADDER

NORMAL PASSENGER  
EGRESS LADDER

R

FOLDOUT FRAME 2



ENCAPSULATED SEAT

HATCH

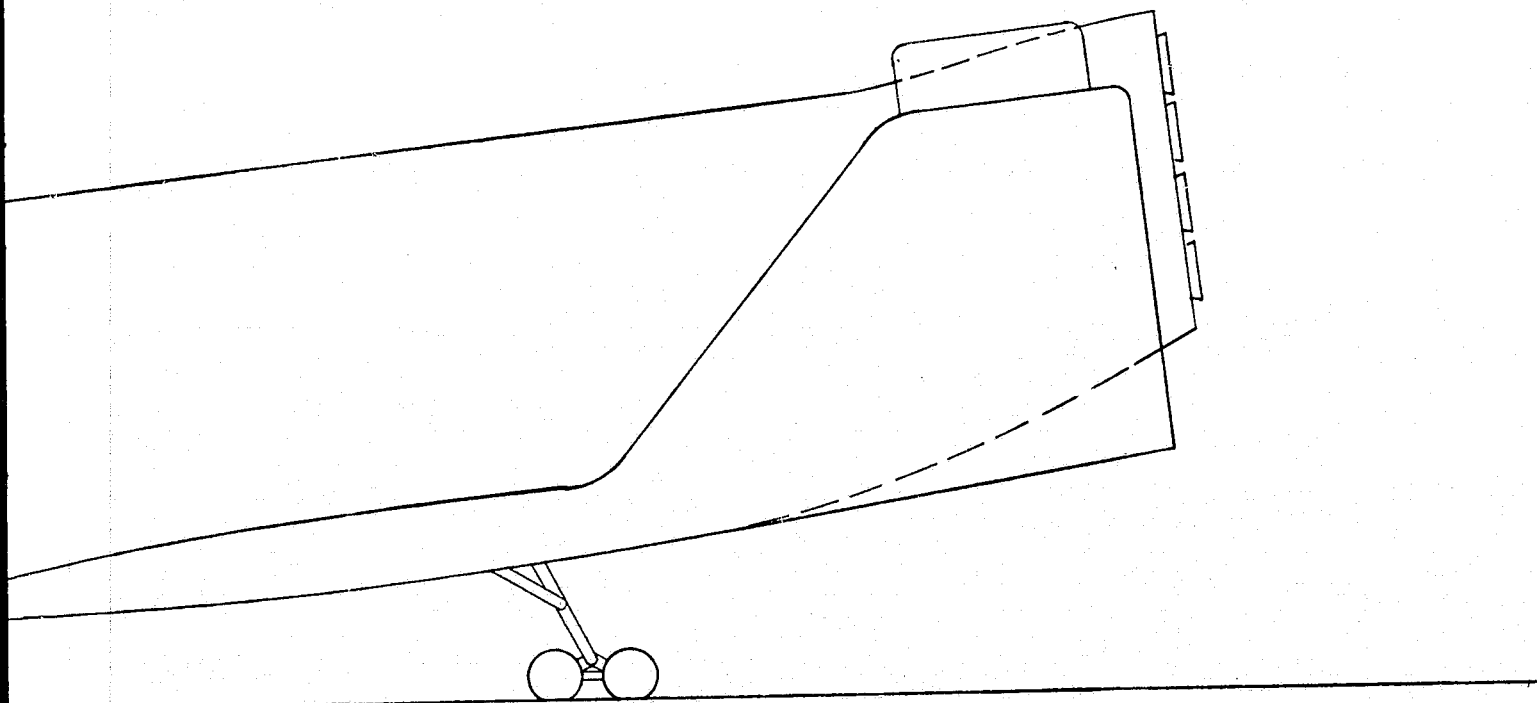
GROUND LEVEL

21 FT

INFLATED SLIDE (I)

BOOSTER

FOLDOUT FRAME 3



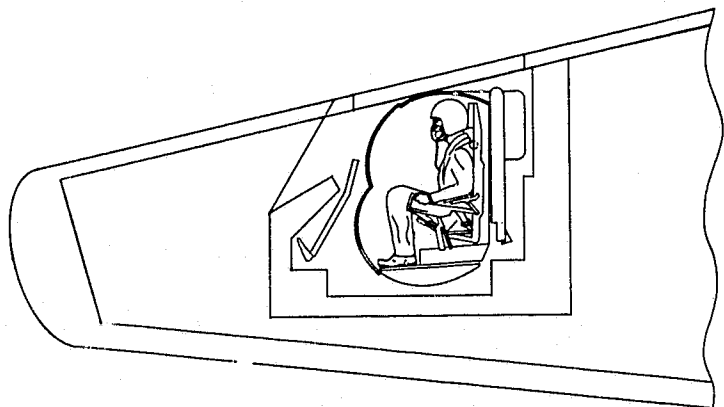
STER

FOLDOUT FRAME

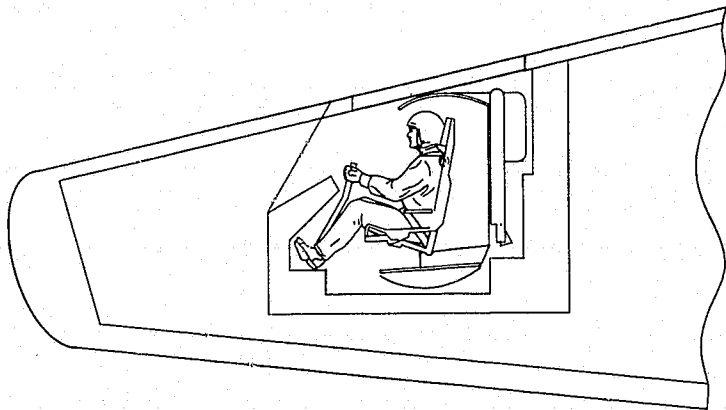
4

POST LANDING  
PERS. ESCAPE PROVISIONS  
1/20 SKJ 100269

A-17

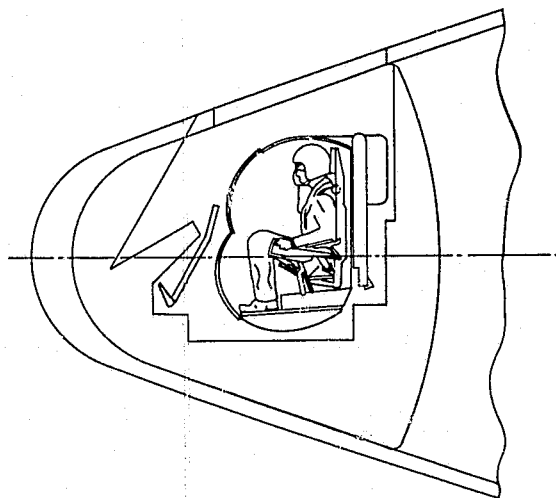


RETRACTED EJECTION POSITION  
ORBITER

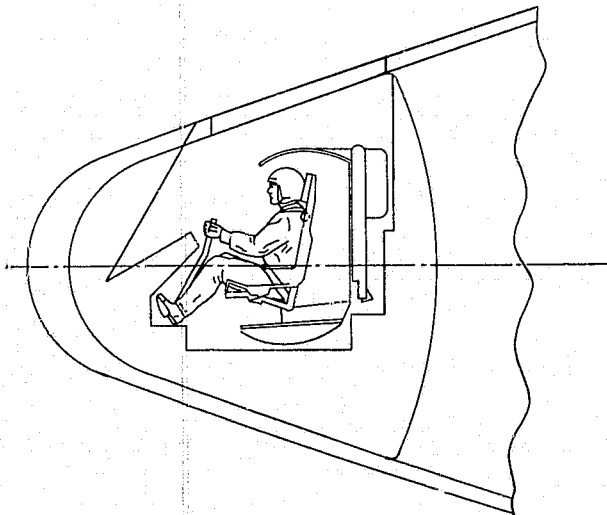


NORMAL FLIGHT POSITION  
ORBITER

FOLDOUT FRAME |



RETRACTED EJECTION POSITION  
BOOSTER



NORMAL FLIGHT POSITION  
BOOSTER

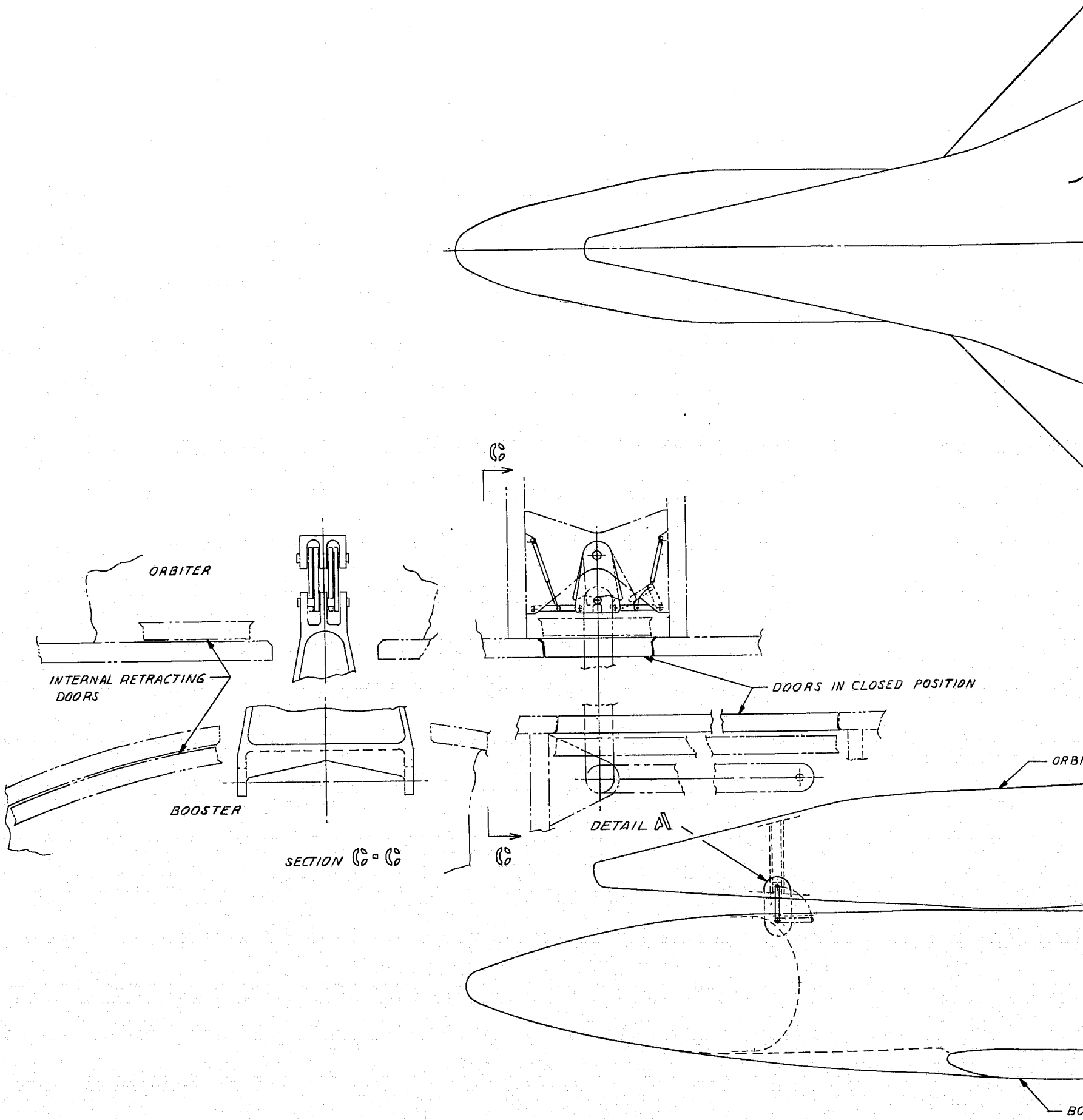
ENCAPSULATED SEAT INSTL.  
PERS. ESCAPE PROVISIONS

A-18

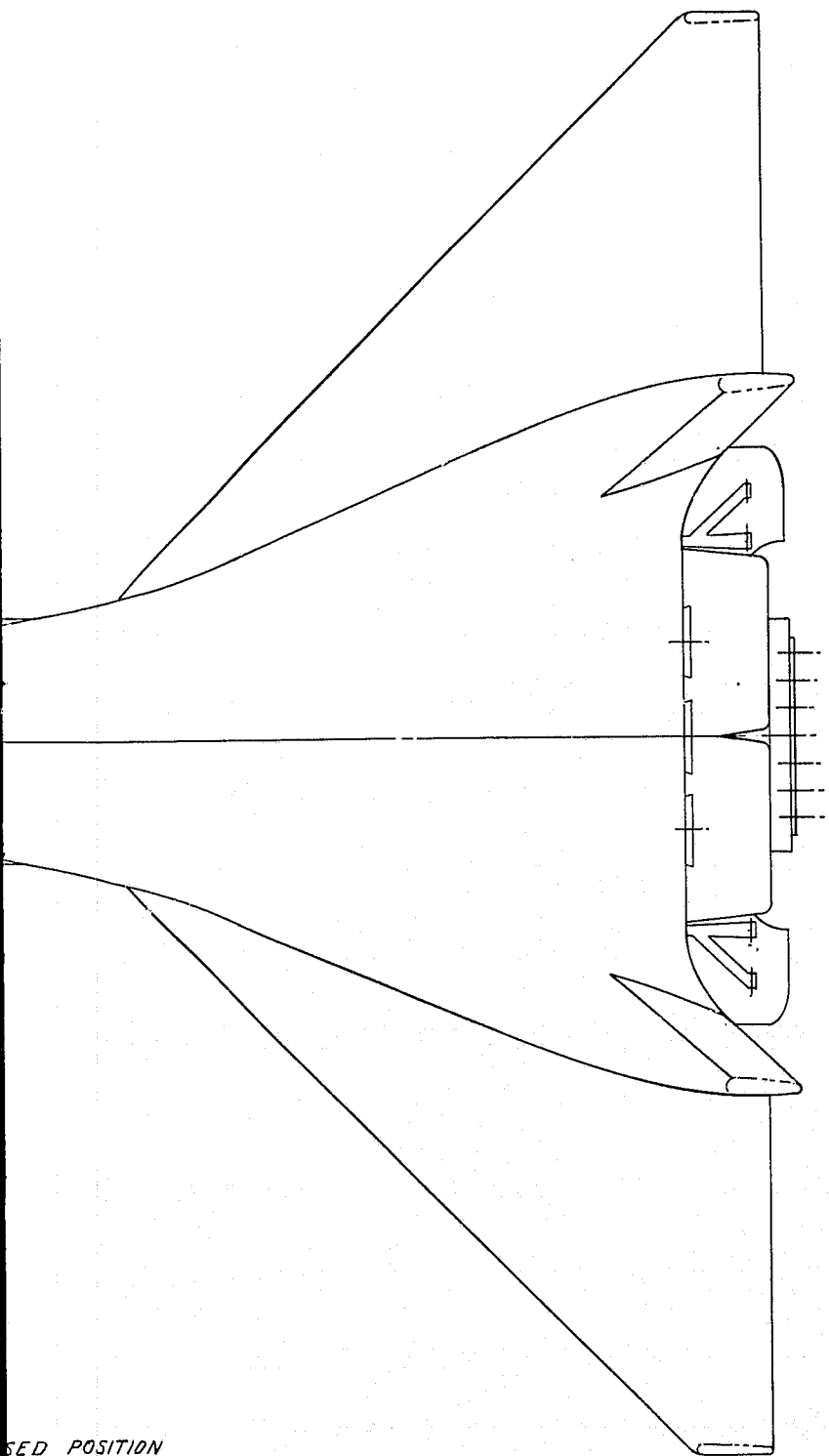
1/30

SKJ 100369

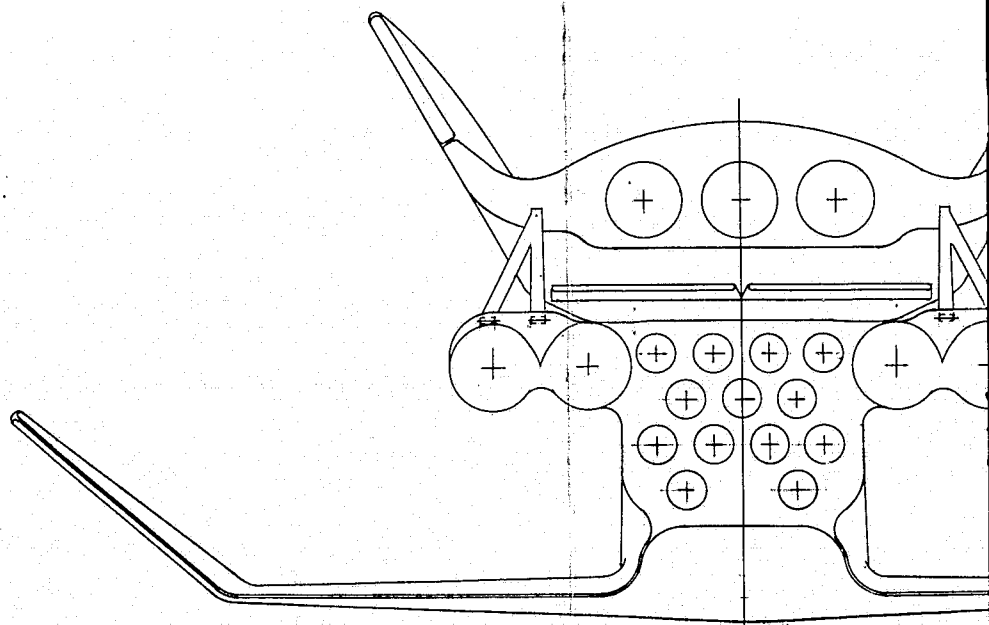
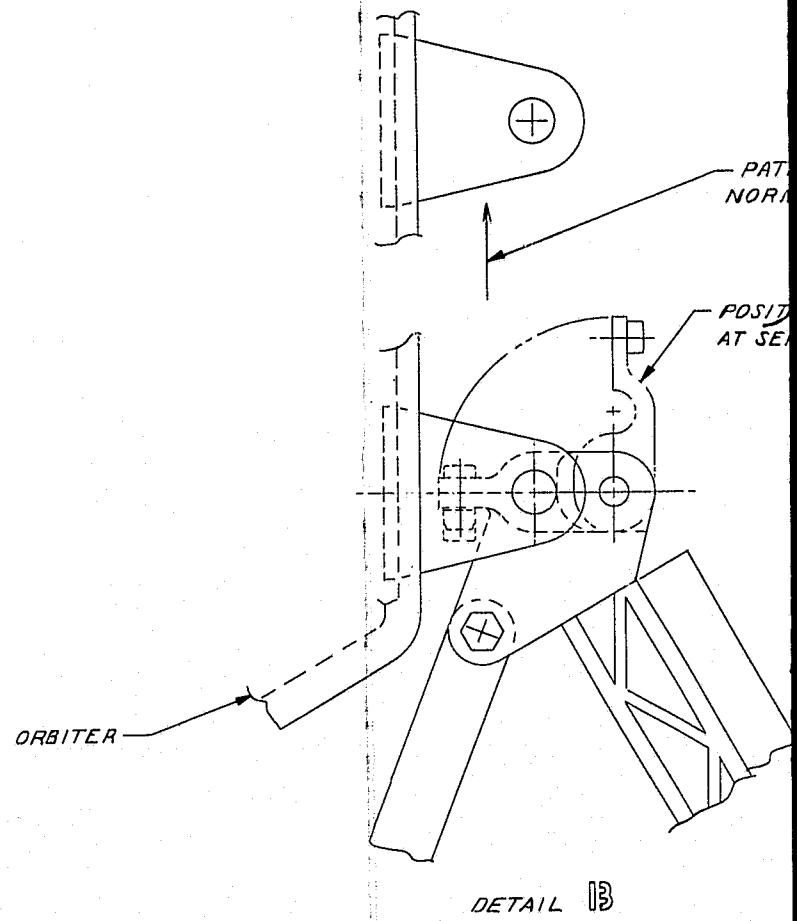
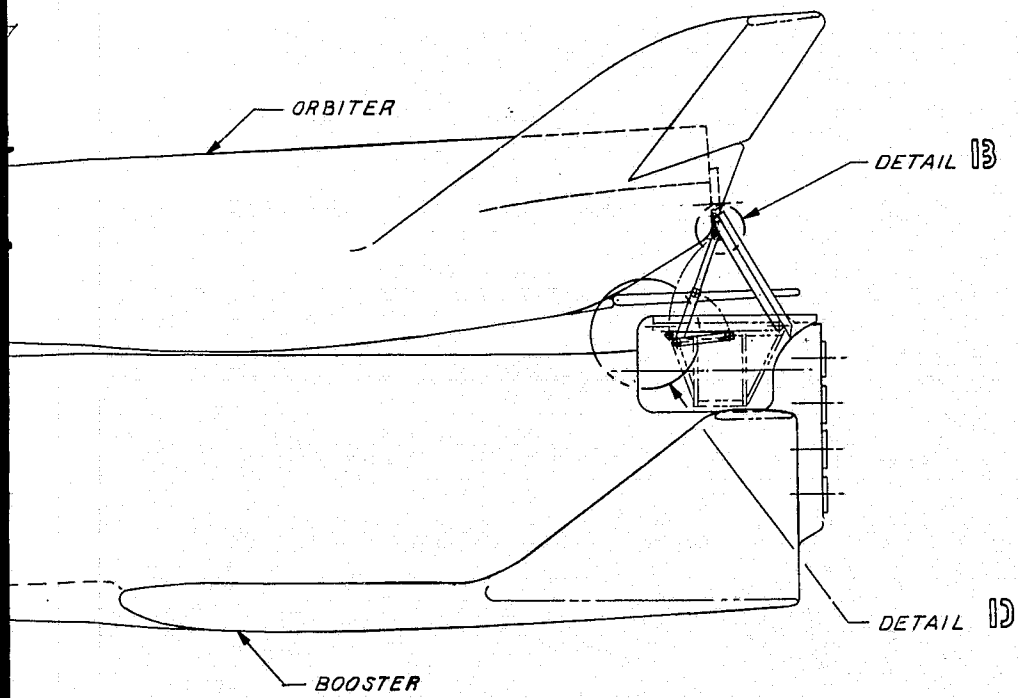
FOLDOUT FRAME 2



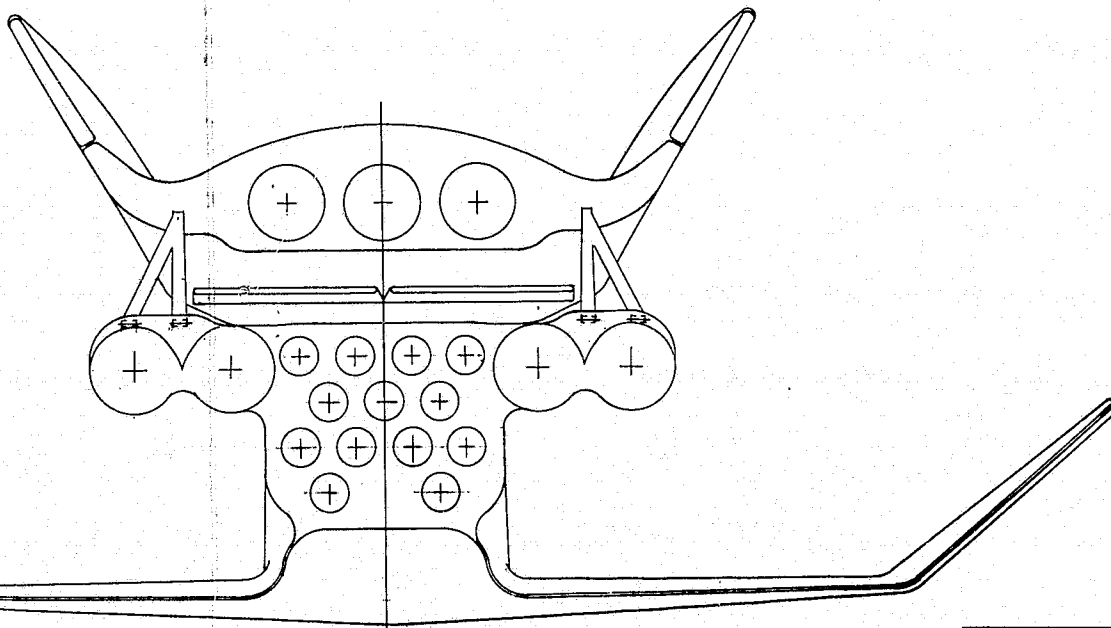
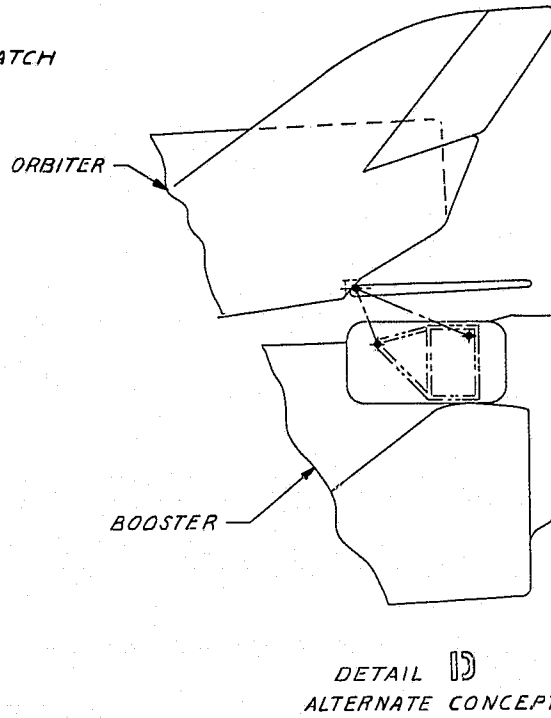
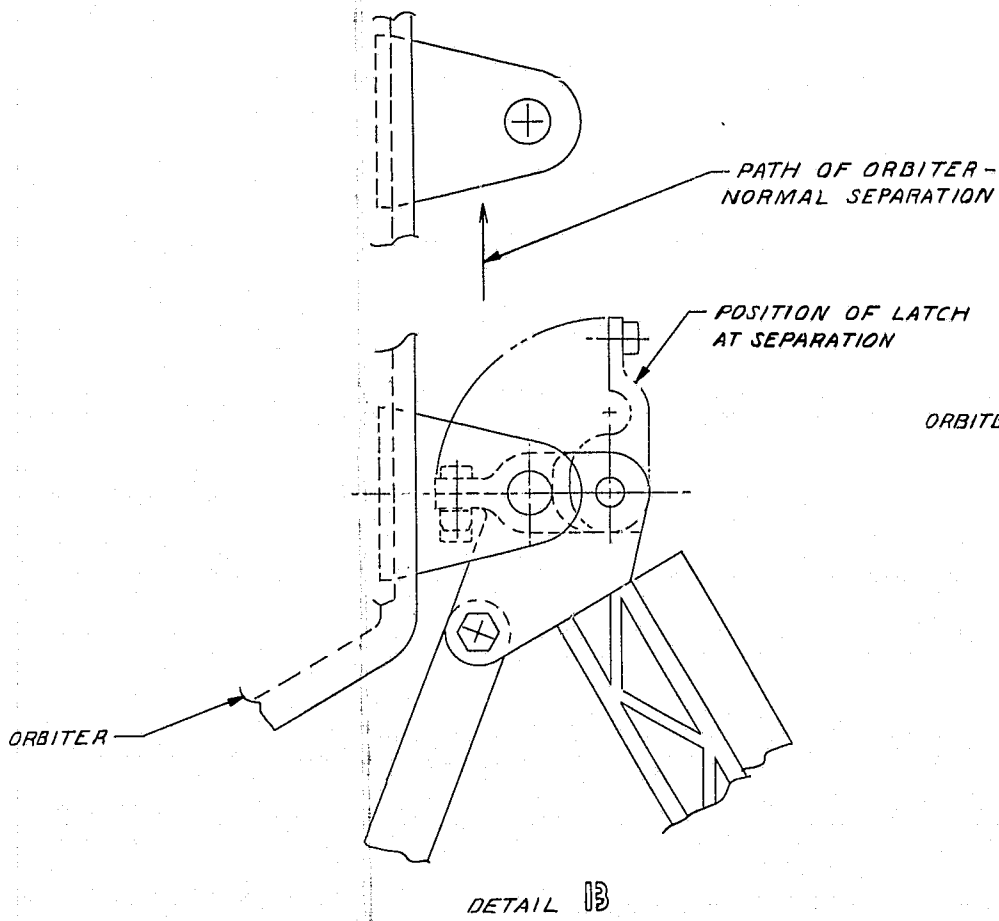
FOLDOUT FRAME |



SED POSITION



FOLDOUT FRAME 2

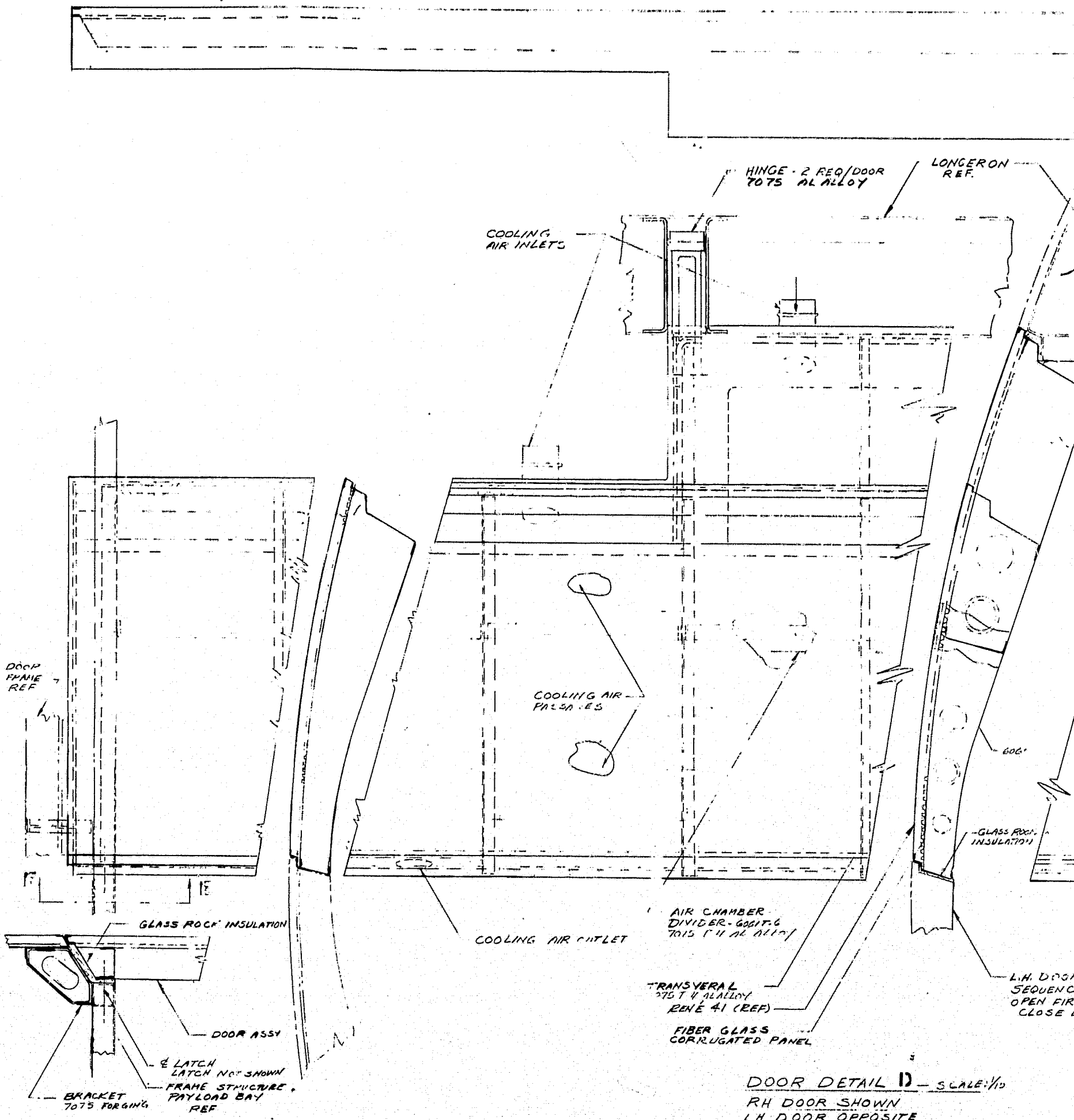


DATE	10/10/69	LOCKHEED MISSILES & SPACE COMPANY						
DR.	J. K. Brainerd	A GROUP DIVISION OF LOCKHEED AIRCRAFT CORPORATION						
		SUNNYVALE, CALIFORNIA						
APPD		<b>3 POINT ATTACHMENT CONCEPT 2 STAGE SYSTEM</b>						
ENGRG								
CHK								
APPD					SIZE	CODE IDENT	DRAWING NO.	REV
APPD							SKB101069	
		SCALE		SHEET	1 of 1			

FOLDOUT FRAME 3

A-19

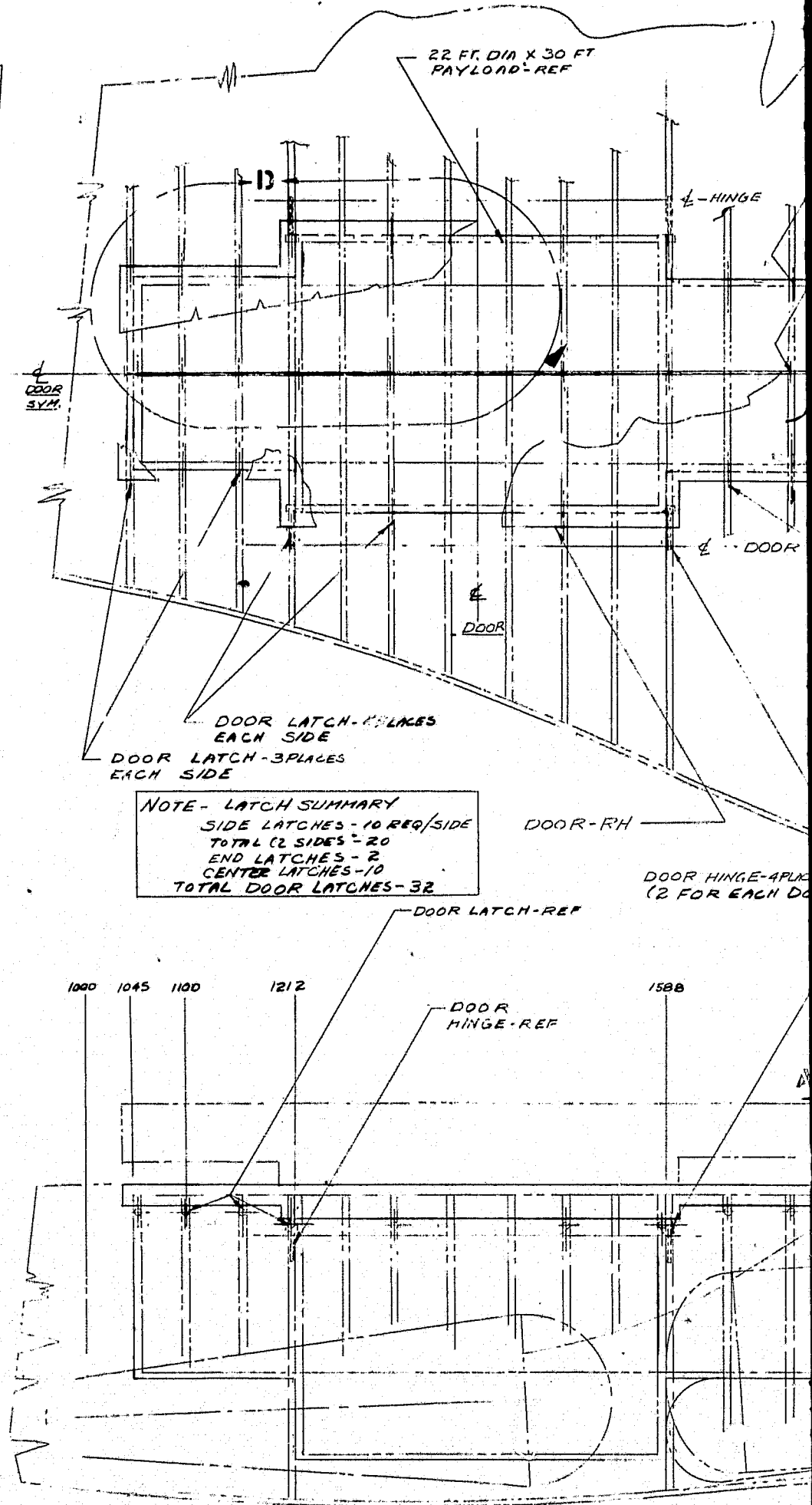
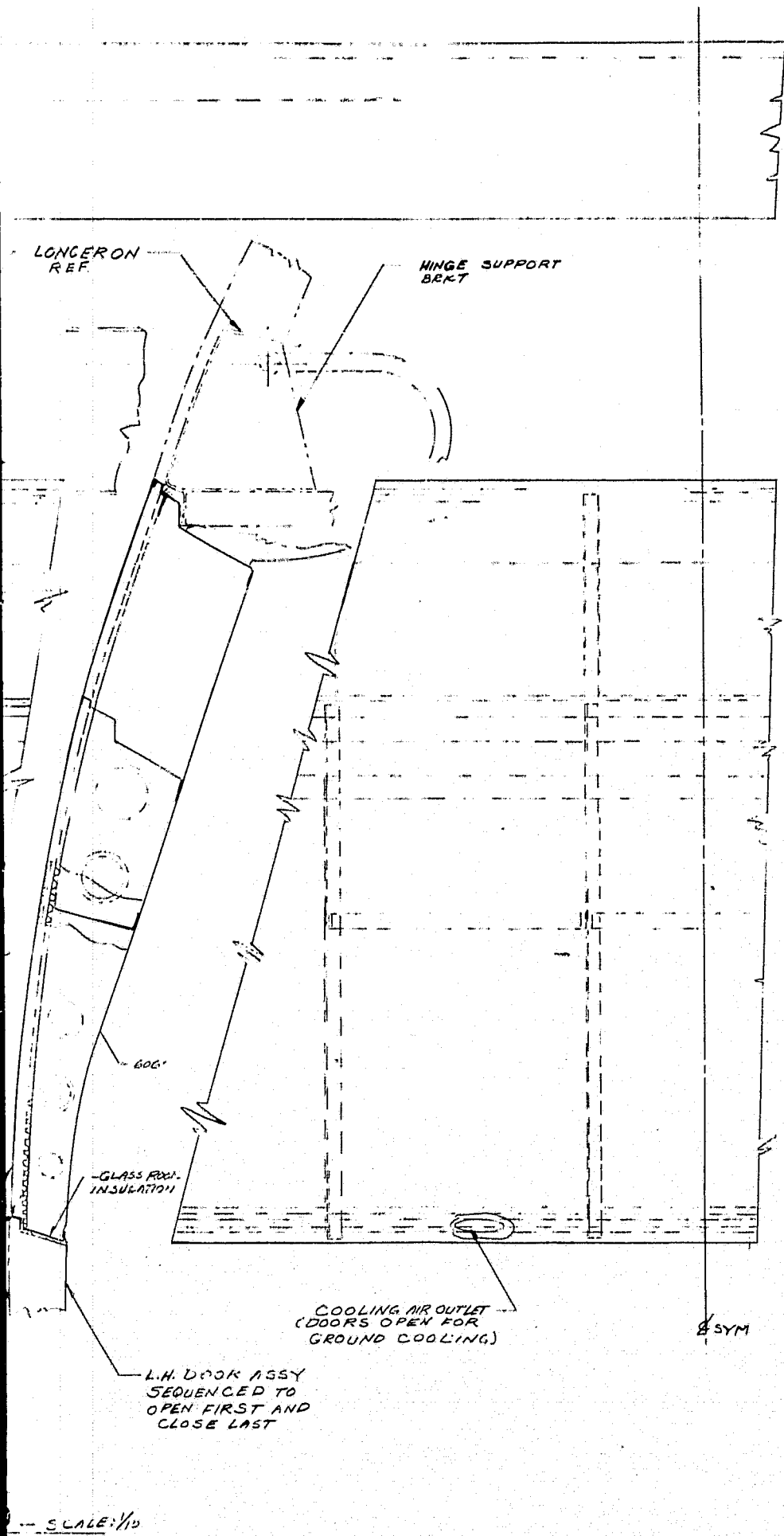


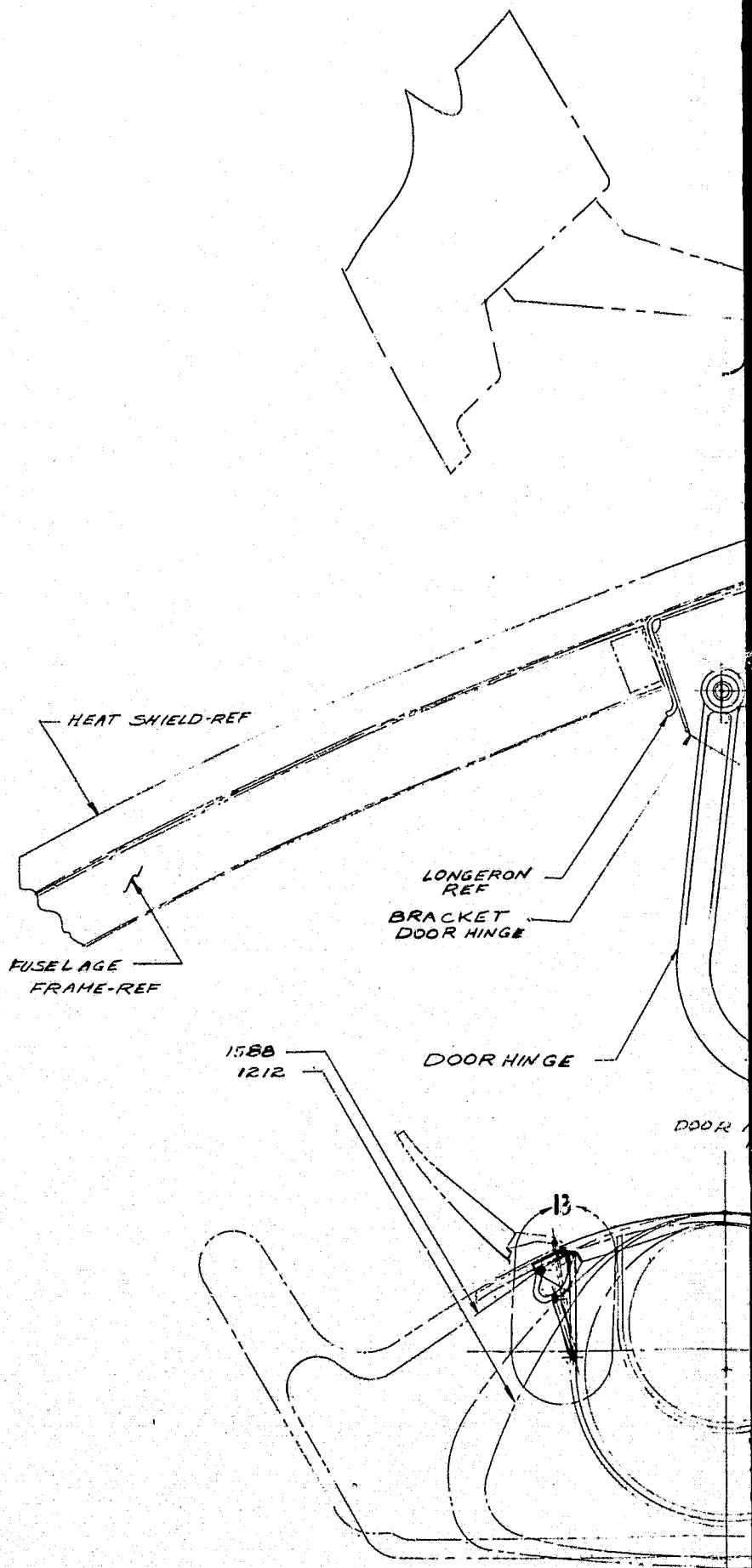
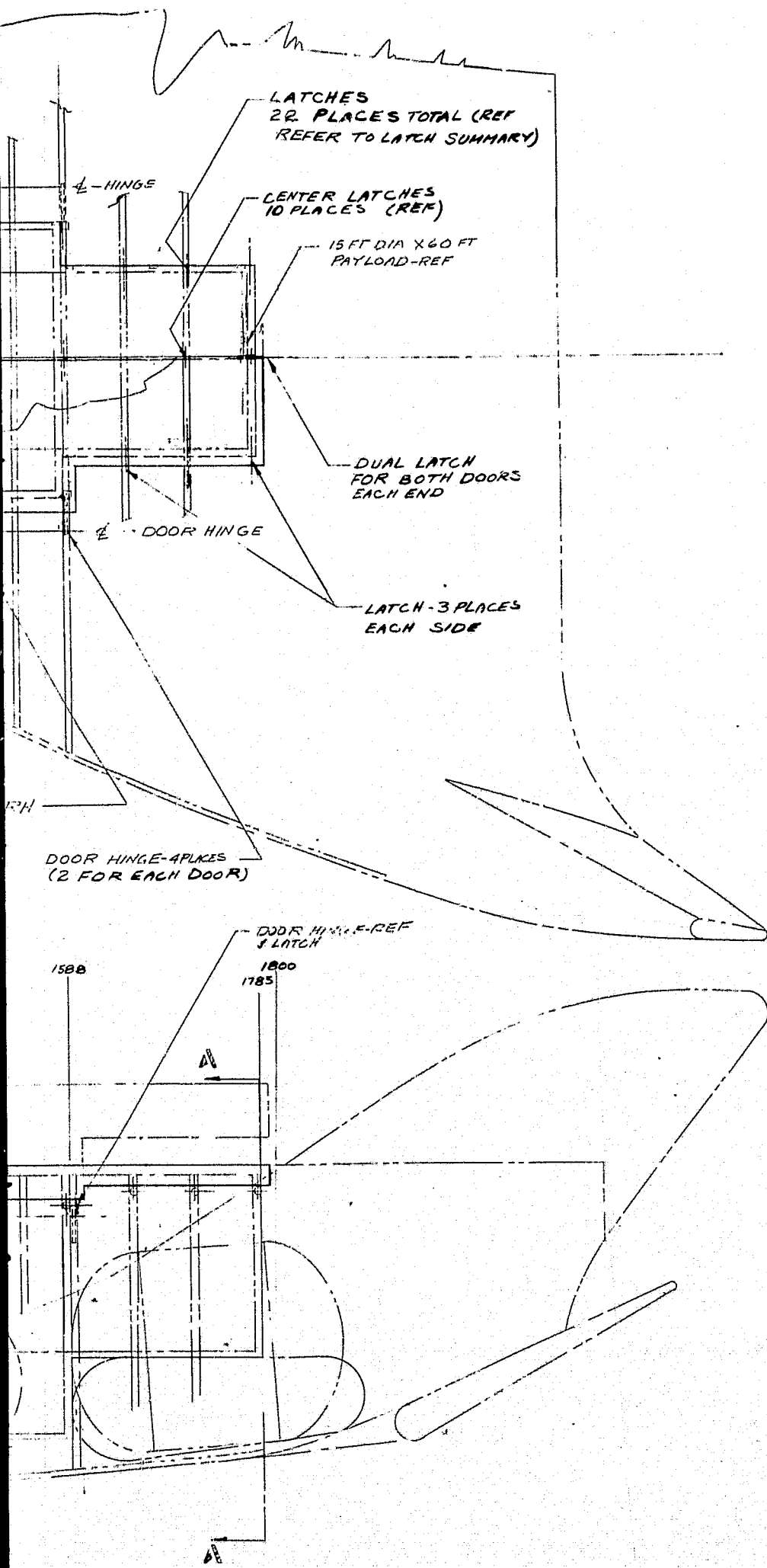


**VIEW E E**  
 SCALE 1/16

**DOOR DETAIL D** - SCALE 1/16  
 RH DOOR SHOWN  
 LH DOOR OPPOSITE  
 EXCEPT AS NOTED

**FOLDOUT FRAME**

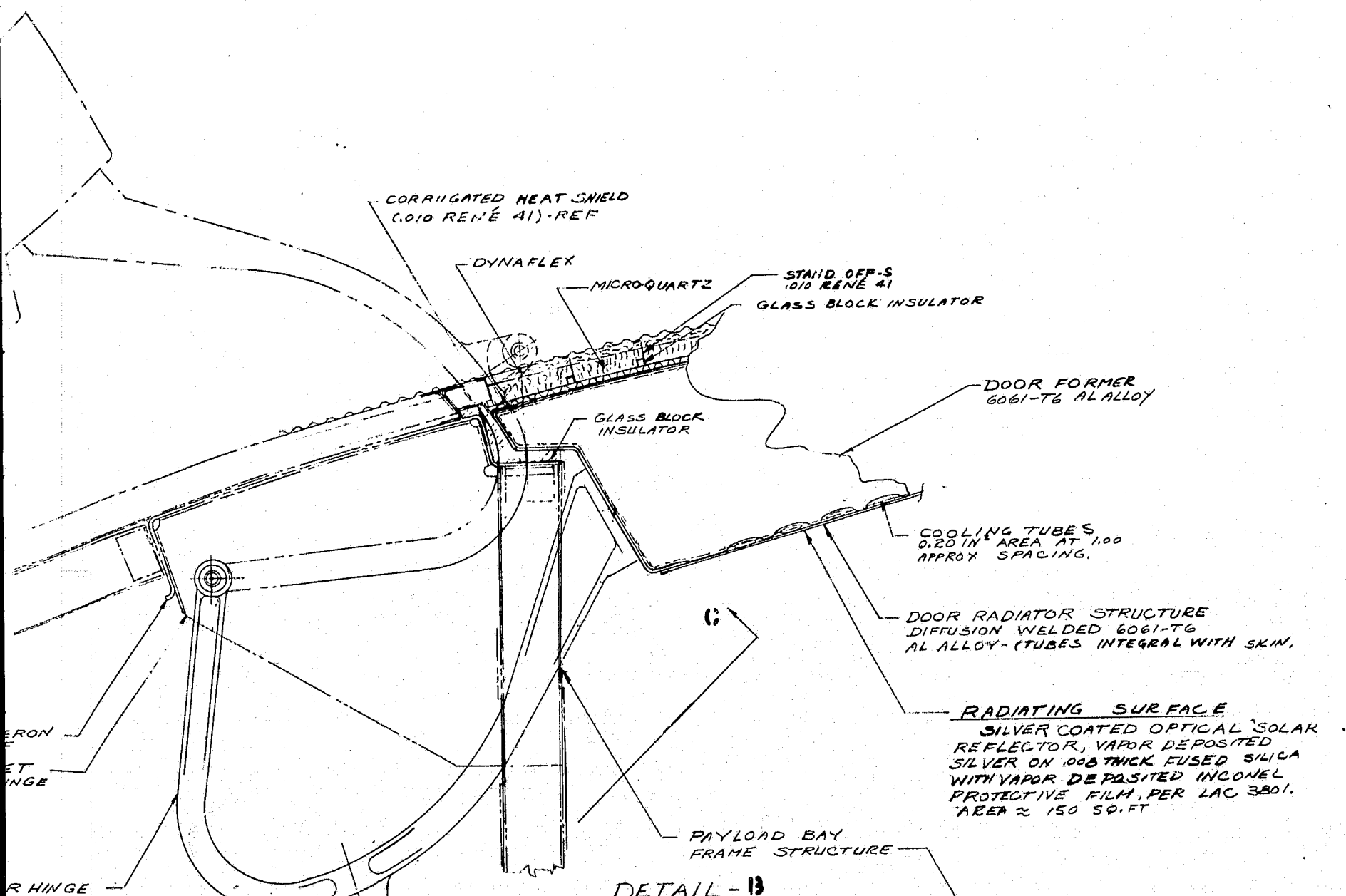




VIEW A  
 LOOKING F  
 @ STA 178

**FOLDOUT FRAME 3**

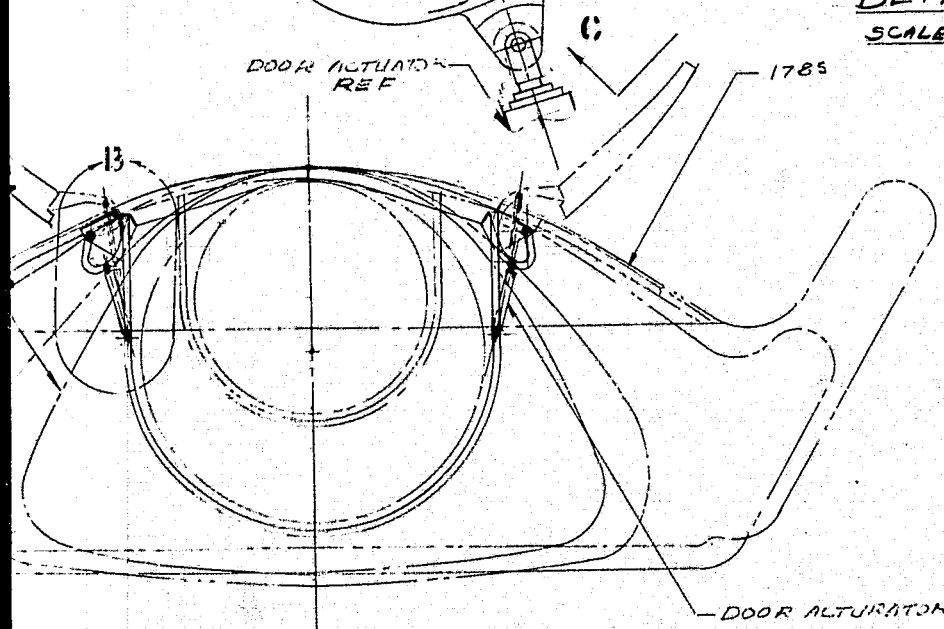
FOLDOUT FRA



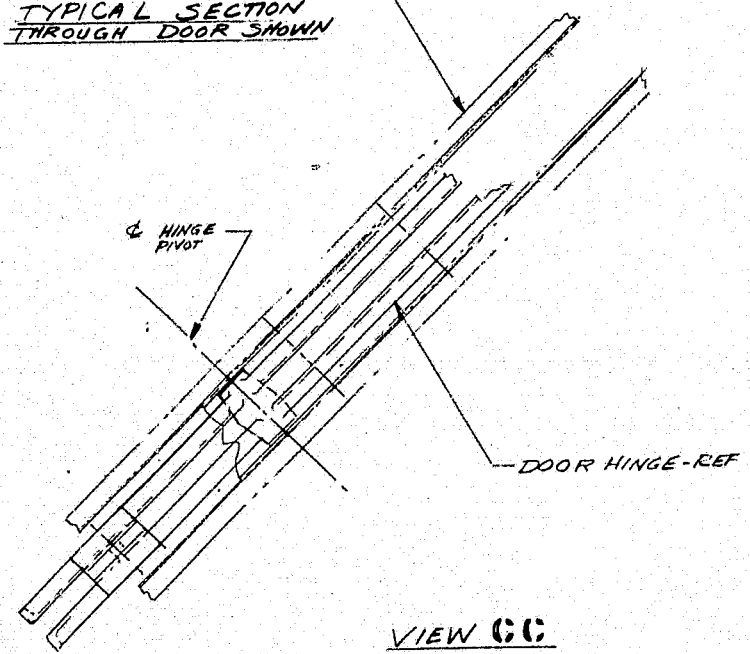
**DETAIL - 13**

SCALE ≈ 1/4

TYPICAL SECTION  
THROUGH DOOR SHOWN



VIEW A-A  
LOOKING FWD  
@ STA 1785



VIEW CC  
SCALE ≈ 1/4

FOLDOUT FRAME

FOLDOUT FRAME 4

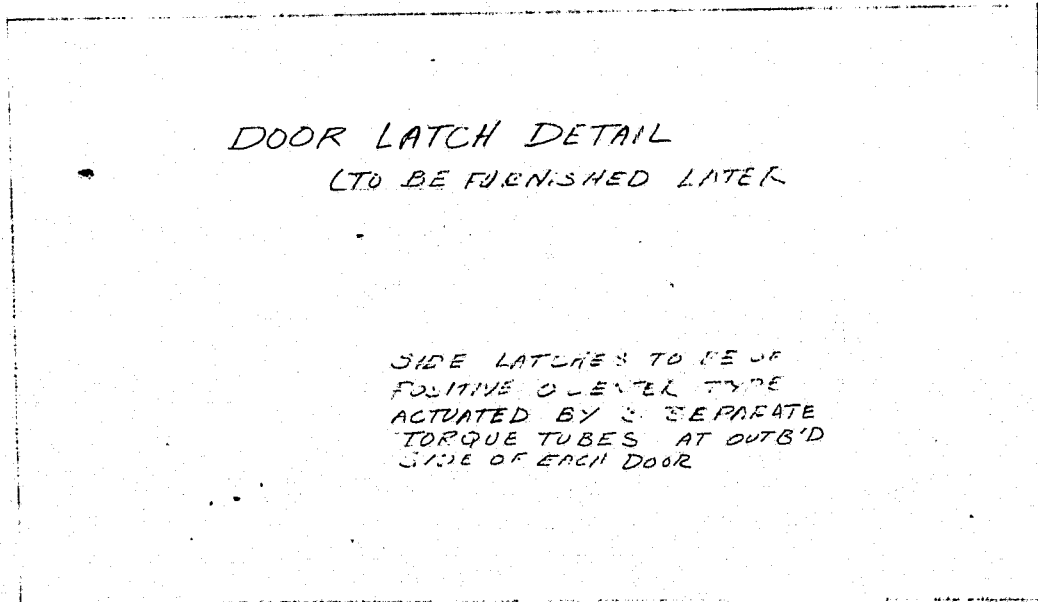
FORMER  
ALLOY

S  
1.00  
G.

STRUCTURE  
ED 6061-T6  
INTEGRAL WITH SKIN.

SURFACE  
ATED OPTICAL SOLAR  
VAPOR DEPOSITED  
PB THICK FUSED SILICA  
E POSITED INCONEL  
FILM, PER LAC 3801.  
SQ. FT

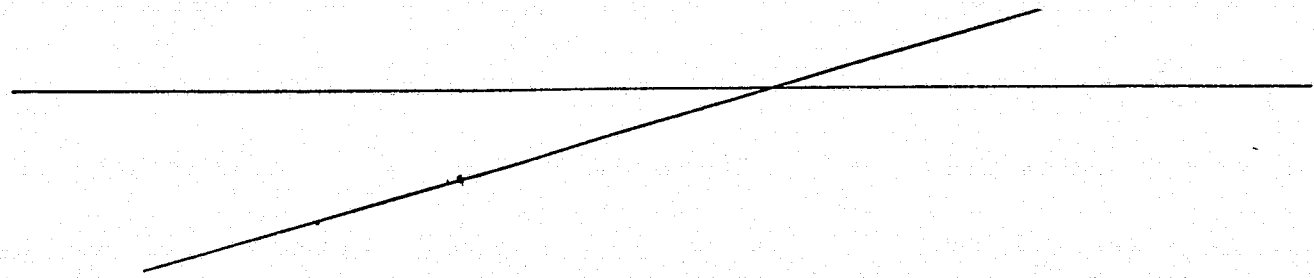
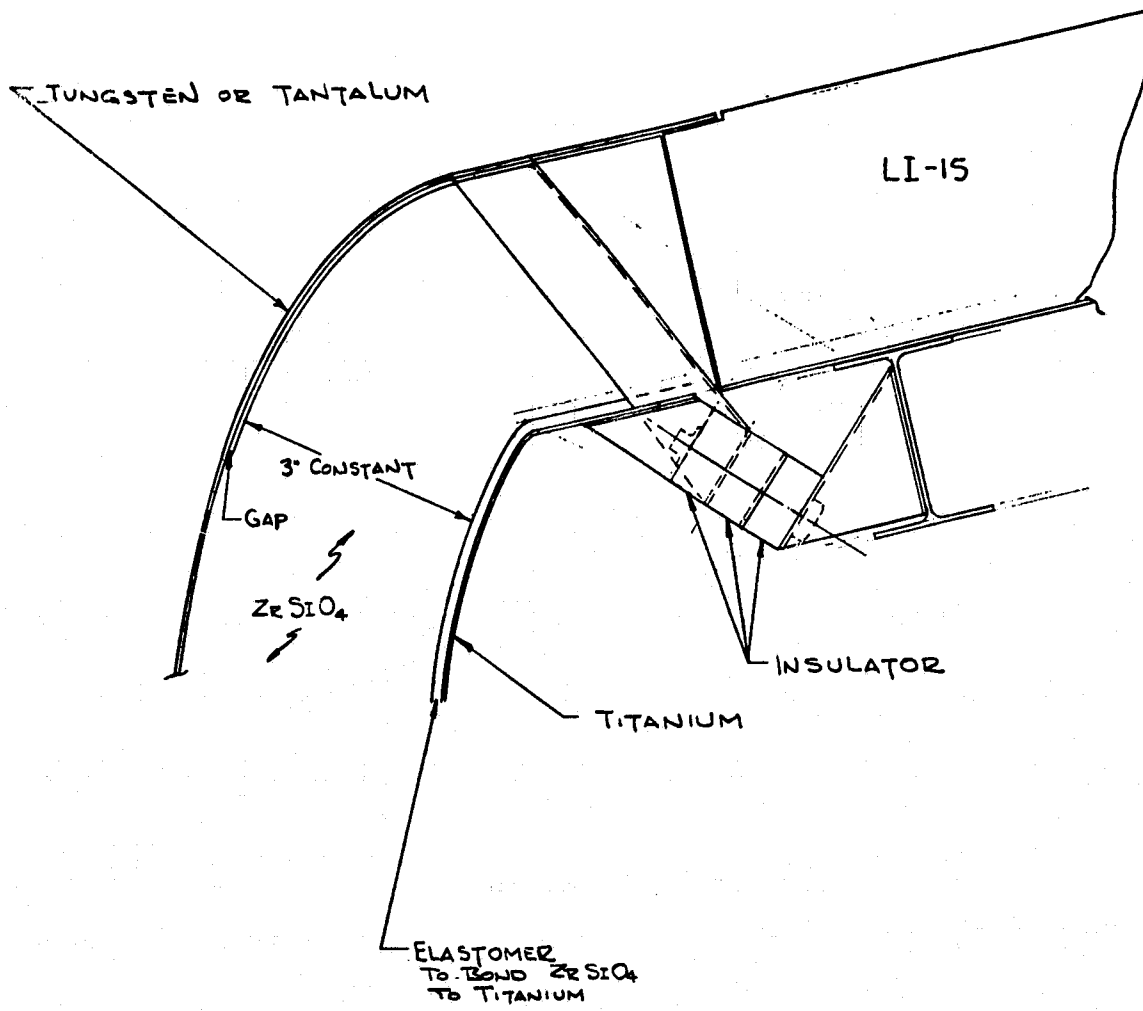
OR HINGE-REF



UNLESS OTHERWISE SPECIFIED DIM. ARE IN INCHES. TOLERANCES ON:	DATE 10-15-69	LOCKHEED MISSILES & SPACE COMPANY A GROUP DIVISION OF LOCKHEED AIRCRAFT CORPORATION SUNNYVALE, CALIFORNIA	
FRACTIONS = ± 1/16	DR H.K. Moss	DOOR STRUCTURE	
DECIMALS: .X = ± .1	APPD	PAYLOAD BAY	
.XX = ± .03	APPD	2 STAGE SYSTEM	
.XXX = ± .010	ENGRG	SIZE	CODE IDENT
ANGLES = ± 2 DEG	CHK	DRAWING NO.	REV
CONTR	APPD	SKM 10156	
CCA/CEI	APPD	SCALE: 1/2" = 1'-0"	SHEET 1 of 1

FOLDOUT FRAME 5

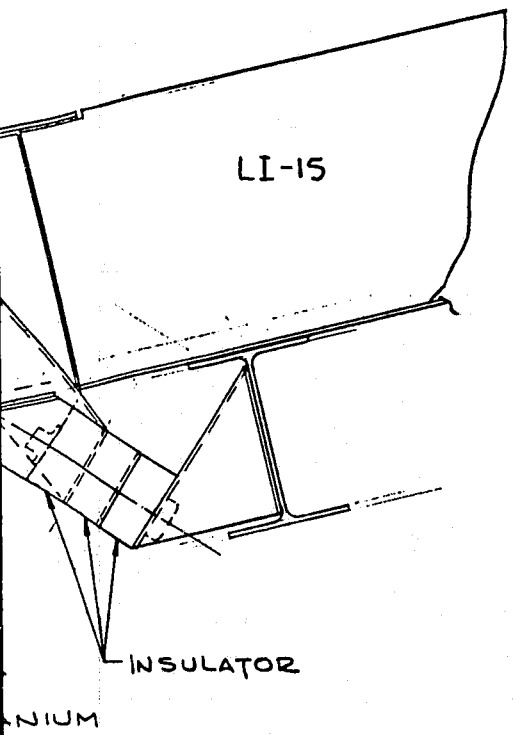
A-20



DATE	6-
DR	R. H.
APPD	
APPD	
ENGRG	
CHK	
APPD	
APPD	

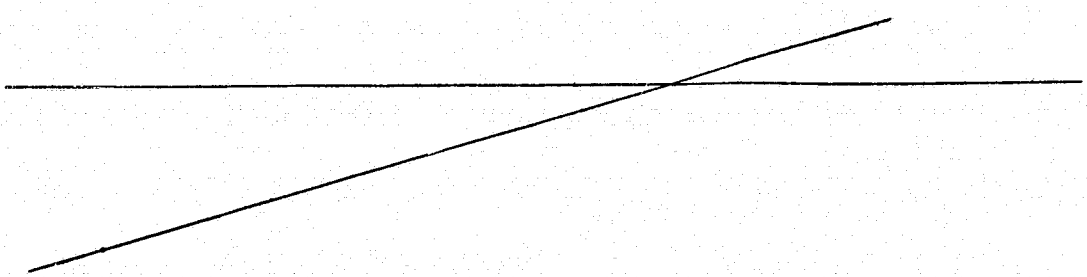
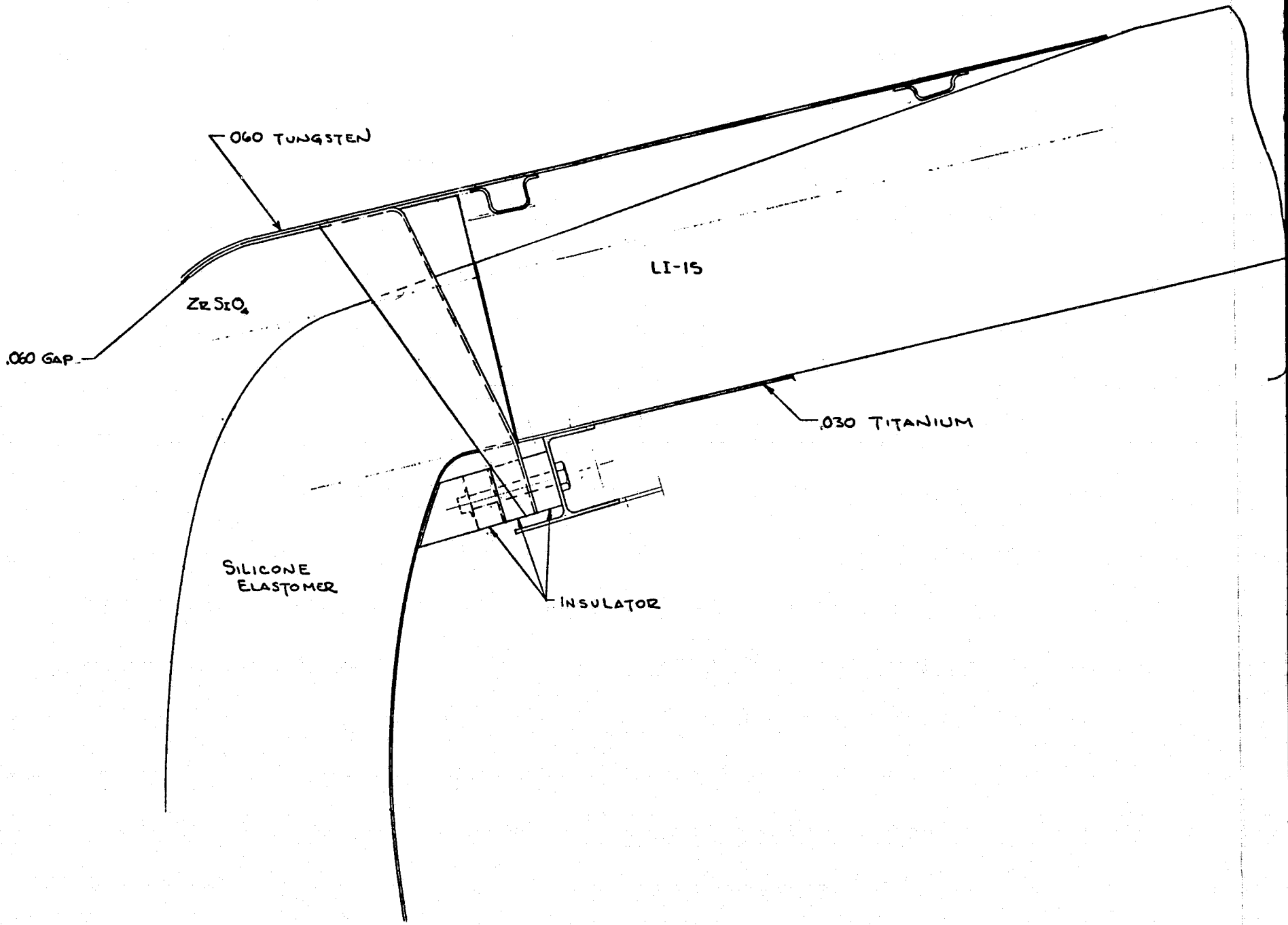
FOLDOUT FRAME 1

FOLDO



DATE	6-9-69			LOCKHEED MISSILES & SPACE COMPANY	
DR	R. HADLER			A GROUP DIVISION OF LOCKHEED AIRCRAFT CORPORATION	
APPD				SUNNYVALE, CALIFORNIA	
ENGRG				NOSE CAP CONCEPT 1	
CHK				W-ZR S±Q <sub>4</sub> - TI	
APPD	SIZE	CODE IDENT	DRAWING NO.	REV	
APPD			SKR 060969		
	SCALE	1/1		SHEET	

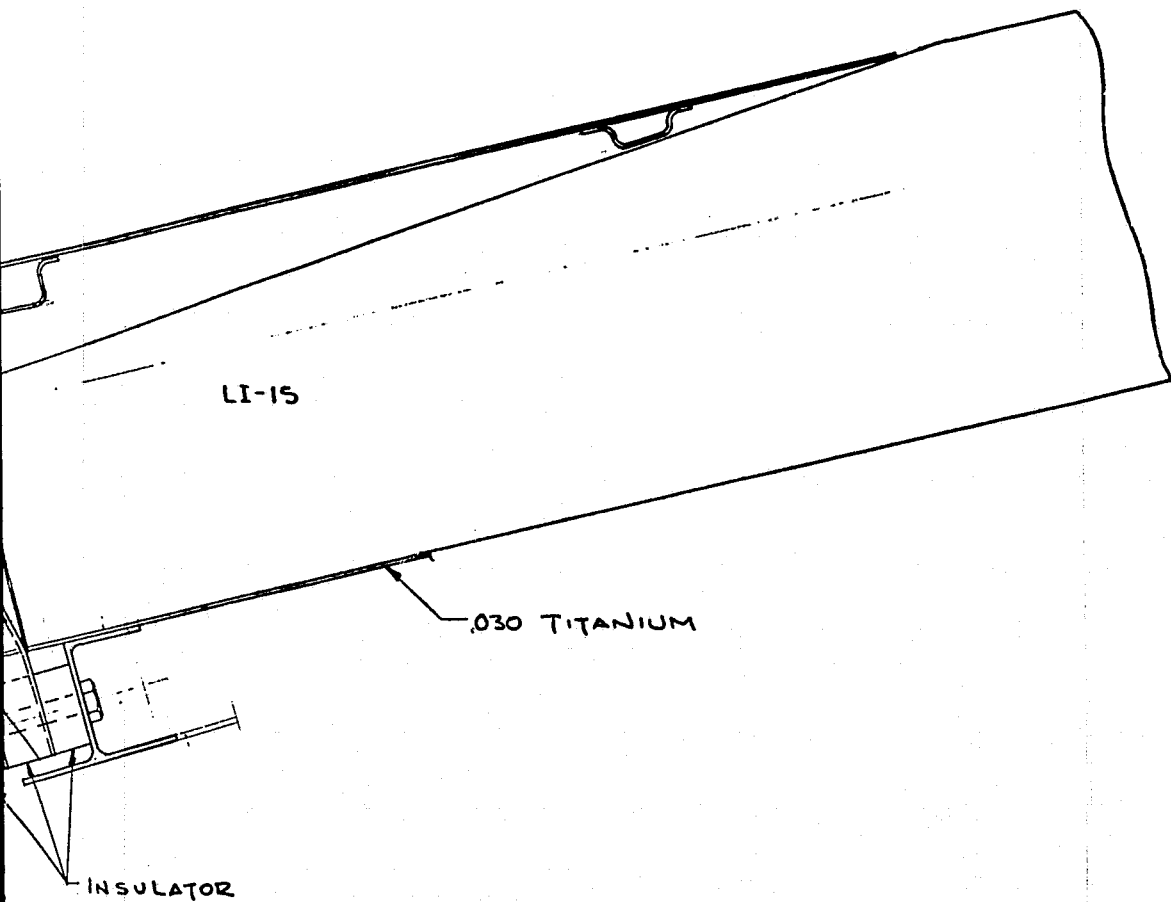
FOLDOUT FRAME 2A-21



DATE	6-6-69	LOCKHEED MISSILES & SPACE	
DR	R. HACKER	A GROUP DIVISION OF LOCKHEED CORP. SUNNYVALE, CALIF.	
APPD		NOSE CAP	
ENGRG		W-ZrSiO <sub>4</sub>	
CHK			
APPD		SIZE	CODE IDENT
APPD		SCALE	1/1

FOLDOUT FRAME 1



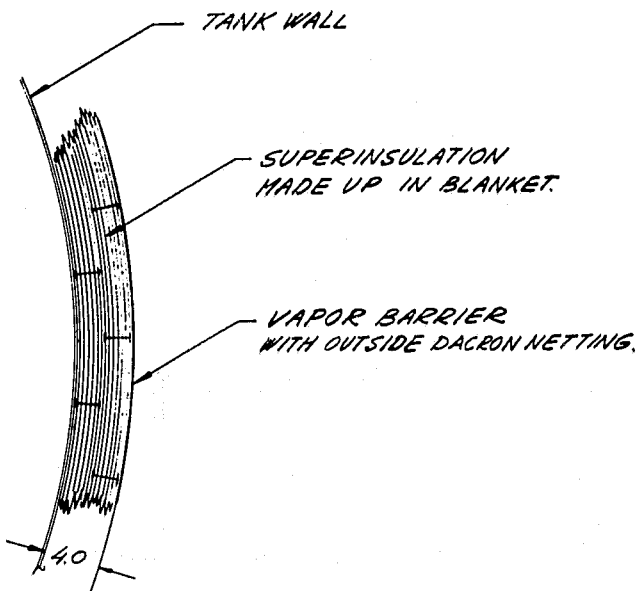


DATE	6-6-69			LOCKHEED MISSILES & SPACE COMPANY	
DR	R HACKER			A GROUP DIVISION OF LOCKHEED AIRCRAFT CORPORATION	
APPD				SUNNYVALE, CALIFORNIA	
ENGRG				NOSE CAP CONCEPT 3	
CHK				W-ZrSiO <sub>4</sub> -SILICONE ELASTOMER-Ti	
APPD	SIZE	CODE IDENT	DRAWING NO.	REV	
APPD			SKR060669		
	SCALE	1/1		SHEET	

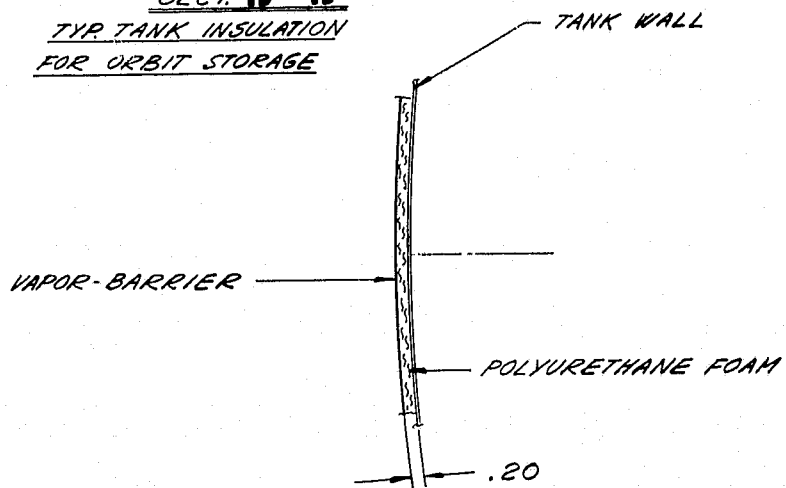
A-22

FRONT FRAME 2

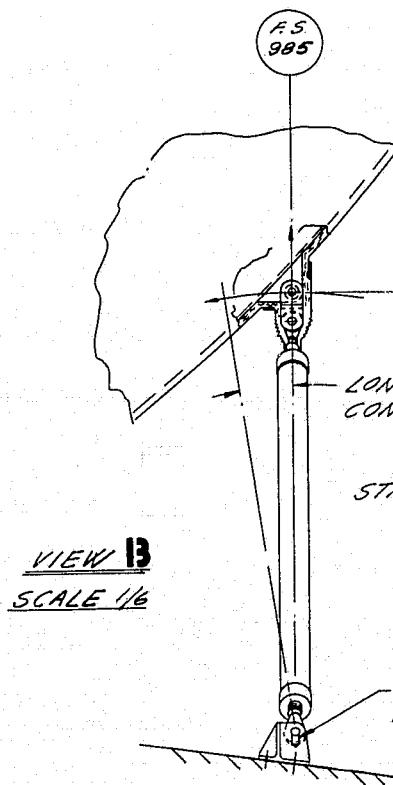
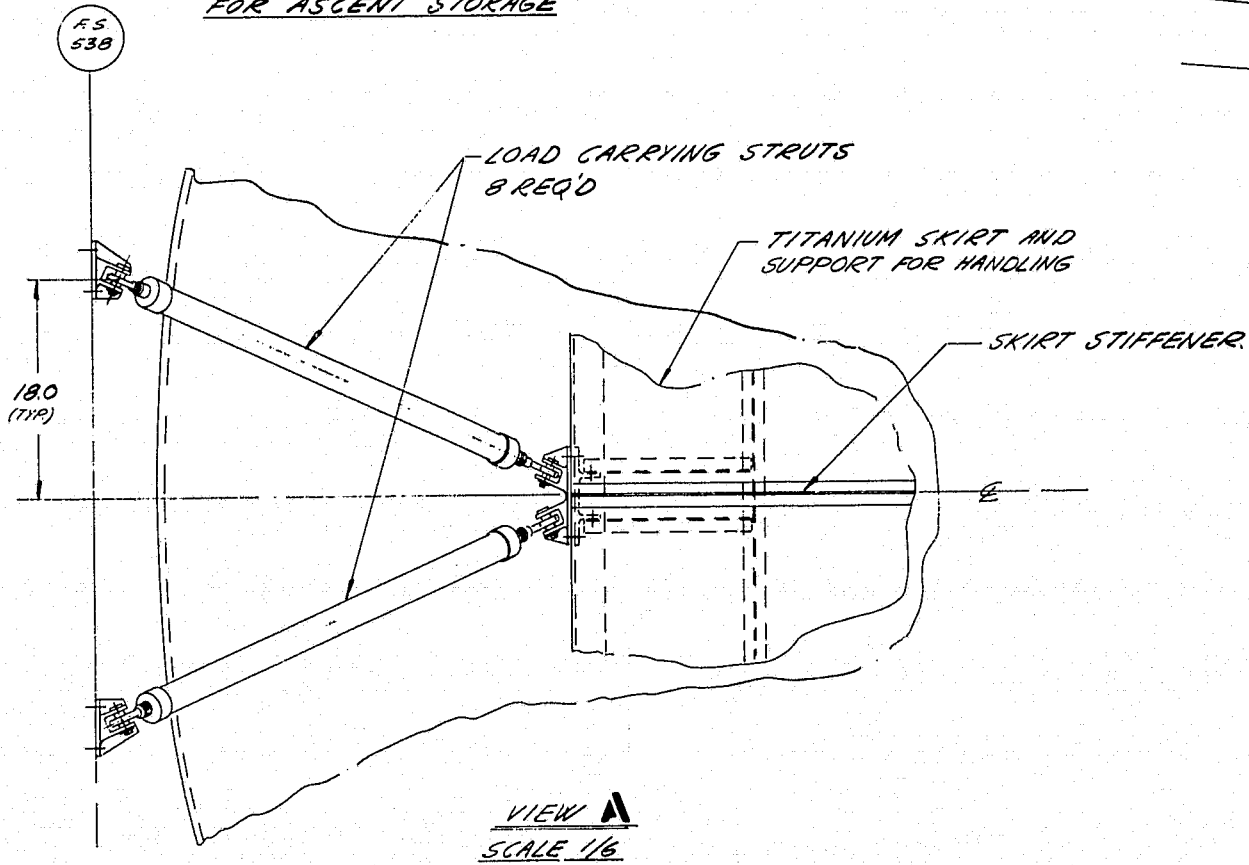
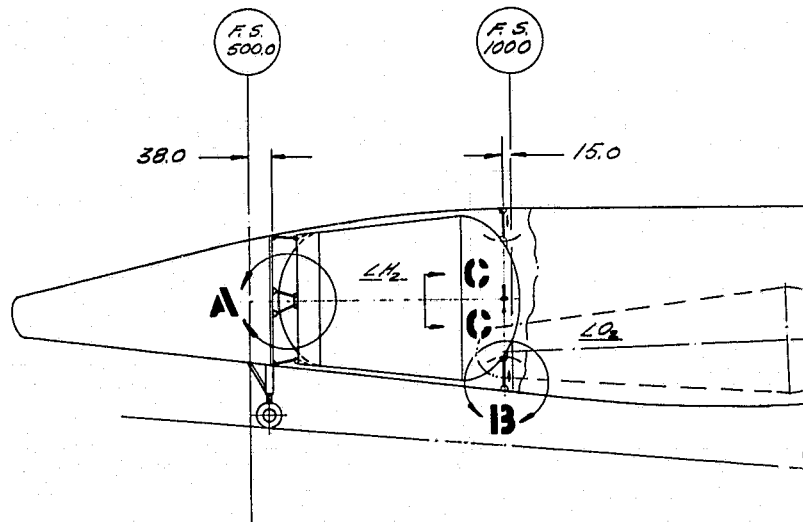
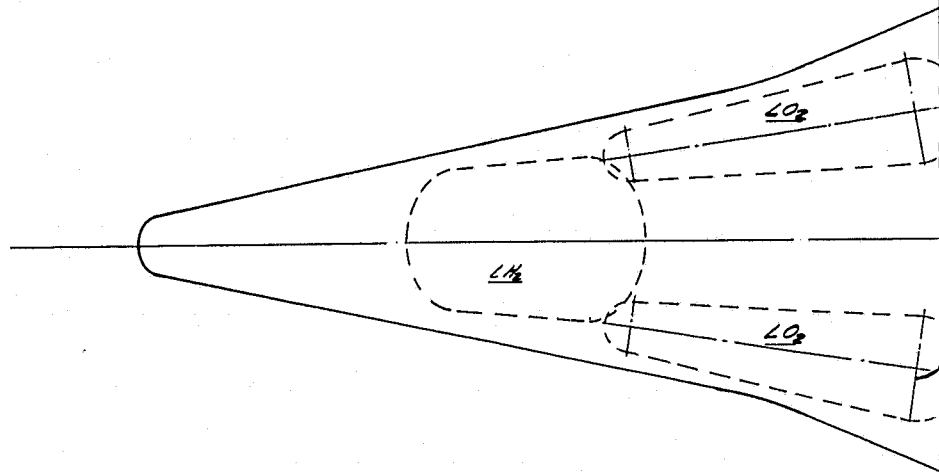
FRAME 1



**SECT D-D**  
TYP. TANK INSULATION  
FOR ORBIT STORAGE

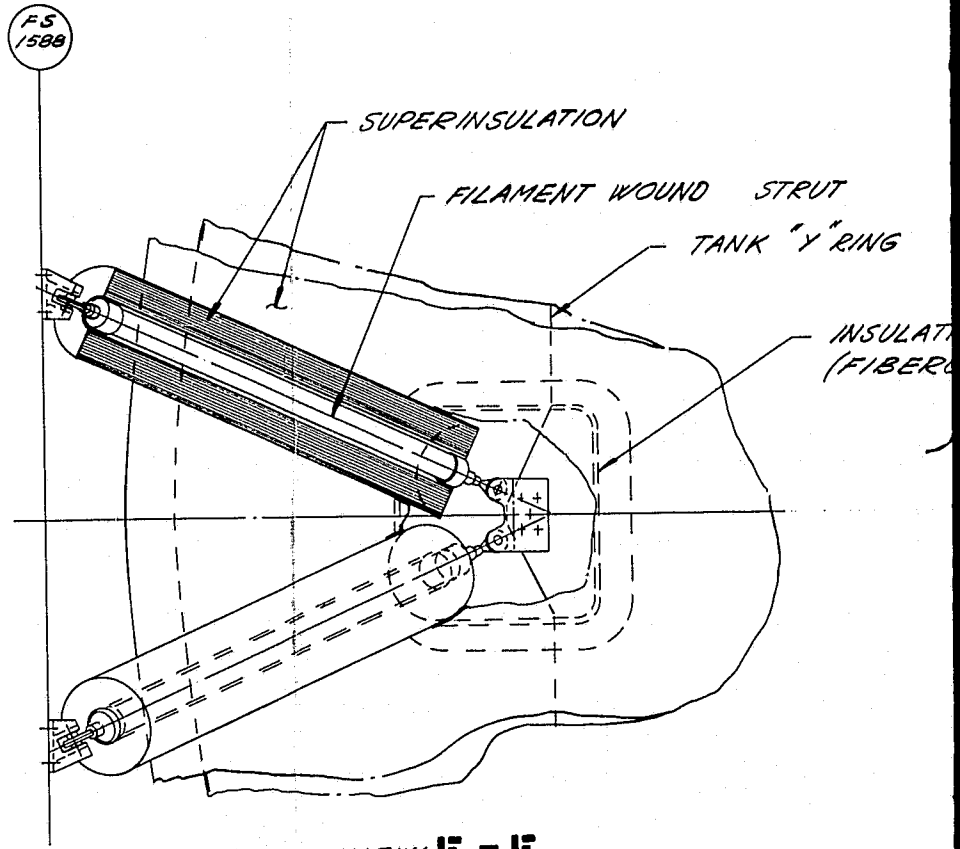
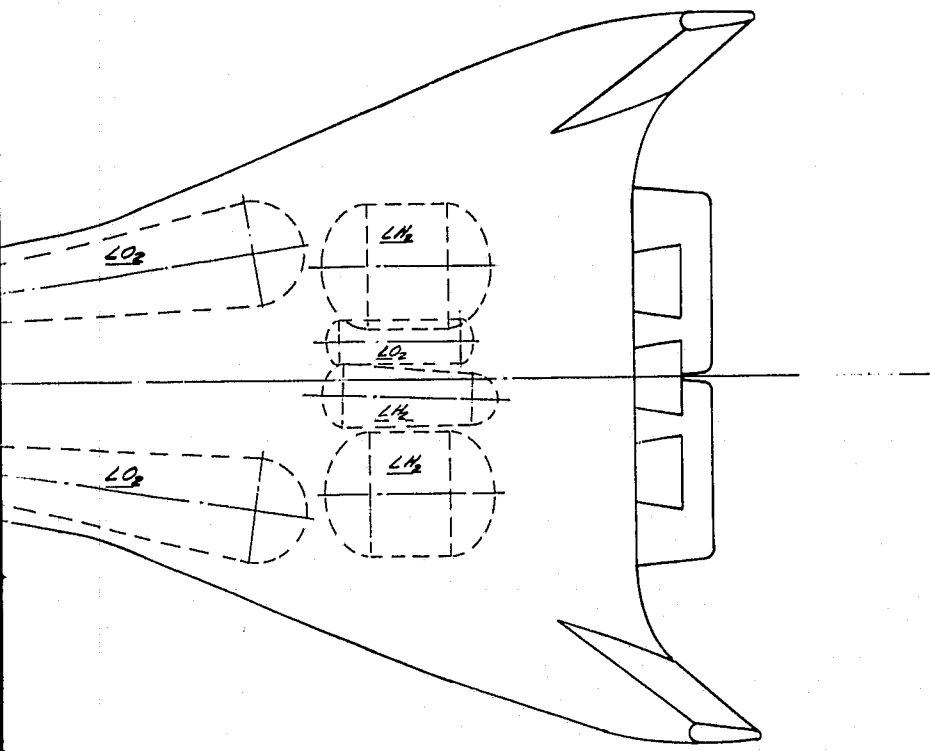


**SECT G-G**  
TYP. TANK INSULATION  
FOR ASCENT STORAGE

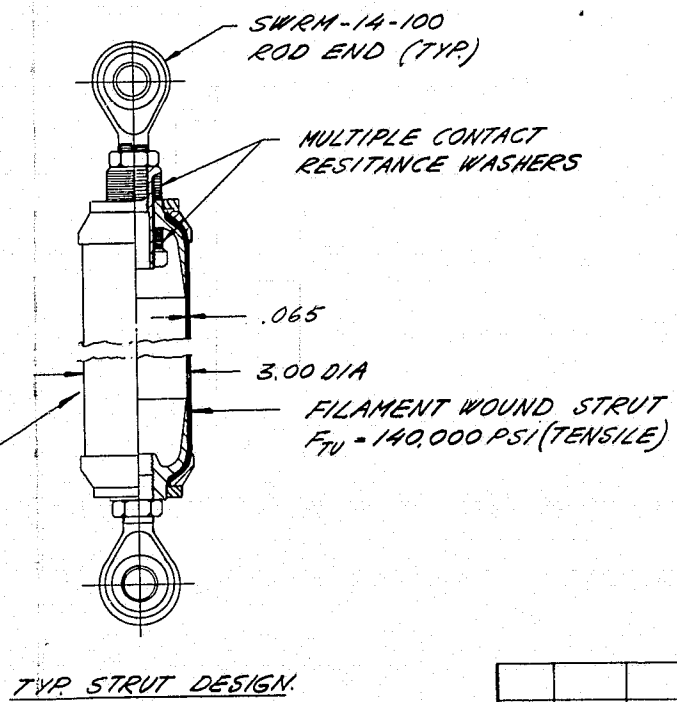
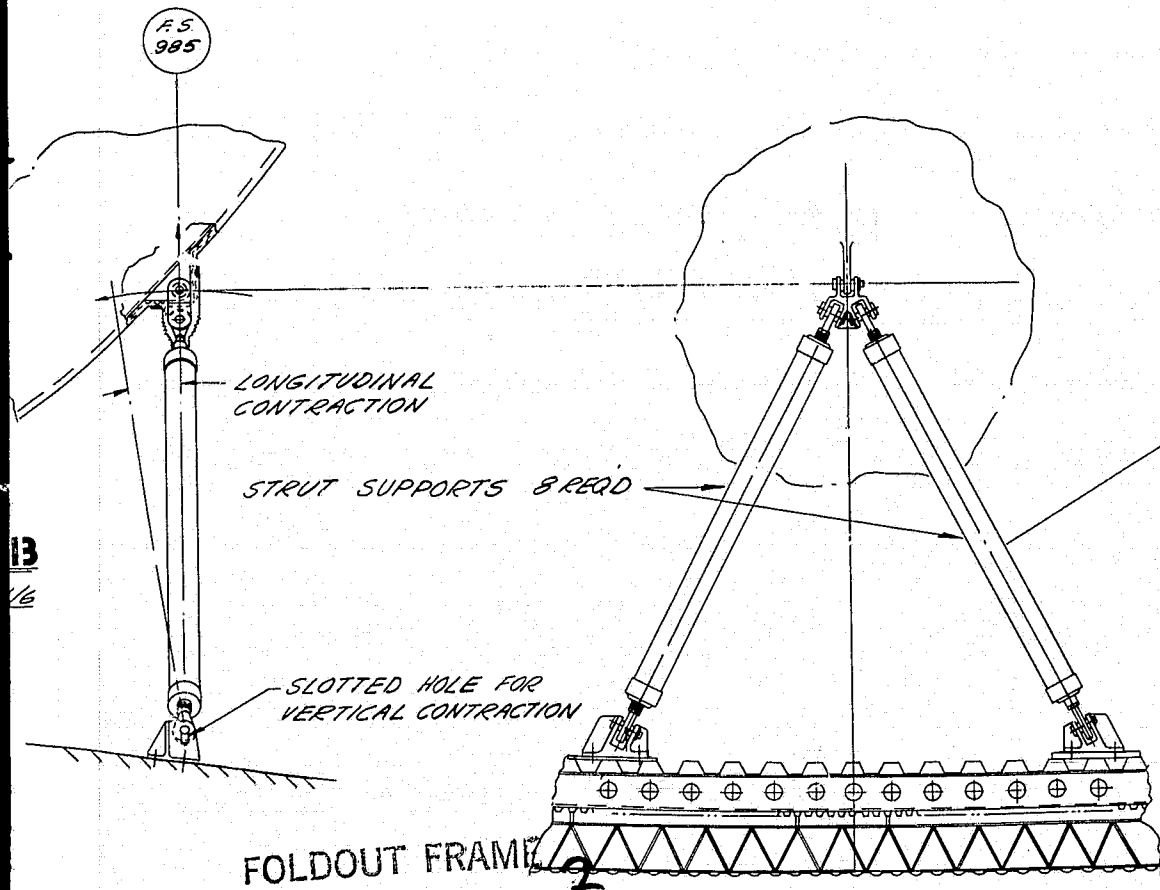
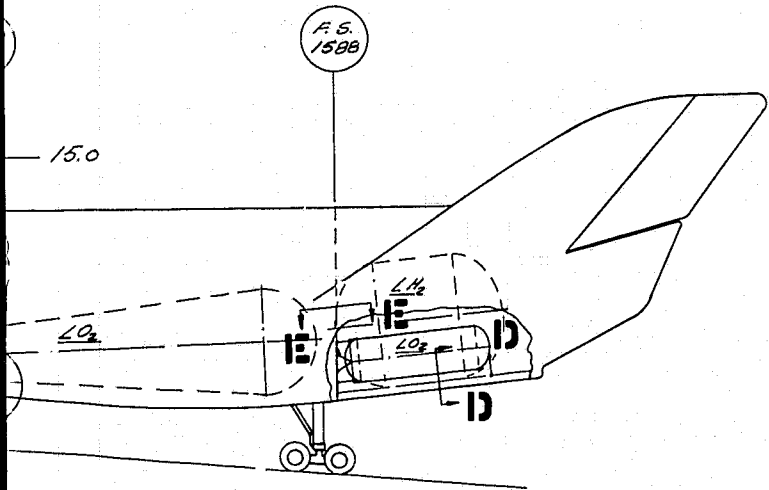


FOLDOUT FRAME /

FO



**VIEW E-E**  
 TYP TANK STRUTS FOR  
 ORBIT STORAGE

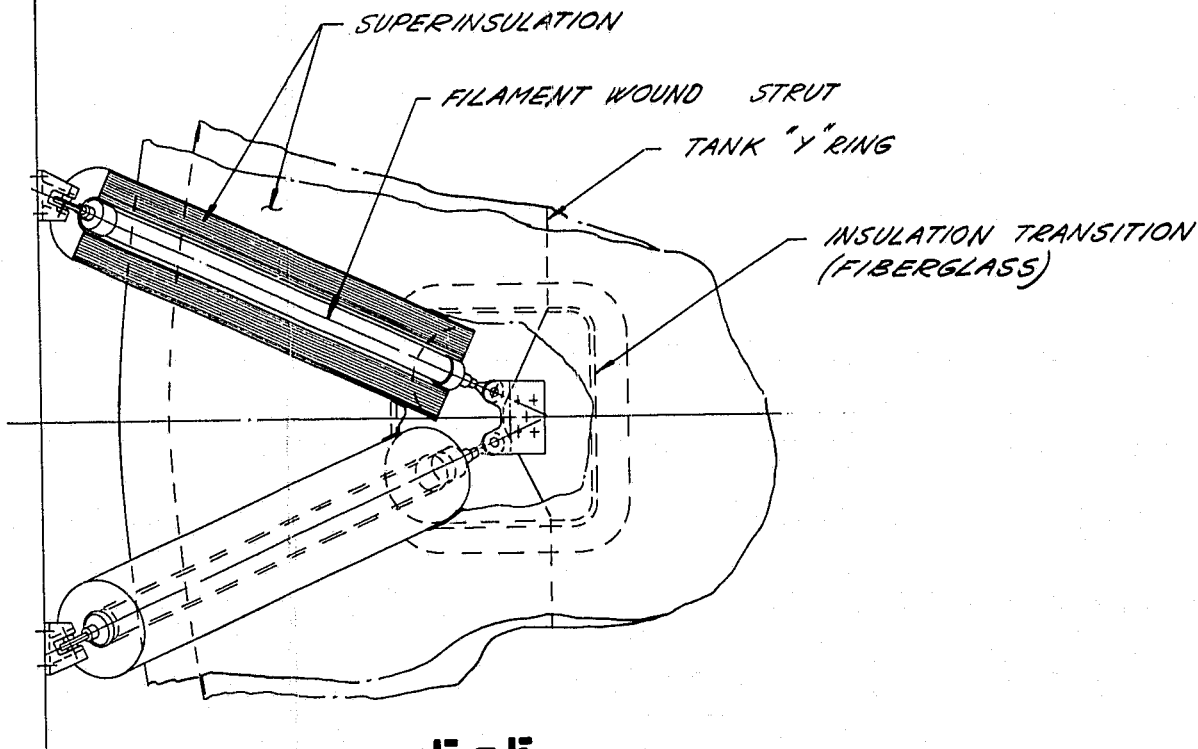


QTY REQD	CODE IDENT	PART IDENT

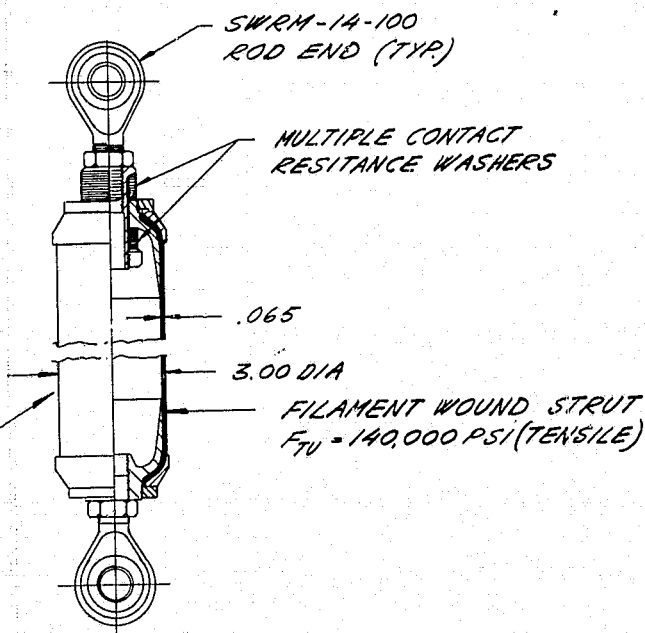
INTERPRET DWG PER		UNLESS OTHERWISE SPECIFIED DIMENSIONS, TOLERANCES, FRACTIONS = DECIMALS: .X .XX .XXX ANGLES = ±
NEXT ASSY APPLICATION	USED ON	
		CONTR
		CCA/CEI

FOLDOUT FRAME

FS  
1588



VIEW E - E  
TYP TANK STRUTS FOR  
ORBIT STORAGE



TYP. STRUT DESIGN.

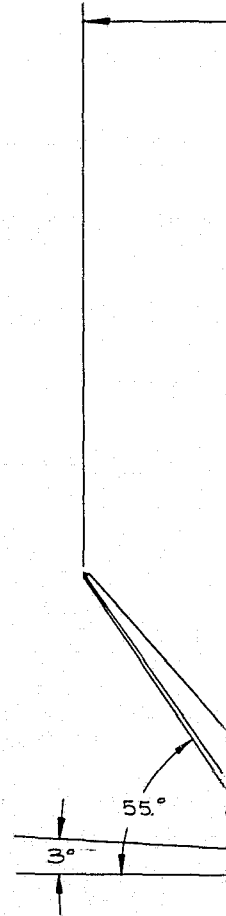
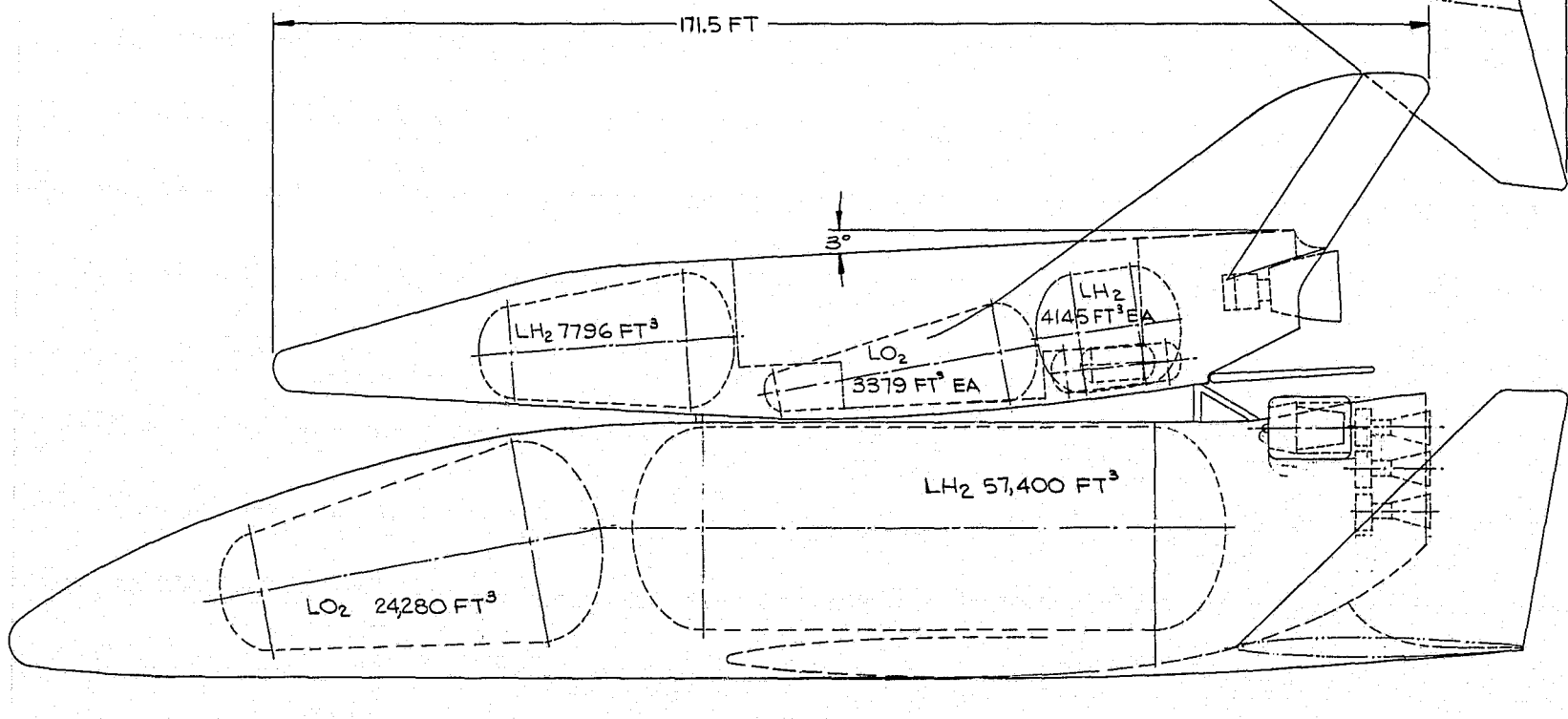
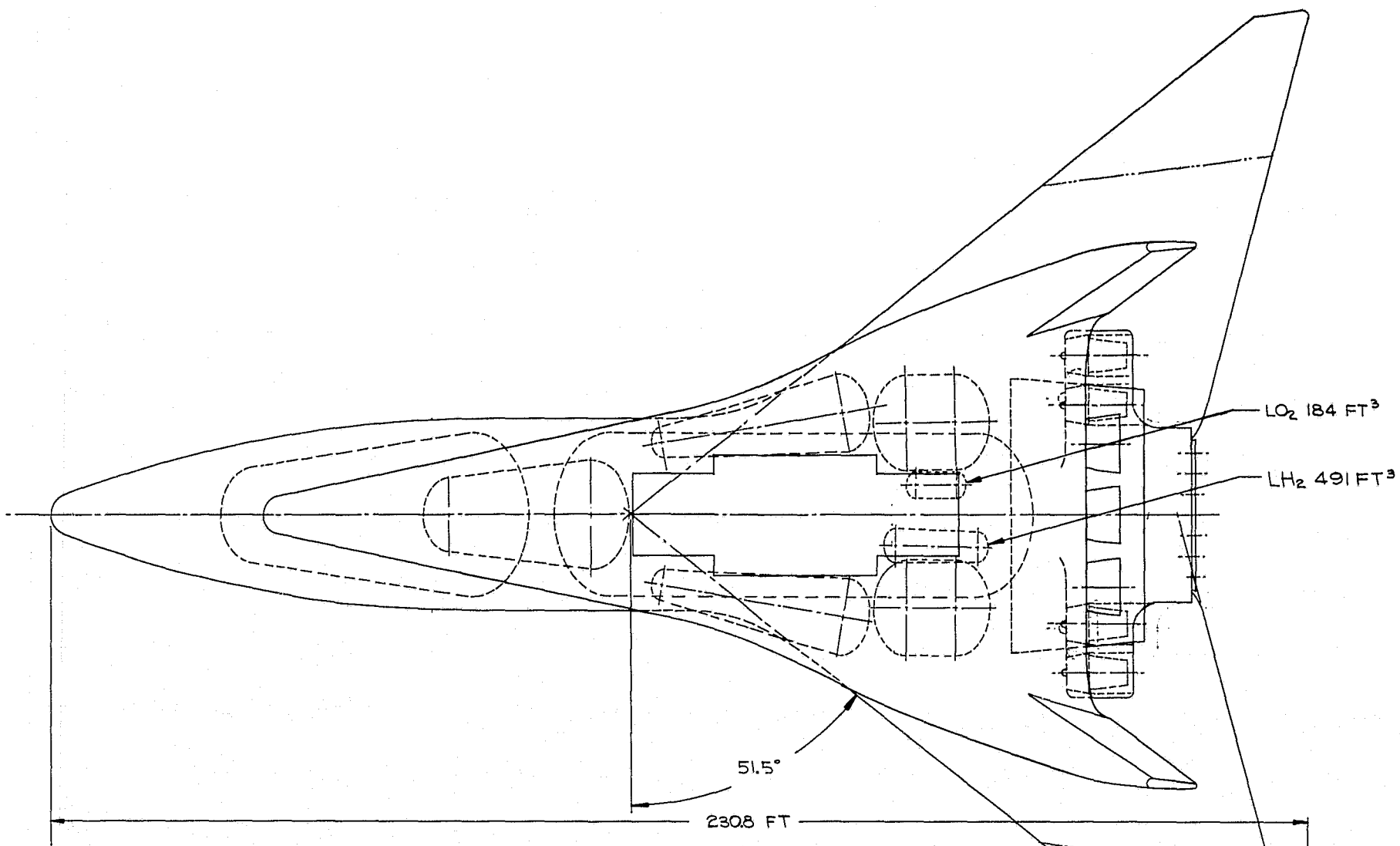
QTY REQD	CODE IDENT	PART OR IDENTIFYING NO.	NOMENCLATURE OR DESCRIPTION	MATERIAL DESCRIPTION OR NOTE	MATERIAL SPECIFICATION	ZONE	ITEM NO.
PARTS LIST							
INTERPRET DWG PER			UNLESS OTHERWISE SPECIFIED DIM. ARE IN INCHES. TOLERANCES ON:		DATE 10-8-69		
			FRACTIONS = ± 1/16		DR KARL TOLLO		
			DECIMALS: .X = ± .1		APPD		
			.XX = ± .03		ENGRG		
			.XXX = ± .010		CHK		
			ANGLES = ± 2 DEG		APPD		
NEXT ASSY			CONTR		SIZE CODE IDENT		
APPLICATION			CCA/CEI		DRAWING NO.		
					7 SKT 100969		
					SCALE 1/200 UNITS		
					SHEET 1 OF 1		

LOCKHEED MISSILES & SPACE COMPANY  
A GROUP DIVISION OF LOCKHEED AIRCRAFT CORPORATION  
SUNNYVALE, CALIFORNIA

**TANK SUPPORT**  
SPACECRAFT 2 STAGE SYSTEM

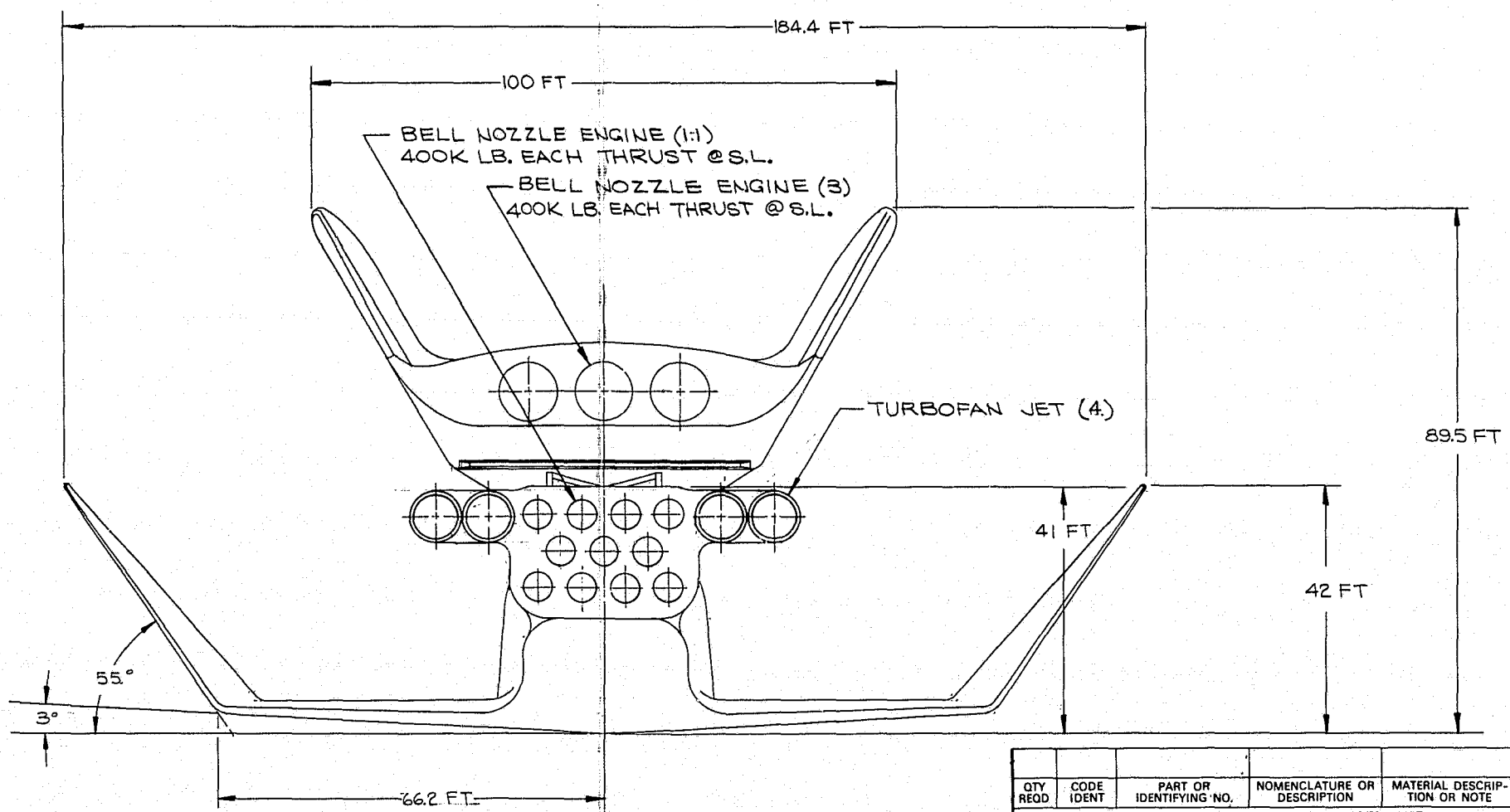
FOLDOUT FRAME 3

A-23



FOLDOUT FRAME /

LO<sub>2</sub> 184 FT<sup>3</sup>  
 LH<sub>2</sub> 491 FT<sup>3</sup>



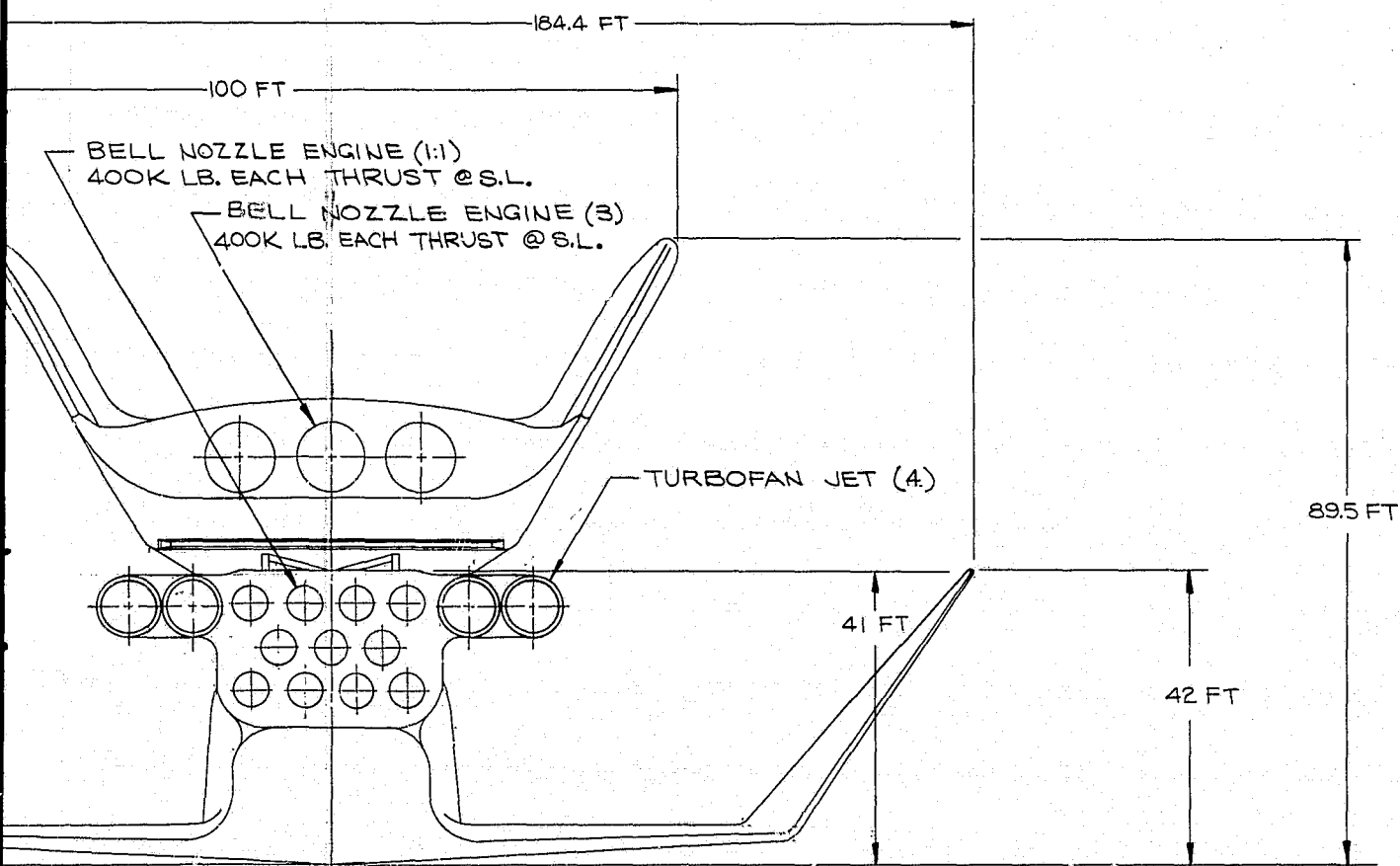
QTY REQD	CODE IDENT	PART OR IDENTIFYING NO.	NOMENCLATURE OR DESCRIPTION	MATERIAL DESCRIPTION OR NOTE	M SPE
PARTS LIST					

INTERPRET DWG PER	UNLESS OTHERWISE SPECIFIED DIM. ARE IN INCHES. TOLERANCES ON:	DATE 10-16-69	LOCKHEED MISSILE
	FRACTIONS = ± 1/16	DR. K. L. JOHNSON	A GROUP DIVISION OF LOCKHEED
	DECIMALS: .X = ± .1	APPD	SUNNYVALE, CALIF.
	.XX = ± .03	ENGRG	LAUNCH V
	.XXX = ± .010	CHK	2 STAGE SYSTEM
	ANGLES = ± 2 DEG	APPD	SIZE CODE IDENT
NEXT ASSY	CONTR	APPD	SK
APPLICATION	CCA/CEI	APPD	SCALE 1/120

A-24

FOLDOUT FRAME 2

FOLDOUT FRAME



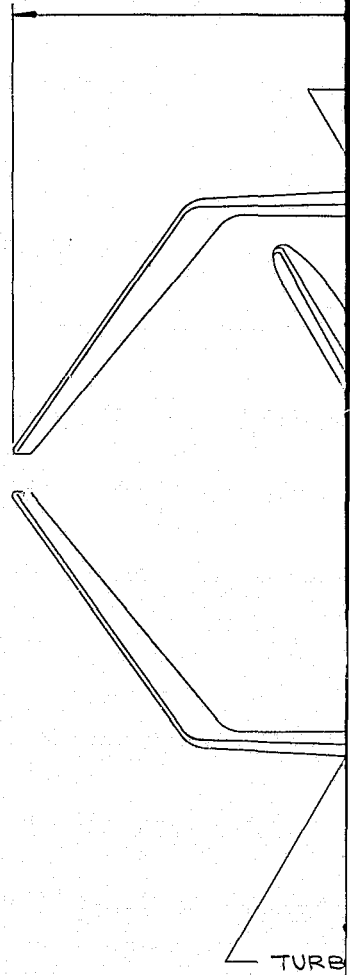
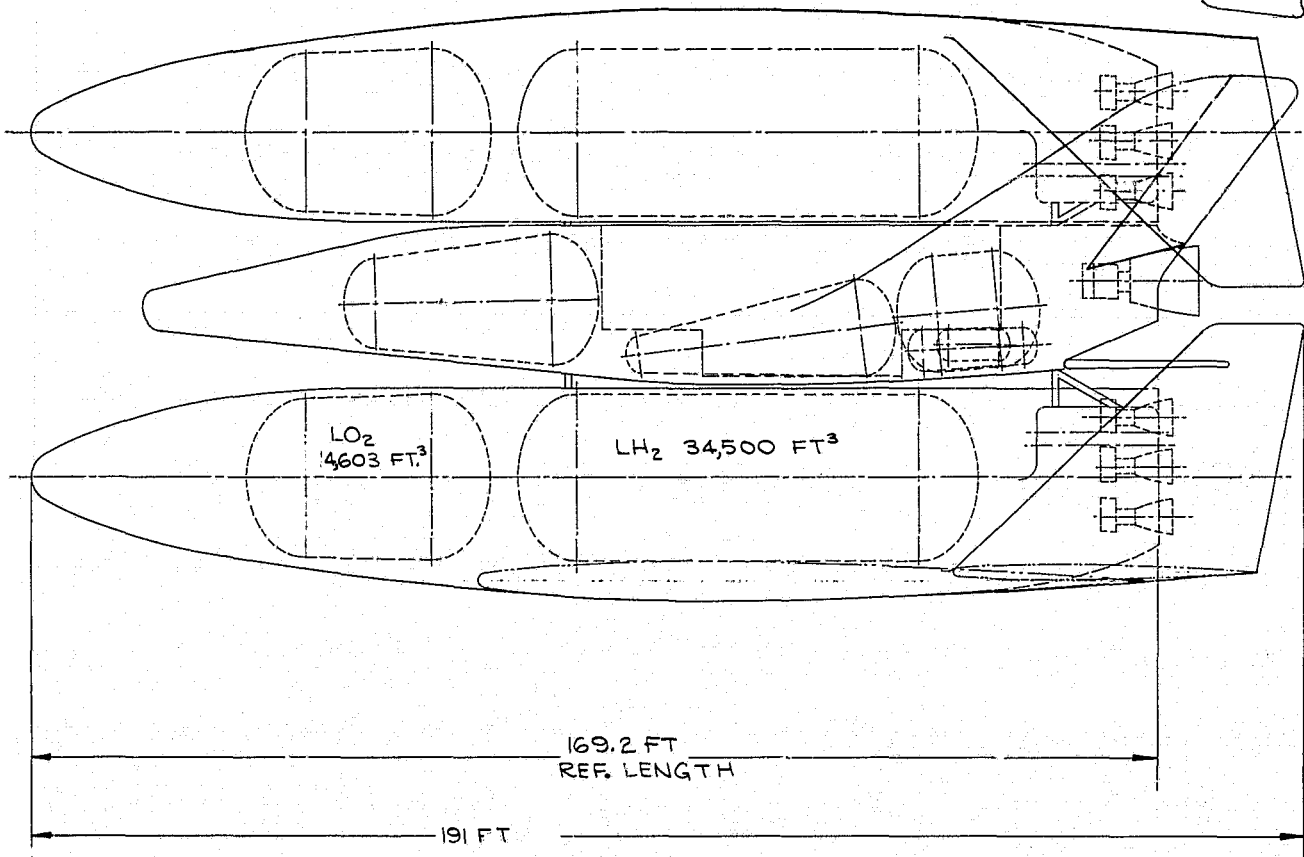
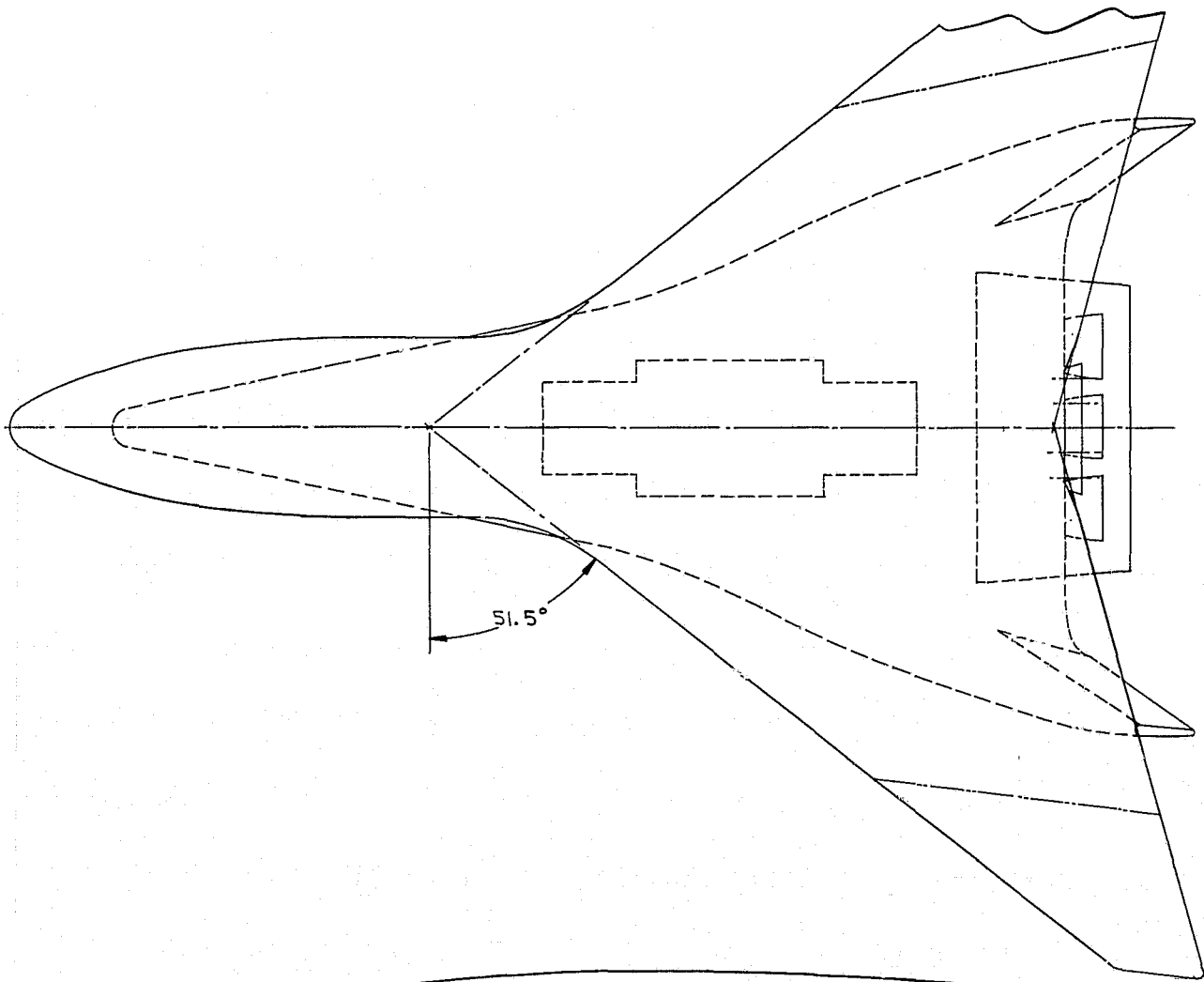
QTY REQD	CODE IDENT	PART OR IDENTIFYING NO.	NOMENCLATURE OR DESCRIPTION	MATERIAL DESCRIPTION OR NOTE	MATERIAL SPECIFICATION	ZONE	ITEM NO.
PARTS LIST							

INTERPRET DWG PER	UNLESS OTHERWISE SPECIFIED, DIM. ARE IN INCHES. TOLERANCES ON: FRACTIONS = ± 1/16 DECIMALS: .X = ± .1 .XX = ± .03 .XXX = ± .010 ANGLES = ± 2 DEG	DATE 10-16-69 DR K.L. JOHNSON	LOCKHEED MISSILES & SPACE COMPANY A GROUP DIVISION OF LOCKHEED AIRCRAFT CORPORATION SUNNYVALE, CALIFORNIA
NEXT ASSY USED ON APPLICATION	CONTR CCA/CEI	APPD ENGRG CHK APPD APPD	LAUNCH VEHICLE 2 STAGE SYSTEM 25K P/L
		SIZE CODE IDENT	DRAWING NO. SKJ 101669
		SCALE 1/120	REV SHEET 1 OF 1

A-24

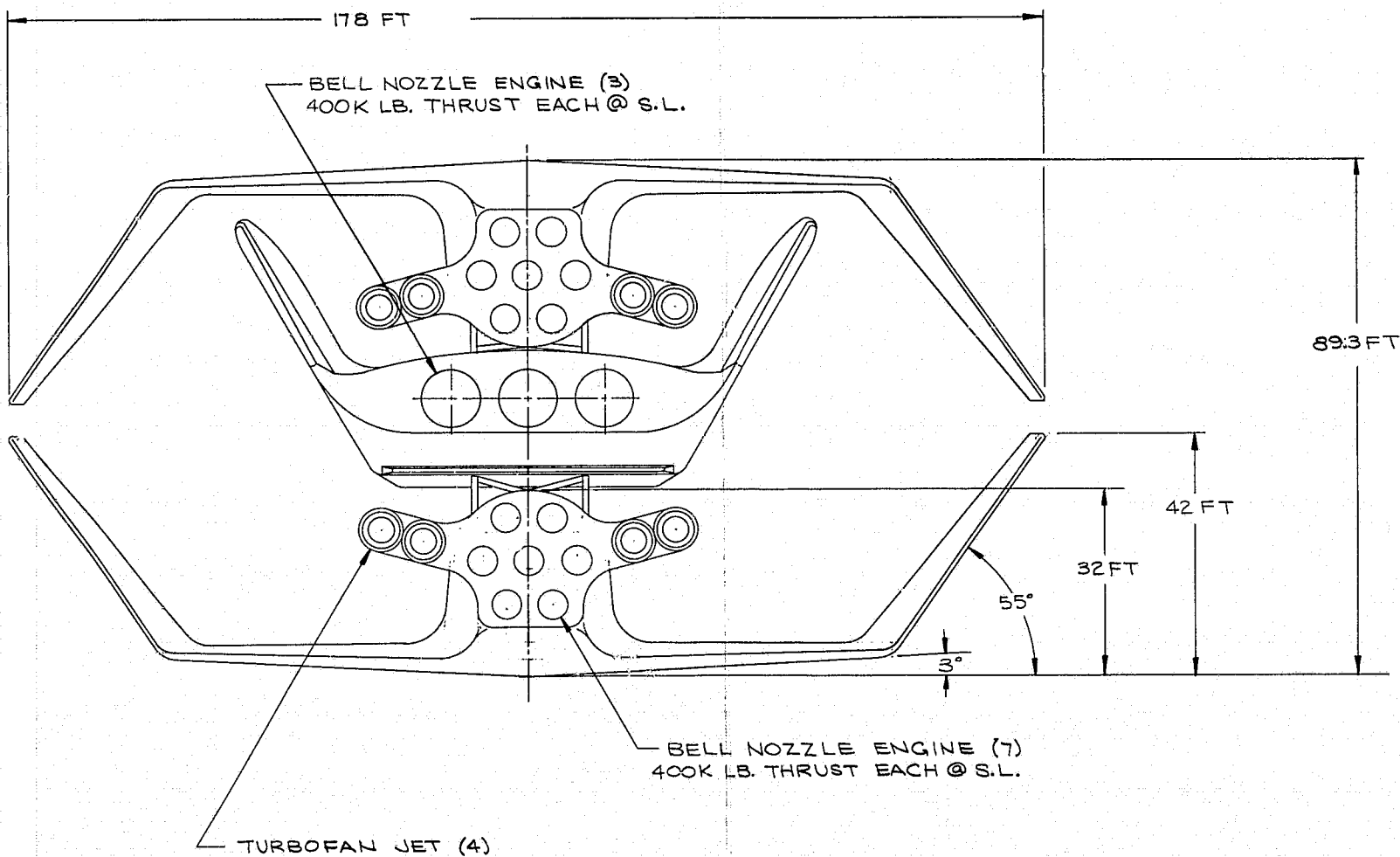
FRAME 2

FOLDOUT FRAME 3



FOLDOUT FRAME /



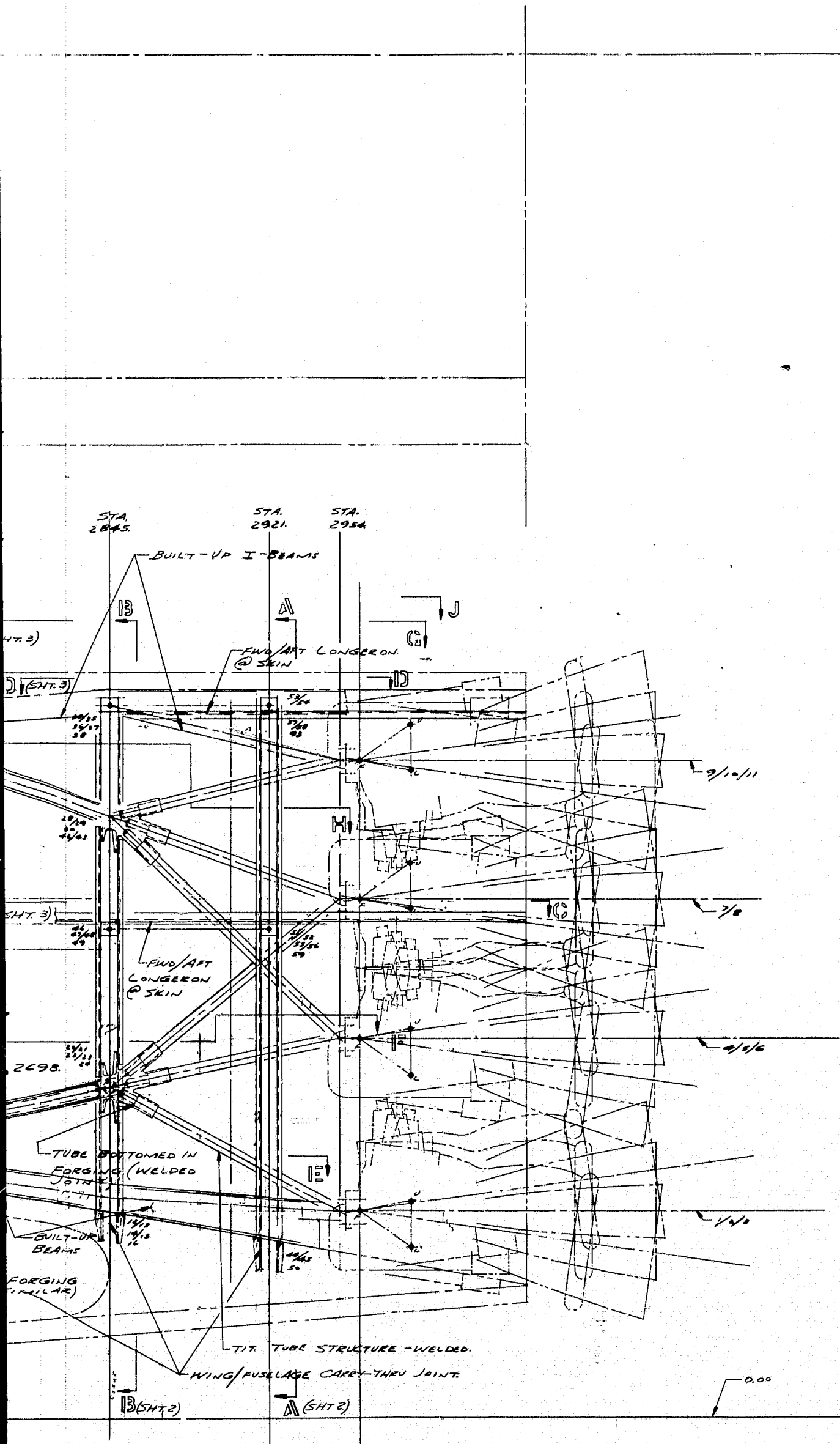


FOLDOUT FRAME 2

A-25

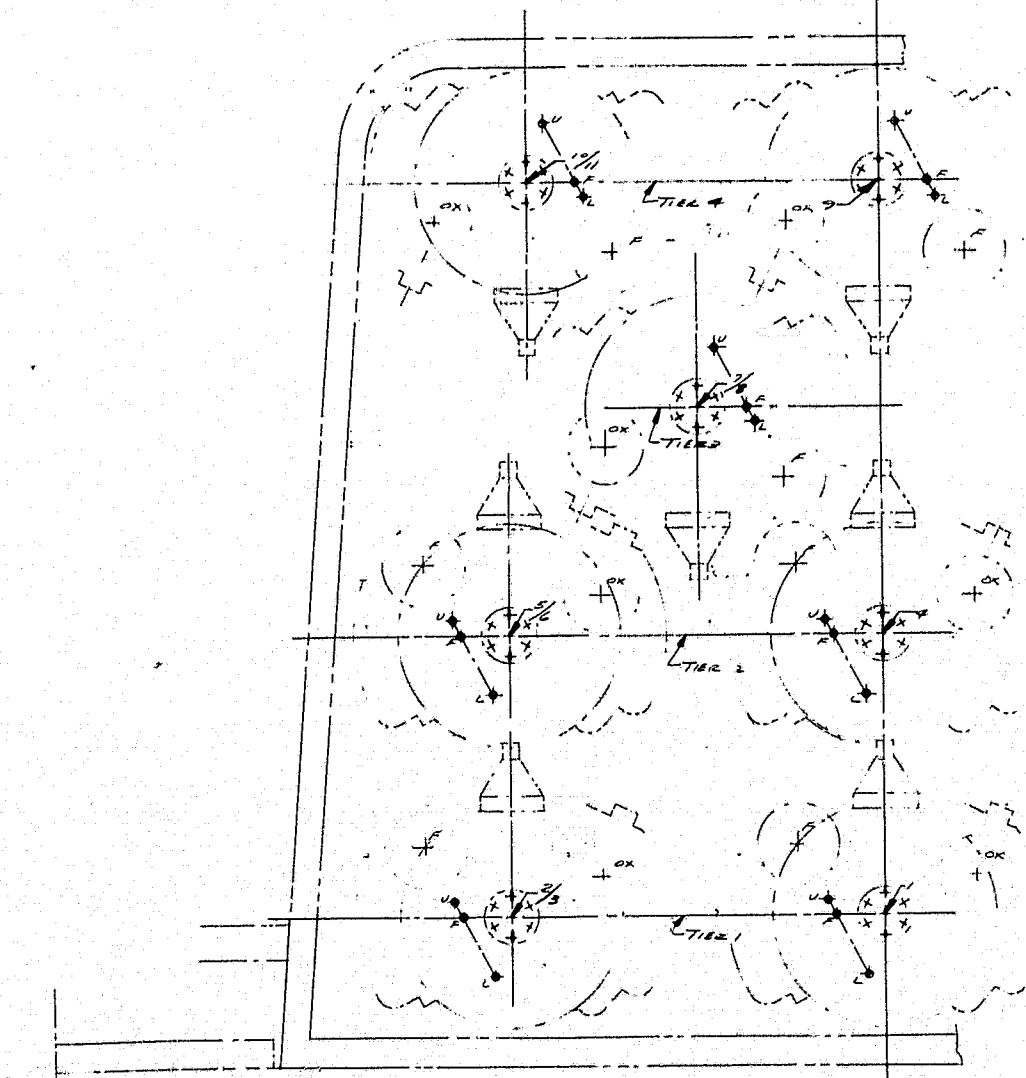
QTY REQD	CODE IDENT	PART OR IDENTIFYING NO.	NOMENCLATURE OR DESCRIPTION	MATERIAL DESCRIPTION OR NOTE	MATERIAL SPECIFICATION	ZONE	ITEM NO.
PARTS LIST							
INTERPRET DWG PER	UNLESS OTHERWISE SPECIFIED DIM. ARE IN INCHES. TOLERANCES ON:		DATE 10-17-69	LOCKHEED MISSILES & SPACE COMPANY			
	FRACTIONS = ± 1/16		DR <i>K.K. Johnson</i>	A GROUP DIVISION OF LOCKHEED AIRCRAFT CORPORATION			
	DECIMALS: .X = ± .1		APPD	SUNNYVALE, CALIFORNIA			
	.XX = ± .03		APPD	LAUNCH VEHICLE			
	.XXX = ± .010		ENGRG	DISSIMILAR TRIAMESE SYS.			
	ANGLES = ± 2 DEG		CHK	25K P/L			
	CONTR		APPD	SIZE CODE IDENT	DRAWING NO.	REV	
NEXT ASSY USED ON APPLICATION	CCA/CEI		APPD	SCALE 1/120	SKJ101769	SHEET 1 OF 1	





FOLDOUT FRAME 2

E 5/6



500  
1002

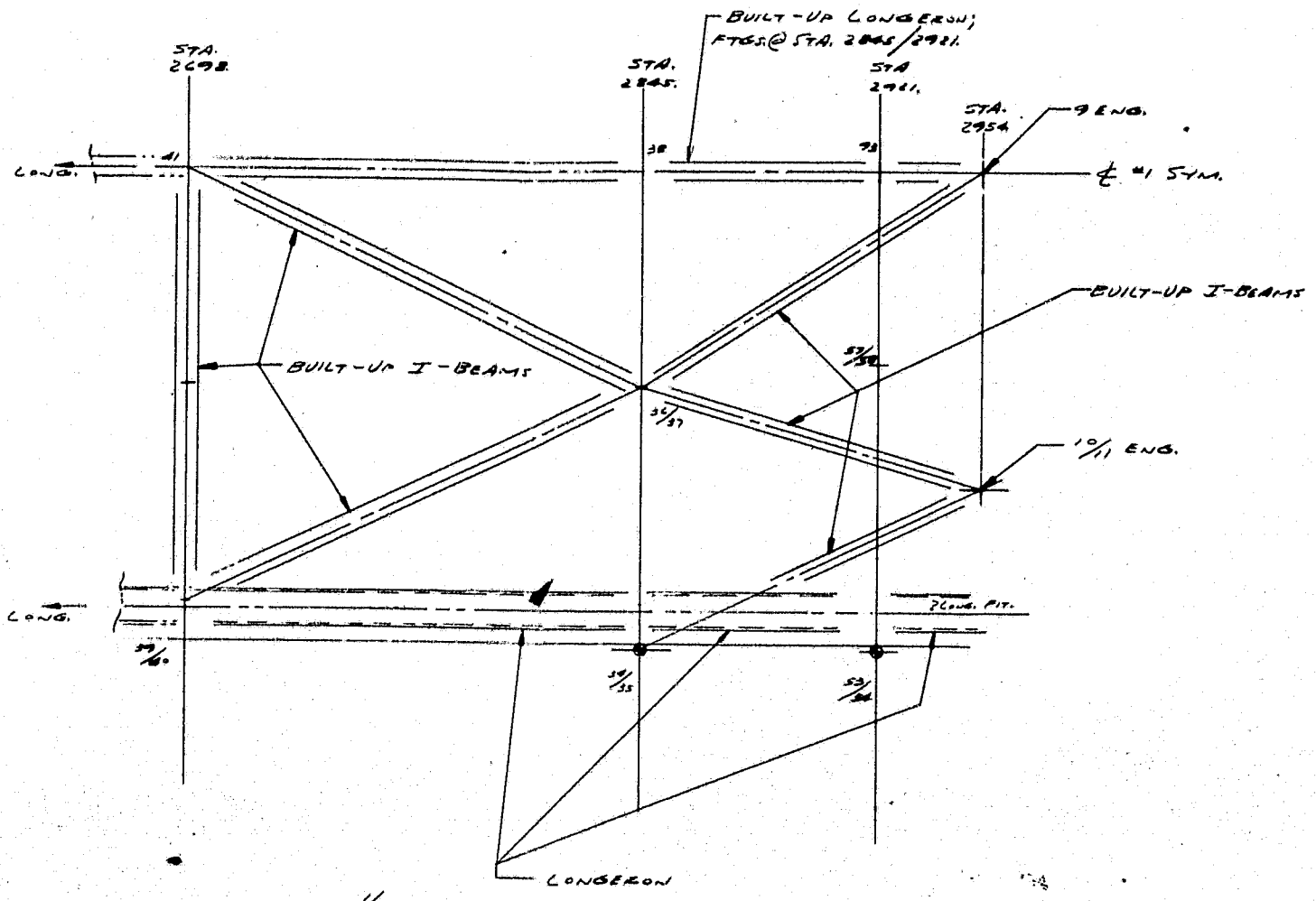
VIEW LOOKING FWD

500

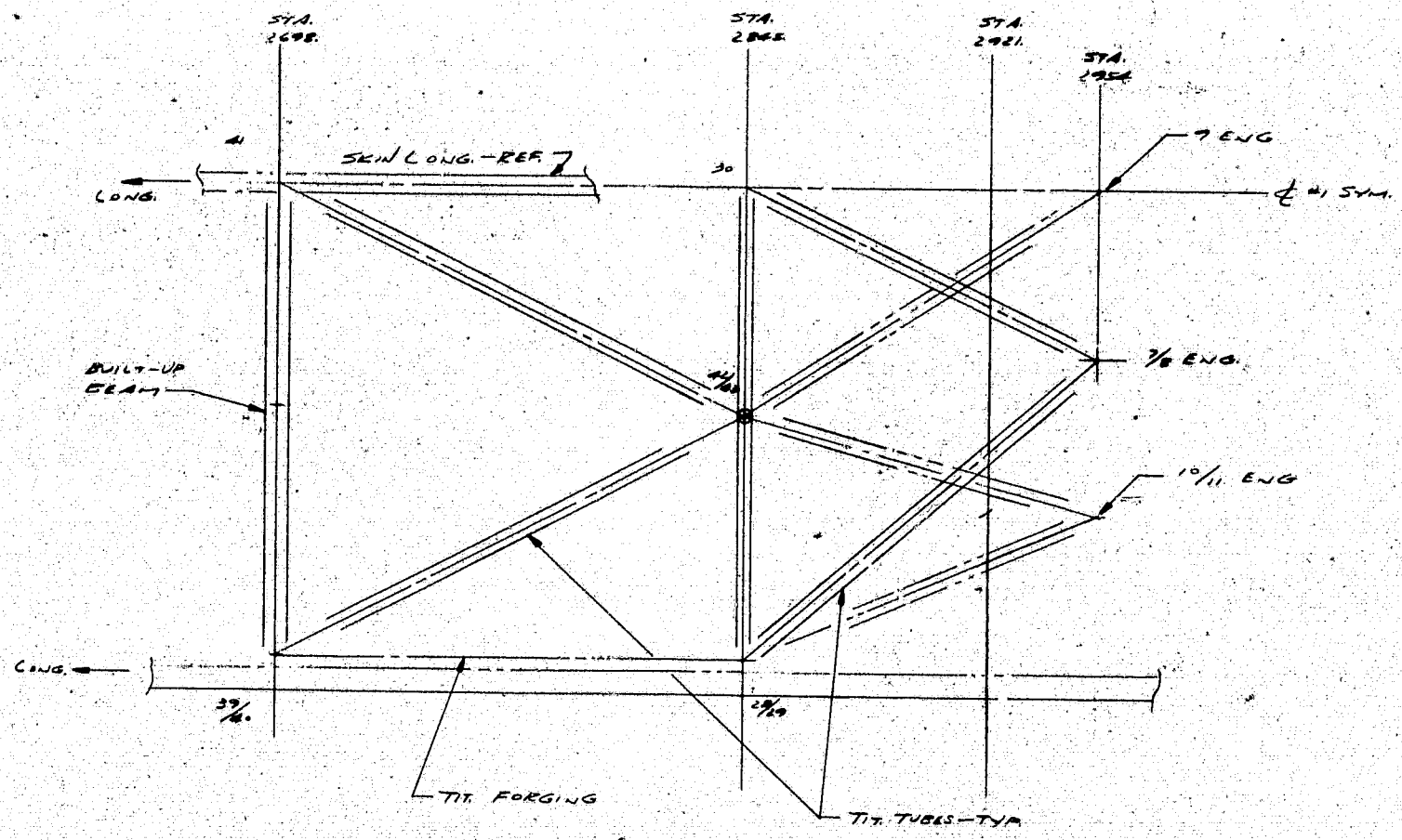
EOLDOUT FRAME 3

DATE 29/SEPT. 69	LOCKHEED MISSILES & SPACE COMPANY	
DR SWEET & BLOOMFELD	A GROUP DIVISION OF LOCKHEED AIRCRAFT CORPORATION	
	SUNNYVALE, CALIFORNIA	
APPD	THRUST STRUCTURE-	
APPD	SPACE, BOOSTER,	
ENGRG	11 ENGINE SYSTEM	
CHK	SIZE CODE IDENT	DRAWING NO.
APPD		SKQ092969
APPD	SCALE 1/20	SHEET 1003

A-26.1

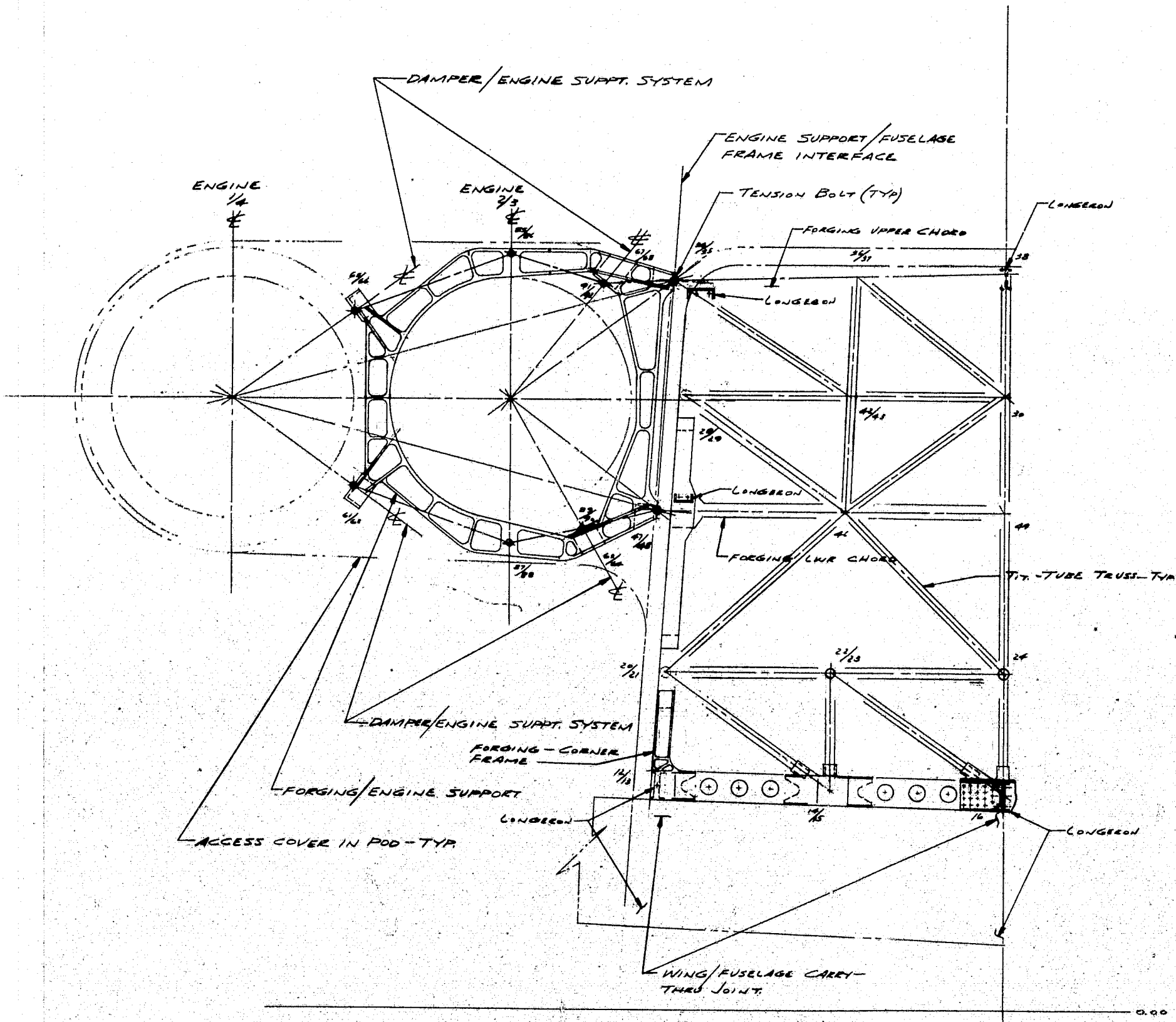


1/20 SCALE  
 VIEW J = J (SHT. 1)



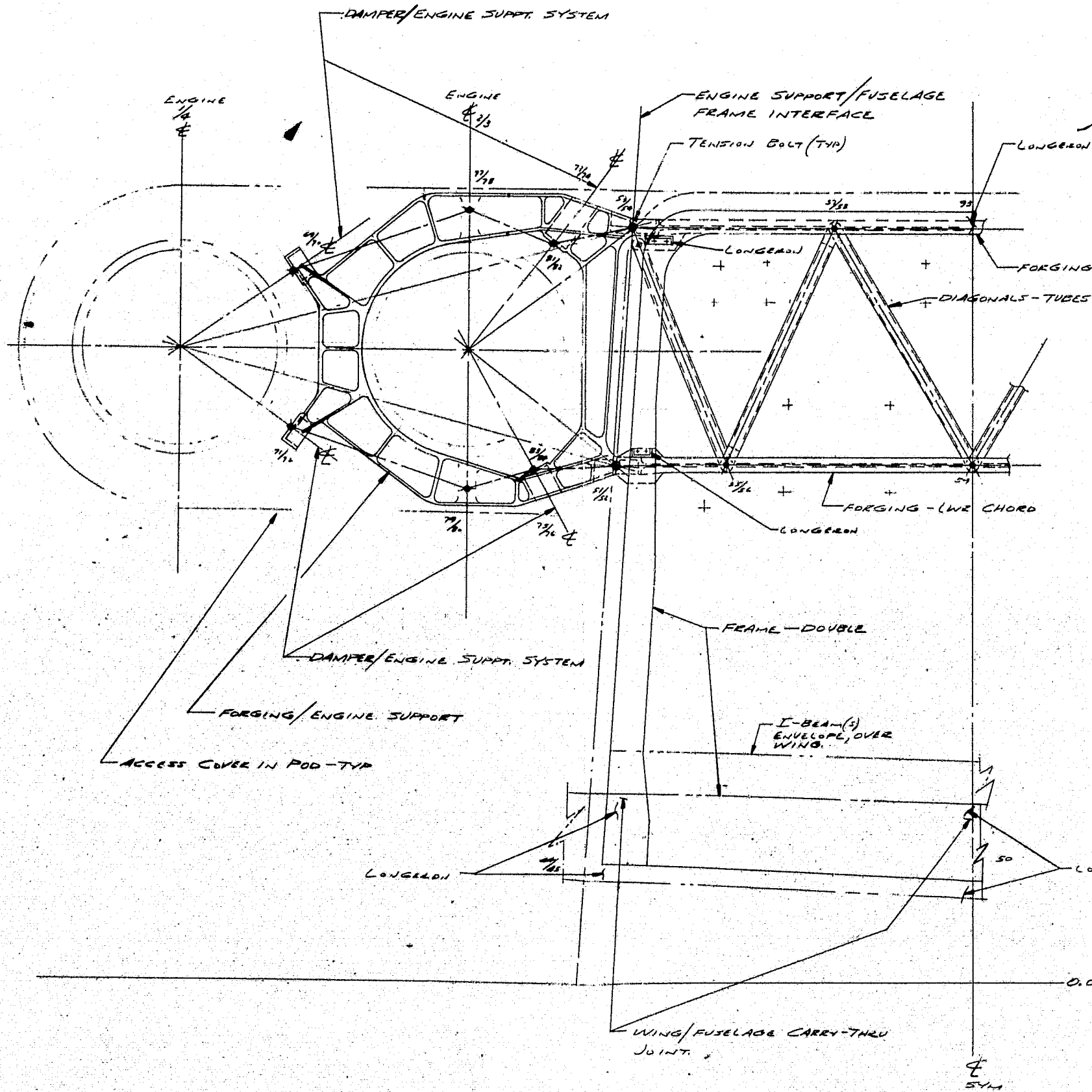
1/20 SCALE  
 VIEW H = H (SHT. 1)

FOLDOUT FRAME 1



0.00  
 & SYM.  
 STA. 2845.  
 1/20 SCALE  
 VIEW B - B (SHT. 1)

FOLDOUT FRAME 2



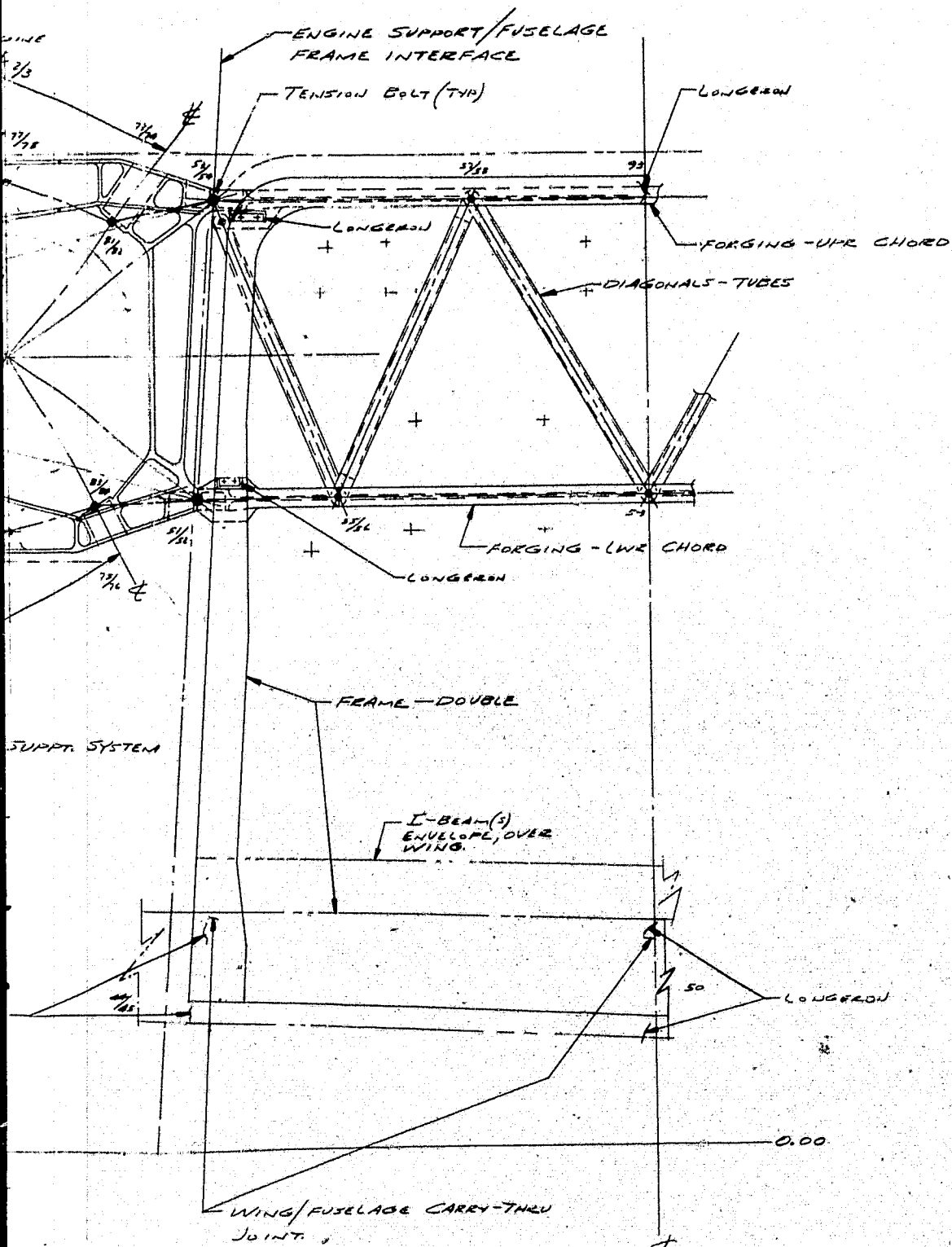
STA. 2921.

1/10 SCALE

VIEW A = A (SHT. 1)

FOLDOUT FRAME 3

SUPPT. SYSTEM



SUPPT. SYSTEM

WING/FUSELAGE CARRY-THRU JOINT

STA. 2921

1/20 SCALE

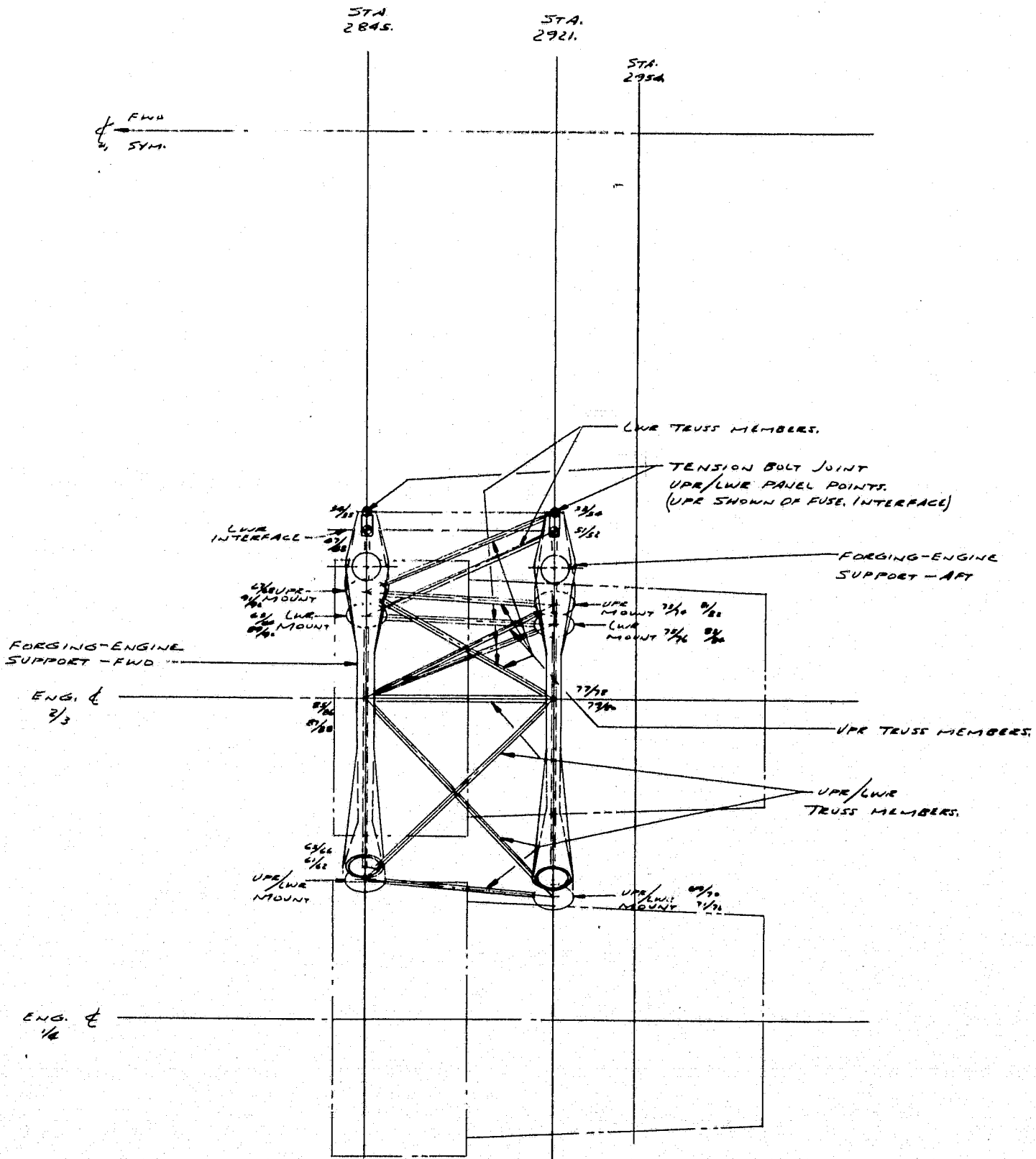
VIEW A = A (SHT 1)

WING/FUSELAGE CARRY-THRU JOINT

DATE	SEPT 69	LOCKHEED MISSILES & SPACE COMPANY	
DR	STEVEN G. CAMPBELL	A GROUP DIVISION OF LOCKHEED AIRCRAFT CORPORATION	
		SUNNYVALE, CALIFORNIA	
APPD		THRUST STRUCTURE - SPACE BOOSTER, 11 ENGINE SYSTEM	
ENGRG		SIZE CODE IDENT	DRAWING NO.
CHK			SKQ092969
APPD		SCALE	SHEET
APPD		1/20	2000

A-26 ?

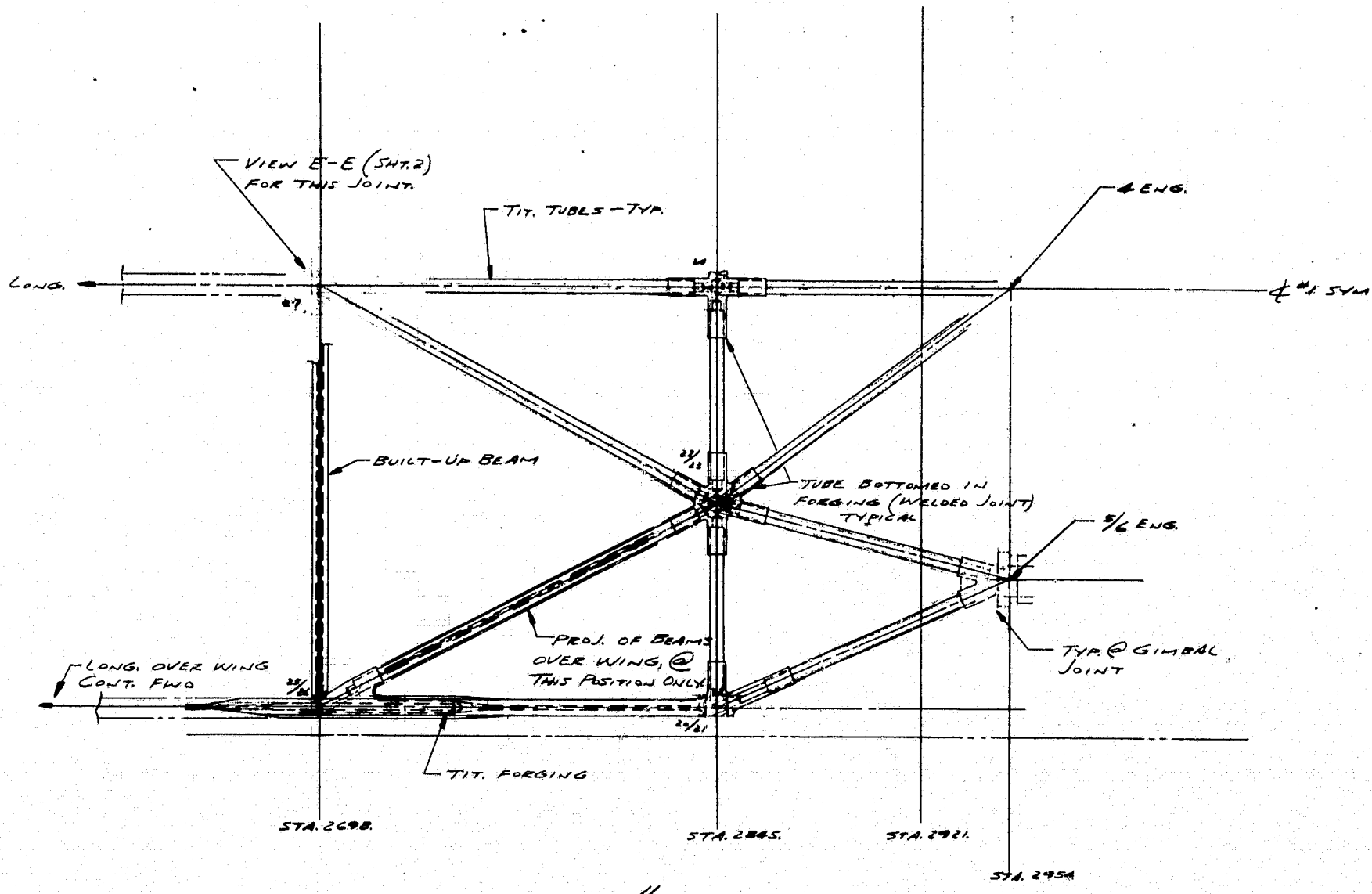




THRUST STRUCTURE FOR JET ENGINES

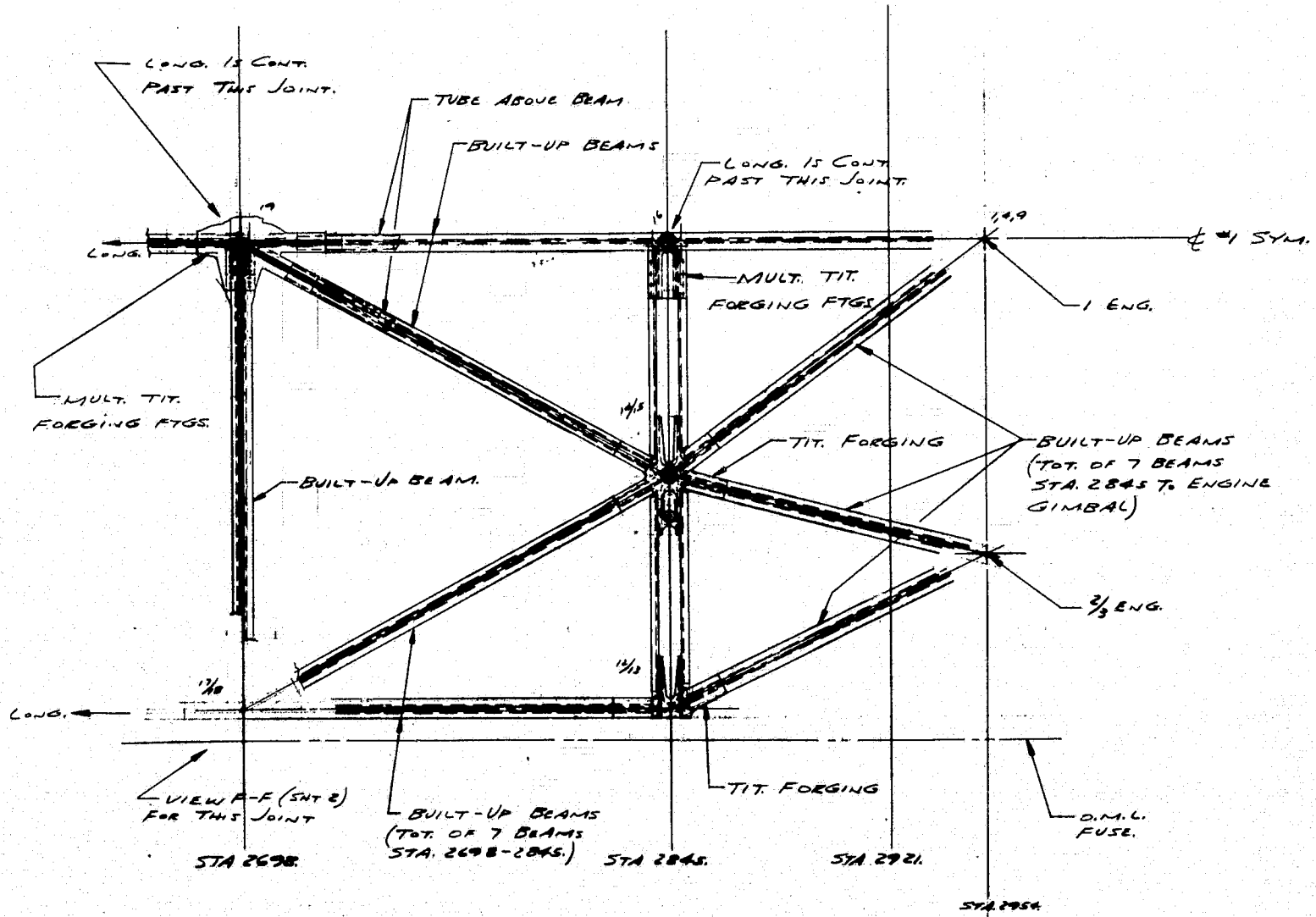
1/20 SCALE  
 VIEW (A) = (A) (SHT. 1)

FOLDOUT FRAME |



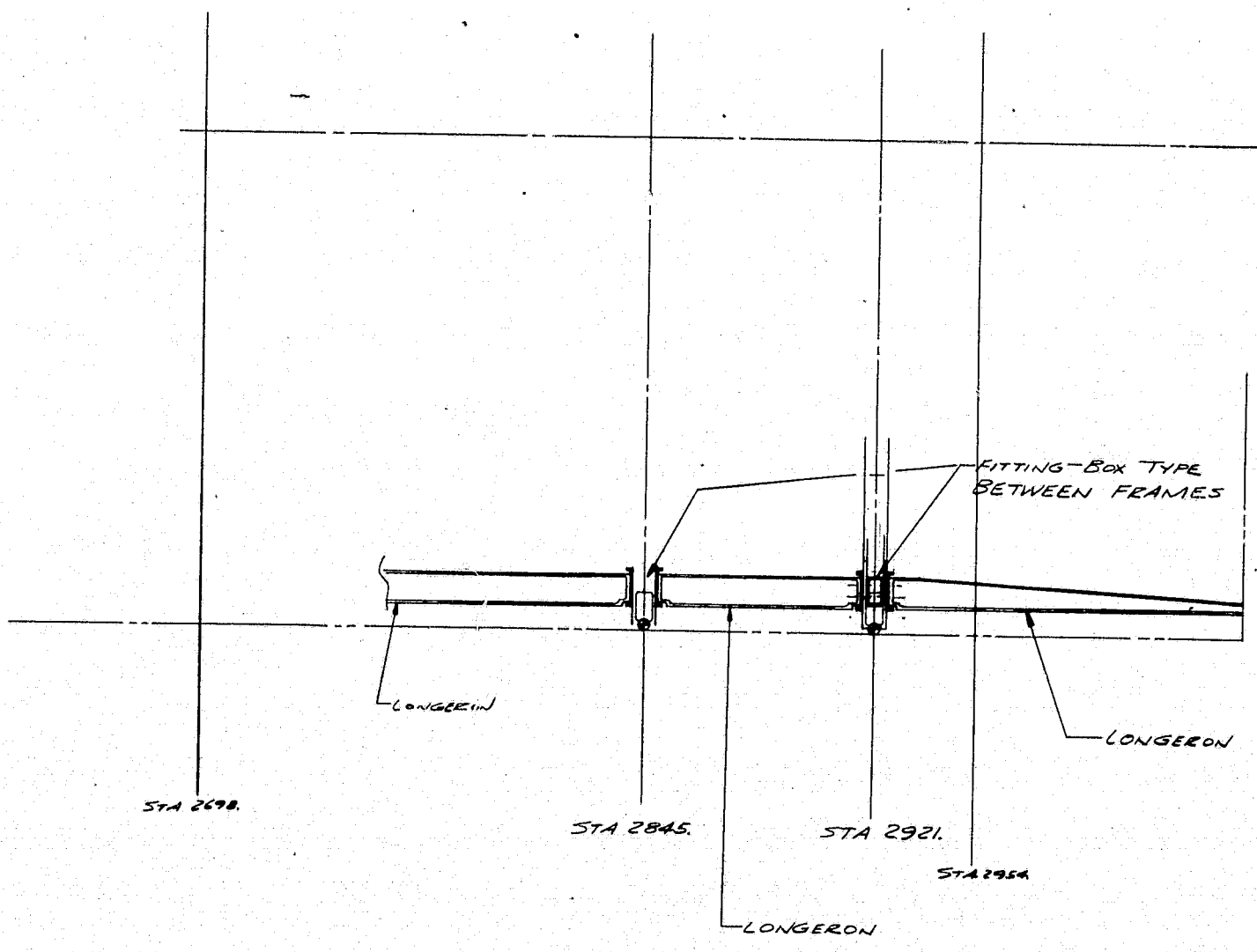
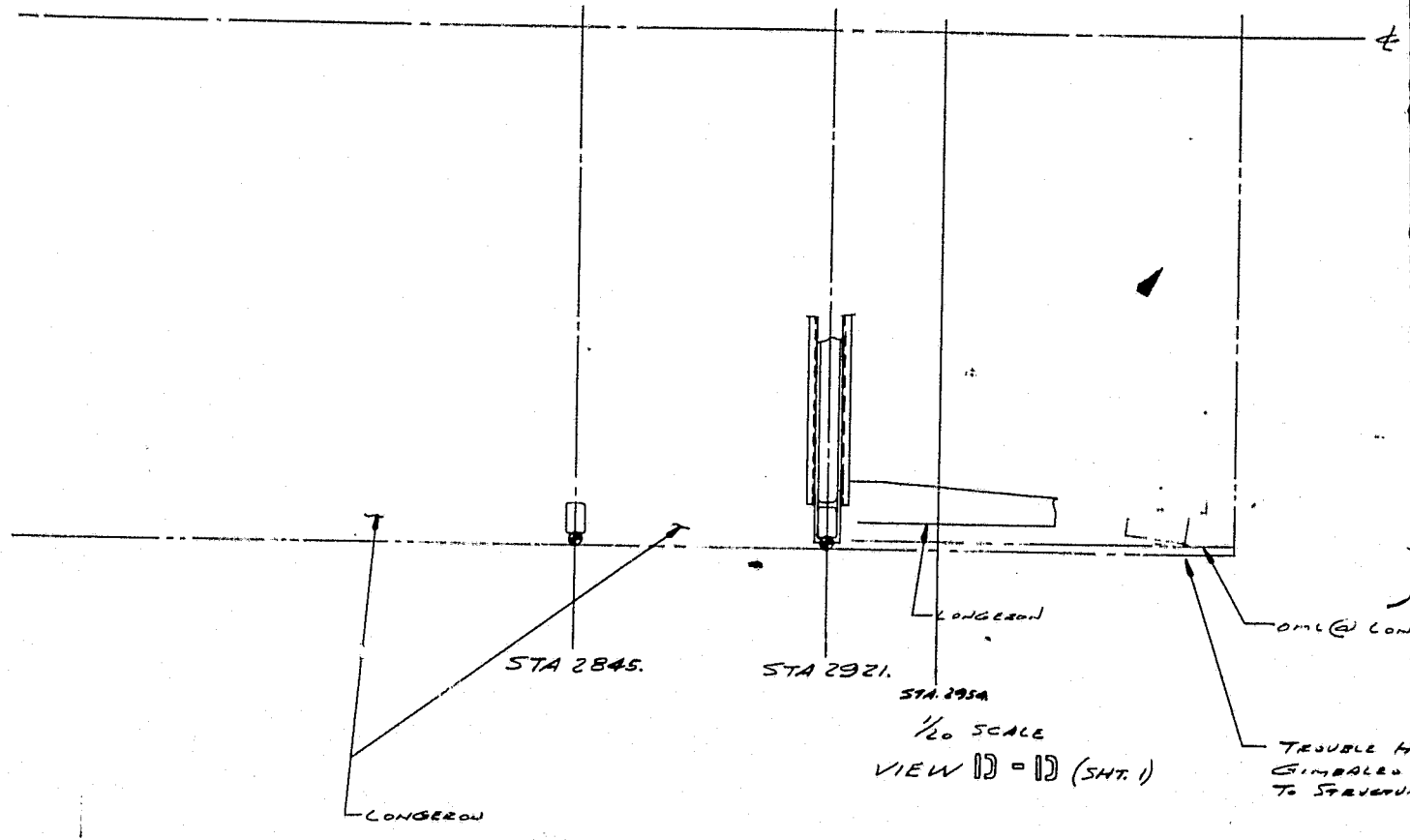
1/20 SCALE  
 VIEW  $\square = \square$  (SHT. 1)

FOLDOUT FRAME 2

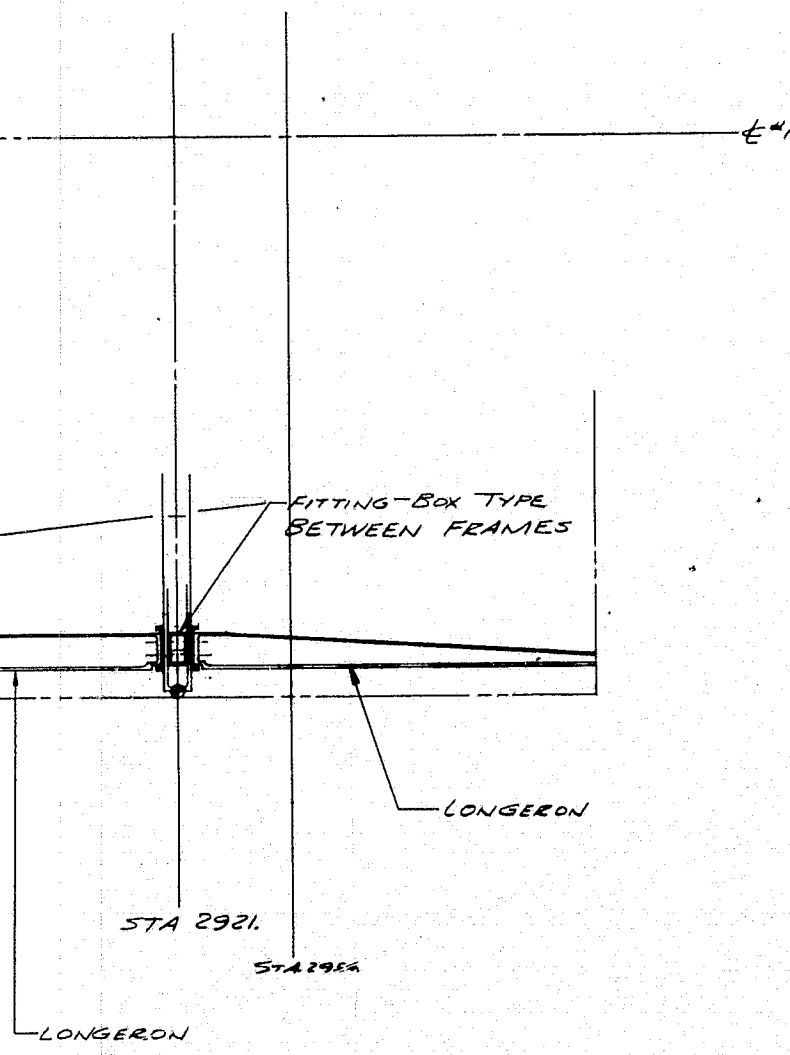
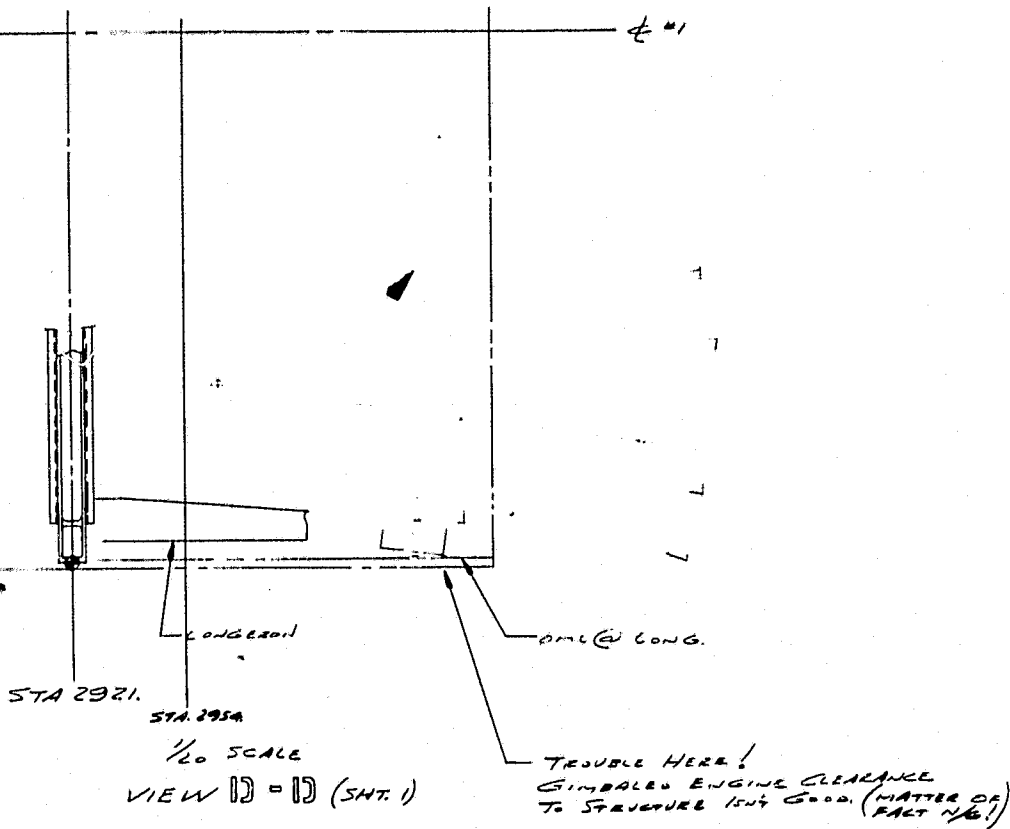


1/20 SCALE  
 VIEW  $\begin{matrix} \square \\ \square \end{matrix} - \begin{matrix} \square \\ \square \end{matrix}$  (SHT. 1)

FOLDOUT FRAME 3



FOLDOUT FRAME 4

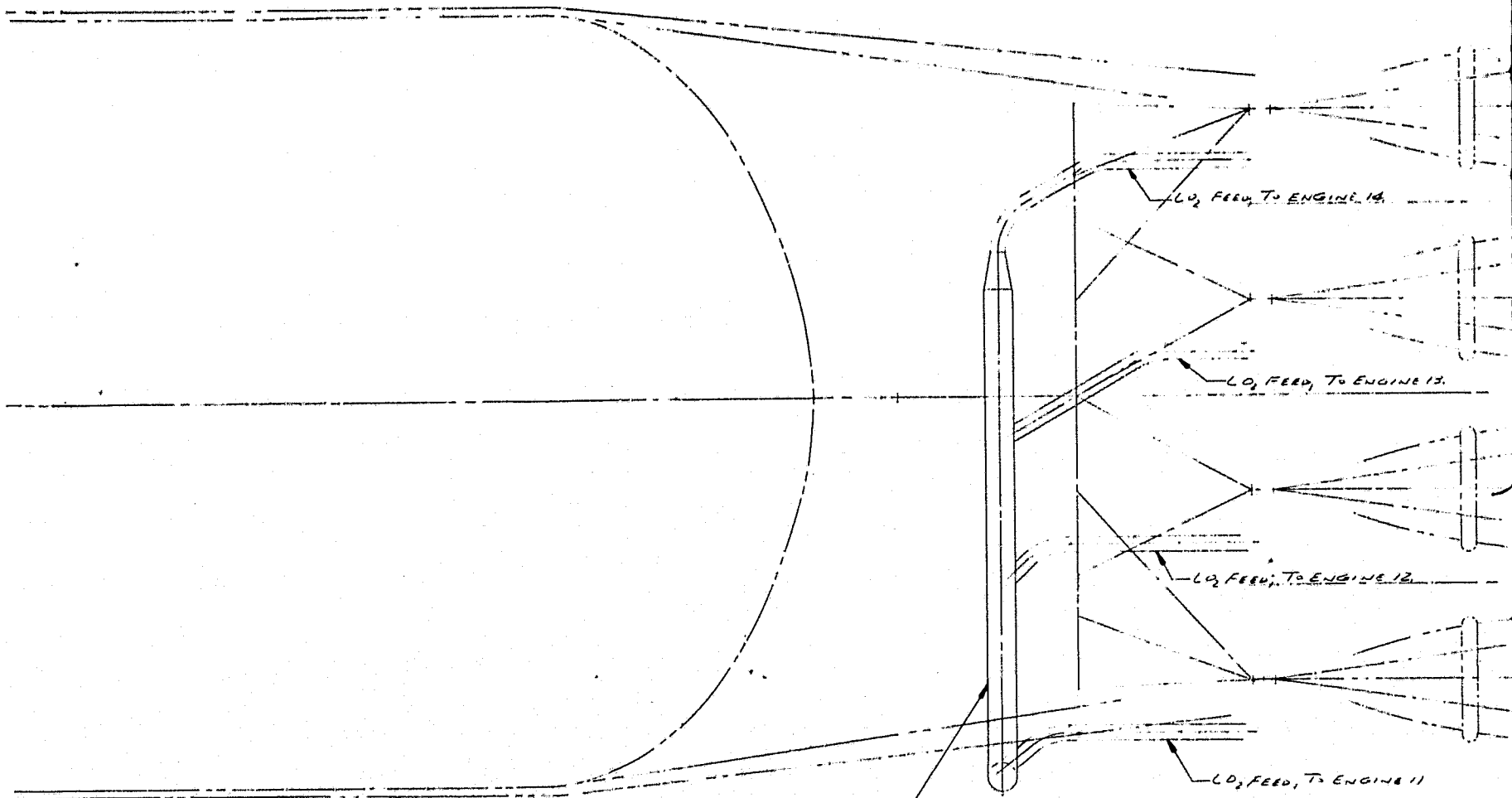


DATE <i>29 Sept 69</i>	LOCKHEED MISSILES & SPACE COMPANY A GROUP DIVISION OF LOCKHEED AIRCRAFT CORPORATION SUNNYVALE, CALIFORNIA		
DR <i>SVEN G. OLSSON</i>	THRUST STRUCTURE- SPACE BOOSTER, I1 ENGINE SYSTEM		
APPD	SIZE	CODE IDENT	DRAWING NO.
ENGRG			<i>SKQ092969</i>
CHK			REV
APPD			
APPD	SCALE NOTE:		SHEET <i>3028</i>

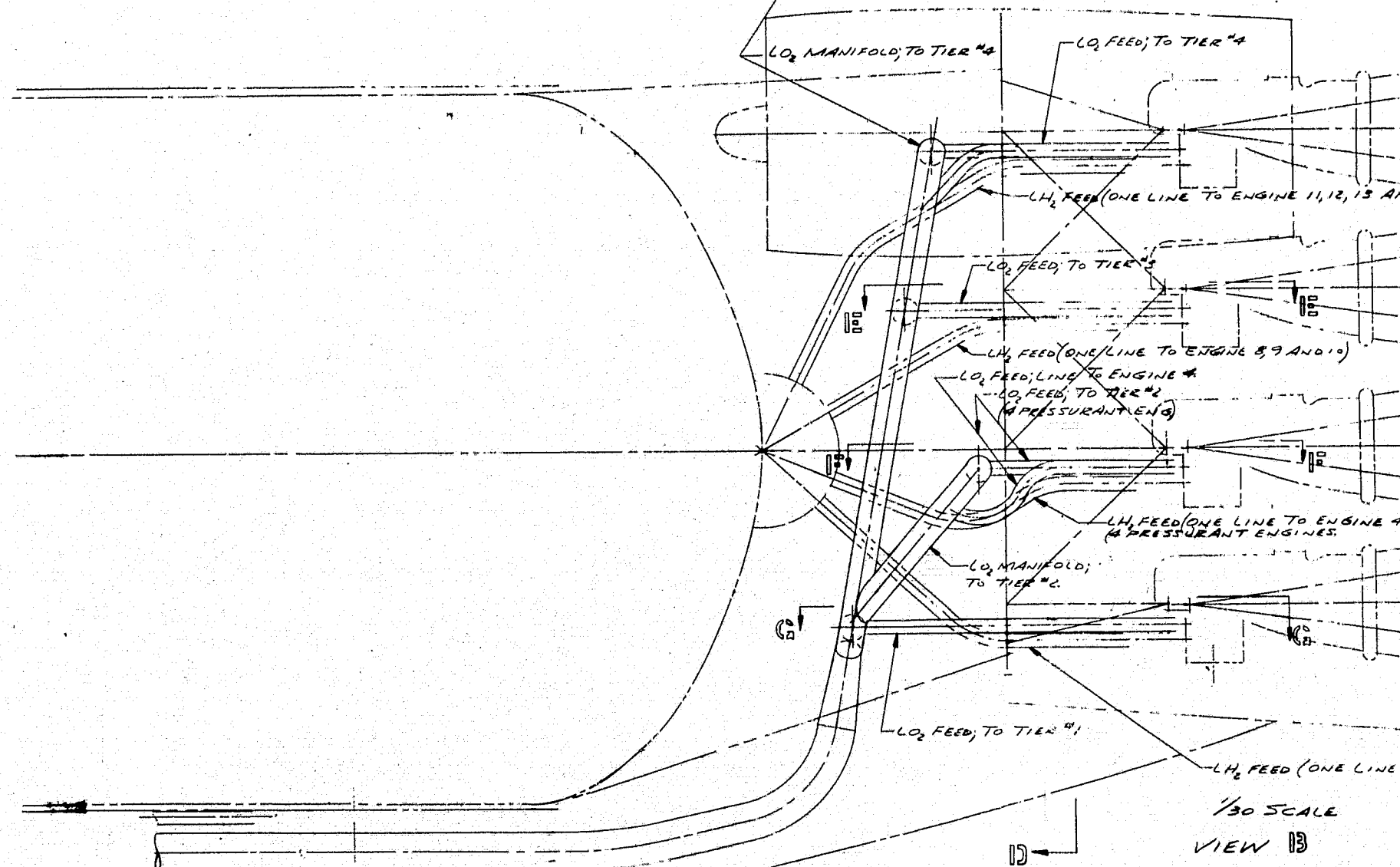
A-26.3

OUT FRAME 4

FOLDOUT FRAME 5



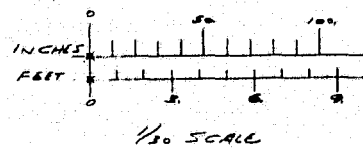
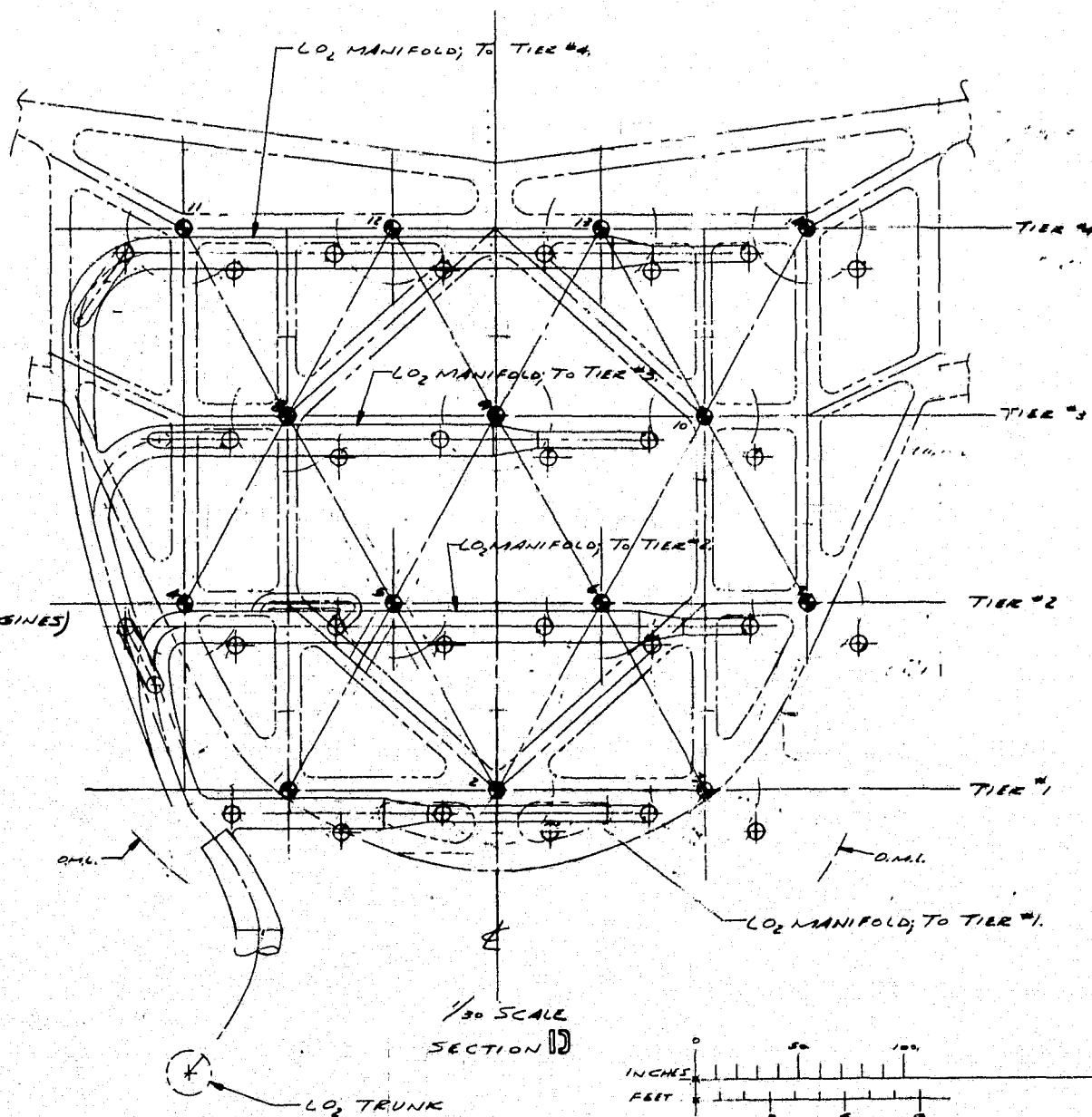
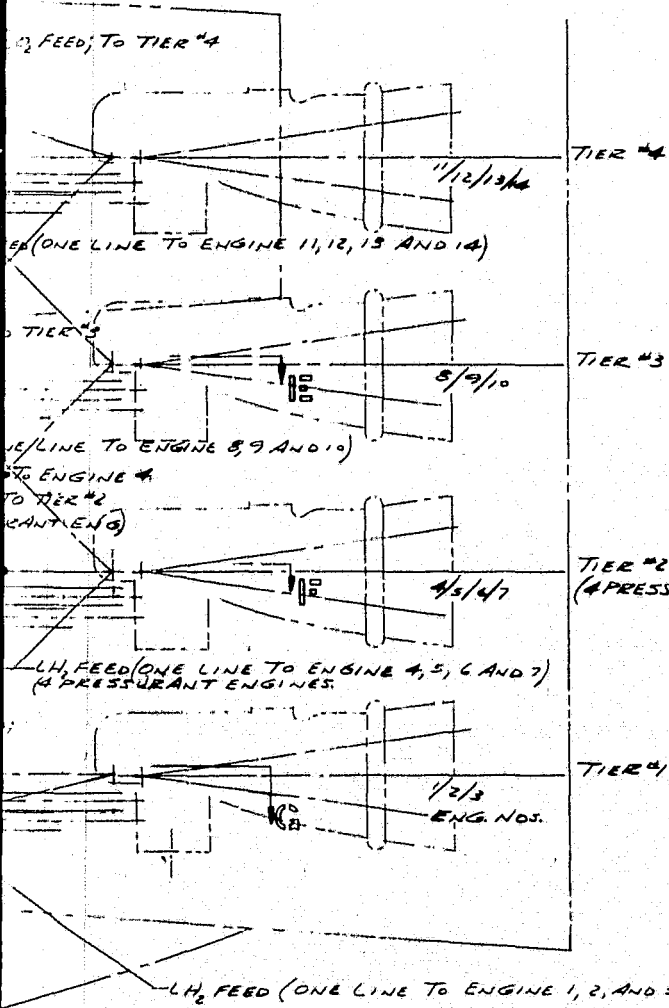
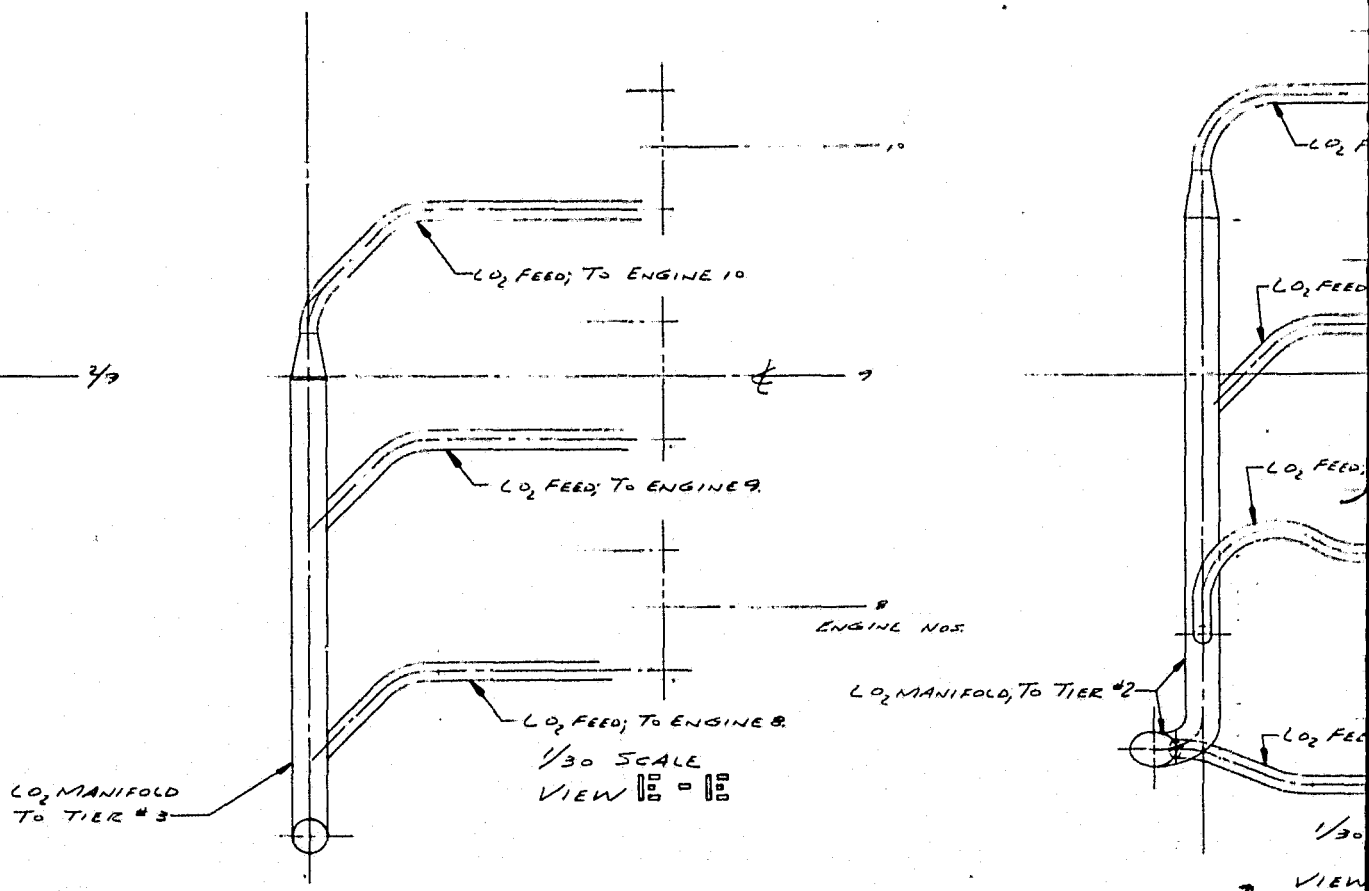
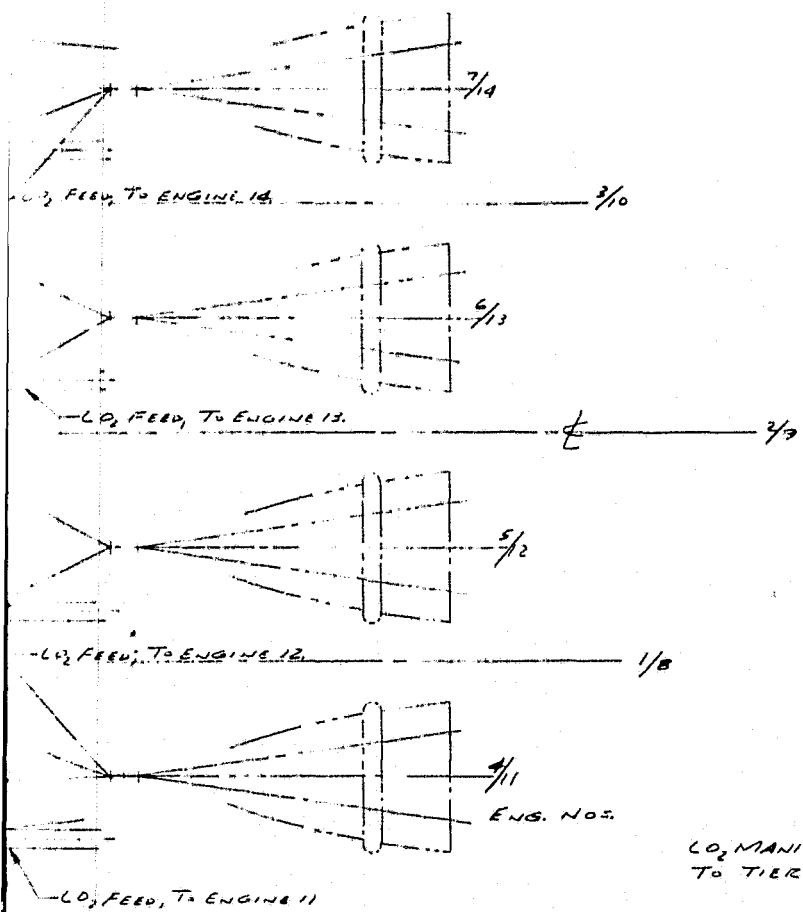
1/30 SCALE  
VIEW 6



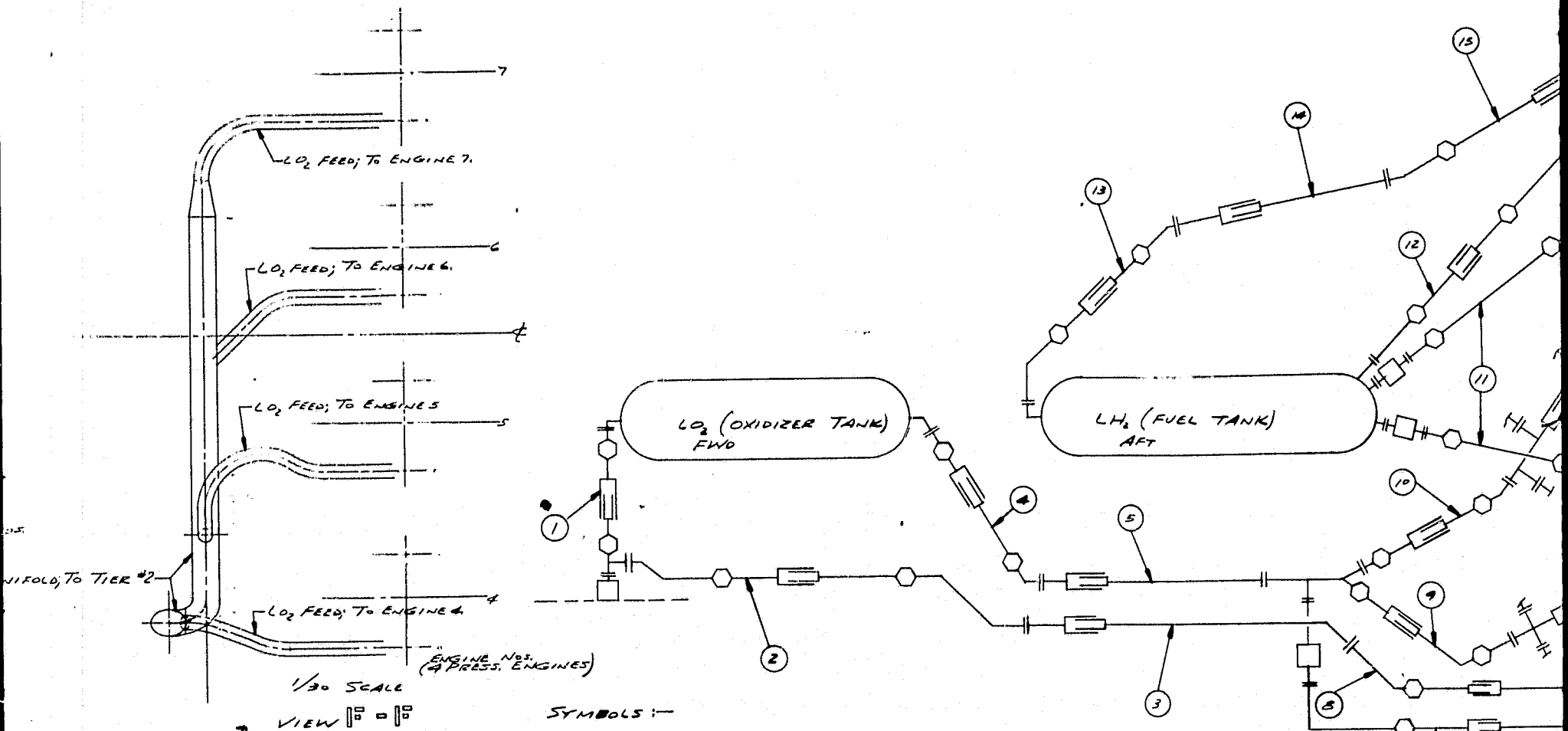
1/30 SCALE  
VIEW 13

**FOLDOUT FRAME**

LO<sub>2</sub> TRUNK (LEFT SIDE VEHICLE)

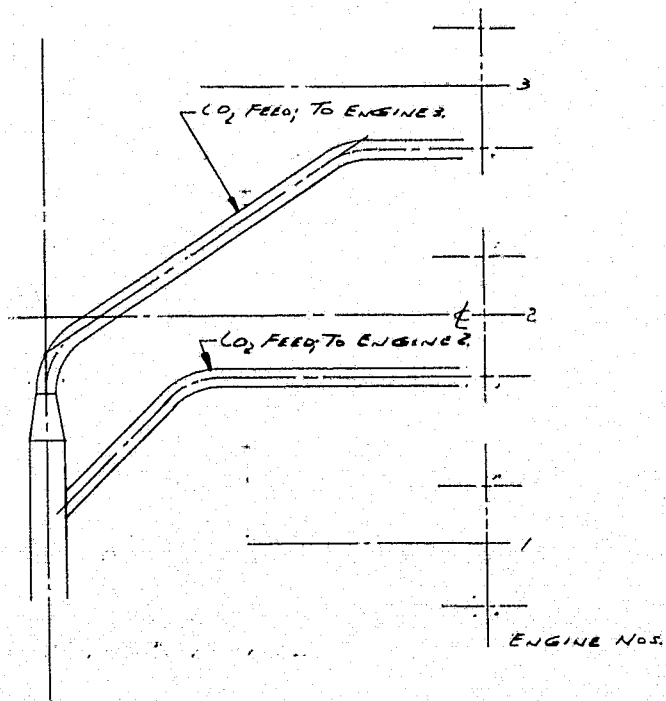
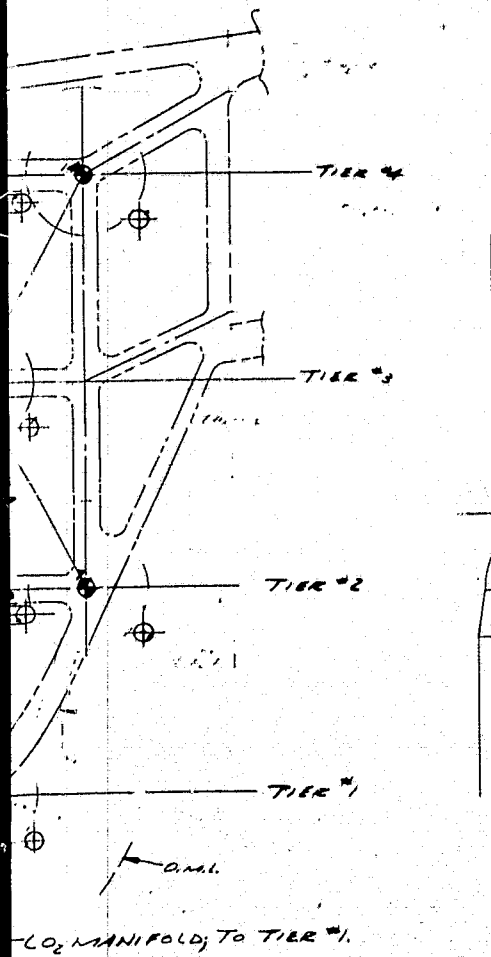


FOLDOUT FRAME 2

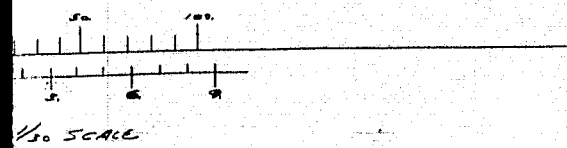
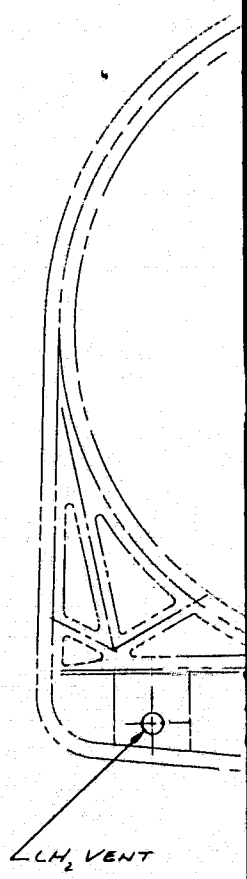


- SYMBOLS :-
- GIMBAL JOINT.
  - SLIDING JOINT.
  - PRESSURE, VOLUME COMPENSATING JOINT.
  - VALVE.
  - JOINT, MECHANICAL.

CRYOGENIC SCHEMATIC  
PRIMARY PROPULSION SYSTEM

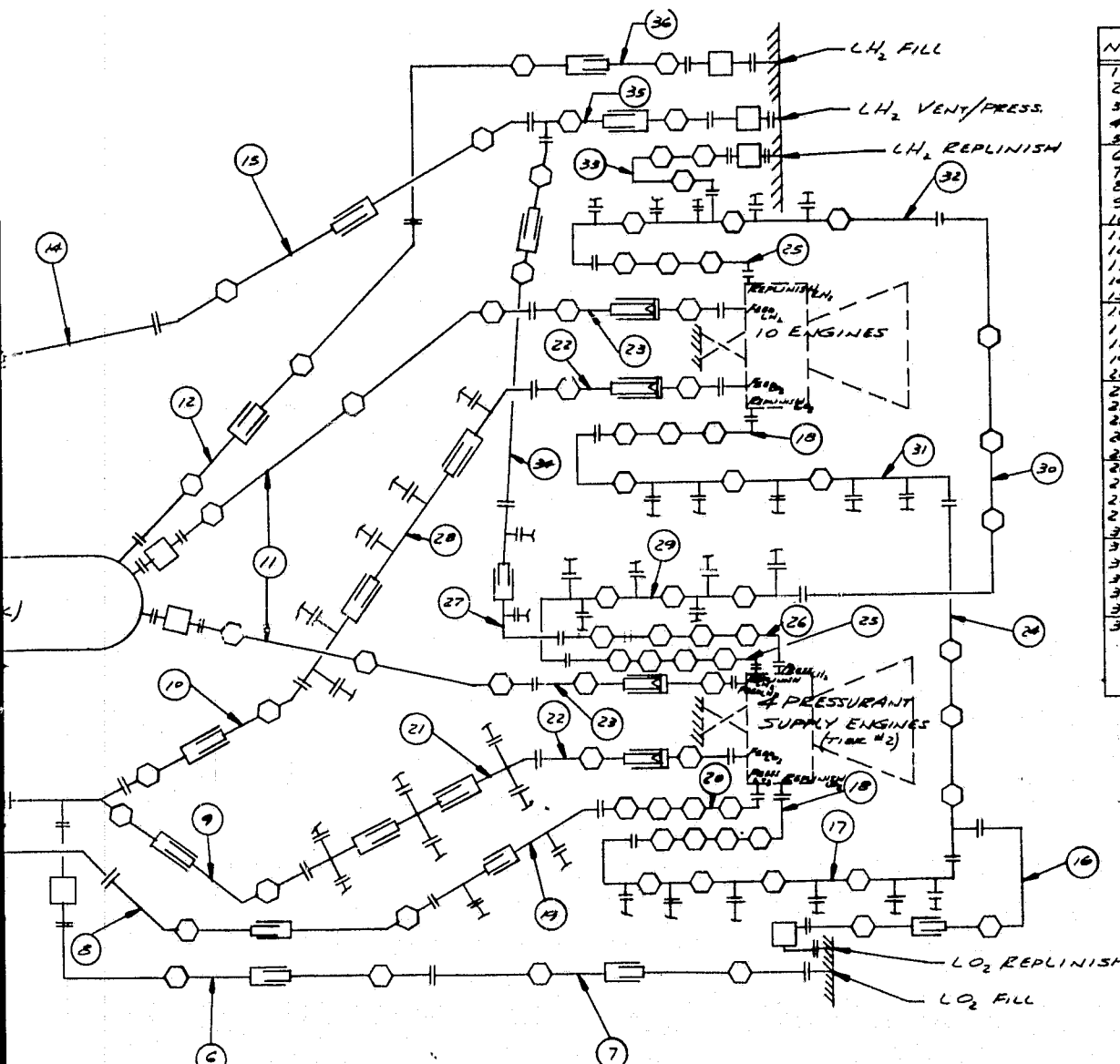


1/30 SCALE  
VIEW Q = Q

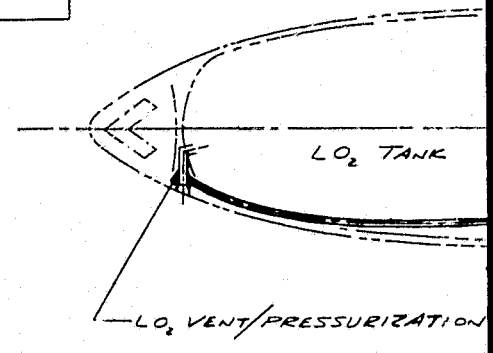


FOLDOUT FRAME 3

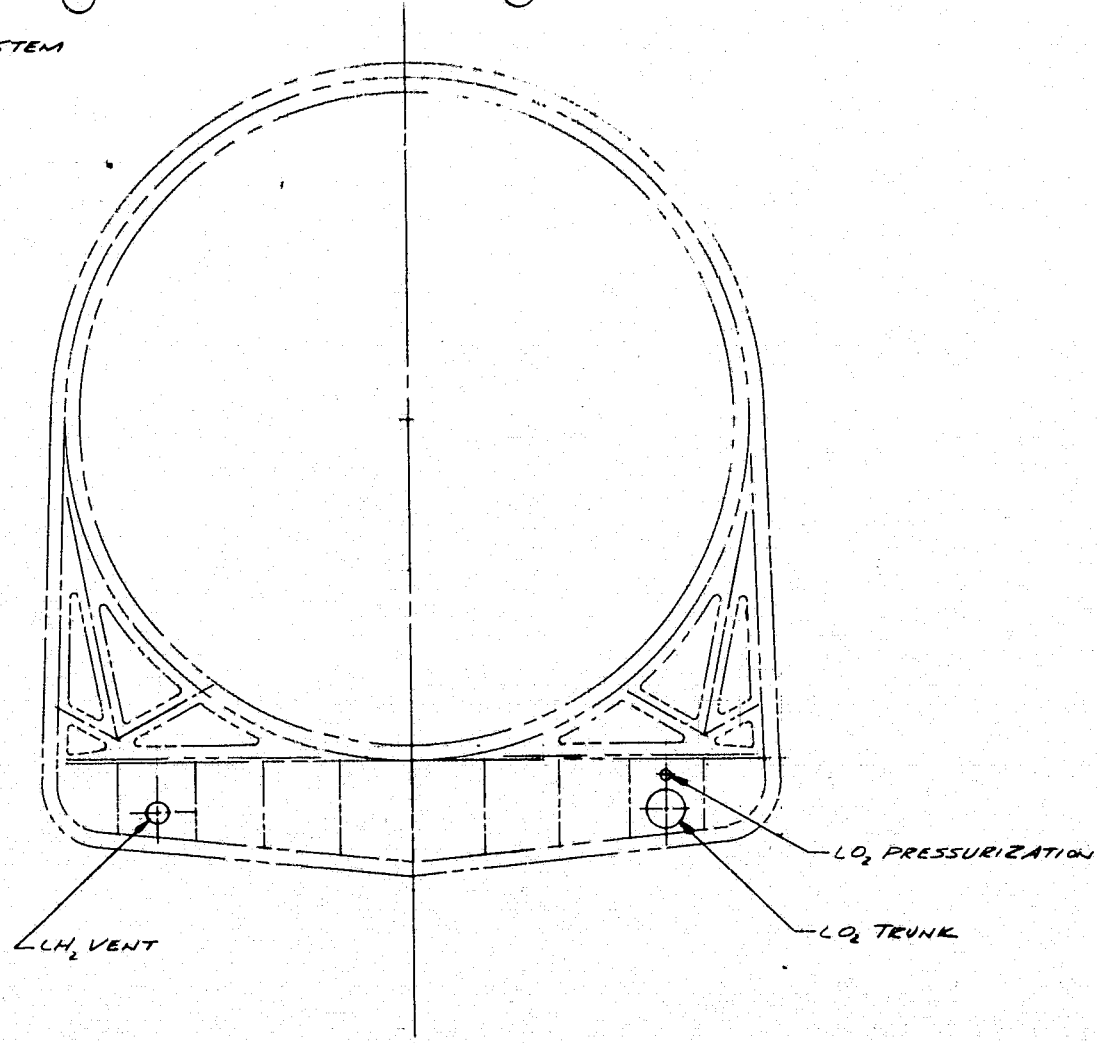




No	NOMENCLATURE
1	LOX VENT
2	LOX PRESSURIZATION, FWD
3	LOX PRESS., LONG
4	LOX TRUNK, FWD
5	LOX TRUNK, LONG
6	LOX FILL, FWD
7	LOX FILL, AFT
8	LOX PRESS., FWD
9	LOX MANIFOLD FEED, LONG
10	LOX MANIFOLD FEED, SHORT
11	FUEL FEED, FWD
12	FUEL FILL, FWD
13	FUEL VENT, FWD
14	FUEL VENT, LONG
15	FUEL VENT, MID
16	LOX REPLINISH
17	LOX REPLINISH, MANIFOLD
18	LOX REPLINISH, ENGINE
19	LOX PRESS., MANIFOLD
20	LOX PRESS., ENGINE
21	LOX FEED, MANIFOLD
22	LOX FEED, ENGINE
23	FUEL FEED, ENGINE
24	LOX REPLINISH MANIFOLD FEED
25	FUEL REPLINISH, ENGINE
26	FUEL PRESS., ENGINE
27	FUEL PRESS., MANIFOLD
28	LOX FEED, MANIFOLD
29	FUEL REPLINISH, MANIFOLD
30	FUEL REPLINISH, MANIFOLD FEED
31	LOX REPLINISH, MANIFOLD
32	FUEL REPLINISH, MANIFOLD
33	FUEL REPLINISH, MANIFOLD FEED
34	FUEL PRESS., AFT
35	FUEL VENT, AFT
36	FUEL FILL, AFT

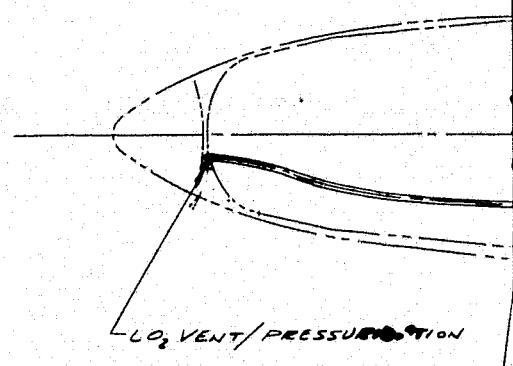


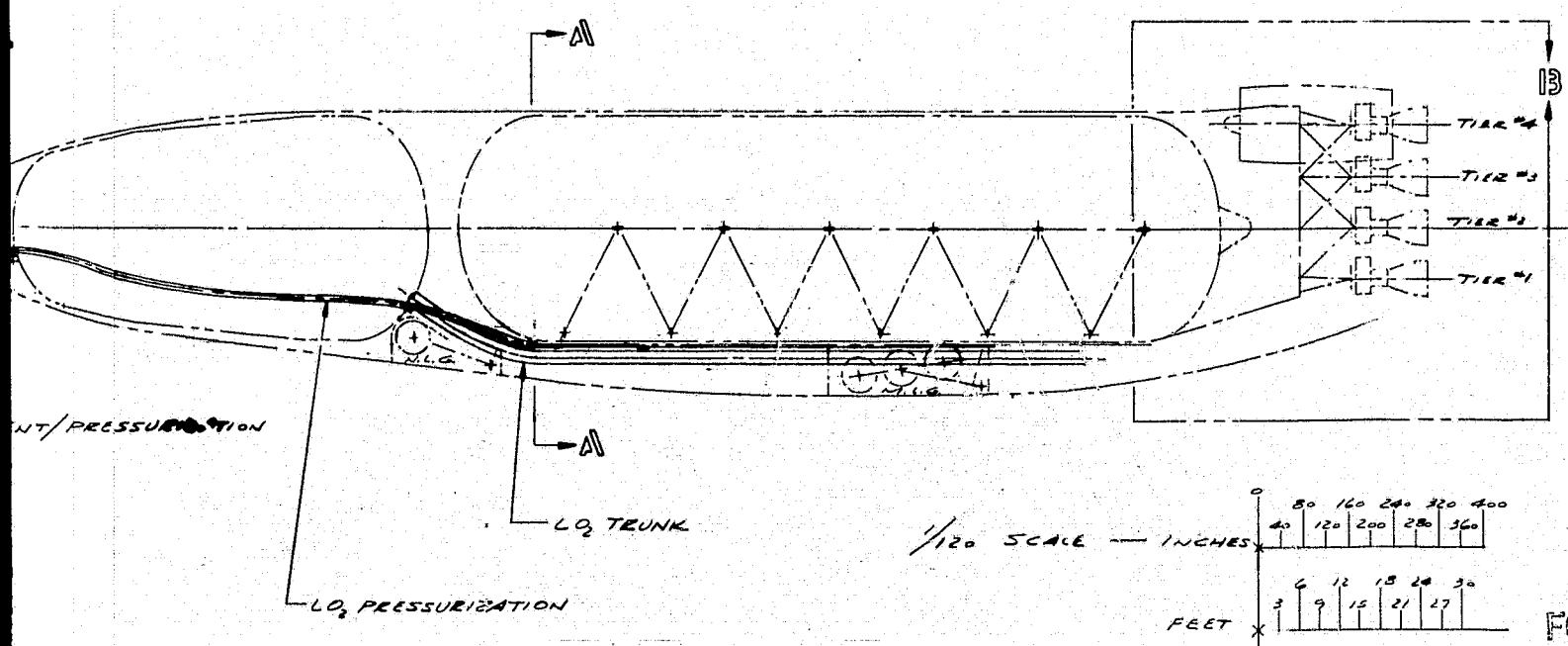
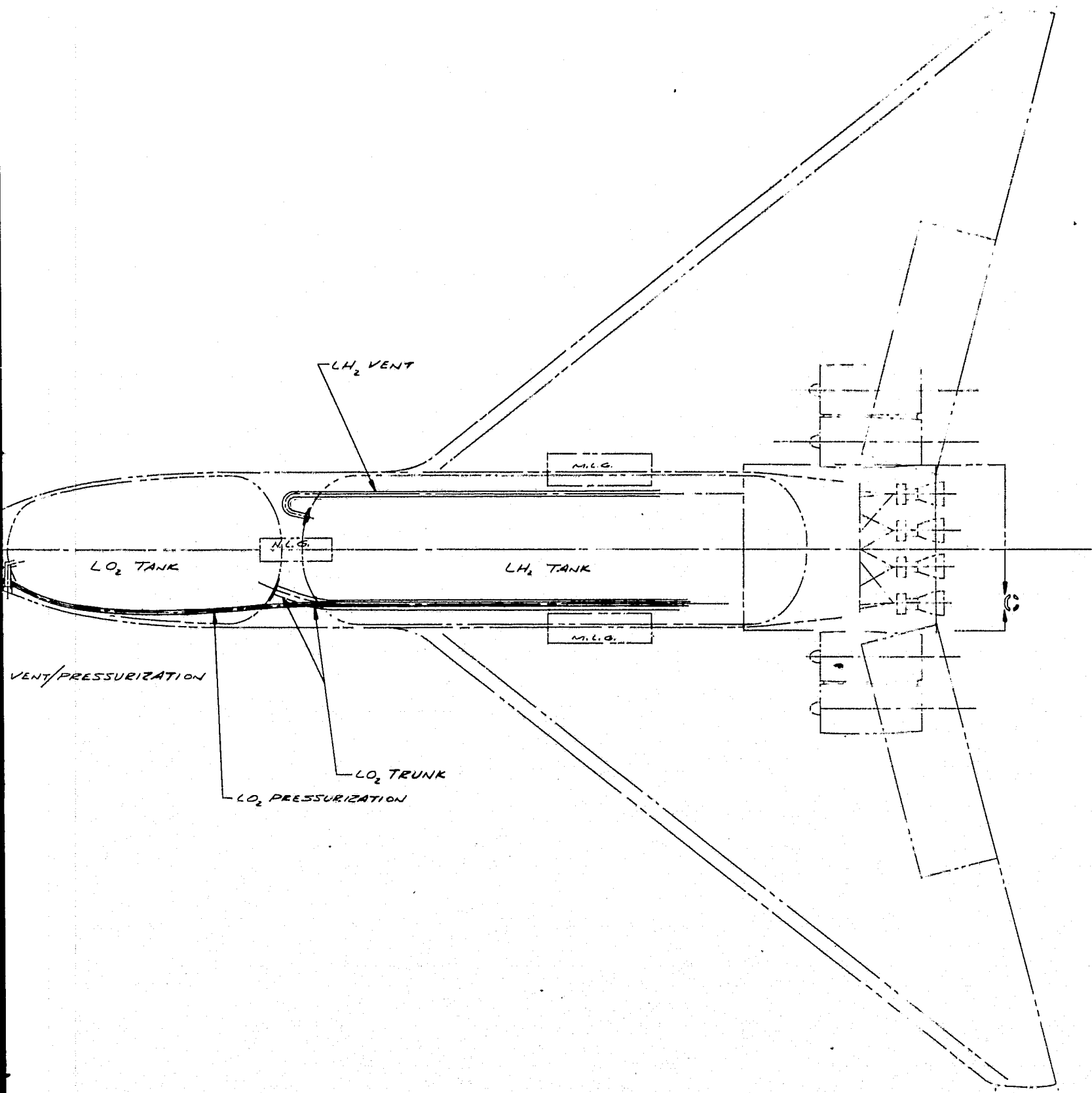
EMATIC  
SION SYSTEM



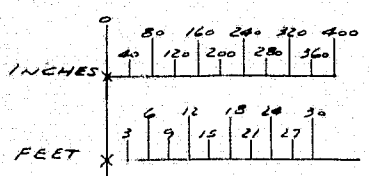
SECTION A-A  
1/40 SCALE

FOLDOUT FRAME 4

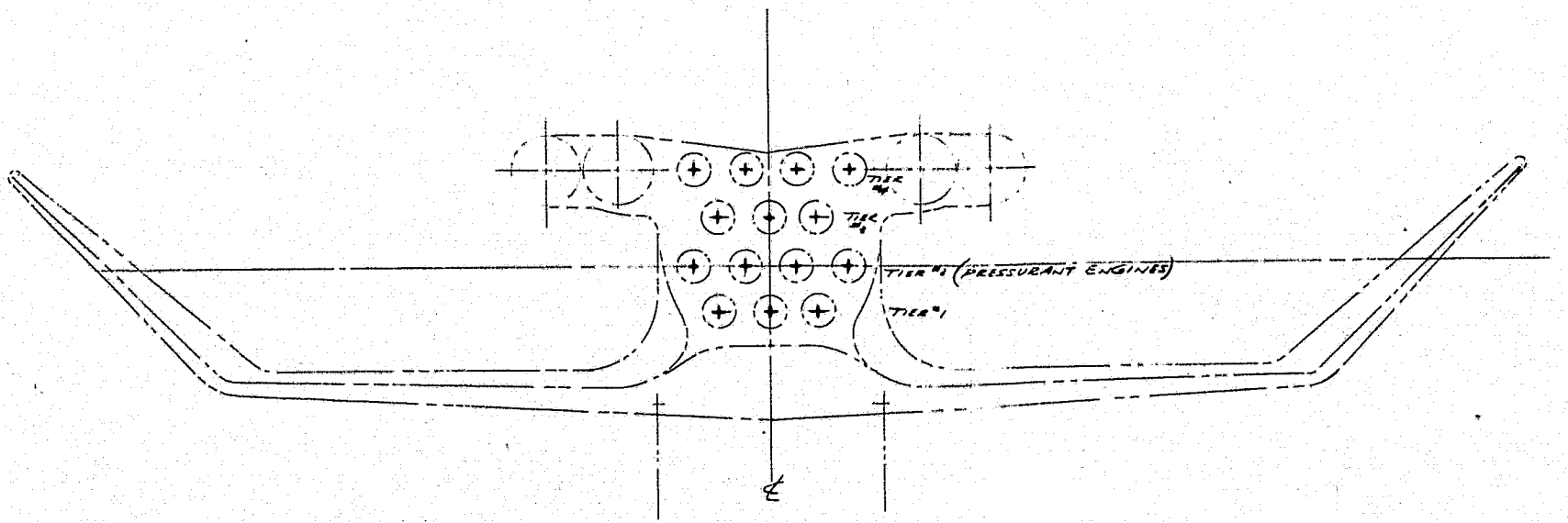




1/120 SCALE — INCHES

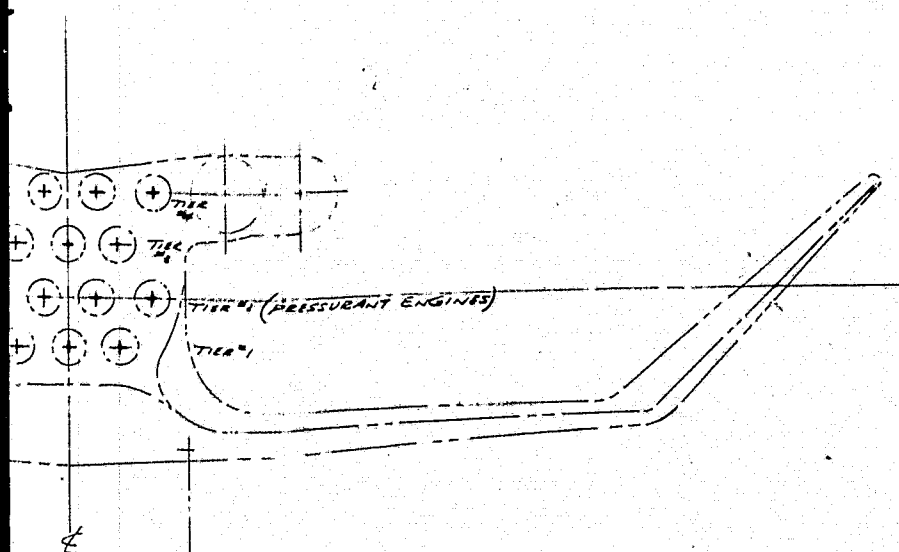


FOLDOUT FRAME 5



FRAME 5

FOLDOUT FRAME 6



FOLDOUT FRAME 6

DATE	OCT 69 W	LOCKHEED MISSILES & SPACE COMPANY	
DR	Sven G. Blomquist	A GROUP DIVISION OF LOCKHEED AIRCRAFT CORPORATION	
		SUNNYVALE, CALIFORNIA	
APPD		PRIMARY PROPULSION	
ENGRG		SYSTEM - BOOSTER, TWO	
CHK		STAGE VEHICLE, 1 ENGINE ST.	
APPD		SIZE CODE IDENT	DRAWING NO.
APPD			SKQ 101569
		SCALE 1/2" = 1"	SHEET 1 OF 1

A-27

FOLDOUT FRAME 7